THE UNIVERSITY OF NEW SOUTH WALES

Technical Report on the Development of a Geochemical Atlas of Cyprus

Volume 2 – Tables and Figures

David Cohen

and

Neil Rutherford

School of Biological, Earth and Environmental Sciences
The University of New South Wales

With contributions by

E. Morisseau, A.M. Zissimos, S. Laffan, S.G. Gatehouse and L. Ren

and other staff of the Geological Survey Department of Cyprus and the University of New South Wales

A report to the
Ministry of Agriculture, Natural Resources and Environment,
Geological Survey Department
(Tender AR 2005/12)

1 June 2011

Geochemical Atlas of Cyprus

Periodic Table of Elements

Atomic number: 79 — Symbol: Au — Element: gold — Atomic weight: 197.0

1 H hydrogen 1.0																	2 He helium 4.0
3 Li lithium 6.9	4 Be beryllium 9.0											5 B boron 10.8	6 C carbon 12.0	7 N nitrogen 14.0	8 O oxygen 16.0	9 F fluorine 19.0	10 Ne neon 20.2
11 Na sodium 23.0	12 Mg magnesium 24.3											13 Al aluminum 27.0	14 Si silicon 28.1	15 P phosphorus 31.0	16 S sulfur 32.1	17 Cl chlorine 35.5	18 Ar argon 40.0
19 K potassium 39.1	20 Ca calcium 40.1	21 Sc scandium 45.0	22 Ti titanium 47.9	23 V vanadium 50.9	24 Cr chromium 52.0	25 Mn manganese 54.9	26 Fe iron 55.9	27 Co cobalt 58.9	28 Ni nickel 58.7	29 Cu copper 63.6	30 Zn zinc 65.4	31 Ga gallium 69.7	32 Ge germanium 72.6	33 As arsenic 74.9	34 Se selenium 79.0	35 Br bromine 79.9	36 Kr krypton 83.8
37 Rb rubidium 85.5	38 Sr strontium 87.6	39 Y yttrium 88.91	40 Zr zirconium 91.2	41 Nb niobium 92.9	42 Mo molybdenum 95.9	43 Tc technetium 98	44 Ru ruthenium 101.1	45 Rh rhodium 102.9	46 Pd palladium 106.4	47 Ag silver 107.9	48 Cd cadmium 112.4	49 In indium 114.8	50 Sn tin 118.7	51 Sb antimony 121.8	52 Te tellurium 127.6	53 I iodine 126.9	54 Xe xenon 131.3
55 Cs cesium 132.9	56 Ba barium 137.3		72 Hf hafnium 178.5	73 Ta tantalum 180.9	74 W tungsten 183.8	75 Re rhenium 186.2	76 Os osmium 190.2	77 Ir iridium 192.2	78 Pt platinum 195.1	79 Au gold 197.0	80 Hg mercury 200.6	81 Tl thallium 204.4	82 Pb lead 207.2	83 Bi bismuth 209	84 Po polonium 209	85 At astatine 210	86 Rn radon 222
87 Fr francium 223	88 Ra radium 226																
			57 La lanthanum 138.9	58 Ce cerium 140.1	59 Pr praseodymium 140.9	60 Nd neodymium 144.2	61 Pm promethium 145	62 Sm samarium 150.4	63 Eu europium 152	64 Gd gadolinium 157.3	65 Tb terbium 158.9	66 Dy dysprosium 162.5	67 Ho holmium 164.9	68 Er erbium 167.3	69 Tm thulium 168.9	70 Yb ytterbium 173.0	71 Lu lutetium 175
			89 Ac actinium 227	90 Th thorium 232	91 Pa protactinium 231	92 U uranium 238	93 Np neptunium 237	94 Pu plutonium 239	95 Am americium 243	96 Cm curium 247	97 Bk berkelium 247	98 Cf californium 251	99 Es einsteinium 252	100 Fm fermium 257	101 Md mendelevium 258	102 No nobelium 259	103 Lr lawrencium 262

- alkali metals
- rare earth elements
- transition metals
- semi-metals
- noble gases
- Chalcophile
- alkaline earth metals
- actinides
- other metals
- non-metals
- halogens
- Siderophile

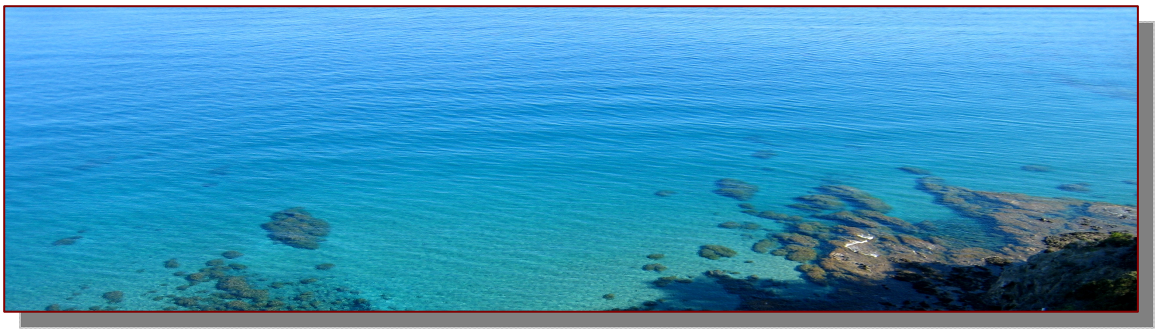

CONTENTS

Page 2-__

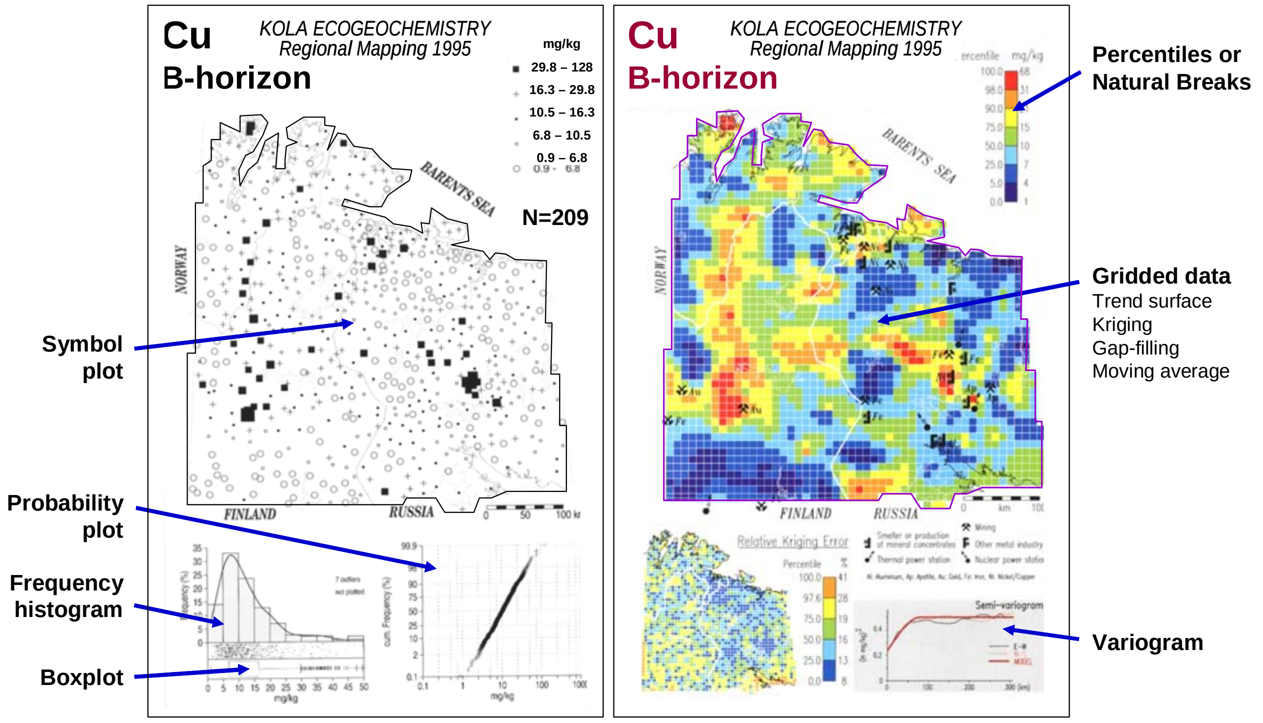

Figure 1.1 Data presentation formats for the Central Barents geochemical atlas. Modified from Reimann *et al.* (1998).

Table 1.1 Examples of large scale geochemical atlases. Main source: Garrett *et al.* (2008).

Year	Author (s)	Atlas title
1978	Instit. of Geological Sci.	*Regional Geochemical Atlas Series*: *Shetland and Orkneys*
1978	Webb *et al.*	*The Wolfson Geochemical Atlas of England and Wales*
1983	Weaver *et al.*	*The Geochemical Atlas of Alaska*
1985	Fauth *et al.*	*Geochemischer Atlas Bundesrepublik Deutschland*
1985	Instit. of Geophysical and Geochemical Exploration	*Provisional Geochemical Atlas of Northwestern Jiangxi*
1986	Bølviken *et al.*	*Geochemical Atlas of Northern Fennoscandia*
1987	Bolivar *et al.*	*Geochemical Atlas of San Jose and Golfito Quadrangle, Costa Rica*
1989	Tan	*The Atlas of Endemic Diseases and Their Environments in the Republic of China*
1989	Thalmann *et al.*	*Geochemischer Atlas der Republik Österreich*
1990	Lahermo *et al.*	*The Geochemical Atlas of Finland, Part 1: Groundwater*
1992	Koljonen	*The Geochemical Atlas of Finland, Part 2: Till*
1992	McGrath and Loveland	*The soil geochemical atlas of England and Wales*
1994	National EPA, People's Republic of China	*The Atlas of the Soil Environmental Background Value in the People's Republic of China*
1995	Lalor *et al.*	*A Geochemical Atlas of Jamaica*
1995	Lis and Pasieczna	*Geochemical Atlas of Poland*
1996	Lahermo *et al.*	*Geochemical Atlas of Finland, Part 3: Environmental Geochemistry stream waters and sediments*
1996	Mankovská	*Geochemical Atlas of Slovakia: Forest Biomass*
1996	Rapant *et al.*	*Geochemical Atlas of Slovakia: Groundwater*
1997	Cohen *et al.*	*Stream Sediment Geochemical Survey of the NE region of NSW*
1998	Reimann *et al.*	*Environmental Geochemical Atlas of the Central Barents Region*
1999	Aurlík and Šefčík	*Geochemical Atlas of the Slovak Republic Part V: Soils*
1999	Kadunas *et al.*	*Geochemical Atlas of Lithuania*
1999	Li and Wu	*Atlas of the Ecological Environmental Geochemistry of China*
1999	Rank *et al.*	*Bodenatlas des Freistaates Sachsen*
2000	Ottesen *et al.*	*Geochemical Atlas of Norway. Part 1: Chemical Composition of Overbank Sediments*
2003	De Vivo *et al.*	*Geochemical environmental atlas of Campania Region* (in Italian)
2003	Reimann *et al.*	*Agricultural Soils in Northern Europe: A Geochemical Atlas*
2004	Imai *et al.*	*Geochemical Map of Japan*
2004	Salminen *et al.*	*Geochemical Atlas of Eastern Barents Region*
2005	Salminen *et al.*	*Geochemical Atlas of Europe*
2007	Cornelius *et al.*	*Regolith Geochemical Mapping of the Yilgarn Craton*
2007a	Caritat *et al.*	*National Geochemical Survey of Australia* (in progress)
2007b	Caritat *et al.*	*Riverina Region Geochemical Survey, Southwestern NSW and Northern Victoria*
2008	Caritat *et al.*	*Thompson Region Geochemical Survey, Northwestern NSW*
2009	Smith *et al.*	*North American Soil Geochemical Landscape Project* (in progress)

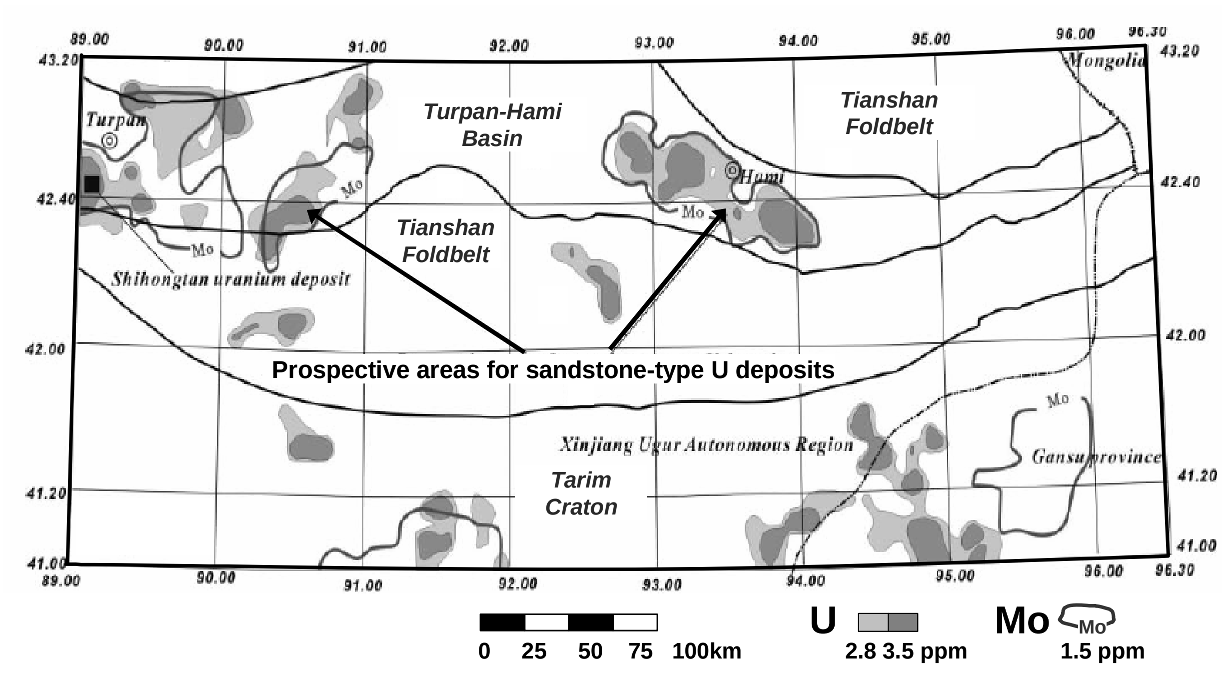

Figure 1.2 Mobile metal distributions for U and Mo from a low-density regional reconnaissance survey in NW China, showing prospective areas for sandstone-hosted U-Cu mineralisation in the vicinity of the Shihongtan U deposit. Modified from Wang *et al.* (2007).

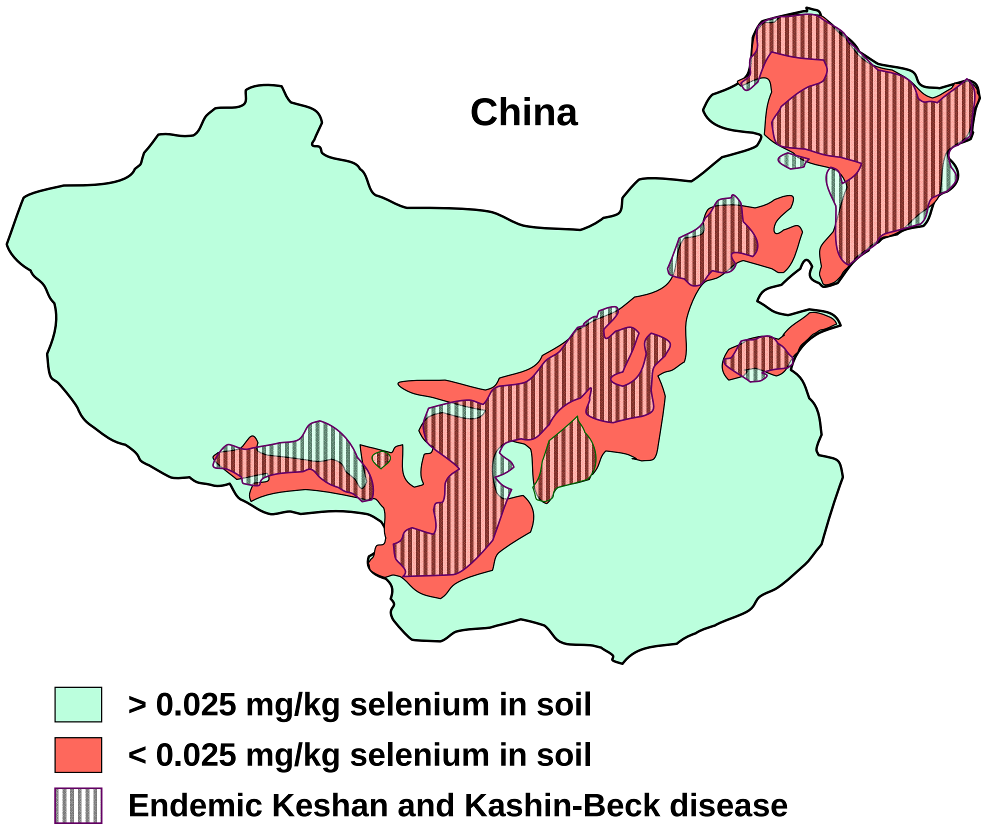

Figure 1.3 Distribution of Se in soils across China and endemic diseases related to Se deficiencies. Modified from Tan (1989).

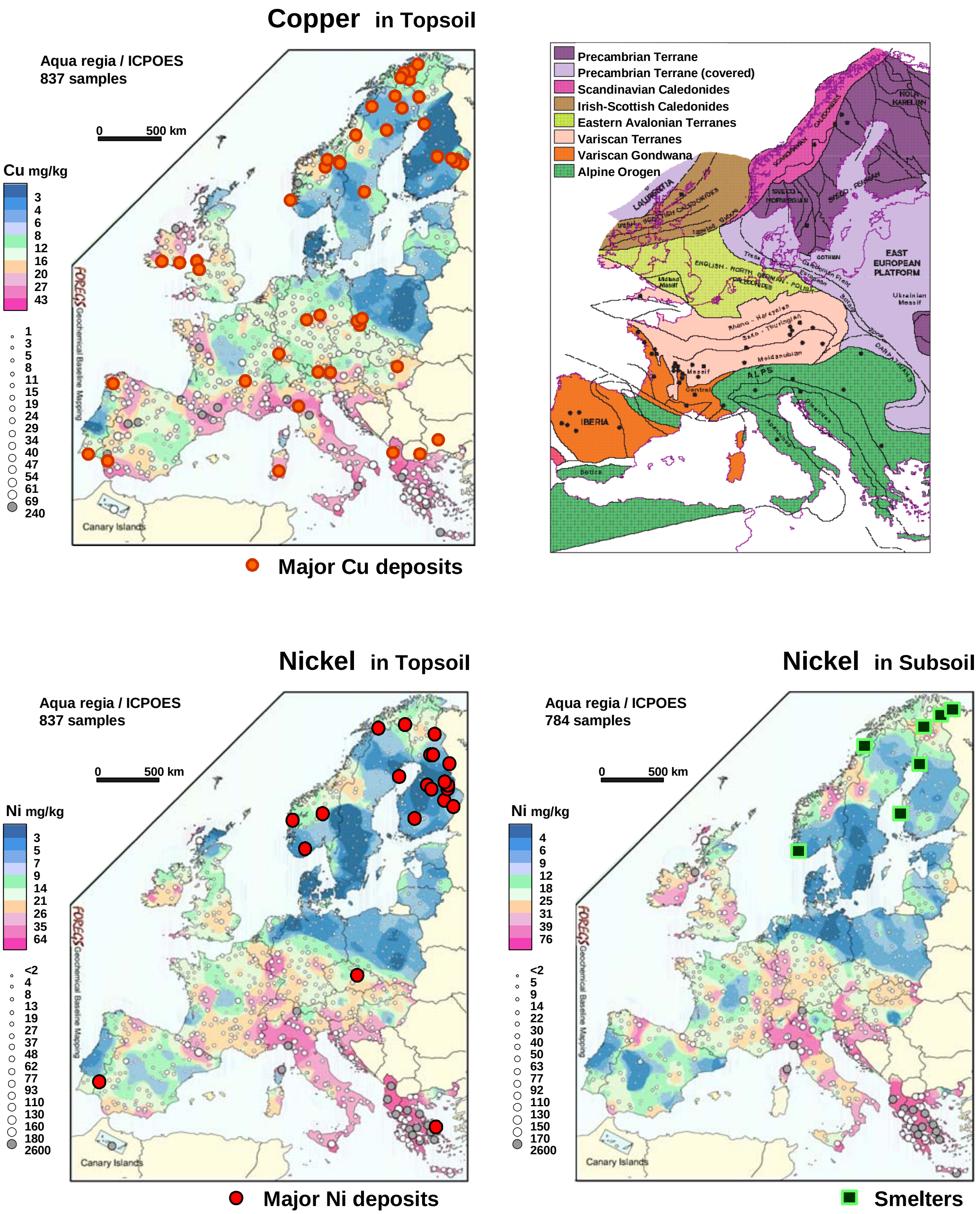

Figure 1.4 Copper and Ni in top soil and sub soil samples from the Geochemical Atlas of Europe, along with simplified geological terrane map. Modified from www.gtk.fi/publ/foregsatlas/ and Plant *et al.* (2007).

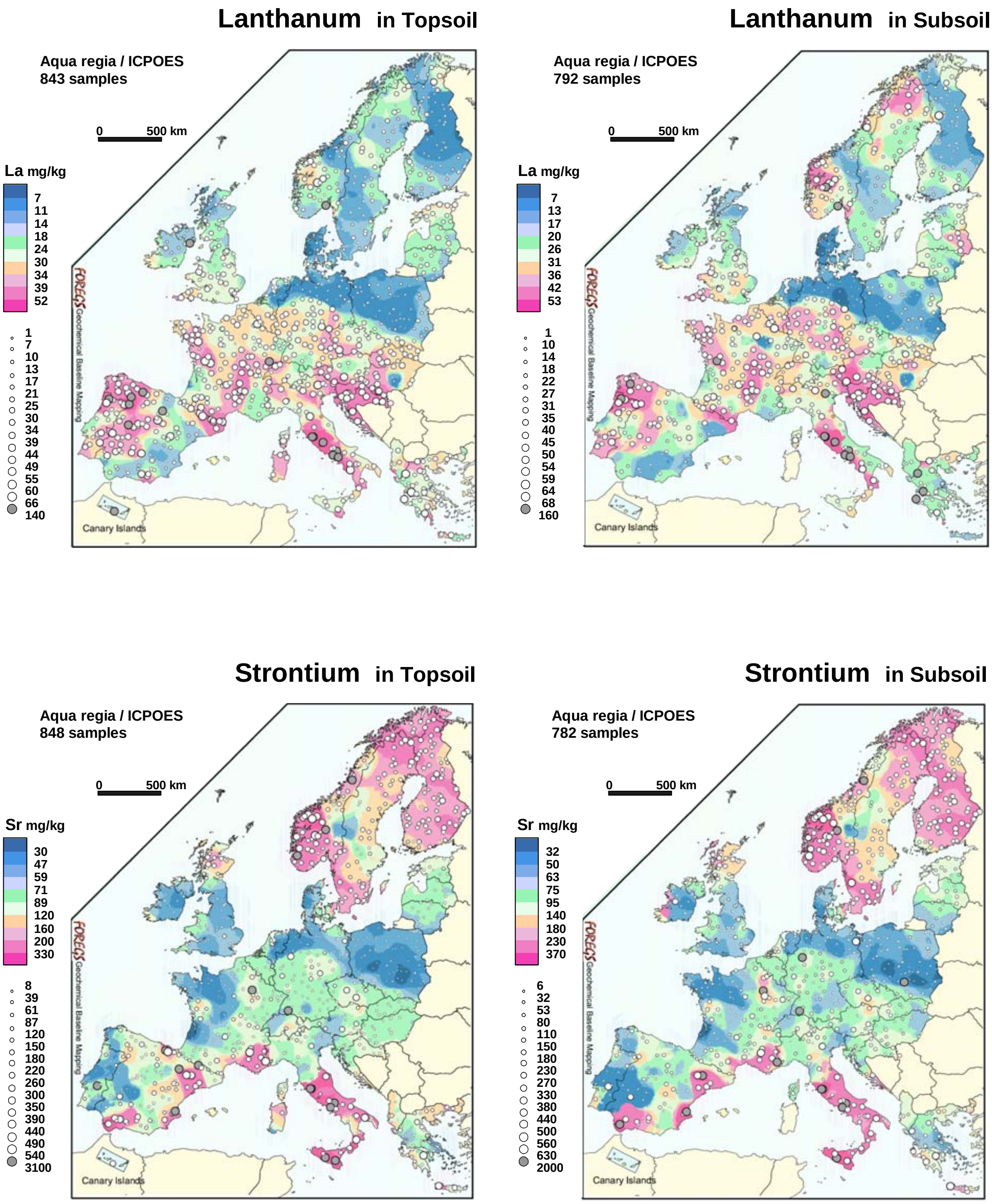

Figure 1.5 Lanthanum and Sr in top soil and sub soil samples from the Geochemical Atlas of Europe. Modified from Salminen *et al.* (2007) and www.gtk.fi/publ/foregsatlas/.

Table 1.2 Environmental risk assessment and clean-up standards for residential land use for selected elements from various European countries. Data compiled by Rapant *et al.* (2008). Values in mg/kg.

Element	**Risk limit value**	**Excess of risk value limit**		**European content level**		**National clean-up standards for residential land use**									
	(50th %ile)	**n**	**%**	**Median**	**Mean**	**Slovakia**	**Finland**	**Belgium**	**Canada**	**France**	**Germany**	**Italy**	**Netherlands**	**Sweden**	**UK**
As	33.5	39	4.7	7.03	11.6	30	50	110	12	37	50	20	55	15	20
Ba	625	81	9.8	375	400	1000			500	625			625		
Cd	9	1	0.1	0.145	0.284	5	10	6	10	20	20	2	12	0.4	8
Co	75	3	0.4	7.78	10.4	50	100			240		20	240	30	
Cr	175	46	5.6	60	94.8	250	200	300	64	130	400	150	380	120	130
Cu	135	2	0.2	13	17.3	100	150	400	63	190		120	190	100	
Hg	6.8	0	0	0.037	0.061	2	2	15	6.6	7	20	1	10	1	8
Mo	200	0	0	0.62	0.943	40	200	200							
Ni	110	32	3.9	18	37.3	100	100	470	50	140	140	120	210	35	50
Pb	300	6	0.7	22.6	32.6	150	200	700	140	400	400	100	530	80	450
V	130	65	7.8	60.4	68.1	200	150		130			90		120	
Zn	425	4	0.5	52	68.1	500	250	1000	200	9000		150	720	350	

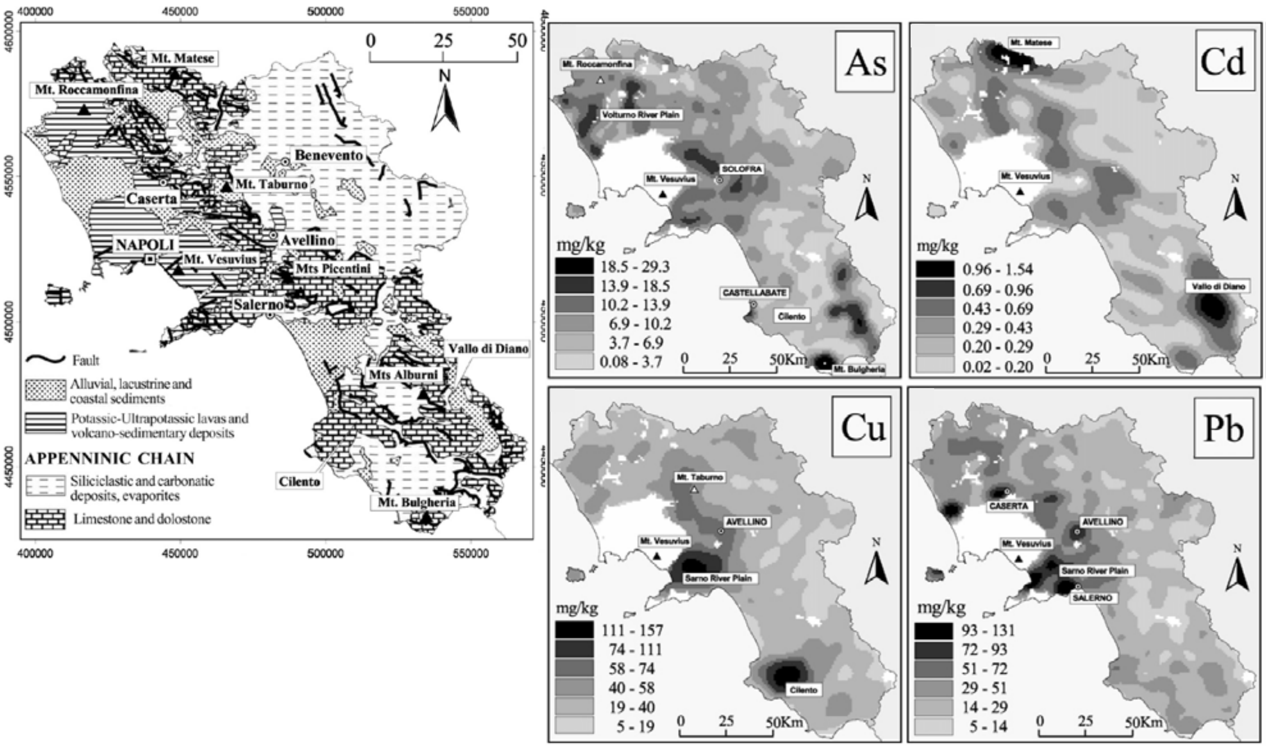

Figure 1.6 Comparison between geology and distribution of various trace elements in stream sediments of the Campania region of Italy. From Albanese *et al.* (2007).

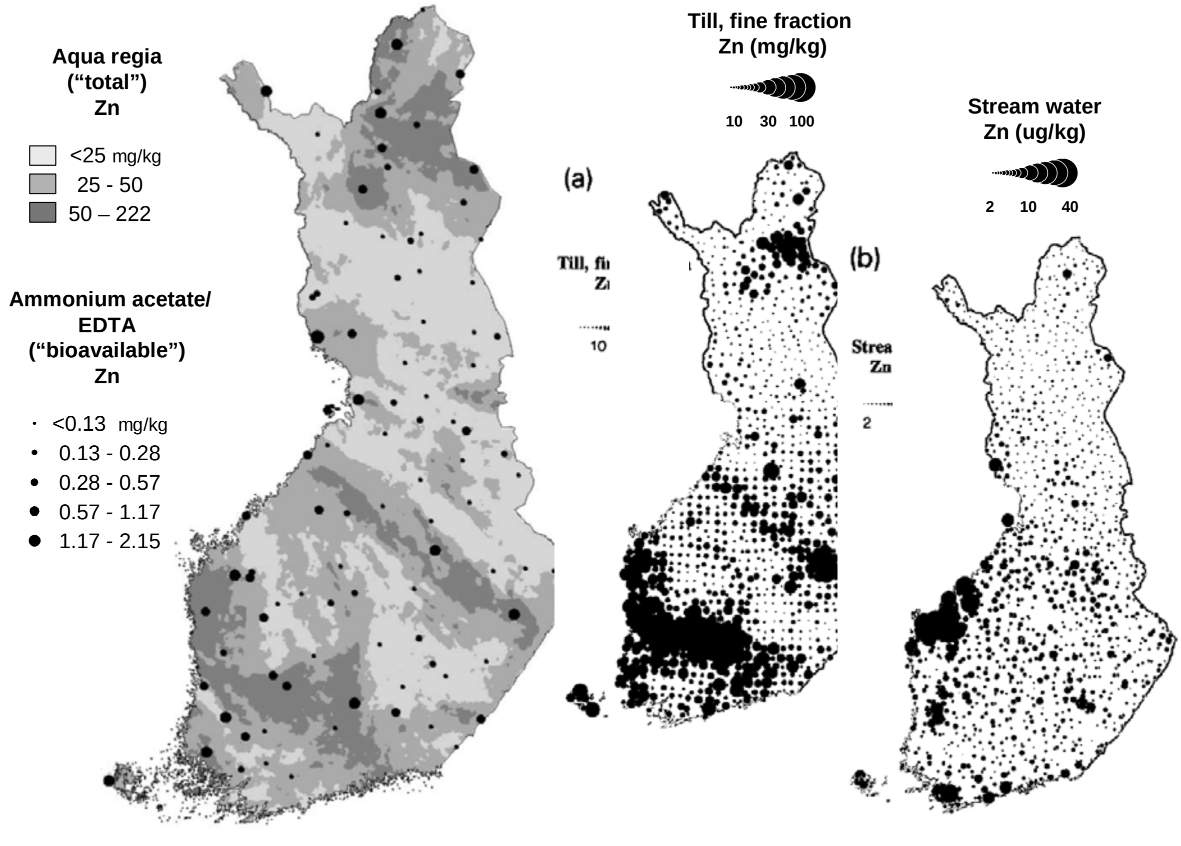

Figure 1.7 Comparison between aqua regia ("total") and ammonium acetate/EDTA-extractable ("bioavailable") Zn in tills of Finland and between till and stream waters. Modified from Salminen and Tarvainen (1995).

Table 1.3 Comparison between means for the original detailed regional dataset and 90-sample subset (Fig 1.7). From Salminen and Tarvainen (1995).

Element	Regional data	Subset
Samples	82,062	90
Cr	31.3	30.5
Cu	21.8	15.6
Ni	17.2	14.1
V	38.0	38.1
Zn	30.8	24.6

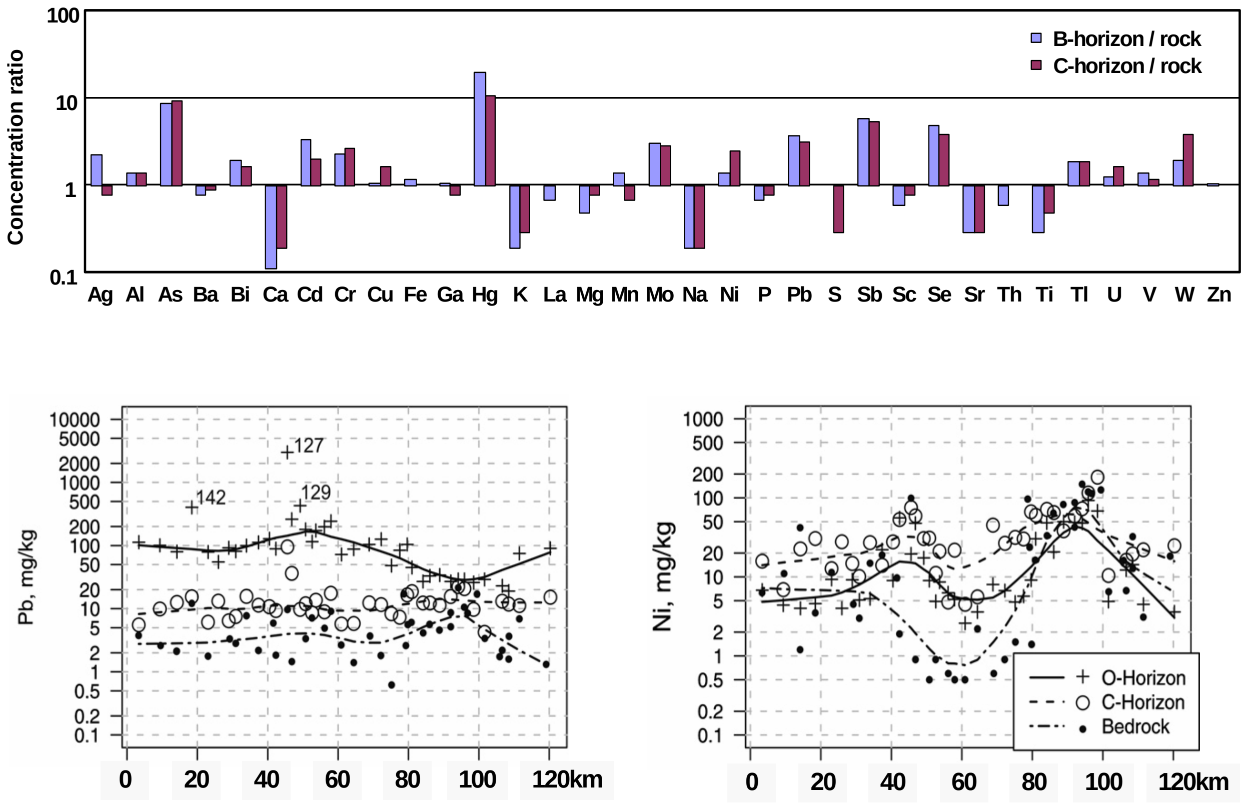

Figure 1.8 Concentration ratios between B-horizon and C-horizon soil samples and parent rock for 40 samples from Norway, and traverse plots for Pb and Ni. Data and figures after Reimann *et al.* (2007).

Bismuth in organics horizon

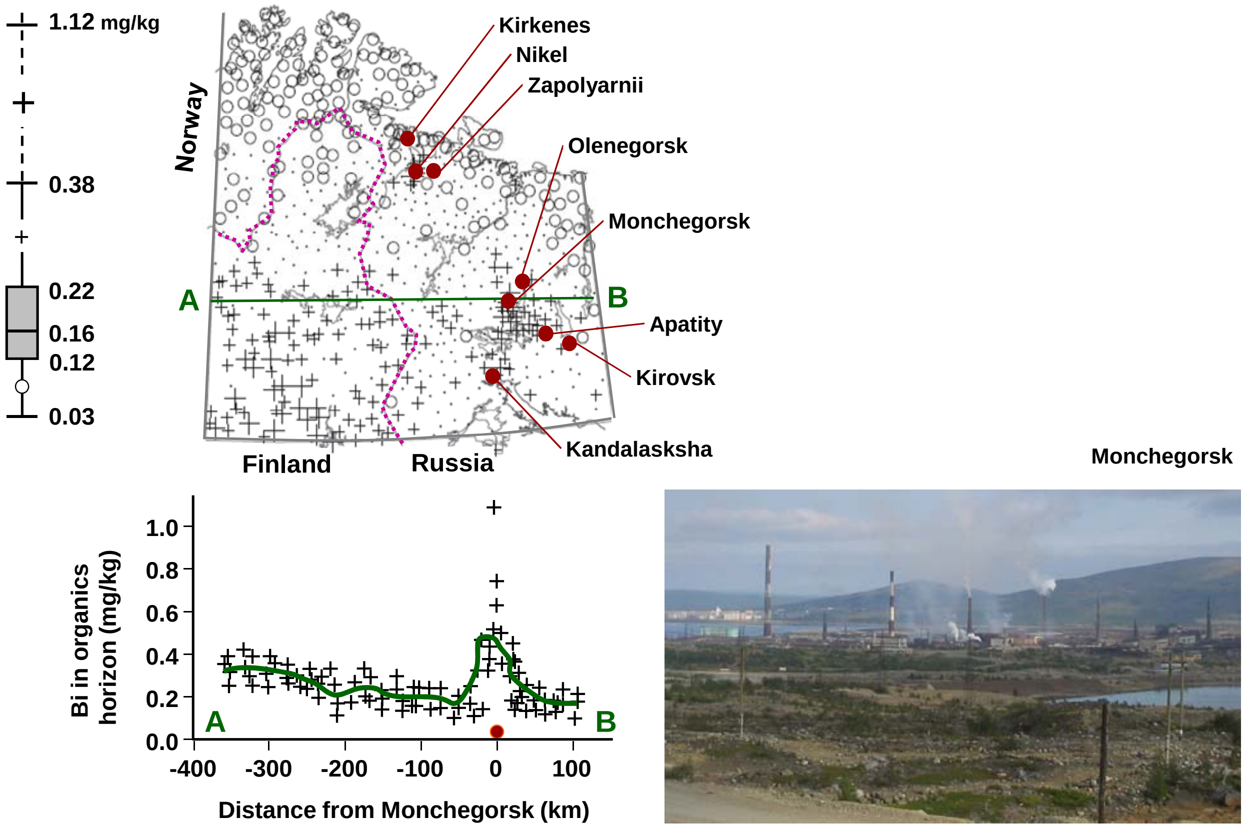

Figure 1.9 Soil organic (A_o) Bi contents for the Central Barents region, and E-W traverse across the Monchegorsk smelter area. Modified from Reimann and de Caritat (2005).

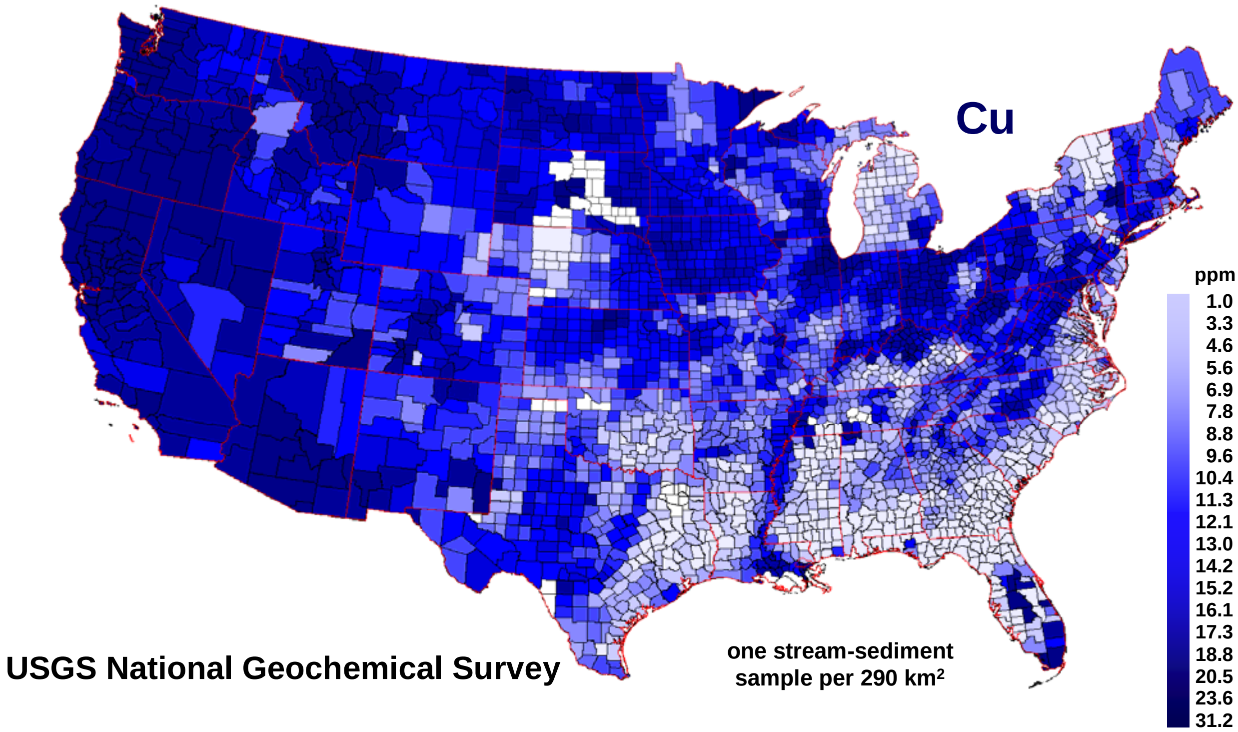

Figure 1.10 Stream sediment geochemistry for the conterminous USA. Data from USGS national geochemical survey.

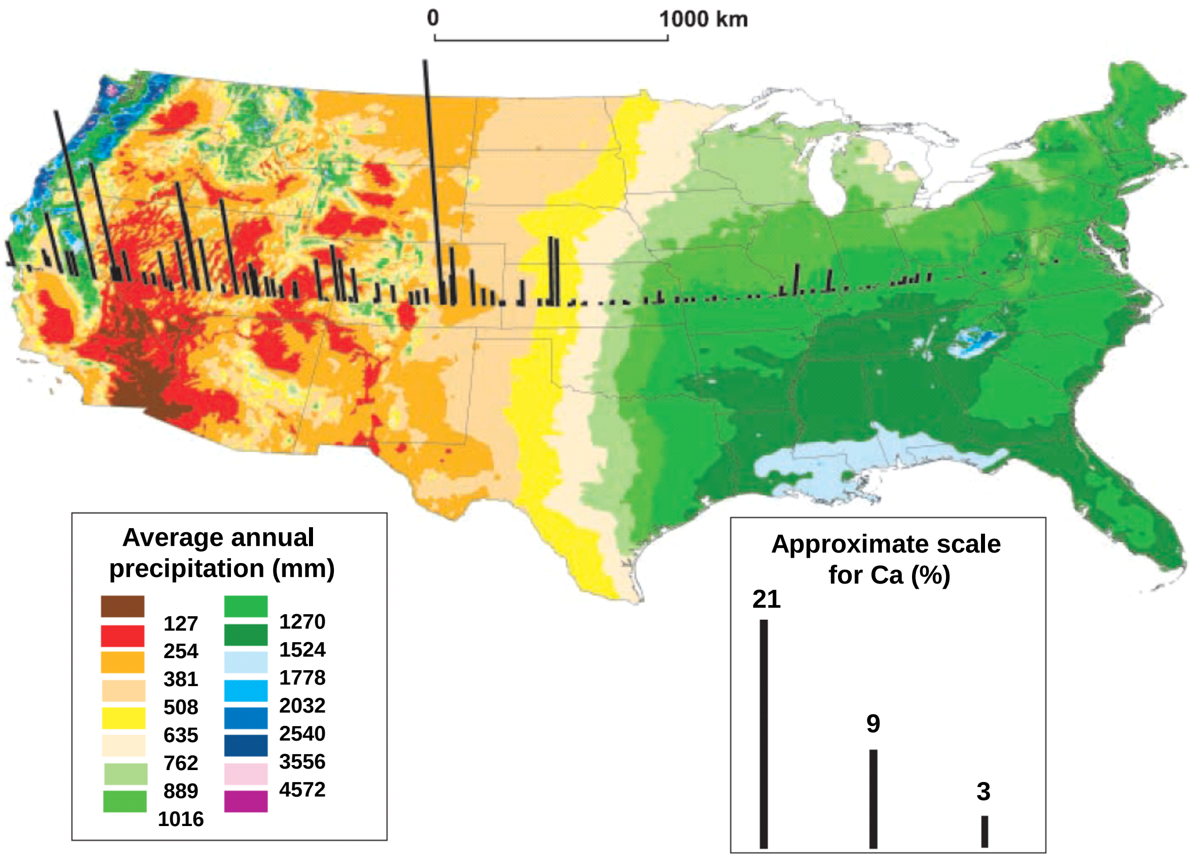

Figure 1.11 Calcium content in top soils from E-W traverse across the USA compared with rainfall patterns. Modified from Smith (2005, 2006).

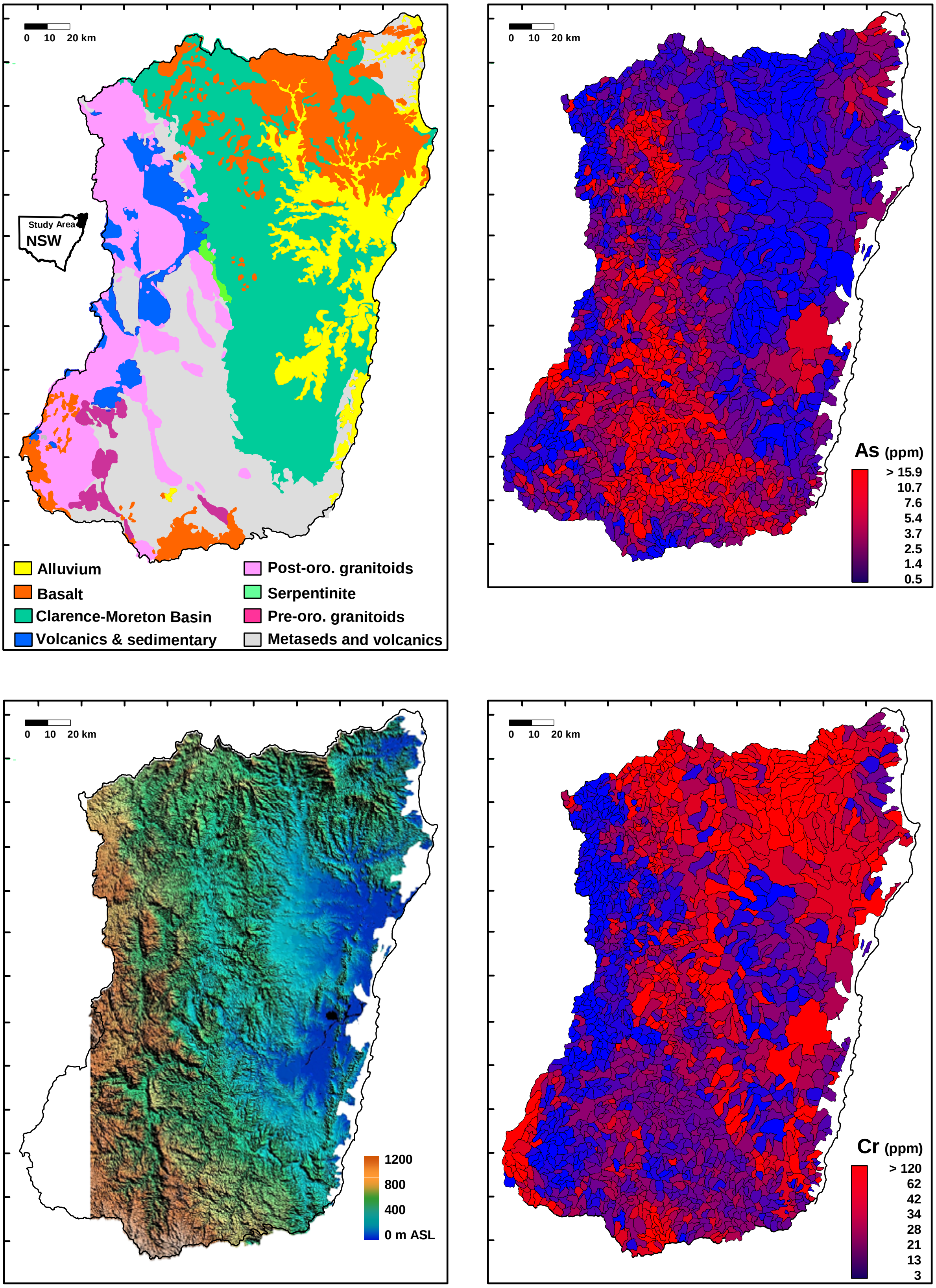

Figure 1.12 General geology and topography of the north-east region of NSW and distribution of total As and Cr in stream sediments. From Cohen *et al.* (1995).

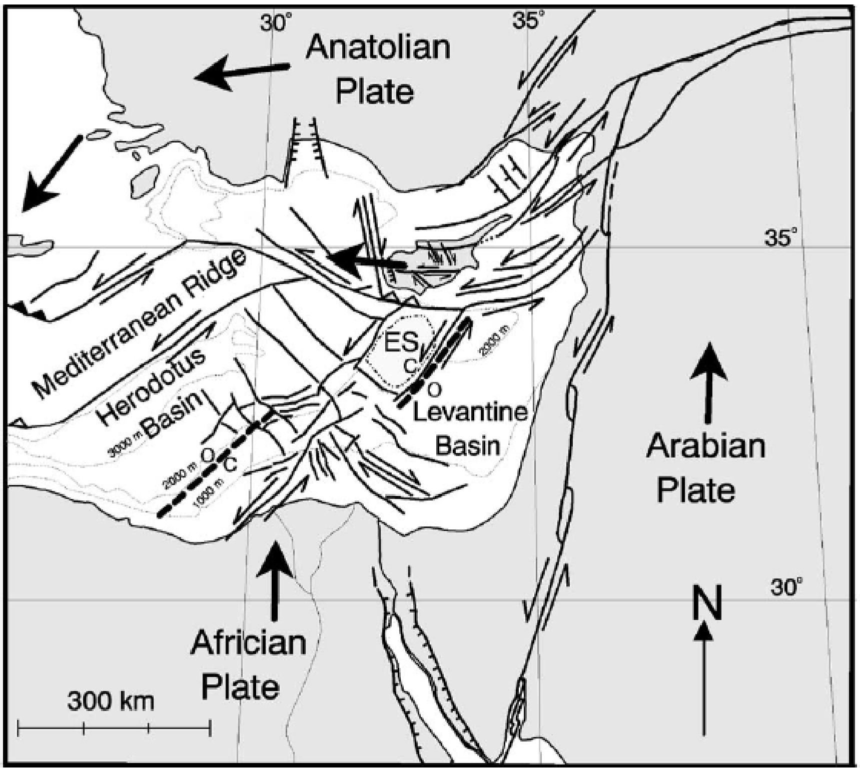

Figure 1.13 General tectonic setting and major features of the eastern Mediterranean. From Harrison *et al*. (2004).

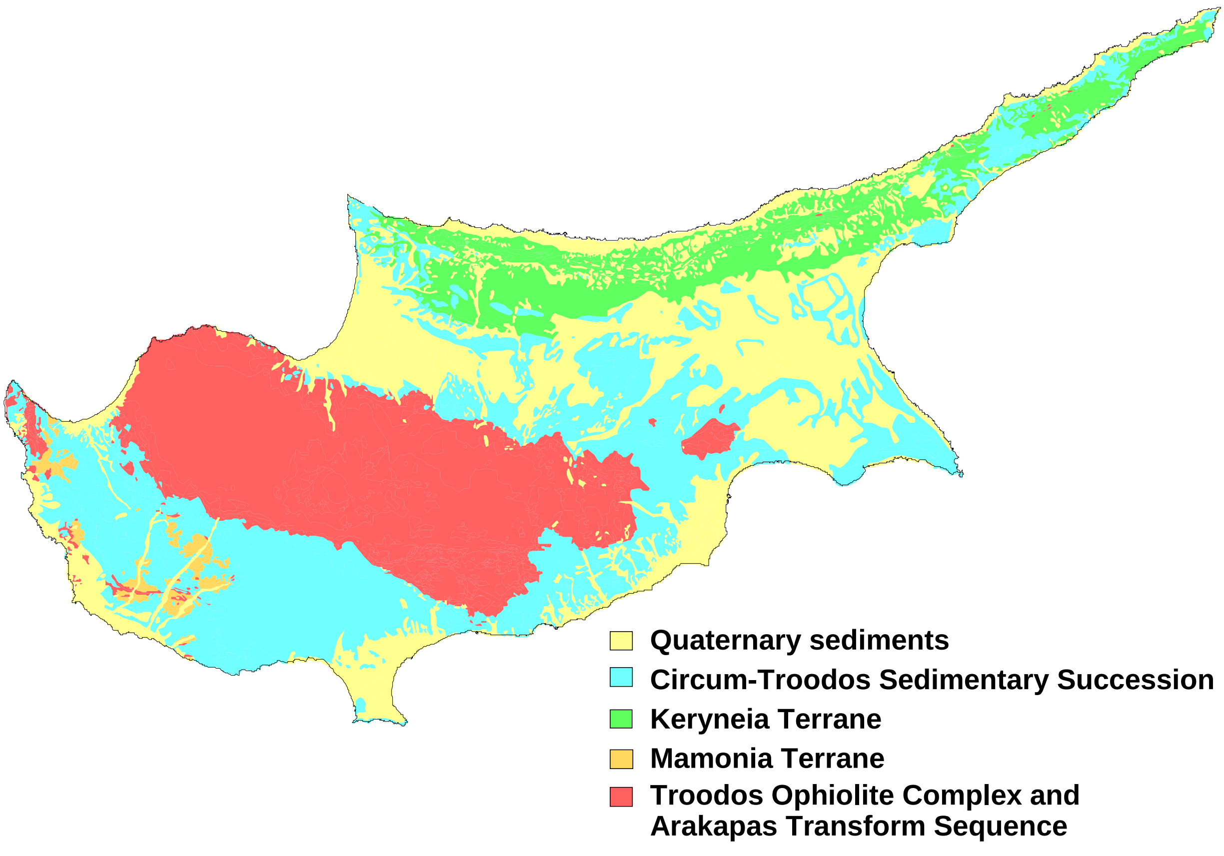

Figure 1.14 Main geological terranes of Cyprus.

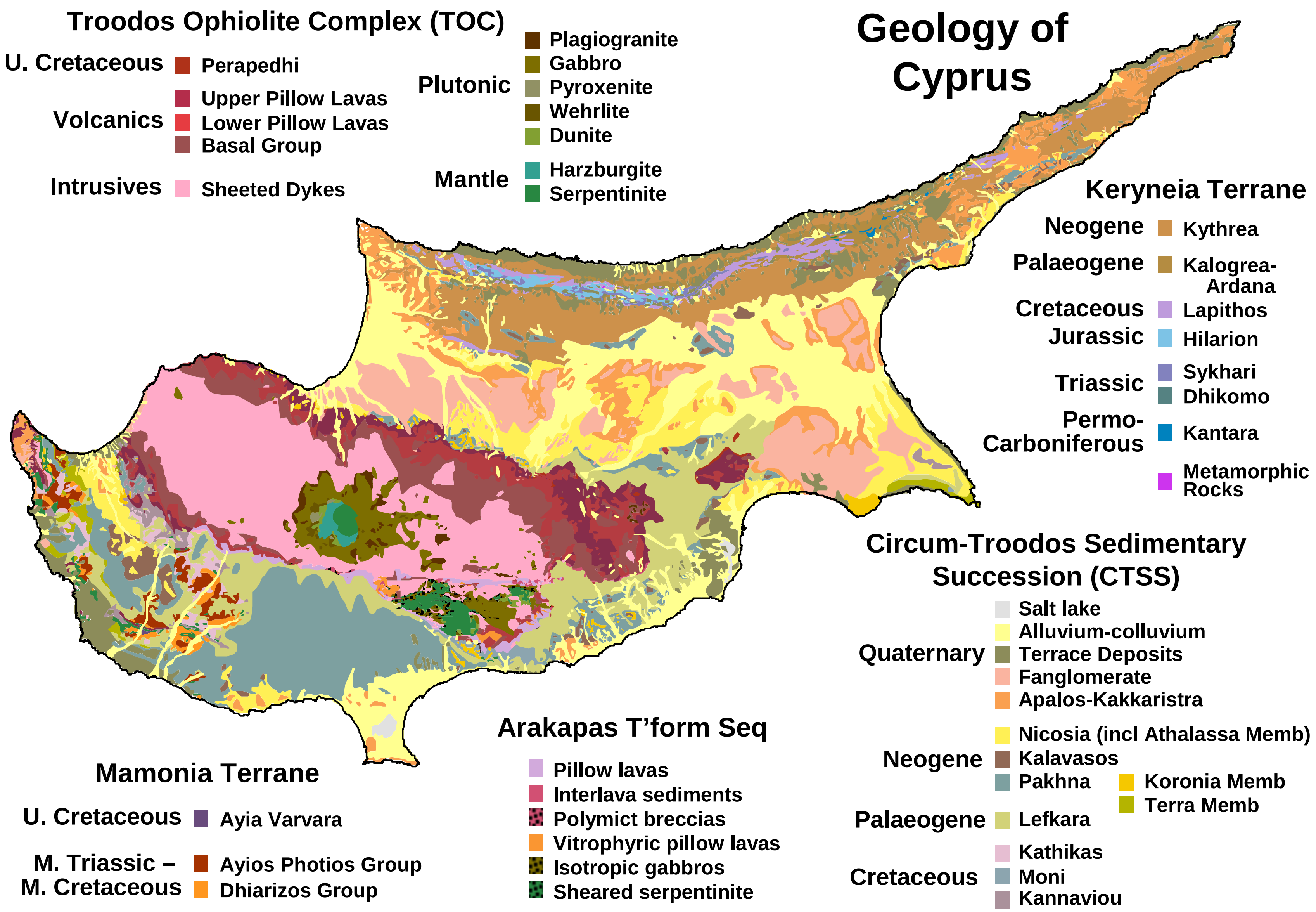

Figure 1.15 Detailed geological map with formations colour coded according to the 1995 1:250,000 geological map of Cyprus. Data from the GSD.

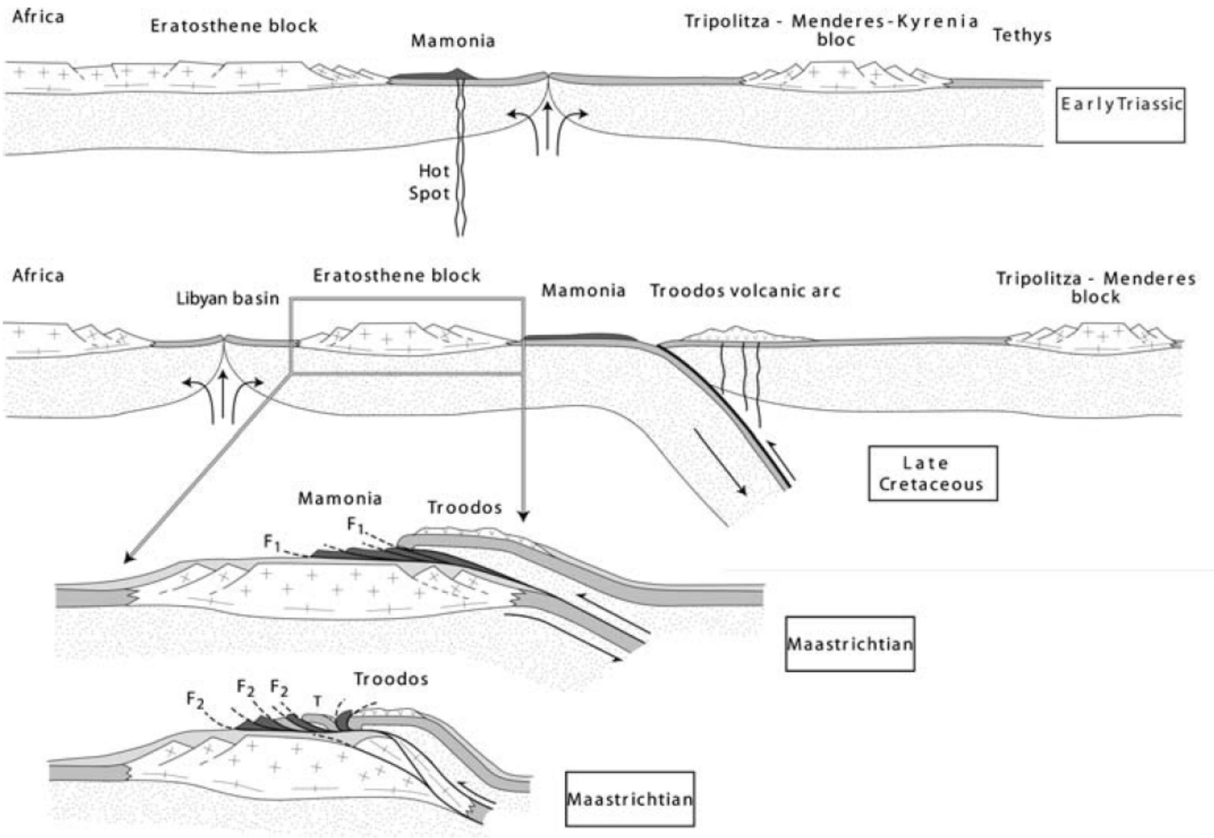

Figure 1.16 Schematic reconstruction of structural and tectonic events from the early Triassic to Maastrictian. From Lapierre *et al.* (2007).

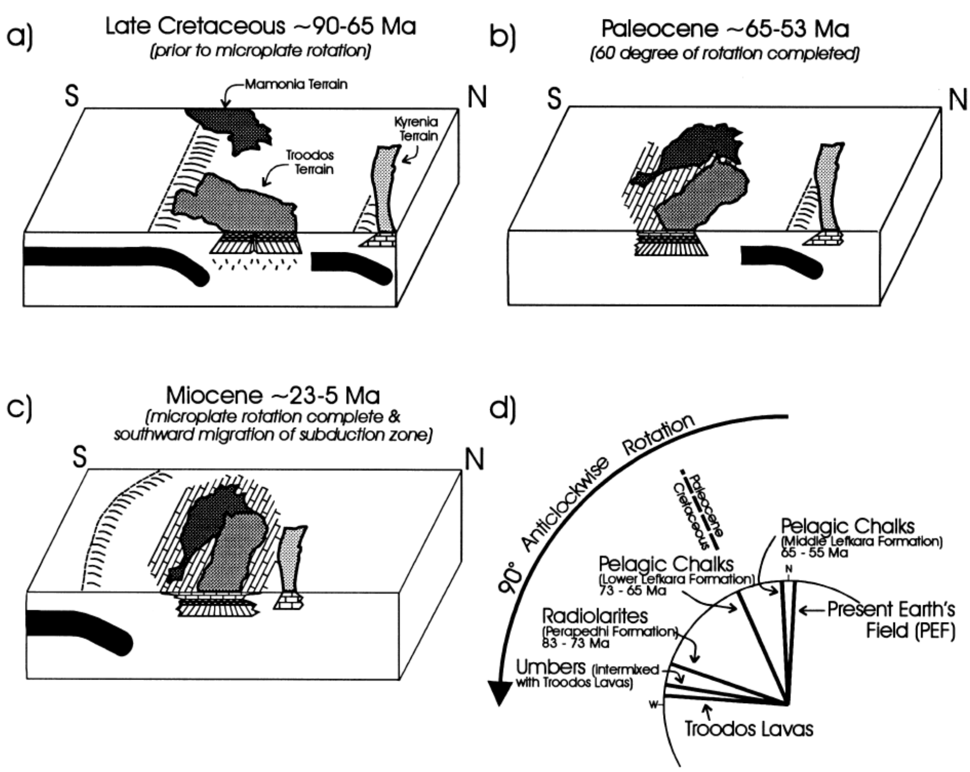

Figure 1.17 Alternative model for terrane accretion involving the Troodos, Mamonia and Keryneia Terranes. From Lagroix and Borradaile (2000).

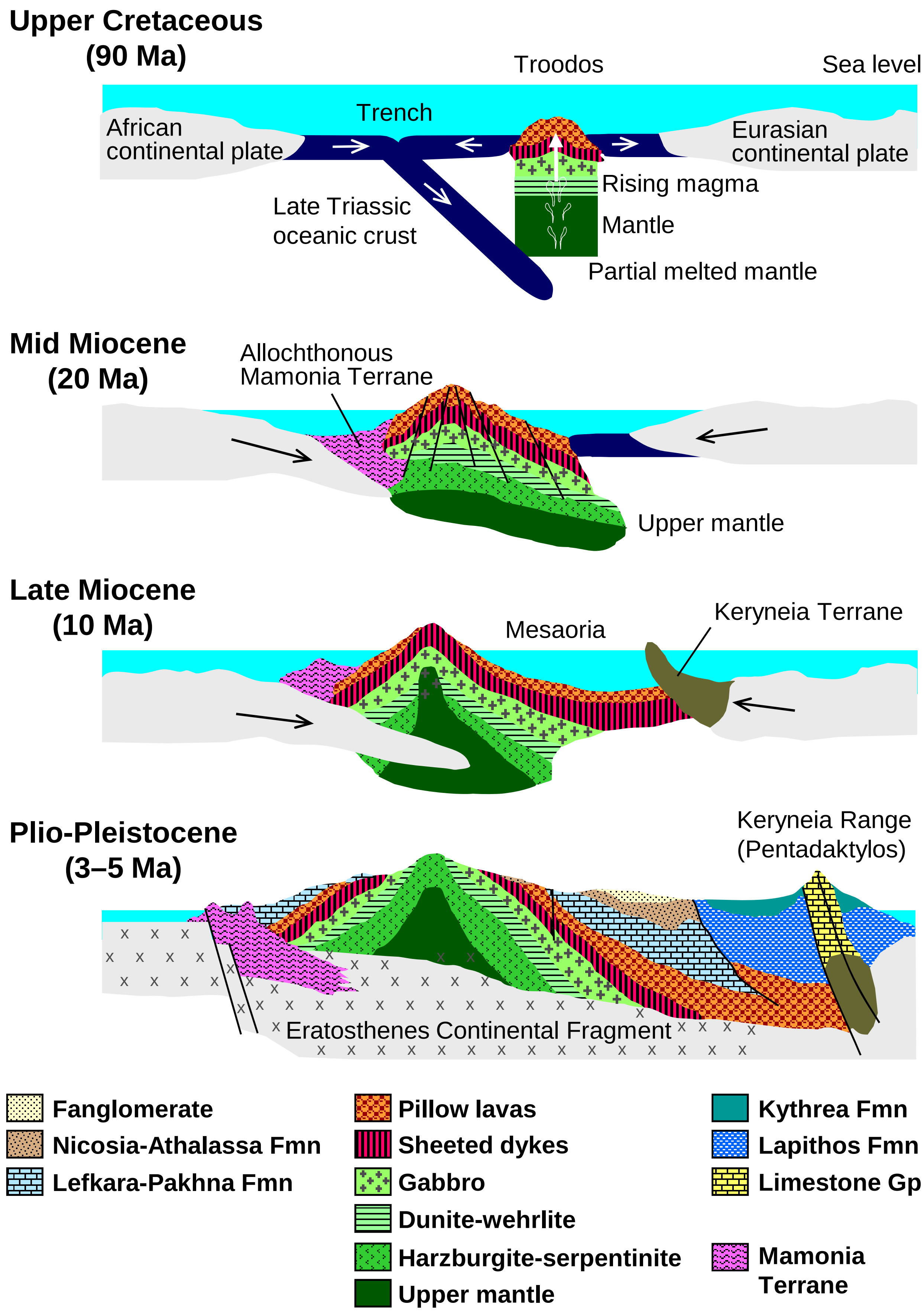

Figure 1.18 Geological evolution of Cyprus. Modified from the GSD original figure.

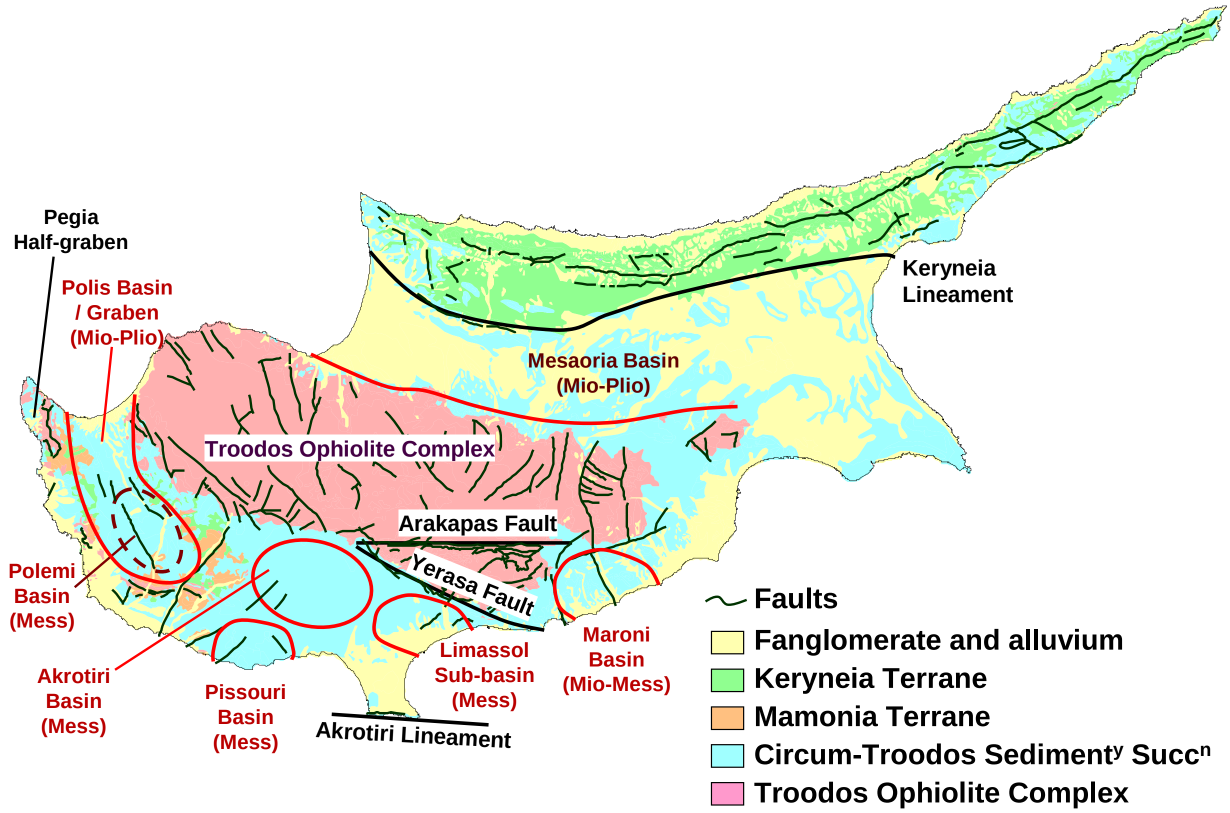

Figure 1.19 Main structural units and depositional basins of Cyprus. Based on Eaton and Robertson (1993) and Lagroix and Borradaile (2000).

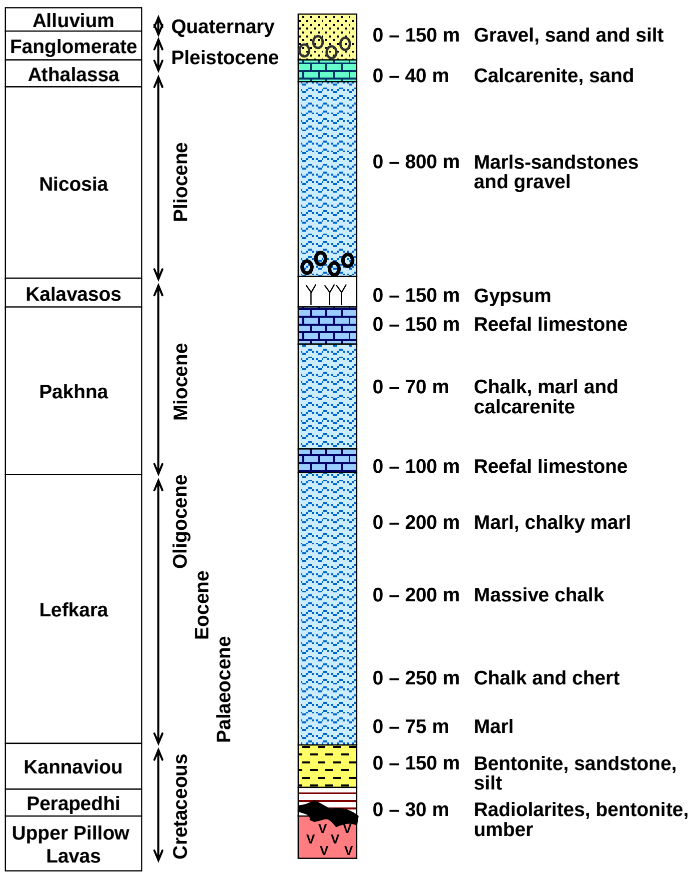

Figure 1.20 Stratigraphy of the Circum-Troodos Sedimentary Succession (CTSS) and Holocene units. Modified from Malpas *et al.* (1992).

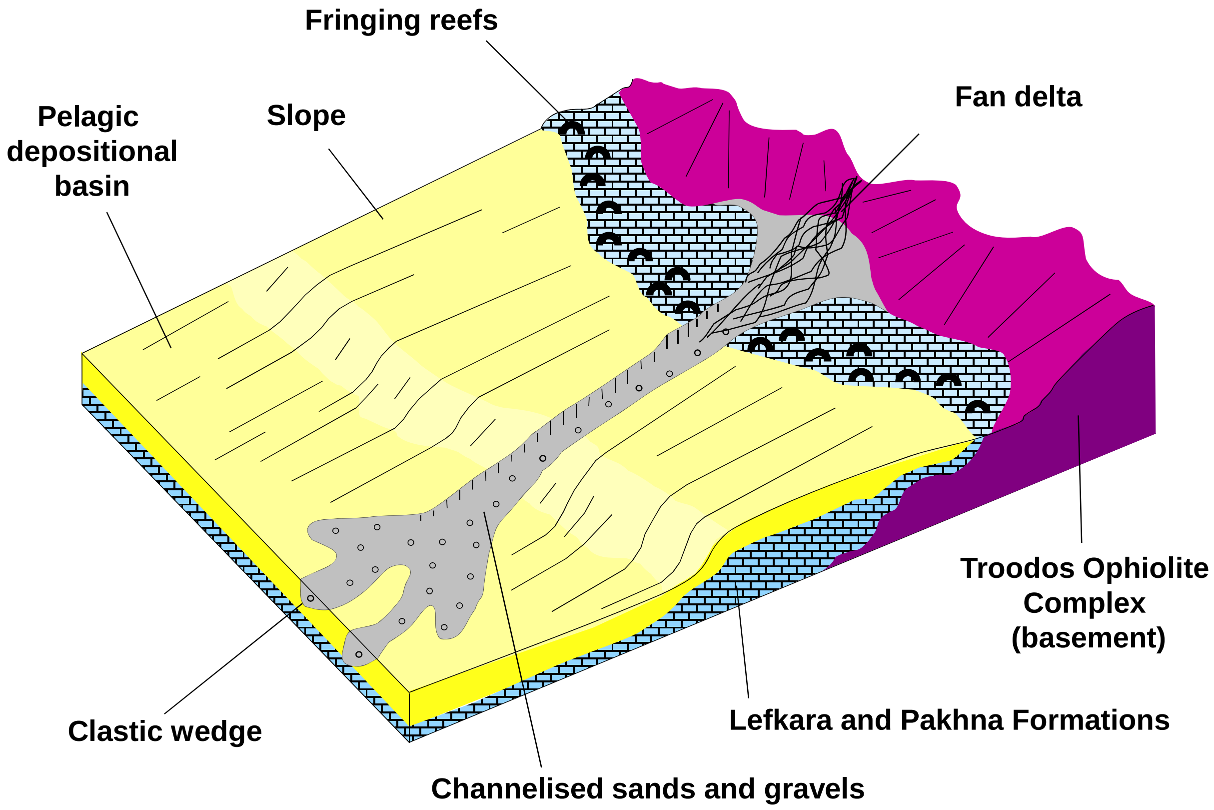

Figure 1.21 Schematic of CTSS depositional environments. Modified from Eaton and Robertson (1993).

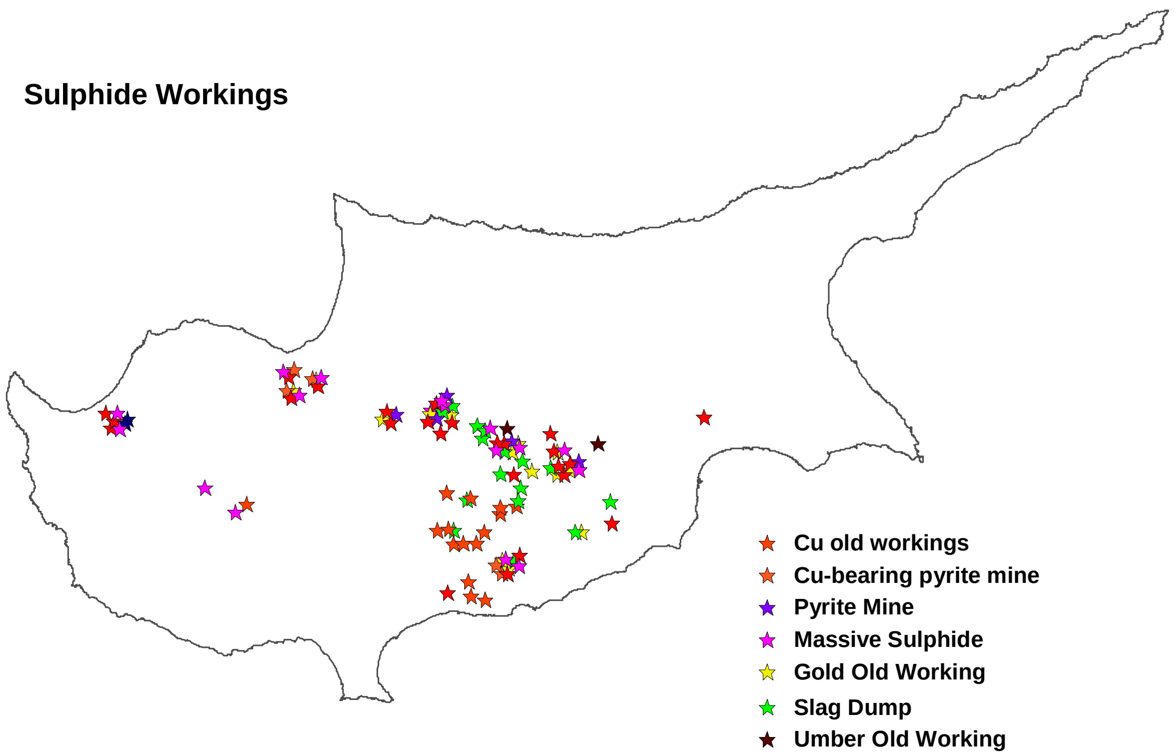

Figure 1.22 Main mineral deposits of Cyprus. Data from GSD.

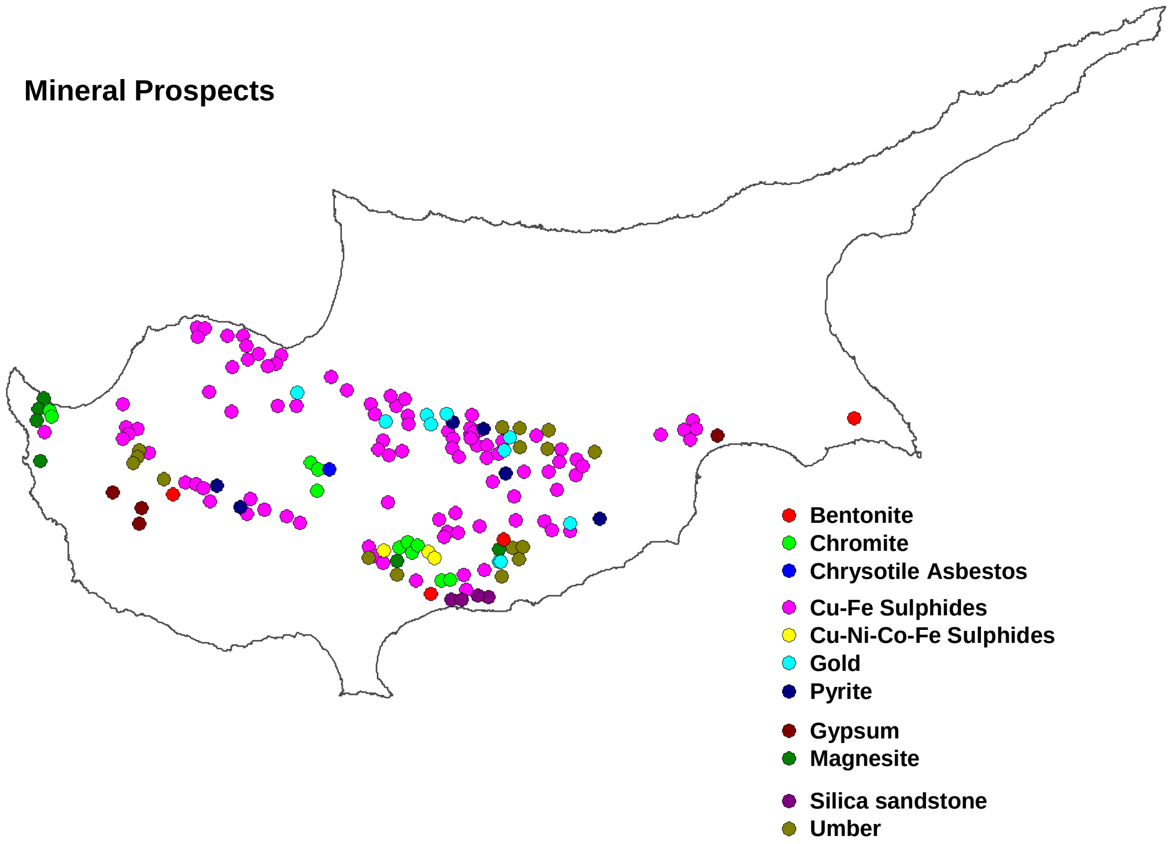

Figure 1.23 Sulphide workings in Cyprus. Data from GSD.

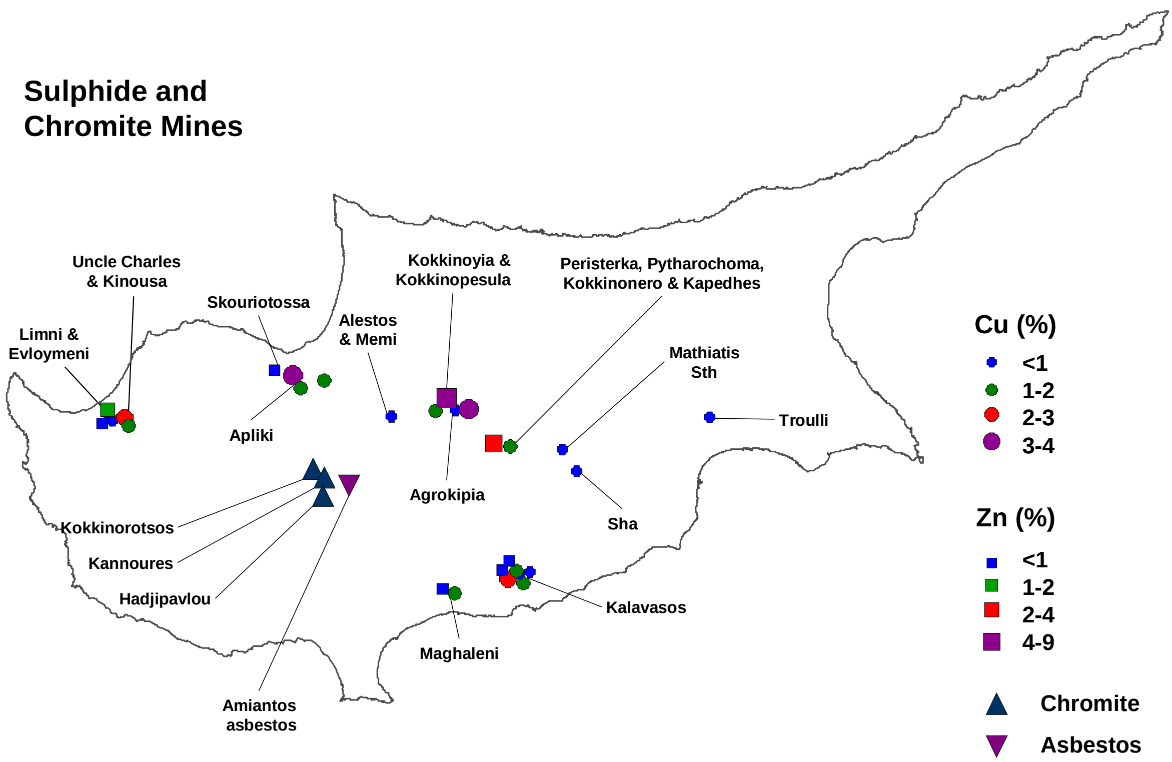

Figure 1.24 Sulphide, chromite and asbestos mines (mainly historical). Data from the GSD.

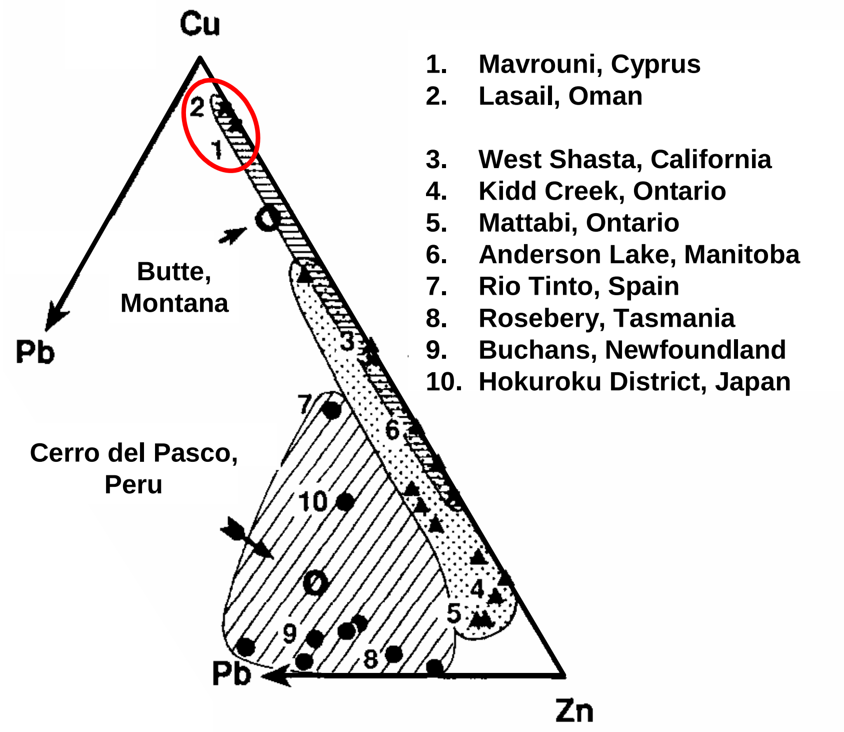

Figure 1.25 Relative Cu-Pb-Zn contents of various examples within the spectrum of VMS deposits. Modified from Sawkins (1980).

Kalavasos Mine Samples
(Adamides 1980)

1	**Lefkara Fmn chalk**
2	**Gossan / goethitic breccia**
3	**Mn oxides**
4	**Oxide zone malachite and gypsum**
5-12	**Hypogene ore, stringers, disseminated sulphides py > ccpyr**
13,14	**Altered footwall, jasper breccia**
15	**Altered and leached basalt**
16	**Silicified sample**
17-20	**Pillow basalts – smectite-chlorite alteration, py and cc veining**

Images © Data Metallogenica (AMIRA)

Figure 1.26 Examples of main lithologies, including the mineralised zone, from the Kalavasos Mine. Data Metallogenica (AMIRA) with descriptions by Adamides (1980).

Agrokipia Mitsero Mine Samples
(Adamides 1980)

1-3	**Goethite and jarosite**
4	**Gypsum breccia**
5	**Malachite-stained basalt**
6-8	**Leached and sericitised basalt**
9-11	**Massive sulphide zone; porous, crystalline massive py**
12	**Quartz-sericite-py altered basalt**
13-16	**Chloritised (propylitised) basalt, py**
17	**Pillow basalt host rocks**
18,19	**Amygdaloidal basalt**
20	**?Dacitic porphyry**

Images © Data Metallogenica (AMIRA)

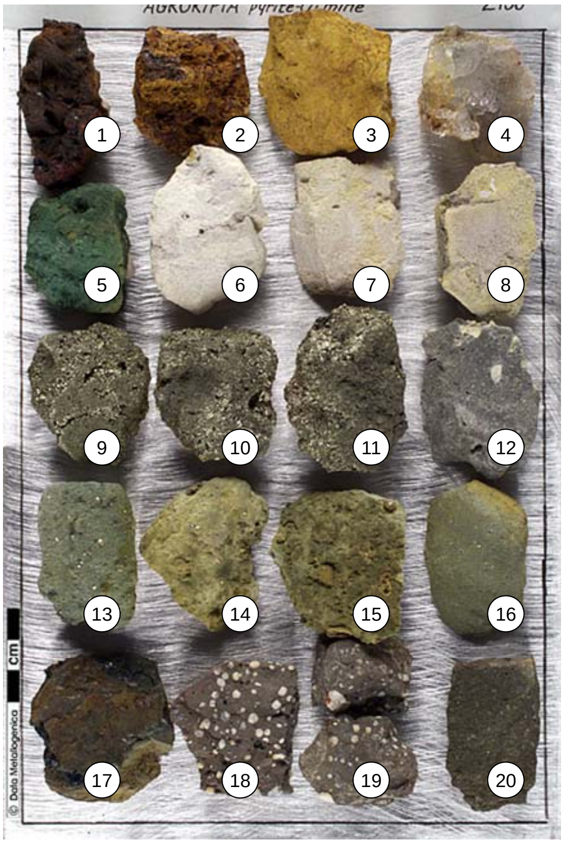

Figure 1.27 Examples of main lithologies, including the mineralised zone, from the Agrolipia-Mitsero Mine. Data Metallogenica (AMIRA) with descriptions by Adamides (1980).

Mathiatis Mine Samples
(Lydon and Galley 1986)

1,2	**Lefkara Fmn chalk**
3	**Oxide zone gypsum**
4,5	**Acid leached basalt**
6	**Massive ore; py > sph > ccpyr >**
7-16	**Silicified breccia to stockwork; py > ccpyr**
17	**Jasper**
18	**Chloritised basalt**
19	**Amygdaloidal basalt**

Images © Data Metallogenica (AMIRA)

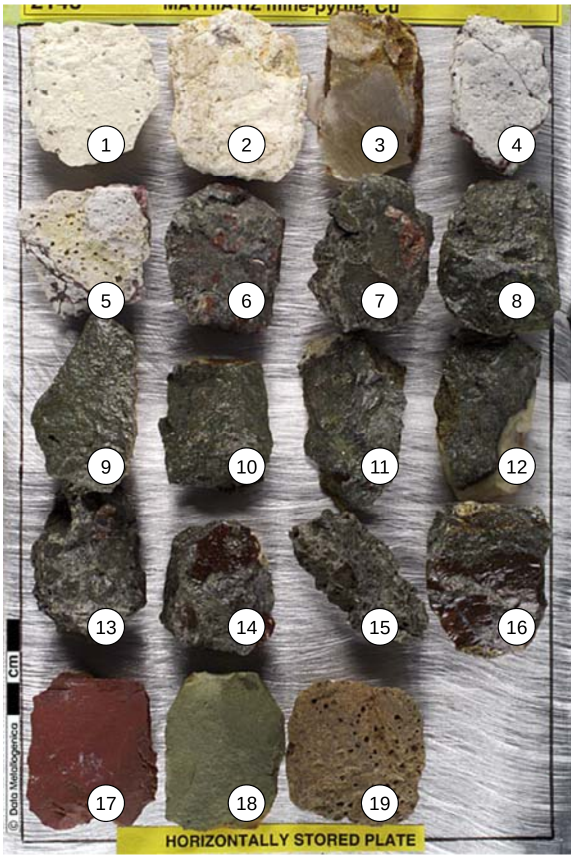

Figure 1.28 Examples of main lithologies, including the mineralised zone, from the Mathiatis Mine. Data Metallogenica (AMIRA) with descriptions by Lydon and Galley (1986).

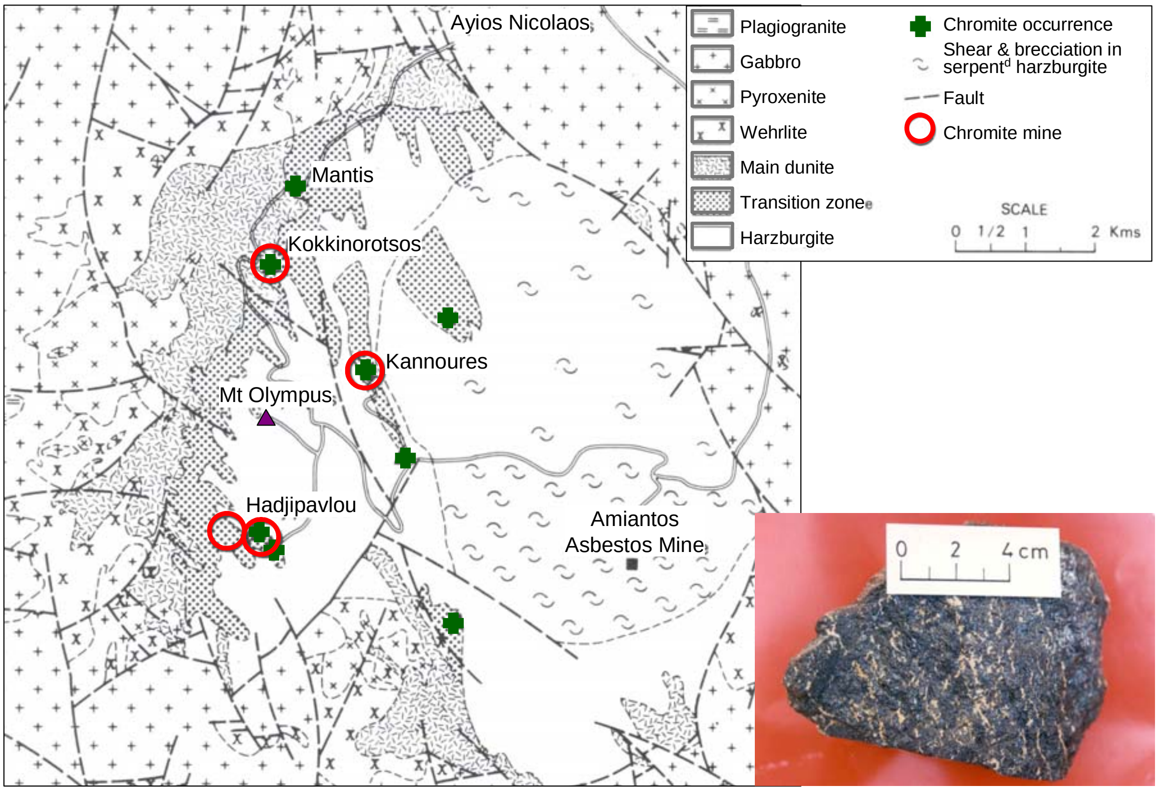

Figure 1.29 Location and geological setting of the Troodos chromite and asbestos mines. From Morisseau (2007).

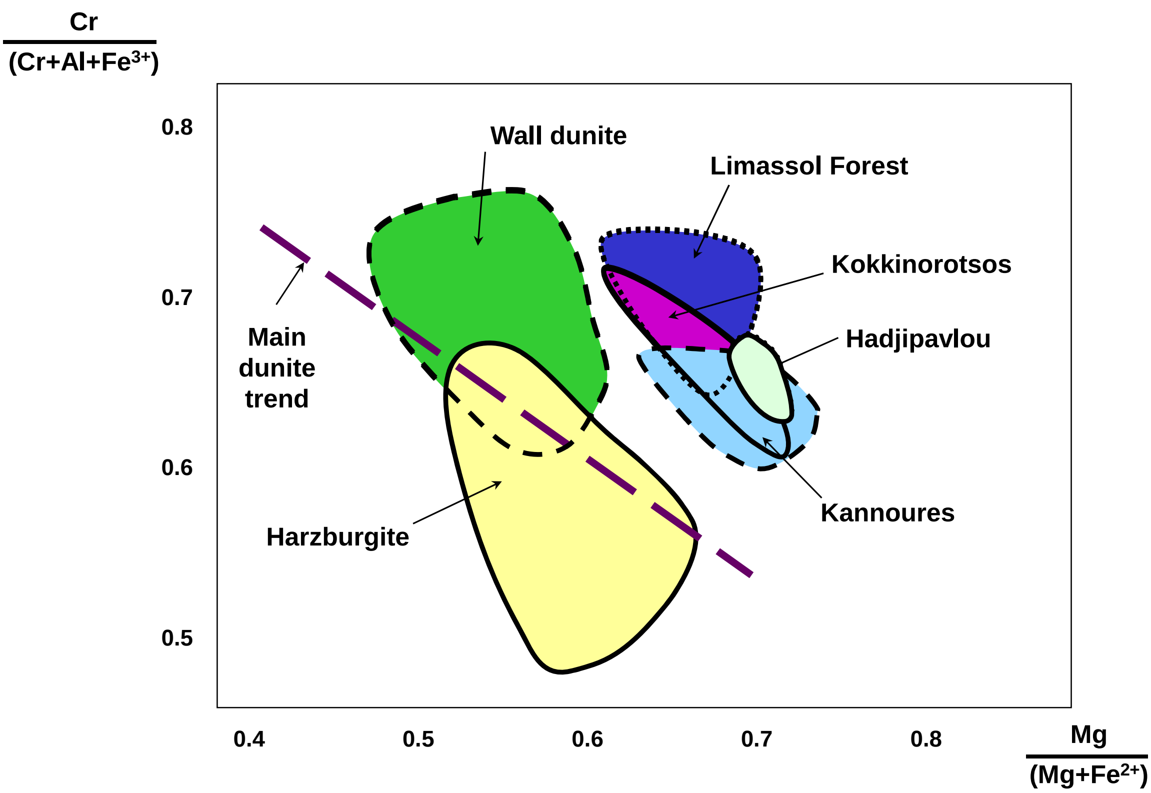

Figure 1.30 Compositional variations in chromites in Cyprus. From Morisseau (2007).

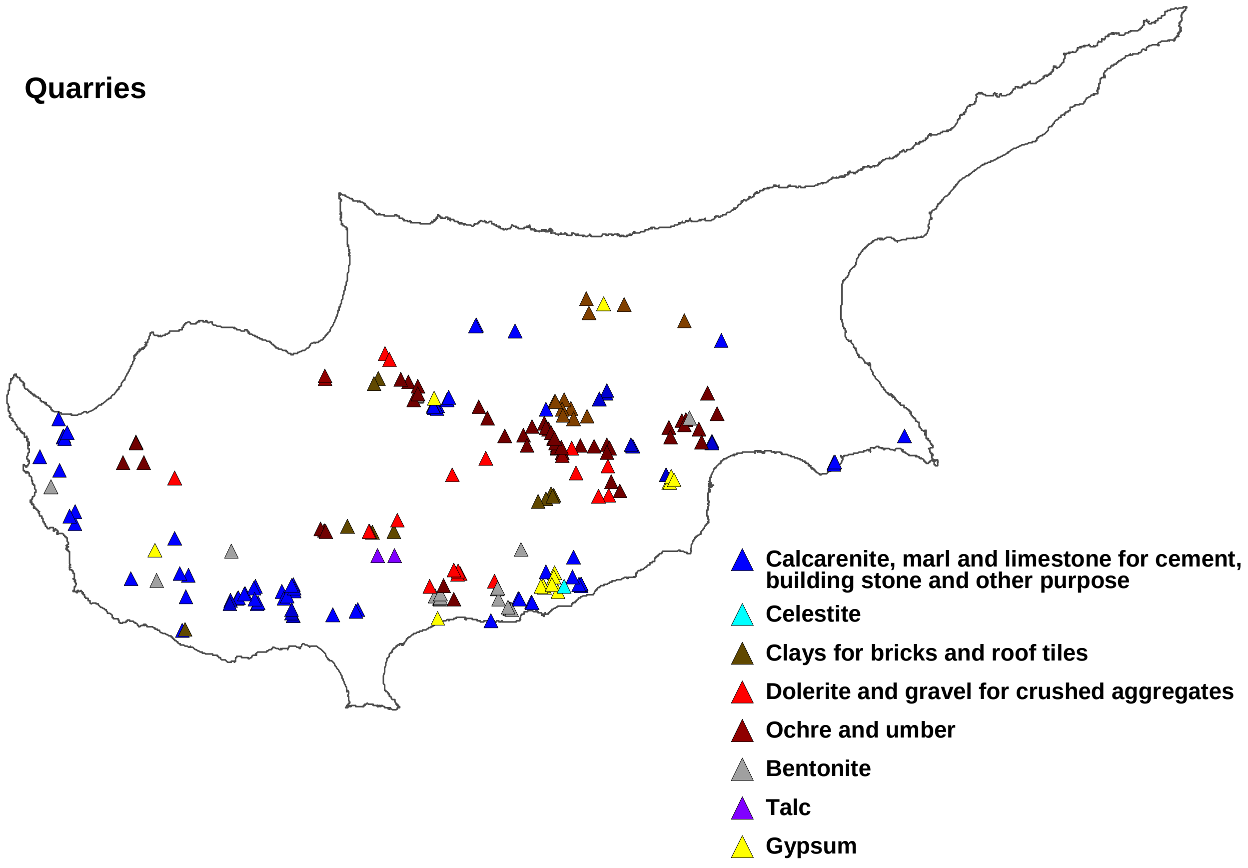

Figure 1.31 Location of major quarries in Cyprus. Data from GSD.

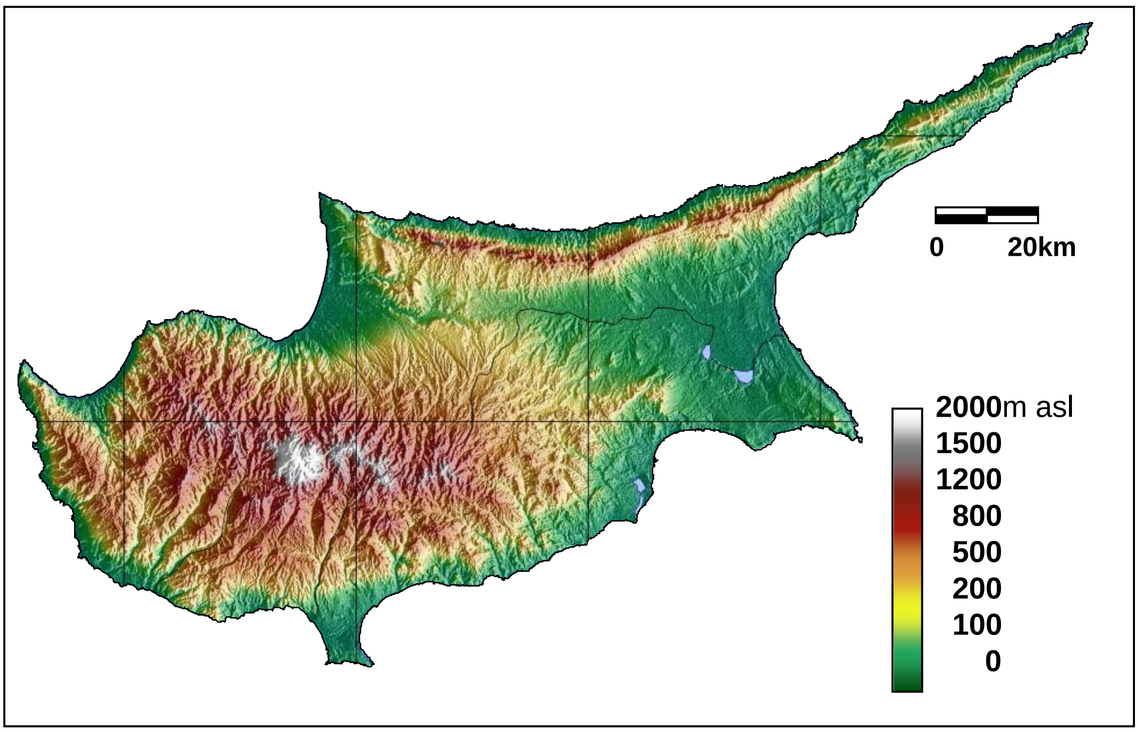

Figure 1.32 Topographic relief map of Cyprus.

Figure 1.33 Modified Google™ image of Cyprus.

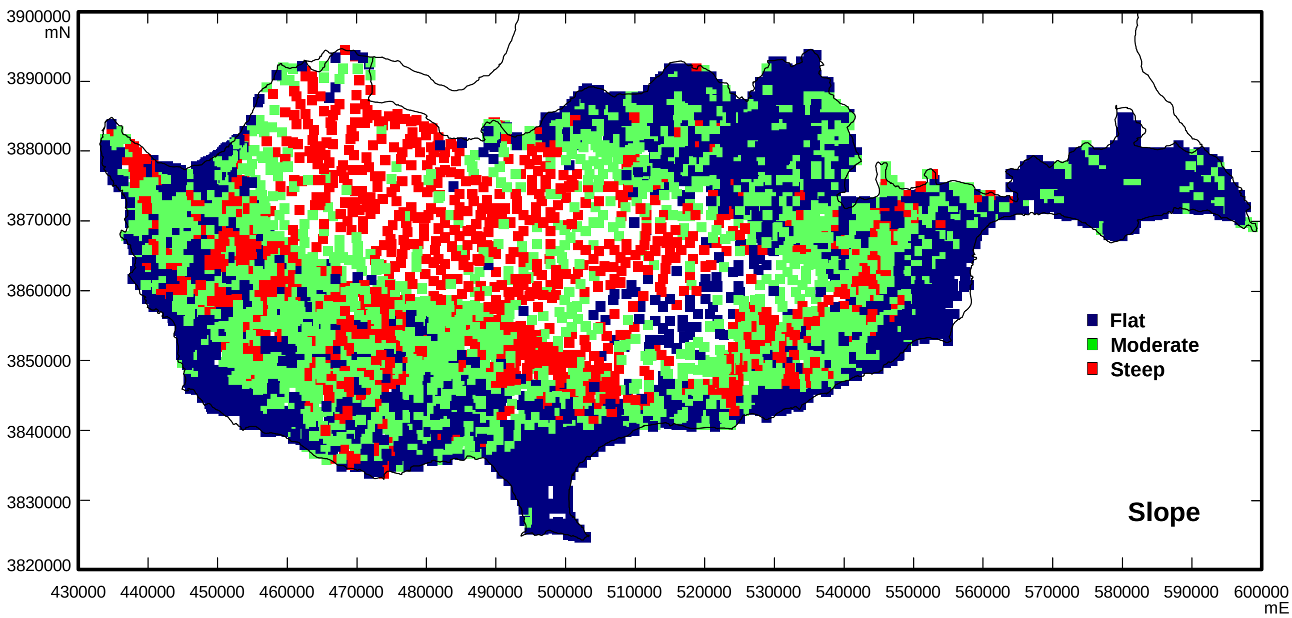

Figure 1.34 Variation in typical land slopes observed the sampling region.

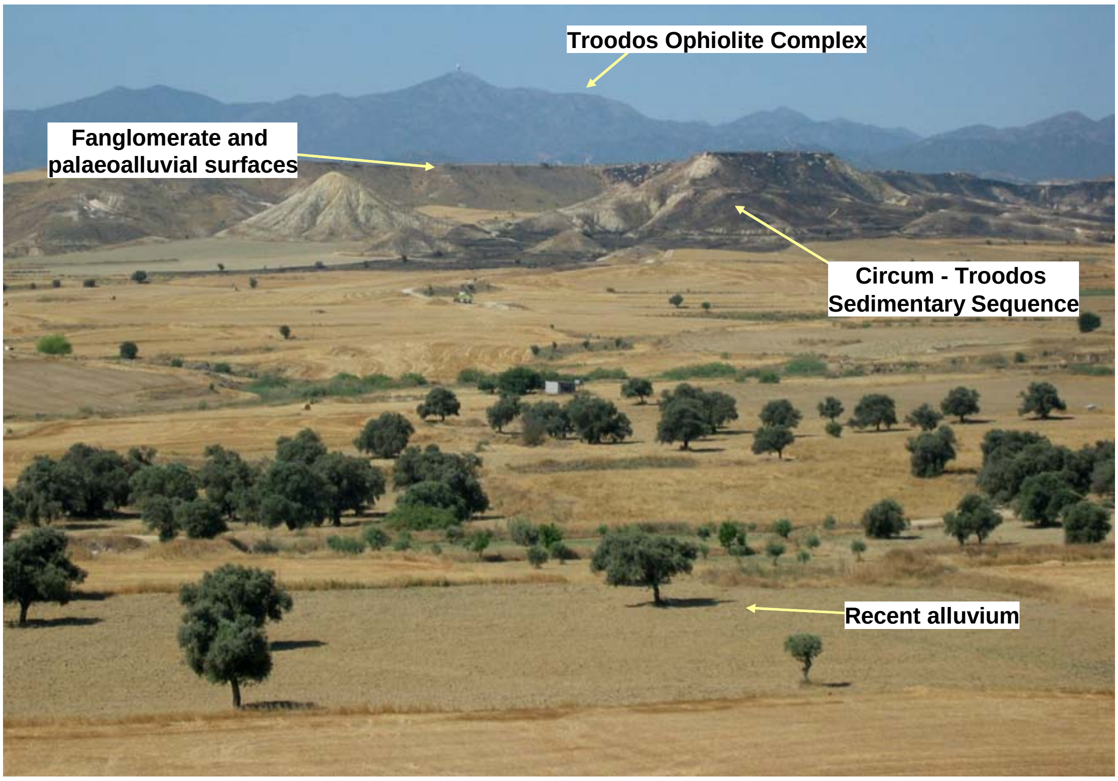

Figure 1.35 View from near Tseri looking south and showing the Troodos Massif in the background, the dissected fanglomerate palaeosurface developed on the CTSS on-lap sequence in the middle ground, and mixed colluvial and alluvial fill in the valley containing the wheat fields and olives trees.

Figure 1.36 Skeletal regolith (C/D horizon) and localised scree patches on steep-sided hills, with areas that have been largely stripped of original forest cover, northern side of the Troodos Mountains.

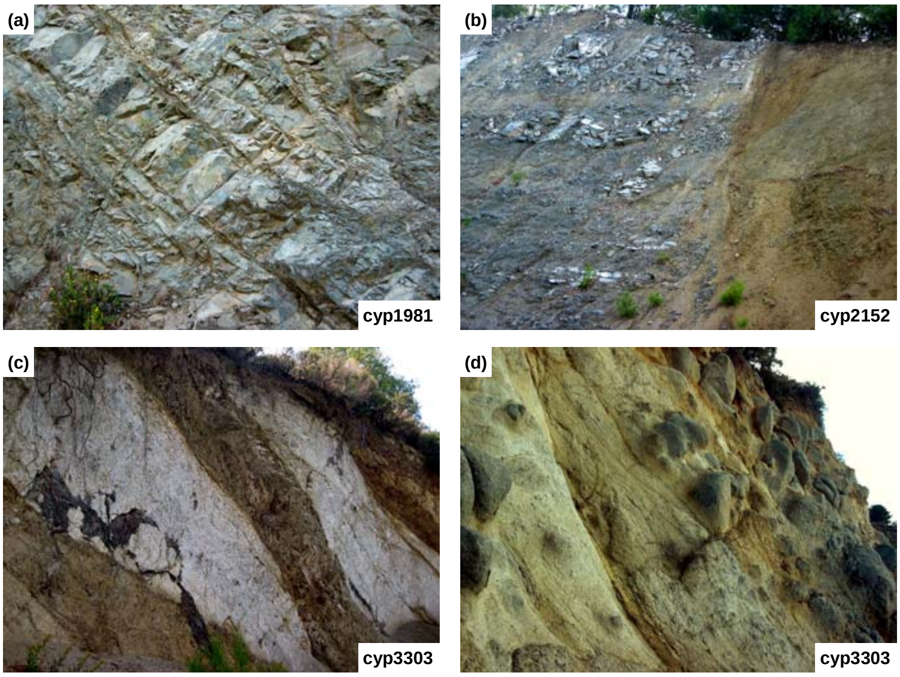

Figure 1.37 Profile exposures on Troodos; (a) Sheeted dolerite dykes with minor development of secondary Fe-oxides along fractures and the edges of individual dykes. (b) fault-bounded block of weakly weathered gabbro adjacent to more strongly weathered gabbro. (c and d) Skeletal A-horizon and transported B-horizon overlying preferentially weathered dolerite dykes and more massive gabbro, with weathering extending down to at least 5 m depth.

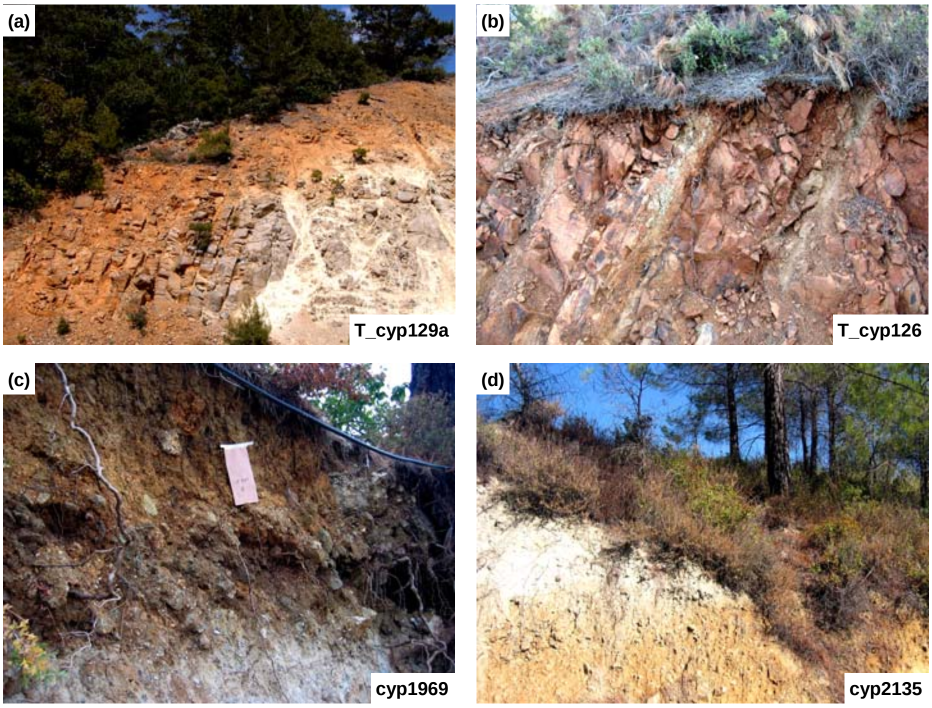

Figure 1.38 Profile exposures on Troodos; (a) 2 to 5 m thick C-horizon developed within gabbro, capped by a thin A-horizon and incipient development of a B-horizon with Fe-oxide accumulation; (b) Skeletal A-horizon in thin colluvial veneer overlying slightly weathered dolerite dykes; (c) Zone of residual regolith and soil development in dunite on the top of a ridge; (d) Exposure of 80 cm thick B-horizon in gabbro with upper clay-rich and lower ferruginous zones.

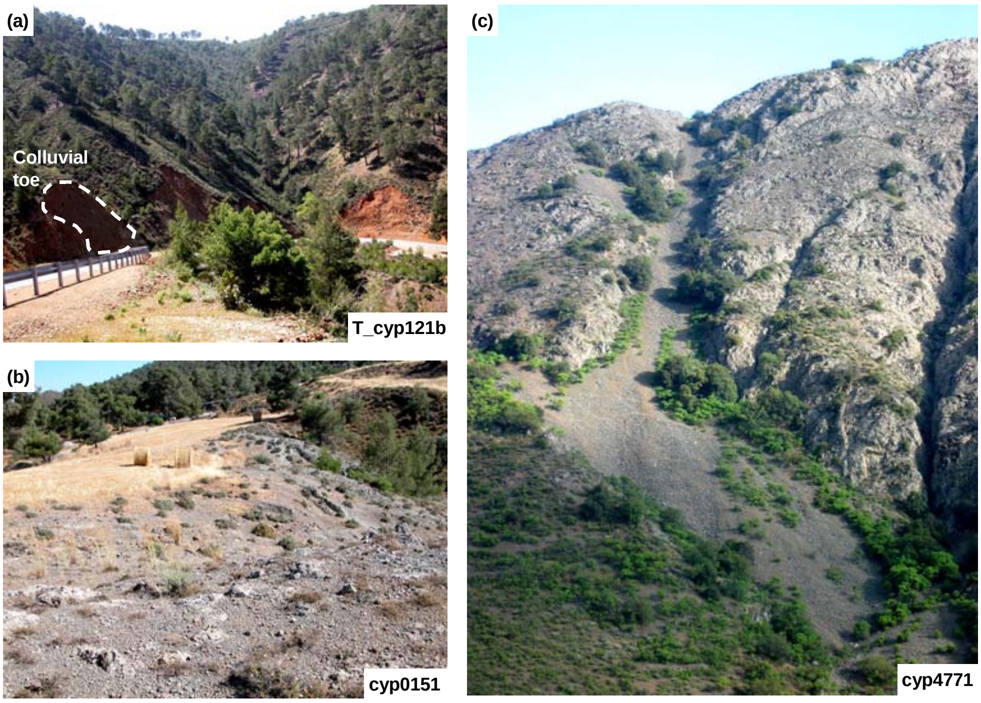

Figure 1.39 (a) Skeletal regolith cover on Troodos with zones of up to 2 m of local colluvial material infilling depressions or forming toe to slopes, exposed in road cutting north of Platres; (b) Thin local colluvium developed over basalt with recently harvested small wheat field adjacent to forest; (c) Exposed gabbro with scree chute from western side of Troodos near Prodromos. Active scree and exposed rock surfaces are both stripped of vegetation.

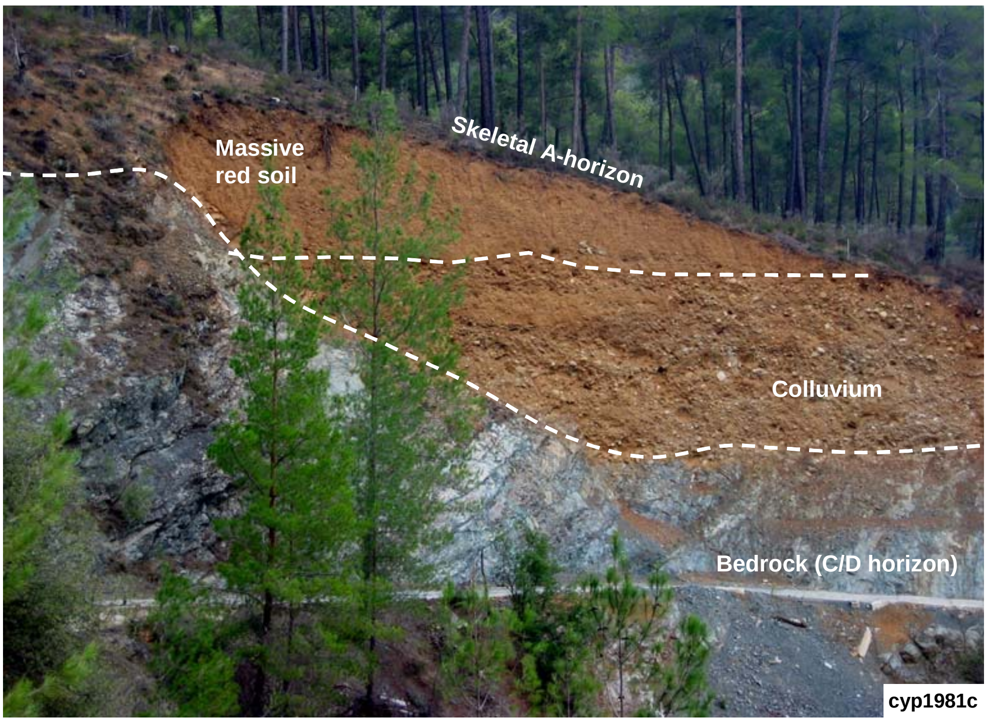

Figure 1.40 Multi-layered colluvial infill of depression in weathered gabbro, near Palaiomylos. The gabbro is weathered down to ~5 m depth along joints. Lower transported layer contains large, sub-rounded clasts of weathered mafics whereas the upper layer is dominated by massive red sands. A thin A-horizon overlies the area. Age relationship between the colluvium and massive red soil unknown.

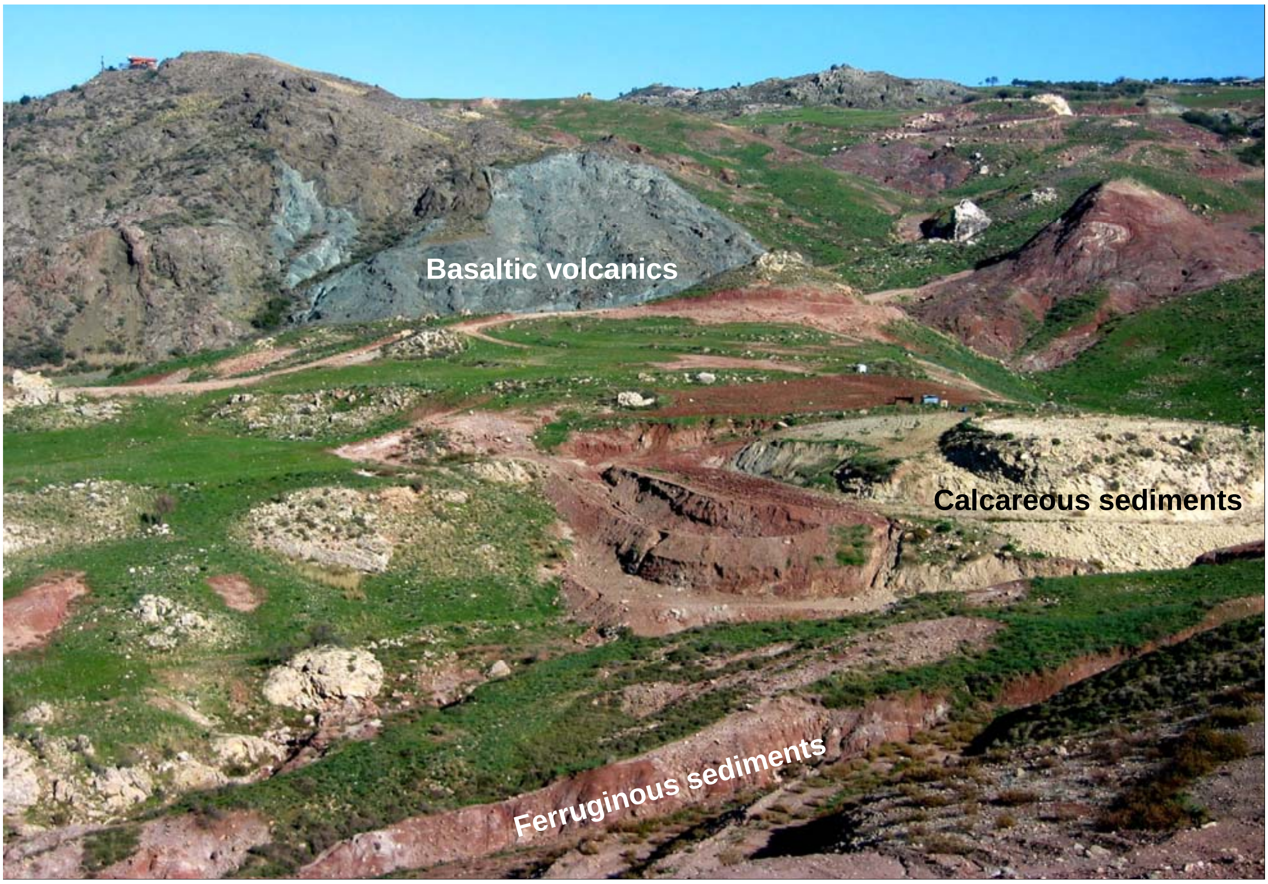

Figure 1.41 Outcrops of weathered mafic volcaniclastics, sediments and vesicular basalts of the Dhiarizos Group (lower unit within the Mamonia Terrane) near Pano Panagia. Small outliers of Ayios Photios Group clastics and calcareous sedimentary units outcrop on the right of the photo. Soils are skeletal on upper slopes. There is up to 2 m of colluvial cover at the base of slope, although there is deep dissection of the colluvium along streams.

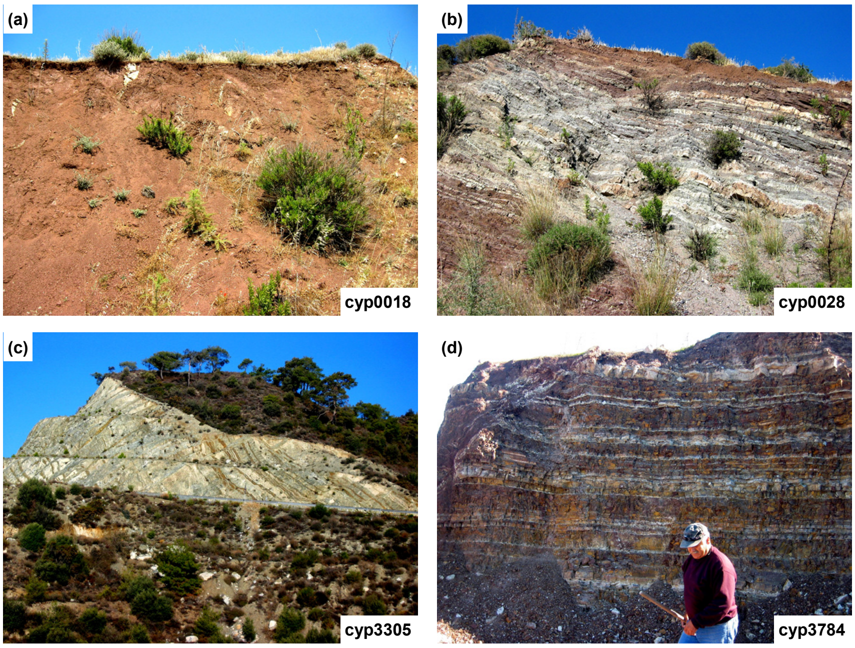

Figure 1.42 (a) Dhiarizos Group; ferruginous and mafic sediments (volcaniclastics and bentonitic clays) with cherty or siliciclastic units, near Fasoula. (b) Ayios Photios Group; mudstones with carbonate and silty layers, near Kidasi. (c) Folded and weathered dolerite dykes in basalts exposed on hill top, near Sanida. (d) Kathikas Fmn; folded (soft-sediment slumping) and later faulted mafic-derived ferruginous sediments and volcaniclastics of the, near Pentalia.

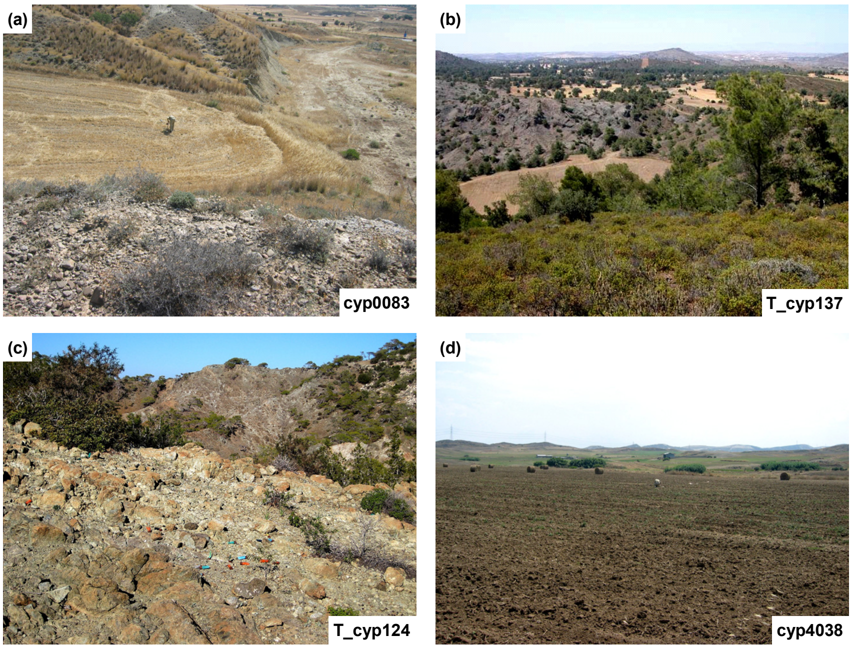

Figure 1.43 (a) View down from palaeosurface mesa on Nicosia Fmn carbonates to wheat field in recent alluvial plains containing a mixture of carbonate and basalt-derived soil, near Tseri; (b) Undulating terrane over pillow basalts on NE edge of Troodos looking towards Morfou Bay. Depth of regolith cover ranges from 1-2 m (small wheat field) to <50 cm (garrigue vegetation cover) to skeletal (exposed C-horizon basalts); (c) Weathered basalts with shotgun cartridges; (d) Fallow wheat field near Troulloi containing basaltic colluvium and alluvium (used for variation test site 1).

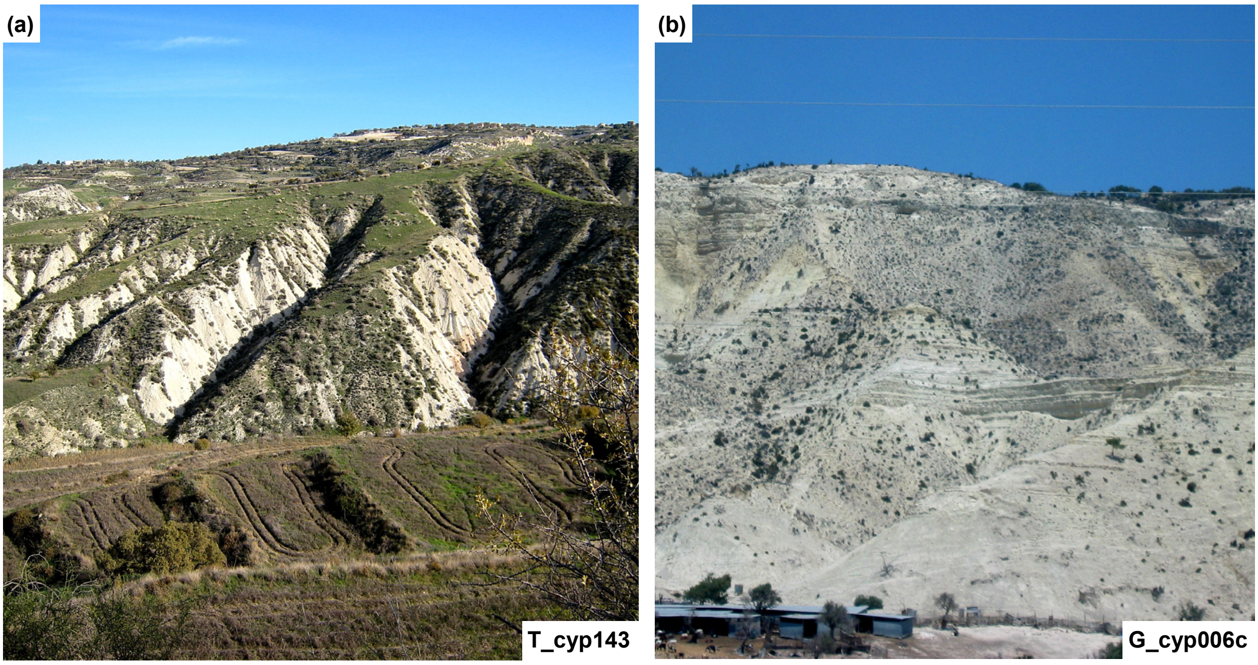

Figure 1.44 Exposures of dissected Pakhna Fmn calcareous sediments (mainly calcarenites) in (a) Polis Valley and (b) north of Episkopi, where there is also locally-derived scree covering much of the exposure.

Figure 1.45 Slumped limestone block (olistolith) in Mamonia Terrane near Episkopi Pafos.

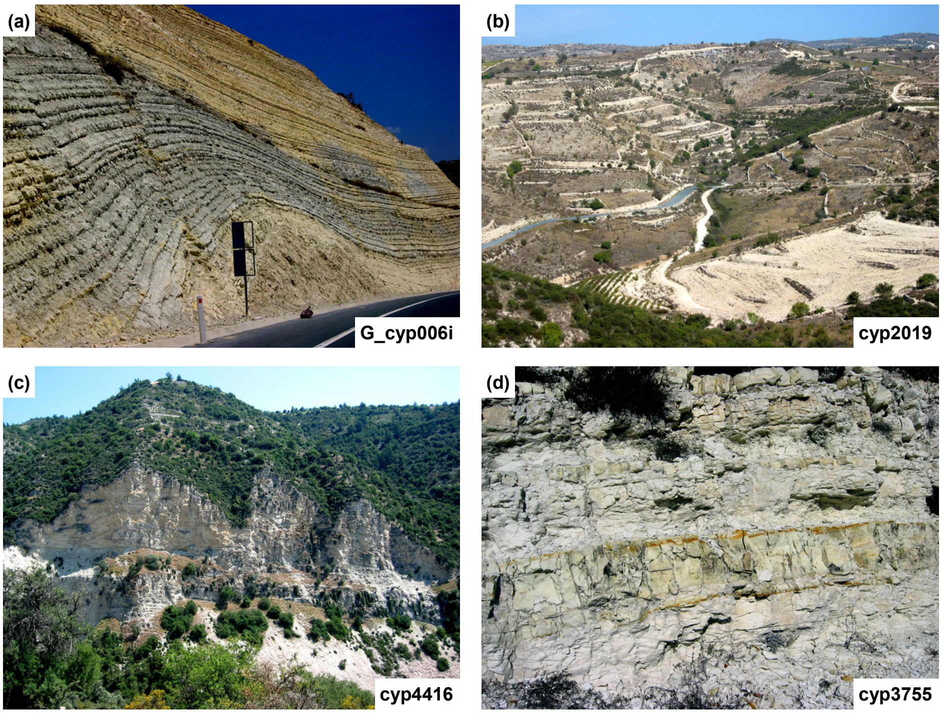

Figure 1.46 (a) Exposure of well-bedded Pakhna Fmn calcareous sediments with drape structure, on main highway near Episkopi Lemesos; (b) extensive terracing in Pakhna Formation near Prastio; (c) Cliff exposures of CTSS carbonates of the Lefkara Fmn on NW flank of Troodos near Arminou; (d) Ferruginisation of more siliceous beds within carbonate sequences of the Lefkara Fmn near Stavrokonnou.

Figure 1.47 View into Secret Valley and the exposed contact between Pakhna Fmn carbonates and underlying Mamonia Terrane mafics and sedimentary rocks of the Dhiarizos Gp.

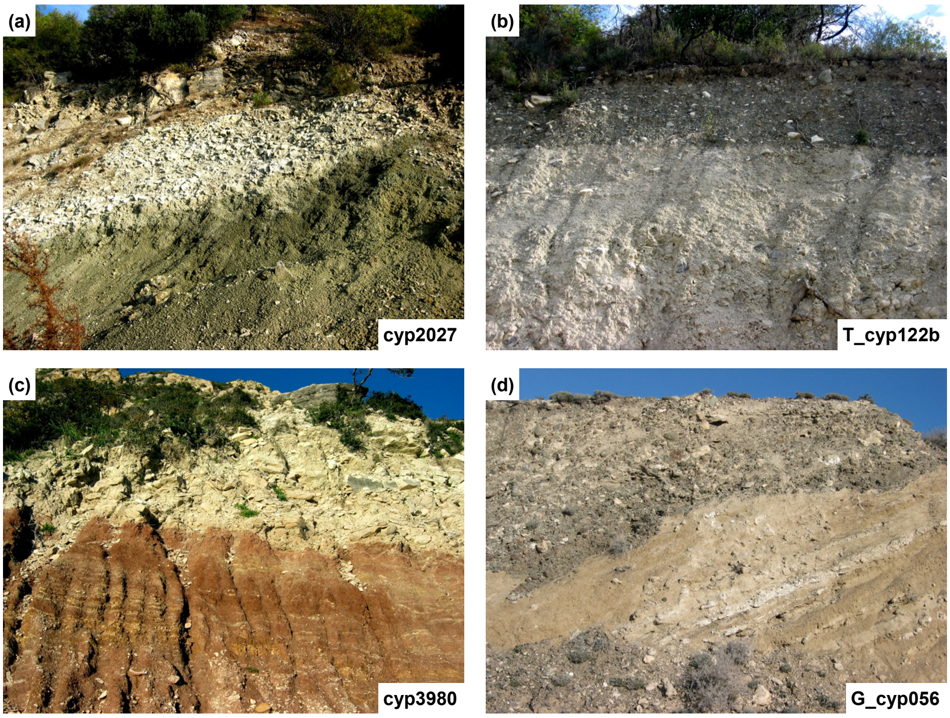

Figure 1.48 Examples of mixed regolith profiles. (a) Carbonate-rich colluvium overlying weathered basalts and basaltic colluvium, near Dora; (b) Mafic-rich gravels overlying carbonate-rich gravels on the Mesaoria Plain; (c) Carbonate-rich colluvium overlying ferruginous to volcaniclastic-derived sediments of the Dhiarizos Gp; (d) Perched mixed palaeogravels containing both cobbles and matrix of carbonate and mafic clasts, north of Mitsero.

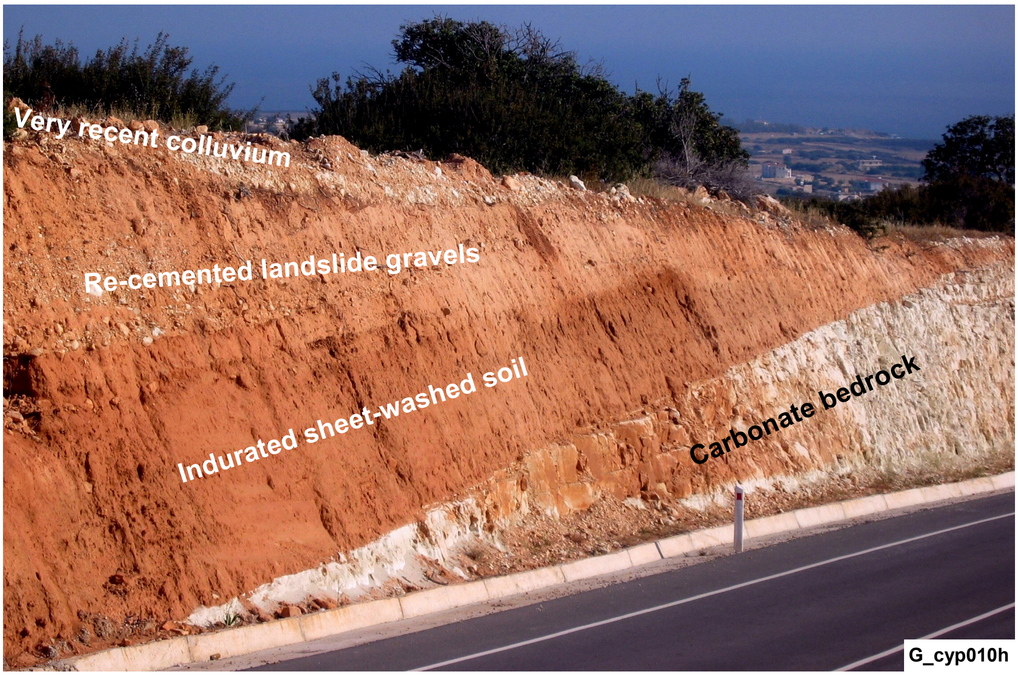

Figure 1.49 Road cut near Coral Beach, Pegeia, displaying bleached calcareous sediments overlain by massive red soils (which may have an aeolian component), recent cemented gravels and recent gravels above a soft-sediment unconformity. The indurated red soils may be derived from sheetwashing of fines from Troodos after de-forestation.

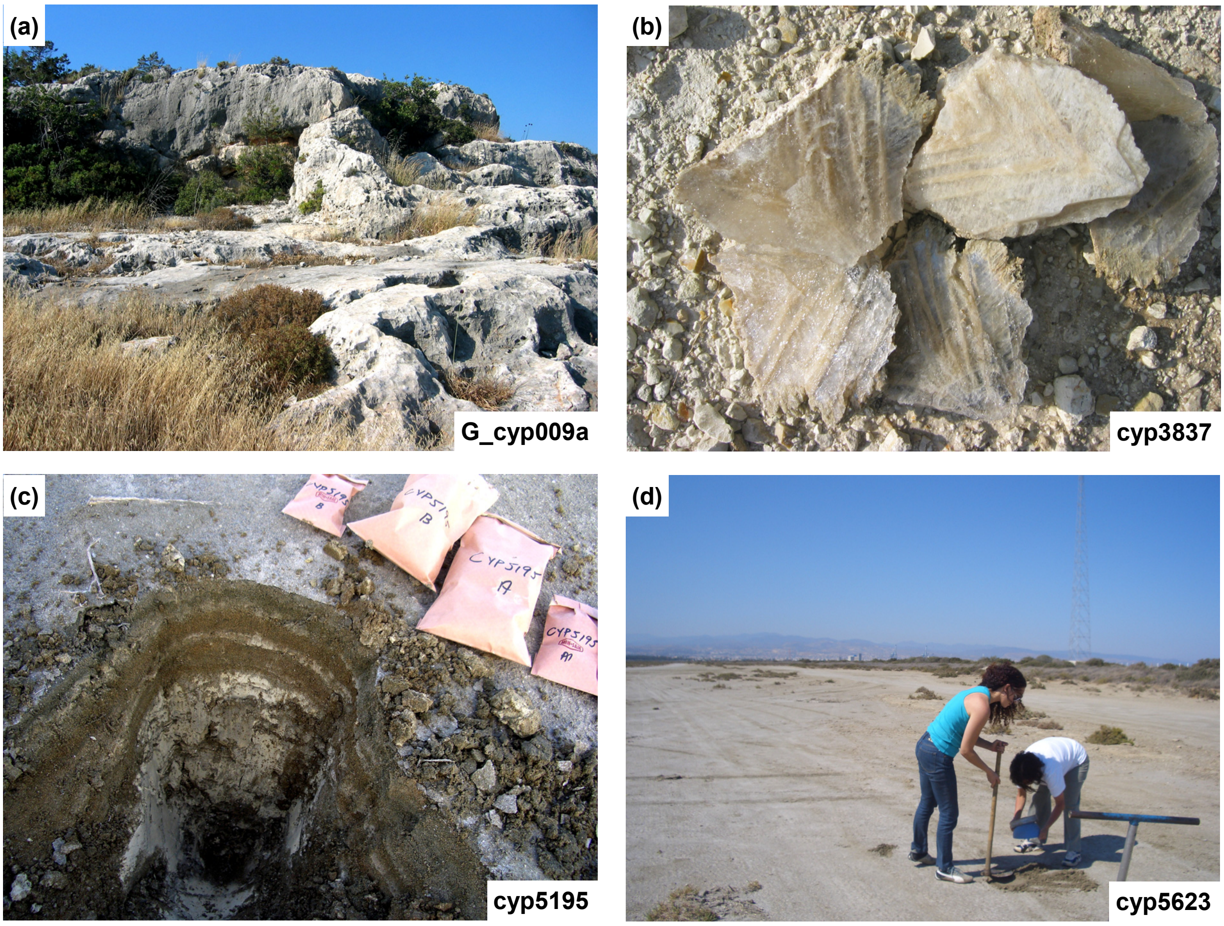

Figure 1.50 (a) Karstic limestones with skeletal soil/colluvial cover, Coral Bay; (b) Gypsum layers within Kalavasos Fmn, near Amargeti; (c and d) Section through salt pan at Akrotiri and sampling by C. Kapodistria and Dr E. Morisseau (GSD).

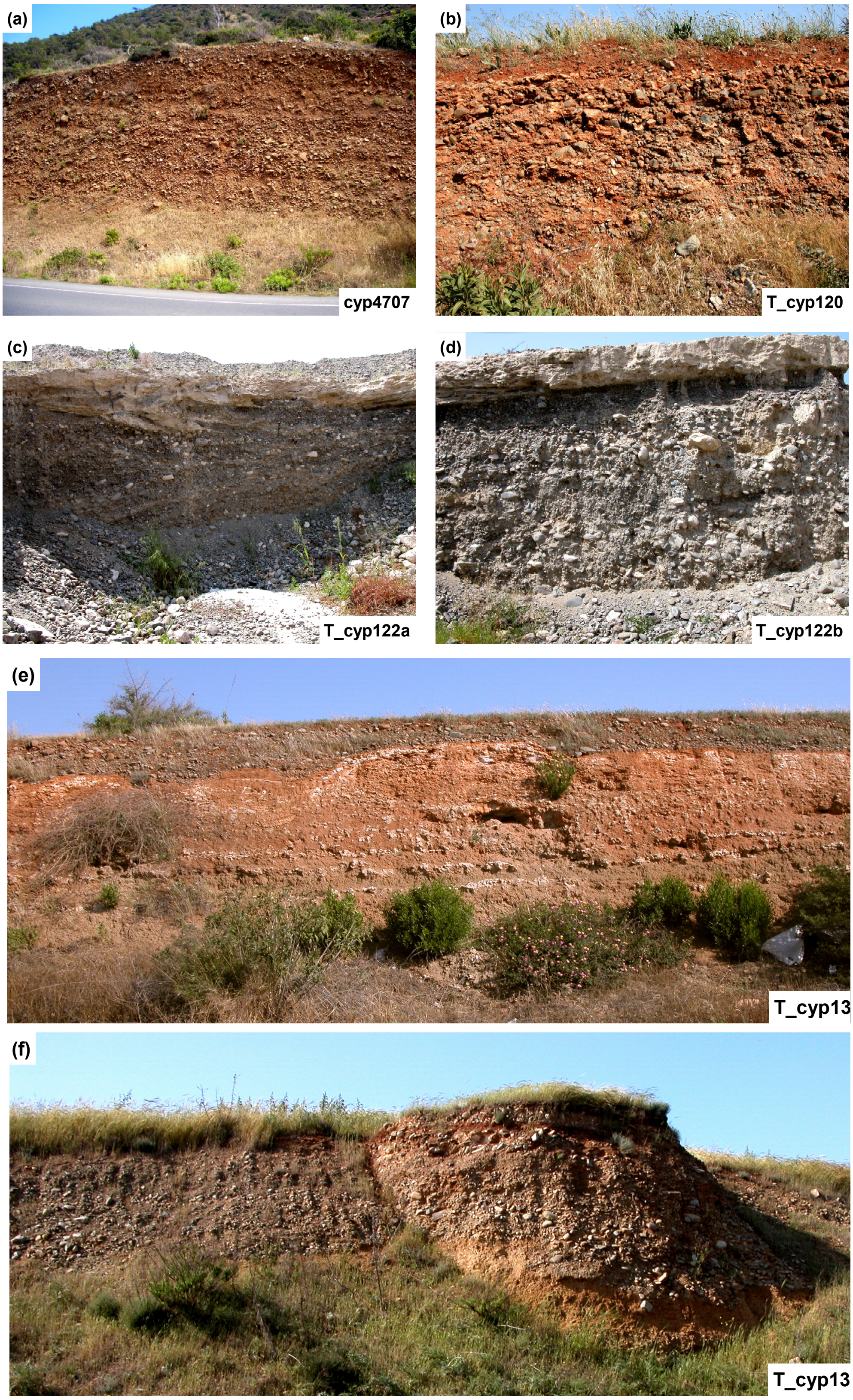

Figure 1.51 Gravel beds of the Mesaoria Plain with layers of calcrete and surface disturbance to a depth of ~25 cm. Gravel clasts include TOC mafics and CTSS calcareous sedimentary rocks.

Figure 1.52 Saline lake next to Larnaka Airport (with flamingos).

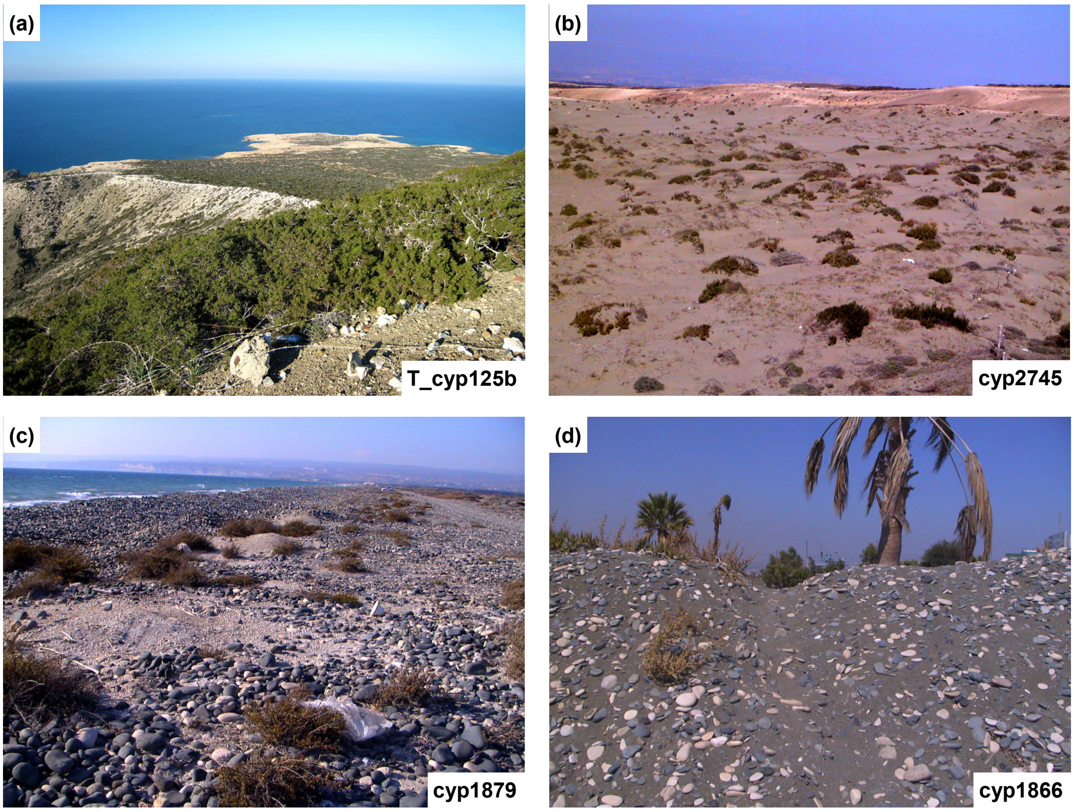

Figure 1.53 (a) Cape Arnaoutis at the end of the Akamas Peninsula with thin carbonate cover overlying basalts; (b and c) Dune sands and cobble+sand beaches on the southwest corner of the Akrotiri Peninsula; (d) Mixed gravels containing both TOC and CTSS clasts and beach sands with high mafic component, Lady's Mile Beach, Akrotiri Peninsula.

Table 1.4 Main soil groups in Cyprus, based on the FAO (1998) classification. Data from Hadjiparaskevas (2008).

Soil Order	Sub-order	Characteristics
Lithosols	Calcaric Eutric	Limited in depth by continuous coherent and hard rock within 10 cm of the surface.
Fluvisols	Calcaric Eutric	Recent alluvial deposits, having no diagnostic horizons other than an Ochric A or a histic H horizon.
Regosols	Calcaric Eutric	Unconsolidated material, having no diagnostic horizons other than an ochric A horizon.
Rendzinas		Mollic horizon immediately overlying extremely calcareous material.
Solonchaks	Gleyic Orthic	High salinity within 125 cm of the surface (EC > 15 mmhos).
Solonetz		Natric B-horizon.
Vertisols		40 % or more clay in all horizons, developing wide cracks from the soil surface downwards.
Cambisols	Vertic Calcaric Calcic Eutric Chromic	Cambic B-horizon and no diagnostic horizon other than an ochric or an umbric A horizon, a calcic or a gypsic horizon.
Luvisols	Vertic Calcic Chromic	Argillic B-horizon.

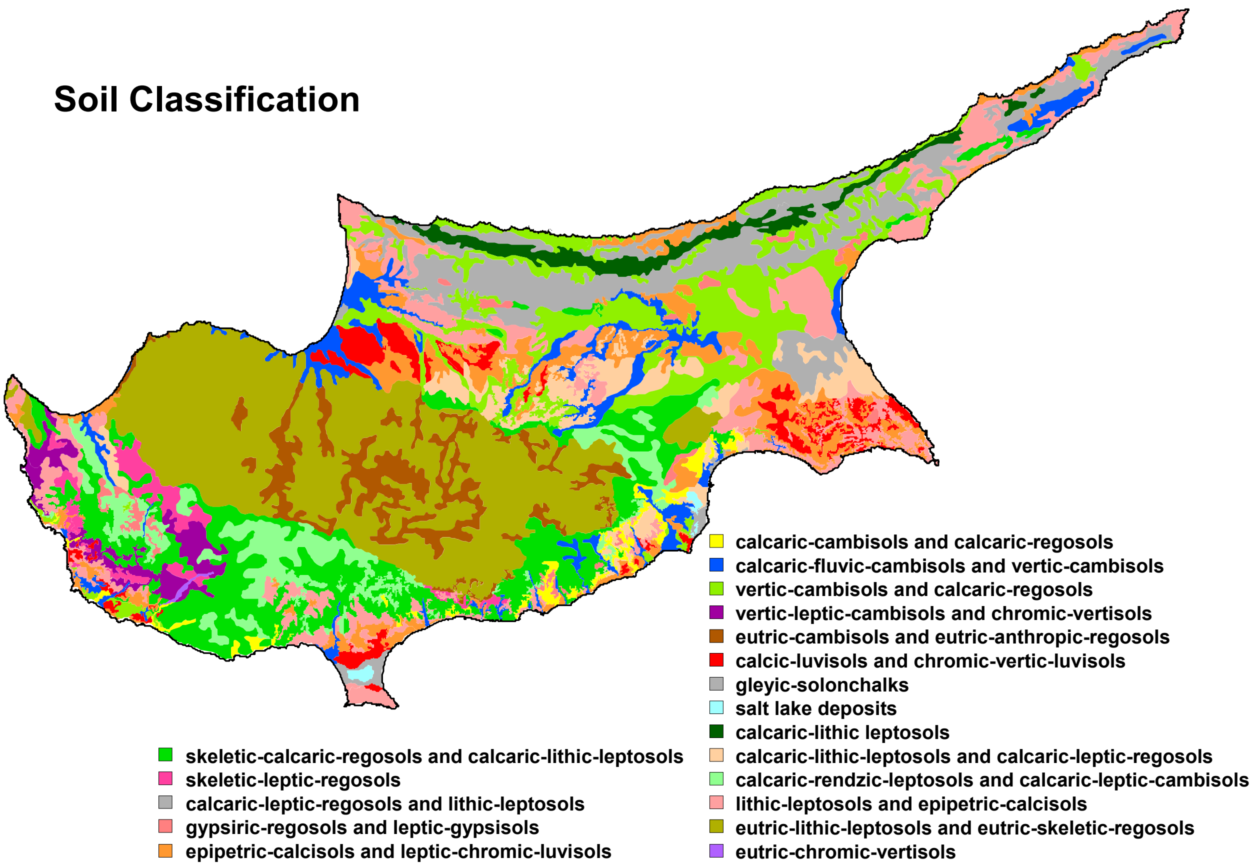

Figure 1.54 Soil classification and distribution for the TOC, Mamonia and CTSS terranes, Cyprus.

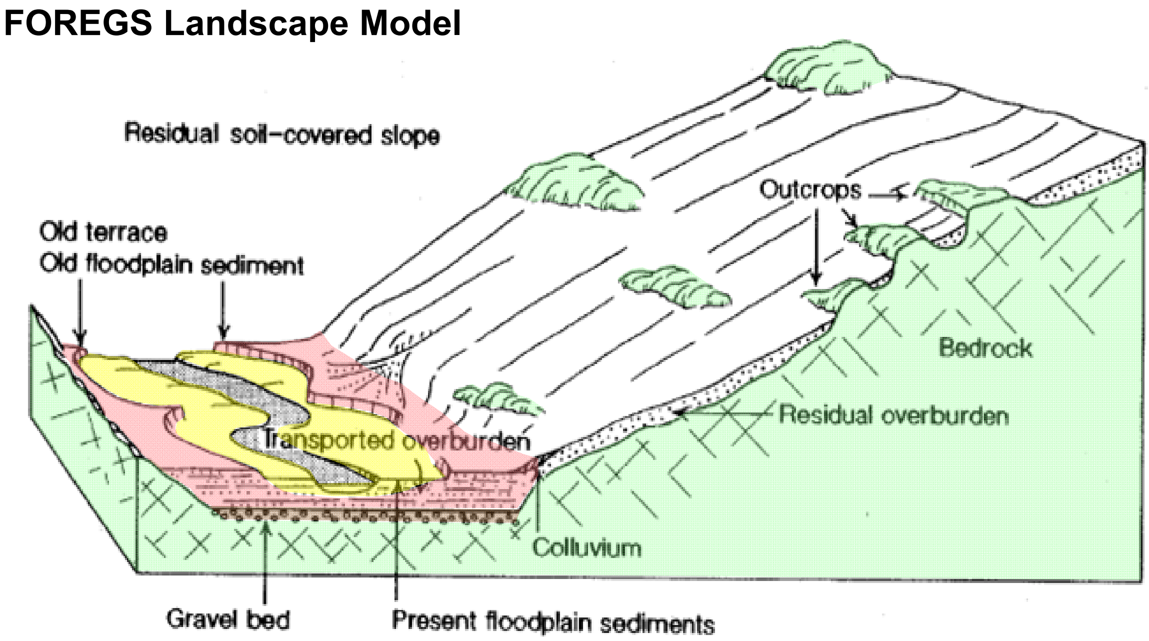

Figure 1.55 Conceptual regolith-landform model for the FOREGS project. After Salminen *et al.* (2005) and Strahler (1969).

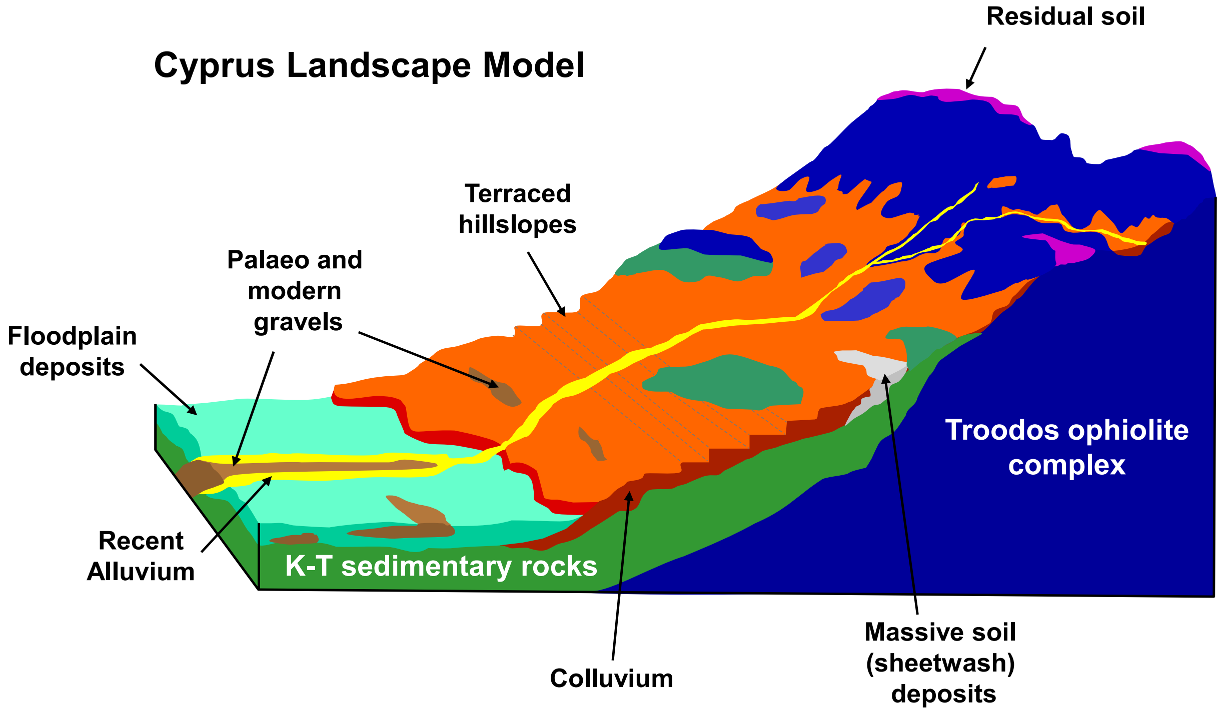

Figure 1.56 Conceptual model of the Cyprus landscape-regolith, showing the relationship between landforms and underlying geology. With the exception of the residual soils on the ridges in Troodos and exposed C-horizon, nearly all regolith is transported, whether colluvium or alluvium.

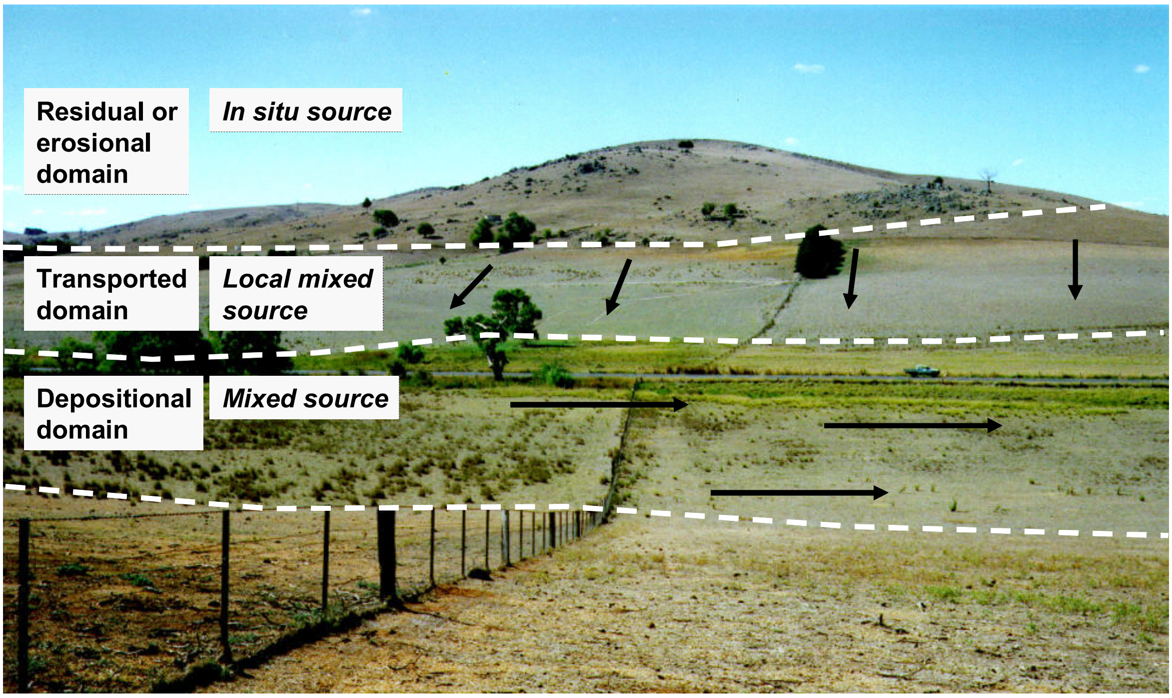

Figure 1.57 Division of landscape into residual, transported and depositional terranes.

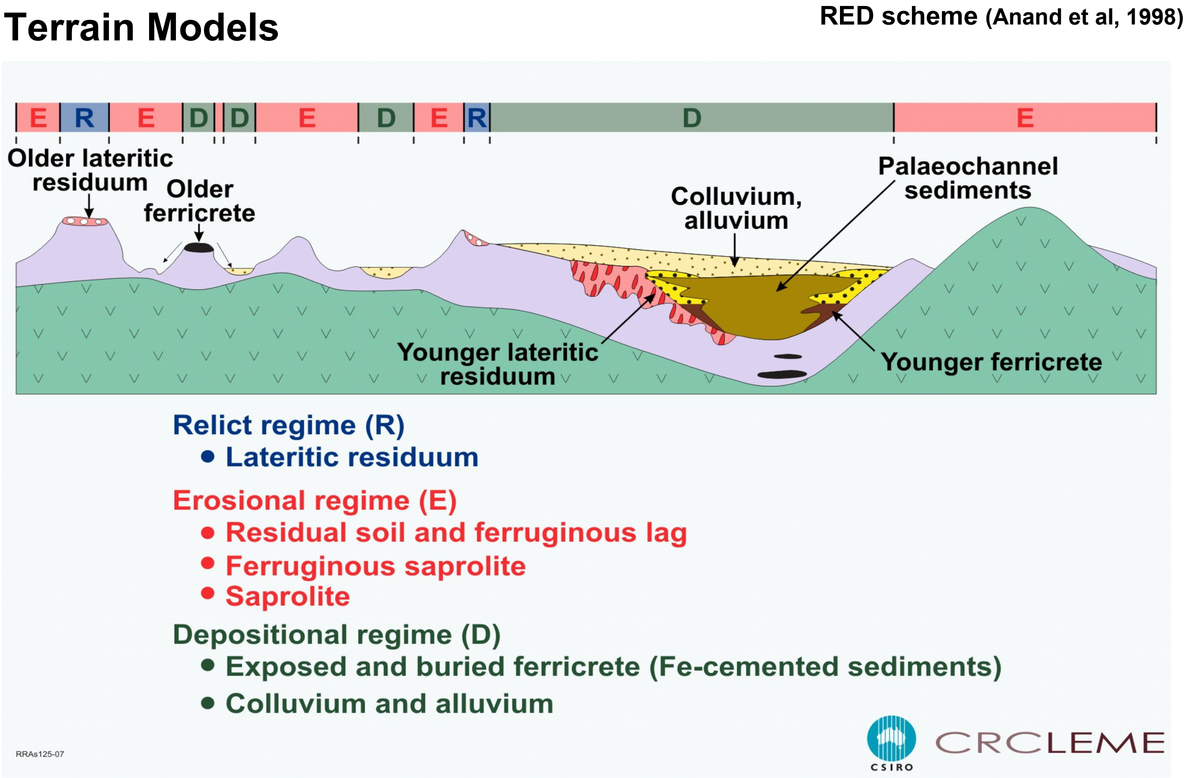

Figure 1.58 RED scheme (residual – erosional – depositional) classification of regolith terrains. From Anand *et al.* (1990).

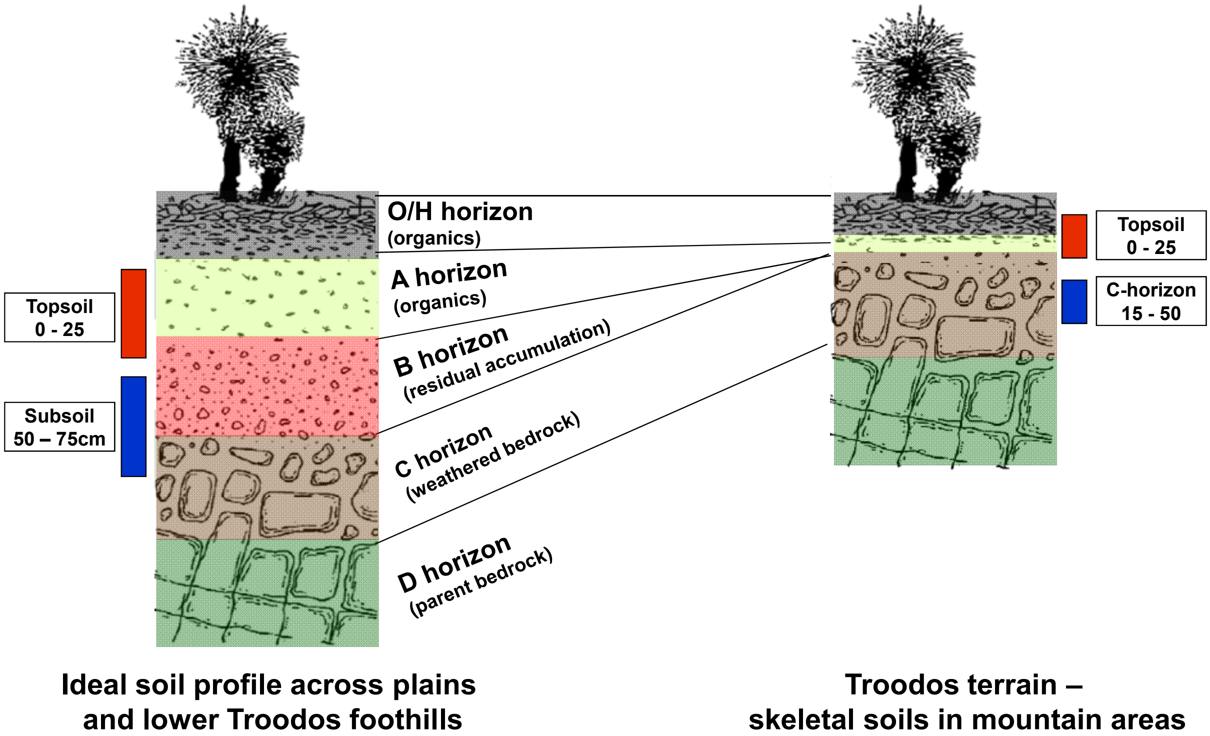

Figure 1.59 Comparison of typical soil profiles.

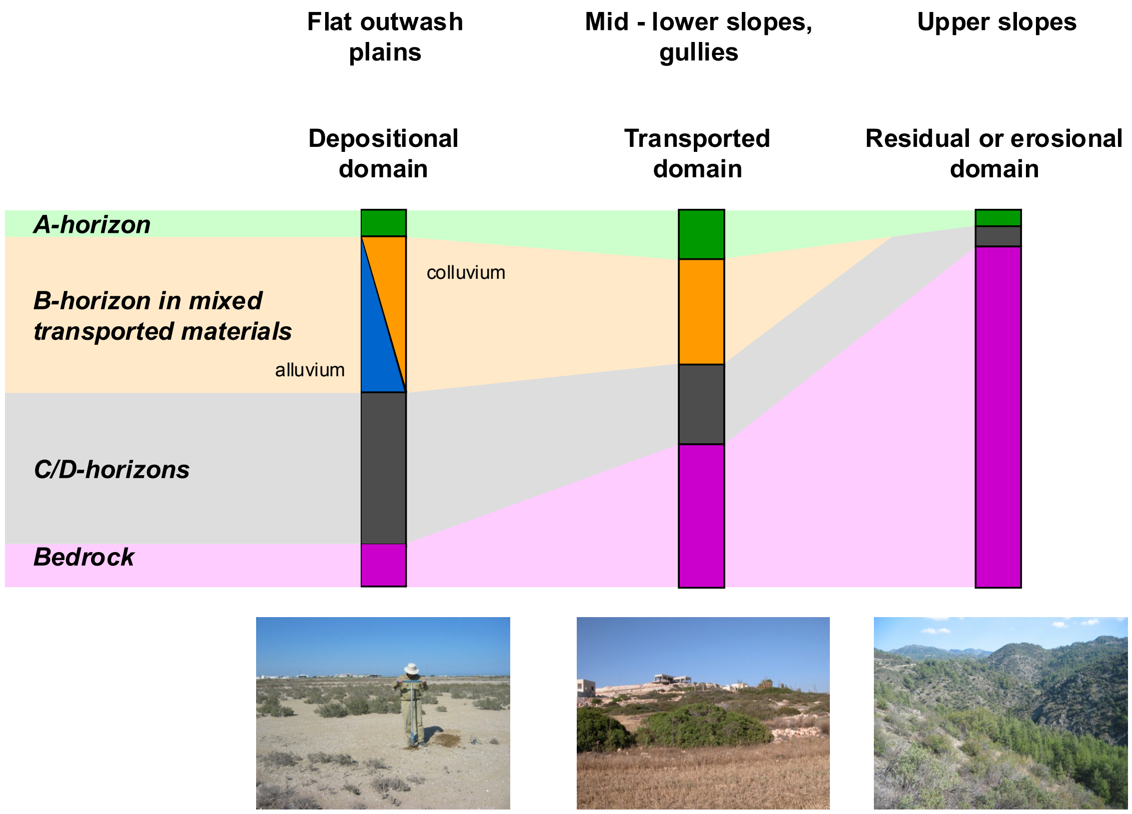

Figure 1.60 Soil profile variation from outwash plains to the Troodos upper slopes.

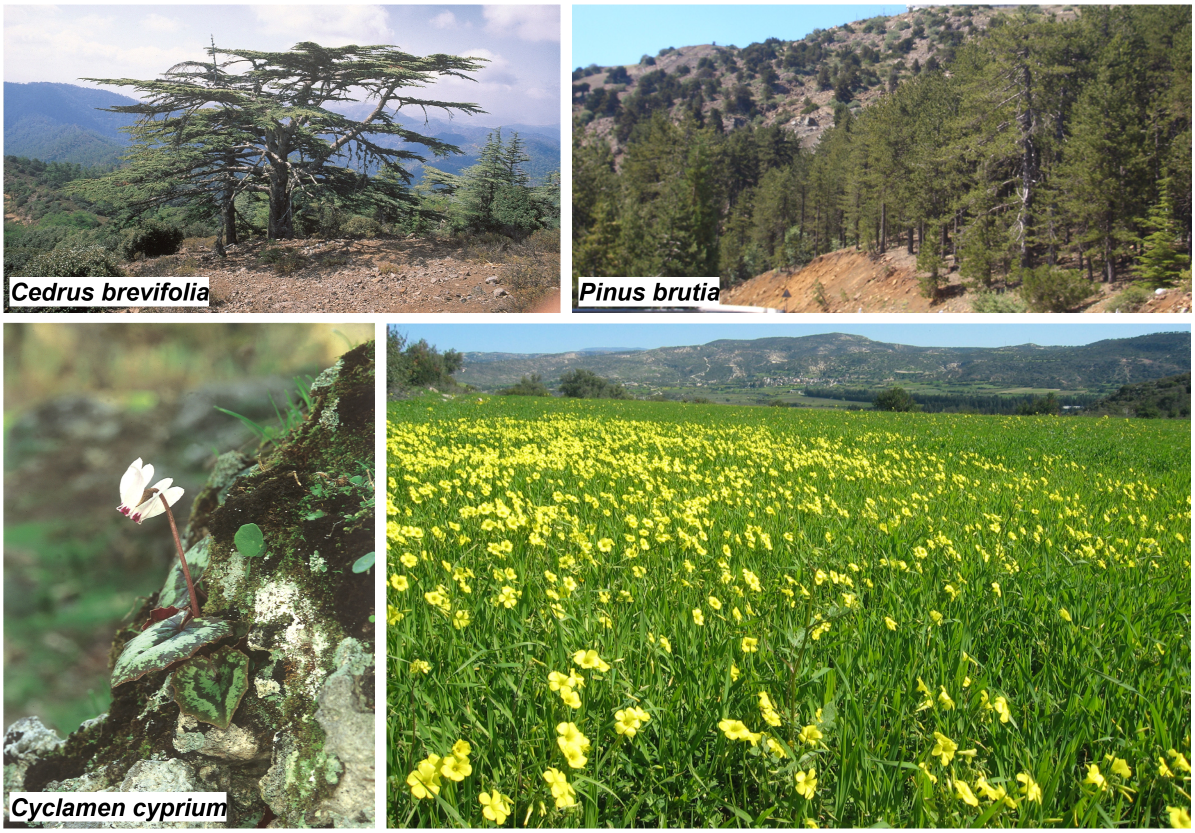

Figure 1.61 *Cyclamen cypria* (the national flower of Cyprus); *Cedrus brevifola* (endemic to the Pafos Forest); one of the common pine species (*Pinus brutia*).

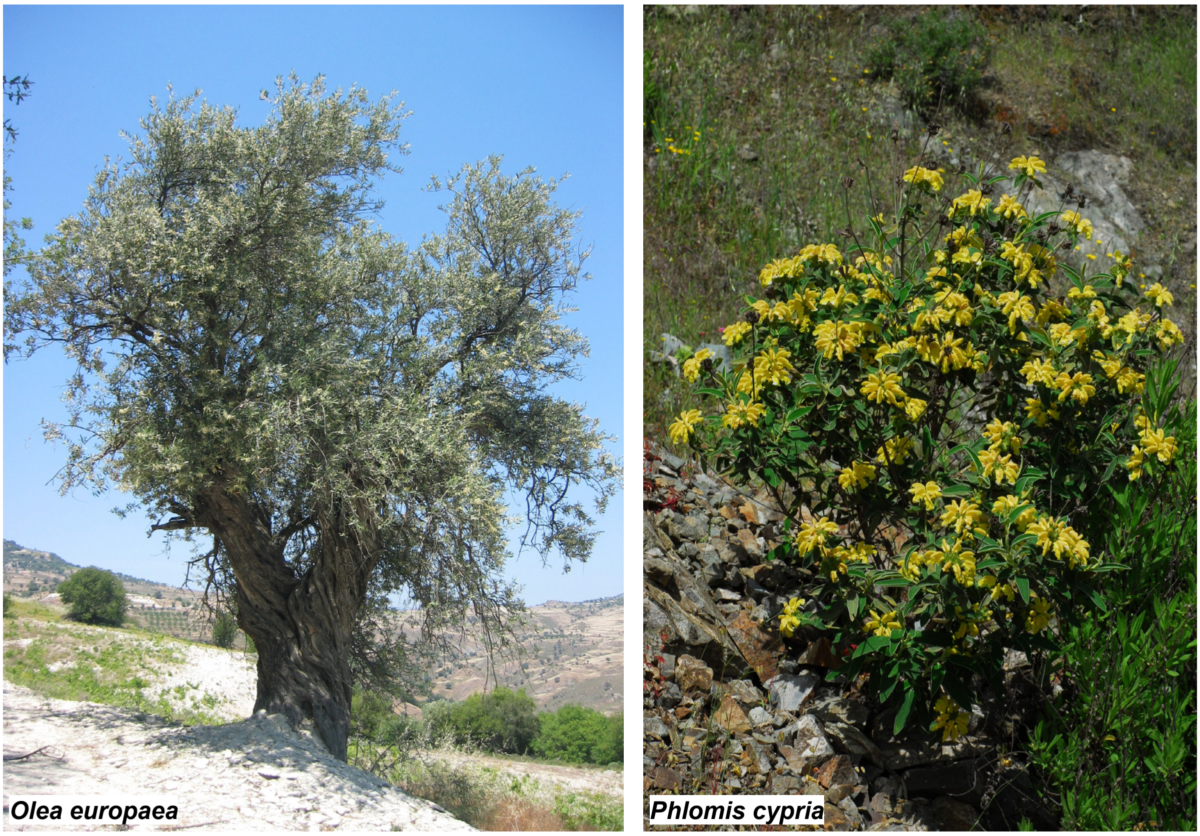

Figure 1.62 Two species extremes – the introduced *Olea europaea* (widely distributed across all continents) and *Phlomis cypria* (an endangered species endemic to Cyprus).

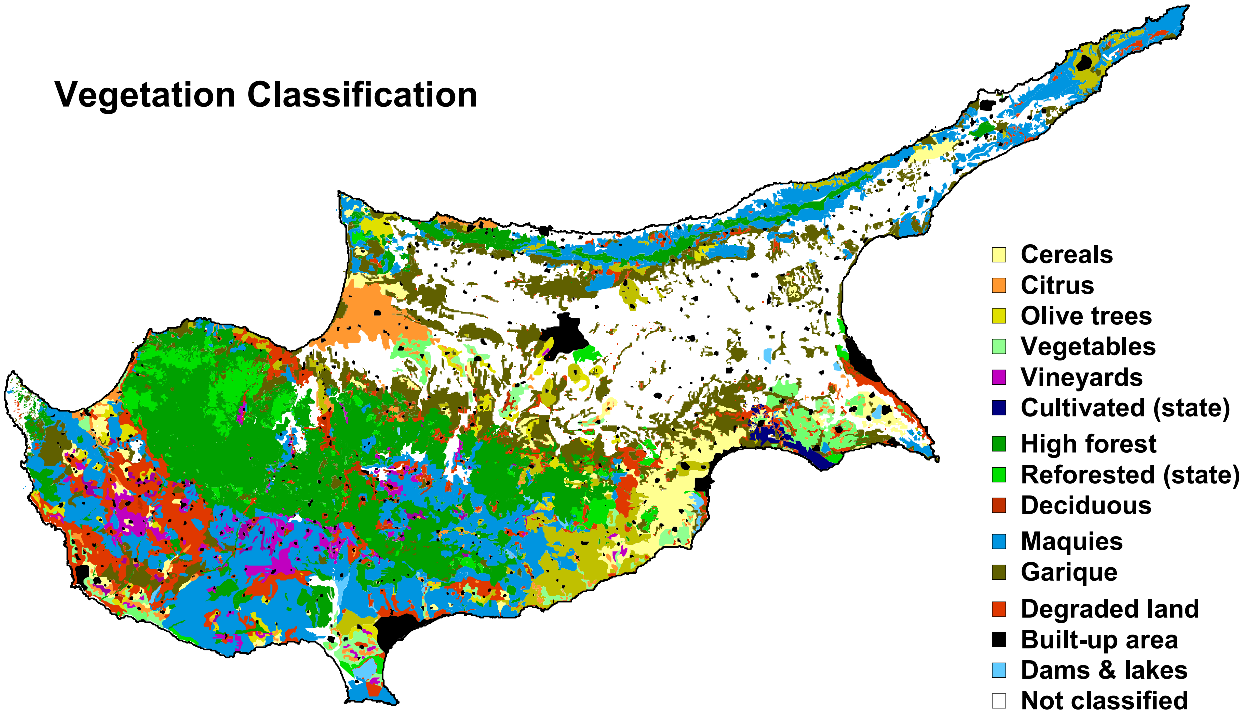

Figure 1.63 Vegetation association classification map for Cyprus.

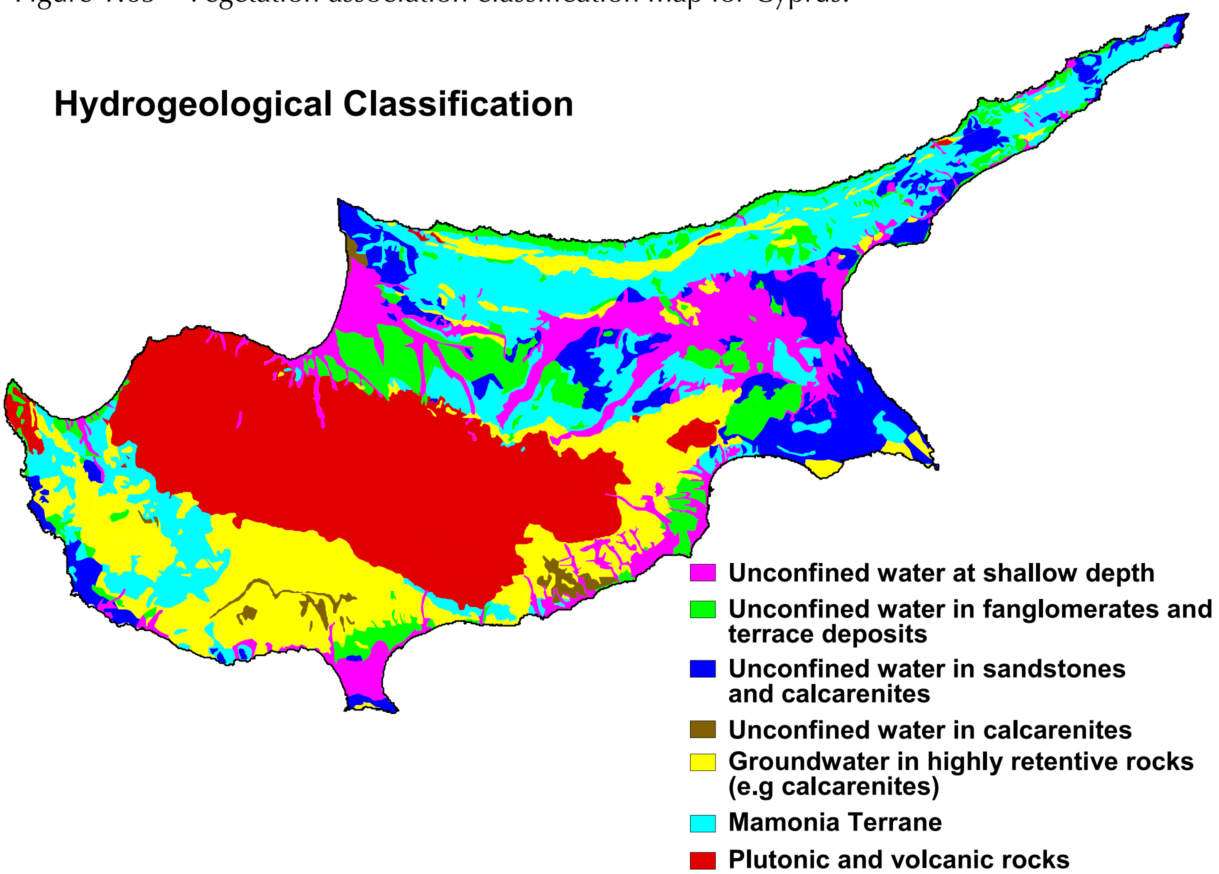

Figure 1.64 Hydrological classification map for Cyprus.

Figure 1.65 (a) Entrance to Kikkos monastery; (b) Larnaka Castle; (c) Mosaics from Ancient Kourion; (d) Aqueduct in western Larnaca.

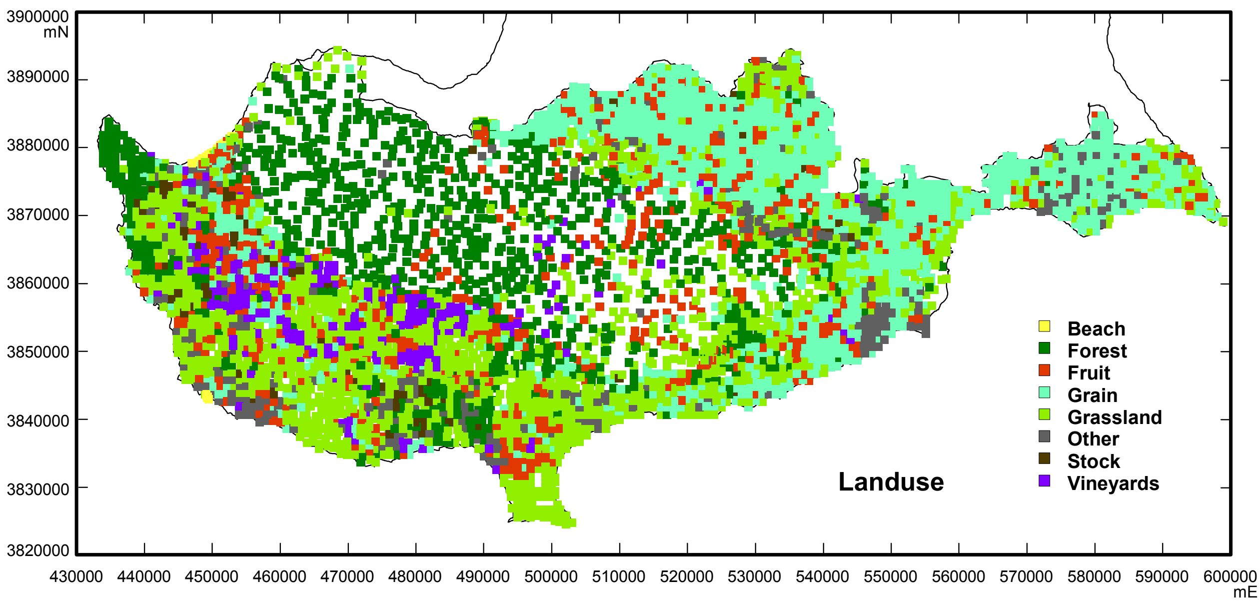

Figure 1.66 Principal landuse classifications observed for the part of Cyprus covered by the atlas.

Figure 1.67 Extensive terracing along the sides of Pakhna Fmn ridges and spurs, with vines, near Amargeti. A large proportion of older terraces are abandoned.

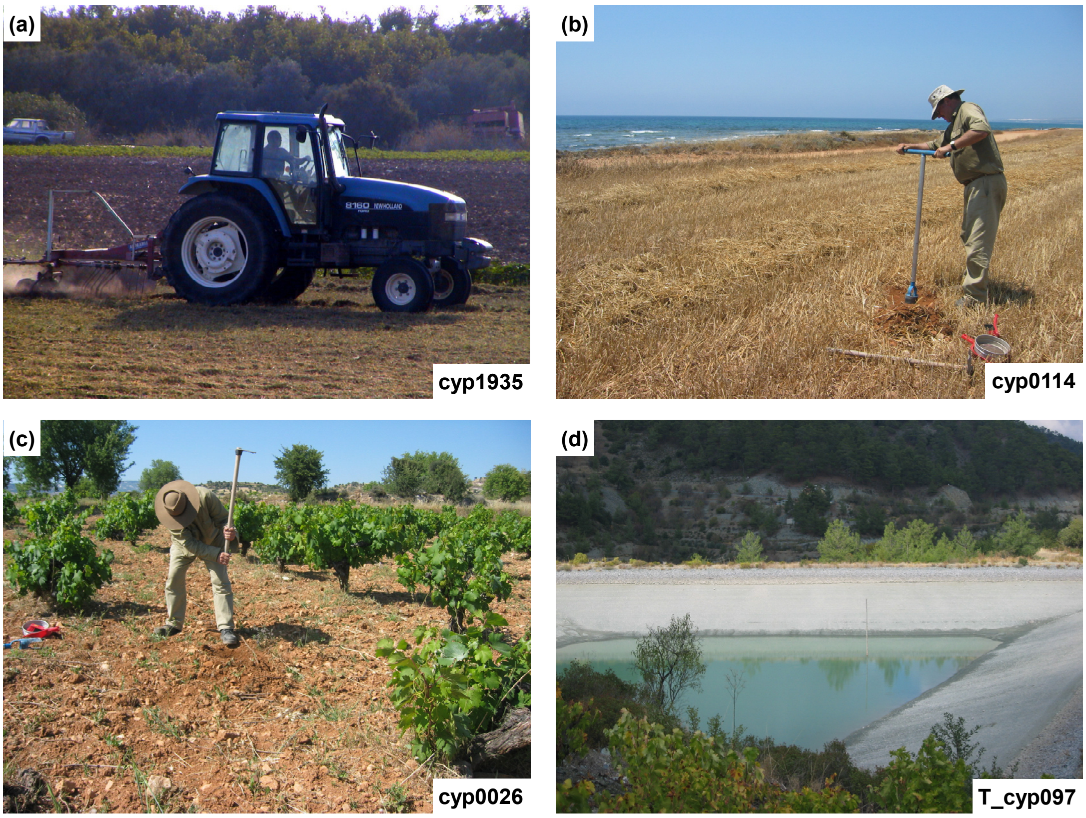

Figure 1.68 (a) Plowing of fields – typically at a depth of 25 cm; (b) Sampling in a fallow wheat field on the coast near Ayia Napa; (c) sampling in a vineyard, near Kelokedara; (d) a small dam near Alona.

Figure 1.69 Mining operations. (a) Amiantos asbestos mine (abandoned) currently under remediation; (b) pit at the Sha Cu mine (abandoned); (c) limestone quarry near Ayios Georgios of Alamanos; (d) Old workings at the Kannoures Cr mine (abandoned).

Figure 1.70 Kokkinopezoula Cu mine (abandoned), Mitsero. Fe-stained mine waters have a pH around 3. Pit walls and benches are being recolonised by *Picea brutia*.

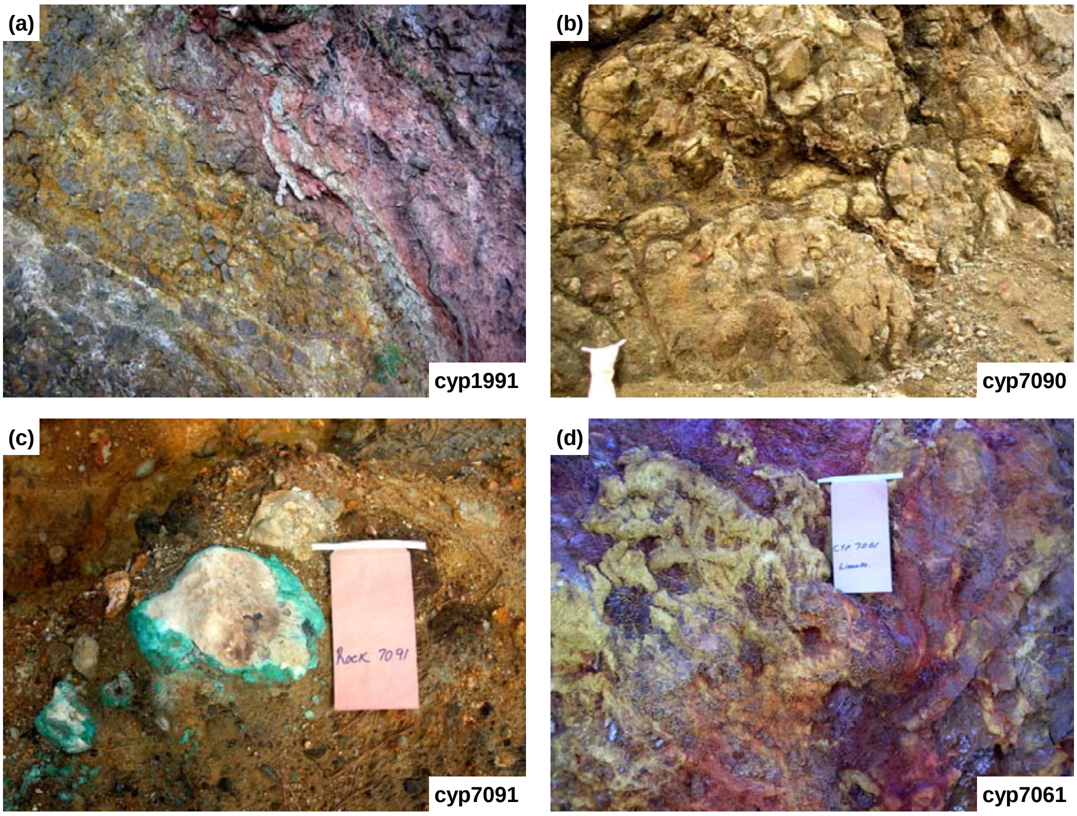

Figure 1.71 (a) Umbers and ochres associated with altered basalts near Mandria; (b and c) pillow lavas and malachite staining in Limni pit; (d) limonitic and goethitic coating on footwall rocks from Kokkinopesula mine.

Figure 1.72 Effects of acid mine drainage and wall-rock leaching at Limni and Sha mines.

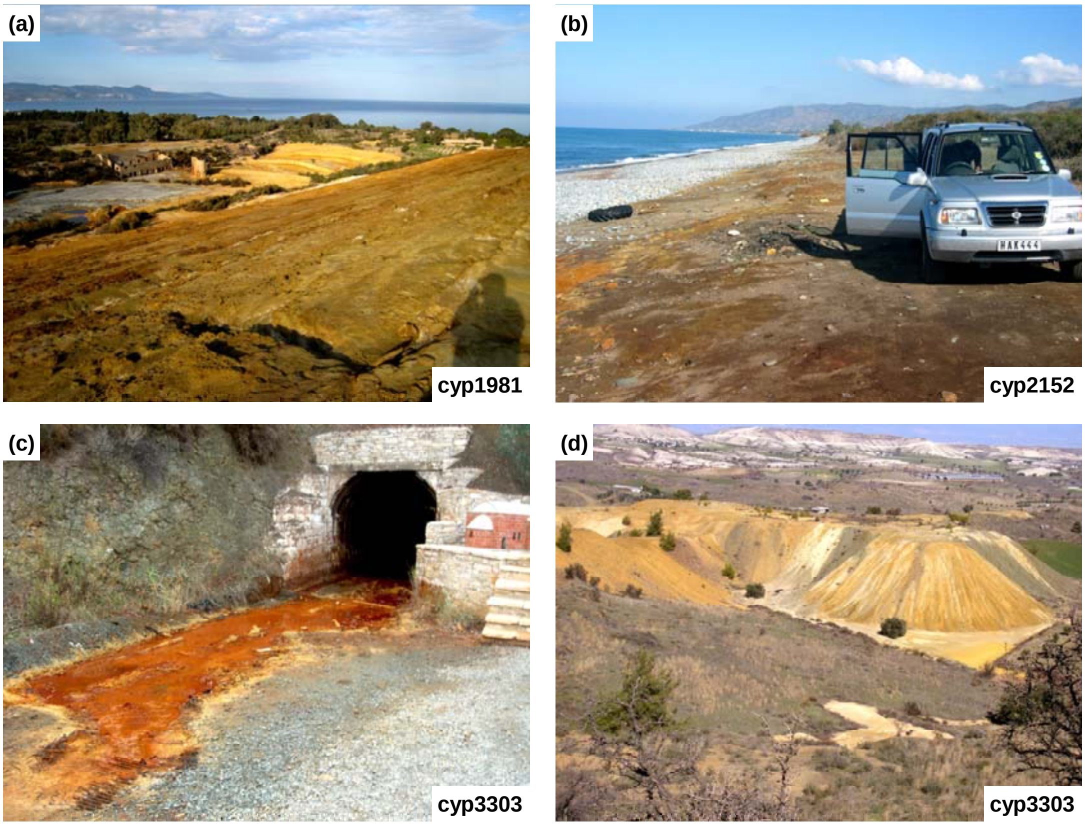

Figure 1.73 Effects of abandoned Cu mine wastes. (a and b) tailings dump at the Limni mine and dispersing across the beach below the mine dump; (c) AMD runoff from the Kalavasos mine; (d) Waste dump at the Mathiatis mine.

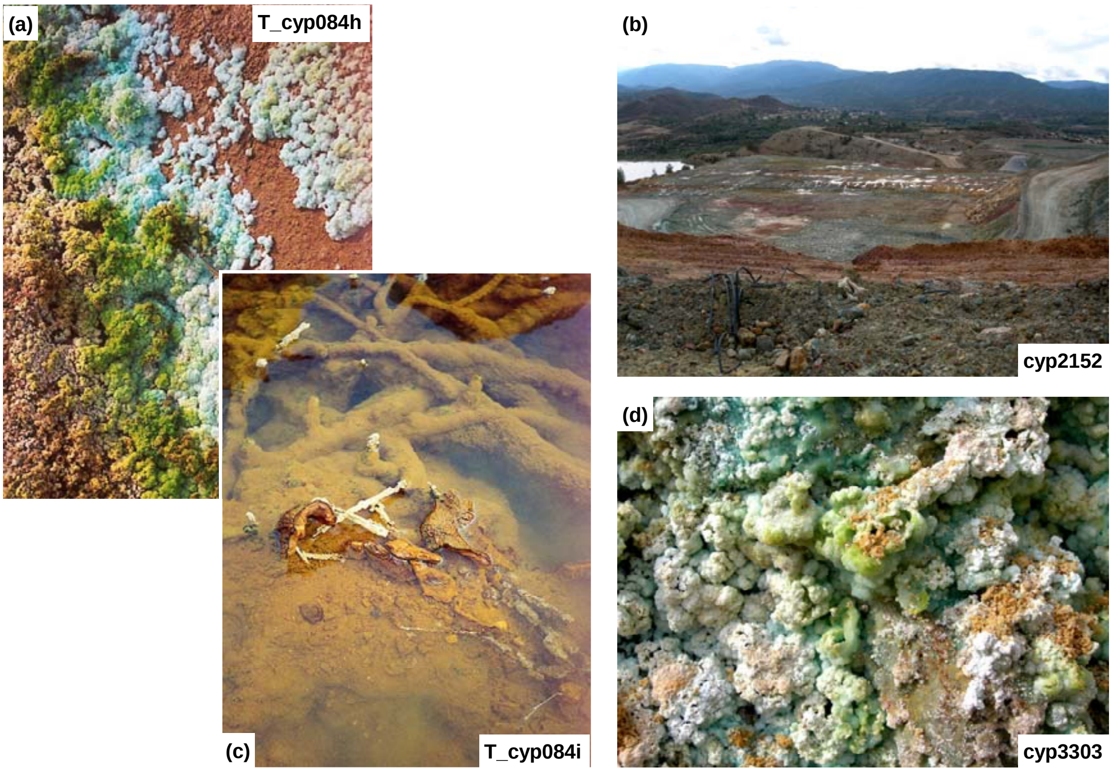

Contamination from the Skouriotissa Mine. (a and d) Efflorescence of Cu sulphates in soils near mine waste dumps; (b) Leach pads; (c) secondary Fe-oxyhydroxides coatings in streams below the

mine.

Figure 1.75 Modified environments. (a) View from GSD building in Strovolos south across Lefkosia towards Troodos; (b) Donkeys passing through historical Omodos; (c) Commercial vessel harbour at Paphos; (d) Kouris Dam.

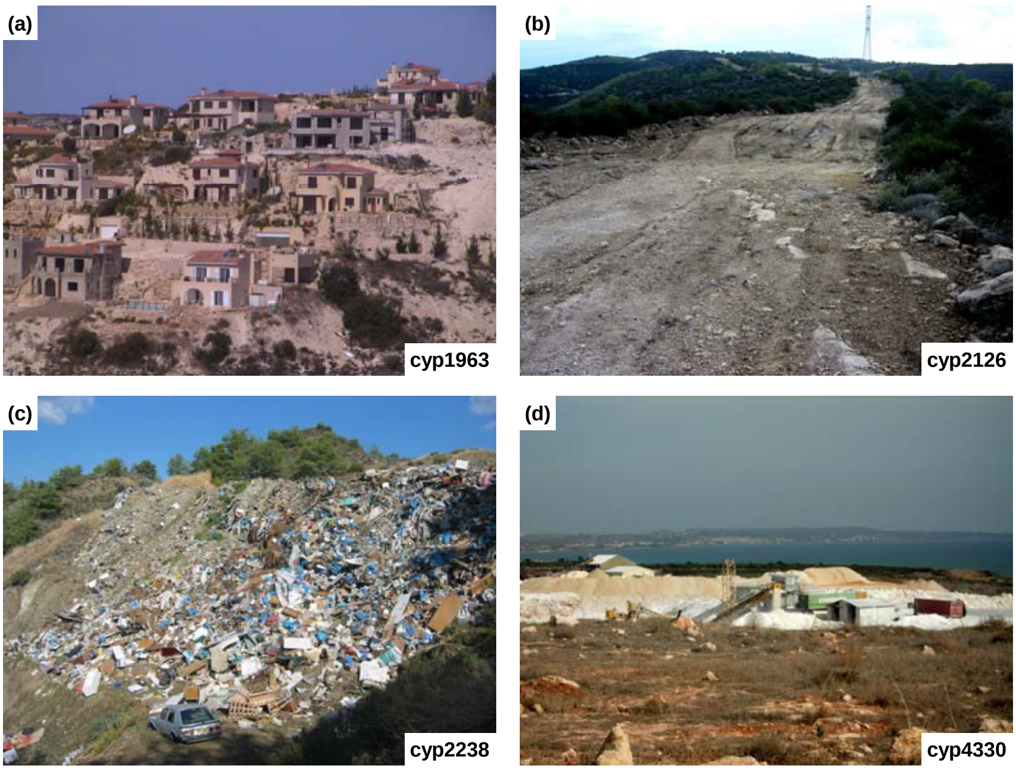

Figure 1.76 New housing developments (typical of large parts of the southern coast); (b) Clearing for new housing developments to commence, near Pano Archimandrita; (c) rubbish dump; (d) Limestone quarry near Cape Pyla.

Figure 1.77 Zivania still at Eledio; (b) Abandoned house, Phalia; (c) Old olive press; (d) traditional olive harvesting, near Anogyra.

Table 1.5 The Dutch Government intervention levels for soils.

Species	**Target values**	**Intervention value for soils** (10% organic and 25% clay)	**Indicative levels for serious contamination for soils** (10% organic and 25% clay)
		(mg/kg)	(mg/kg)
As	30	55	
Ba	200	625	
Cd	0.8	12	
Co	20	240	
Cr	100	380	
Cu	36	190	
Hg (inorganic)	0.3	10	
Mo	10	200	
Ni	35	210	
Pb	85	530	
Sb	5	22	
Zn	140	720	
Ag			15
Be			30
Se			100
Sn			900
Te			600
Tl			15
V			250

Table 1.6 Summary table of statutory limits of toxic elements in soil established by different European countries and Canada, their phytotoxic levels, and global soil. From Demetriades *et al.* (2006). Values in mg/kg.

Species	**Italy**		**Canada**		**Denmark**	**Finland**		**Switzerland**		**Global soil mean**
	Parks & Resid[1]	*Indust & Commerc*[1]	*Federal*	*Ontario Residential*		*Guide*	*Limit*	*Trigger*	*Clean-up*	
Ag	-	-	-	-	-	-	2	-	-	0.07
As	20	50	20	25	20	10	20	-	-	5
Ba	-	-	-	-	-	600	600	-	-	500
Be	2	10	-	-	-	-	10	-	-	3
Br	-	-	-	-	-	-	10	-	-	
Cd	2	15	3	4	5	0.5	3	2	20	0.3
Co	20	250	40	50	-	50	50	-	-	10
Cr (tot.)	150	800	750	1000	1000	100	100	-	-	80
Cr (VI)	2	15	-	-	-	-	-	150	1000	-
Cu	50	140	150	200	500	100	100	-	-	25
F	-	-	-	-	-	-	200	-	-	-
Ga	-	-	-	-	-	-	10	-	-	15
Hg	1	5	0.8	1	3	0.2	2	-	-	0.05
Mn	-	-	-	-	-	-	-	-	-	530
Mo	-	-	5	5	-	5	5	-	-	1.2
Ni	120	500	150	200	30	60	100	200	1000	20
Pb	100	1000	375	500	400	60	100	-	-	17
Sb	10	30	-	-	-	5	40	-	-	0.5
Sc	-	-	2	2	-	-	-	-	-	12
Se	3	15	-	-	-	-	10	-	-	0.3
Sn	-	-	-	-	-	50	50	-	-	10
Tl	1	10	-	-	-	-	1	-	-	0.5
U	-	-	-	-	-	-	5	-	-	2.7
V	90	250	-	-	-	-	50	-	2000	90
Zn	150	1500	600	800	1000	150	300	-	-	70
Zr	-	-	-	-	-	-	300	-	-	300

Species	**G e r m a n y**				**Nether-lands**	**United Kingdom**		**Phytotoxic levels**	
	Play-ground	*Resi-dential*	*Parks & Rec*	*Indust & Commerc*[1]	Action	*Residential*[3]	*Indust & Commerc*[1]	*Min*	*Max*
Ag	-	-	-	-	-	-	-	-	2
As	25	50	125	140	55	20	500	15	50
Ba	-	-	-	-	625	-	-	-	-
Be	-	-	-	-	-	-	-	-	10
Cd	10[2]	20[2]	50	60	12	1 or 2 or 8[4]	1400	3	8
Co	-	-	-	-	240	-	25	50	
Cr (tot.)	200	400	1000	1000	380	130	5000	75	100
Cu	-	-	-	-	190	130	-	60	125
Hg	10	20	50	80	10	8	480	0.2	0.5
Mn	-	-	-	-	-	-	-	1500	3000
Mo	-	-	-	-	200	-	-	2	10
Ni	-	-	-	-	210	50	5000	100	100
Pb	200	400	1000	2000	530	450	750	100	400
Sb	-	-	-	-	-	-	-	5	10
Se	-	-	-	-	35	8000	5	10	
Sn	-	-	-	-	-	-	-	50	50
Tl	-	-	-	-	-	-	-	-	1
V	-	-	-	-	-	-	-	50	100
Zn	-	-	-	-	720	-	-	70	400

Global soil means from Levinson (1980). Phytotoxic levels from Kabatas-Pendias and Pendias (1984).

Table 1.7 Risk-based soil guideline values for metals for Cyprus, developed for residential and industrial landuse. From Wcislo and Korcz (2006).

	Risk Based Soil Guideline Values	
	Residential mg/kg	**Industrial** mg/kg
Ag	0.23	2.1
As	39	180
B	15	210
Ba	11	120
Be	31	220
Cd	70	900
CrIII	37	280
CrIV	0.11	0.53
Cu	300	4300
Fe	23000	320000
Hg	1.9	14
Hg (chloride)	0.017	0.18
Mn	920	8600
Mo	0.38	5.3
Ni	920	8600
Pb	400	800
Sb	26	320
Se	0.38	5.3
Sn	46	640
Tl (chloride)	6.1	85
Zn	23	320

Table 1.8 Ultramafic geochemistry from Troodos Igneous Complex. Data from Moore and Vines (1971).

	Gabbro *Saittas*	**Olivine gabbro** *Platres*	**Horn-blende trond-hjemite** *Khandria*	**Olivine pyrox-enite 1** *Troodos village*	**Olivine pyrox-enite 2** *Troodos village*	**Dunite** *Troodos village*	**Harz-burgite 1** *Troodos village*	**Harz-burgite 2** *Lemesos Forest*	**Serpent-inite** *Lemesos Forest*
%									
SiO_2	46.07	48.16	73.06	46.27	39.54	33.72	37.68	42.93	38.59
TiO_2	0.08	0.01	0.28	0.06	0.03			0.11	0.07
$A1_2O_3$	22.21	9.35	12.3	2.31	5.15	0.51	0.56	4.43	1.97
Fe_2O_3	0.87	9.58	2.32	2.74	3.48	4.06	4.8	4.13	8.51
FeO	2.74	0.00	2.23	3.76	4.39	3.21	2.88	5.24	2.00
MnO	0.08	0.27	0.05	0.13	0.14	0.11	0.11	0.13	0.15
MgO	8.82	17.18	0.65	29.24	32.71	41.82	39.32	28.3	33.24
CaO	17.48	13.6	3.56	12.12	4.06	0.15	0.54	7.30	1.28
Na_2O	0.68	0.05	3.90	0.15	0.14			0.15	0.04
K_2O	0.11	0.10	0.18	0.07	0.09			0.15	0.04
P_2O_5	0.05	0.13	0.07	0.20	0.04	0.04	0.03	0.03	
mg/kg									
Cr_2O_3	270			320	260	8000	1650		
NiO				800	980	700	2300		

Table 1.9 PGE contents of chromitites in the TOC. From Büchel *et al.* (2004).

PGE	ug/kg
Pd	11.1–76.8
Ru	34.3–83.6
Ir	11.3–19.0
Pt	0.41–9.07
Os	13.7–104

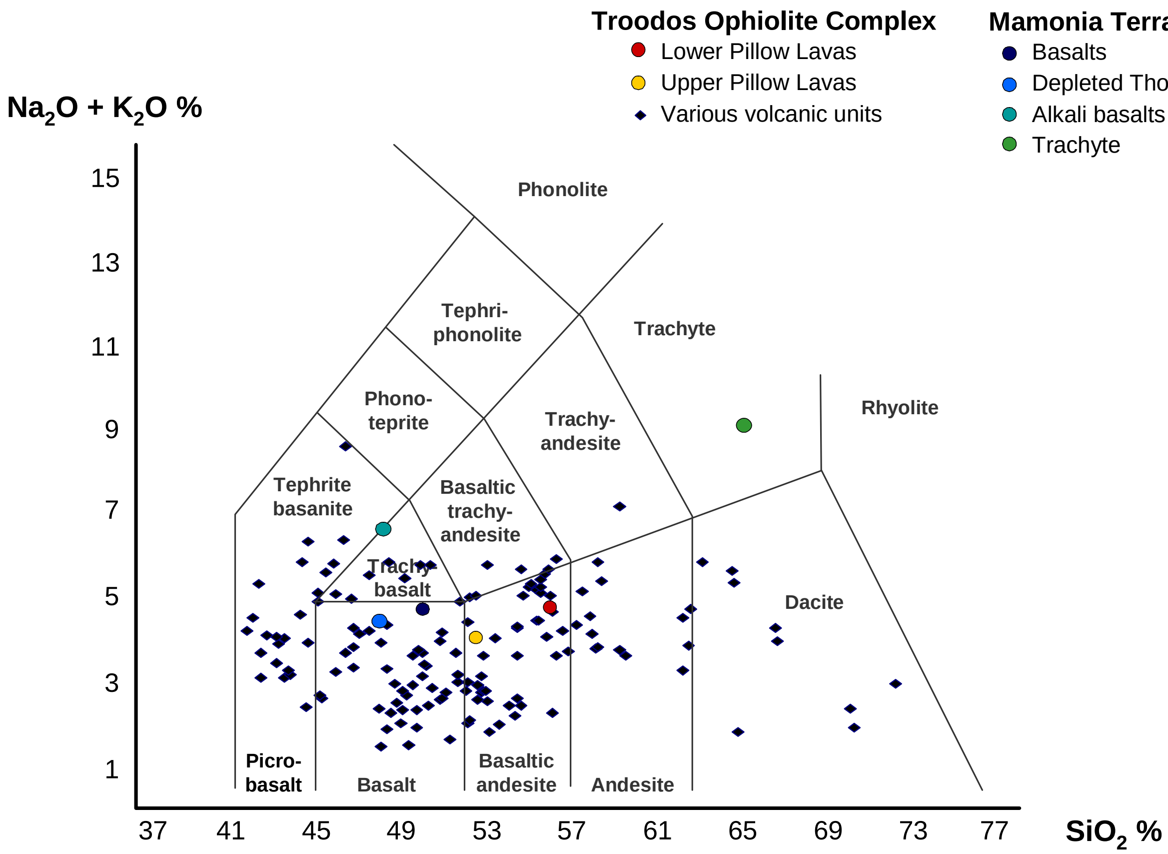

Figure 1.78 TAS diagram with average compositions plotted for the TOC pillow lavas and Mamonia Terrain basalts. Data from Pearce (1975; Lapierre *et al.* (2007); EMED (2008).

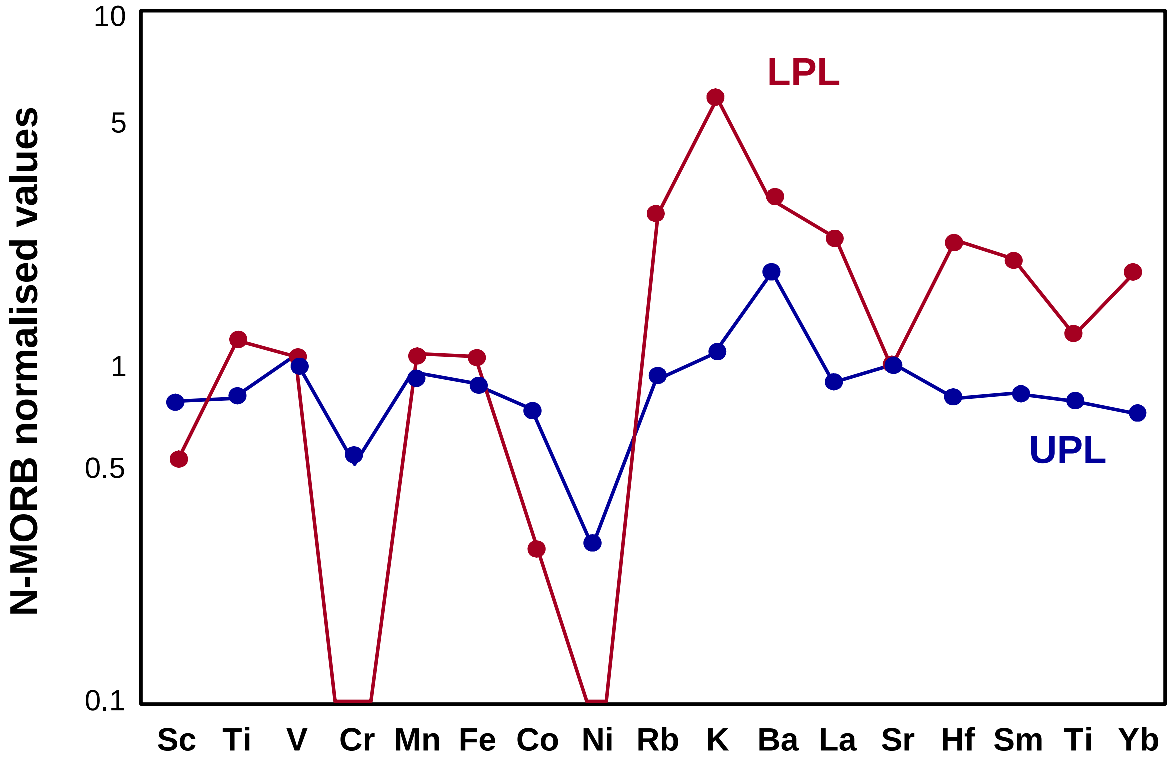

Figure 1.79 N-MORB normalized major and trace element distributions in upper and lower pillow lavas. Modified from Thy and Moore (1988).

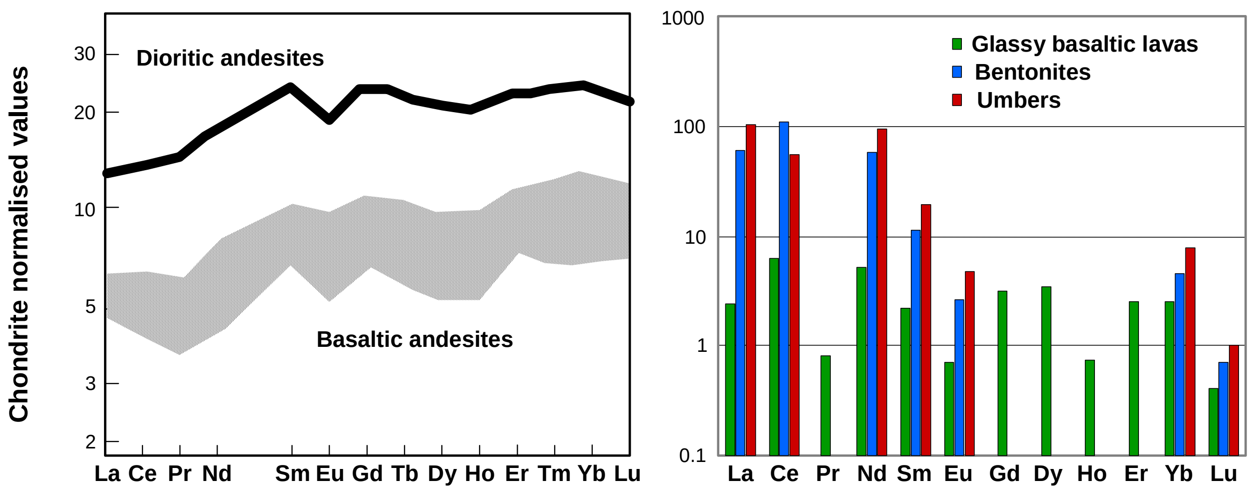

Figure 1.80 Chondrite normalized REE values for dioritic andesites and basaltic andesites and average REE values in glassy basaltic lavas, bentonites and umbers in TOC. Data from Thy *et al.* (1985) and Robertson and Fleet (1995).

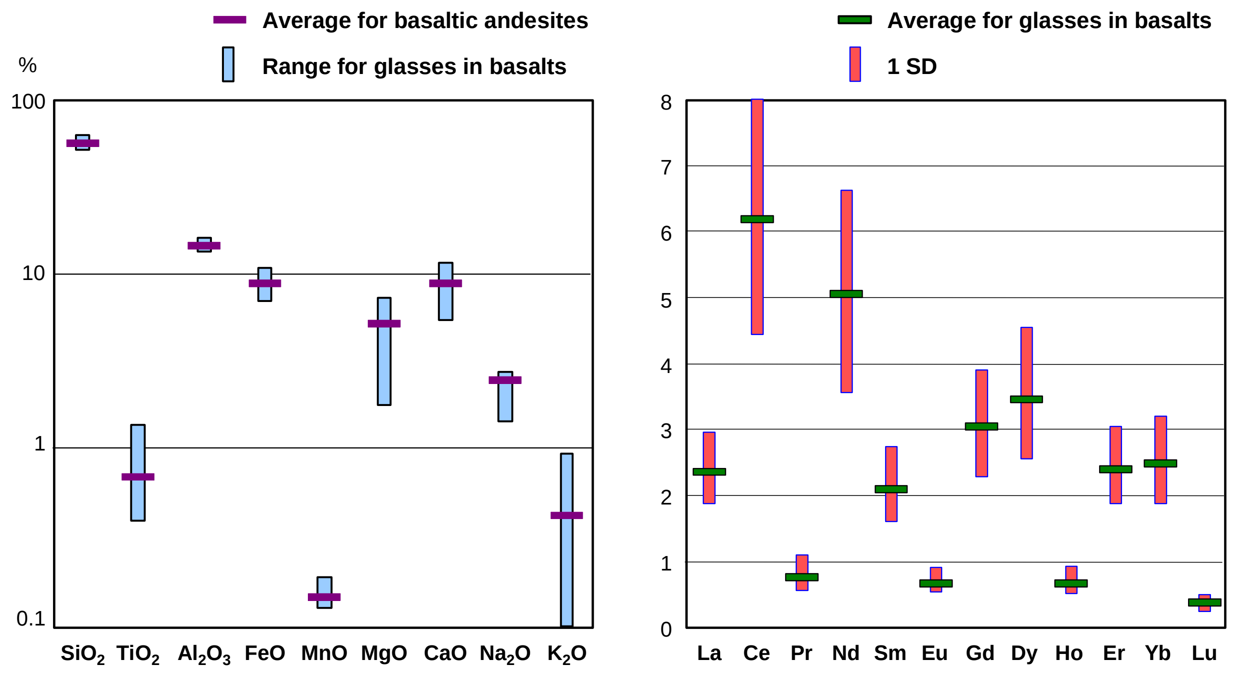

Figure 1.81 Distribution of major oxides and REE in basaltic glasses and average for TOC basaltic andesites. Data from Thy *et al.* (1985).

Table 1.10 Troodos Ophiolite Complex lithogeochemistry. Data from Pearce (1975).

	Major oxides (%)							
	SiO_2	***TiO_2***	***Al_2O_3***	***FeO***	***MgO***	***CaO***	***Na_2O***	***K_2O***
Lower Pillow Lavas	56.36	1.03	16.49	10.37	7.07	4.63	3.65	0.99
Upper Pillow Lavas	52.65	0.42	15.70	9.56	8.13	9.36	1.73	2.37
Mamonia Terrain Mafics	50.68	2.83	15.83	9.82	5.54	9.91	2.90	2.69
Dolerites		1.07						0.20

	Trace elements (mg/kg)						***Ratios***	
	Cr	***Nb***	***Rb***	***Sr***	***Y***	***Zr***	***Ti/Zr***	***Ti/Y***
Lower Pillow Lavas	*105*	*1*	*18*	*117*	*27*	*61*	*110*	224
Upper Pillow Lavas	*383*	*1*	*29*	*109*	*14*	*20*	*124*	175
Mamonia Terrain Mafics	*80*	*70*	*38*	*317*	*33*	*282*	*66*	504
Dolerites	*97*	*1*	*2*	*92*	*29*	*69*	*92*	217

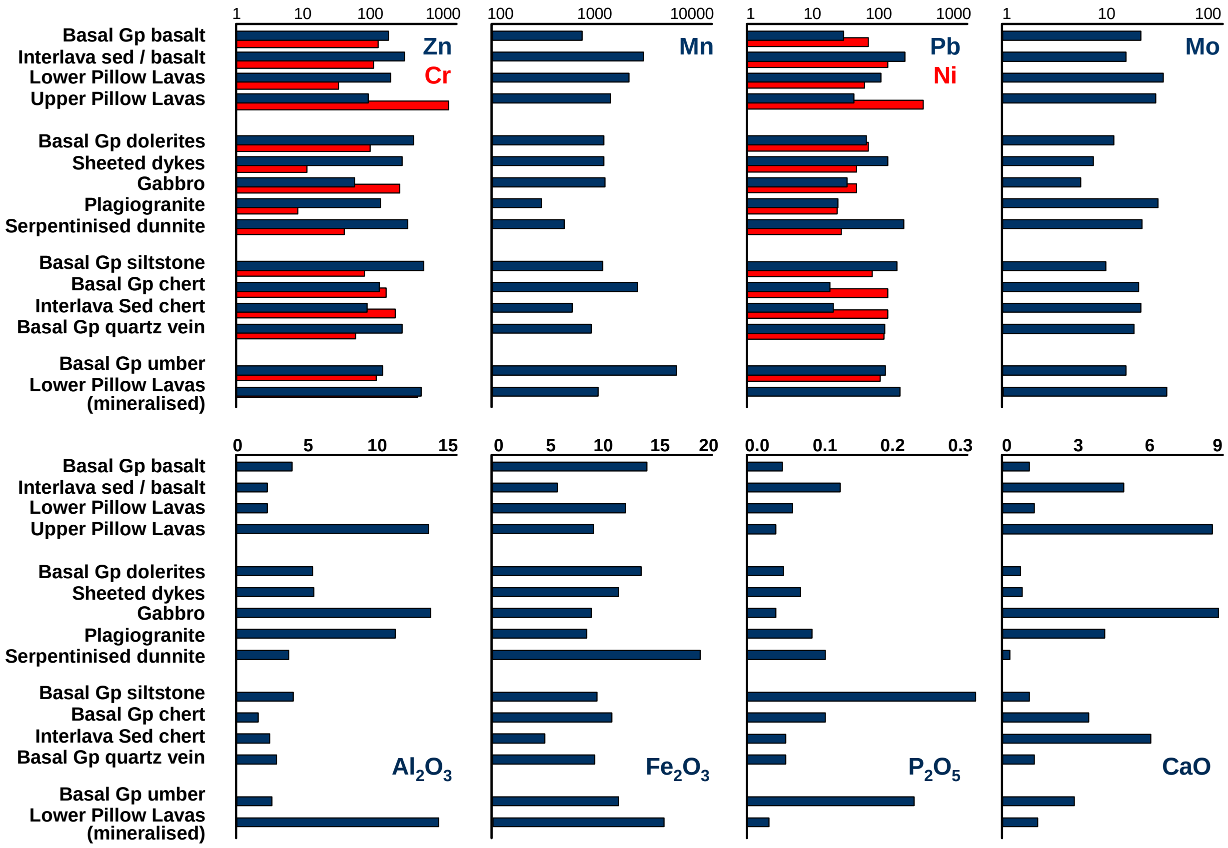

Figure 1.82 Distribution of selected elements within various lithologies of TOC. Data compiled by EMED Ltd (2008).

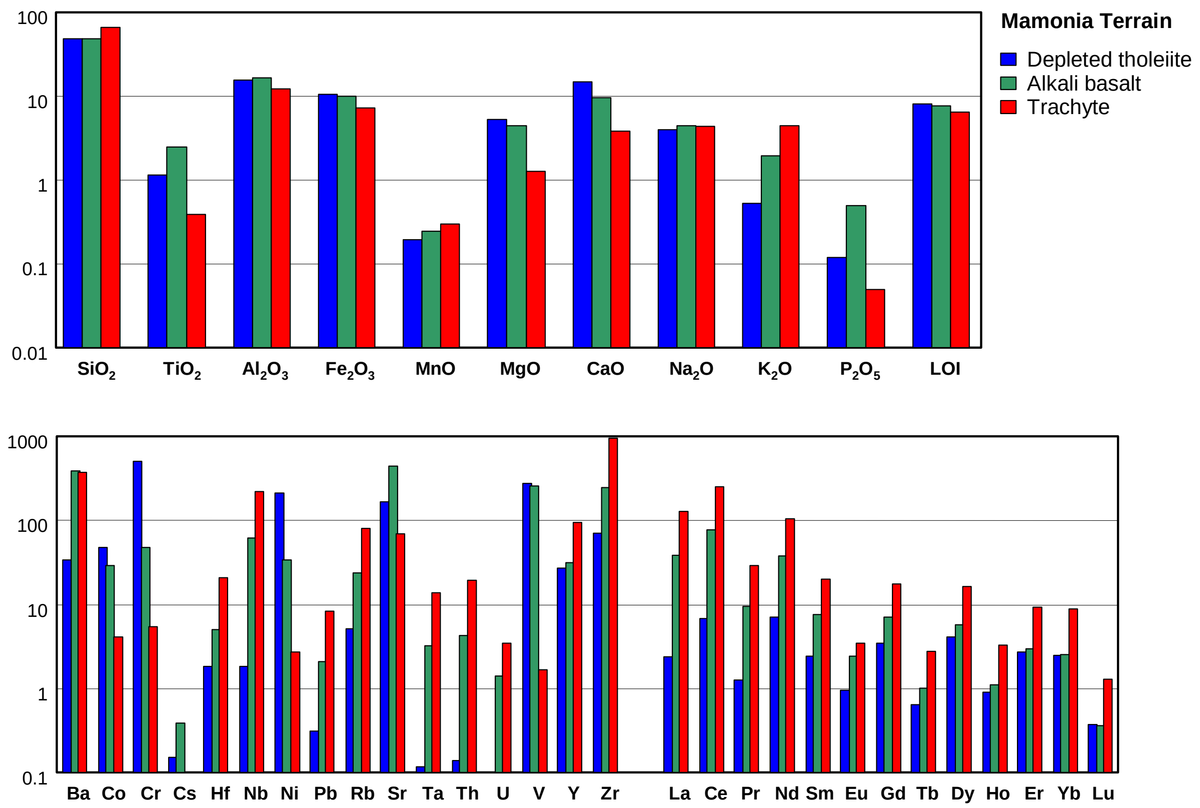

Figure 1.83 Average major and trace element distributions in Mamonia Terrain lithologies. Data from Lapierre *et al*. (2007).

Table 1.11 Trace-element content of Ayia Varvara Fmn amphibolitic basaltic rocks and amphibolites. Data from Malpas *et al*. (1992).

	Amphibolitic Basalts				**Amphibolite**
	Type 1	*Type 2*	*Type 3*	*Type 4*	
n	*3*	*2*	*4*	*4*	*6*
Values in mg/kg					
Ba	89	164	173	9	41
Ce	30	47	51	14	11
Cr	453	82	84	607	161
Cu	87	70	77	98	60
Ga	9	18	15	6	9
La	14	32	30	14	13
Nb	7	49	36	4	6
Ni	137	45	45	194	61
Pb	6	2	3	4	2
Rb	5	11	11	3	3
Sr	257	203	411	51	124
Tb	15	6	9	8	5
V	222	248	282	246	330
Y	36	26	40	14	48
Zn	62	43	66	49	81
Zr	30	62	208		60
Values in %					
K_2O	0.60	0.85	0.70	0.23	0.42
P_2O_5	0.05	0.06	0.25	0.02	0.07
TiO_2	0.81	1.18	2.07	0.21	1.10

Type 1 Olivine-phyric, varioiitic basalts.
Type 2 Plagioclase-augite pillow basalts with calcitic amygdales.
Type 3 Altered feldspar-phyric basalts.
Type 4 Olivine-phyric basaltic lavas with augite.

Table 1.12 Geochemistry of umbers and associated lithologies. Data from Robertson and Hudson (1972).

	Umbers							
	1	*2*	*3*	*4*	*5*	*6*	*7*	*8*
(%)								
Ca	0.4	0.7	0.9	1.5	1.2	0.7	1	1.3
K	0.57	0.57	0.62	1.9	1.9	0.21	0.21	0.32
Fe	44	30.7	28.6	11	5.3	32.5	37.7	35.3
Ti	0.13	0.95	0.11	0.35	0.35	0.06	0.89	0.16
Si	7	6.1	6.1	22.9	22.8	4.9	5.6	7
Al	2	1	1.7	6.2	6.6	0.95	1.2	1
Mg	0.5	0.5	0.4	2.3	1.8	0.4	0.5	0.7
P	0.26	0.21	0.18	0.22	0.13	0.28	0.53	0.12
Mn	1.6	11.2	12.5	3.4	2.9	2.4	2.4	10.9
(mg/kg)								
Ba	756	1190	1180	310	225	58	45	1190
Co	129	133	104	74	57	76	145	85
Cr	8	9	9	41	35	38	69	4
Cu	803	1400	1180	420	280	1180	1200	1180
Ni	336	368	335	152	100	163	130	164
Pb	179	190	246	183	158	122	77	155
V	886	689	613	152	189	1493	1490	597
Zn	467	381	404	414	306	289	386	301
Zr	1102	798	591	89	92	427	363	340

	Radiolarian mudstone				Calcareous sedimentary rocks		
	9	*10*	*11*	*12*	*13*	*14*	*15*
(%)							
Ca	1	0.4	1.2	1.3	35	23.2	22.9
K	1.72	0.33	1.39	1.1	0.37	0.19	0.31
Fe	7.5	1.4	4.1	4	1.2	9.3	9.5
Ti	0.3	0.03	0.13	0.35	0.96	0.05	0.05
Si	25.6	43.9	35	34.5	6	2.5	4.7
Al	5.5	1.3	2.6	6.5	1.6	0.6	1.1
Mg	2.9	0.2	1.2	1.7	0.6	0.3	1.3
P	0.18	0.04	0.18	0.16	0.05	0.04	0.06
Mn	3.5	0.71	0.12	0.36	0.37	0.36	0.27
(mg/kg)							
Ba	80	40	82	71	57	61	98
Co	68	16	17	20	33	37	33
Cr	28	24	63	71	48	66	65
Cu	342	67	68	183	68	183	18
Ni	139	24	35	33	65	78	73
Pb	114	51	22	41	5	6	1
V	179	38	33	39	88	109	37
Zn	308	134	221	230	5	5	5
Zr	93	31	79	46	161	167	145

Table 1.13 Radiometric-based analysis of Th, U and K for various lithologies in Cyprus. Data from Tzotzis and Tsertos (2004).

	Calcarenite, marl, chalk and related sediments	Silici-clastic sediments	Ultramafics (incl. serpentinites)	Upper and lower pillow lavas
Th	1 – 8	0.1 – 3	<0.2	0.1 – 1
U	0.3 – 3	0.1 – 2	0.05 – 0.2	0.08 – 0.8
K	0.2 – 1	0.07 - 1	0.001 – 0.2	0.04 - 1

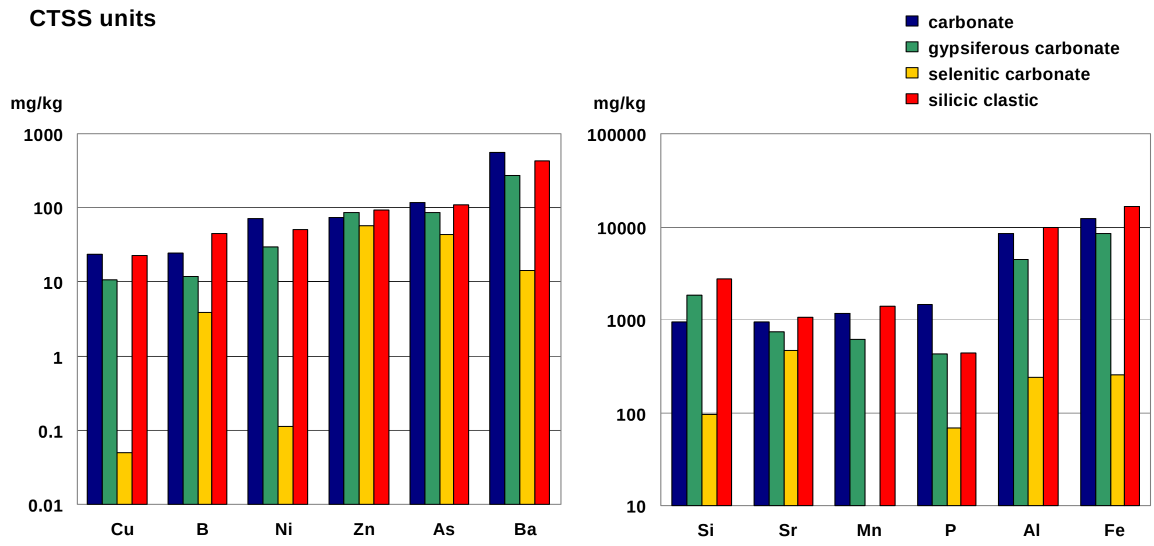

Figure 1.84 Varition in mean values for major and trace elements in CTSS carbonates. Data from various PhD thesis held by the GSD.

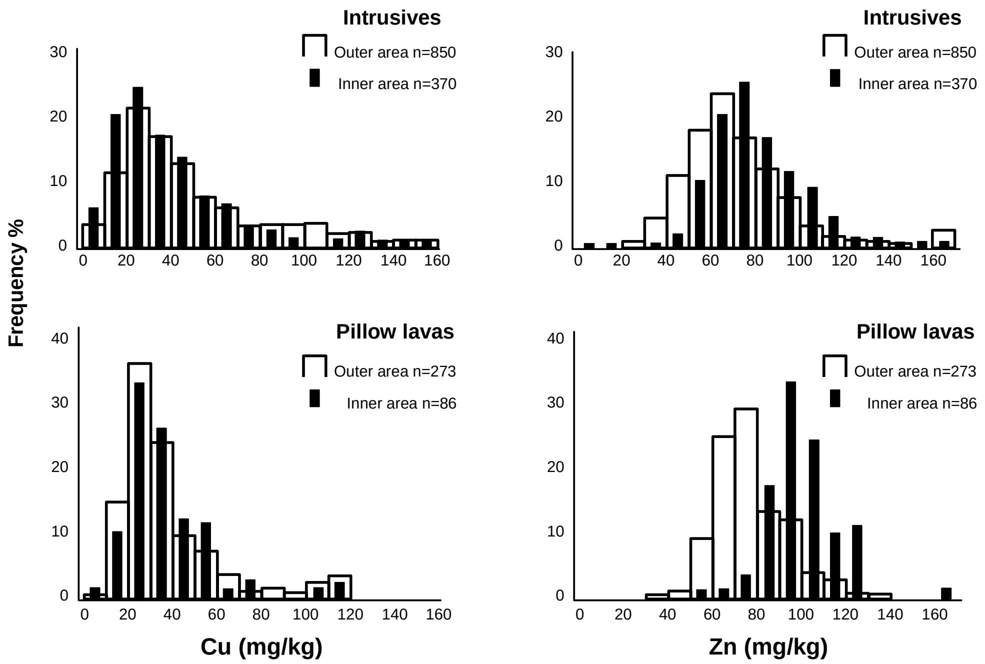

Figure 1.85 Comparitive distributions of Cu and Zn in intrusives (dolerites and other dykes) and pillow lavas in the vicinity of Mathiatis Mine. From Pantazis and Govett (1973).

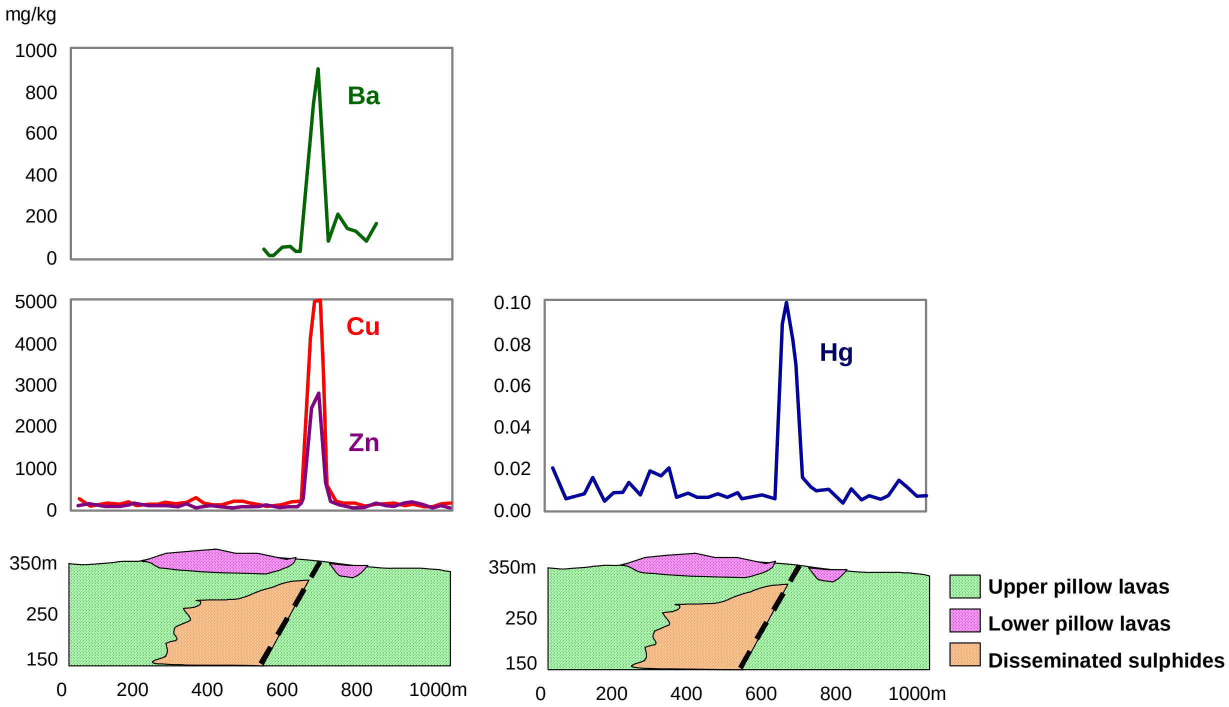

Figure 1.86 Soil geochemistry from traverse over buried sulphide mineralisation at the Sha Mine. Modified from Friedrich *et al.* (1985).

Table 1.14 Summary of metal contents of soils, Vassiliko Industrial site, Cyprus. Data from Demetriades and Charalambides (2006). 79 samples; values in mg/kg, P_2O_5 in %.

	As	*Cd*	*Co*	*Cr*	*Cu*	*Pb*	*Ni*	*P_2O_5*	*Zn*
Minimum	15	1.3	<d.l.	12	3	2.5	17	<d.l.	19
Maximum	697	45.5	70.7	243	2176	317.5	286	1.66	2850
Mean	180	10.7	21.3	97	269	57.3	87	0.26	341

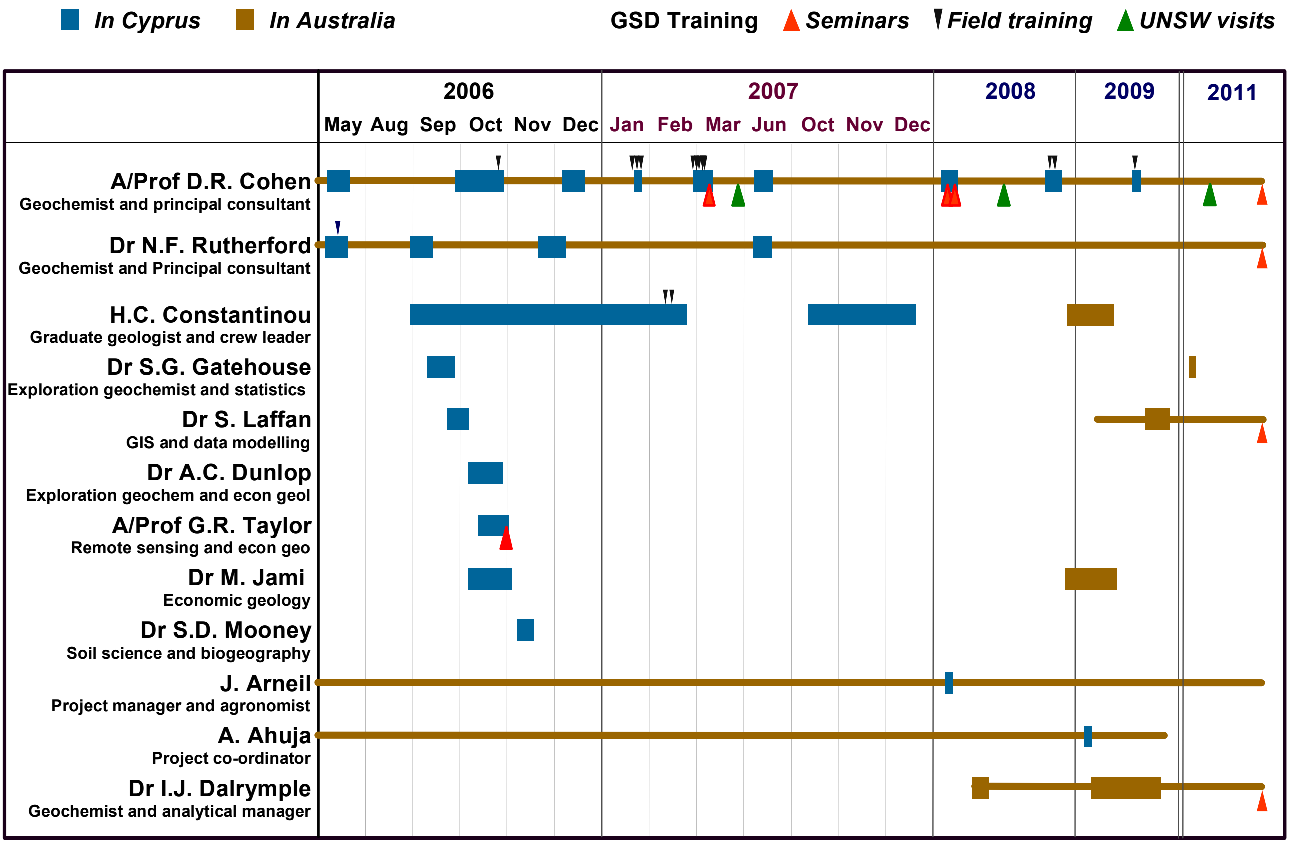

Figure 2.2 Project advisor and consultant activity in the project.

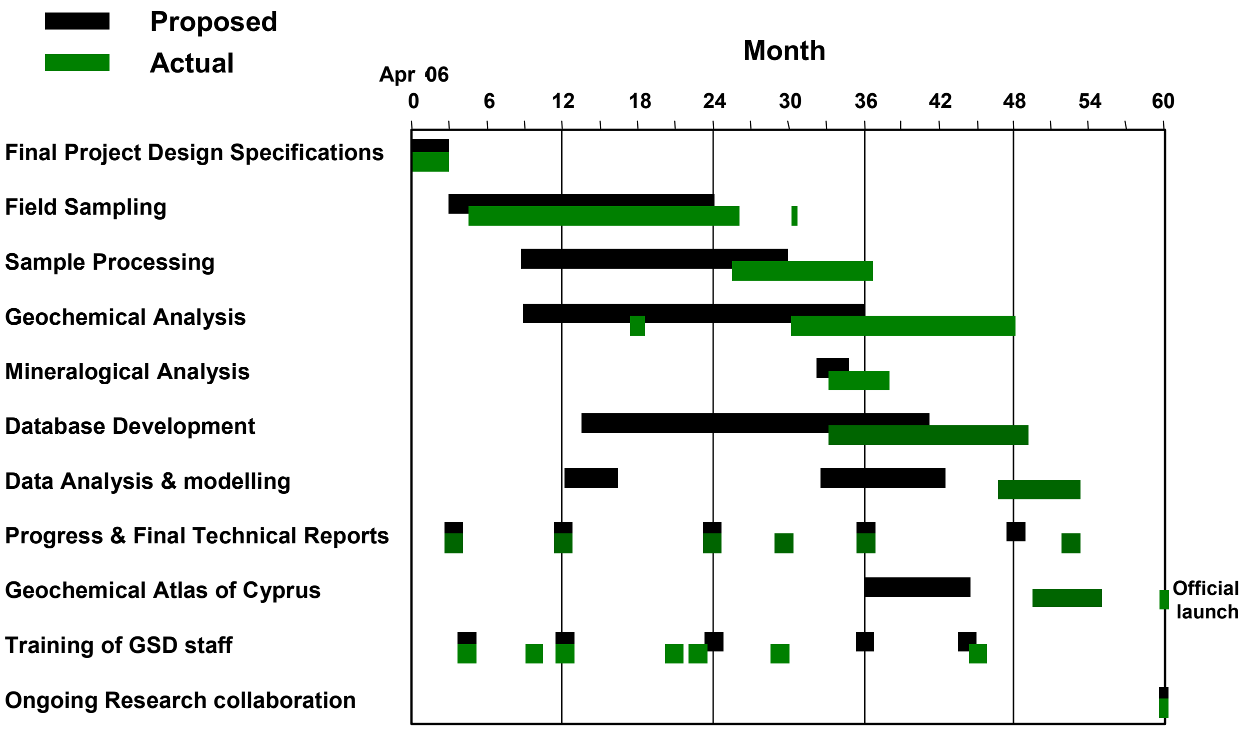

Figure 2.3 Timing of key stages in the project (proposed versus actual).

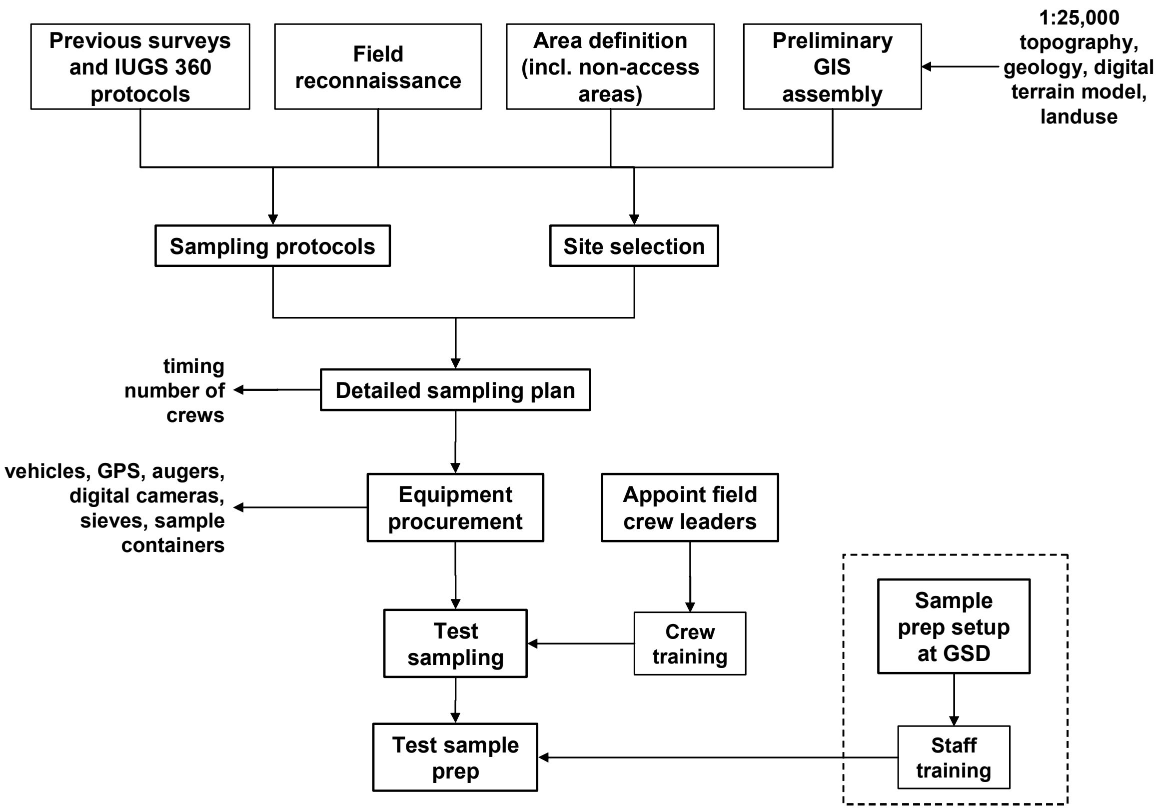

Figure 2.4 Key stages and components of Task 1.

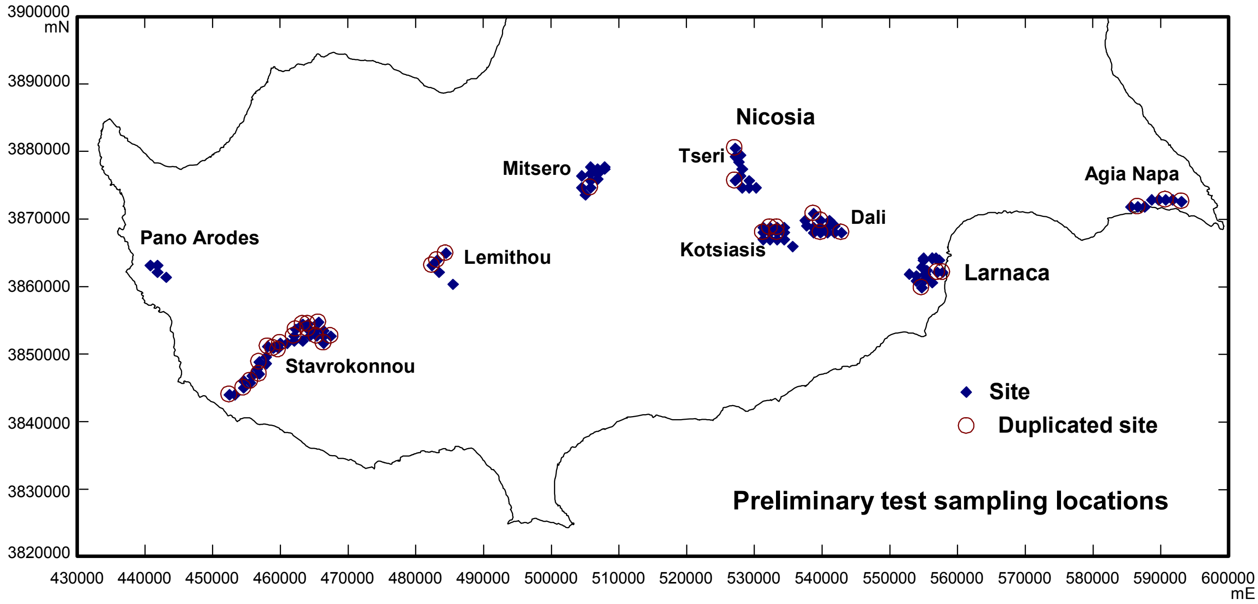

Figure 2.5 Sampling undertaken as part of the orientation survey, May 2006.

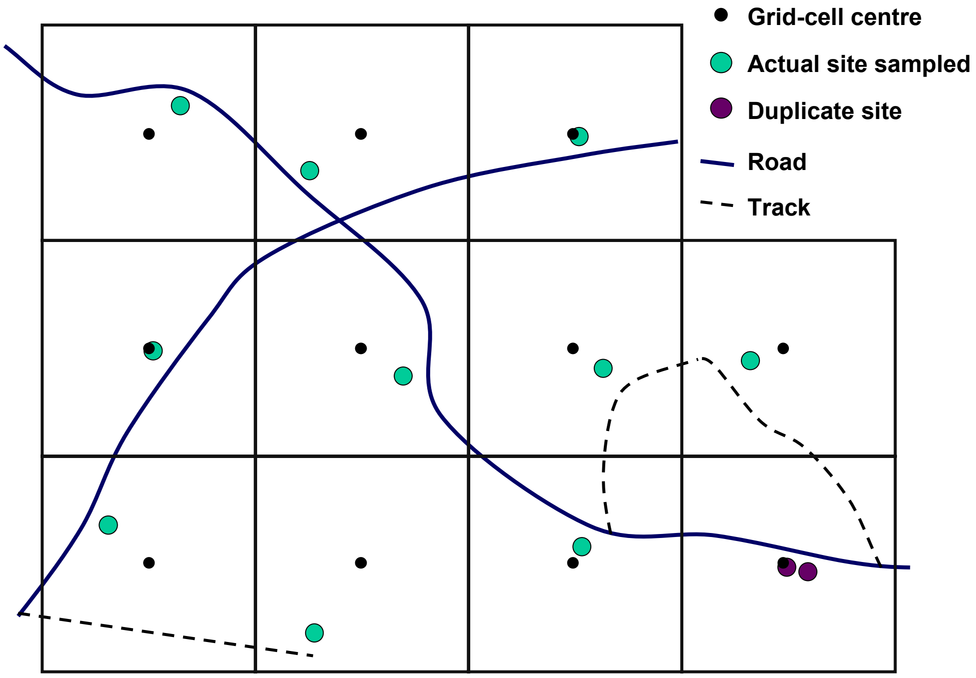

Figure 2.6 Grid cell sampling model.

Table 2.2 Summary of sampling sites.

Zone	Sites
Circum-Troodos sedimentary sequence, Quaternary & Troodos margins	3,857
Troodos Ophiolite Complex	903
Mines suite	386
Other special samples	370
Total	**5,516**
Plus stream sediments	*(89)*

Figure 2.7 (a) Field navigation based on 1:50,000 topographic maps and Garmin GPS; (b and c) Recovery or awaiting recovery of bogged vehicles.

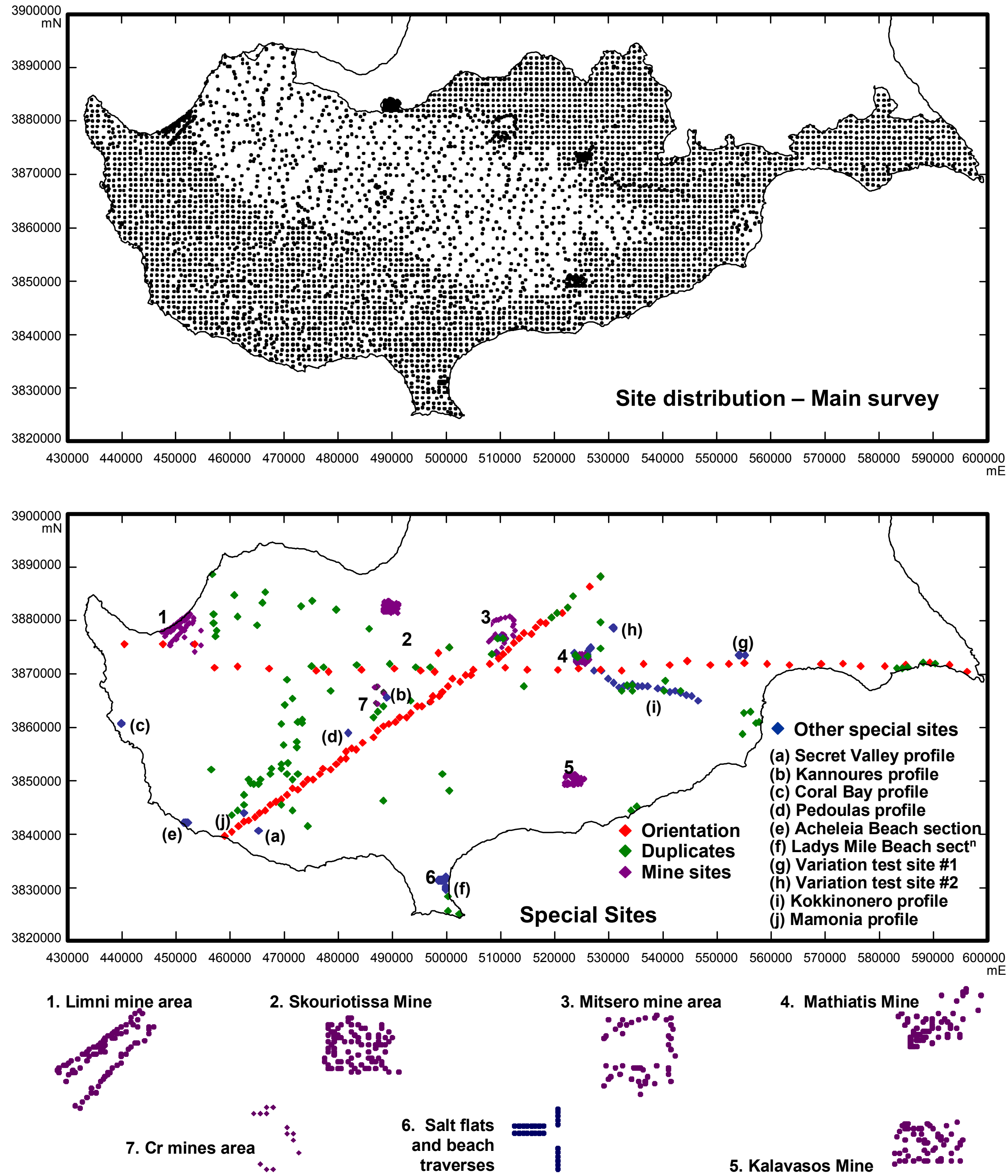

Figure 2.8 (a) Site distribution for the main survey and (b) the distribution of orientation, duplicates, mines and other special sites.

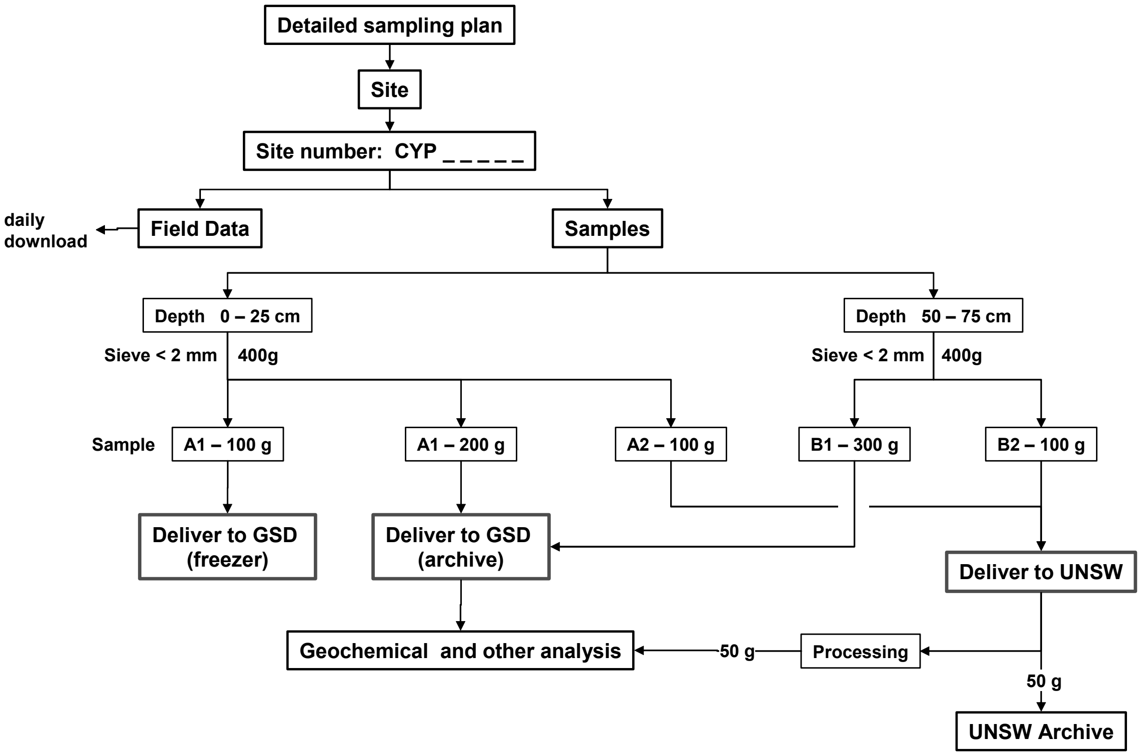

Figure 2.9 Sampling flow diagram.

Figure 2.10 (a) and (b) stripping of recent organic deposits from the surface and excavation of upper 25 cm using pick or spade; (c) sieved materials (~400g); (d and e) excavation by auger and packing soil down in auger with cleaned pick handle (f) Jarrett-type steel augers with 20 cm steel flights and W-tipped cutting edges. Intermediate 20-cm intervals between the top and sub sample were also examined.

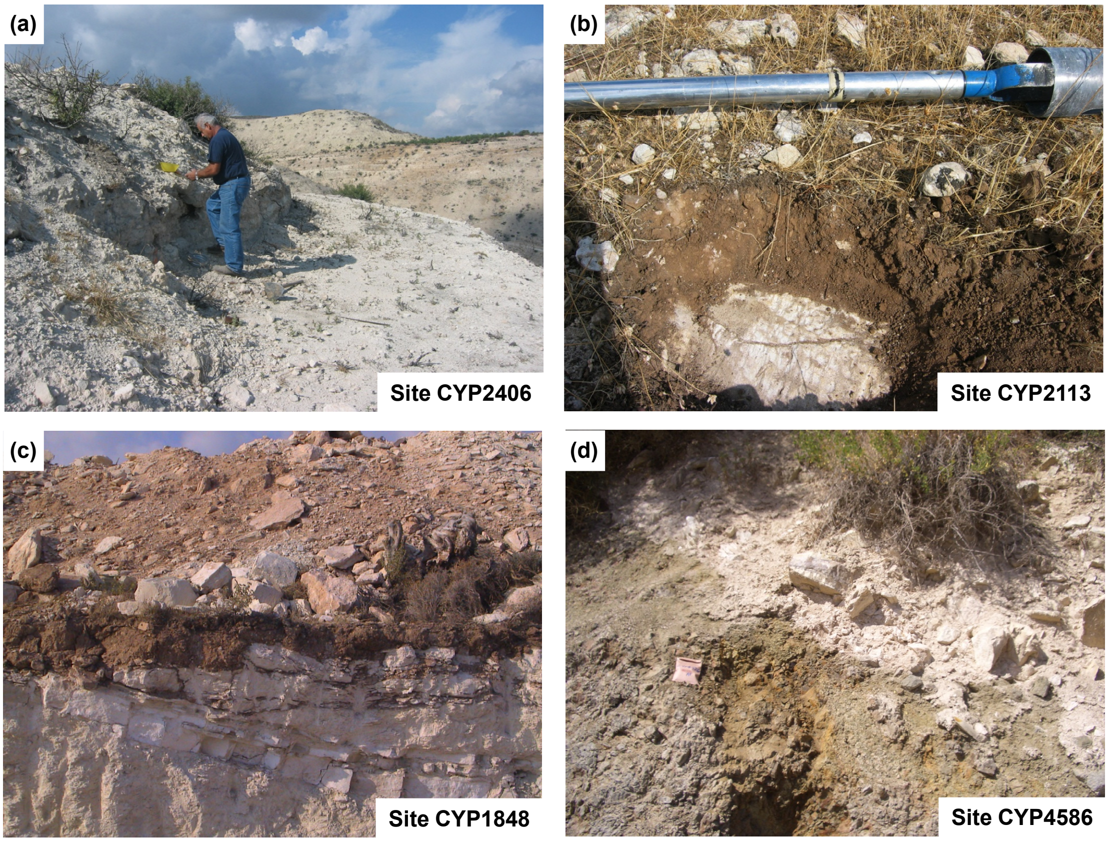

Figure 2.11 Sampling site examples - 1.

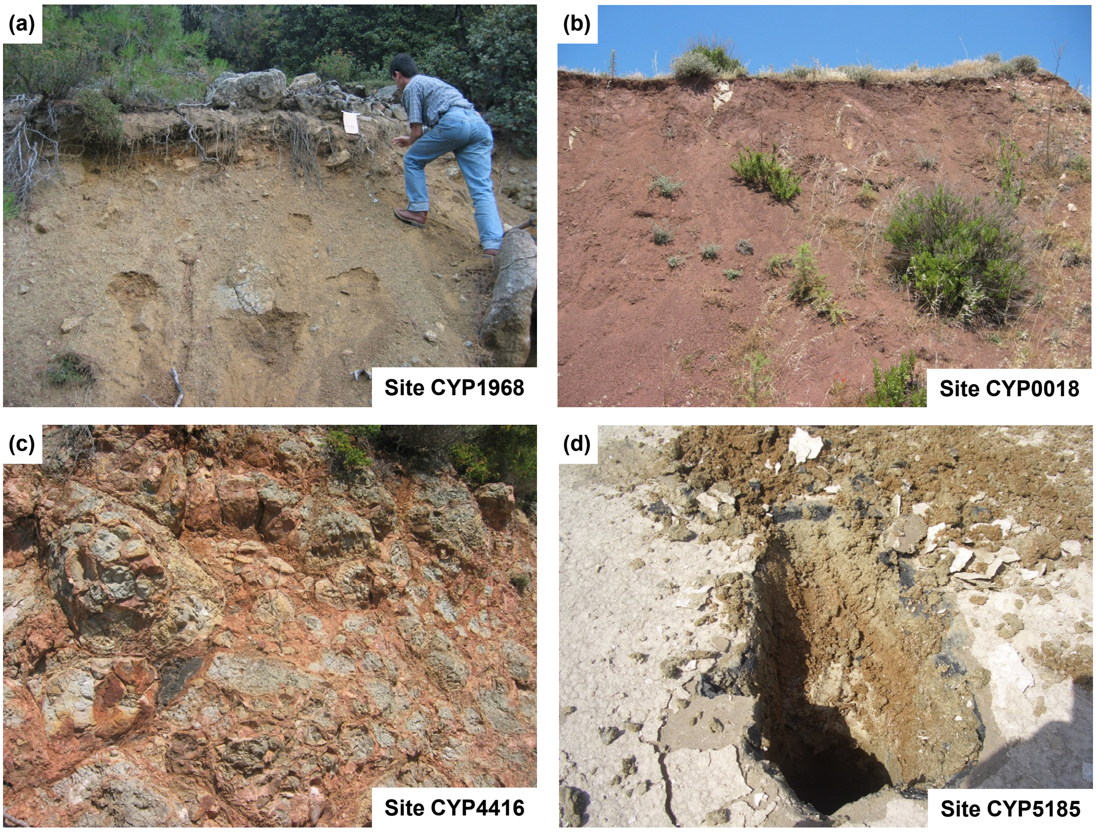

Figure 2.12 Sampling site examples - 2.

Figure 2.13 Sampling site examples - 3.

Figure 2.14 Sampling site examples - 4.

Figure 2.15 Sampling site examples - 5.

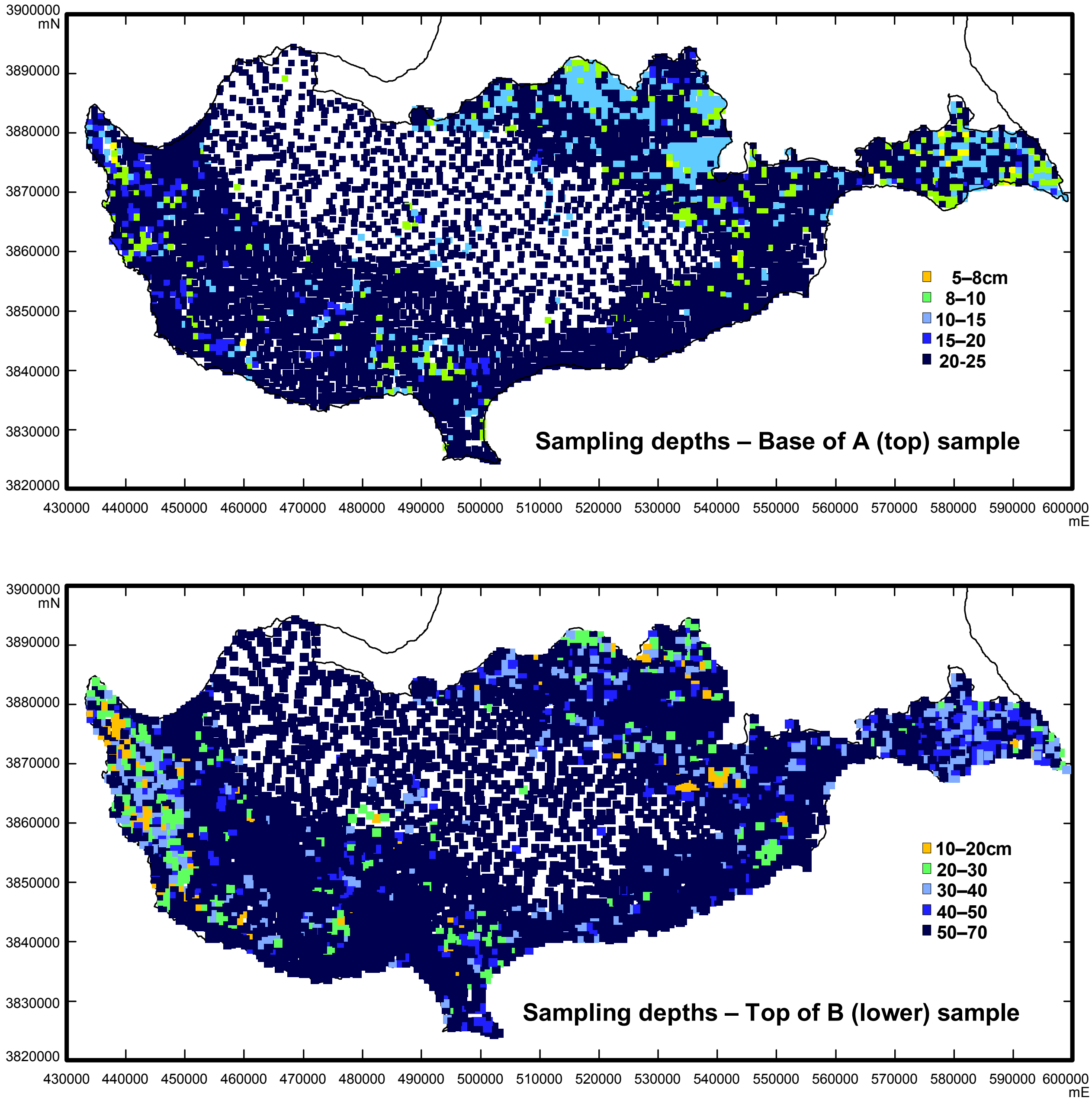

Figure 2.16 Distribution of sampling depths (base of top sample and starting depth of lower sample).

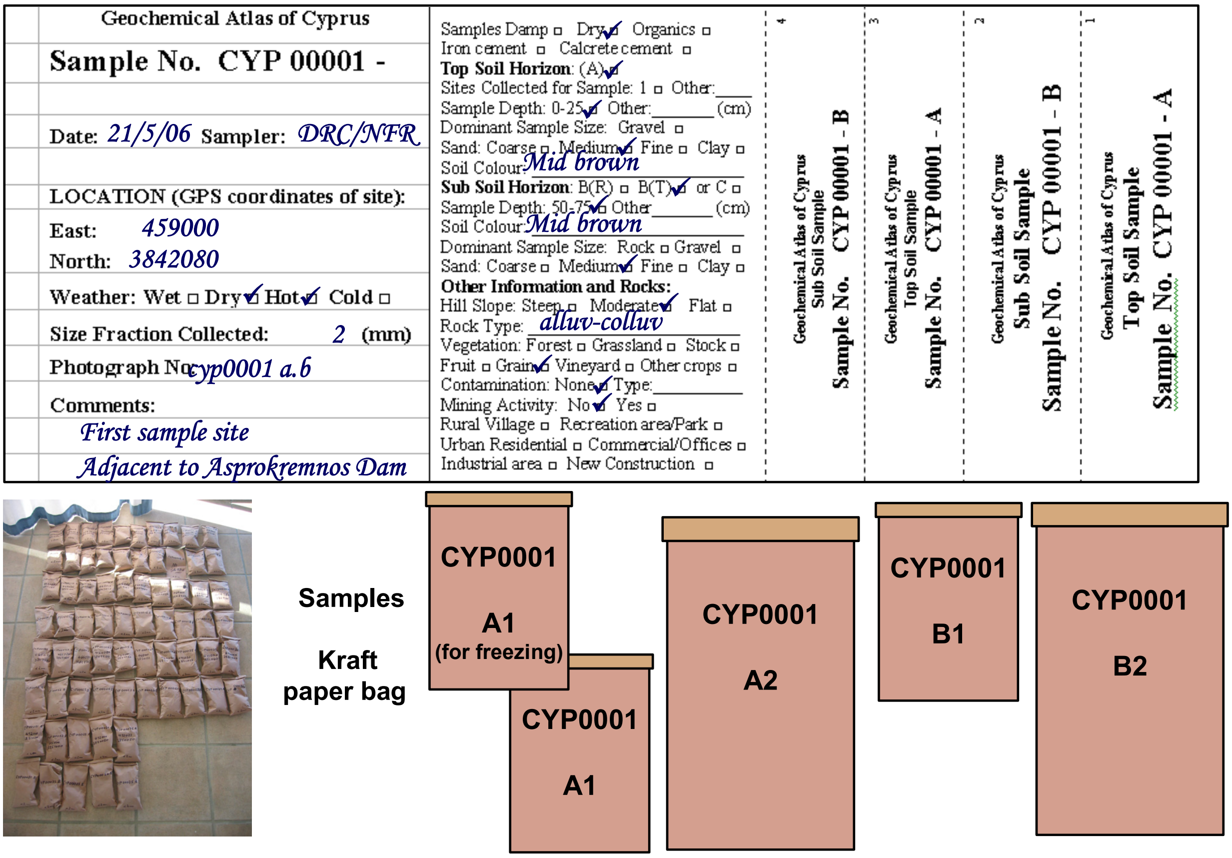

Figure 2.17 Sample tick book and numbered soil sample packets.

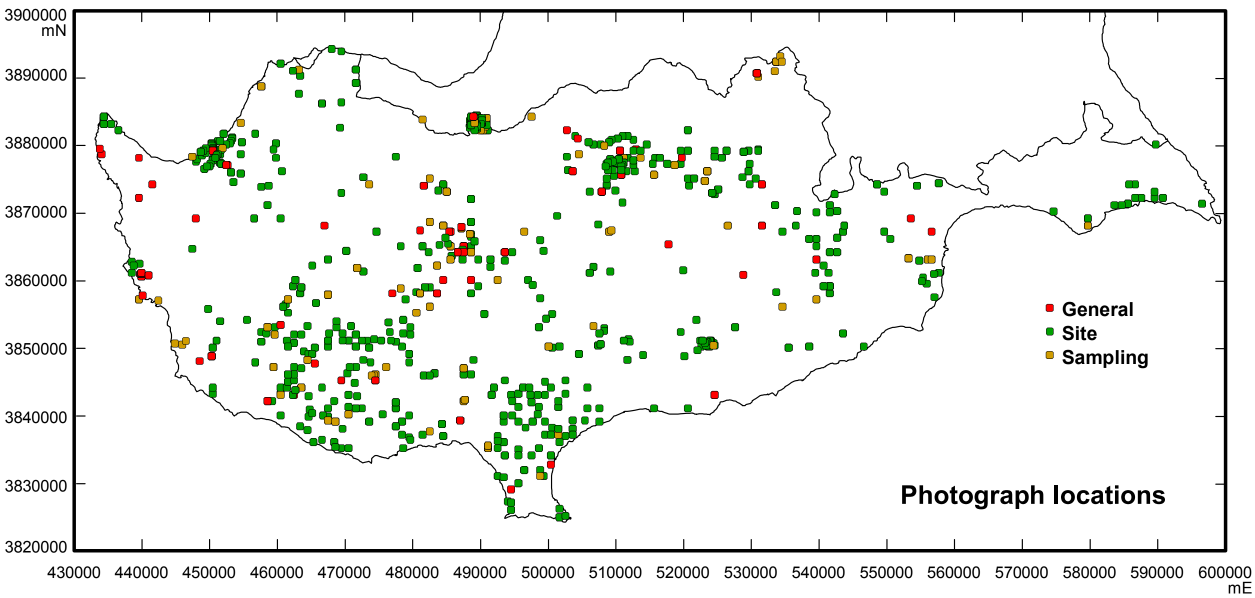

Figure 2.18 Distribution of sites with photographic records.

Figure 2.19 (a) Site CYP0001 samples;

(b and c) Penultimate site collected at the GSD with A. Demetriades (ADCS), C. Kapodistria (GSD), Dr A. Zissimos (GSD), Dr P. Michailides (former Director GSD), Dr E. Morisseau (Director GSD), E. Stavrou (GSD) and E. Demetriou (Central Govt Labs);

(d and e) Final site, CYP5516, collected from the Presidential Garden by the President of Cyprus, the Minister for Agriculture Natural Resources and Environment, the Australian Consul, staff of the GSD, ADCS and the project team.

Table 2.3 Breakdown of sampling sites for the project.

Zone	Total sites	Material	Samples collected	
Circum-Troodos sequences, Quaternary, Mamonia and Troodos margins	3,857	Soil	Top	3,857
			Base	3,856
Troodos Ophiolite Complex	903	Soil	Top	903
			Base	903
Mines suite	386	Soil	Top	386
			Base	386
Other special soil samples	231	Soil		231
Sub-Total	**5,377**			**10,522**

Other special samples	19	Rock		48
	120	Vegetation		120
Sub-total	**139**			**168**

Total	**5,516**			**10,690**

Stream sediments	89	Sediment	Top	89
			Base	88

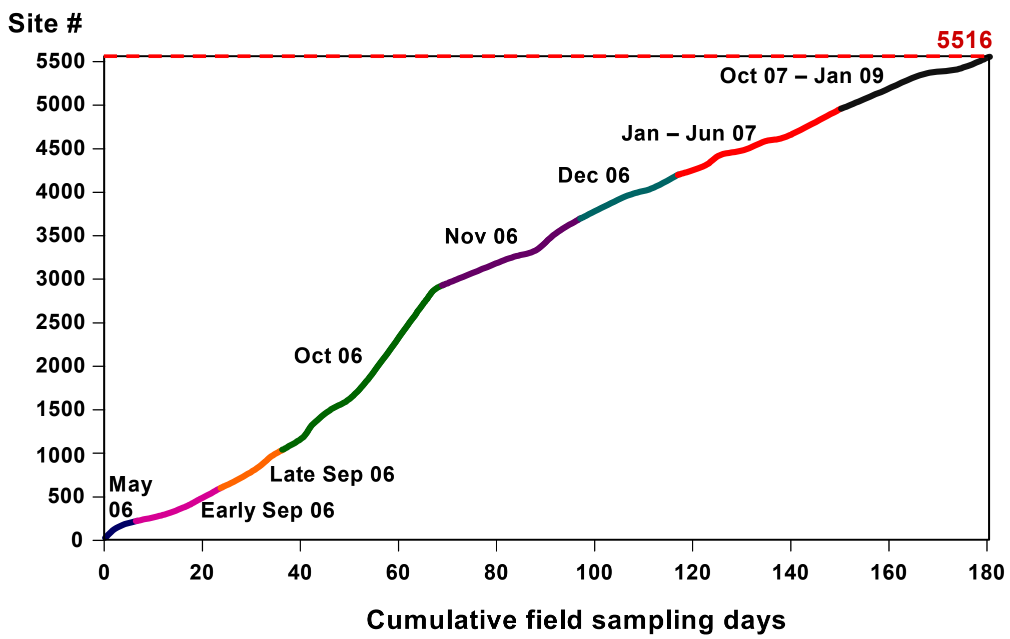

Figure 2.20 Cumulative samples versus number of days in which crews were deployed.

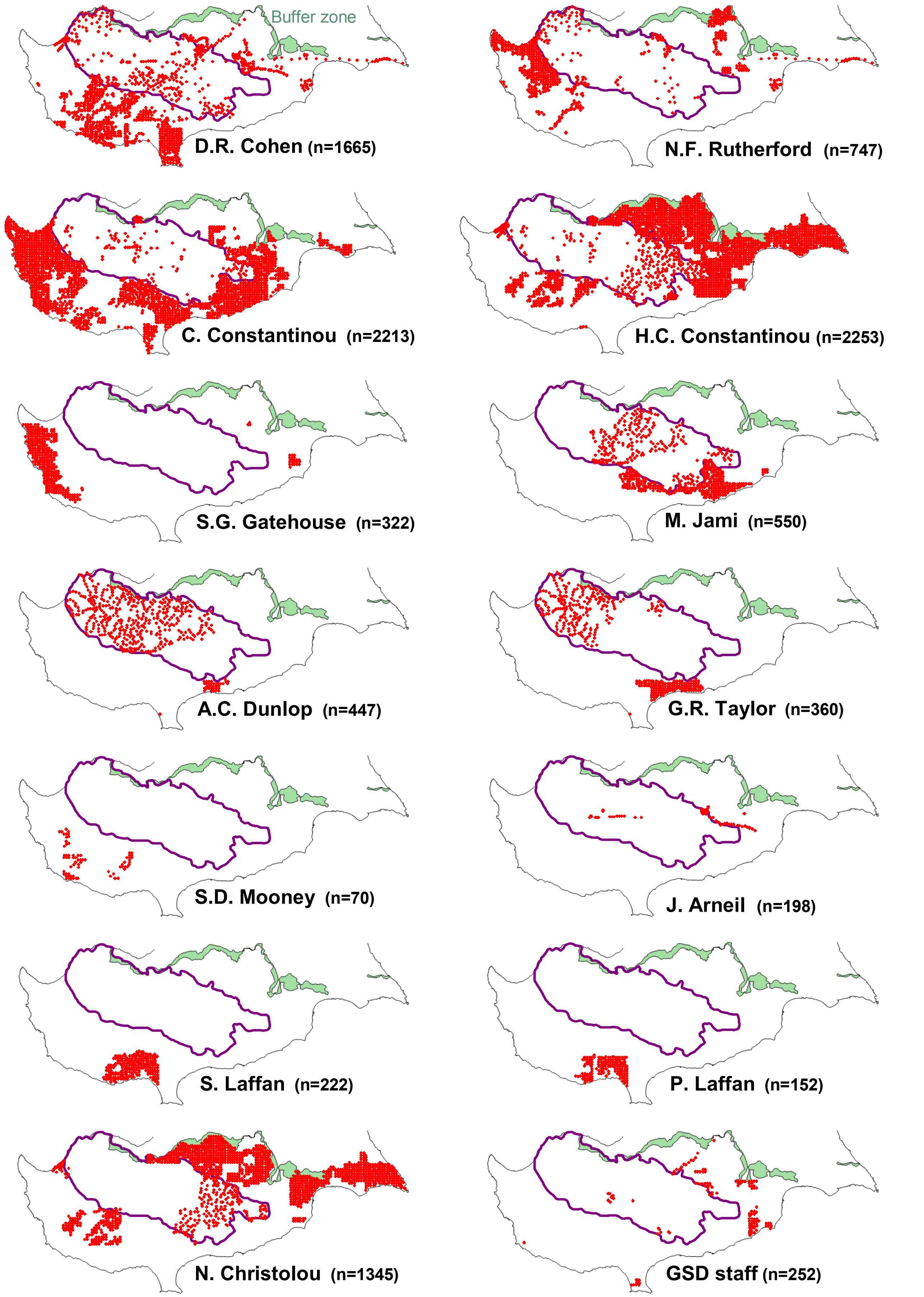

Figure 2.21 Distribution of sites collected under the supervision of UNSW advisors and crew leaders. Troodos was mainly sampled by teams of two advisors.

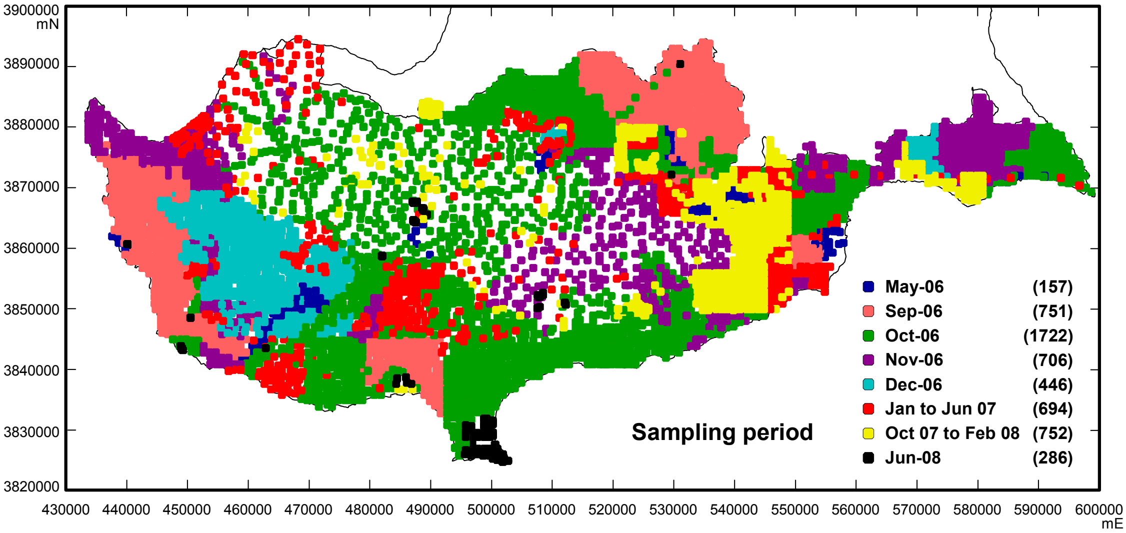

Figure 2.22 Distribution of samples with the month of sampling.

Figure 2.23 (a and b) Sample archive at the GSD store, Geri; (c) pallet with crates ready for transportation to UNSW.

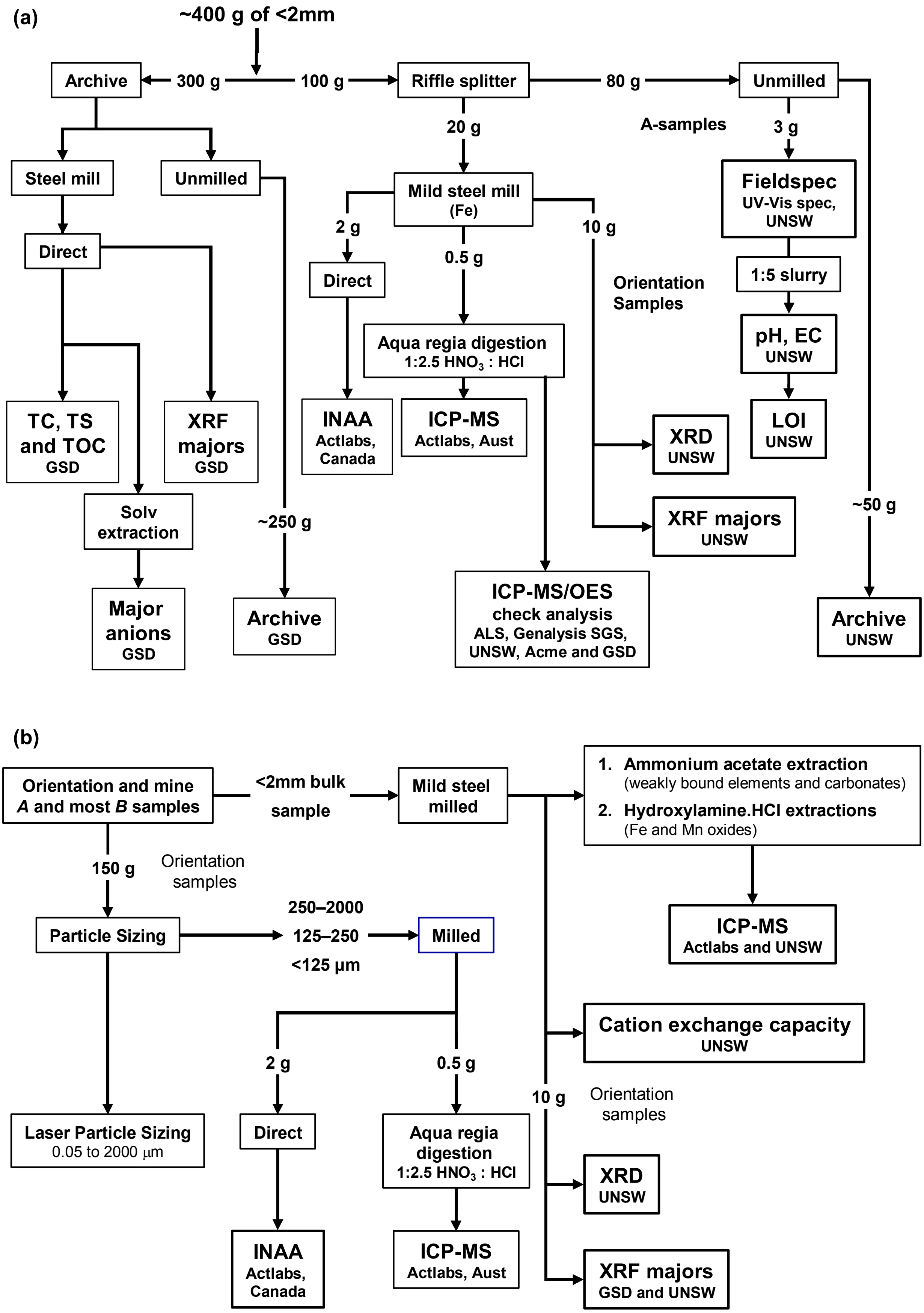

Figure 2.24 (a) Analytical scheme; (b) special processing of orientation suite.

Figure 2.25 Splitting and milling. (a) After drying, the original field samples have an analytical number assigned (CYPAyyyy) and split using a Laval Labs aluminium riffle splitter (b) with ~20g being placed in a Ziploc bag (c) prior to milling in Rocklabs mild steel mills and returned to the plastic bag ready for shipment to Actlabs (d).

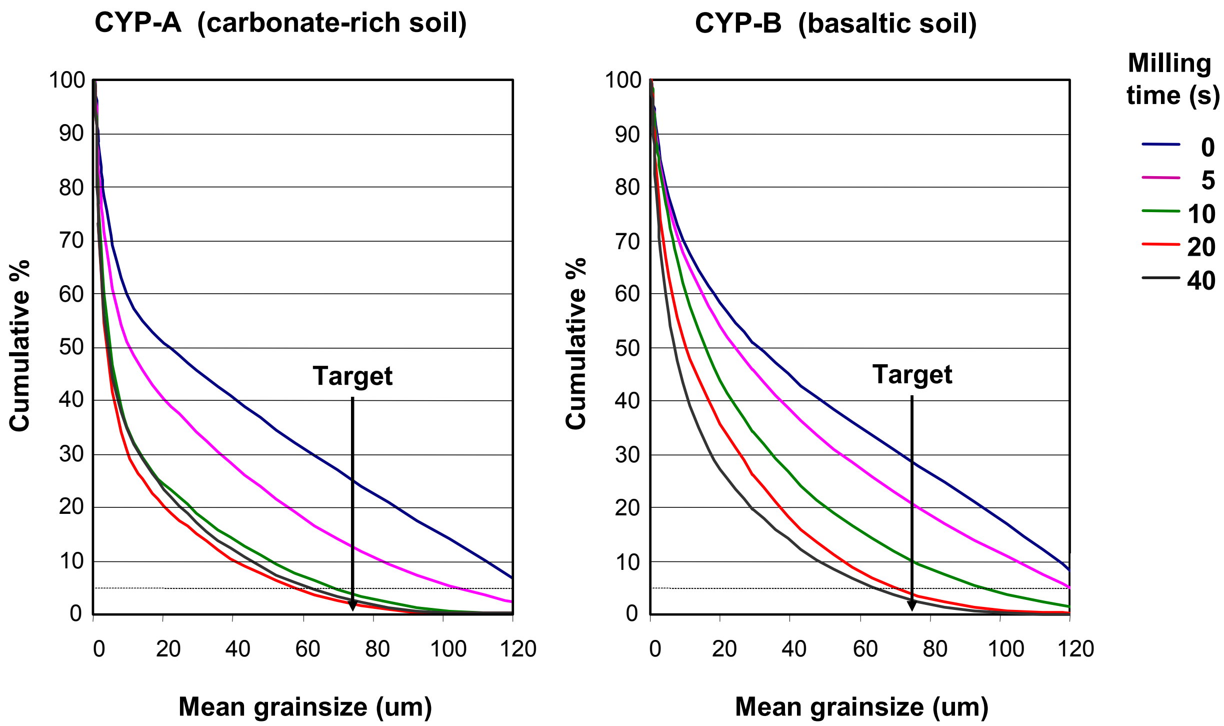

Figure 2.26 Variations in particle size distribution with milling time.

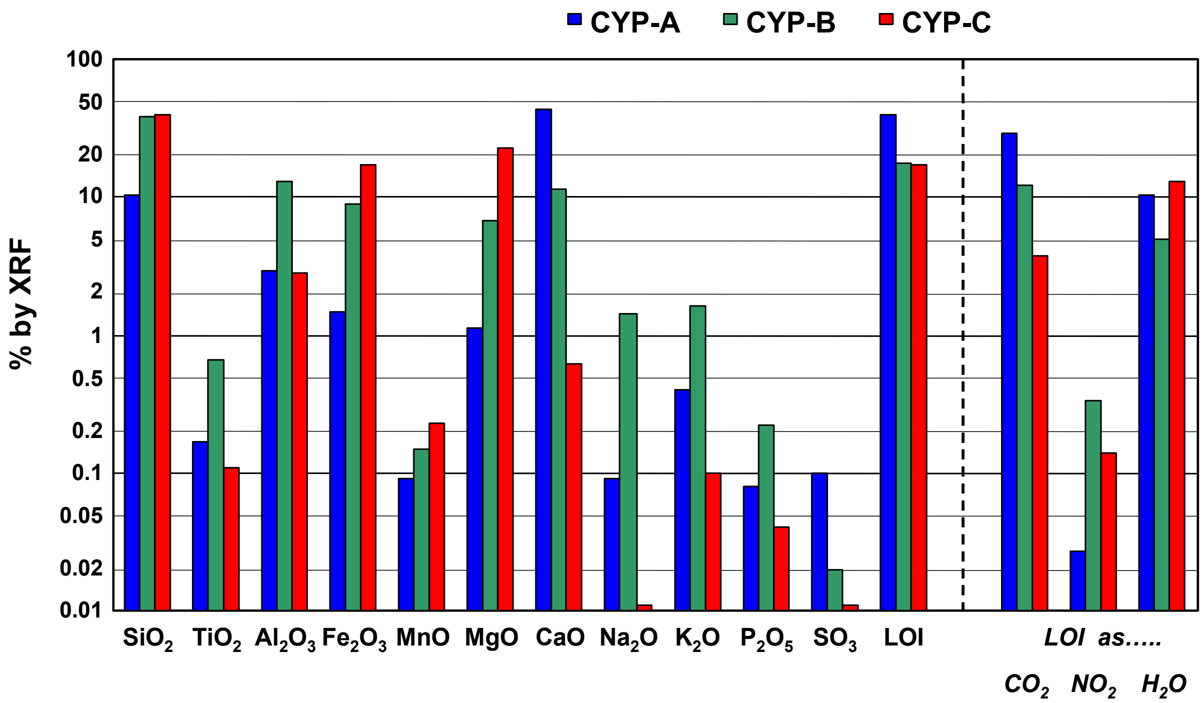

Figure 2.27 XRF major oxide and Leco CNS volatile data for reference materials (based on sub-sample duplicate analyses and an average of three readings).

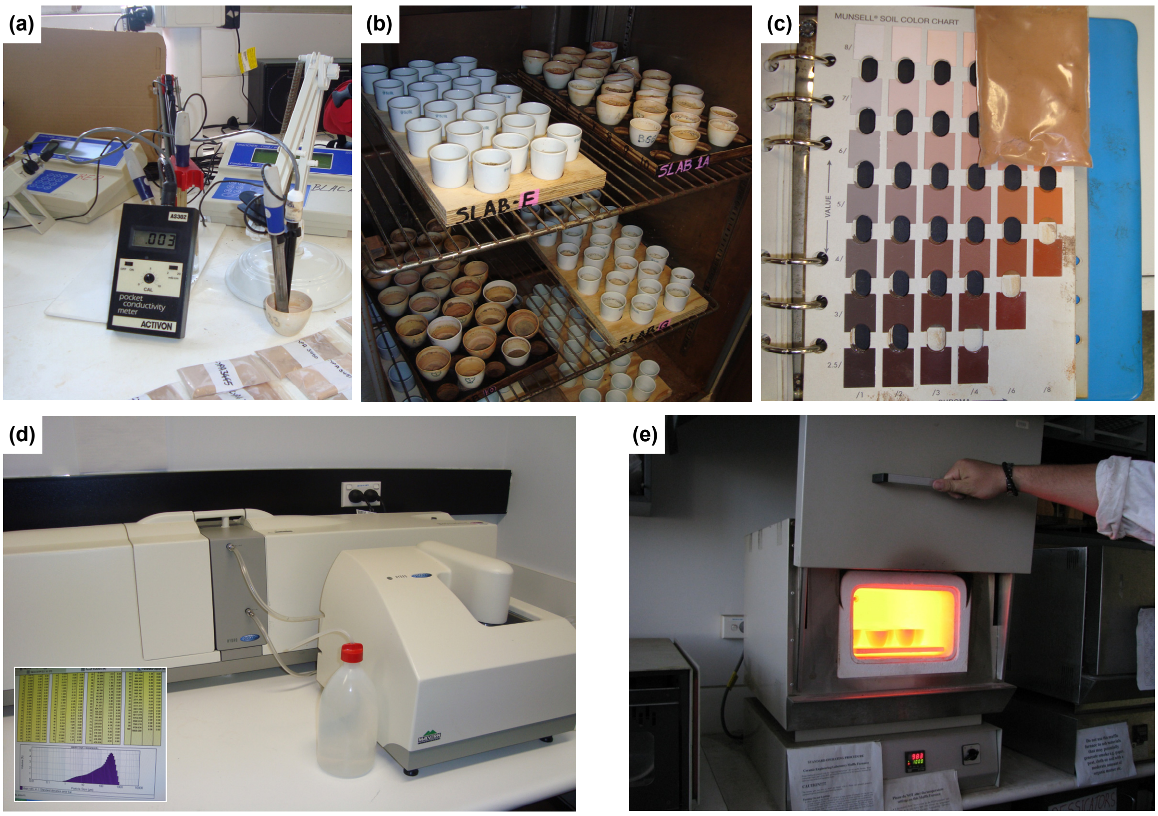

Figure 2.28 (a) Surry pH and EC conduced on 1:5 solid:water mix in pre-weighed crucibles for unmilled A-samples; (b and e) Drying the slurry at 80°C prior to determination of LOI at 1000°C in a muffle furnace; (c) Slightly dampened split used to determine Munsell soil colour; (d) Malvern 2000 laser particle sizer with ultrasonic pre-treatment cell, used on orientation samples (range form 0.05–2000µm).

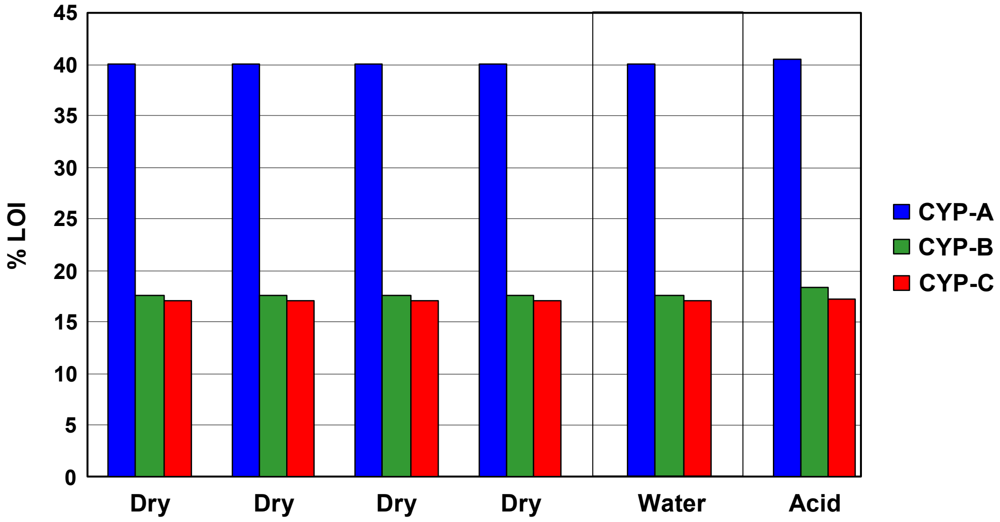

Figure 2.29 Effect of the addition of (a) 15 ml of water and (b) 15 ml of 40% nitric acid on 3 g samples of the reference materials, on LOI @ 1000°C.

Table 2.4 Comparison of aqua regia (with refluxing) versus microwave three-acid digestion on various regolith materials (data from Sastre *et al.* 2002).

Ref mat.	Digestion	Cd	Cu	Pb	Zn
CRM 141R Calcareous Soil	**Aqua regia**	**13.4 ± 0.6 (0.7)**	**45 ± 4 (4)**	**57 ± 5 (4)**	**284 ± 16 (19)**
	Microwave total	**14.3 ± 0.8 (0.7)**	**48 ± 1 (3)**	**59 ± 2 (4)**	**260 ± 19 (20)**
CRM 142R Light sandy soil	**Aqua regia**	**0.24 ± 0.02 (0.08)**	**74 ± 3 (5)**	**26 ± 3 (2)**	**111 ± 9 (9)**
	Microwave total	**0.32 ± 0.02 (0.08)**	**70 ± 0.3 (0.9)**	**42 ± 3 (2)**	**105 ± 1 (3)**
CRM 320 River sediment	**Aqua regia**	**0.45 ± 0.10 (0.08)**	**44 ± 1 (1.1)**	**31 ± 1 (2)**	**121 ± 4 (5)**
	Microwave total	**0.59 ± 0.03 (0.07)**	**48 ± 0.9 (3)**	**45 ± 3 (2)**	**150 ± 2 (10)**

Table 2.5 Correlation between total analysis and aqua regia extractable metals in soils from a transect across Manitoba (data from Klassen 2009).

Element	R^2 Value	Comment
Na	-0.016	Bound in plagioclase feldspars
Sr	0.256	Associated with a mixture of resistate and
As	0.272	(e.g. feldspar or rutile) and aqua regia
Ti	0.564	soluble phases
Ba	0.734	Associated with clays and correlated
K	0.769	
Al	0.867	
Fe	0.971	Correlated with secondary Fe minerals
Cr	0.900	adsorbed to secondary minerals
Co	0.960	
Ni	0.975	
Zn	0.975	
Cu	0.977	
Mn	0.984	
P	0.989	
La	0.976	Present in carbonates
Mg	0.994	(high correlation with CO_2)
Ca	0.995	

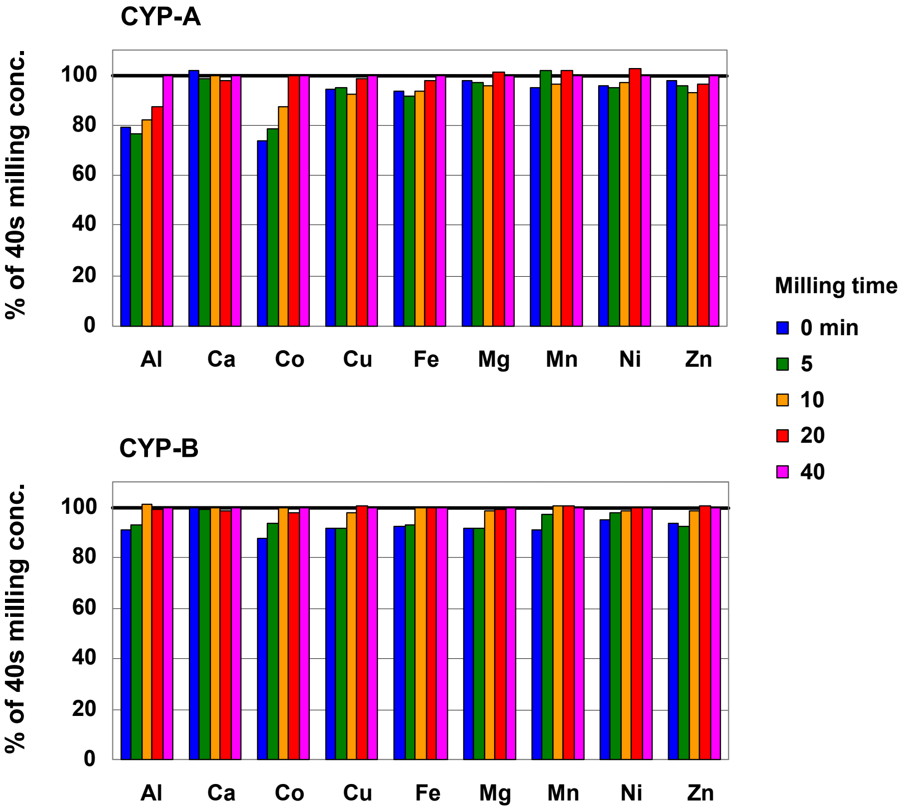

Figure 2.30 Effect of grain size (milling time on 20g samples) on metal extractability for CYP-A and CYP-B.

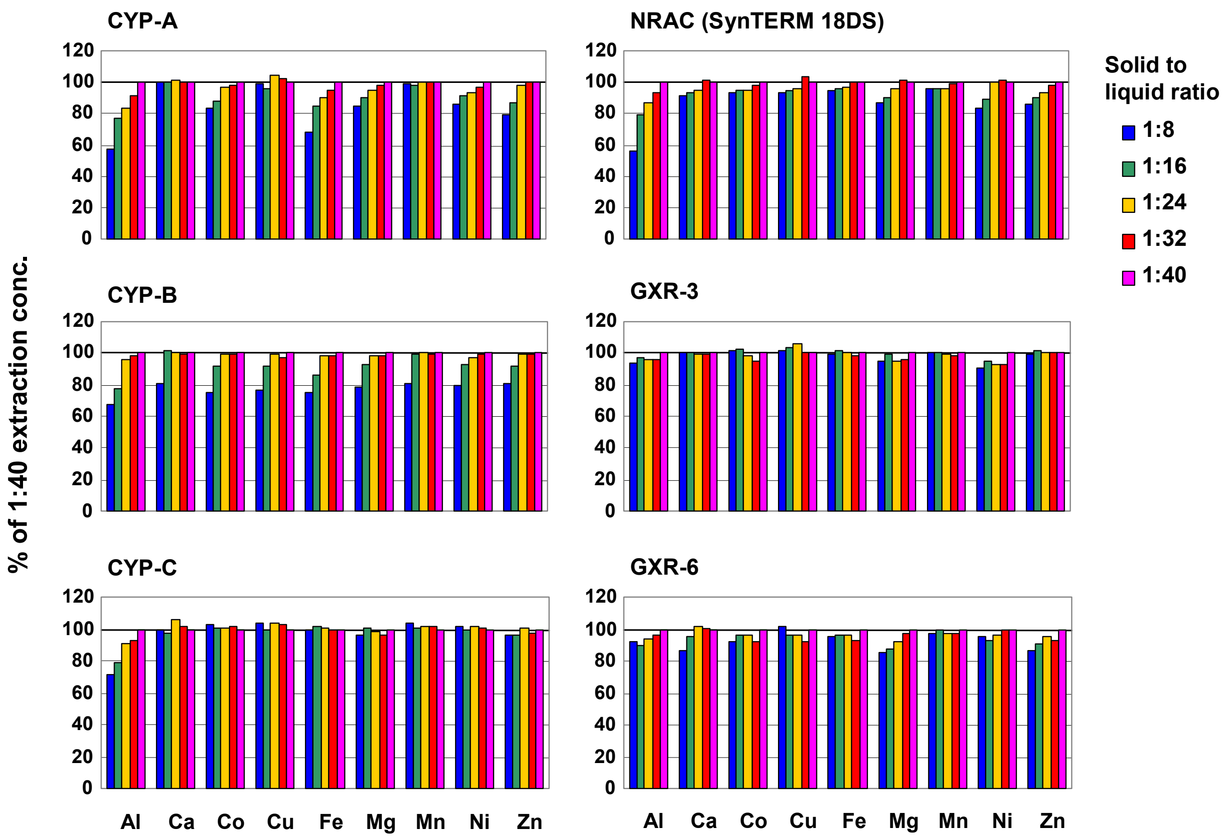

Figure 2.31 Variations in element extraction with changing solid:liquid ratios for aqua regia.

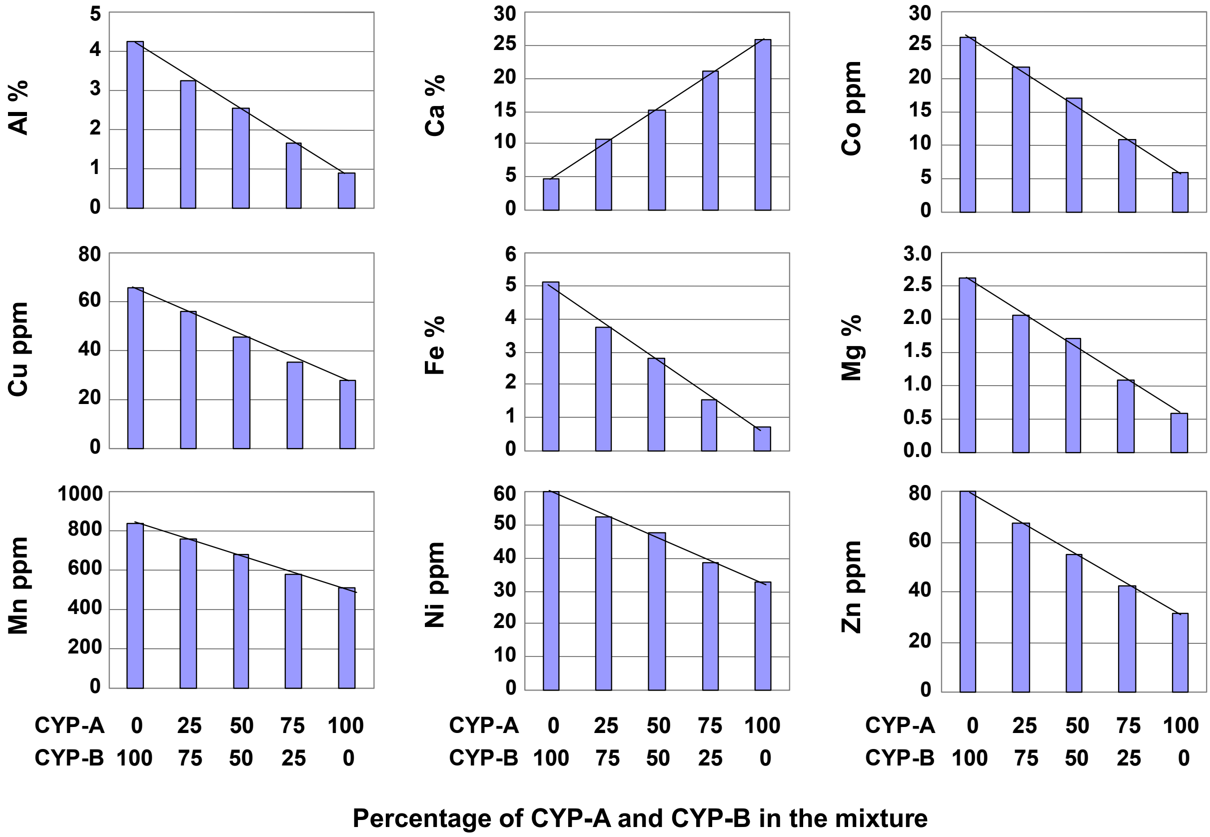

Figure 2.32 Response of mixtures of CYP-B and CYP-A in various proportions to aqua regia digestion.

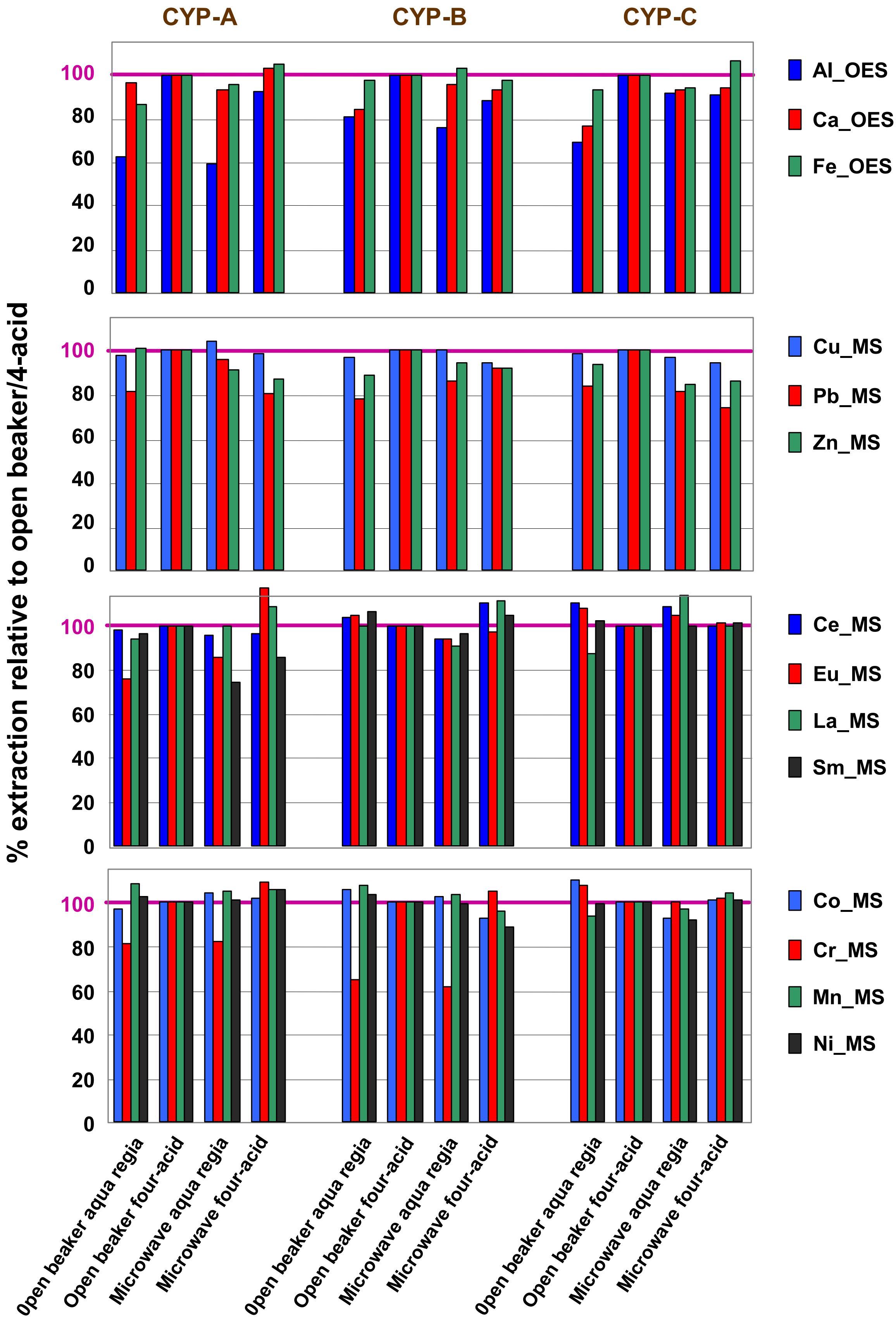

Figure 2.33 Comparison of the extraction of elements from the three reference materials using four different methods. Data presented as extraction % relative to open beaker four-acid digestion values.

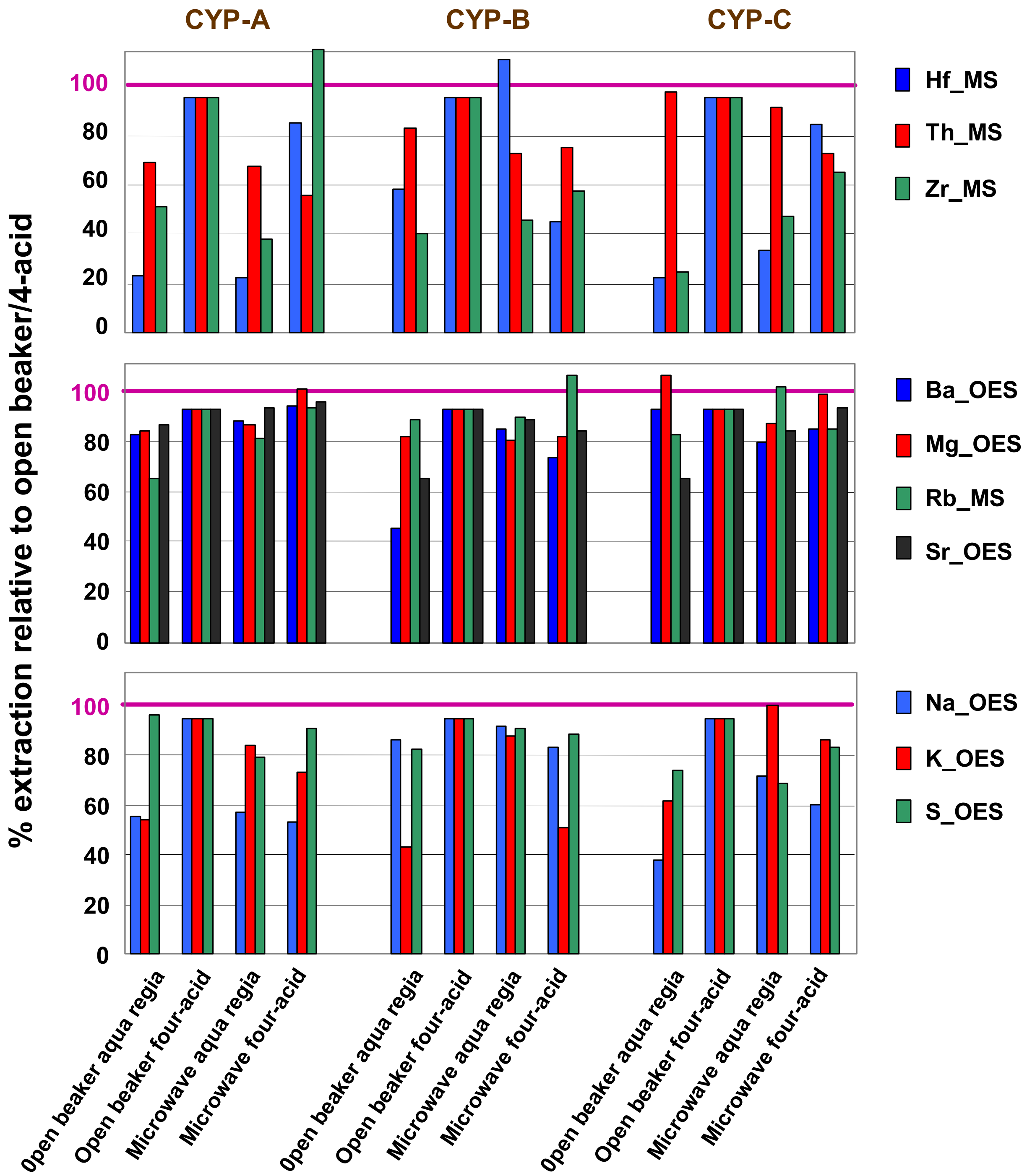

Figure 2.33 Ctd...

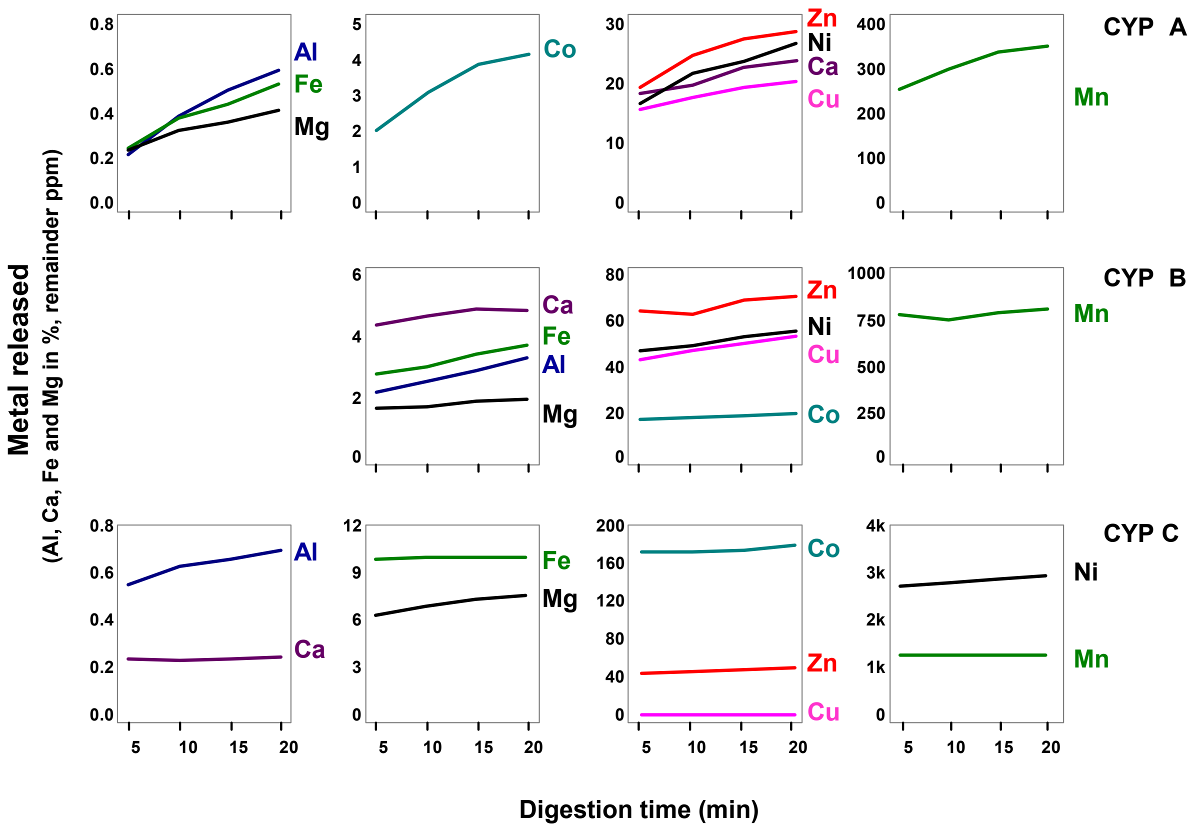

Figure 2.34 Time-dependence on aqua regia extraction of elements for project reference materials.

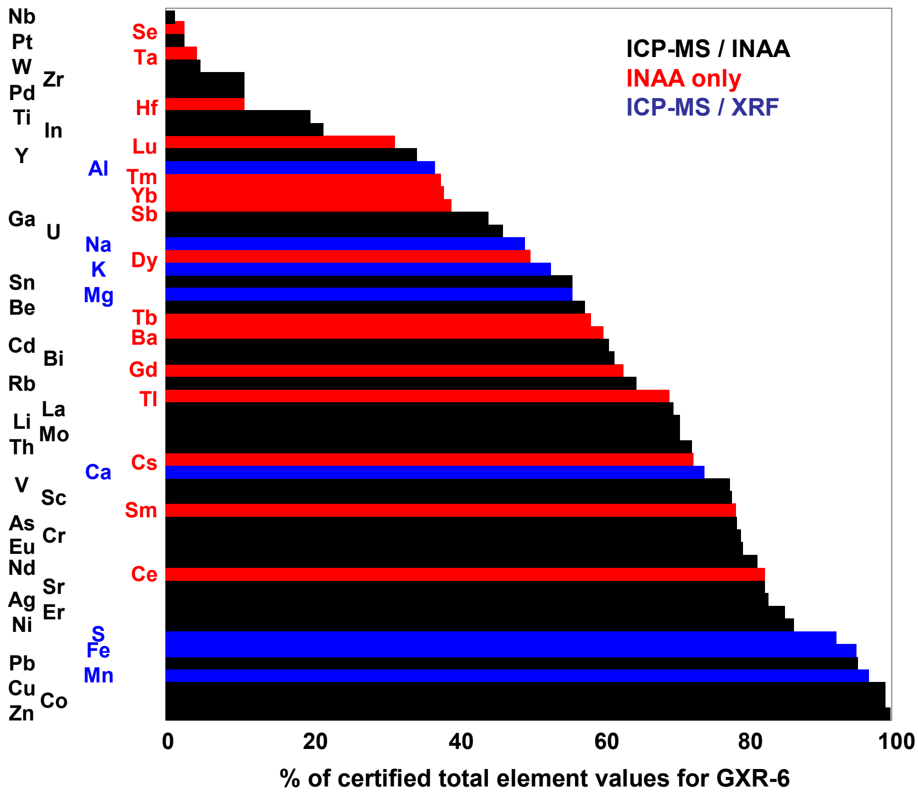

Figure 2.35 Proportion of total element contents (as per certified or recommended GXR-6 values) extracted on average by the seven commercial laboratories using nitric-rich aqua regia.

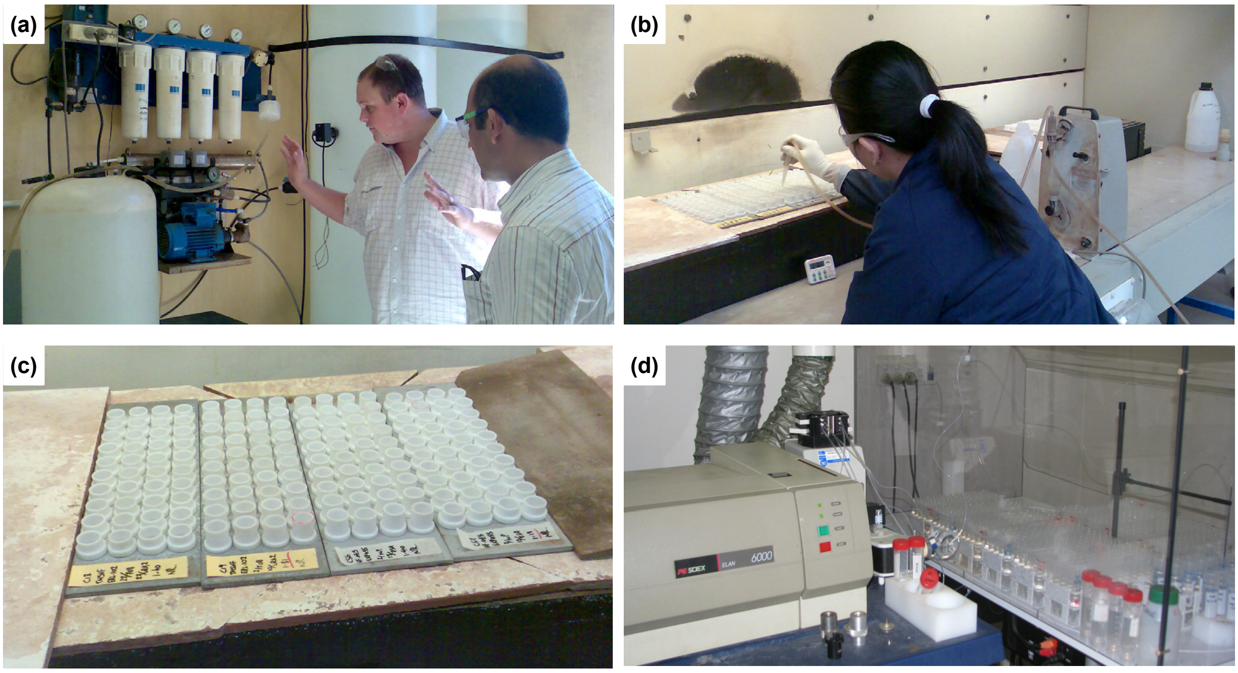

Figure 2.36 (a) Millipore water deionisation unit. (b) Addition of HCl to samples in polythene tubes, Actlabs (c) heat f reaction tubes in heating bath after addition of HNO_3. (d) Perkin Elmer Optima 5000 ICP-OES unit for analysis of major and high concentration elements.

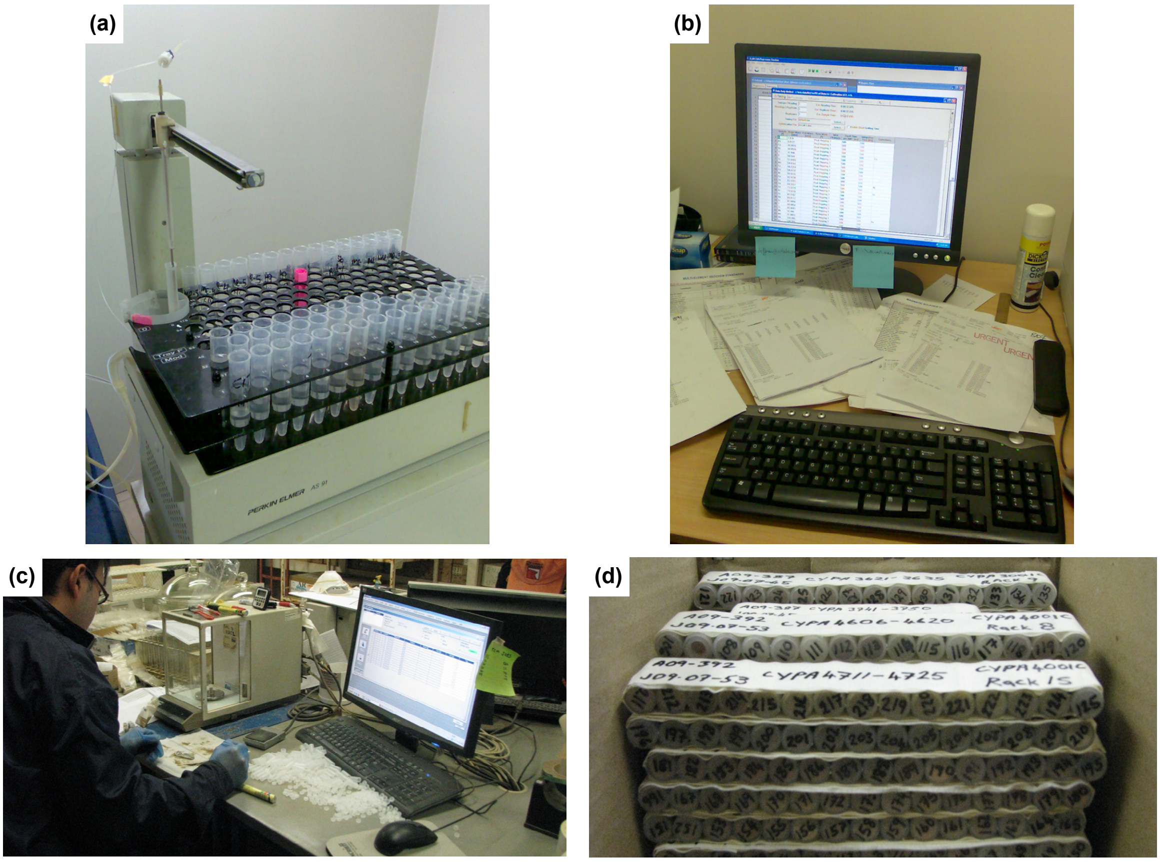

Figure 2.37 (a) Autodilution prior to running ICP-MS; (b) Actlabs LIMS system handles all data capture, result collation and QC monitoring; (c) Weighing room; (d) INAA vials in sub-batches packaged for shipment to Canada.

ICP-MS

Group	Element	Detection Limit (mg/kg)
Major and minor	Al	100
	Ba	0.5
	Ca	100
	Cr^	0.5
	Cu	0.01
	Fe^	100
	K	100
	Mg	100
	Mn	1
	Na	10
	Ni	0.1
	P	100
	Pb	0.01
	Rb^	0.1
	Sr	0.5
	Ti^	1
	Zn	0.1
	Zr	0.1
Trace	Ag	0.002
	As^	0.1
	B	1.0
	Be	0.1
	Bi	0.02
	Cd	0.01
	Co^	0.1
	Cs^	0.02
	Ga	0.02
	Ge	0.1
	Hf^	0.1
	Hg	0.01
	In	0.02
	Li	0.1
	Mo	0.01
	Nb	0.1
	Re^	0.001
	Sb^	0.02
	Sc	0.1
	Se	0.1
	Sn	0.2
	Ta^	0.05
	Te	0.02
	Th	0.1
	Tl	0.02
	U	0.1
	V	1.0
	W	0.1
	Y	0.01
REE	Ce^	0.01
	Dy^	0.1
	Er^	0.1
	Eu^	0.1
	Gd^	0.1
	Ho^	0.1
	La^	0.5
	Lu^	0.1
	Nd^	0.1
	Sm^	0.1
	Tb^	0.1
	Tm^	0.1
	Yb^	0.1

^elements in addition to TOR

INAA

Group	Element	Detection Limit (mg/kg)
Major and minor	Ba	50
	Cr	5
	Fe	100
	Na	100
	Ni	20
	Sr	500
	Zn	50
Trace	Ag	5
	As	0.5
	Au	0.002
	Br^	0.5
	Co	1
	Cs^	0.5
	Hf^	0.5
	Ir^	0.005
	Mo	1
	Rb	15
	Sb	0.1
	Sc	0.1
	Se	3
	Ta^	0.5
	Th	0.2
	U	0.5
	W	1
REE	Ce^	3
	Eu^	0.2
	La	0.5
	Lu^	0.05
	Nd^	5
	Sm^	0.1
	Tb^	0.5
	Yb^	0.2

Figure 2.38 Listing of analytes and expected detection limits under aqua regia ICP-MS and INAA analysis (Actlabs and UNSW Analytical Centre).

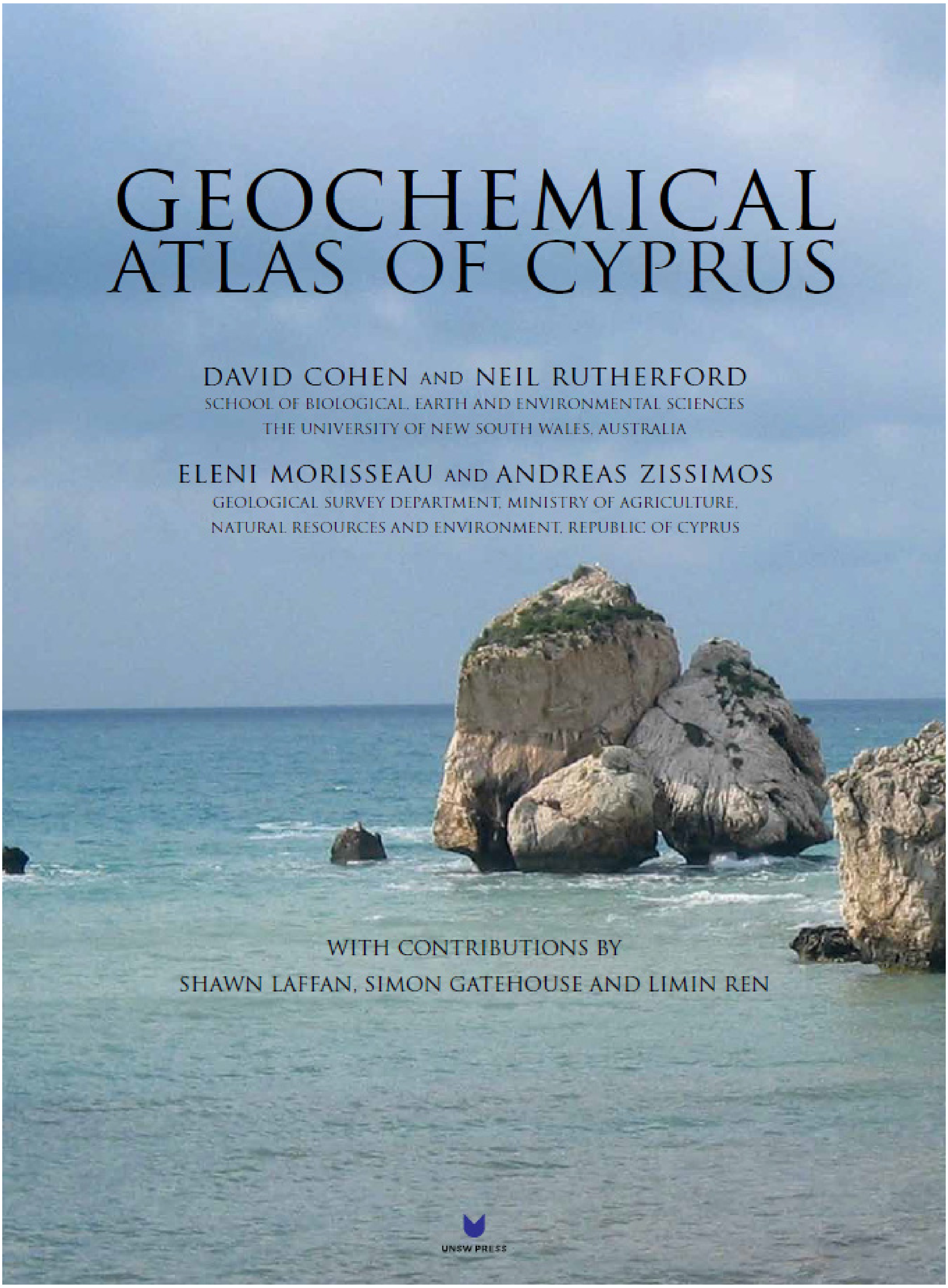

Figure 2.39 Title page of the Geochemical Atlas of Cyprus.

Table 2.6 Comparison between detection limits of this study and the FOREGS atlas.

Element	This Study			FOREGS soils		Units
	INAA	XRF	ar-ICPMS	Total (XRF or ICP-MS)	ar-ICPMS	
Ag	5	n/a	0.002	0.01	n/a	mg/kg
Al, Al_2O_3	n/a	0.01	0.01	0.05	n/a	%
As	0.5	n/a	0.1	0.2	5	mg/kg
Au	0.002	n/a	n/a	n/a	n/a	ug/kg
B	n/a	n/a	1	n/a	n/a	mg/kg
Ba	50	n/a	0.5	5	1	mg/kg
Be	n/a	n/a	0.1	2	n/a	mg/kg
Br	0.5	n/a	n/a	n/a	n/a	mg/kg
Bi	n/a	n/a	0.02	0.5	n/a	mg/kg
Ca, CaO	1	0.01	0.01	0.01	n/a	%
Cd	n/a	n/a	0.01	0.01	n/a	mg/kg
Ce	3	n/a	0.01	0.15	n/a	mg/kg
Co	1	n/a	0.1	3	1	mg/kg
Cr	5	n/a	0.5	3	1	mg/kg
Cs	1	n/a	0.02	0.5	n/a	mg/kg
Cu	n/a	n/a	0.1	0.01	1	mg/kg
Dy	n/a	n/a	0.1	0.1	n/a	mg/kg
Er	n/a	n/a	0.1	0.1	n/a	mg/kg
Eu	0.2	n/a	0.1	0.05	n/a	mg/kg
Fe, Fe_2O_3	0.01	0.01	0.01	0.01	0.002	%
Ga	n/a	n/a	0.02	0.2	n/a	mg/kg
Gd	n/a	n/a	0.1	0.1	n/a	mg/kg
Ge	n/a	n/a	0.1	n/a	n/a	mg/kg
Hf	1	n/a	0.1	0.2	n/a	mg/kg
Hg	1	n/a	0.01	0.0001	n/a	mg/kg
Ho	n/a	n/a	0.1	0.02	n/a	mg/kg
In	n/a	n/a	0.02	0.01	n/a	mg/kg
Ir	0.005	n/a	n/a	n/a	n/a	ug/kg
K	n/a	n/a	0.01	n/a	n/a	%
La	0.5	n/a	0.5	n/a	n/a	mg/kg
Li	n/a	n/a	0.1	n/a	n/a	mg/kg
Lu	0.05	n/a	0.1	0.02	n/a	mg/kg
Mg, MgO	n/a	0.01	0.01	0.01	n/a	%
Mn, MnO	n/a	100	10	10	10	mg/kg
Mo	1	n/a	0.01	0.1	n/a	mg/kg
Na, Na_2O	0.01	n/a	0.001	0.01	n/a	%
Nb	n/a	n/a	0.1	0.1	n/a	mg/kg
Nd	5	n/a	0.02	0.15	n/a	mg/kg
Ni	20	n/a	0.1	2	2	mg/kg
P_2O_5	n/a	0.01	n/a	0.001	n/a	%
Pb	n/a	n/a	0.1	3	3	mg/kg
Pr	n/a	n/a	0.1	0.1	n/a	mg/kg
Pt	n/a	n/a	0.002	n/a	n/a	ug/kg
Rb	15	n/a	0.1	2	n/a	mg/kg
Re	n/a	n/a	0.001	n/a	n/a	mg/kg
S	n/a	n/a	n/a	n/a	50	mg/kg
Sb	0.1	n/a	0.02	0.02	n/a	mg/kg
Sc	0.1	n/a	0.1	0.5	n/a	mg/kg
Se	3	n/a	0.1	n/a	n/a	mg/kg
SiO_2	n/a	0.01	n/a	0.1	n/a	%
Sm	0.1	n/a	0.1	0.1	n/a	mg/kg
Sn	200	n/a	0.2	2	n/a	mg/kg
Sr	500	n/a	0.5	2	n/a	mg/kg
Ta	0.5	n/a	0.05	0.05	n/a	mg/kg
Tb	0.5	n/a	0.1	0.02	n/a	mg/kg
Te	n/a	n/a	0.02	0.02	n/a	mg/kg
Th	0.2	n/a	0.1	0.1	n/a	mg/kg
Ti, TiO_2	n/a	0.001	1	0.001	n/a	%
Tl	n/a	n/a	0.02	0.01	n/a	mg/kg
Tm	n/a	n/a	0.1	0.02	n/a	mg/kg
U	0.5	n/a	0.1	0.1	n/a	mg/kg
V	n/a	n/a	1	0.5	1	mg/kg
W	1	n/a	0.1	5	n/a	mg/kg
Y	n/a	n/a	0.1	3	n/a	mg/kg
Yb	0.2	n/a	0.1	0.05	n/a	mg/kg
Zn	50	n/a	0.1	3	1	mg/kg
Zr	n/a	n/a	0.1	3	n/a	mg/kg

Table 2.6 Summary of analyses completed in the project.

Zone	Material	Samples collected		Fractions analysed	Physical Analysis					Geochemical Analyses							
					EC (UNSW)	pH (UNSW)	Mussel color (UNSW)	Laser particle sizing	LOI (UNSW)	AAC (Actlabs)	HXL (Actlabs)	AQR + INAA (Actlabs)	XRF (UNSW)	TC (UNSW)	XRF (GSD)*	TC, TOC and TS (GSD)*	CEC (UNSW)
Circum-Troodos sew, Quaternary, Mamonia and Troodos margins	Soil	Top soil	3,857	Bulk	3,857	3,857	3,857		3,857			3,857			3,857	3,857	
		Sub soil	3,847	Bulk								3,847					
		Total	**7,704**		**3,857**	**3,857**	**3,857**	**0**	**3,857**	**0**	**0**	**7,704**	**0**	**0**	**3,857**	**3,857**	**0**
Troodos Ophiolite Complex	Soil	Top soil	903	Bulk	903	903	903		903			903			903	903	
		Sub soil	903	Bulk								903					
		Total	**1,806**		**903**	**903**	**903**	**0**	**903**	**0**	**0**	**1,806**	**0**	**0**	**903**	**903**	**0**
Orientation suite (in additional to analysis for main set of samples)	Soil	Top soil	104	Bulk				104		104	104		37	37			104
				< 125 um								104					
				125-250 um								104					
				250-2000 um								104					
		Sub soil	104	Bulk	104	104	104	104	104	104	104		37	37			104
				< 125 um								104					
				125-250 um								104					
				250-2000 um								104					
		Total	**208**		**104**	**104**	**104**	**208**	**104**	**208**	**208**	**624**	**74**	**74**	**0**	**0**	**208**
Mines suite	Soil	Top soil	386	Bulk	386	386	386		386	264	264	386	10	10	386	386	
		Sub soil	386	Bulk							232	386	10	10			
		Total	**772**		**386**	**386**	**386**	**0**	**386**	**264**	**496**	**772**	**20**	**20**	**386**	**386**	**0**
Other special samples	Soil		231	bulk	231	231	231		231			231			231	231	
	Rock		48	bulk								48					
	Vegetation		120	leaves								120					
		Total	**399**		**231**	**231**	**231**	**0**	**231**	**0**	**0**	**399**	**0**	**0**	**231**	**231**	**0**
Stream sediments	Sediment	Top soil	89	Bulk								89					
		Sub soil	88	Bulk								88					
		Total	**177**		**0**	**0**	**0**	**0**	**0**	**0**	**0**	**177**	**0**	**0**	**0**	**0**	**0**
Total			**11,066**		**5,481**	**5,481**	**5,481**	**208**	**5,481**	**472**	**704**	**11,482**	**94**	**94**	**5,377**	**5,377**	**208**

Table 2.7 Structure of analytical data spreadsheet.

Variable	Description	Units
Anal No	Unique analytical number for Actlabs and UNSW Analytical Centre	
Site No	Field sample	
East	Easting (WGS86 Zone 36N)	m
North	Northing (WGS86 Zone 36N)	m
Lvl	Sampling level - A = top 25 cm; B = 50 - 75 cm (nominal) depth	
Frac	Size fraction	um
Colour	Munsell colour chart value	
Rec	Record sequence	
Sample Dup	Sample duplicate	
Site Dup	Site duplicate	
Test site	Test site	
GRMs	Reference material	
Sizing	Particle sizing completed	
Orient	Orientation site	
Mines	Mine site	
Rocks	Rock sample collected	
Traverse	Traverse site	
Stream seds	Stream sediment sample	
LOI %	Loss on ignition at 1000°C (UNSW AC)	%
pH	pH for 1:5 slurry on 2.00 ± 0.20 g sample in crucible (UNSW AC)	
EC	EC for 1:5 slurry on 2.00 ± 0.20 g sample in crucible (UNSW AC)	mS
Ag_ICP	Ag by aqua regia ICP-MS (Actlabs, Australia)	*mg/kg*
Etc		
Zr_ICP	Zr by aqua regia ICP-MS (Actlabs, Australia)	*mg/kg*
Ag_INAA	Au by INAA (Actlabs, Canada)	*mg/kg*
Etc		
Zn_INAA	Lu by INAA (Actlabs, Canada)	*mg/kg*

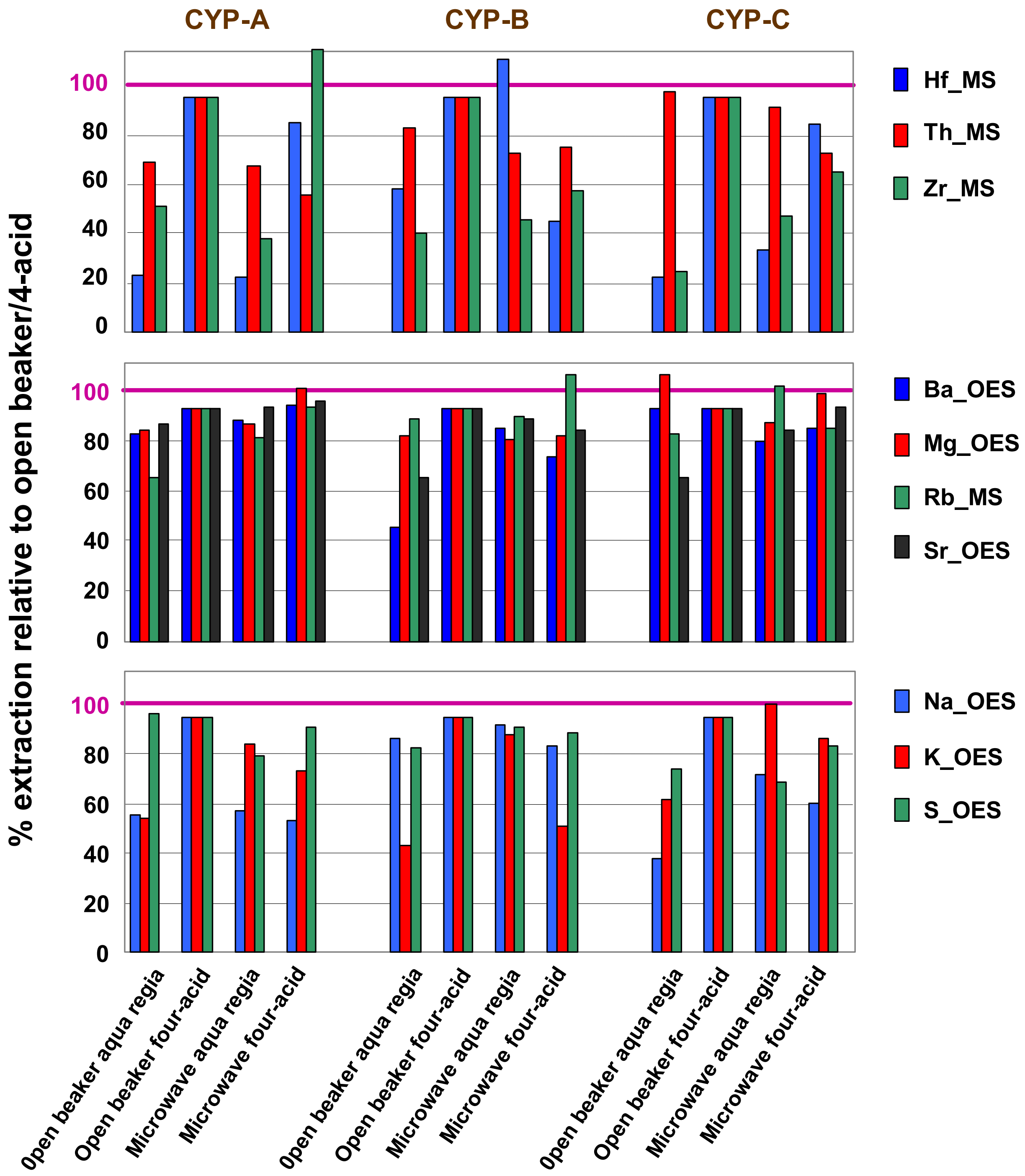

Figure 2.33 Ctd...

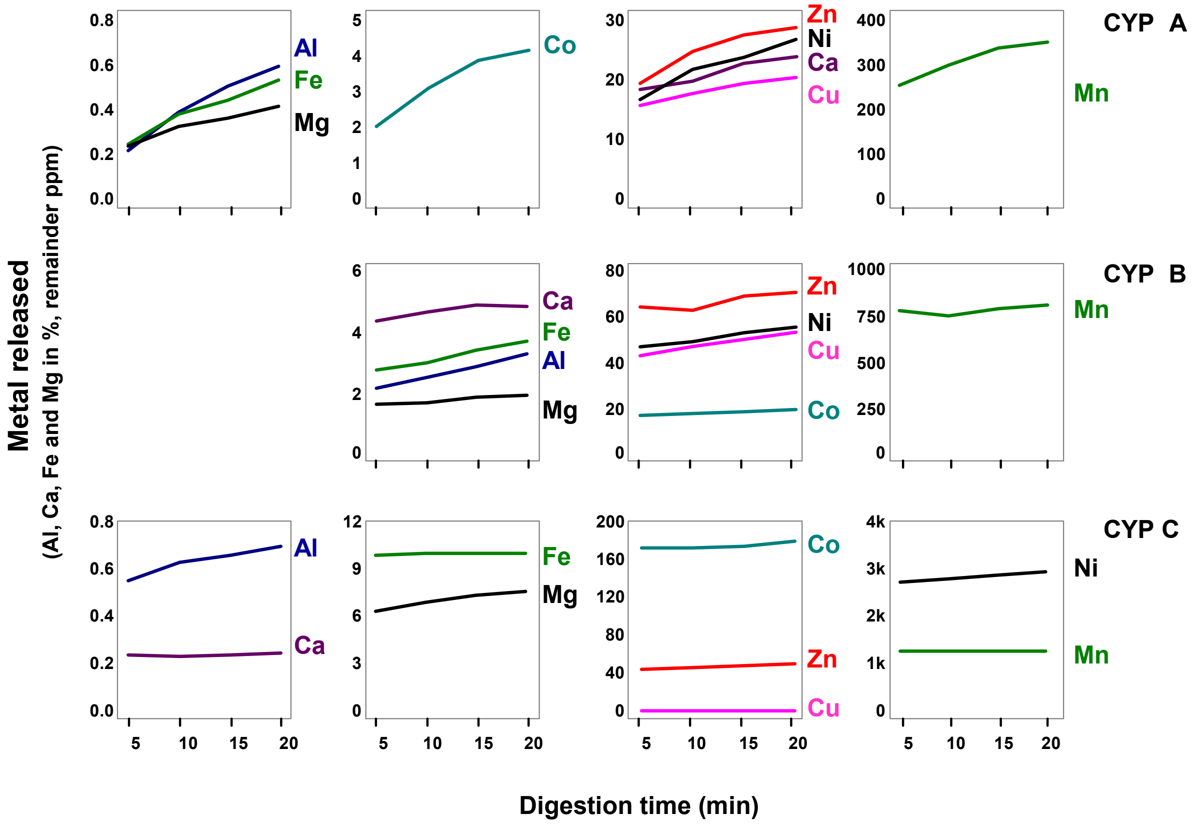

Figure 2.34 Time-dependence on aqua regia extraction of elements for project reference materials.

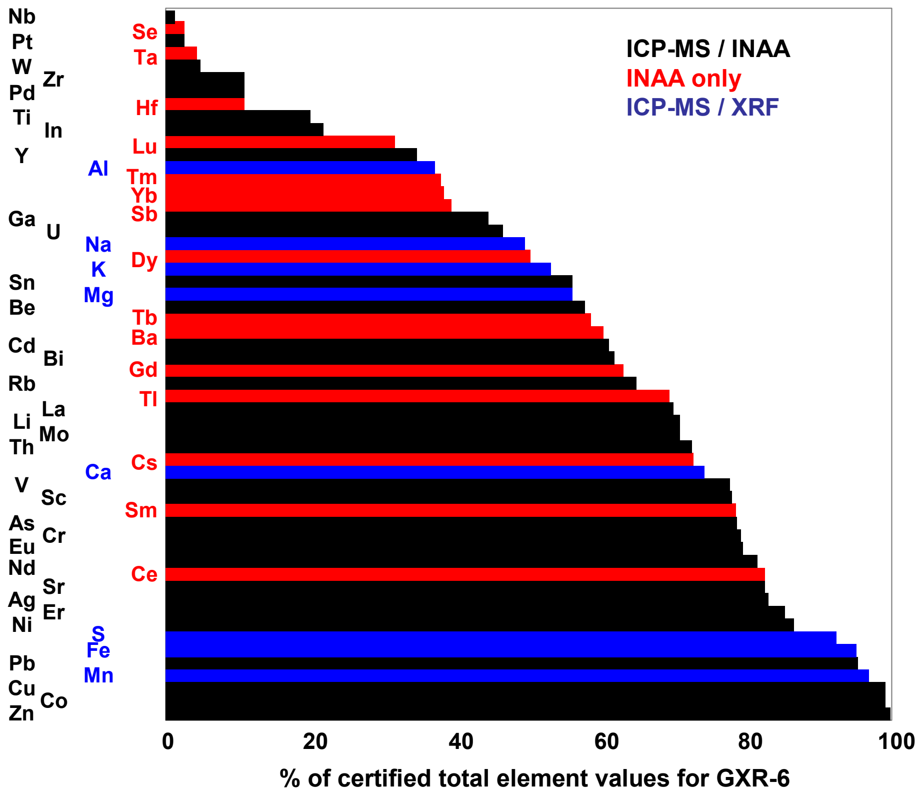

Figure 2.35 Proportion of total element contents (as per certified or recommended GXR-6 values) extracted on average by the seven commercial laboratories using nitric-rich aqua regia.

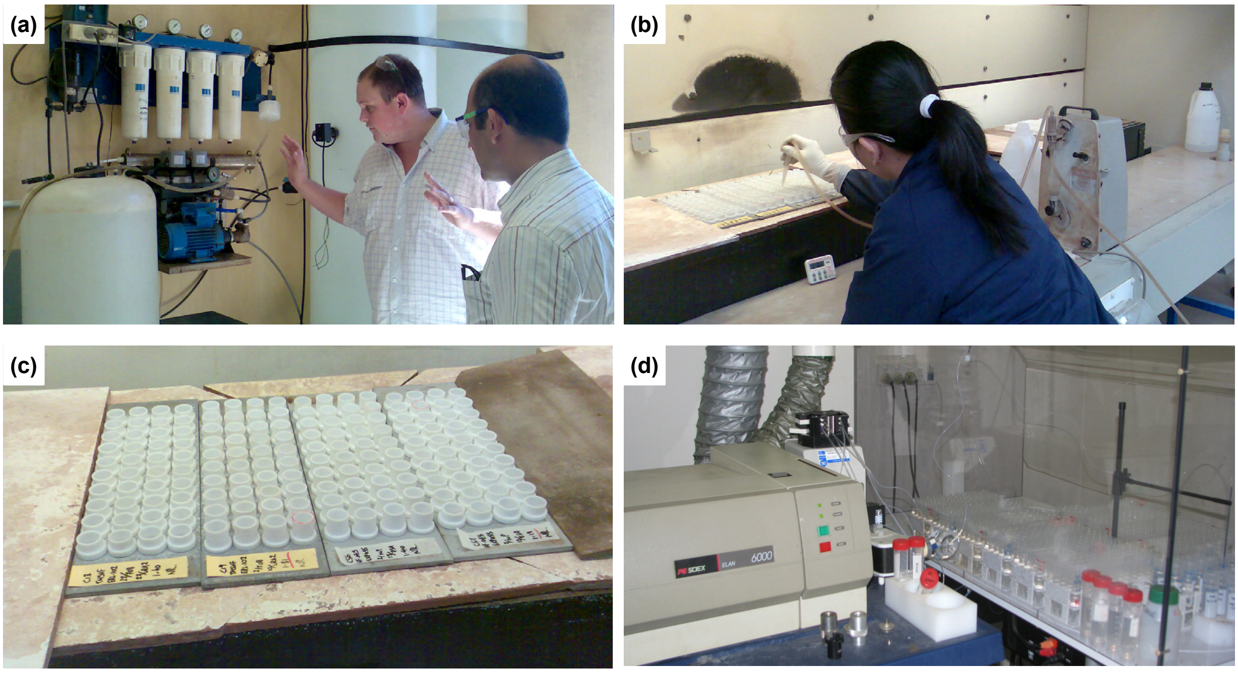

Figure 2.36 (a) Millipore water deionisation unit. (b) Addition of HCl to samples in polythene tubes, Actlabs (c) heat f reaction tubes in heating bath after addition of HNO_3. (d) Perkin Elmer Optima 5000 ICP-OES unit for analysis of major and high concentration elements.

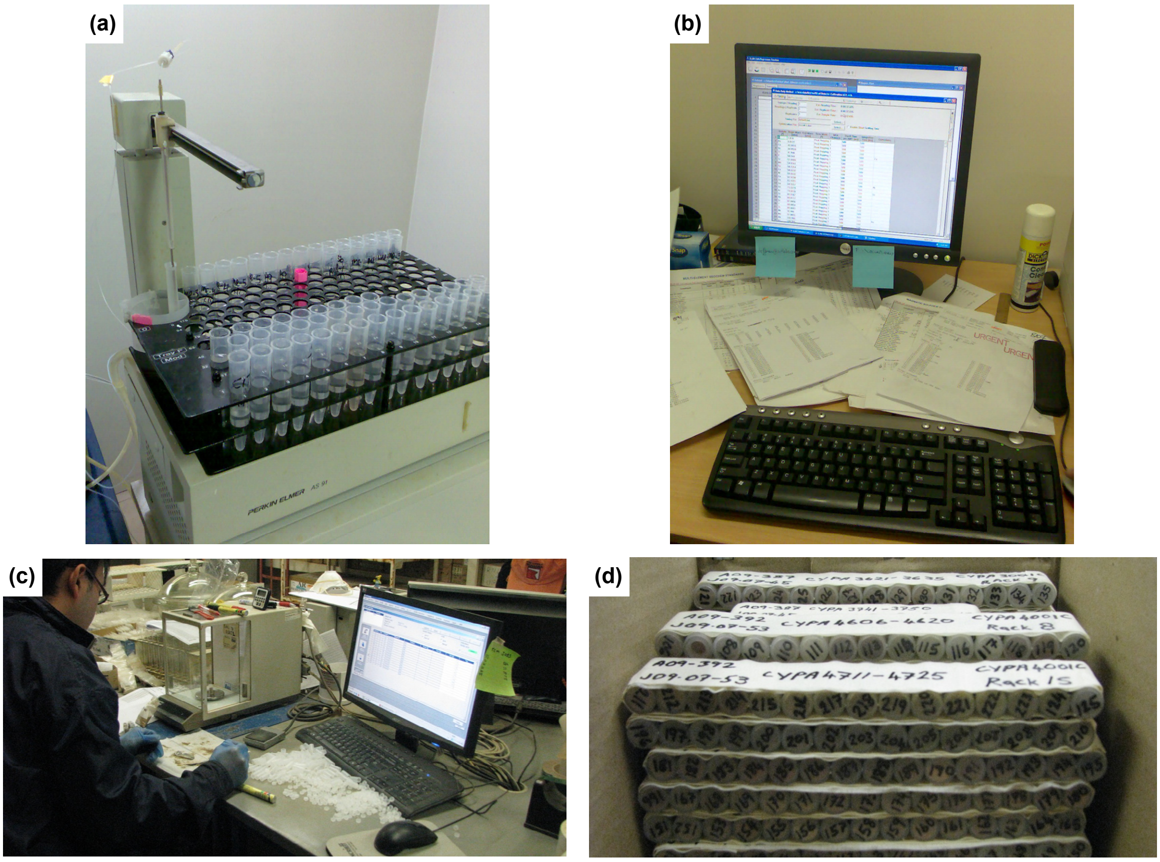

Figure 2.37 (a) Autodilution prior to running ICP-MS; (b) Actlabs LIMS system handles all data capture, result collation and QC monitoring; (c) Weighing room; (d) INAA vials in sub-batches packaged for shipment to Canada.

ICP-MS

Group	Element	Detection Limit (mg/kg)
Major and minor	Al	100
	Ba	0.5
	Ca	100
	Cr^	0.5
	Cu	0.01
	Fe^	100
	K	100
	Mg	100
	Mn	1
	Na	10
	Ni	0.1
	P	100
	Pb	0.01
	Rb^	0.1
	Sr	0.5
	Ti^	1
	Zn	0.1
	Zr	0.1

Group	Element	Detection limit (mg/kg)
Trace	Ag	0.002
	As^	0.1
	B	1.0
	Be	0.1
	Bi	0.02
	Cd	0.01
	Co^	0.1
	Cs^	0.02
	Ga	0.02
	Ge	0.1
	Hf^	0.1
	Hg	0.01
	In	0.02
	Li	0.1
	Mo	0.01
	Nb	0.1
	Re^	0.001
	Sb^	0.02
	Sc	0.1
	Se	0.1
	Sn	0.2
	Ta^	0.05
	Te	0.02
	Th	0.1
	Tl	0.02
	U	0.1
	V	1.0
	W	0.1
	Y	0.01

Group	Element	Detection limit (mg/kg)
REE	Ce^	0.01
	Dy^	0.1
	Er^	0.1
	Eu^	0.1
	Gd^	0.1
	Ho^	0.1
	La^	0.5
	Lu^	0.1
	Nd^	0.1
	Sm^	0.1
	Tb^	0.1
	Tm^	0.1
	Yb^	0.1

^elements in addition to TOR

INAA

Group	Element	Detection Limit (mg/kg)
Major and minor	Ba	50
	Cr	5
	Fe	100
	Na	100
	Ni	20
	Sr	500
	Zn	50
Trace	Ag	5
	As	0.5
	Au	0.002
	Br^	0.5
	Co	1
	Cs^	0.5
	Hf^	0.5
	Ir^	0.005
	Mo	1
	Rb	15
	Sb	0.1
	Sc	0.1
	Se	3
	Ta^	0.5
	Th	0.2
	U	0.5
	W	1
REE	Ce^	3
	Eu^	0.2
	La	0.5
	Lu^	0.05
	Nd^	5
	Sm^	0.1
	Tb^	0.5
	Yb^	0.2

Figure 2.38 Listing of analytes and expected detection limits under aqua regia ICP-MS and INAA analysis (Actlabs and UNSW Analytical Centre).

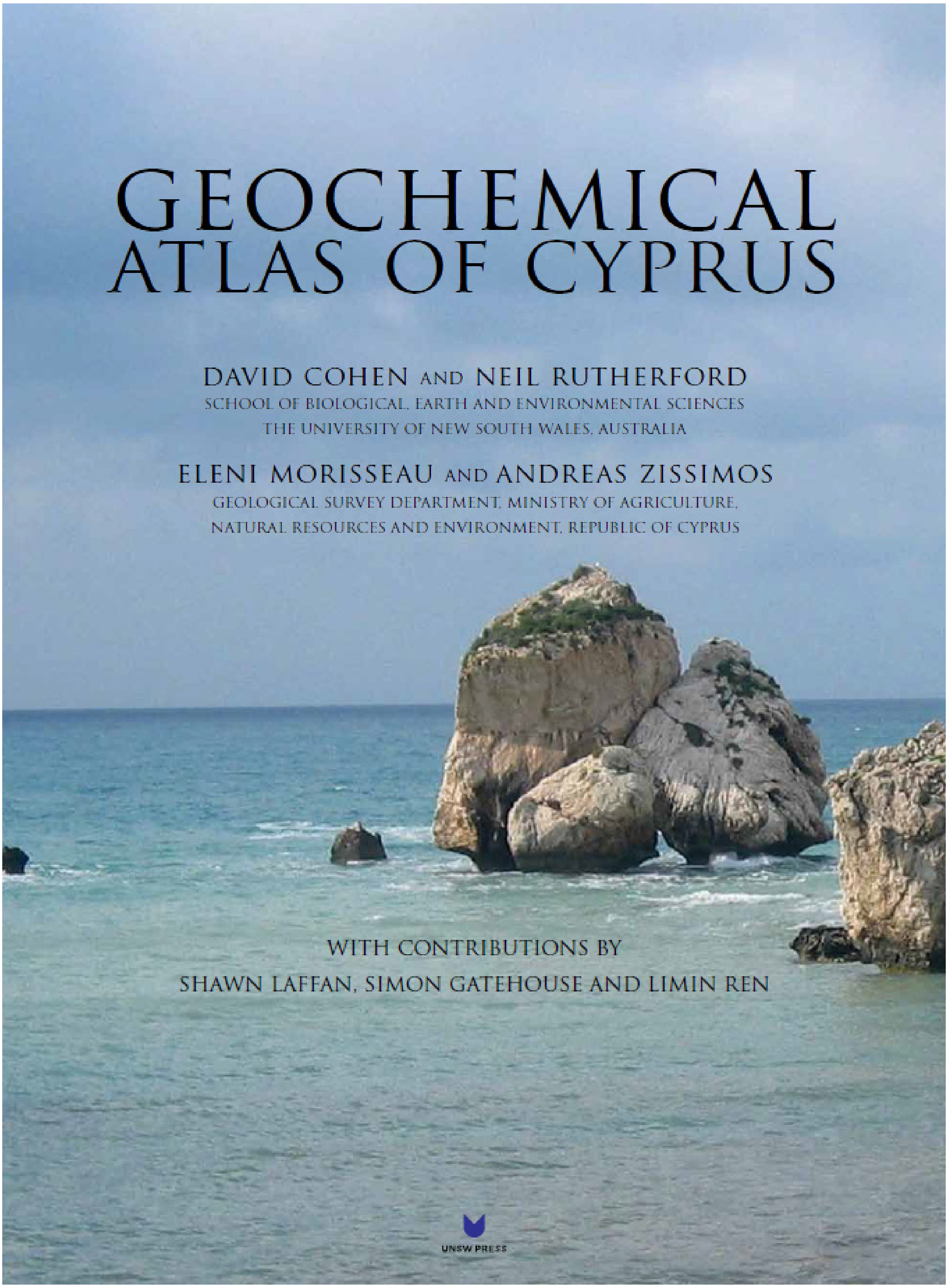

Figure 2.39 Title page of the Geochemical Atlas of Cyprus.

Table 2.6 Comparison between detection limits of this study and the FOREGS atlas.

Element	This Study			FOREGS soils		Units
	INAA	XRF	ar-ICPMS	Total (XRF or ICP-MS)	ar-ICPMS	
Ag	5	n/a	0.002	0.01	n/a	mg/kg
Al, Al_2O_3	n/a	0.01	0.01	0.05	n/a	%
As	0.5	n/a	0.1	0.2	5	mg/kg
Au	0.002	n/a	n/a	n/a	n/a	ug/kg
B	n/a	n/a	1	n/a	n/a	mg/kg
Ba	50	n/a	0.5	5	1	mg/kg
Be	n/a	n/a	0.1	2	n/a	mg/kg
Br	0.5	n/a	n/a	n/a	n/a	mg/kg
Bi	n/a	n/a	0.02	0.5	n/a	mg/kg
Ca, CaO	1	0.01	0.01	0.01	n/a	%
Cd	n/a	n/a	0.01	0.01	n/a	mg/kg
Ce	3	n/a	0.01	0.15	n/a	mg/kg
Co	1	n/a	0.1	3	1	mg/kg
Cr	5	n/a	0.5	3	1	mg/kg
Cs	1	n/a	0.02	0.5	n/a	mg/kg
Cu	n/a	n/a	0.1	0.01	1	mg/kg
Dy	n/a	n/a	0.1	0.1	n/a	mg/kg
Er	n/a	n/a	0.1	0.1	n/a	mg/kg
Eu	0.2	n/a	0.1	0.05	n/a	mg/kg
Fe, Fe_2O_3	0.01	0.01	0.01	0.01	0.002	%
Ga	n/a	n/a	0.02	0.2	n/a	mg/kg
Gd	n/a	n/a	0.1	0.1	n/a	mg/kg
Ge	n/a	n/a	0.1	n/a	n/a	mg/kg
Hf	1	n/a	0.1	0.2	n/a	mg/kg
Hg	1	n/a	0.01	0.0001	n/a	mg/kg
Ho	n/a	n/a	0.1	0.02	n/a	mg/kg
In	n/a	n/a	0.02	0.01	n/a	mg/kg
Ir	0.005	n/a	n/a	n/a	n/a	ug/kg
K	n/a	n/a	0.01	n/a	n/a	%
La	0.5	n/a	0.5	n/a	n/a	mg/kg
Li	n/a	n/a	0.1	n/a	n/a	mg/kg
Lu	0.05	n/a	0.1	0.02	n/a	mg/kg
Mg, MgO	n/a	0.01	0.01	0.01	n/a	%
Mn, MnO	n/a	100	10	10	10	mg/kg
Mo	1	n/a	0.01	0.1	n/a	mg/kg
Na, Na_2O	0.01	n/a	0.001	0.01	n/a	%
Nb	n/a	n/a	0.1	0.1	n/a	mg/kg
Nd	5	n/a	0.02	0.15	n/a	mg/kg
Ni	20	n/a	0.1	2	2	mg/kg
P_2O_5	n/a	0.01	n/a	0.001	n/a	%
Pb	n/a	n/a	0.1	3	3	mg/kg
Pr	n/a	n/a	0.1	0.1	n/a	mg/kg
Pt	n/a	n/a	0.002	n/a	n/a	ug/kg
Rb	15	n/a	0.1	2	n/a	mg/kg
Re	n/a	n/a	0.001	n/a	n/a	mg/kg
S	n/a	n/a	n/a	n/a	50	mg/kg
Sb	0.1	n/a	0.02	0.02	n/a	mg/kg
Sc	0.1	n/a	0.1	0.5	n/a	mg/kg
Se	3	n/a	0.1	n/a	n/a	mg/kg
SiO_2	n/a	0.01	n/a	0.1	n/a	%
Sm	0.1	n/a	0.1	0.1	n/a	mg/kg
Sn	200	n/a	0.2	2	n/a	mg/kg
Sr	500	n/a	0.5	2	n/a	mg/kg
Ta	0.5	n/a	0.05	0.05	n/a	mg/kg
Tb	0.5	n/a	0.1	0.02	n/a	mg/kg
Te	n/a	n/a	0.02	0.02	n/a	mg/kg
Th	0.2	n/a	0.1	0.1	n/a	mg/kg
Ti, TiO_2	n/a	0.001	1	0.001	n/a	%
Tl	n/a	n/a	0.02	0.01	n/a	mg/kg
Tm	n/a	n/a	0.1	0.02	n/a	mg/kg
U	0.5	n/a	0.1	0.1	n/a	mg/kg
V	n/a	n/a	1	0.5	1	mg/kg
W	1	n/a	0.1	5	n/a	mg/kg
Y	n/a	n/a	0.1	3	n/a	mg/kg
Yb	0.2	n/a	0.1	0.05	n/a	mg/kg
Zn	50	n/a	0.1	3	1	mg/kg
Zr	n/a	n/a	0.1	3	n/a	mg/kg

Table 2.6 Summary of analyses completed in the project.

Zone	Material	Samples collected		Fractions analysed	Physical Analysis					Geochemical Analyses							
					EC (UNSW)	pH (UNSW)	Mussel color (UNSW)	Laser particle sizing	LOI (UNSW)	AAC (Actlabs)	HXL (Actlabs)	AQR + INAA (Actlabs)	XRF (UNSW)	TC (UNSW)	XRF (GSD)*	TC, TOC and TS (GSD)*	CEC (UNSW)
Circum-Troodos sew, Quaternary, Mamonia and Troodos margins	Soil	Top soil	3,857	Bulk	3,857	3,857	3,857		3,857			3,857			3,857	3,857	
		Sub soil	3,847	Bulk								3,847					
		Total	**7,704**		**3,857**	**3,857**	**3,857**	**0**	**3,857**	**0**	**0**	**7,704**	**0**	**0**	**3,857**	**3,857**	**0**
Troodos Ophiolite Complex	Soil	Top soil	903	Bulk	903	903	903		903			903			903	903	
		Sub soil	903	Bulk								903					
		Total	**1,806**		**903**	**903**	**903**	**0**	**903**	**0**	**0**	**1,806**	**0**	**0**	**903**	**903**	**0**
Orientation suite (in additional to analysis for main set of samples)	Soil	Top soil	104	Bulk				104		104	104		37	37			104
				< 125 um								104					
				125-250 um								104					
				250-2000 um								104					
		Sub soil	104	Bulk	104	104	104	104	104	104	104		37	37			104
				< 125 um								104					
				125-250 um								104					
				250-2000 um								104					
		Total	**208**		**104**	**104**	**104**	**208**	**104**	**208**	**208**	**624**	**74**	**74**	**0**	**0**	**208**
Mines suite	Soil	Top soil	386	Bulk	386	386	386		386	264	264	386	10	10	386	386	
		Sub soil	386	Bulk							232	386	10	10			
		Total	**772**		**386**	**386**	**386**	**0**	**386**	**264**	**496**	**772**	**20**	**20**	**386**	**386**	**0**
Other special samples	Soil		231	bulk	231	231	231		231			231			231	231	
	Rock		48	bulk								48					
	Vegetation		120	leaves								120					
		Total	**399**		**231**	**231**	**231**	**0**	**231**	**0**	**0**	**399**	**0**	**0**	**231**	**231**	**0**
Stream sediments	Sediment	Top soil	89	Bulk								89					
		Sub soil	88	Bulk								88					
		Total	**177**		**0**	**0**	**0**	**0**	**0**	**0**	**0**	**177**	**0**	**0**	**0**	**0**	**0**
Total			**11,066**		**5,481**	**5,481**	**5,481**	**208**	**5,481**	**472**	**704**	**11,482**	**94**	**94**	**5,377**	**5,377**	**208**

Table 2.7 Structure of analytical data spreadsheet.

Variable	Description	Units
Anal No	Unique analytical number for Actlabs and UNSW Analytical Centre	
Site No	Field sample	
East	Easting (WGS86 Zone 36N)	m
North	Northing (WGS86 Zone 36N)	m
Lvl	Sampling level - A = top 25 cm; B = 50 - 75 cm (nominal) depth	
Frac	Size fraction	um
Colour	Munsell colour chart value	
Rec	Record sequence	
Sample Dup	Sample duplicate	
Site Dup	Site duplicate	
Test site	Test site	
GRMs	Reference material	
Sizing	Particle sizing completed	
Orient	Orientation site	
Mines	Mine site	
Rocks	Rock sample collected	
Traverse	Traverse site	
Stream seds	Stream sediment sample	
LOI %	Loss on ignition at 1000°C (UNSW AC)	%
pH	pH for 1:5 slurry on 2.00 ± 0.20 g sample in crucible (UNSW AC)	
EC	EC for 1:5 slurry on 2.00 ± 0.20 g sample in crucible (UNSW AC)	mS
Ag_ICP	Ag by aqua regia ICP-MS (Actlabs, Australia)	*mg/kg*
Etc		
Zr_ICP	Zr by aqua regia ICP-MS (Actlabs, Australia)	*mg/kg*
Ag_INAA	Au by INAA (Actlabs, Canada)	*mg/kg*
Etc		
Zn_INAA	Lu by INAA (Actlabs, Canada)	*mg/kg*

Table 2.8 Structure of a nalytical quality control data spreadsheet.

Shee t	Sheet tab	Data	Materials
1	ICP GRMs	Sequence of GRMs used to monitor ICP-MS analyses	CYP-A, CYP-B, CYP-C, USGS GXR-6, ORES100P, ORES45A, blanks
2	INAA GRMs	Sequence of GRMs used to monitor INAA analyses	CYP-A, CYP-B, CYP-C, USGS GXR-6, Till-1, Till-2, Till-3, Till-4, blanks
3	GRM summary	Analysis of GRM data and quality acceptance decision	
4	GRM round-robin	Round-robin analysis of CYP-A, CYP-B and CYP-C (plus USGS GXR-6) from seven labs	
5	ICP sam dup	ICP-MS duplicates (sample processing and analytical)	
6	ICP site dup	ICP-MS site duplicates	
7	INAA sam dup	INAA duplicates (sample processing and analytical)	
8	INAA site dup	INAA site duplicates	
9	XRF vs INAA	Comparison of XRF and INAA data for selected elements	
10	Resampled sites	Sites sampled and processed by separate teams	
11	Sel extract GRM	ICP-MS analyses of GRMs under selective extractions (AAC and HXL)	CYP-A, CYP-B, CYP-C, blanks
12	Sel extract dup	ICP-MS duplicate sample analyses under selective extractions (AAC and HXL)	
13	Veg dup	Vegetation sample duplicates for ICP-MS	
14	Sizing dup	Laser particle sizing duplicates	
15	Var test sites	Soil geochemical variation test site data	
16	DL	Detection limits and practical quantification limits for ICP-MS and INAA	

Table 2.9 Structure of analytical sample sequence spreadsheet.

Variable	Description	Units
Anal No	Unique analytical number for Actlabs and UNSW Analytical Centre	
Site No	Field sample	
East	Easting (WGS86 Zone 36N)	m
North	Northing (WGS86 Zone 36N)	m
Lvl	Sampling level - A = top 20 cm; B = 50 - 70 cm (nominal) depth	
Frac	Fraction (um)	um
Colour	Munsell colour chart value	
Rec	Record sequence	
Sample Dup	Sample duplicate	
Site Dup	Site duplicate	
Test site	Test site	
GRMs	Reference material	
Sizing	Particle sizing completed	
Orient	Orientation site	
Mines	Mine site	
Rocks	Rock sample collected	
Traverse	Traverse site	
Stream seds	Stream sediment sample	

Table 2.10 Structure of field data logs spreadsheet.

Geochemical Atlas of Cyprus - Field Data UTM Zone 36N, WGS84

Sample Site No	Date	Sampler	50k Map Sheet	Municipality	Weather	Temp	GPS Location Easting	Northing	Bulk Character Size	State	Orgs	Fe cem	Calc
CYP0001	21-May-06	DRC-NFR	Pissouri	Mandria Pafou	dry	hot	459000	3842080	<2mm	dry	n	n	n
CYP0002	21-May-06	DRC-NFR	Pissouri	Mandria Pafou	dry	hot	459120	3842005	<2mm	dry	n	n	n
CYP0003	21-May-06	DRC-NFR	Pissouri	Nikokleia	dry	hot	459760	3842020	<2mm	dry	n	n	n
CYP0004	21-May-06	DRC-NFR	Pissouri	Nikokleia	dry	hot	460980	3843140	<2mm	dry	n	n	n
CYP0005	21-May-06	DRC-NFR	Pissouri	Nikokleia	dry	hot	460970	3843160	<2mm	dry	n	n	n
CYP0006	21-May-06	DRC-NFR	Pissouri	Nikokleia	dry	hot	461070	3844090	<2mm	dry	n	n	y
CYP0007	21-May-06	DRC-NFR	Pissouri	Souskiou	dry	hot	461870	3844000	<2mm	dry	n	n	y
CYP0008	21-May-06	DRC-NFR	Pissouri	Souskiou	dry	hot	461870	3844050	<2mm	dry	n	n	y
CYP0009	21-May-06	DRC-NFR	Pissouri	Souskiou	dry	hot	462130	3844930	<2mm	dry	n	n	y

Top Soil Horizon Sam Meth	Up Depth	Bot Depth	Dom Size	Colour Soil	Sub Soil Sample Samp Meth	Horiz	Up Depth	Bot Depth	Colour Soil	Dom Size	Other Information & Rocks Hill Slope	Rock Type	Rock Group
Spade	0	25	med	br	auger	B(t)	50	75		med	flat	gravels	alluvium-colluvium
Spade	0	25	med	br	auger	B(t)	50	75		med	flat	gravels	alluvium-colluvium
Spade	0	25	med	br	auger	B(t)	50	75		med	flat	gravels	alluvium-colluvium
Spade	0	25	med	lt-br	auger	B(t)	50	75	lt-br	med	flat	calcarenite	calcarenite
Spade	0	25	med	lt-br	auger	B(t)	50	75	lt-br	med	flat	calcarenite	calcarenite
Spade	0	25	med	br	auger	B(t)	50	75	rd-br	fine	mod	gravels	alluvium-colluvium
Spade	0	25	fine	lt-br	auger	B(t)	50	75	rd-br	fine	flat	calcarenite	calcarenite
Spade	0	25	fine	lt-br	auger	B(t)	50	75	rd-br	fine	flat	calcarenite	calcarenite
Spade	0	25	fine	rd-br	auger	B(t)	30	40	rd-br	fine	flat	gravels	alluvium-colluvium

Other Information & Rocks Formation name	Formation Age	Formation type	Landuse	Vegetation Types	Contam	Mining	Urban Setting	General Photo	Site Comments
Pakhna	MI-Mu	calcarenite	grain	cereals	none	no	nil	cyp0001ab	1st sampling site. Gravel over calcar.
Pakhna	MI-Mu	calcarenite	grain	garigue-maquis	none	no	nil	cyp0002	Sampling on terraced wheat field
Pakhna	MI-Mu	calcarenite	other	degraded	none	no	nil	cyp0003	Sampling on terraced wheat field
Pakhna	MI-Mu	calcarenite	grass	degraded	none	no	nil	cyp0004	Exposed section through calcarenites
Pakhna	MI-Mu	calcarenite	grass	degraded	none	no	nil		
Lefkara	Ku3-Ou	calcarenite	grain	garigue-maquis	plow	no	nil	cyp0006	Sampling in fallow field.
Dhiarizos Group	Tm-Km	basalt-volcaniclastic	grain	garigue-maquis	none	no	nil	cyp0007ab	Incised valleys in calcarenites.
Dhiarizos Group	Tm-Km	basalt-volcaniclastic	grain	garigue-maquis	none	no	nil		
Ayios Photios Group	Tm-Km	calcarenite-clastic	other	tall forest	none	no	nil	cyp0009ab	

Table 2.11 Structure of ICP-MS_data spreadsheet.

Variable	Ag_ICP	Al_ICP	As_ICP	etc	Zn_ICP	Zr_ICP			
Element	Ag	Al	As		Zn	Zr			
Units	mg/kg	%	mg/kg		mg/kg	mg/kg			
Detection Limit	0.002	0.01	0.1		0.1	0.1			
Analysis Method	ICPMS	ICPMS	ICPMS		ICPMS	ICPMS	**Batch**	**Seq**	**Date**
CYPA01001	0.038	1.03	3.4		178.0	1.3	A09-377	1001	24-Jun-10
CYPA01002	0.194	2.71	10.1		194.0	4.0	A09-377	1002	24-Jun-10
CYPA01003	0.001	3.55	0.7		103.0	9.2	A09-377	1003	24-Jun-10
CYPA01004	0.001	4.64	1.1		98.8	7.1	A09-377	1004	24-Jun-10
CYPA01005	0.006	3.91	0.7		19.6	2.8	A09-377	1005	24-Jun-10
CYPA01006	0.010	4.14	2.3		16.7	3.2	A09-377	1006	24-Jun-10

Table 2.12 Structure of INAA_data spreadsheet.

Variable	Ag_ INAA	As_ INAA	Au_ INAA	etc	Yb_ INAA	Zn_ INAA			
Element	Ag	As	Au		Yb	Zn			
Units	mg/kg	mg/kg	ug/kg		mg/kg	mg/kg			
Detection Limit	5	0.5	2		0.2	50			
Analysis Method	INAA	INAA	INAA		INAA	INAA	**Batch**	**Seq**	**Date**
CYPA01001	3	4.5	14		2.4	210	A09_5396	1001	23-Dec-09
CYPA01002	3	13.6	28		2.4	230	A09_5396	1002	23-Dec-09
CYPA01003	3	0.3	1		3.2	25	A09_5396	1003	23-Dec-09
CYPA01004	3	0.3	1		2.3	260	A09_5396	1004	23-Dec-09
CYPA01005	3	0.3	1		2.0	25	A09_5396	1005	23-Dec-09
CYPA01006	3	0.3	1		2.4	25	A09_5396	1006	23-Dec-09

Table 2.13 Structure of main geochemical data spreadsheet.

Variable	Description	Units
Site No	Field sample	
East	Easting (WGS84 Zone 36N)	m
North	Northing (WGS84 Zone 36N)	m
Lvl	Sampling level: A = top 25 cm; B = 50 - 75 cm (nominal) depth	
Anal No	Unique analytical number for Actlabs and UNSW Analytical Centre	
Colour	Munsell colour chart value	
Rec	Sequential record number	
LOI %	Loss on ignition at 1000°C	%
pH	pH for 1:5 slurry on 2.00 ± 0.20 g sample in crucible	
EC	EC for 1:5 slurry on 2.00 ± 0.20 g sample in crucible	mS/cm
Ag_ICP	Ag by aqua regia ICP-MS (Actlabs, Australia)	mg/kg
etc		
Zr_ICP	Zr by aqua regia ICP-MS (Actlabs, Australia)	mg/kg
Ag_INAA	Au by INAA (Actlabs, Canada)	mg/kg
etc		
Zn_INAA	Lu by INAA (Actlabs, Canada)	mg/kg

Table 2.14 Structure of orientation sites spreadsheet.

Variable	Description	Level	Units
Site	Field site		
East	Easting (WGS84 Zone 36N)		m
North	Northing (WGS84 Zone 36N)		m
Line	1 or 2		
Station	Station number		
Distance	Distance along Line 1 or 2		m
Analysis_A	Actlabs analytical number	A	
Analysis_B	Actlabs analytical number	B	
Munsell_A	Munsell soil colour	A	
Munsell_B	Munsell soil colour	B	
LOI_A	Loss on ignition (1000°C)	A	%
LOI_B	Loss on ignition (1000°C)	B	%
pH_A	pH (slurry)	A	
pH_B	pH (slurry)	B	
EC_A	Electrical conductivity (slurry)	A	mS/cm
EC_B	Electrical conductivity (slurry)	B	mS/cm
CEC_A	Cation exchange capacity	A	cmol/kg
CEC_B	Cation exchange capacity	B	cmol/kg
<125_A	Laser particle sizing <125µm	A	%
125-250_A	Laser particle sizing 125-250µm	A	%
etc			
SiO2_A	XRF major oxides for level A	A	%
SiO2_B	XRF major oxides for level B	B	%
etc			
CO2_A	LECO major oxides for level A	A	%
CO2_B	LECO major oxides for level B	B	%
Ag_ICP_A	Ag by ICPMS for sample from level A	A	mg/kg
Ag_ICP_B	Ag by ICPMS for sample from level B	B	mg/kg
Ag_INAA_A	Ag by INAA for sample from level A	A	mg/kg
etc			
Zr_ICP_B	Zr by ICPMS for sample from level B	B	mg/kg

Table 2.15 Structure of particle sizing spreadsheet.

Variable	Description	Units
Analytical	Analytical No.	
Site	Field site	
East	Easting (WGS84 Zone 36N)	m
North	Northing (WGS84 Zone 36N)	m
Lvl	Sampling level: A = top 20 cm; B = 50 - 70 cm (nominal) depth	
Line	Orientation line (1=NE-SW; 2=E-W)	
Station	Station along line	
Distance	Distance from end of line	m
10^{th} %ile	10th percentile of particle sizes	µm
median	median particle sizes	µm
90^{th} %ile	90th percentile of particle sizes	µm
0-15	Proportion of sample in size range 0-15 µm	%
etc		
500-2000	Proportion of sample in size range 500-2000 µm	%
0.200	Proportion of sample in size range <0.2 µm	%
0.023	Proportion of sample in size range 0.2 to <0.023 µm	%
etc		
1660	Proportion of sample in size range 1445.439 to <1659.586 µm	%
1905	Proportion of sample in size range 1659.586 to <1905.46 µm	%
Obscuration	Malvern sample parameters	
Residual	Malvern sample parameters	
Conc	Malvern sample parameters	
Span	Malvern sample parameters	
Vol wt mean	Malvern sample parameters	
Uniformity	Malvern sample parameters	
Spec surf area	Malvern sample parameters	m2
Surf wt mean	Malvern sample parameters	g
pH		
EC		mS/cm
Ba_ICP < 2000µm	Ba by ICP-MS in the <2000µm (bulk) fraction	mg/kg
etc		
Zn_ICP < 2000µm	Zn by ICP-MS in the <2000µm (bulk) fraction	mg/kg
Ba_ICP < 125µm	Ba by ICP-MS in the < 125µm fraction	mg/kg
Ba_ICP 125-250µm	Ba by ICP-MS in the 125-250µm fraction	mg/kg
Ba_ICP 250-2000µm	Ba by ICP-MS in the 250-2000µm fraction	mg/kg
etc		
Zn_ICP < 125µm	Zn by ICP-MS in the < 125µm fraction	mg/kg
Zn_ICP 125-250µm	Zn by ICP-MS in the 125-250µm fraction	mg/kg
Zn_ICP 250-2000µm	Zn by ICP-MS in the 250-2000µm fraction	mg/kg

Table 2.16 Structure of photograph logs spreadsheet (UTM Zone 36N, WGS84).

Sites

Site	Easting	Northing	Photo	Caption	Size (Mb)	Resolution	By	Date
CYP0001	459000	3842080	cyp0001a	First sampling site, below Asprokremnos Dam. Recemented gravels. Wheat-field and olive groves in background.	1.69	2272 x 1704	DRC	21-May-06
CYP0001	459000	3842080	cyp0001b	Weathered Pakhna Fmn carbonate overlain by 2 m of indurated recent gravels. The gravels are mainly composed of carbonate clasts but there may be Troodos materials, which are typically more rounded.	1.84	2272 x 1704	DRC	21-May-06
etc								

Sampling and Processing

Site	Easting	Northing	Photo	Caption	Size (Mb)	Resolution	By	Date
Skouriotissa	489500	3884000	G_cyp001a	Collection of Cu-rich leachate waters, Skouriotissa	1.18	3072 x 2304	CC	4-Dec-07
Skouriotissa	489500	3884000	G_cyp001b	Accumulations of Fe oxides above leached and altered basalts, Phoucassa Pit, Skouriotissa	1.35	3072 x 2304	CC	4-Dec-07
Asprokremnos Dam	459000	3842080	G_cyp003	Packing down soil in auger to allow removal of B sample	1.33	1704 x 2272	DRC	21-May-06
etc					1.02	1704 x 2272	DRC	22-May-06

General

Site	Easting	Northing	Photo	Caption	Size (Mb)	Resolution	By	Date
Coral Bay	440000	3857000	T_cyp001a	Field base (Andreas' villa) near Coral Bay	0.66	2272 x 1704	DRC	20-Mar-06
Coral Bay	440000	3857000	T_cyp001c	Data entry each evening. Site numbers and coordinates checked against tick books and topographic maps	0.65	1704 x 2272	DRC	20-Mar-06
Expressway	535000	3856000	T_cyp003	Junctions of A1 and A5	1.74	3264 x 2448	MJ	14-Oct-06
etc					0.97	2272 x 1704	DRC	22-May-06

Analysis

Site	Photo	Caption	Size (Mb)	Resolution	By	Date
UNSW	A_cyp001	Sample splits with analytical number (CYPAxxx) assigned ready for milling	2.56	3072 x 2304	DRC	14-Apr-09
UNSW	A_cyp002	Laval Lab Jones-type riffle minisplitter. Aluminium composition.	2.41	3072 x 2304	DRC	14-Apr-09
UNSW	A_cyp004	Rocklabs Carbon 40, mild steel milling bowl, puck and lid.	2.60	3072 x 2304	DRC	14-Apr-09
etc						

Sample archive

Site	Photo	Caption	Size (Mb)	Resolution	By	Date
Tseri	S_cyp002	Unpacking drying boxes for repacking in crates	0.93	2272 x 1704	DRC	28-Jan-07
Tseri	S_cyp003	Samples arranged in shipping crates	0.84	2272 x 1704	DRC	28-Jan-07
Geri, GSD sample store	S_cyp007a	Sample archive, GSD	1.18	2272 x 1704	DRC	29-Jan-07
etc						

Table 2.17 Structure of reference material testing spreadsheet.

Sheet	Sheet tab	Data	Materials
1	Round-robins	Data from round-robin testing of ar-ICPMS for seven commercial laboratories	CYP-A, CYP-B, CYP-C, USGS GXR-6
2	Round-robin RSDs	Summary of round-robin RSDs	CYP-A, CYP-B, CYP-C, USGS GXR-6
3	Interlab comparison	Summary of round-robin tests	CYP-A, CYP-B, CYP-C, USGS GXR-6
4	Milling test	ar-ICPMS data versus milling time	CYP-A, CYP-B
5	Sizing test	Milling time versus particle sizing	CYP-A, CYP-B
6	LOI test	Testing of LOI method	CYP-A, CYP-B, CYP-C
7	Digest test	Comparison of selected elements released under different digest conditions	CYP-A, CYP-B, CYP-C
8	Digest time test	Comparison of selected elements released under different digest times	CYP-A, CYP-B, CYP-C
9	Solid-liquid test	Comparison of XRF and INAA data for selected elements	CYP-A, CYP-B, CYP-C, USGS GXR-6, Synterm-12
10	Mixing ratio test	Testing of mixing ratios	CYP-A, CYP-B
11	XRF	XRF data	CYP-A, CYP-B, CYP-C, blanks
12	GXR-6	Percent of total extraction by ar-ICPMS	USGS GXR-6
13	Actlabs seq	Sequencing of Actlabs sub-batches	

Table 2.18 Structure of vegetation data spreadsheet.

Variable	Description	Units
Site	Field sample	
East	Easting (WGS84 Zone 36N)	m
North	Northing (WGS84 Zone 36N)	m
Spec	Species (Olive [*Olea europaea*]; Pine [*Pinus brutia*])	
Organ	Plant organ; leaves/needles, fruit	
Sub-site	**A-C** Mitsero Mine; **X-Z** Limni Mine; **Mat** Mathiatis Mine area; **Trav** Traverse from coast to Mathiatis Mine	
Ash %	Percent ash in organ sample	**%**
Ag _VEG	Ag by aqua regia (ashed sample) ICP-MS	mg/kg
etc	As by aqua regia (ashed sample) ICP-MS	mg/kg
Zr _VEG	B by aqua regia (ashed sample) ICP-MS	mg/kg

Table 2.19 Structure of selective extractions spreadsheet.

Variable	Description	Units
Site	Field site	
East	Easting (WGS84 Zone 36N)	m
North	Northing (WGS84 Zone 36N)	m
Type	Orientation or Mine Site	
Lvl	Sampling level: A = top 20 cm; B = 50 - 70 cm (nominal) depth	
Ag_ AAC	Ag by pH 5.5 ammonium acetate extraction ICP-MS	mg/kg
Ag_ HXL	Ag by pH 1 / 1M hydoxylamine.HCl extraction ICP-MS (post AAC)	mg/kg
Ag_ HXLt	Ag by AAC plus HXL	mg/kg
Ag_ AQR	Ag by aqua regia extraction ICP-MS	mg/kg
etc		
Zr_ AAC	Au by pH 5.5 ammonium acetate extraction ICP-MS	mg/kg
Zr_ HXL	Au by pH 1 / 1M hydoxylamine.HCl extraction ICP-MS (post AAC)	mg/kg
Zr_ HXLt	Au by AAC plus HXL	mg/kg
Zr_ INAA	Au by INAA	mg/kg

Table 2.20 Structure of XRD_data spreadsheet.

Variable	Description	Units
Seq	Data sequence	
Task file	XRD output file	
Site	Site number	
Lvl	Sampling level: A = top 25 cm; B = 50 - 75 cm (nominal) depth	
Line	Orientation line (1=ne-sw; 2=E-W)	
Station	Station along line	
Distance	Distance from end of line	m
Actinolite	XRD Actinolite based on SIROQUANT methods	%
etc		
Talc	XRD Talc based on SIROQUANT methods	%
Actinolite	Error of fit for Actinolite	%
etc		
Talc	Error of fit for Talc	%
Global χ^2	Chi-squared total error in model	
Quartz	Total Quartz	%
Carbonate	Total Carbonate	%
Feldspar	Total Feldspar	%
Ferro-mags	Total Ferromags	%
Kaolinite + illite	Total Kaolinite + illite	%
Montmorillonite	Total Montmorillonite	%
Talc	Total Talc	%
Other	Total Other	%

Figure 2.40 MapInfo shading for rock groups.

Rock Group	Colour		Foreground			Background			
	MI Code	Shading	Red	Green	Blue	Red	Green	Blue	Mapinfo instruction
alluvium-colluvium	34,16777104,10	34	255	255	144	0	0	0	"alluvium-colluvium" Symbol (34,16777104,10),
carbonates	34,8233120,10	34	125	160	160	0	0	0	"carbonates" Symbol (34,8233120,10),
limestone	34,33470,10	34	0	130	190	0	0	0	"limestone" Symbol (34,33470,10),
carbonates-clastics	34,11509880,10	34	175	160	120	0	0	0	"carbonates-clastics" Symbol (34,11509880,10),
silicic clastics	34,13472075,10	34	205	145	75	0	0	0	"silicic clastics" Symbol (34,13472075,10),
gypsiferous clastics	34,14448715,10	34	220	120	75	0	0	0	"gypsiferous clastics" Symbol (34,14448715,10),
carbonates-basalt	34,10503760,10	34	160	70	80	0	0	0	"carbonates-basalt" Symbol (34,10503760,10),
mafic clastics	34,11481625,10	34	175	50	25	0	0	0	"mafic clastics" Symbol (34,11481625,10),
basalt	34,15088705,10	34	230	60	65	0	0	0	"basalt" Symbol (34,15088705,10),
dolerite	34,16755400,10	34	255	170	200	0	0	0	"dolerite" Symbol (34,16755400,10),
gabbro	34,8220160,10	34	125	110	0	0	0	0	"gabbro" Symbol (34,8220160,10),
basalt-dol-gab	34,10849330,10	34	165	140	50	0	0	0	"basalt-dol-gab" Symbol (34,10849330,10),
metamorphics	34,9211020,10	34	140	140	140	0	0	0	"metamorphics" Symbol (34,9211020,10)
ultramafics	34,3317905,10	34	50	160	145	0	0	0	"ultramafics" Symbol (34,3317905,10),
serpentinites	34,3323060,10	34	50	180	180	0	0	0	"serpentinites" Symbol (34,3323060,10),

Table 2.21 List of geological formations of Cyprus and the assigned MapInfo code for colour and symbolling.

Formation	Age	Symbol	*MI Code*
Circum Troodos Sedimentary Succession			
Alluvium - Colluvium	Holocene	H	2,16777104,0
Terrace Deposits	Pleistocene	Q2	2,9210970,0
Fanglomerate	Pleistocene	Q1	2,16430240,0
Apalos - Athalassa - Kakkaristra	Pleistocene	Q	2,16425040,0
Nicosia	Pliocene	Pl	2,16773205,0
Kalavasos	Upper Miocene	Mu1	2,9529685,0
Pakhna	Miocene	Ml-Mu	2,8233120,0
Pakhna (Koronia Member)	Miocene	Mu	2,16107520,0
Pakhna (Terra Member)	Miocene	Ml	2,11842560,0
Lefkara	Palaeogene-Oligocene	Ku3-Ou	2,13816440,0
Kathikas	Upper Cretaceous	Ku3	2,15122130,0
Moni	Upper Cretaceous	Ku2	2,9217455,0
Kannaviou	Upper Cretaceous	Ku1	2,11178395,0
Salt lake	Holocene	Hs	2,14803425,0
Troodos Ophiolite			
Perapedhi	Upper Cretaceous	Ku	2,11481625,0
Upper Pillow Lavas	Upper Cretaceous	UPL	2,11808075,0
Lower Pillow Lavas	Upper Cretaceous	LPL	2,15088705,0
Basal Group	Upper Cretaceous	BG	2,10178640,0
Sheeted Dykes (Diabase)	Upper Cretaceous	Db	2,16755400,0
Plagiogranite	Upper Cretaceous	?	2,6238720,0
Gabbro	Upper Cretaceous	d	2,8220160,0
Pyroxenite	Upper Cretaceous	s4	2,9539940,0
Wehrlite	Upper Cretaceous	s3	2,6903040,0
Dunite	Upper Cretaceous	s2	2,8560690,0
Harzburgite	Upper Cretaceous	s1	2,3317905,0
Serpentinite	Upper Cretaceous	s	2,2656065,0
Arakapas Transform Sequence			
Pillow Breccias	Upper Cretaceous	Plb	2,2954260,0
Interlava Sediments	Upper Cretaceous	Vis(a)	2,13783155,0
Polymict Breccia	Upper Cretaceous	Vis(b)	48,0,13783155
Pillow Lavas	Upper Cretaceous	Lvs	2,13806300,0
Vitrophyric Pillow Lavas	Upper Cretaceous	Vpl	2,16422450,0
Isotropic Gabbros	Upper Cretaceous	I?	48,0,8220160
Isotropoc Wehrlites	Upper Cretaceous	Is3	48,0,6903040
Sheared Serpentinite	Upper Cretaceous	s_	48,0,2656065
Kyrenia			
Kythrea	Miocene	Mm	2,13472075,0
Kalogrea - Ardana	Oligocene-Lower Miocene	Ol-Ml	2,11832385,0
Lapithos	Upper Cretaceous-Eocene	Ku-Eu	2,12491740,0
Lapithos (B)	Upper Cretaceous-Eocene	Ku-Eu	2,12491740,0
Lapithos (R)	Upper Cretaceous-Eocene	Ku-Eu	2,12491740,0
Hilarion	Jurassic-Lower Cretaceous	Jl-Kl	2,8242150,0
Sykhari	Upper Triassic	Tu	2,8553150,0
Dhikomo	Lower Triassic	Tl-Tu	2,5603970,0
Kantara	Permo-Carboniferous	C-P	2,33470,0
Mammonia			
Ayia Varvara	Upper Cretaceous	Ku	2,6900605,0
Ayios Photios Group	Triassic-Mid Cretaceous	Tm- km	2,10826240,0
Dhiarizos Group	Triassic-Mid Cretaceous	Tm- km	2,16750110,0
Metamorphic Rocks	Upper Cretaceous	Sc	2,13448430,0

Table 2.22 Listing of rock types indicated in field tick books by the advisors and simplified rock groupings to be used in maps and statistical work. The digital field data logs have both datasets.

Rocktype (field notes)	**Rocktype (standardised)** *alluvm-colluvm*	*carbonate*	*limestone*	*carbonate-clastic*	*carbonate-basalt*	*silicic clastic*	*mafic clastic*	*gypsif' clastic*	*basalt*	*dolerite*	*gabbro*	*basalt-dol-gab*	*metamorphic*	*ultra-mafic*	*serpentinite*
alluvium	X														
colluvium	X														
Fe-rich_sands	X														
gravels	X														
silt-sand-gravel	X														
beach_sands	X														
calcarenite		X													
calcarenite-volcanic_seds		X													
calcrete		X													
calcsiltstone		X													
limestone			X												
calcarenite-chert				X											
calcarenite-limestone				X											
calcarenite-mudstone				X											
calcarenite-qtz_veins				X											
calcarenite-shale				X											
calcarenite-basalt					X										
chert						X									
glauconitic_sandstones						X									
glauconitic_siltstones						X									
micaceous_siltstone						X									
mudstone						X									
sandstone						X									
sandstone-siltstone						X									
shale						X									
siltstone						X									
siltstone-mudstone						X									
siltstone-sandstone						X									
basaltic colluv							X								
basaltic conglomerate							X								
basalt-sandstone							X								
basalt-shale							X								
mafic_colluvium							X								
mafic_sediments							X								
gypsiferous_calcarenite								X							
gypsiferous_mudstone								X							
gypsiferous_sandstone								X							
gypsiferous_siltstone								X							
basalt									X						
basalt (altered)									X						
basalt (chloritic)									X						
basalt (sulphidic)									X						
basalt-chert									X						
metabasalt									X						
pillow_basalt									X						
dolerite										X					
sheeted_dykes										X					
gabbro											X				
gabbro-dolerite											X				
basalt-dolerite												X			
basalt-gabbro												X			
gabbro-basalt												X			
amphibolite													X		
chloritic_schist													X		
schist													X		
dunite														X	
dunite-chromite														X	
harzburgite														X	
plagiogranite														X	
plagiogranite-dolerite														X	
pyroxenite														X	
pyroxenite-dunite														X	
pyroxenite-dunite-chromite														X	
pyroxenite-gabbro														X	
pyroxenite-wehrlite														X	
serpentinised_dunite															X
serpentinised_gabbro															X
serpentinised_harzbergite															X
serpentinised_pyroxenite-dunite															X
serpentinite															X

Table 2.23 Correlation between geological description for tick books and formation type indicated in the GSD digital geological map.

Rock_Group UNSW	alluvium-colluvium	calcarenite	calcarenite-clastic	calcarenites-gyp	clastic-mixed	limestone	basalt	basalt-dolerite	basalt-dol-gab	basalt-volcaniclastic	mafic volcs	volcaniclastic	volcaniclastic-bent	gabbro	metamorphic	ultramafic
alluvium-colluvium	730	111	257	6	12	17	50		21	2	1		3	1		8
carbonates	251	851	190	22	27	85	82		6	8	9	1	10	2		5
limestone	73	170	45	1	7	34	4			1			3			5
gypsiferous clastics	1	11	4	12												
carbonates-basalt	7	4	7	1	3	1	33		5	1			3			3
silicic clastics	93	229	143	23	20	10	11	3	6	5		1	15			8
mafic clastics	7	4	10		10		1		1	5	1		1			9
basalt	95	42	33	1	17	3	547	140	140	13	9	1	25	2		19
basalt-dol-gab	5					2	23		57					27		
dolerite	1	4	1		2		18	43	198		1			15	1	6
gabbro		6					4	5	48					54		11
metamorphics	3															2
ultramafics	1	1					2		1					5		73
serpentinite		1					1							2		53

Table 2.24 List of report and GAC numbers.

Number	Report
GAC01-2006	Manual of Sampling
GAC02-2006	First Progress Report
GAC03-2006	Manual of Analysis
GAC04-2007	Second Progress Report
GAC05-2008	Third Progress Report
GAC06-2008	QAQC Progress Report
GAC07-2009	Manual for Sample Preparation and Analysis
GAC08-2009	Fourth Progress Report
GAC09-2010	Fifth Progress Report
GAC10-2010	Final Technical Report
GAC11-2011	The Geochemical Atlas of Cyprus
GAC12-2008	Theses

Table 2.25 Digital Data Archive

Oct 2006	Feb 2008
Air Photos 1963	Amiandos-Paleochori geology (10k)
Air Photo Flights 1963	Ancient slags (5k)
Air Photos 1994	Aster (remote sensing) imagery
Air Photos Flights 1994	Copper mining centres (250k)
British Bases (50k)	Dams
Buffer Zone (50k)	DEM (25m 50k)
Built Up Areas (50k)	General Geology (25k)
Coastline (50k)	Geological memoir
Contours (50k)	Geological zones (500k)
Faults (250k)	Gossan areas
Geology (250k)	Hillshade (25m 50k)
Hydrogeology (250k)	Karapasia geology (31k)
Hydrological Regions (50k)	Landsat TM 5
Municipalities (5k)	Landsat TM 7
QuickBird 2003Index	Lefkosia bedrock geology (25k)
Rivers (50k)	Lefkosia surficial geology (25k)
Roads (50k)	Mining activities
Salt Lakes (5k)	Mining leases
Soils (250k)	Pafos Forestry and geology (10k)
Topo Maps (50k) Index	Parcel permits
Topo Maps (5k) Index	Pentadaktylos geology (50k)
Vegetation (250k)	Polis-Kathikas geology (31k)
Watershed (50k)	Quarry licenses
Quarry zones	
S Troodos TFZ geology (25k)	
Spot elevation (50k)	
Sulphide workings	
Trig Points (50k)	

3 QUALITY CONTROL

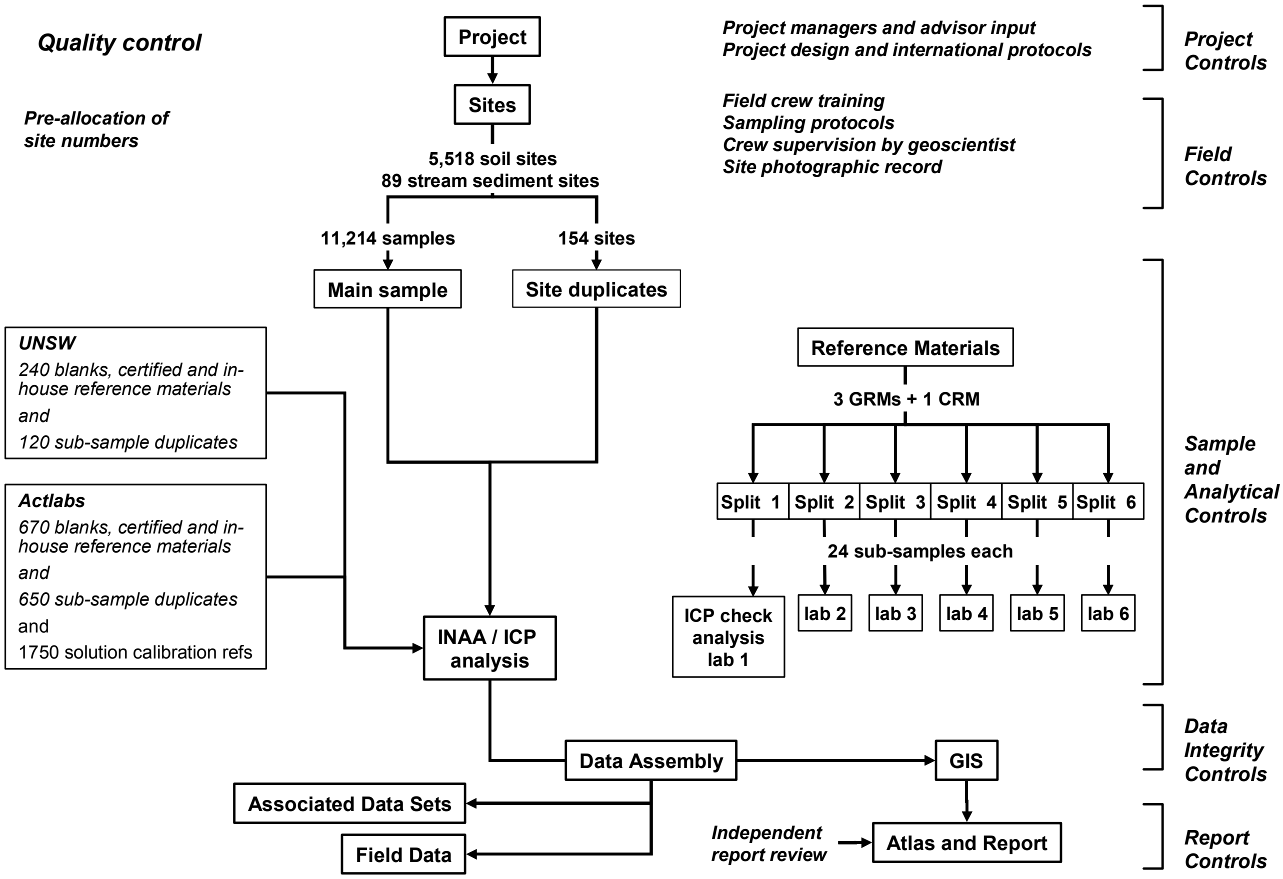

Figure 3.1 Outline of project quality control procedures.

Table 3.1 Summary of analytical and QC samples.

	ICP-MS	INAA
MAIN DATASET		
Total "unknown" samples ICP-MS / INAA	**11,482**	**11,482**
Quality control analyses		
CYP-A	56	56
CYP-B	61	61
CYP-C	53	53
USGS GXR-6	8	8
ORES100 A	179	
ORES47 P	194	
Till-1 to Till-4		244
UNSW blanks	55	57
Actlabs blanks	383	40
UNSW processing duplicates	119	121
Actlabs analytical duplicates	630	805
Total quality control analyses (main set)	**1,738**	**1,445**
SPECIAL SAMPLES ANALYSIS		
Ammonium acetate	472	
Hydroxylamine	704	
Aqua regia	168	
Total special analyses	**1,344**	
Total quality control analyses (special set)	**107**	
Total samples	12,836	11,482
Total quality control samples	1,845	1,445
TOTAL ANALYSES	**14,681**	**12,927**

Table 3.2 Proportion of quality control samples in analytical program.

Type	**Geochemical Atlas of Cyprus**		**FOREGS project**	**NASGLP project**
	ICP-MS (aqua regia and selective extractions)	*INAA*	*Various*	*ICP-MS (4-acid)*
Reference materials	5.2%#	4.3%	~2%	6%
Inter-laboratory comparisons	0.2%^	-	~8%	-
Duplicates (at various scales of sampling)	6.9%	7.2%	~5%	4%
Total	**12.3%**	**11.5%**	**~15%**	**10%**

excluding blanks and other reference materials used by Actlabs to monitor instrumental drift.
^ as part of round-robin to determined expected values for project-specific in-house reference materials and check of Actlabs method precision.

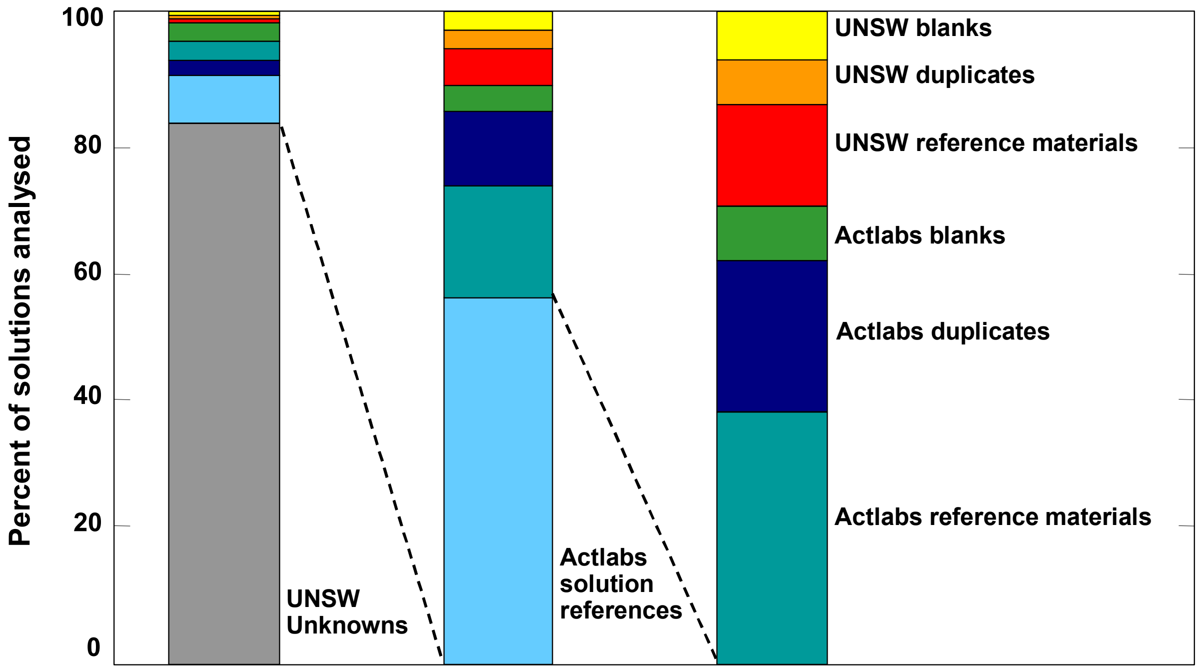

Figure 3.2 Relative percentages of quality control samples within the total analytical program.

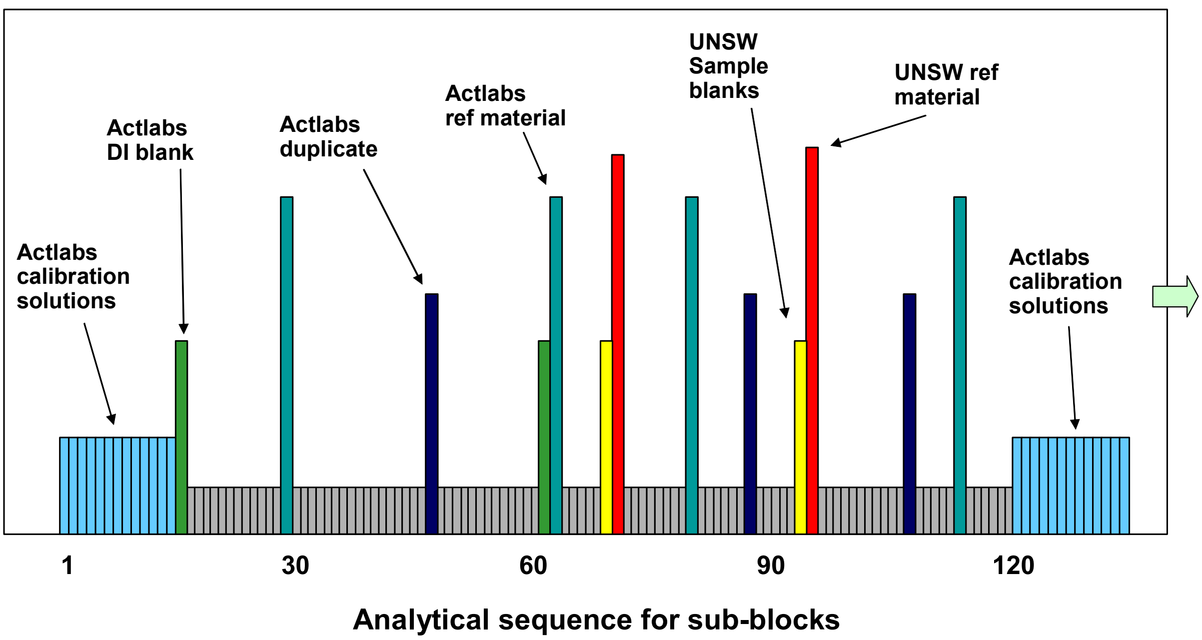

Figure 3.3 Analytical sequence QC samples for each sub-block of 180 samples.

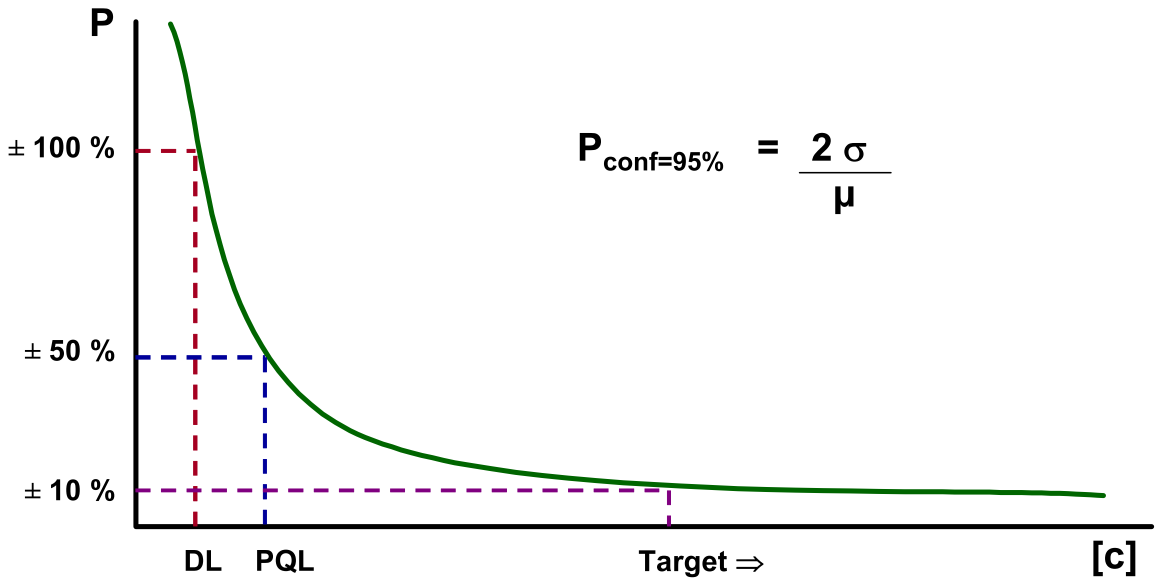

Figure 3.4 Typical relationship between precision (P) and concentration (c).

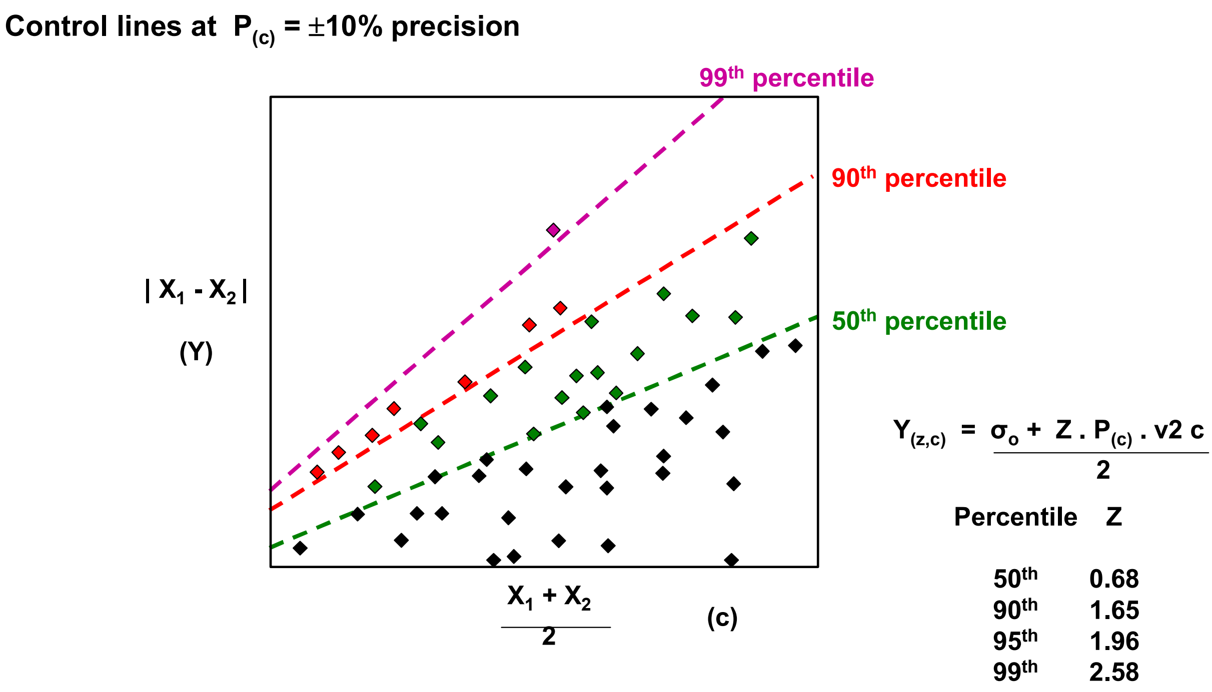

Figure 3.5 Thompson-Howarth plots of absolute difference between duplicates versus mean duplicate value showing fitting of probability lines for a chosen precision level.

Table 3.3 Summary of analytical round-robin ICP-MS results.

(a) Elements where the Actlabs analyses were statistically equivalent to the other six laboratories (ALS-Chemex Brisbane, ALS-Chemex Vancouver, SGS Toronto, Genalysis Perth, Acme Vancouver and UNSW AC).

Ag	Co	Eu	La	Nb	Sr	U	Zr
Al	Cr	Gd	Li	Ni	Tb	V	
Ba	Cs	Ge	Lu	Rb	Te	W	
Be	Cu	Ho	Mg	Sb	Ti	Y	
Cd	Dy	In	Mo	Sc	Tl	Yb	
Ce	Er	K	Na	Sm	Tm	Zn	

(b) Elements displaying variations between Actlabs values and one or more of the remaining six laboratories.

B	All labs except Actlabs report B at detection limits of 10 or 20 ppm. The capacity of Actlabs to detect B is related to their use of non borosilicate glass digestion tubes and longer flushing times in the ICP solution tubes.
Bi	Actlabs values are significantly higher than for the other labs. This may be attributed to the generally immobility of Bi and the soaking for some hours in HCl. Values are within 5x detection limit.
Ca	Actlabs values are slightly higher than for the other laboratories – see Bi. This is also attributed to the Actlabs digestion procedure delivering slightly higher extraction of Ca from clays.
Fe	Actlabs values are significantly higher than for the other labs (~20%) in the basaltic soil (CYP-A) and ultramafic soil (CYP-C) GRMs in which there is magnetite and other resistate Fe phases present. This is attributed to the kinetics of Fe extraction from those phases and the soaking for some hours in HCl.
Ga	Actlabs is consistently but marginally lower than other labs. This is attributed to the more complex and robust calibration method used by Actlabs
Hg	It is difficult to assess due to the high DL used by the other labs. The only other lab with low DL (Lab 3) has similar values to Actlabs.
Mn	As for Fe, Mn values are slightly higher than other labs but is a function of longer digestion times
P	As for Fe and Mn, P values are slightly higher than other labs but is a function of longer digestion times
Pb	As for Fe, Mn values are slightly higher than other labs but this is a function of longer digestion times. Pb is also likely to be mostly associated with the products of alumino-silicate weathering than Fe oxides in Cyprus.
Sn	Actlabs values are slightly low for CYP-C but similar for the other GRMs
Th	Actlabs values are slightly lower than the other labs
As	Actlabs values are slightly low for CYP-C but similar for the other GRMs
Se	Actlabs value are low, however their procedure for calibration limits the problem of the mass interference corrections for Se.
Ta	Detection limits are too high to evaluate

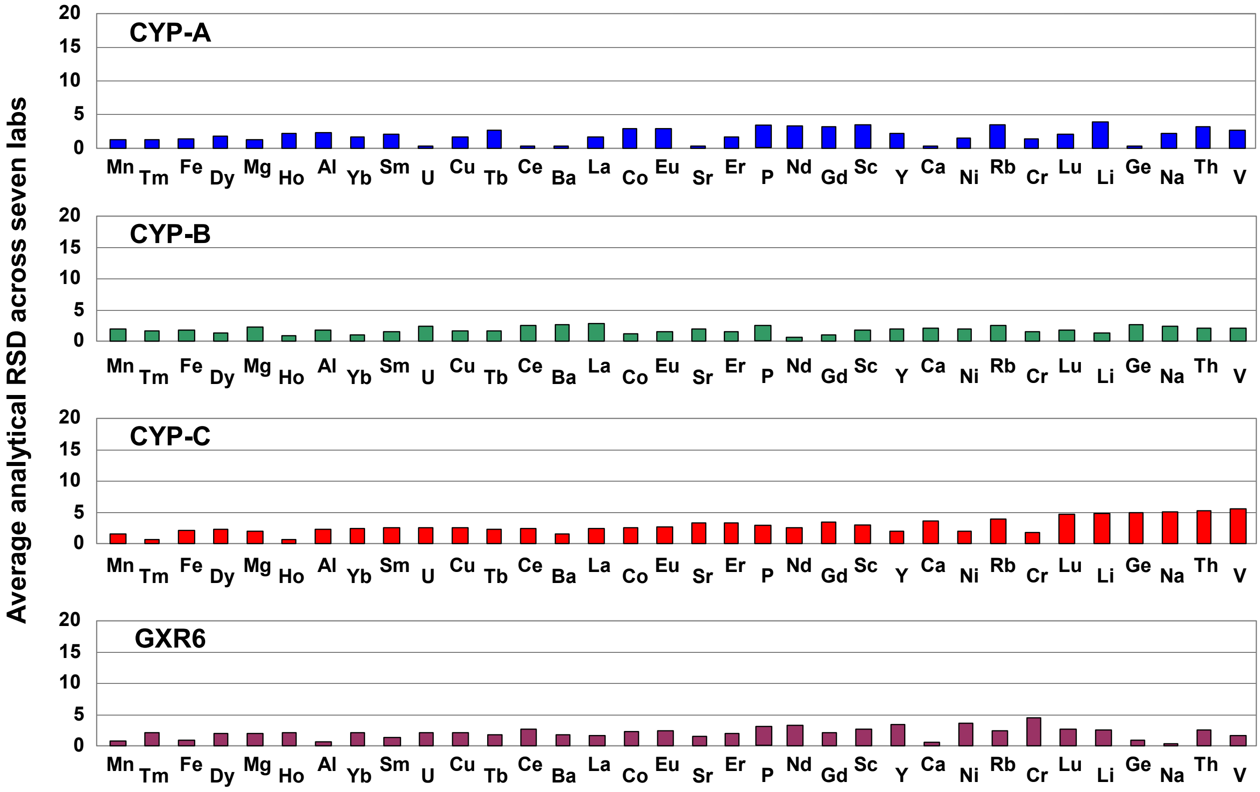

Figure 3.6 Average RSDs (based on triplicate analyses) for elements on reference materials for the seven commercial laboratories.

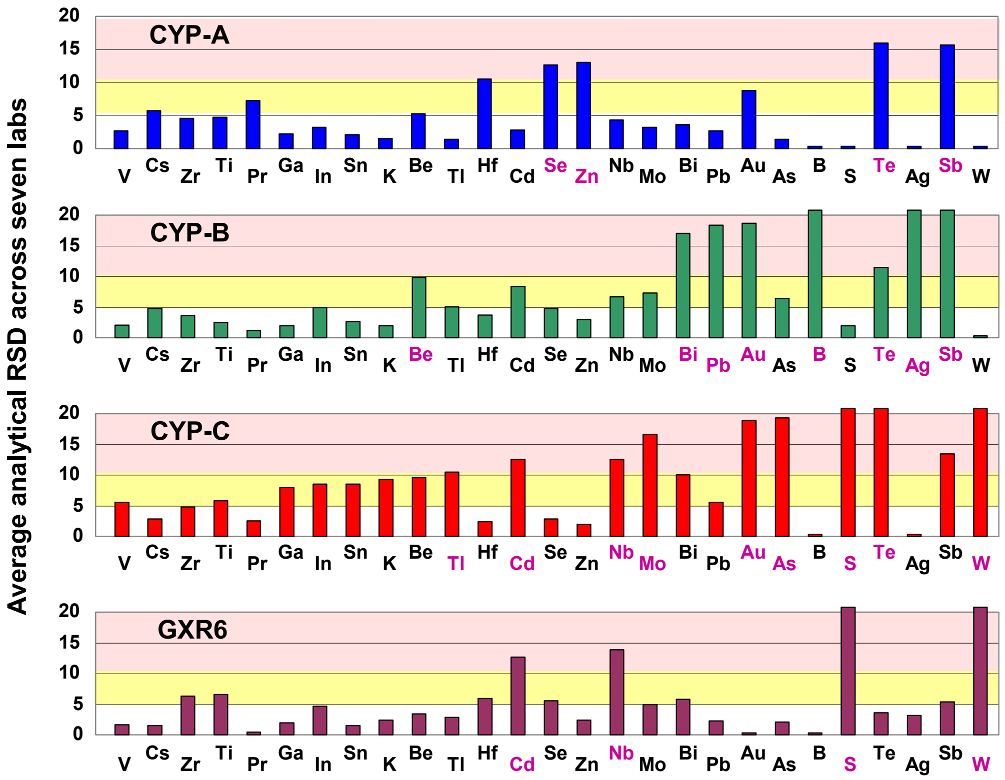

Figure 3.7 Average RSDs (based on triplicate analyses) on reference materials for the seven commercial laboratories, for elements where at least one reference material displayed an RSD > 5%.

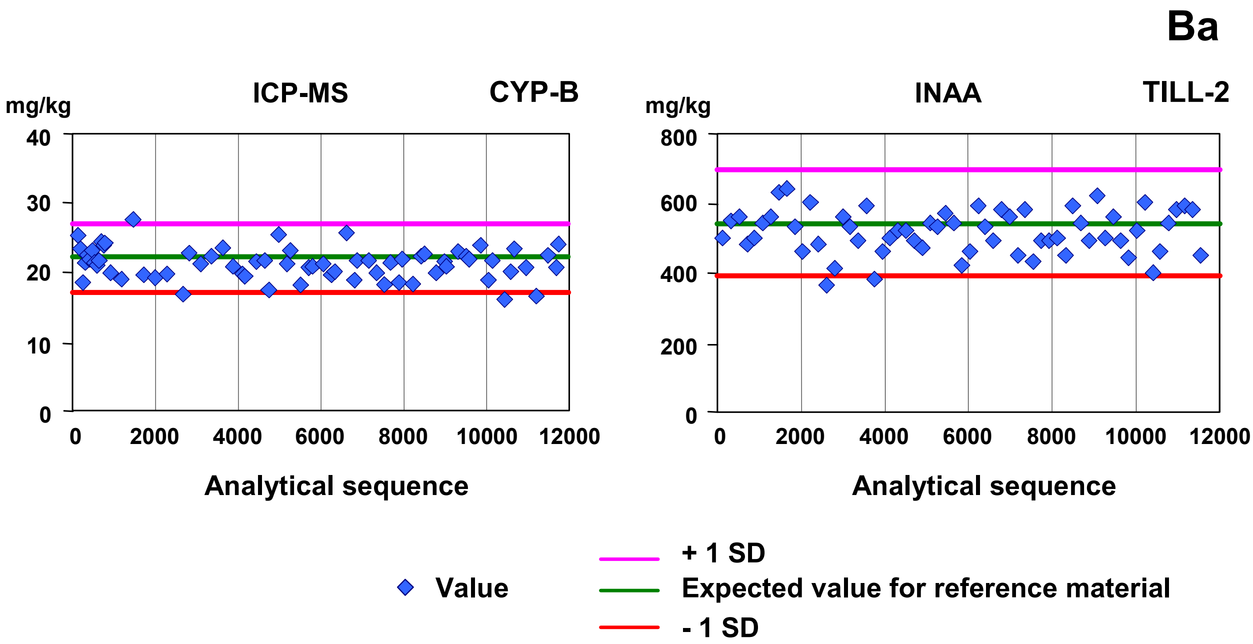

Figure 3.8 Example of analytical control charts.

Reference material
Specified by Actlabs
Analysis of all samples of reference material
Determine if **rec**ommended or **cert**ified value is within the range **analytical mean ± standard dev**
Difference between rec / cert value and analytical mean
Comparison of analytical mean with rec or cert value in relation to DQOs set
If either "OK" then **Accept** DQO

CYP-A	**Ag ICPMS** mg/kg	**Al ICPMS** %	**As ICPMS** mg/kg	**Ba ICPMS** mg/kg
Detection limits	*0.003*	*0.01*	*0.1*	*0.5*
Mean	0.011	0.66	1.9	1182.9
Standard deviation	0.010	0.10	0.3	85.6
Rec / cert value	0.013	0.71	1.7	1205.0
Rec vs mean ± 1SD	OK	OK	OK	OK
Abs % diff from Mean	17.2	6.3	8.9	1.9
Mean / DL	4	66	19	2366
Mean vs rec/cert value	OK	OK	High	OK
Decision	**Accept**	**Accept**	**Accept**	**Accept**

Figure 3.9 Structure of the reference materials summary tables and DQO decisions in Appendix 9.10.

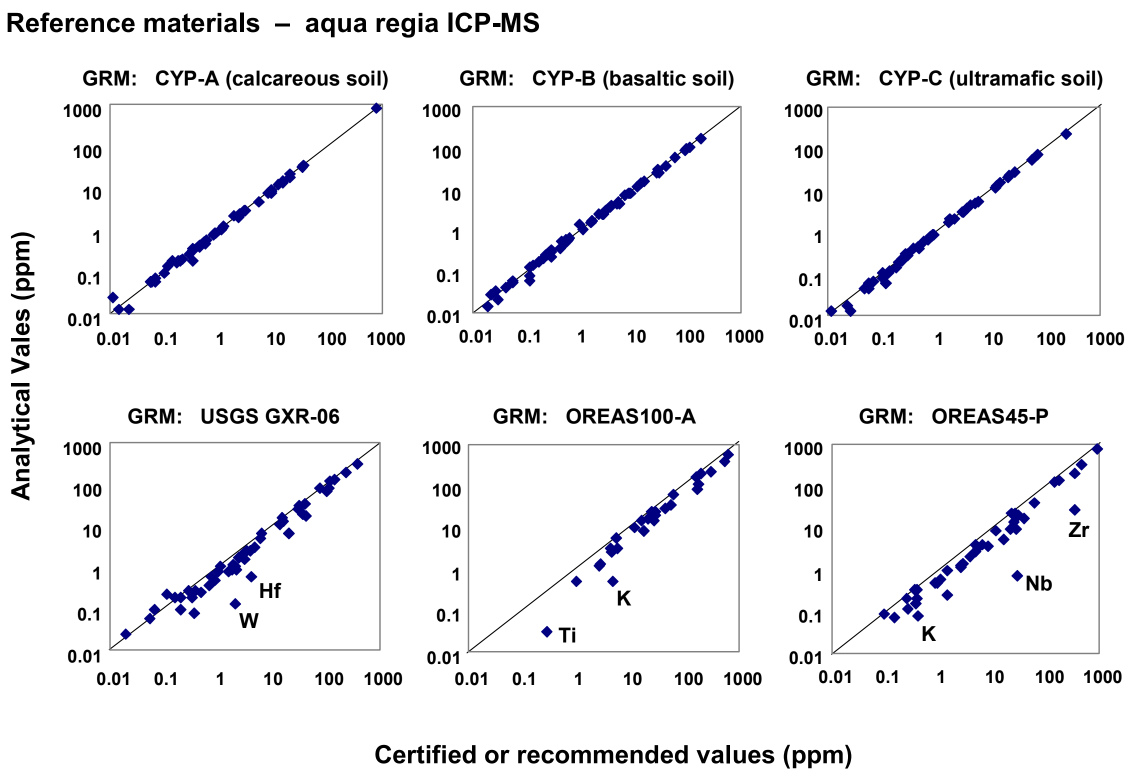

Figure 3.10 Plot of average analytical value versus certified or recommended values for all elements for six GRMs used during ICP-MS analysis program at Actlabs. Data based on 8 analyses of GXR-06 and >50 analyses of the other reference materials.

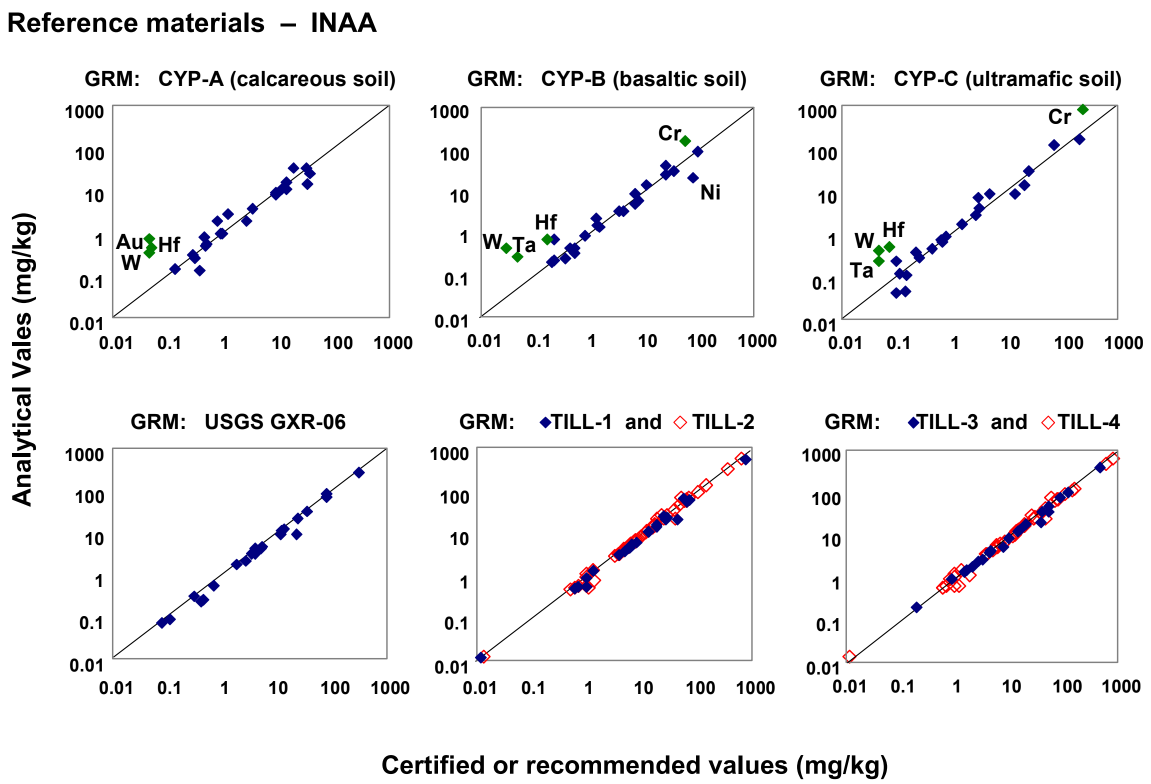

Figure 3.11 Plot of average analytical value versus certified or recommended values for all elements for six GRMs used during INAA analysis program at Actlabs. Data based on 8 analyses of GXR-06 and >50 analyses of the other reference materials.

INAA versus XRF

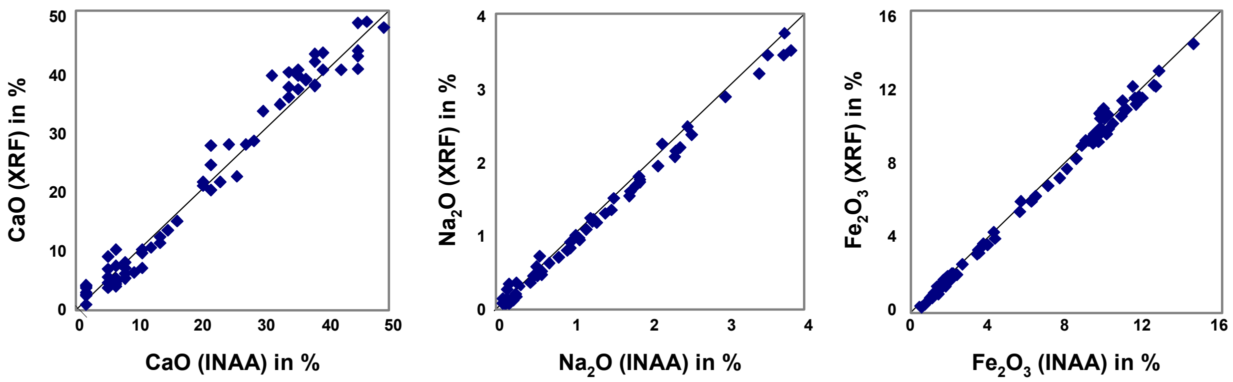

Figure 3.12 XRF versus INAA for selected elements.

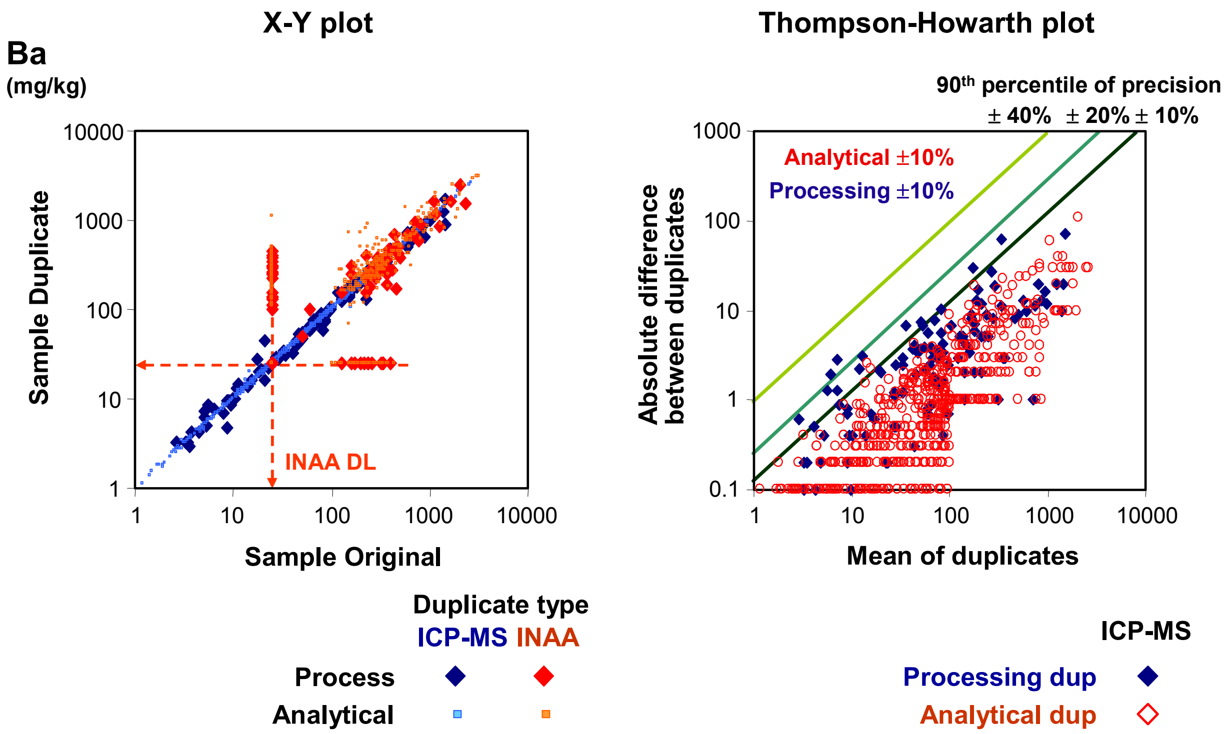

Figure 3.13 Examples of duplicate analysis scatter plots and associated Thompson-Howarth plots with the 90th percentiles plotted for precision control lines of 10, 20 and 40%.

Table 3.4 Actlabs analytical detection limits (DLs) and practical quantification limits (PQLs) which combine the effects of detection limits with natural sample variability and processing errors at the scale of the analytical sub-samples.

ICP-MS			
Element	**Units**	**Actlabs Analytical DL**	**Method DL**
Ag	mg/kg	0.002	0.004
Al	%	0.01	0.01
As	mg/kg	0.1	0.3
B	mg/kg	1	1
Ba	mg/kg	0.5	0.5
Be	mg/kg	0.1	0.1
Bi	mg/kg	0.02	0.02
Ca	%	0.01	0.01
Cd	mg/kg	0.01	0.01
Ce	mg/kg	0.01	0.01
Co	mg/kg	0.1	0.1
Cr	mg/kg	0.5	0.5
Cs	mg/kg	0.02	0.04
Cu	mg/kg	0.01	0.01
Dy	mg/kg	0.1	0.1
Er	mg/kg	0.1	0.3
Eu	mg/kg	0.1	0.1
Fe	%	0.01	0.01
Ga	mg/kg	0.02	0.02
Gd	mg/kg	0.1	0.2
Ge	mg/kg	0.1	0.2
Hf	mg/kg	0.1	0.1
Hg	mg/kg	0.01	0.01
Ho	mg/kg	0.1	0.1
In	mg/kg	0.02	0.05
K	%	0.01	0.01
La	mg/kg	0.5	0.5
Li	mg/kg	0.1	0.1
Lu	mg/kg	0.1	0.1
Mg	%	0.01	0.01
Mn	mg/kg	1	1
Mo	mg/kg	0.01	0.04

ICP-MS			
Element	**Units**	**Actlabs Analytical DL**	**Method DL**
Na	%	0.001	0.005
Nb	mg/kg	0.1	0.3
Nd	mg/kg	0.02	0.02
Ni	mg/kg	0.1	0.1
P	%	0.01	0.01
Pb	mg/kg	0.01	0.01
Pr	mg/kg	0.1	0.2
Pt	ug/kg	0.002	0.002
Rb	mg/kg	0.1	0.2
Re	mg/kg	0.001	0.003
Sb	mg/kg	0.02	0.04
Sc	mg/kg	0.1	0.1
Se	mg/kg	0.1	0.1
Sm	mg/kg	0.1	0.1
Sn	mg/kg	0.2	0.2
Sr	mg/kg	0.5	0.5
Ta	mg/kg	0.05	0.05
Tb	mg/kg	0.1	0.5
Te	mg/kg	0.02	0.02
Th	mg/kg	0.1	0.3
Ti	mg/kg	1	1
Tl	mg/kg	0.02	0.06
Tm	mg/kg	0.1	0.4
U	mg/kg	0.1	0.3
V	mg/kg	1	5
W	mg/kg	0.1	0.3
Y	mg/kg	0.01	0.04
Yb	mg/kg	0.1	0.1
Zn	mg/kg	0.1	1
Zr	mg/kg	0.1	0.1

INAA			
Element	**Units**	**Actlabs Analytical DL**	**Method DL**
Ag	mg/kg	5	5
As	mg/kg	0.5	2
Au	mg/kg	0.002	0.002
Ba	mg/kg	50	200
Br	mg/kg	0.5	2
Ca	%	1	2
Ce	mg/kg	3	3
Co	mg/kg	1	1
Cr	mg/kg	5	5
Cs	mg/kg	1	1
Eu	mg/kg	0.2	1
Fe	%	0.01	0.01
Hf	mg/kg	1	1
Hg	mg/kg	1	1
Ir	mg/kg	0.005	0.005
La	mg/kg	0.5	2
Lu	mg/kg	0.05	0.05
Mo	mg/kg	1	1
Na	%	0.01	0.01
Nd	mg/kg	5	5
Ni	mg/kg	20	50
Rb	mg/kg	15	50
Sb	mg/kg	0.1	0.4
Sc	mg/kg	0.1	0.1
Se	mg/kg	3	3
Sm	mg/kg	0.1	0.1
Sn	mg/kg	200	200
Sr	mg/kg	500	500
Ta	mg/kg	0.5	0.5
Tb	mg/kg	0.5	0.5
Th	mg/kg	0.2	0.5
U	mg/kg	0.5	2
W	mg/kg	1	1
Yb	mg/kg	0.2	0.2
Zn	mg/kg	50	150

Table 3.5 Comparative detection limits (this study and FOREGS) and RSDs on duplicates (this study).

Element	Units	This Study			FOREGS		This Study							
		INAA	XRF	ar-ICPMS	Total (XRF or ICP-MS)	ar-ICPMS	INAA sample prep	INAA analyt.	INAA sample prep	INAA analyt.	ar-ICPMS sample prep	ar-ICPMS analyt.	ar-ICPMS sample prep	ar-ICPMS analyt.
		Detection Limits					Global means on duplicates		Global RSDs on duplicates (%)		Global means on duplicates		Global RSDs on duplicates (%)	
Ag	mg/kg	5	n/a	0.002	0.01	n/a	5.0	5.0	0.0	4.8	0.08	0.04	26.8	2.8
Al / Al_2O_3	%	n/a	0.01	0.01	0.05	n/a					2.01	1.96	6.7	1.9
As	mg/kg	0.5	n/a	0.1	0.2	5	9.3	6.8	22.8	20.7	8.69	4.71	16.2	2.0
Au	ug/kg	0.002	n/a	n/a	n/a	n/a	21.4	5.5	110.4	95.1				
B	mg/kg	n/a	n/a	1	n/a	n/a					1.48	1.68	76.2	19.4
Ba	mg/kg	50	n/a	0.5	5	1	236.8	205.2	49.2	45.8	187.6	168.9	4.2	2.8
Be	mg/kg	n/a	n/a	0.1	2	n/a					0.34	0.33	31.1	8.9
Br	mg/kg	0.5	n/a	n/a	n/a	n/a	10.4	11.8	12.9	16.3				
Bi	mg/kg	n/a	n/a	0.02	0.5	n/a					0.10	0.09	12.4	9.0
Ca / CaO	%	1	0.01	0.01	0.01	n/a	12.8	12.9	11.4	11.3	12.2	11.8	6.7	2.1
Cd	mg/kg	n/a	n/a	0.01	0.01	n/a					0.31	0.27	20.3	4.3
Ce	mg/kg	3	n/a	0.01	0.15	n/a	21.6	23.3	17.4	10.7	11.9	13.1	10.8	2.2
Co	mg/kg	1	n/a	0.1	3	1	27.1	29.0	8.2	7.2	21.4	21.8	4.9	2.0
Cr	mg/kg	5	n/a	0.5	3	1	403.5	452.5	9.0	13.0	63.3	71.8	11.9	2.3
Cs	mg/kg	1	n/a	0.02	0.5	n/a	1.3	1.3	67.7	49.4	0.36	0.41	13.2	4.6
Cu	mg/kg	n/a	n/a	0.01	0.01	1					152.4	71.9	15.5	1.6
Dy	mg/kg	n/a	n/a	0.1	0.1	n/a					1.89	1.89	7.8	2.2
Er	mg/kg	n/a	n/a	0.1	0.1	n/a					1.08	1.09	9.2	2.9
Eu	mg/kg	0.2	n/a	0.1	0.05	n/a	0.7	0.7	20.8	19.6	0.47	0.49	11.5	5.0
Fe / Fe_2O_3	%	0.01	0.01	0.01	0.01	0.002	4.5	4.5	3.9	3.2	3.61	3.62	9.6	2.3
Ga	mg/kg	n/a	n/a	0.02	0.2	n/a					5.25	5.34	13.3	2.8
Gd	mg/kg	n/a	n/a	0.1	0.1	n/a					2.39	2.42	8.5	2.3
Ge	mg/kg	n/a	n/a	0.1	n/a	n/a					0.07	0.07	94.9	13.5
Hf	mg/kg	1	n/a	0.1	0.2	n/a	1.5	1.8	42.6	30.9	0.11	0.12	28.1	13.1
Hg	mg/kg	1	n/a	0.01	0.0001	n/a	0.5	0.5	0.0	27.2	0.04	0.03	67.3	8.8
Ho	mg/kg	n/a	n/a	0.1	0.02	n/a					0.39	0.41	12.1	6.4
I	mg/kg	n/a	n/a	n/a	2	n/a								
In	mg/kg	n/a	n/a	0.02	0.01	n/a					0.03	0.03	27.0	8.6
Ir	ug/kg	0.005	n/a	n/a	n/a	n/a	3.0	3.0	0.0	28.1				
K	%	n/a	n/a	0.01	n/a	n/a					0.22	0.23	16.0	2.9
La	mg/kg	0.5	n/a	0.5	n/a	n/a	11.3	11.8	9.2	5.6	7.17	7.69	7.0	2.5
Li	mg/kg	n/a	n/a	0.1	n/a	n/a					9.05	8.83	25.2	3.1
Lu	mg/kg	0.05	n/a	0.1	0.02	n/a	0.3	0.3	20.0	21.9	0.14	0.14	20.8	11.6
Mg / MgO	%	n/a	0.01	0.01	0.01	n/a					1.25	1.27	14.0	2.2
Mn / MnO	mg/kg	n/a	0.01	1	10	10					1040	972	5.6	1.7
Mo	mg/kg	1	n/a	0.01	0.1	n/a	1.7	1.2	182.8	147.4	1.01	0.90	15.6	7.3
Na / Na_2O	%	0.01	n/a	0.001	0.01	n/a	0.8	0.7	7.0	4.2	0.27	0.25	38.9	5.2
Nb	mg/kg	n/a	n/a	0.1	0.1	n/a					0.19	0.24	31.6	10.1
Nd	mg/kg	5	n/a	0.02	0.15	n/a	9.2	9.7	35.1	36.1	6.51	6.70	10.6	3.0
Ni	mg/kg	20	n/a	0.1	2	2	129.4	164.8	42.4	44.4	110	132	13.0	5.4
P_2O_5	%	n/a	0.01	n/a	0.001	n/a								
Pb	mg/kg	n/a	n/a	0.01	3	3					10.3	7.1	40.5	2.5
Pr	mg/kg	n/a	n/a	0.1	0.1	n/a					1.59	1.67	9.2	3.3
Pt	ug/kg	n/a	n/a	0.002	n/a	n/a					1.99	1.49	56.6	40.8
Rb	mg/kg	15	n/a	0.1	2	n/a	30.8	36.0	188.6	222.0	8.24	8.95	18.7	3.2
Re	mg/kg	n/a	n/a	0.001	n/a	n/a					0.002	0.002	55.2	25.8
S	mg/kg	n/a	n/a	n/a	n/a	50								
Sb	mg/kg	0.1	n/a	0.02	0.02	n/a	0.8	0.5	34.0	38.4	0.50	0.29	20.7	4.2
Sc	mg/kg	0.1	n/a	0.1	0.5	n/a	19.0	18.3	6.8	3.7	11.4	11.0	17.0	4.1
Se	mg/kg	3	n/a	0.1	n/a	n/a	2.3	2.2	19.4	14.1	0.84	0.54	41.6	10.3
SiO_2	%	n/a	0.01	n/a	0.1	n/a								
Sm	mg/kg	0.1	n/a	0.1	0.1	n/a	2.3	2.4	14.1	10.5	1.67	1.71	9.5	3.0
Sn	mg/kg	200	n/a	0.2	2	n/a	100.8	101.8	0.0	37.4	0.87	0.64	29.1	8.8
Sr	mg/kg	500	n/a	0.5	2	n/a	386.4	412.1	37.1	31.6	333	308	10.8	2.2
Ta	mg/kg	0.5	n/a	0.05	0.05	n/a	0.4	0.4	113.9	81.9	0.03	0.03	0.0	0.9
Tb	mg/kg	0.5	n/a	0.1	0.02	n/a	0.4	0.4	50.1	45.4	0.30	0.31	11.5	6.5
Te	mg/kg	n/a	n/a	0.02	0.02	n/a					0.08	0.05	42.8	9.5
Th	mg/kg	0.2	n/a	0.1	0.1	n/a	2.5	2.6	18.3	15.8	1.16	1.26	16.2	6.0
Ti / TiO_2	mg/kg	n/a	0.01	1	0.001	n/a					0.09	0.09	34.1	14.5
Tl	mg/kg	n/a	n/a	0.02	0.01	n/a					0.16	0.10	12.5	5.7
Tm	mg/kg	n/a	n/a	0.1	0.02	n/a					0.15	0.15	16.0	9.2
U	mg/kg	0.5	n/a	0.1	0.1	n/a	1.1	1.0	46.3	44.5	0.58	0.63	38.5	5.3
V	mg/kg	n/a	n/a	1	0.5	1					101	95	10.9	3.3
W	mg/kg	1	n/a	0.1	5	n/a	0.6	0.8	113.5	76.8	0.10	0.34	22.1	28.7
Y	mg/kg	n/a	n/a	0.01	3	n/a					10.56	10.94	10.2	1.9
Yb	mg/kg	0.2	n/a	0.1	0.05	n/a	1.9	1.9	10.4	9.9	0.99	0.98	7.6	3.1
Zn	mg/kg	50	n/a	0.1	3	1	122.5	85.2	42.0	52.3	86.3	54.3	34.1	1.8
Zr	mg/kg	n/a	n/a	0.1	3	n/a					4.53	4.65	20.8	3.9

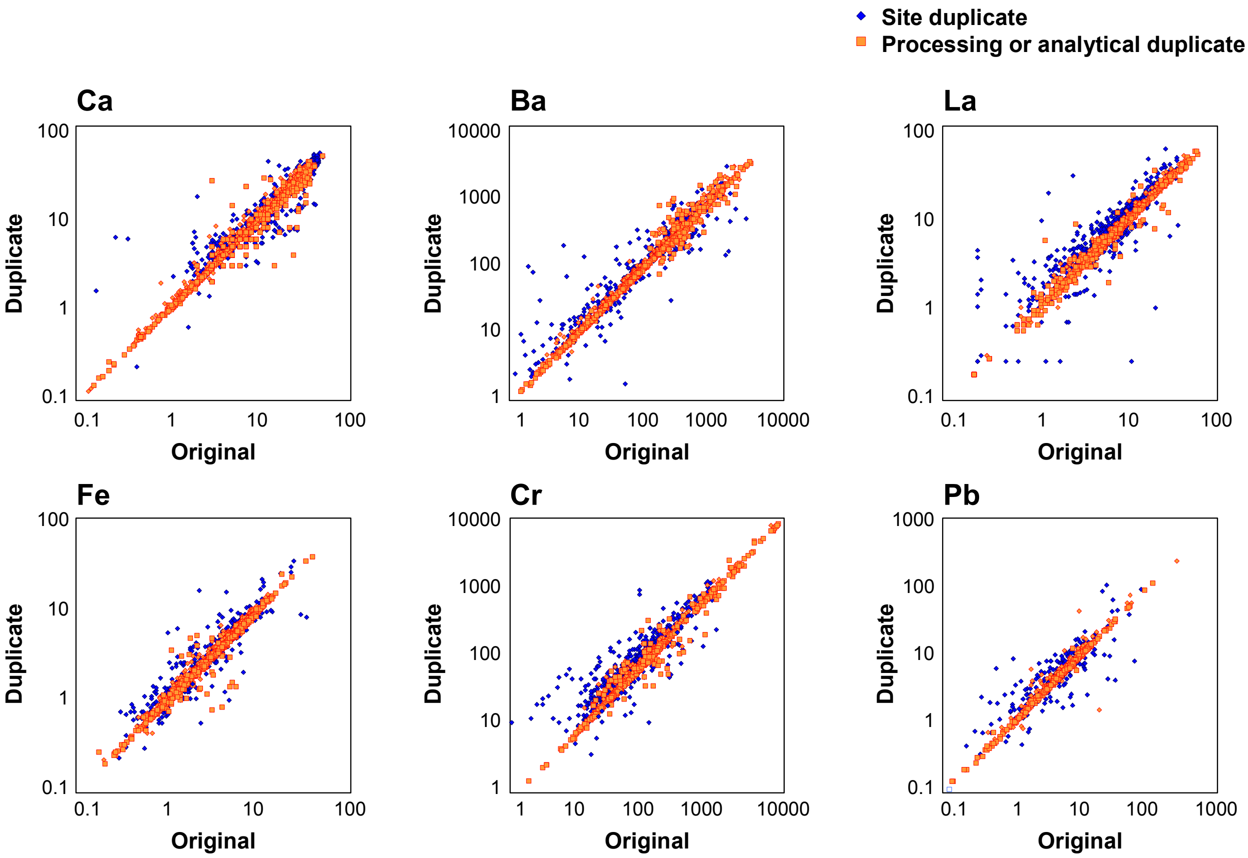

Figure 3.14 Comparison between analytical or processing duplicates (■) and site duplicates (◆).

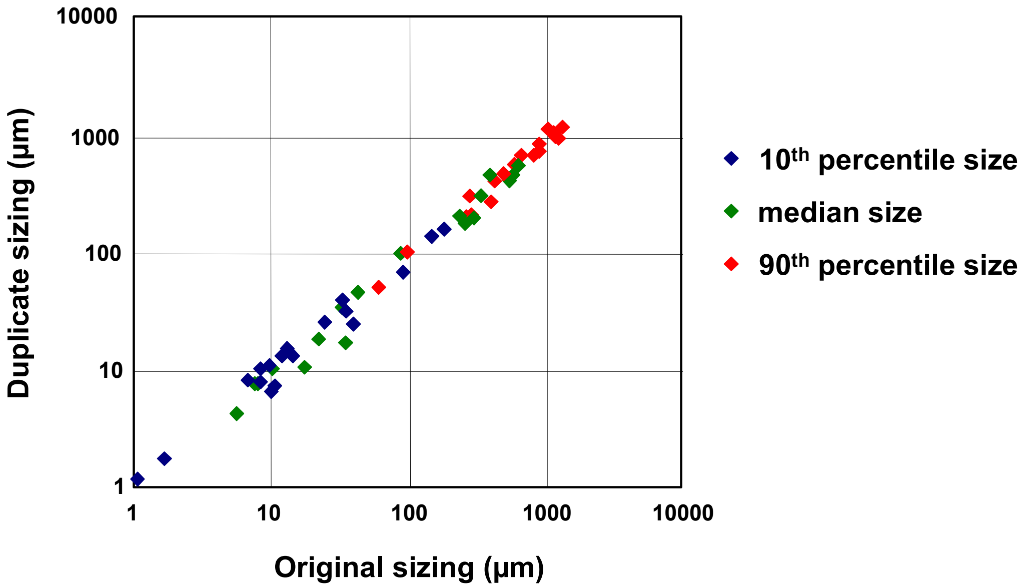

Figure 3.15 Particle sizing duplicates.

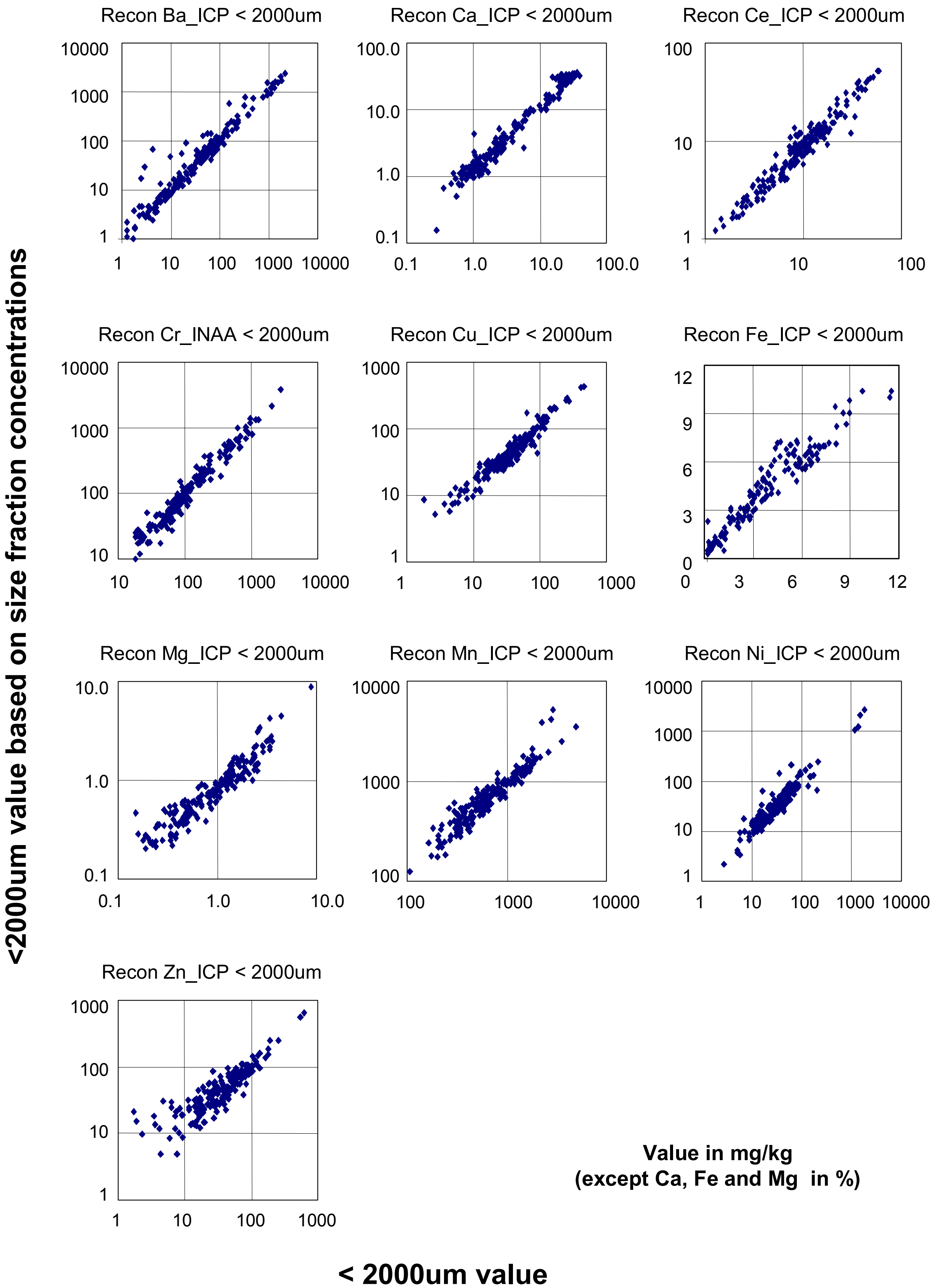

Figure 3.16 Reconstituted bulk sample (<2000um) geochemistry based on analytical values and weight proportions of component fractions.

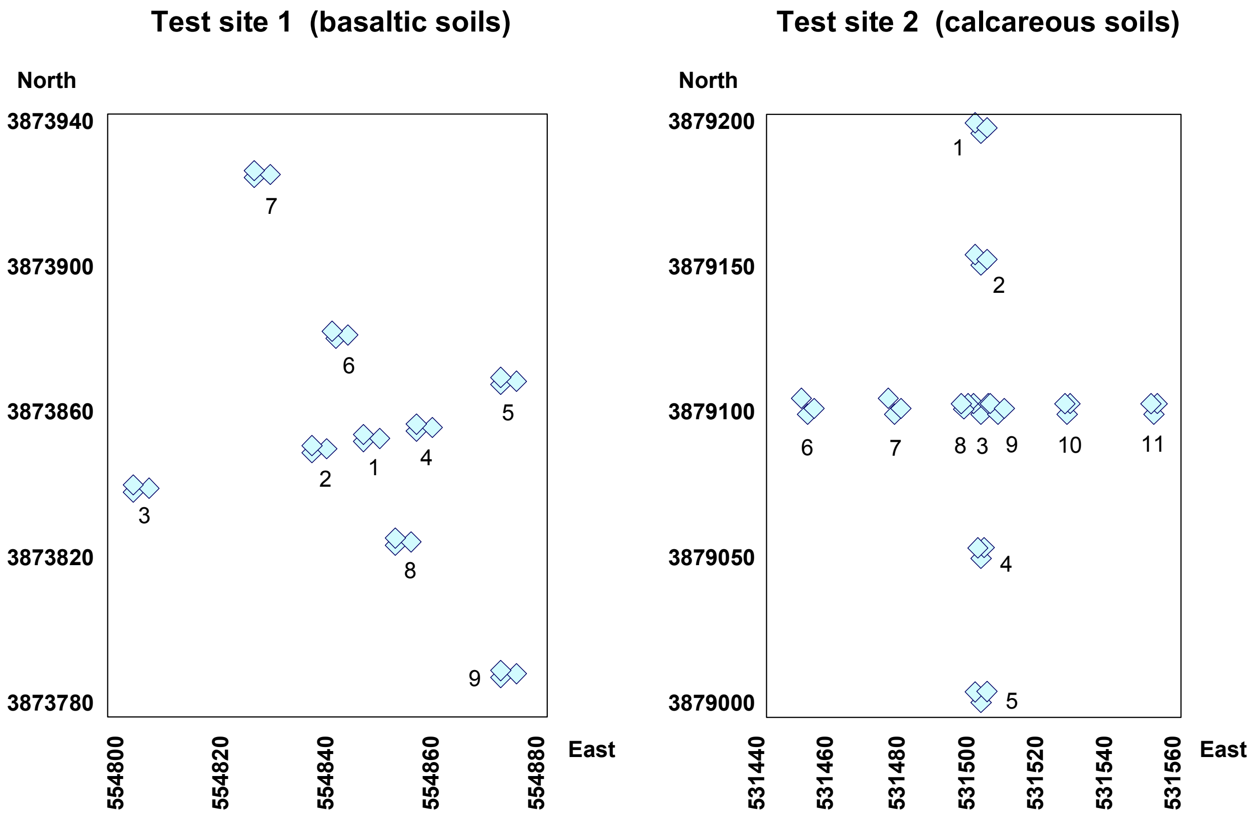

Figure 3.17 Test site layout showing the 9 or 11 sets of three sub-site duplicates.

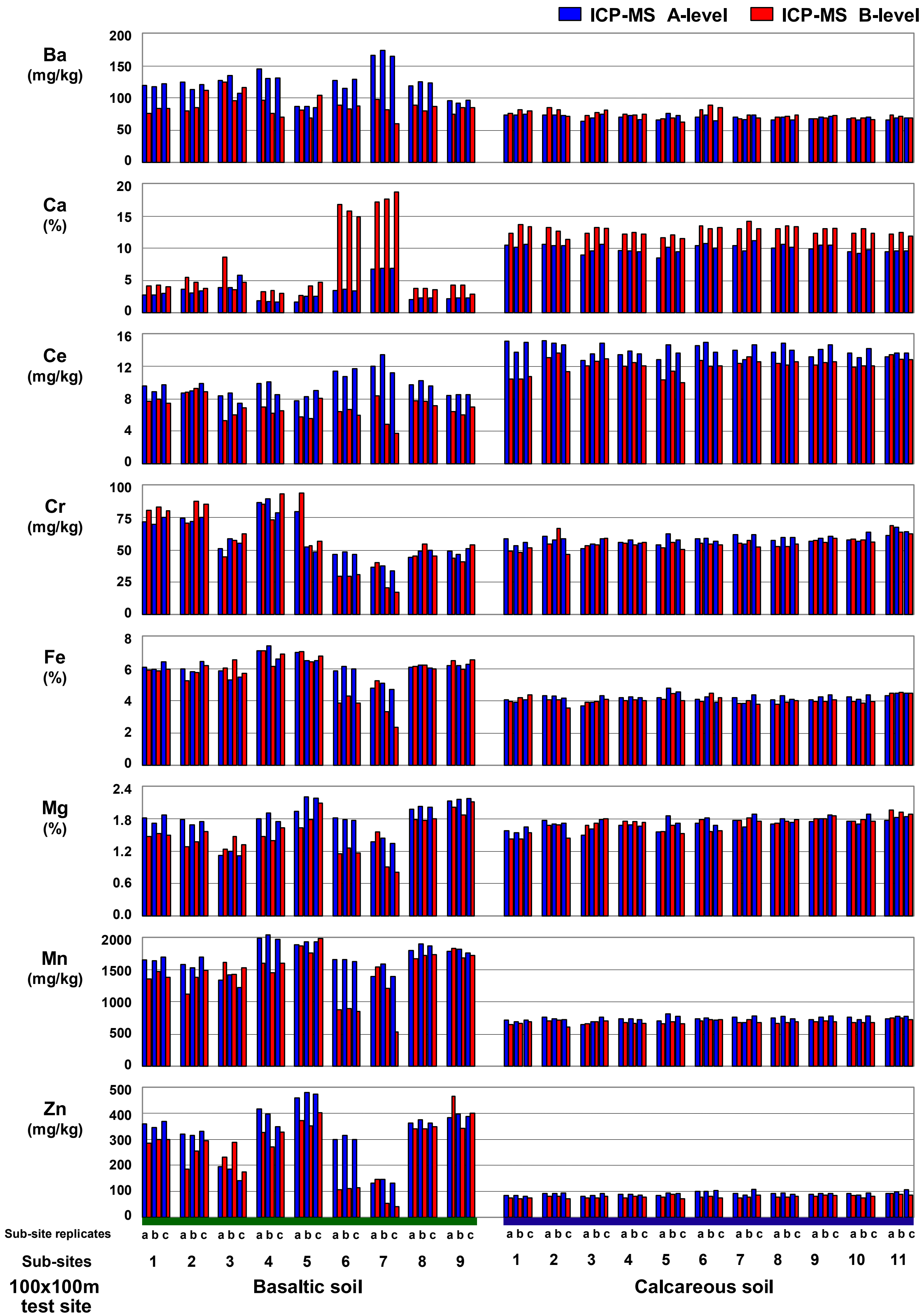

Figure 3.18 Variation between test site samples for selected elements.

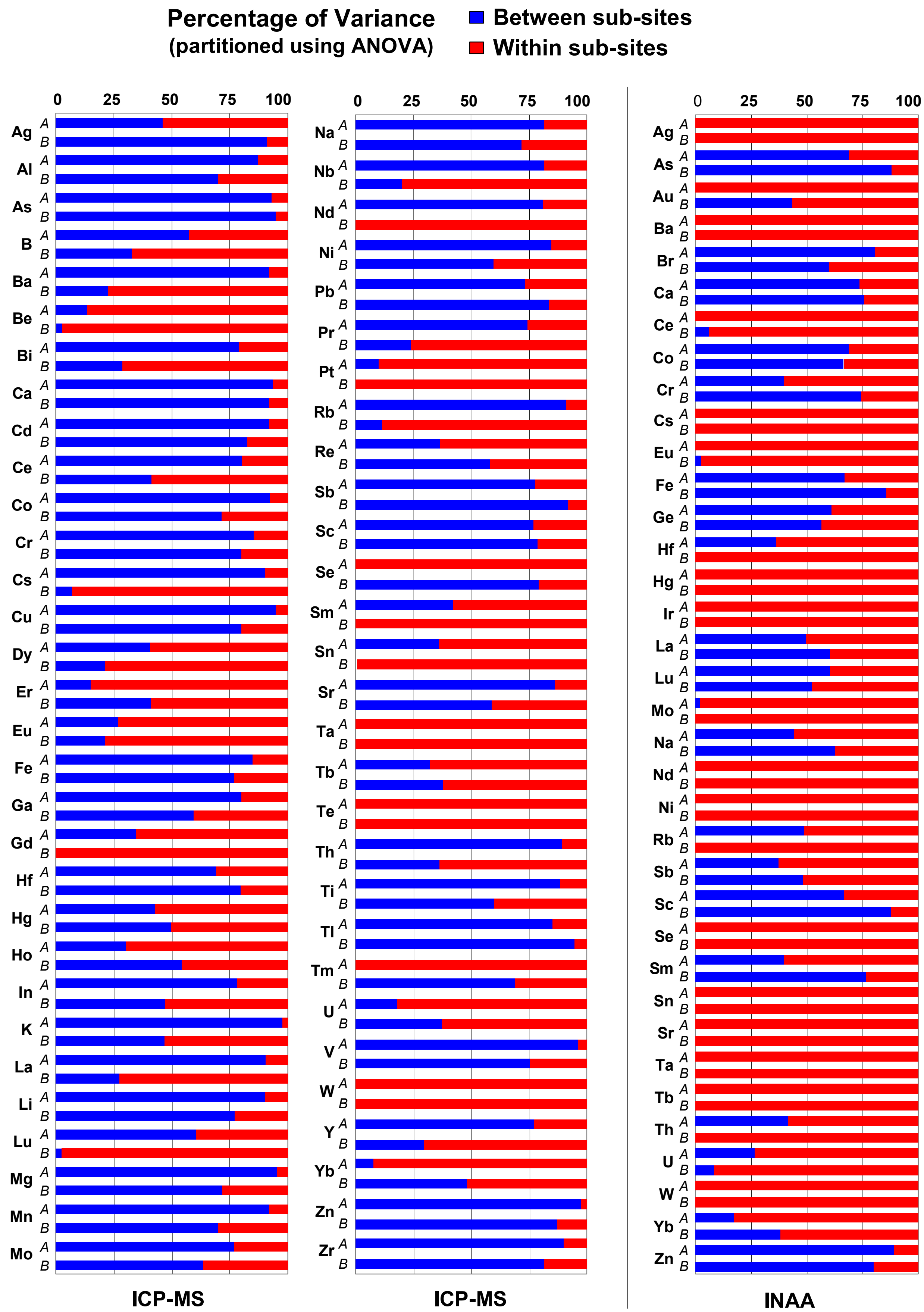

Figure 3.19 Partitioning of variance between sites (scale of 10 to 100 m) versus sub-site variation (scale of 1m). Subsite variance includes processing and analytical errors.

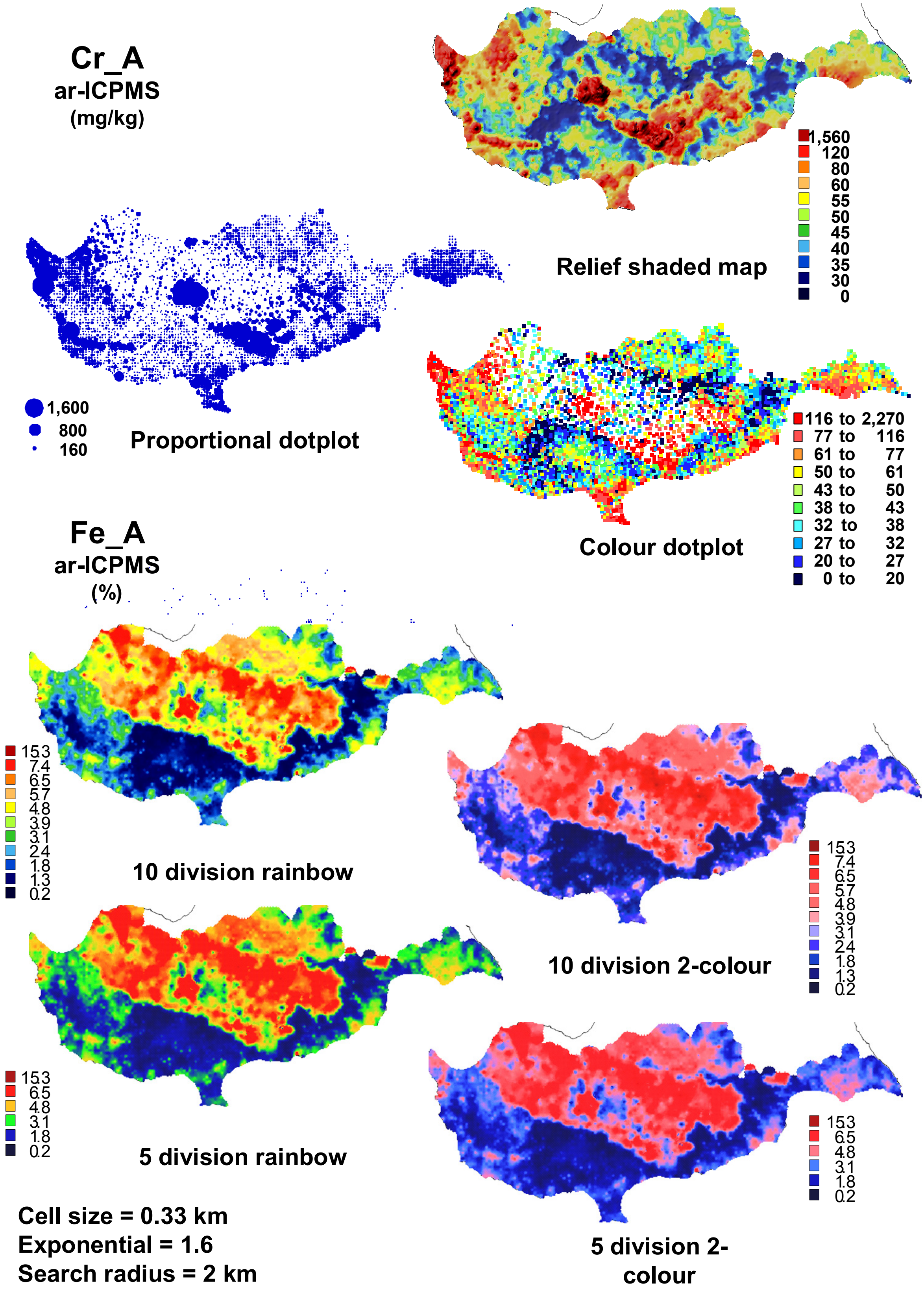

Figure 4.1 Comparison of various methods for plotting high-density spatial geochemical data and the number of colour slices and slicing schemes for plotting high-density spatial geochemical data.

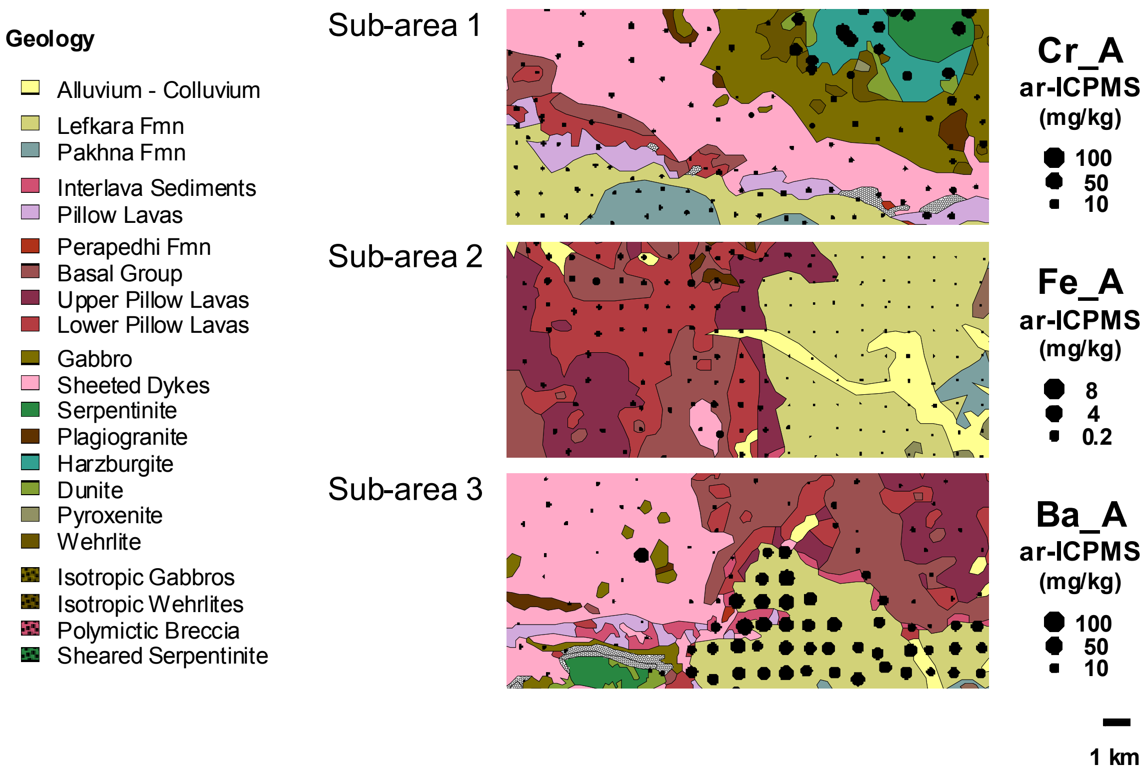

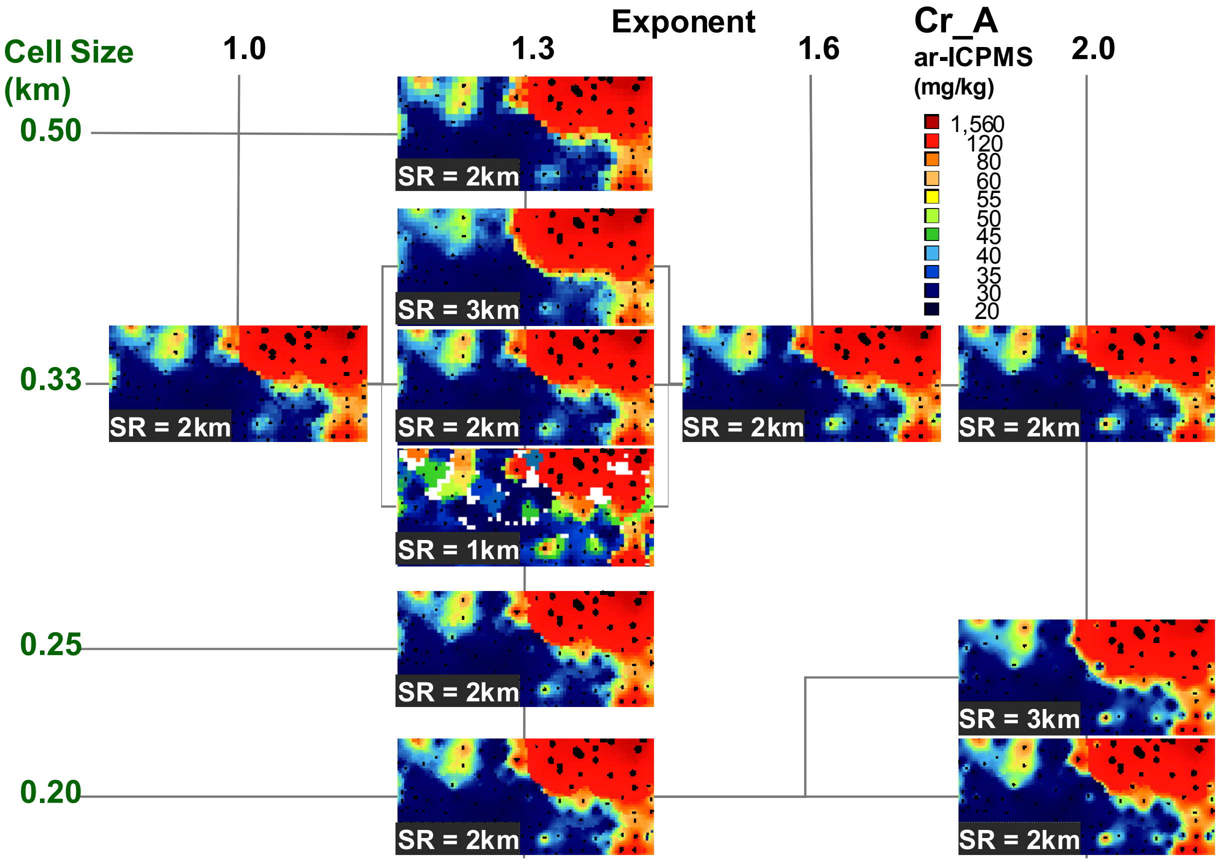

Figure 4.2 (i) Sub-areas used to test gridding procedures; (ii) Effect of variation in *MapInfo* IDW gridding parameters on *ar*-Cr_ICP_A in sub area 1 (south-western transect from ultramafic core of Troodos to CTSS).

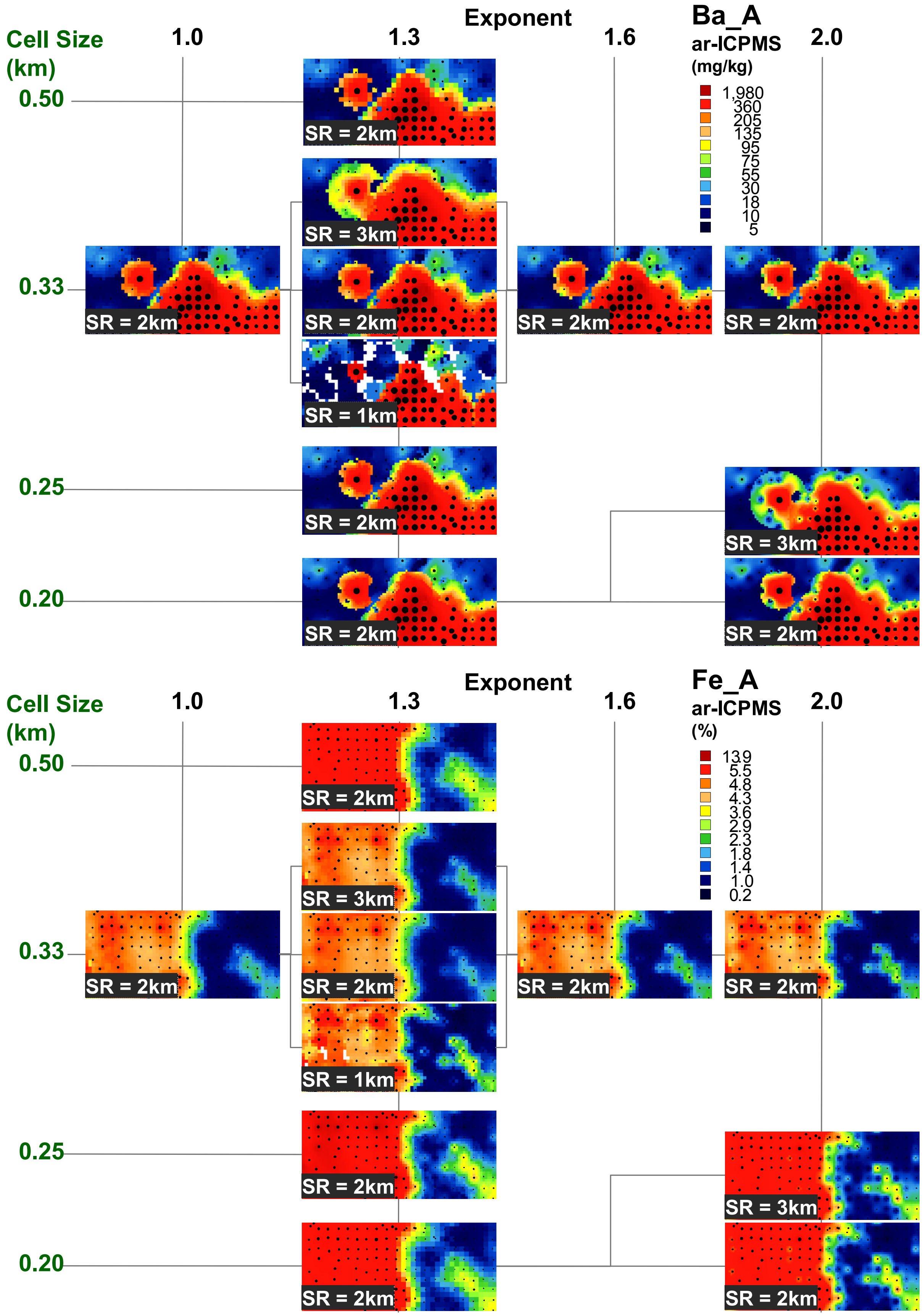

Figure 4.3 (i) Effect of variation in *MapInfo* IDW gridding parameters on *ar*-Fe_A in sub-area 2 across the basalt carbonate boundary and (ii) *ar*-Ba_A in sub area 3 (region where the TOC, Arakapas Transform zone and CTSS intersect).

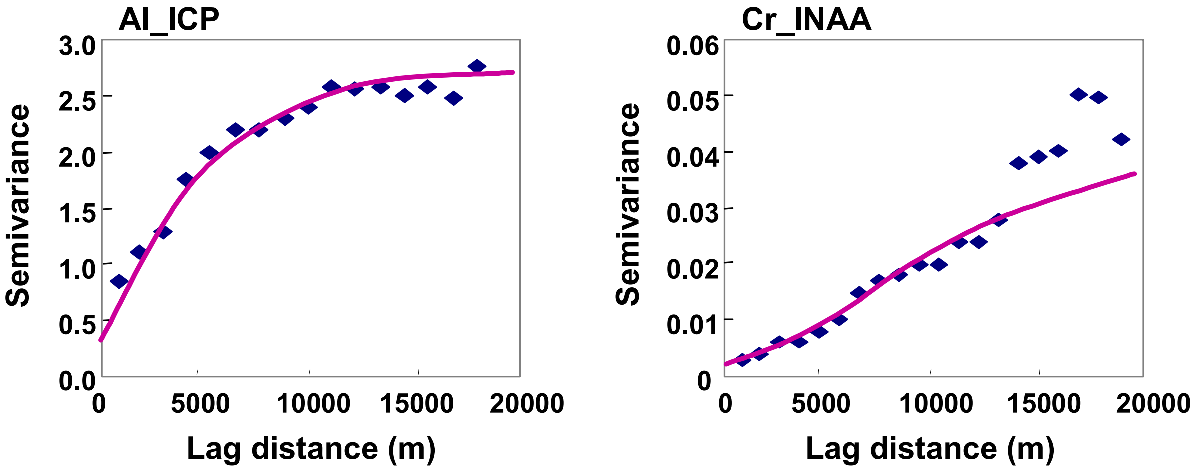

Model	Al_ICP	Cr_INAA
Nugget	0.300	0.003
Type	Exponential	Gaussian
Sill	2.300	0.035
Range	10,000	20,000

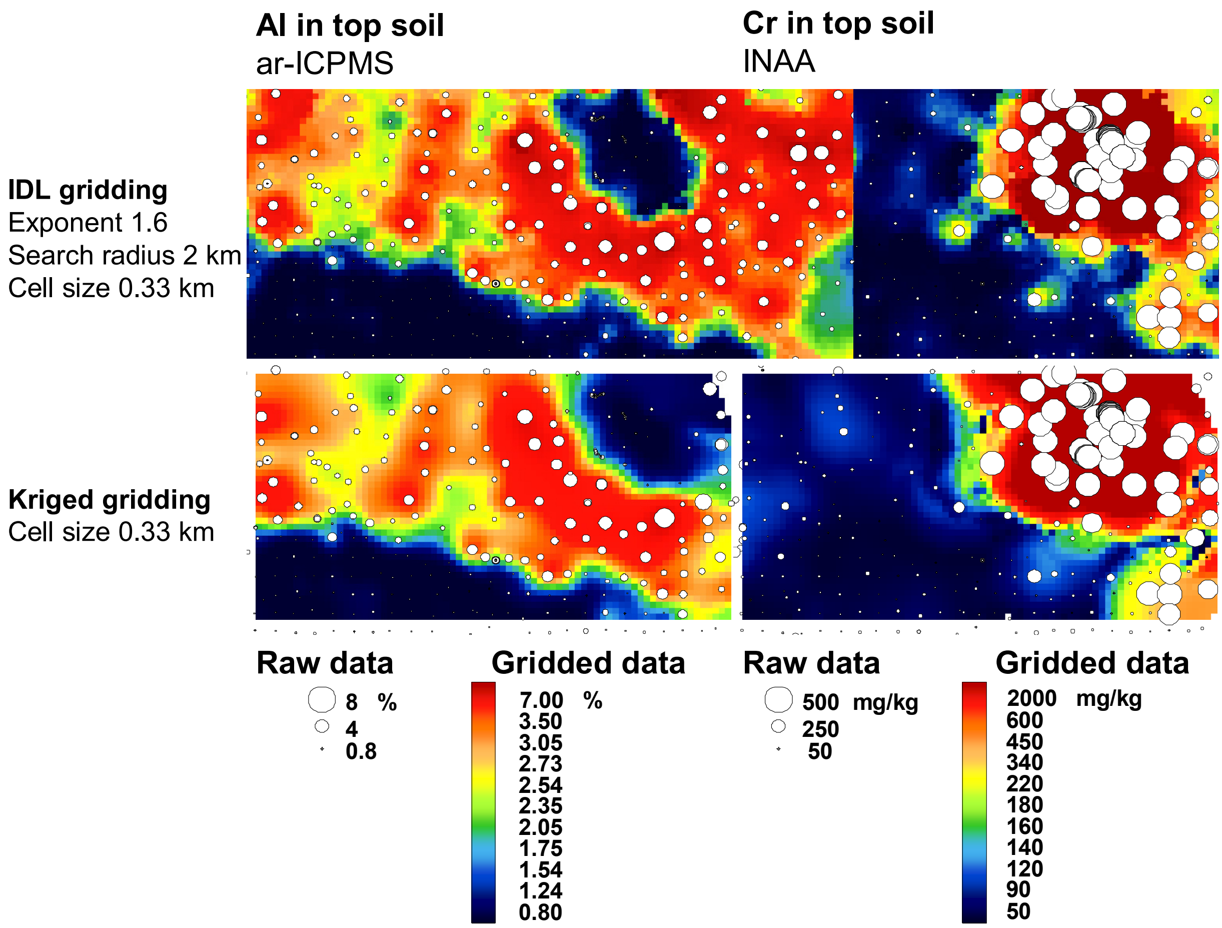

Figure 4.4 (i) Variograms and models for Al_ICP_A and Cr_INAA_A for sample suite in sub-area 1; (ii) Comparison between raw data, *MapInfo* IDW gridding and variography/kriging grid for *ar*-Al_A and *tot*-Cr_A in sub-area 1.

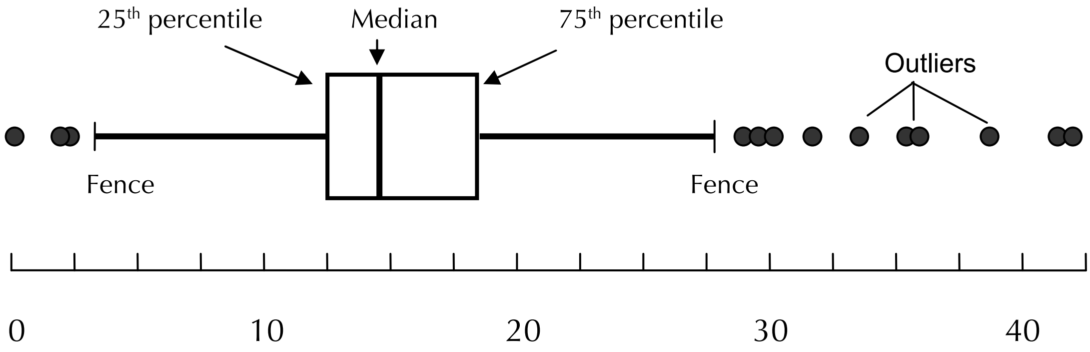

Figure 4.5 Standard Tukey boxplot.

See Volume 3 of this Report for the Maps

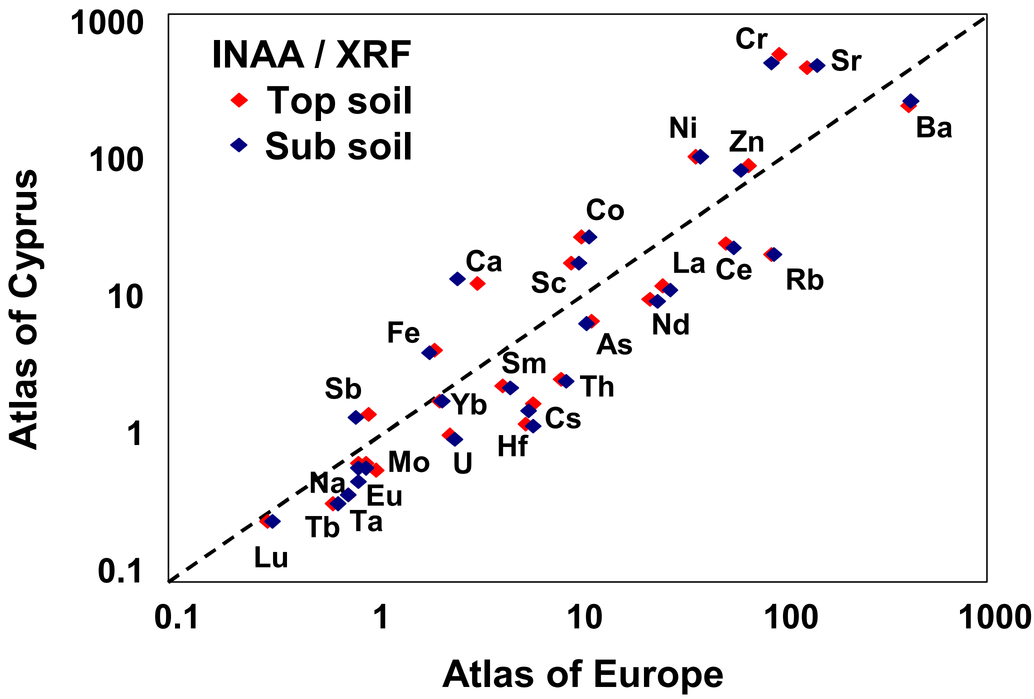

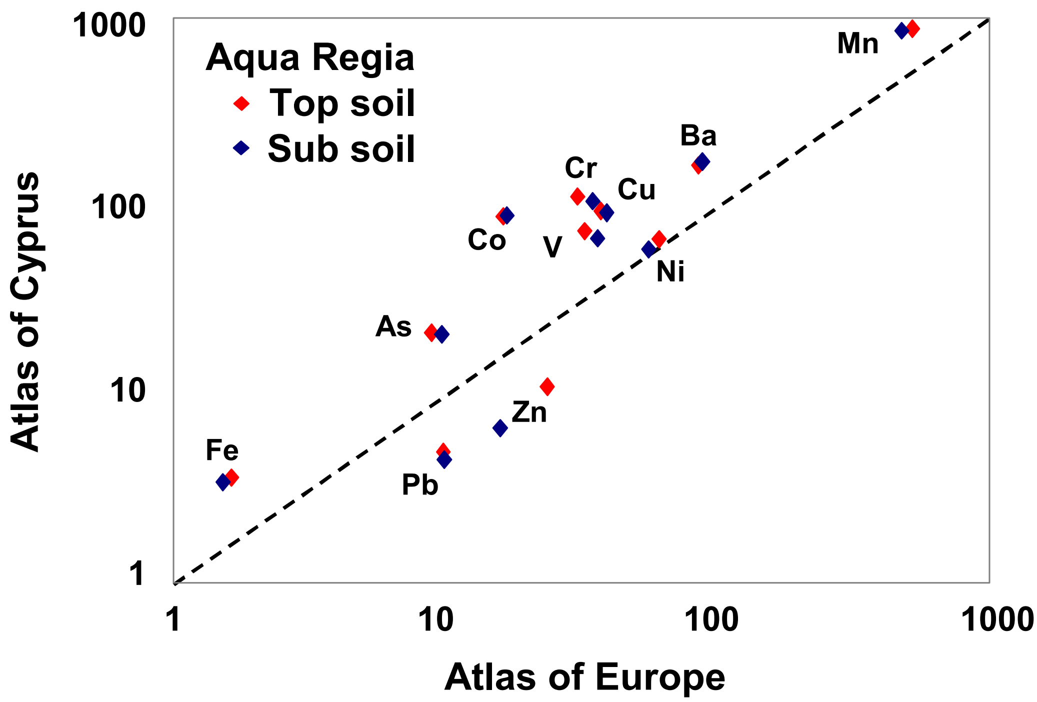

Figure 5.1 Comparison between the mean geochemical values (total and aqua regia extractable) of the FOREGS Atlas of Europe and the Cyprus dataset.

Table 5.1 Basic statistics for the main geochemical dataset.

(a) Top soil (0 – 25 cm)

Variable	Units	N	Mean	Min	Max	Std Dev	RSD (%)	Skew	Kurt
LOI	%	5339	23	0.66	44.51	10.80	47	0	-1
pH		5339	8.32	1.85	10.78	0.80	10	-1	6
EC	mS/cm	5339	0.42	0.00	29.23	1.86	438	10	113
Ag_ICP	mg/kg	5340	0.043	0.001	5.020	0.159	367	16	356
Ag_INAA	mg/kg	5340	3	3	13	0	6	43	1949
Al_ICP	%	5340	1.88	0.12	8.61	1.14	61	1	1
As_ICP	mg/kg	5340	4.90	0.05	230.0	7.00	143	13	301
As_INAA	mg/kg	5340	6.9	0.3	224.0	7.7	113	9	173
Au_INAA	ug/kg	5340	6	1	1080	35	615	19	438
B_ICP	mg/kg	5340	2.0	0.5	38.0	2.2	108	5	52
Ba_ICP	mg/kg	5340	163	0	2490	265	163	3	14
Ba_INAA	mg/kg	5340	227	25	5150	340	150	3	20
Be_ICP	mg/kg	5340	0.4	0.1	10.2	0.3	93	8	161
Bi_ICP	mg/kg	5340	0.09	0.01	5.96	0.14	163	20	628
Br_INAA	mg/kg	5340	10.9	0.3	282.0	13.7	126	9	117
Ca_ICP	%	5340	11.9	0.1	41.2	10.4	87	1	-1
Ca_INAA	%	5340	12.7	0.5	41.0	10.2	80	0	-1
Cd_ICP	mg/kg	5340	0.3	0.0	15.5	0.5	164	12	269
Ce_ICP	mg/kg	5340	14.2	0.3	353.0	11.8	83	6	129
Ce_INAA	mg/kg	5340	24.6	2.0	393.0	18.8	76	3	30
Co_ICP	mg/kg	5340	21.2	1.4	311.0	22.5	106	5	29
Co_INAA	mg/kg	5340	27.4	2.0	331.0	26.1	95	4	26
Cr_ICP	mg/kg	5340	73.7	0.3	2270.0	129.9	176	7	60
Cr_INAA	mg/kg	5340	518	3	100000	2809	542	28	924
Cs_ICP	mg/kg	5340	0.42	0.01	7.22	0.37	90	4	33
Cs_INAA	mg/kg	5340	1.31	0.50	11.00	1.17	89	1	2
Cu_ICP	mg/kg	5340	87.9	1.9	12000	332.7	379	19	482
Dy_ICP	mg/kg	5340	1.96	0.03	11.90	0.94	48	2	8
Er_ICP	mg/kg	5340	1.12	0.05	7.30	0.55	50	2	10
Eu_ICP	mg/kg	5340	0.50	0.05	3.30	0.26	54	2	9
Eu_INAA	mg/kg	5340	0.69	0.10	3.60	0.38	56	1	2
Fe_ICP	%	5340	3.57	0.15	31.20	2.60	73	2	8
Fe_INAA	%	5340	4.3	0.4	32.4	2.6	60	1	5
Ga_ICP	mg/kg	5340	5.31	0.24	16.30	2.90	55	1	-1
Gd_ICP	mg/kg	5340	2.54	0.05	19.4	1.3	52	2	11
Ge_ICP	mg/kg	5340	0.1	0.0	1.6	0.1	80	6	105
Hf_ICP	mg/kg	5340	0.1	0.0	1.1	0.1	104	3	10
Hf_INAA	mg/kg	5340	1.8	0.5	12.0	1.5	84	1	2
Hg_ICP	mg/kg	5340	0.03	0.00	4.52	0.08	235	38	1958
Hg_INAA	mg/kg	5340	0.5	0.5	4.0	0.1	18	32	1074
Ho_ICP	mg/kg	5340	0.4	0.1	2.5	0.2	49	2	9
In_ICP	mg/kg	5340	0.03	0.00	23.10	0.31	985	72	5194
Ir_INAA	ug/kg	5340	3	3	12	0	4	73	5340
K_ICP	%	5340	0.24	0.00	1.33	0.16	66	1	2
La_ICP	mg/kg	5340	8.3	0.3	191.0	6.8	82	5	103
La_INAA	mg/kg	5340	12.4	0.3	205.9	9.6	77	3	34
Li_ICP	mg/kg	5340	9.3	0.1	117.0	7.7	82	3	25
Lu_ICP	mg/kg	5340	0.14	0.05	1.60	0.09	66	2	16
Lu_INAA	mg/kg	5340	0.27	0.03	1.48	0.16	61	1	1

Mg_ICP	%	5340	1.32	0.06	13.40	1.63	124	4	24
Mn_ICP	mg/kg	5340	981	28	12000	857	87	6	68
Mo_ICP	mg/kg	5340	0.95	0.00	58.40	1.91	201	10	202
Mo_INAA	mg/kg	5340	1.53	0.50	66.00	3.10	202	6	62
Na_ICP	%	5340	0.25	0.00	7.00	0.37	148	8	103
Na_INAA	%	5340	0.70	0.02	6.59	0.68	96	1	2
Nb_ICP	mg/kg	5340	0.28	0.05	3.50	0.27	97	3	17
Nd_ICP	mg/kg	5339	7.16	0.18	99.20	4.89	68	3	29
Nd_INAA	mg/kg	5340	10.1	3.0	97.0	9.3	92	3	11
Ni_ICP	mg/kg	5340	111	0	3990	374	337	6	41
Ni_INAA	mg/kg	5340	102	10	4900	429	422	6	43
P_ICP	%	5340	0.04	0.00	0.31	0.03	92	2	2
Pb_ICP	mg/kg	5340	10.90	0.04	4490.00	76.62	703	47	2490
Pr_ICP	mg/kg	5340	1.79	0.05	32.90	1.33	75	4	60
Pt_ICP	ug/kg	5340	0.000	0.000	2.870	0.040	1794	61	4007
Rb_ICP	mg/kg	5340	9.5	0.2	51.3	6.5	68	1	4
Rb_INAA	mg/kg	5340	20.7	8.0	131.0	21.8	105	2	2
Re_ICP	mg/kg	5340	0.002	0.000	0.116	0.004	195	16	341
Sb_ICP	mg/kg	5340	0.41	0.01	97.10	2.11	516	31	1187
Sb_INAA	mg/kg	5340	0.62	0.05	91.60	2.05	328	30	1145
Sc_ICP	mg/kg	5340	11.2	0.1	853.0	14.3	128	39	2275
Sc_INAA	mg/kg	5340	18.0	1.2	74.1	11.6	65	1	-1
Se_ICP	mg/kg	5340	0.66	0.04	70.00	1.63	246	22	696
Se_INAA	mg/kg	5340	2.16	2.00	92.00	2.47	115	21	530
Sm_ICP	mg/kg	5340	1.80	0.05	16.60	1.05	58	2	13
Sm_INAA	mg/kg	5340	2.45	0.05	18.30	1.28	52	2	9
Sn_ICP	mg/kg	5340	0.81	0.03	96.30	2.50	308	22	632
Sn_INAA	mg/kg	5340	102	100	1600	39	38	23	658
Sr_ICP	mg/kg	5340	335	2	1200	370	110	1	0
Sr_INAA	mg/kg	5340	426	300	42900	729	171	41	2242
Ta_ICP	mg/kg	5340	0.03	0.01	0.08	0.00	4	36	1419
Ta_INAA	mg/kg	5340	0.42	0.30	7.50	0.45	106	5	29
Tb_ICP	mg/kg	5340	0.32	0.05	2.10	0.16	52	2	8
Tb_INAA	mg/kg	5340	0.36	0.30	2.60	0.20	57	4	20
Te_ICP	mg/kg	5340	0.06	0.01	5.34	0.18	298	16	336
Th_ICP	mg/kg	5340	1.32	0.05	47.70	1.43	108	8	206
Th_INAA	mg/kg	5340	2.74	0.10	19.00	2.48	90	2	3
Ti_ICP	%	5340	0.09	0.00	1.18	0.08	92	3	16
Tl_ICP	mg/kg	5340	0.09	0.01	4.53	0.15	159	18	458
Tm_ICP	mg/kg	5340	0.16	0.05	1.70	0.09	61	2	17
U_ICP	mg/kg	5340	0.69	0.05	129.00	1.93	280	55	3613
U_INAA	mg/kg	5340	1.10	0.30	11.20	1.20	109	2	9
V_ICP	mg/kg	5340	96	1	485	70	73	1	1
W_ICP	mg/kg	5340	0.06	0.04	3.30	0.08	143	23	684
W_INAA	mg/kg	5340	0.57	0.50	17.00	0.55	97	13	237
Y_ICP	mg/kg	5340	11.4	0.2	79.2	5.3	46	2	15
Yb_ICP	mg/kg	5340	1.01	0.05	10.00	0.53	52	3	23
Yb_INAA	mg/kg	5340	1.9	0.1	9.7	0.9	47	1	3
Zn_ICP	mg/kg	5340	66.8	0.1	4990.0	117.5	176	21	689
Zn_INAA	mg/kg	5340	87.7	25.0	5720.0	149.7	171	16	470
Zr_ICP	mg/kg	5340	4.62	0.05	44.90	4.68	101	3	9

(b) Sub soil (25 – 50 cm)

Variable	Units	N	Mean	Min	Max	Std Dev	RSD (%)	Skew	Kurt
LOI	%	209	20	5.66	42.33	10.48	52	1	-1
pH		209	8.33	3.11	10.50	1.12	13	-2	7
EC	mS/cm	209	0.27	0.01	5.64	0.57	205	6	43
Ag_ICP	mg/kg	5197	0.044	0.001	8.230	0.200	451	21	661
Ag_INAA	mg/kg	5197	3	3	11	0	4	62	4073
Al_ICP	%	5197	1.94	0.06	8.71	1.25	65	1	1
As_ICP	mg/kg	5197	4.77	0.05	259.00	9.52	199	16	343
As_INAA	mg/kg	5197	6.7	0.3	267.0	10.1	151	13	273
Au_INAA	ug/kg	5197	6	1	1670	43	682	22	648
B_ICP	mg/kg	5197	1.8	0.5	19.0	1.7	92	3	12
Ba_ICP	mg/kg	5197	179	0	3010	330	185	3	14
Ba_INAA	mg/kg	5197	250	25	4770	431	173	4	16
Be_ICP	mg/kg	5197	0.4	0.1	16.6	0.4	112	16	556
Bi_ICP	mg/kg	5197	0.08	0.01	9.40	0.17	202	32	1566
Br_INAA	mg/kg	5197	12.8	0.3	175.0	11.3	88	4	34
Ca_ICP	%	5197	13.0	0.0	48.4	11.0	85	0	-1
Ca_INAA	%	5197	13.7	0.5	42.0	10.8	78	0	-1
Cd_ICP	mg/kg	5197	0.3	0.0	21.3	0.7	236	16	378
Ce_ICP	mg/kg	5197	13.0	0.1	101.0	11.0	85	2	6
Ce_INAA	mg/kg	5197	23.0	2.0	162.0	19.0	82	2	4
Co_ICP	mg/kg	5197	21.9	0.3	1630.0	35.6	163	25	979
Co_INAA	mg/kg	5197	27.8	0.5	1570.0	37.1	133	19	680
Cr_ICP	mg/kg	5197	70.5	0.3	1810.0	128.3	182	7	54
Cr_INAA	mg/kg	5197	456	3	100000	2768	607	29	992
Cs_ICP	mg/kg	5197	0.44	0.01	6.74	0.39	90	3	26
Cs_INAA	mg/kg	5197	1.30	0.50	12.00	1.21	93	2	4
Cu_ICP	mg/kg	5197	91.4	0.6	12000.0	400.8	438	19	456
Dy_ICP	mg/kg	5197	1.96	0.02	14.80	1.03	53	2	9
Er_ICP	mg/kg	5197	1.13	0.05	7.80	0.62	55	2	9
Eu_ICP	mg/kg	5197	0.49	0.05	4.80	0.29	60	2	17
Eu_INAA	mg/kg	5197	0.66	0.10	5.30	0.41	62	1	5
Fe_ICP	%	5197	3.54	0.05	23.80	2.62	74	1	3
Fe_INAA	%	5197	4.2	0.1	22.0	2.7	63	1	1
Ga_ICP	mg/kg	5197	5.38	0.01	23.40	3.13	58	1	0
Gd_ICP	mg/kg	5197	2.50	0.05	21.6	1.4	57	2	11
Ge_ICP	mg/kg	5197	0.1	0.1	6.0	0.1	134	36	1937
Hf_ICP	mg/kg	5197	0.1	0.1	1.4	0.1	106	3	10
Hf_INAA	mg/kg	5197	1.7	0.5	11.0	1.5	89	2	2
Hg_ICP	mg/kg	5197	0.03	0.00	3.62	0.08	265	29	1059
Hg_INAA	mg/kg	5197	0.5	0.5	5.0	0.1	20	32	1170
Ho_ICP	mg/kg	5197	0.4	0.1	2.7	0.2	54	2	8
In_ICP	mg/kg	5197	0.02	0.01	0.79	0.03	124	10	170
Ir_INAA	ug/kg	5197	3	3	25	0	12	57	3359
K_ICP	%	5197	0.22	0.00	1.37	0.16	74	1	3
La_ICP	mg/kg	5197	7.7	0.3	115.0	6.7	86	3	20
La_INAA	mg/kg	5197	11.7	0.3	112.0	9.7	83	2	6
Li_ICP	mg/kg	5197	9.8	0.1	119.0	8.6	88	4	23
Lu_ICP	mg/kg	5197	0.14	0.05	4.10	0.11	79	9	264
Lu_INAA	mg/kg	5197	0.27	0.03	1.65	0.18	66	1	2
Mg_ICP	%	5197	1.31	0.02	12.90	1.60	122	4	23

Mn_ICP	mg/kg	5197	951	15	12000	944	99	6	62
Mo_ICP	mg/kg	5197	0.93	0.00	78.50	2.57	275	13	250
Mo_INAA	mg/kg	5197	1.47	0.50	99.00	3.63	246	10	158
Na_ICP	%	5197	0.24	0.00	4.22	0.28	114	5	41
Na_INAA	%	5197	0.66	0.01	3.71	0.66	100	1	2
Nb_ICP	mg/kg	5197	0.20	0.05	2.40	0.21	105	3	14
Nd_ICP	mg/kg	5197	6.84	0.03	87.40	5.04	74	2	18
Nd_INAA	mg/kg	5197	9.8	3.0	105.0	9.6	98	3	12
Ni_ICP	mg/kg	5197	110	0	6900	398	361	7	65
Ni_INAA	mg/kg	5197	100	10	5660	447	449	7	54
P_ICP	%	5197	0.04	0.00	0.38	0.03	95	2	4
Pb_ICP	mg/kg	5197	6.83	0.00	2040.00	30.19	442	60	3968
Pr_ICP	mg/kg	5197	1.70	0.05	20.20	1.33	78	2	13
Pt_ICP	ug/kg	5197	0.000	0.000	1.380	0.020	1192	38	1615
Rb_ICP	mg/kg	5197	9.1	0.1	57.6	6.8	74	1	4
Rb_INAA	mg/kg	5197	20.4	8.0	152.0	22.2	109	2	4
Re_ICP	mg/kg	5197	0.002	0.001	0.299	0.005	255	36	1734
Sb_ICP	mg/kg	5197	0.32	0.01	51.80	1.08	335	28	1111
Sb_INAA	mg/kg	5197	0.52	0.05	27.90	0.88	169	13	313
Sc_ICP	mg/kg	5197	11.6	0.1	450.0	11.0	95	13	480
Sc_INAA	mg/kg	5197	18.0	0.3	69.8	12.2	68	1	-1
Se_ICP	mg/kg	5197	0.64	0.05	98.60	1.90	295	32	1440
Se_INAA	mg/kg	5197	2.18	2.00	238.00	4.02	185	44	2352
Sm_ICP	mg/kg	5197	1.75	0.05	17.70	1.10	63	2	13
Sm_INAA	mg/kg	5197	2.37	0.05	20.80	1.37	58	2	10
Sn_ICP	mg/kg	5197	0.61	0.03	52.80	1.49	244	19	480
Sn_INAA	mg/kg	5197	102	100	1400	43	42	21	485
Sr_ICP	mg/kg	5197	344	1	1200	373	108	1	0
Sr_INAA	mg/kg	5197	440	300	45800	967	220	35	1493
Ta_ICP	mg/kg	5197	0.03	0.03	0.19	0.00	11	42	1877
Ta_INAA	mg/kg	5197	0.42	0.30	6.60	0.45	108	5	30
Tb_ICP	mg/kg	5197	0.32	0.05	2.70	0.18	57	2	11
Tb_INAA	mg/kg	5197	0.36	0.30	3.10	0.22	61	5	31
Te_ICP	mg/kg	5197	0.06	0.01	13.50	0.26	429	32	1360
Th_ICP	mg/kg	5197	1.34	0.05	10.70	1.42	106	2	5
Th_INAA	mg/kg	5197	2.63	0.10	17.30	2.58	98	2	3
Ti_ICP	%	5197	0.09	0.00	1.08	0.08	91	3	12
Tl_ICP	mg/kg	5197	0.09	0.01	19.90	0.33	334	45	2484
Tm_ICP	mg/kg	5197	0.16	0.05	1.60	0.10	67	2	16
U_ICP	mg/kg	5197	0.62	0.05	19.60	0.91	146	6	65
U_INAA	mg/kg	5197	1.05	0.30	18.50	1.29	123	3	22
V_ICP	mg/kg	5197	96	1	618	74	77	1	2
W_ICP	mg/kg	5197	0.08	0.05	33.30	0.57	707	48	2523
W_INAA	mg/kg	5197	0.60	0.50	35.00	1.03	171	19	464
Y_ICP	mg/kg	5197	11.5	0.2	80.6	5.9	51	2	12
Yb_ICP	mg/kg	5197	1.03	0.05	9.60	0.60	59	3	20
Yb_INAA	mg/kg	5197	1.9	0.1	10.4	1.0	53	1	4
Zn_ICP	mg/kg	5197	61.5	0.1	7650.0	174.8	284	30	1182
Zn_INAA	mg/kg	5197	81.3	25.0	8410.0	205.2	252	27	976
Zr_ICP	mg/kg	5197	5.06	0.05	57.80	5.31	105	3	10

(c) Stream sediments top sample (0-25 cm)

Variable	Units	N	Mean	Min	Max	Std Dev	RSD (%)	Skew	Kurt
LOI	%								
pH									
EC	mS/cm								
Ag_ICP	mg/kg	88	0.029	0.001	0.596	0.072	245	6	45
Ag_INAA	mg/kg	88	3	3	3	0	0	0	0
Al_ICP	%	88	1.80	0.50	4.23	0.93	52	1	0
As_ICP	mg/kg	88	4.24	0.05	12.40	2.56	61	1.2	1.1
As_INAA	mg/kg	88	5.8	0.3	17.4	3.8	65.7	0.6	0.5
Au_INAA	ug/kg	88	6	1	205	25	422	7	52
B_ICP	mg/kg	88	0.9	0.5	6.0	1.0	106	4	15
Ba_ICP	mg/kg	88	126	5	970	144	114	3	15
Ba_INAA	mg/kg	88	160	25	1000	177	110	2	5
Be_ICP	mg/kg	88	0.3	0.1	1	0.2	68	1	2
Bi_ICP	mg/kg	88	06	01	0.22	04	72	1	1
Br_INAA	mg/kg	88	10.6	0.3	84.5	10.8	102	4.2	25.4
Ca_ICP	%	88	11.7	0.6	29.5	8.8	75.5	0.5	-1.1
Ca_INAA	%	88	12.6	0.5	31	8.8	69.9	0.5	-0.9
Cd_ICP	mg/kg	88	0.2	0	0.9	0.2	78	2	2
Ce_ICP	mg/kg	88	9.5	1.6	30.2	6	63.3	1.1	1.3
Ce_INAA	mg/kg	88	19.8	2	55	12.9	65.2	0.6	-0.4
Co_ICP	mg/kg	88	17.4	4.6	43.3	7.6	43.8	0.7	0.5
Co_INAA	mg/kg	88	23.8	6	71	10.9	45.9	1.1	2.7
Cr_ICP	mg/kg	88	59.5	9.8	580	68.1	114.4	5.5	39.5
Cr_INAA	mg/kg	88	328	34	2230	316	96	3	14
Cs_ICP	mg/kg	88	0.32	05	0.93	0.20	63	1	0
Cs_INAA	mg/kg	88	1.10	0.50	40	0.98	89	1	0
Cu_ICP	mg/kg	88	73.1	12.7	811	101.6	139	5.4	35.2
Dy_ICP	mg/kg	88	1.71	0.66	3.50	0.53	31	1	1
Er_ICP	mg/kg	88	0.94	0.50	1.90	0.28	30	1	1
Eu_ICP	mg/kg	88	0.43	0.10	10	0.18	42	0	0
Eu_INAA	mg/kg	88	0.58	0.10	1.40	0.29	50	0	0
Fe_ICP	%	88	3.16	0.60	7.34	1.67	53	0.6	-0.5
Fe_INAA	%	88	4.1	1.3	8.5	1.9	47	0.3	-1
Ga_ICP	mg/kg	88	4.84	1.32	11.50	2.13	44	0.6	0.1
Gd_ICP	mg/kg	88	2.14	0.60	4.4	0.9	41	0	0
Ge_ICP	mg/kg	88	0.1	0.1	0.2	0	57	3	7
Hf_ICP	mg/kg	88	0.1	0.1	0.4	0.1	76	2	2
Hf_INAA	mg/kg	88	1.4	0.5	5	1.2	86	1	1
Hg_ICP	mg/kg	88	01	00	06	01	77	1	0
Hg_INAA	mg/kg	88	0.5	0.5	0.5	0	0	0	0
Ho_ICP	mg/kg	88	0.4	0.2	0.7	0.1	32	1	0
In_ICP	mg/kg	88	01	01	06	01	63	1	2
Ir_INAA	ug/kg	88	3	3	3	0	0	0	0
K_ICP	%	88	0.18	03	0.49	08	49	1	1
La_ICP	mg/kg	88	5.3	0.7	15.6	3.4	63.3	0.8	0.2
La_INAA	mg/kg	88	10.6	1.1	30.1	6.6	62.1	0.6	-0.5
Li_ICP	mg/kg	88	8.3	1	26.7	4.1	49.6	1.4	4.1
Lu_ICP	mg/kg	88	0.11	05	0.30	06	62	1	1
Lu_INAA	mg/kg	88	0.29	03	0.78	0.10	35	1	5
Mg_ICP	%	88	1.33	0.32	3.75	0.77	58	1	1

Mn_ICP	mg/kg	88	919	207	2300	423	46	1	2
Mo_ICP	mg/kg	88	0.62	00	3.45	0.61	99	2	5
Mo_INAA	mg/kg	88	1.43	0.50	140	2.83	198	3	11
Na_ICP	%	88	0.38	05	2.30	0.31	82	3	15
Na_INAA	%	88	0.93	0.13	3.79	0.71	77	1	2
Nb_ICP	mg/kg	88	0.16	05	0.80	0.14	85	2	5
Nd_ICP	mg/kg	88	5.63	0.90	12.70	2.90	52	0.4	-0.4
Nd_INAA	mg/kg	88	8.9	3	26	7	78	0.8	-0.6
Ni_ICP	mg/kg	88	73	12	386	72	99	2	5
Ni_INAA	mg/kg	88	22	10	420	60	269	5	28
P_ICP	%	88	03	00	0.11	02	74	1	0
Pb_ICP	mg/kg	88	5.89	0.60	19.20	3.81	65	1.1	1.2
Pr_ICP	mg/kg	88	1.27	0.20	3.20	0.70	55	1	0
Pt_ICP	ug/kg	88	000	000	000	000	0	-1	-2
Rb_ICP	mg/kg	88	7.8	1	21.1	4.5	57.8	0.8	0.7
Rb_INAA	mg/kg	88	21	8	85	21.5	102.2	1.4	0.6
Re_ICP	mg/kg	88	001	001	007	001	71	3	8
Sb_ICP	mg/kg	88	0.28	01	6.18	0.66	232	8	71
Sb_INAA	mg/kg	88	0.35	05	10	0.27	76	0	-1
Sc_ICP	mg/kg	88	10.4	1.8	24.9	6.2	60	0.7	-0.6
Sc_INAA	mg/kg	88	19	4.4	37.3	10.7	56	0.2	-1.5
Se_ICP	mg/kg	88	0.47	05	1.70	0.35	74	1	2
Se_INAA	mg/kg	88	23	20	50	0.31	16	9	88
Sm_ICP	mg/kg	88	1.42	0.30	30	0.64	45	0	-1
Sm_INAA	mg/kg	88	2.32	0.60	4.80	0.95	41	1	0
Sn_ICP	mg/kg	88	0.50	05	3.36	0.47	94	4	16
Sn_INAA	mg/kg	88	100	100	100	0	0	0	0
Sr_ICP	mg/kg	88	345	14	1200	327	95	1	1
Sr_INAA	mg/kg	88	374	300	2000	253	68	5	23
Ta_ICP	mg/kg	88	03	03	03	00	0	1	-2
Ta_INAA	mg/kg	88	0.34	0.30	1.60	0.20	60	5	21
Tb_ICP	mg/kg	88	0.29	05	0.60	0.10	36	0	0
Tb_INAA	mg/kg	88	0.33	0.30	1.20	0.15	47	5	21
Te_ICP	mg/kg	88	03	01	0.21	03	100	2	8
Th_ICP	mg/kg	88	1.13	05	3.50	0.84	74	1	0
Th_INAA	mg/kg	88	2.28	0.10	7.60	1.85	81	1	0
Ti_ICP	%	88	08	00	0.34	06	74	2	3
Tl_ICP	mg/kg	88	07	01	0.29	05	71	2	4
Tm_ICP	mg/kg	88	0.11	05	0.30	05	50	1	0
U_ICP	mg/kg	88	0.53	05	2.10	0.52	98	1	1
U_INAA	mg/kg	88	15	0.30	4.50	12	96	1	2
V_ICP	mg/kg	88	90	18	272	57	64	1	1
W_ICP	mg/kg	88	05	05	0.30	03	67	6	40
W_INAA	mg/kg	88	0.51	0.50	20	0.15	31	9	88
Y_ICP	mg/kg	88	7.2	2.3	15.6	2.9	40.1	0.7	0.4
Yb_ICP	mg/kg	88	0.86	0.40	1.80	0.29	35	1	1
Yb_INAA	mg/kg	88	1.7	0.8	4.1	0.5	31	1	4
Zn_ICP	mg/kg	88	55.6	16.2	213	35.5	63.8	2.4	7
Zn_INAA	mg/kg	88	59.5	25	240	56.4	94.8	1.6	1.5
Zr_ICP	mg/kg	88	4.22	0.60	14.50	2.94	70	1.2	1.4

(d) Stream sediments sub sample (25 - 50 cm)

Variable	Units	N	Mean	Min	Max	Std Dev	RSD (%)	Skew	Kurt
LOI	%	89	20	3.33	380	9.46	47	0	-1
pH		89	8.57	7.13	9.56	0.44	5	0	1
EC	mS/cm	89	0.33	06	60	0.65	193	8	65
Ag_ICP	mg/kg	89	038	001	0.376	062	162	3	11
Ag_INAA	mg/kg	89	3	3	3	0	0	0	0
Al_ICP	%	89	1.74	0.35	3.89	0.86	50	1	0
As_ICP	mg/kg	89	4.46	0.40	18.40	2.76	62	2	6
As_INAA	mg/kg	89	5.9	0.3	22.2	3.9	67	1	3
Au_INAA	ug/kg	89	5	1	61	11	212	4	16
B_ICP	mg/kg	89	0.9	0.5	4	0.7	76	2	4
Ba_ICP	mg/kg	89	136	4	1260	162	119	4	26
Ba_INAA	mg/kg	89	163	25	1440	212	130	3	14
Be_ICP	mg/kg	89	0.3	0.1	0.9	0.2	71	1	1
Bi_ICP	mg/kg	89	07	01	0.63	07	103	4	29
Br_INAA	mg/kg	89	11.1	0.3	89.8	10.8	97	5	33
Ca_ICP	%	89	11.5	0.7	29.9	8.5	75	1	-1
Ca_INAA	%	89	12.3	0.5	32	8.3	67	1	-1
Cd_ICP	mg/kg	89	0.3	0	1.2	0.2	84	2	3
Ce_ICP	mg/kg	89	9.3	1.4	43.5	6.4	68	2	9
Ce_INAA	mg/kg	89	19.3	2	60	12.4	64	1	1
Co_ICP	mg/kg	89	17	4.4	40.5	7.2	42	1	1
Co_INAA	mg/kg	89	24.8	6	69	11.2	45	1	2
Cr_ICP	mg/kg	89	61.9	9.3	526	71.8	116	4	23
Cr_INAA	mg/kg	89	441	32	5390	670	152	5	34
Cs_ICP	mg/kg	89	0.30	02	1.56	0.22	74	2	10
Cs_INAA	mg/kg	89	1.16	0.50	50	1.13	97	1	1
Cu_ICP	mg/kg	89	66.6	11.5	492	68.4	103	4	21
Dy_ICP	mg/kg	89	1.65	0.70	4.30	0.52	32	2	6
Er_ICP	mg/kg	89	0.91	0.40	2.20	0.27	30	2	5
Eu_ICP	mg/kg	89	0.42	0.20	1.30	0.17	41	2	6
Eu_INAA	mg/kg	89	0.53	0.10	1.30	0.28	54	0	0
Fe_ICP	%	89	3.14	0.54	6.72	1.50	48	0	-1
Fe_INAA	%	89	4.2	1	7.7	1.9	45	0	-1
Ga_ICP	mg/kg	89	4.64	1.34	10.80	1.97	42	1	0
Gd_ICP	mg/kg	89	24	0.70	6	0.8	40	1	5
Ge_ICP	mg/kg	89	0.1	0.1	0.2	0	54	3	10
Hf_ICP	mg/kg	89	0.1	0.1	0.4	0.1	81	2	6
Hf_INAA	mg/kg	89	1.5	0.5	5	1.2	82	1	1
Hg_ICP	mg/kg	89	02	00	09	01	74	1	1
Hg_INAA	mg/kg	89	0.5	0.5	0.5	0	0	0	0
Ho_ICP	mg/kg	89	0.3	0.2	0.9	0.1	32	2	7
In_ICP	mg/kg	89	02	01	0.19	02	101	5	36
Ir_INAA	ug/kg	89	3	3	3	0	0	0	0
K_ICP	%	89	0.19	03	0.64	0.11	58	1	3
La_ICP	mg/kg	89	5.2	0.6	21.9	3.5	67	2	5
La_INAA	mg/kg	89	10.3	1.6	31	6.5	63	1	0
Li_ICP	mg/kg	89	7.6	1.5	21.1	4.1	54	1	1
Lu_ICP	mg/kg	89	0.10	05	0.30	05	54	1	2
Lu_INAA	mg/kg	89	0.29	03	0.59	09	32	1	1
Mg_ICP	%	89	1.35	0.39	6.56	0.94	70	3	11

Mn_ICP	mg/kg	89	909	237	2850	438	48	2	4
Mo_ICP	mg/kg	89	0.64	00	3.63	0.67	105	2	6
Mo_INAA	mg/kg	89	18	0.50	130	1.95	180	4	18
Na_ICP	%	89	0.31	05	1.66	0.21	70	3	16
Na_INAA	%	89	0.89	0.12	3.47	0.73	82	1	1
Nb_ICP	mg/kg	89	0.20	05	0.90	0.16	79	2	4
Nd_ICP	mg/kg	89	5.47	15	21.50	38	56	2	7
Nd_INAA	mg/kg	89	7.5	3	28	6.4	86	1	1
Ni_ICP	mg/kg	89	82	9	671	109	133	3	12
Ni_INAA	mg/kg	89	48	10	790	137	288	4	17
P_ICP	%	89	03	00	0.12	02	81	1	1
Pb_ICP	mg/kg	89	9.43	0.86	83.30	11.60	123	4	22
Pr_ICP	mg/kg	89	1.23	0.20	5.10	0.74	60	2	7
Pt_ICP	ug/kg	89	000	000	000	000	10	9	89
Rb_ICP	mg/kg	89	7.8	0.7	42.5	5.8	75	3	13
Rb_INAA	mg/kg	89	17.7	8	103	19.3	109	2	5
Re_ICP	mg/kg	89	001	001	008	001	78	3	10
Sb_ICP	mg/kg	89	0.28	01	2.34	0.31	111	4	21
Sb_INAA	mg/kg	89	0.44	05	2.30	0.40	91	2	4
Sc_ICP	mg/kg	89	9.5	1.7	23.5	5.3	56	1	-1
Sc_INAA	mg/kg	89	19.1	4.2	43	10.3	54	0	-1
Se_ICP	mg/kg	89	0.44	05	2.20	0.37	84	2	4
Se_INAA	mg/kg	89	20	20	20	00	0	0	0
Sm_ICP	mg/kg	89	1.37	0.30	4.40	0.65	47	1	4
Sm_INAA	mg/kg	89	2.30	0.80	5.80	0.89	39	1	2
Sn_ICP	mg/kg	89	0.70	07	7.37	11	144	5	27
Sn_INAA	mg/kg	89	100	100	100	0	0	0	0
Sr_ICP	mg/kg	89	316	15	1200	287	91	1	1
Sr_INAA	mg/kg	89	353	300	1900	213	60	5	33
Ta_ICP	mg/kg	89	03	03	03	00	0	1	-2
Ta_INAA	mg/kg	89	0.37	0.30	2.20	0.30	81	4	19
Tb_ICP	mg/kg	89	0.26	0.10	0.80	0.10	38	2	7
Tb_INAA	mg/kg	89	0.30	0.30	1.10	08	27	9	89
Te_ICP	mg/kg	89	04	01	0.80	08	198	7	63
Th_ICP	mg/kg	89	0.97	0.10	5.20	0.82	84	2	7
Th_INAA	mg/kg	89	2.19	0.10	8.20	1.90	87	1	1
Ti_ICP	%	89	08	00	0.30	06	74	1	1
Tl_ICP	mg/kg	89	07	01	0.35	06	83	2	6
Tm_ICP	mg/kg	89	0.11	05	0.30	05	50	1	2
U_ICP	mg/kg	89	0.47	05	2.10	0.45	96	2	2
U_INAA	mg/kg	89	0.76	0.30	3.10	0.77	101	1	0
V_ICP	mg/kg	89	91	20	233	57	62	1	0
W_ICP	mg/kg	89	05	05	0.30	02	51	9	82
W_INAA	mg/kg	89	0.52	0.50	30	0.26	50	9	89
Y_ICP	mg/kg	89	6.9	2	12.5	2.3	34	0	0
Yb_ICP	mg/kg	89	0.83	0.40	20	0.28	35	1	3
Yb_INAA	mg/kg	89	1.7	0.8	3.6	0.5	31	1	1
Zn_ICP	mg/kg	89	71.7	19.6	561	75.7	106	4	24
Zn_INAA	mg/kg	89	74.8	25	570	93.2	124	3	11
Zr_ICP	mg/kg	89	3.19	0.40	14.60	2.78	87	2	5

Table 5.2 Means for element values in soils within the main lithological group.

	Ultramafic	Mafic intrusive	Basalt	Mafic clastic	Silicic clastic	Carbonate	Alluvium-colluvium
Samples	**149**	**538**	**994**	**44**	**563**	**1,861**	**1,147**
Major elements (values in %)							
Al_ICP top soil	1.28	2.96	2.97	1.52	1.39	1.26	1.81
Al_ICP sub soil	1.49	3.20	3.04	1.58	1.39	1.22	1.89
Ca_ICP top soil	0.9	2.1	4.0	4.6	16.9	19.1	10.9
Ca_ICP sub soil	0.8	2.0	4.6	5.1	18.0	20.6	12.2
Ca_INAA top soil	1.6	3.8	5.0	5.2	17.5	19.7	11.4
Ca_INAA sub soil	1.7	3.7	5.6	5.7	18.7	21.3	12.5
Fe_ICP top soil	7.52	5.29	6.00	3.90	2.44	1.95	3.39
Fe_ICP sub soil	7.88	5.40	5.80	4.30	2.38	1.85	3.47
Fe_INAA top soil	7.99	6.87	6.65	4.36	2.97	2.50	4.30
Fe_INAA sub soil	8.32	7.04	6.48	4.69	2.92	2.44	4.23
K_ICP top soil	0.10	0.11	0.27	0.27	0.25	0.26	0.29
K_ICP sub soil	0.09	0.08	0.25	0.24	0.22	0.23	0.27
Mg_ICP top soil	8.04	1.43	1.85	2.03	0.97	0.67	1.18
Mg_ICP sub soil	7.69	1.54	1.92	2.21	0.96	0.67	1.14
Na_ICP top soil	0.11	0.24	0.32	0.13	0.21	0.18	0.37
Na_ICP sub soil	0.12	0.27	0.35	0.15	0.23	0.18	0.29
Na_INAA top soil	0.26	1.50	1.02	0.47	0.48	0.31	0.91
Na_INAA sub soil	0.27	1.48	0.99	0.50	0.46	0.29	0.80
P_ICP top soil	0.018	0.082	0.071	0.023	0.028	0.024	0.040
P_ICP sub soil	0.016	0.081	0.066	0.024	0.028	0.024	0.039
Ti_ICP top soil	0.03	0.14	0.14	0.05	0.08	0.06	0.09
Ti_ICP sub soil	0.03	0.14	0.13	0.05	0.08	0.06	0.10
Trace elements (values in mg/kg, except Au and Re in ug/kg)							
Ag_ICP top soil	0.012	0.028	0.082	0.013	0.029	0.039	0.038
Ag_ICP sub soil	0.011	0.033	0.099	0.018	0.021	0.032	0.036
As_ICP top soil	1.9	1.7	5.5	3.8	5.0	4.9	6.1
As_ICP sub soil	1.9	1.5	5.6	4.4	4.9	4.7	6.0
As_INAA top soil	3.0	2.4	7.0	5.6	7.0	7.2	8.5
As_INAA sub soil	2.9	2.2	7.1	6.4	6.8	6.9	8.5
B_ICP top soil	2.1	1.1	2.2	2.0	2.1	1.9	2.5
B_ICP sub soil	2.1	1.0	2.2	1.9	2.0	1.7	1.9
Ba_ICP top soil	31.6	23.1	66.6	90.3	284.6	255.0	118.4
Ba_ICP sub soil	26.4	17.8	65.0	104.4	312.0	291.2	121.2
Be_ICP top soil	0.27	0.22	0.25	0.64	0.40	0.45	0.39
Be_ICP sub soil	0.26	0.21	0.26	0.59	0.37	0.43	0.40
Bi_ICP top soil	0.05	0.04	0.10	0.15	0.11	0.10	0.09
Bi_ICP sub soil	0.05	0.04	0.10	0.14	0.10	0.09	0.09
Br_INAA top soil	9.5	5.8	5.9	6.2	10.8	12.6	14.8
Br_INAA sub soil	9.8	7.2	7.3	5.6	13.4	17.4	12.8
Cd_ICP top soil	0.08	0.10	0.24	0.12	0.29	0.43	0.26
Cd_ICP sub soil	0.07	0.13	0.22	0.12	0.25	0.42	0.23

Table 5.2 Ctd…

	Ultramafic	**Mafic intrusive**	**Basalt**	**Mafic clastic**	**Silicic clastic**	**Carbonate**	**Alluvium-colluvium**
Ce_ICP top soil	11.5	6.4	8.2	16.2	13.8	18.4	16.0
Ce_ICP sub soil	10.4	5.6	7.5	14.7	12.9	16.6	15.6
Ce_INAA top soil	22.3	13.4	15.7	43.7	24.9	30.3	26.9
Ce_INAA sub soil	20.4	12.0	15.1	43.0	23.5	27.8	26.3
Co_ICP top soil	114.4	25.0	29.4	30.5	14.5	12.8	17.1
Co_ICP sub soil	117.7	27.4	32.0	34.0	14.7	12.6	17.0
Co_INAA top soil	134.7	37.3	37.1	37.5	18.4	16.5	23.0
Co_INAA sub soil	139.0	39.8	39.4	41.3	18.3	16.0	22.2
Cr_ICP top soil	584	62	73	135	52	51	58
Cr_ICP sub soil	566	60	72	160	52	48	58
Cr_INAA top soil	7473	250	274	990	221	315	415
Cr_INAA sub soil	7379	260	237	805	196	269	340
Cs_ICP top soil	0.7	0.2	0.3	0.5	0.5	0.5	0.4
Cs_ICP sub soil	0.8	0.1	0.3	0.5	0.5	0.5	0.5
Cu_ICP top soil	21.4	128.9	226.7	44.8	51.2	38.5	60.5
Cu_ICP sub soil	21.1	145.1	236.6	42.4	46.2	36.4	60.7
Dy_ICP top soil	0.89	1.79	2.18	1.89	1.84	1.99	1.99
Dy_ICP sub soil	0.89	1.88	2.23	1.83	1.81	1.91	2.05
Er_ICP top soil	0.46	1.10	1.33	0.85	1.01	1.11	1.12
Er_ICP sub soil	0.47	1.17	1.38	0.85	0.99	1.07	1.16
Eu_ICP top soil	0.27	0.40	0.46	0.57	0.48	0.55	0.53
Eu_ICP sub soil	0.26	0.42	0.46	0.56	0.47	0.52	0.54
Eu_INAA top soil	0.4	0.7	0.7	0.9	0.6	0.7	0.8
Eu_INAA sub soil	0.4	0.7	0.6	0.8	0.6	0.7	0.8
Ga_ICP top soil	3.04	8.29	7.88	5.11	4.04	3.78	5.16
Ga_ICP sub soil	3.24	8.68	7.90	5.17	4.02	3.63	5.37
Gd_ICP top soil	1.31	1.86	2.34	2.93	2.49	2.85	2.66
Gd_ICP sub soil	1.26	1.91	2.34	2.81	2.43	2.71	2.74
Hg_ICP top soil	0.07	0.03	0.03	0.03	0.04	0.03	0.03
Hg_ICP sub soil	0.04	0.04	0.04	0.04	0.03	0.03	0.03
Ho_ICP top soil	0.17	0.39	0.46	0.35	0.37	0.40	0.41
Ho_ICP sub soil	0.18	0.41	0.48	0.34	0.37	0.39	0.43

Table 5.2 Ctd…

	Ultramafic	Mafic intrusive	Basalt	Mafic clastic	Silicic clastic	Carbonate	Alluvium-colluvium
La_ICP top soil	5.5	3.0	4.3	7.3	8.6	11.4	9.0
La_ICP sub soil	5.1	2.6	3.9	6.5	8.1	10.5	9.0
La_INAA top soil	9.3	5.3	6.9	20.5	13.3	16.2	13.3
La_INAA sub soil	8.5	4.7	6.6	20.3	12.6	15.1	13.3
Li_ICP top soil	5.0	4.5	11.7	10.0	12.0	8.7	9.7
Li_ICP sub soil	5.2	4.5	12.1	12.8	12.7	9.0	10.4
Lu_INAA top soil	0.15	0.36	0.34	0.28	0.22	0.23	0.31
Lu_INAA sub soil	0.15	0.38	0.35	0.29	0.21	0.22	0.30
Mn_ICP top soil	1303	978	1427	1291	886	768	943
Mn_ICP sub soil	1278	988	1456	1251	853	708	885
Mo_ICP top soil	0.6	0.3	0.9	0.6	1.3	1.1	1.0
Mo_ICP sub soil	0.6	0.3	0.9	0.6	1.3	1.0	1.0
Nb_ICP top soil	0.20	0.16	0.13	0.30	0.27	0.39	0.30
Nb_ICP sub soil	0.16	0.09	0.08	0.20	0.20	0.29	0.21
Nd_ICP top soil	4.5	3.5	4.7	8.5	7.3	9.2	7.7
Nd_ICP sub soil	4.2	3.3	4.5	7.9	7.0	8.6	7.8
Nd_INAA top soil	6.7	5.2	6.7	16.5	10.1	13.1	10.3
Nd_INAA sub soil	6.0	5.2	6.7	15.1	9.7	12.3	10.7
Ni_ICP top soil	1912.2	48.7	70.9	307.7	56.4	54.9	53.7
Ni_ICP sub soil	1987.6	58.1	71.9	358.1	58.1	53.3	52.8
Pb_ICP top soil	6.9	4.5	9.1	8.9	10.3	12.1	13.9
Pb_ICP sub soil	4.4	2.5	6.5	8.1	6.2	8.2	7.5
Pr_ICP top soil	1.20	0.79	1.07	1.95	1.84	2.35	1.94
Pr_ICP sub soil	1.12	0.73	1.00	1.78	1.76	2.19	1.96
Rb_ICP top soil	6.0	3.2	8.1	11.5	10.4	11.3	10.1
Rb_ICP sub soil	5.7	2.5	8.2	10.9	10.1	10.6	10.5
Sb_ICP top soil	0.16	0.15	0.36	0.19	0.46	0.48	0.46
Sb_ICP sub soil	0.12	0.15	0.26	0.28	0.32	0.40	0.37
Sb_INAA top soil	0.21	0.14	0.53	0.46	0.64	0.76	0.74
Sb_INAA sub soil	0.19	0.13	0.45	0.46	0.50	0.65	0.62
Sc_ICP top soil	11.6	18.5	20.7	7.9	7.8	5.8	10.0
Sc_ICP sub soil	12.2	18.5	21.8	8.4	8.0	5.8	10.9
Sc_INAA top soil	17.0	33.5	29.4	13.7	11.9	9.6	18.3
Sc_INAA sub soil	17.7	34.7	29.1	14.3	11.7	9.2	17.9
Se_ICP top soil	0.4	0.6	1.0	0.4	0.6	0.6	0.6
Se_ICP sub soil	0.4	0.5	1.0	0.4	0.5	0.6	0.5
Sm_ICP top soil	1.04	1.10	1.45	2.25	1.83	2.14	1.90
Sm_ICP sub soil	0.99	1.09	1.42	2.17	1.78	2.04	1.94
Sm_INAA top soil	1.7	2.0	2.1	3.4	2.4	2.7	2.6
Sm_INAA sub soil	1.6	2.0	2.1	3.3	2.4	2.5	2.7

Table 5.2 Ctd…

	Ultramafic	Mafic intrusive	Basalt	Mafic clastic	Silicic clastic	Carbonate	Alluvium-colluvium
Sn_ICP top soil	0.78	0.45	0.69	0.78	0.89	0.84	1.00
Sn_ICP sub soil	0.39	0.36	0.53	0.66	0.53	0.65	0.79
Sr_ICP top soil	28.4	58.5	98.7	98.5	465.8	534.1	321.6
Sr_ICP sub soil	27.4	63.3	108.0	123.2	485.4	553.6	318.1
Tb_ICP top soil	0.15	0.27	0.34	0.33	0.31	0.34	0.33
Tb_ICP sub soil	0.15	0.29	0.35	0.32	0.30	0.32	0.34
Te_ICP top soil	0.04	0.05	0.12	0.09	0.05	0.05	0.05
Te_ICP sub soil	0.04	0.05	0.13	0.07	0.04	0.05	0.05
Th_ICP top soil	1.5	0.7	0.8	2.9	1.3	1.6	1.5
Th_ICP sub soil	1.5	0.6	0.8	3.1	1.4	1.5	1.7
Th_INAA top soil	2.3	1.1	1.4	5.5	2.9	3.6	3.0
Th_INAA sub soil	2.1	0.9	1.4	5.5	2.8	3.4	3.1
Tl_ICP top soil	0.05	0.03	0.11	0.11	0.10	0.11	0.09
Tl_ICP sub soil	0.05	0.03	0.13	0.12	0.11	0.11	0.10
Tm_ICP top soil	0.07	0.17	0.20	0.09	0.14	0.15	0.16
Tm_ICP sub soil	0.07	0.18	0.21	0.10	0.14	0.15	0.17
U_ICP top soil	0.36	0.18	0.24	0.32	0.98	0.96	0.76
U_ICP sub soil	0.34	0.17	0.22	0.35	0.98	0.89	0.63
V_ICP top soil	45.9	161.5	155.6	52.5	68.4	53.5	104.2
V_ICP sub soil	44.9	165.1	152.2	51.3	68.3	52.8	104.0
Y_ICP top soil	4.5	10.2	12.4	9.6	10.9	12.1	11.1
Y_ICP sub soil	4.5	11.1	12.8	9.2	10.7	11.6	11.5
Yb_ICP top soil	0.4	1.0	1.3	0.7	0.9	1.0	1.0
Yb_ICP sub soil	0.4	1.1	1.3	0.7	0.9	0.9	1.0
Yb_INAA top soil	1.0	2.4	2.3	1.9	1.6	1.7	2.0
Yb_INAA sub soil	0.9	2.5	2.3	2.0	1.6	1.6	2.0
Zn_ICP top soil	50.0	60.3	124.4	47.5	52.3	46.2	65.4
Zn_ICP sub soil	46.8	64.5	116.1	48.6	44.9	38.2	60.5
Zr_ICP top soil	3.3	5.9	7.8	3.4	3.0	3.3	4.5
Zr_ICP sub soil	3.6	5.7	8.0	4.8	3.7	3.5	5.6

Table 5.3 Results of Box-Cox transformationof variables to de-skew data.

Variable	Box-Cox transformation λ	Mean	Std dev	Skewness	Kurtosis
Ag_ICP sub soil	0.044	-3.59	1.06	0.000	0.601
Ag_ICP top soil	0.063	-3.83	1.20	0.000	1.001
Al_ICP sub soil	0.299	0.52	0.73	0.000	-0.720
Al_ICP top soil	0.264	0.55	0.81	-0.001	-0.771
As_ICP sub soil	0.134	1.38	1.16	0.000	1.611
As_ICP top soil	0.166	1.19	1.21	0.000	1.627
As_INAA sub soil	0.262	2.15	1.71	0.001	1.374
As_INAA top soil	0.325	1.82	1.68	0.000	1.747
B_ICP sub soil	-0.272	0.27	0.78	0.001	-1.399
B_ICP top soil	-0.182	0.16	0.76	-0.001	-1.127
Ba_ICP sub soil	0.045	4.35	1.45	0.000	-0.107
Ba_ICP top soil	0.014	4.52	1.92	-0.001	-0.236
Be_ICP sub soil	0.132	-1.14	0.67	-0.001	-0.048
Be_ICP top soil	0.161	-1.22	0.73	0.000	0.157
Bi_ICP sub soil	0.080	-2.37	0.66	0.001	0.221
Bi_ICP top soil	0.112	-2.58	0.78	-0.001	1.068
Br_INAA sub soil	0.325	2.75	1.44	-0.001	1.616
Br_INAA top soil	0.237	3.48	1.83	-0.001	4.325
Ca_ICP sub soil	0.491	3.48	2.72	0.000	-1.458
Ca_ICP top soil	0.409	4.29	3.33	0.000	-1.447
Ca_INAA sub soil	0.600	4.73	3.45	0.000	-1.336
Ca_INAA top soil	0.542	5.60	4.06	0.000	-1.273
Cd_ICP sub soil	0.028	-1.52	0.83	0.000	1.079
Cd_ICP top soil	0.097	-1.84	1.03	-0.001	3.664
Ce_ICP sub soil	0.236	3.12	1.25	-0.001	0.194
Ce_ICP top soil	0.199	3.07	1.47	0.001	0.470
Ce_INAA sub soil	0.233	4.42	1.58	0.000	-0.009
Ce_INAA top soil	0.244	4.12	1.66	0.000	0.401
Co_ICP sub soil	-0.096	2.07	0.35	0.000	1.768
Co_ICP top soil	-0.218	2.42	0.54	0.000	0.972
Co_INAA sub soil	-0.061	2.32	0.35	0.000	1.413
Co_INAA top soil	-0.186	2.77	0.58	0.001	0.616
Cr_ICP sub soil	-0.074	2.98	0.46	0.000	3.394
Cr_ICP top soil	-0.136	3.27	0.65	0.000	3.907
Cr_INAA sub soil	-0.131	3.38	0.43	0.000	1.887
Cr_INAA top soil	-0.176	3.65	0.59	0.000	1.890
Cs_ICP sub soil	0.295	-1.00	0.68	-0.001	0.295
Cs_ICP top soil	0.224	-0.93	0.67	0.001	0.235
Cu_ICP sub soil	-0.112	2.65	0.41	0.000	2.364
Cu_ICP top soil	-0.195	3.04	0.61	0.000	1.310
Dy_ICP sub soil	0.427	0.69	0.62	0.000	1.623
Dy_ICP top soil	0.416	0.67	0.69	0.000	1.929
Er_ICP sub soil	0.382	0.04	0.51	0.001	1.703
Er_ICP top soil	0.393	0.03	0.56	0.000	2.118
Eu_ICP sub soil	0.352	-0.69	0.41	-0.001	1.144
Eu_ICP top soil	0.331	-0.71	0.45	-0.001	1.203
Eu_INAA sub soil	0.514	-0.39	0.47	0.000	0.161
Eu_INAA top soil	0.591	-0.45	0.52	0.000	0.273
Fe_ICP sub soil	0.330	1.25	1.05	0.000	-0.834
Fe_ICP top soil	0.277	1.27	1.17	0.000	-0.741
Fe_INAA sub soil	0.462	1.77	1.10	0.000	-0.865
Fe_INAA top soil	0.396	1.83	1.26	0.000	-0.656

Table 5.3 Ctd….

Variable	Box-Cox transformation λ	Mean	Std dev	Skewness	Kurtosis
Ga_ICP sub soil	0.474	2.31	1.20	0.000	-0.767
Ga_ICP top soil	0.456	2.36	1.33	0.000	-0.894
Gd_ICP sub soil	0.415	1.01	0.74	0.000	1.254
Gd_ICP top soil	0.399	0.98	0.81	0.000	1.537
Hg_ICP sub soil	-0.676	-6.01	1.73	0.001	-1.475
Hg_ICP top soil	-0.236	-20.48	9.77	0.000	-0.843
Ho_ICP sub soil	0.408	-0.81	0.34	0.000	1.315
Ho_ICP top soil	0.396	-0.81	0.37	-0.001	1.646
K_ICP sub soil	0.322	-1.24	0.43	0.001	-0.230
K_ICP top soil	0.301	-1.31	0.46	0.001	-0.190
La_ICP sub soil	0.286	2.49	1.37	0.000	-0.075
La_ICP top soil	0.278	2.33	1.50	0.000	0.248
La_INAA sub soil	0.254	3.07	1.36	0.000	-0.216
La_INAA top soil	0.240	2.95	1.53	0.000	-0.073
Li_ICP sub soil	0.168	2.33	0.98	-0.001	1.042
Li_ICP top soil	0.142	2.43	1.11	0.000	0.856
Lu_INAA sub soil	0.583	-0.88	0.26	-0.001	-0.183
Lu_INAA top soil	0.686	-0.96	0.32	0.000	-0.158
Mg_ICP sub soil	-0.116	-0.15	0.77	0.000	0.717
Mg_ICP top soil	-0.224	-0.14	0.82	0.001	0.127
Mn_ICP sub soil	0.077	6.80	0.64	0.000	1.668
Mn_ICP top soil	0.005	8.64	1.19	0.001	1.429
Mo_ICP sub soil	0.078	-0.66	1.10	0.000	1.096
Mo_ICP top soil	0.087	-0.93	1.30	0.001	1.696
Na_ICP sub soil	0.195	-1.52	0.73	-0.001	2.151
Na_ICP top soil	0.166	-1.45	0.66	0.000	2.971
Na_INAA sub soil	0.083	-0.77	0.99	0.000	-1.036
Na_INAA top soil	0.084	-0.86	1.03	0.000	-1.066
Nb_ICP sub soil	-0.446	-1.57	0.84	0.000	-1.577
Nb_ICP top soil	0.052	-3.75	2.21	0.000	-0.781
Nd_ICP sub soil	0.318	2.40	1.17	0.000	0.501
Nd_ICP top soil	0.296	2.33	1.31	0.000	0.644
Nd_INAA sub soil	-0.771	1.25	0.35	0.001	-1.792
Nd_INAA top soil	-0.438	0.94	0.19	0.000	-1.644
Ni_ICP sub soil	-0.046	2.95	0.58	0.000	8.103
Ni_ICP top soil	-0.125	3.36	0.90	0.000	10.273
P_ICP sub soil	-0.003	-2.91	0.63	0.000	-0.677
P_ICP top soil	0.113	-3.62	0.94	0.000	0.727
Pb_ICP sub soil	0.193	2.03	0.93	-0.001	8.030
Pb_ICP top soil	0.077	1.75	1.34	-0.001	18.559
Pr_ICP sub soil	0.314	0.42	0.83	0.001	0.342
Pr_ICP top soil	0.285	0.34	0.90	0.000	0.665
Rb_ICP sub soil	0.455	3.31	1.72	0.000	0.002
Rb_ICP top soil	0.407	3.37	2.09	0.000	0.196
Sb_ICP sub soil	0.081	-1.51	0.97	0.000	1.743
Sb_ICP top soil	0.043	-1.63	0.98	-0.001	2.927
Sb_INAA sub soil	0.103	-1.05	1.10	0.001	-0.777
Sb_INAA top soil	0.106	-1.18	1.10	0.000	0.105
Sc_ICP sub soil	0.157	2.40	1.07	0.000	-0.609
Sc_ICP top soil	0.116	2.57	1.23	0.000	-0.337
Sc_INAA sub soil	0.375	4.67	1.92	0.000	-1.206
Sc_INAA top soil	0.359	4.73	2.12	0.000	-1.245
Se_ICP sub soil	-0.002	-0.77	0.81	0.000	0.975
Se_ICP top soil	0.088	-0.86	0.85	0.000	7.734

Table 5.3 Ctd….

Variable	Box-Cox transformation λ	Mean	Std dev	Skewness	Kurtosis
Sm_ICP sub soil	0.369	0.52	0.69	0.000	0.909
Sm_ICP top soil	0.347	0.47	0.76	0.000	1.095
Sm_INAA sub soil	0.297	0.90	0.63	0.000	0.804
Sm_INAA top soil	0.263	0.85	0.72	-0.001	1.140
Sn_ICP sub soil	0.045	-0.74	0.88	0.000	2.495
Sn_ICP top soil	-0.046	-0.91	0.85	0.000	2.770
Sr_ICP sub soil	0.097	6.03	1.76	-0.001	-1.045
Sr_ICP top soil	0.060	6.79	2.14	0.000	-1.061
Tb_ICP sub soil	0.406	-0.96	0.32	0.001	0.863
Tb_ICP top soil	0.410	-0.97	0.35	0.001	1.077
Te_ICP sub soil	-0.176	-4.68	1.67	0.000	-0.847
Te_ICP top soil	-0.164	-4.84	1.74	0.001	-0.764
Th_ICP sub soil	0.055	-0.10	0.89	0.000	-0.365
Th_ICP top soil	0.015	-0.16	1.00	0.000	-0.063
Th_INAA sub soil	0.358	0.84	1.42	0.001	-0.578
Th_INAA top soil	0.404	0.67	1.46	-0.001	-0.340
Ti_ICP sub soil	0.123	-2.21	0.58	0.001	-0.065
Ti_ICP top soil	0.147	-2.28	0.62	0.000	0.603
Tl_ICP sub soil	0.079	-2.27	0.62	0.000	1.205
Tl_ICP top soil	0.129	-2.49	0.78	0.001	1.548
Tm_ICP sub soil	0.064	-1.74	0.46	0.000	-0.749
Tm_ICP top soil	0.137	-1.88	0.57	0.001	-0.622
U_ICP sub soil	-0.001	-0.87	0.99	0.000	-0.320
U_ICP top soil	0.048	-1.08	1.11	0.000	0.225
V_ICP sub soil	0.214	7.00	1.93	0.000	-0.785
V_ICP top soil	0.206	7.08	2.09	0.000	-0.794
Y_ICP sub soil	0.438	4.22	1.36	0.000	1.898
Y_ICP top soil	0.447	4.14	1.48	-0.001	2.538
Yb_ICP sub soil	0.295	-0.07	0.50	-0.001	1.442
Yb_ICP top soil	0.304	-0.08	0.56	0.000	1.799
Yb_INAA sub soil	0.405	0.65	0.59	0.000	0.838
Yb_INAA top soil	0.381	0.61	0.68	0.000	0.890
Zn_ICP sub soil	0.053	4.13	0.83	0.000	6.488
Zn_ICP top soil	0.030	4.15	0.97	0.000	6.172
Zr_ICP sub soil	0.003	1.10	0.89	0.000	-0.301
Zr_ICP top soil	-0.016	1.18	0.96	0.000	-0.301

Table 5.4 Correlation coefficients $r>|0.4|$ between λ-transformed (de-skewed) ar-ICPMS variables. Upper half of table is top soils and lower half is sub soils. Bold values for $r>|0.6|$.

ICP

	Ag	Al	As	B	Ba	Be	Bi	Ca	Cd	Co	Cr	Cs	Cu	Fe	Ga	Hg	K	Li	Mg	Mn	Mo	Na	Nb	Ni	P	Pb	Rb	Sb	Sc	Se	Sn	Sr	Th	Ti	Tl	U	V	Zn	Zr
Ag																																							
Al										**0.62**			0.53	**0.74**	**0.91**				0.55	0.44					0.51				**0.85**					0.40			**0.76**	0.47	0.59
As							0.51		0.43			0.42					0.43				0.57					0.54	0.48	0.59					0.45		**0.65**	0.50			
B																																							
Ba						0.43	0.52	**0.64**	0.49			0.45														0.43	0.47					**0.61**	0.41		0.52	0.47			
Be					0.42		**0.61**					0.58					0.52						**0.61**			0.49	**0.66**				0.47		**0.77**		0.59				
Bi			0.48		0.52	**0.64**			0.47			0.48					0.42						0.44			**0.66**	0.55	0.49			0.49		**0.64**		**0.73**				
Ca					**0.63**				0.46																							**0.91**				0.56			
Cd			0.40		0.49		0.44	0.46													0.43					0.43	0.40	0.58				0.47			0.56	0.51			
Co		**0.62**									0.47		0.47	**0.83**	0.58				**0.72**	**0.64**				0.50					**0.74**								0.57	0.53	0.49
Cr										0.45									0.48					**0.77**															
Cs			0.47		0.48	**0.60**	0.53										0.57	0.43					0.58			0.44	**0.82**	0.43					**0.69**		**0.66**	0.54			
Cu		0.48								0.45				0.49	0.53					0.52									0.54								0.50	**0.66**	
Fe		**0.75**								**0.82**			0.47		**0.79**				**0.67**	0.53					0.49				**0.88**								**0.80**	0.57	**0.64**
Ga		**0.91**								0.58			0.49	**0.79**					0.45	0.43					**0.61**				**0.86**					0.49			**0.83**	0.52	**0.68**
Hg																																							
K			0.46			0.52	0.44					**0.65**						**0.67**					0.40			0.44	**0.86**				0.47		0.52		0.58				
Li				0.41								0.45					**0.65**										**0.65**								0.43				
Mg		0.58								**0.74**	0.43			**0.69**	0.49					0.44				0.41					**0.69**								0.53		
Mn		0.48								**0.68**			0.51	0.57	0.46				0.49										0.53									0.53	0.40
Mo			0.57						0.42																			0.54							0.49	0.55			
Na																																							
Nb					0.42	0.54	0.43					0.54														0.45	0.54				0.42		**0.65**		0.47	0.48			
Ni										0.55	**0.77**								0.44																				
P		0.47												0.42	0.56														0.53					0.52			**0.62**		0.52
Pb			**0.62**		0.47	0.58	**0.74**		0.49			0.58					0.52				0.44		0.46				0.50	**0.60**			0.58		0.52		**0.62**				
Rb			0.51		0.45	**0.64**	0.55					**0.84**					**0.90**	**0.63**					0.46			**0.60**		0.43			0.47		**0.69**		**0.72**	0.43			
Sb			**0.61**		0.40		0.49		0.58			0.49									0.55		0.43			**0.60**	0.46								0.59	0.56			
Sc		**0.85**								**0.73**			0.52	**0.88**	**0.85**				**0.70**	0.57					0.47									0.48			**0.84**	0.56	**0.67**
Se																																							
Sn			0.41			0.56	0.52					0.44					0.48									**0.61**	0.52						0.48		0.43				
Sr					**0.62**			**0.87**	0.47																			0.40								**0.60**			
Th			0.47		0.44	**0.77**	**0.68**					**0.72**					0.54						0.55			**0.65**	**0.68**	0.41			0.57				**0.61**	0.45			
Ti															0.45										0.49				0.45								0.59		0.44
Tl			**0.65**		0.53	0.59	**0.71**		0.54			**0.69**					**0.63**	0.42			0.52		0.47			**0.73**	**0.73**	**0.64**			0.46		**0.63**			0.52			
U			0.48		0.49			0.56	0.50			0.58									0.53		0.52			0.44	0.44	**0.60**				**0.61**	0.50		0.56				
V		**0.76**								0.58			0.48	**0.80**	**0.82**				0.55	0.43					0.56				**0.85**					0.56				0.50	**0.66**
Zn		0.50								0.58			**0.64**	**0.62**	0.56				0.42	**0.60**									**0.61**								0.55		0.44
Zr		0.53								0.44				**0.60**	**0.63**					0.43					0.46				**0.64**					0.42			**0.63**	0.50	
Ce			0.48		0.52	**0.81**	**0.68**		0.41			**0.67**					0.57						**0.72**			0.57	**0.74**	0.42			0.54		**0.88**		**0.66**	0.51			
Dy						0.54									0.45		0.46			0.42							0.47				0.48		0.50						0.56
Er						0.42									0.50		0.42			0.42					0.41						0.43						0.42	0.41	**0.62**
Eu						**0.70**	0.53					0.42					0.52						0.47			0.44	0.59				0.54		**0.70**		0.49				0.40
Gd						**0.72**	0.58					0.45					0.53						0.47			0.46	**0.62**				0.55		**0.71**		0.53				
Ho						0.47									0.51		0.43			0.42							0.42				0.44		0.42						0.58
La			0.44		**0.65**	**0.77**	**0.70**		0.46			**0.68**					0.55						**0.69**			0.57	**0.72**	0.45			0.47		**0.81**		**0.68**	0.53			
Nd			0.43		0.54	**0.80**	**0.70**		0.41			**0.62**					0.55						0.57			0.55	**0.71**	0.40			0.53		**0.82**		**0.65**	0.45			
Pr			0.44		0.58	**0.80**	**0.71**		0.43			**0.66**					0.56						**0.60**			**0.68**	**0.73**	0.42			0.52		**0.83**		**0.67**	0.49			
Sm					0.45	**0.78**	**0.66**					0.54					0.54						0.46			**0.62**	**0.64**				0.55		**0.78**		**0.60**				
Tb						**0.60**	0.46								0.41		0.44			0.43						0.44	0.47				0.59		0.57		0.42				0.48
Tm		0.44												0.45	0.56					0.47					0.42				0.49		0.41						0.47	0.44	**0.61**
Y						0.49									0.42					0.41											0.51								0.50
Yb		0.45												0.45	0.59					0.50					0.47				0.52		0.42			0.42			0.57	0.46	**0.66**

	Ce	Dy	Er	Eu	Gd	Ho	La	Nd	Pr	Sm	Tb	Tm	Y	Yb
Ag														
Al												0.42		0.43
As	0.45						0.43	0.41	0.42					
B														
Ba	0.53						**0.65**	0.57	0.59	0.48				
Be	**0.81**	0.57	0.45	**0.72**	**0.73**	0.50	**0.76**	**0.80**	**0.80**	**0.78**	**0.62**		0.53	
Bi	**0.65**			0.53	0.57		**0.68**	**0.68**	**0.69**	**0.65**	0.46			
Ca														
Cd	0.41						0.47	0.42	0.44					
Co														
Cr														
Cs	**0.69**			0.44	0.46		**0.66**	**0.61**	**0.65**	0.53				
Cu														
Fe														
Ga		0.48	0.54			0.47						0.54		0.57
Hg														
K	0.58	0.43		0.49	0.51		0.55	0.55	0.56	0.55	0.47		0.42	
Li														
Mg														
Mn		0.46	0.47			0.47						0.43		0.44
Mo														
Na														
Nb	**0.64**						**0.63**	**0.65**	**0.67**	0.55				
Ni														
P			0.42									0.42		0.47
Pb	**0.68**			0.52	0.56		**0.68**	**0.67**	0.57	0.52				
Rb	**0.72**	0.43		0.55	0.58		**0.70**	**0.69**	**0.70**	**0.67**	0.52		0.45	
Sb	0.47						0.49	0.44	0.46					
Sc			0.43									0.45		0.47
Se														
Sn	**0.62**	0.56	0.49	**0.63**	**0.64**	0.51	0.54	**0.61**	**0.60**	**0.63**	0.51		0.45	
Sr														
Th	**0.87**	0.47		**0.67**	**0.69**		**0.82**	**0.83**	**0.84**	**0.77**	0.54		0.44	
Ti														0.41
Tl	**0.67**			0.44	0.49		**0.68**	**0.64**	**0.67**	0.58				
U	0.52						0.54	0.45	0.49					
V		0.41	0.49			0.45						0.53		0.51
Zn		0.43	0.46			0.45						0.48		0.51
Zr		**0.61**	**0.65**	0.45	0.45	**0.61**					0.54	**0.63**	0.56	**0.68**
Ce		**0.62**	0.50	**0.80**	**0.83**	0.55	**0.95**	**0.95**	**0.97**	**0.90**	**0.67**		**0.60**	
Dy	**0.60**		**0.96**	**0.89**	**0.92**	**0.96**	0.55	**0.70**	**0.65**	**0.82**	**0.94**	**0.84**	**0.95**	**0.90**
Er	0.48	**0.96**		**0.81**	**0.83**	**0.96**	0.44	0.58	0.53	**0.72**	**0.89**	**0.88**	**0.94**	**0.95**
Eu	**0.77**	**0.89**	**0.81**		**0.95**	**0.84**	**0.73**	**0.85**	**0.81**	**0.91**	**0.90**	**0.68**	**0.84**	**0.71**
Gd	**0.82**	**0.92**	**0.84**	**0.94**		**0.87**	**0.78**	**0.89**	**0.86**	**0.96**	**0.93**	0.69	**0.89**	**0.73**
Ho	0.53	**0.97**	**0.96**	**0.85**	**0.87**		0.48	**0.63**	0.58	**0.76**	**0.92**	**0.86**	**0.94**	**0.92**
La	**0.95**	0.53	0.41	**0.70**	**0.76**	0.46		**0.95**	**0.97**	**0.87**	**0.61**		0.56	
Nd	**0.95**	**0.70**	0.57	**0.83**	**0.89**	**0.63**	**0.95**		**0.98**	**0.95**	**0.75**	0.44	**0.70**	0.46
Pr	**0.97**	**0.64**	0.52	**0.79**	**0.85**	0.57	**0.97**	**0.98**		**0.93**	**0.71**	0.40	**0.65**	0.41
Sm	**0.89**	**0.82**	**0.71**	**0.90**	**0.96**	**0.75**	**0.86**	**0.95**	**0.93**		**0.86**	0.57	**0.80**	**0.60**
Tb	**0.66**	**0.95**	**0.90**	**0.91**	**0.93**	**0.93**	0.59	**0.75**	**0.70**	**0.86**		**0.78**	**0.91**	**0.82**
Tm		**0.84**	**0.89**	**0.69**	**0.69**	**0.86**		0.44		0.56	**0.79**		**0.83**	**0.89**
Y	0.57	**0.95**	**0.95**	**0.84**	**0.88**	**0.95**	0.53	**0.67**	**0.62**	**0.78**	**0.91**	**0.84**		**0.89**
Yb		**0.91**	**0.96**	**0.71**	**0.74**	**0.93**		0.45	0.40	0.59	**0.83**	**0.90**	**0.90**	

Table 5.5 Correlation coefficients r>|0.4| between λ-transformed (de-skewed) INAA variables. Upper half of table is top soils and lower half is sub soils. Bold values for r>|0.6|.

INAA

	As	Br	Ca	Ce	Co	Cr	Eu	Fe	La	Lu	Na	Nd	Sb	Sc	Sm	Th	Yb
As				0.40					0.43				0.58			0.41	
Br																	
Ca		0.42															
Ce	0.44						0.65		0.92			0.67	0.42		**0.79**	**0.88**	
Co								**0.85**			0.44			**0.75**			
Cr																	
Eu				0.66					0.58	0.54		0.51			**0.78**	0.52	**0.70**
Fe					**0.84**					0.50	0.67			**0.88**			0.52
La	0.45			**0.92**			0.59					0.68	0.47		**0.77**	**0.91**	
Lu							0.56	0.54			0.47			0.44	0.43		**0.76**
Na					0.45			0.68		0.51				**0.77**			0.55
Nd				0.65			0.49		0.66						0.59	0.66	
Sb	0.59			0.47					0.50							0.46	
Sc					**0.74**			**0.89**		0.48	**0.78**						0.49
Sm				**0.80**			**0.80**		**0.78**	0.47		0.58				0.69	0.63
Th	0.44			**0.88**			0.50		**0.91**			0.63	0.50		0.68		
Yb							**0.73**	0.57		**0.77**	0.58			0.54	0.66		

Table 5.6 Correlation coefficients r>|0.4| between λ-transformed (de-skewed) ar-ICPMS versus INAA variables. Upper half of table is top soils and lower half of table is sub soils. Bold values for r>|0.6|.

	As _INAA	Ca _INAA	Ce _INAA	Co _INAA	Cr _INAA	Eu _INAA	Fe _INAA	La _INAA	Na _INAA	Nd _INAA	Sb _INAA	Sc _INAA	Sm _INAA	Th _INAA	Yb _INAA
As_ICP	**0.82**		0.44					0.45			0.57			0.44	
Ca_ICP		**0.95**													
Ce_ICP	0.44		**0.89**			0.60		**0.92**		0.64	0.45		**0.77**	**0.85**	
Co_ICP				**0.93**			**0.80**					0.67			
Cr_ICP				0.49	**0.79**										
Eu_ICP			**0.74**			**0.75**		**0.71**		0.55			**0.83**	0.62	0.65
Fe_ICP				**0.81**			**0.95**		0.64			**0.81**			0.52
La_ICP	0.43		**0.82**			0.51		**0.92**		0.63	0.47		**0.71**	**0.81**	
Na_ICP															
Nd_ICP	0.41		**0.86**			0.64		**0.92**		0.65	0.43		**0.81**	**0.81**	
Sb_ICP	0.53							0.40			0.62				
Sc_ICP				**0.71**			**0.83**		0.69			**0.87**			0.48
Sm_ICP			**0.83**			**0.71**		**0.85**		0.62			**0.85**	**0.75**	0.50
Th_ICP	0.43		**0.87**			0.55		**0.87**		0.59			**0.71**	**0.85**	
Yb_ICP						0.56							0.53		**0.74**

	As _INAA	Ca _INAA	Ce _INAA	Co _INAA	Cr _INAA	Eu _INAA	Fe _INAA	La _INAA	Na _INAA	Nd _INAA	Sb _INAA	Sc _INAA	Sm _INAA	Th _INAA	Yb _INAA
As_ICP	**0.82**		0.45					0.45			0.57			0.44	
Ca_ICP		**0.96**													
Ce_ICP	0.46		**0.90**			0.61		**0.92**		0.63	0.50		**0.79**	**0.85**	
Co_ICP				**0.94**			**0.80**					0.67			
Cr_ICP				0.46	**0.83**										
Eu_ICP			**0.74**			**0.78**		**0.70**		0.53			**0.85**	0.60	**0.71**
Fe_ICP				**0.80**			**0.95**		0.63			**0.82**			0.55
La_ICP	0.44		**0.83**			0.53		**0.92**		0.62	0.50		**0.73**	**0.81**	
Na_ICP															
Nd_ICP	0.42		**0.87**			0.66		**0.92**		0.64	0.46		**0.84**	**0.81**	0.40
Sb_ICP	0.57							0.44			0.62			0.42	
Sc_ICP				**0.70**			**0.84**		0.69			**0.88**			0.52
Sm_ICP			**0.84**			**0.73**		**0.86**		0.62	0.40		**0.88**	**0.74**	0.55
Th_ICP	0.44		**0.87**			0.54		**0.89**		0.59	0.45		**0.71**	**0.86**	
Yb_ICP						0.58			0.43				0.56		**0.78**

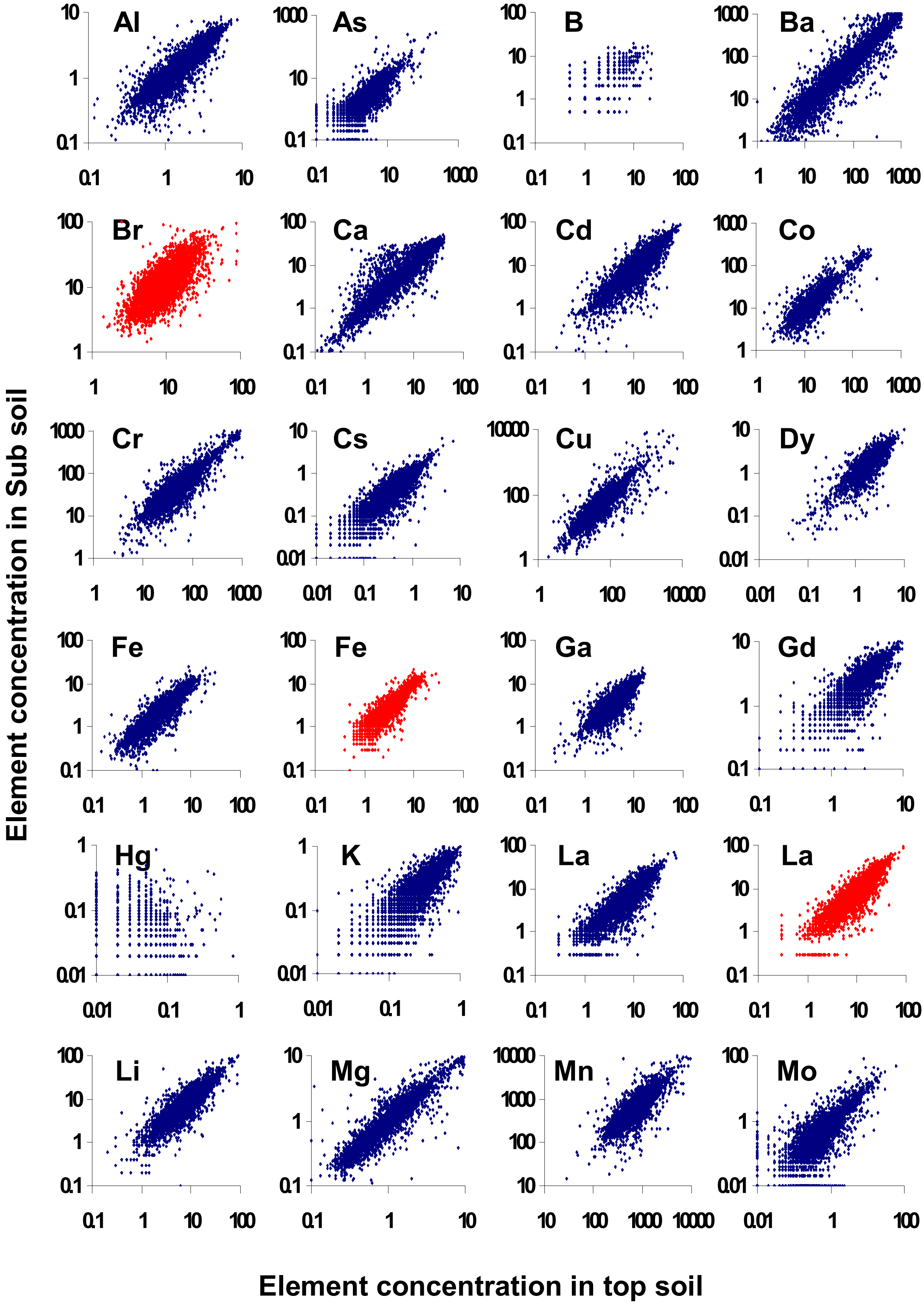

Figure 5.2 Plot of aqua regia-extractable (blue) or total (red) element values in top soil versus sub soil for selected elements.

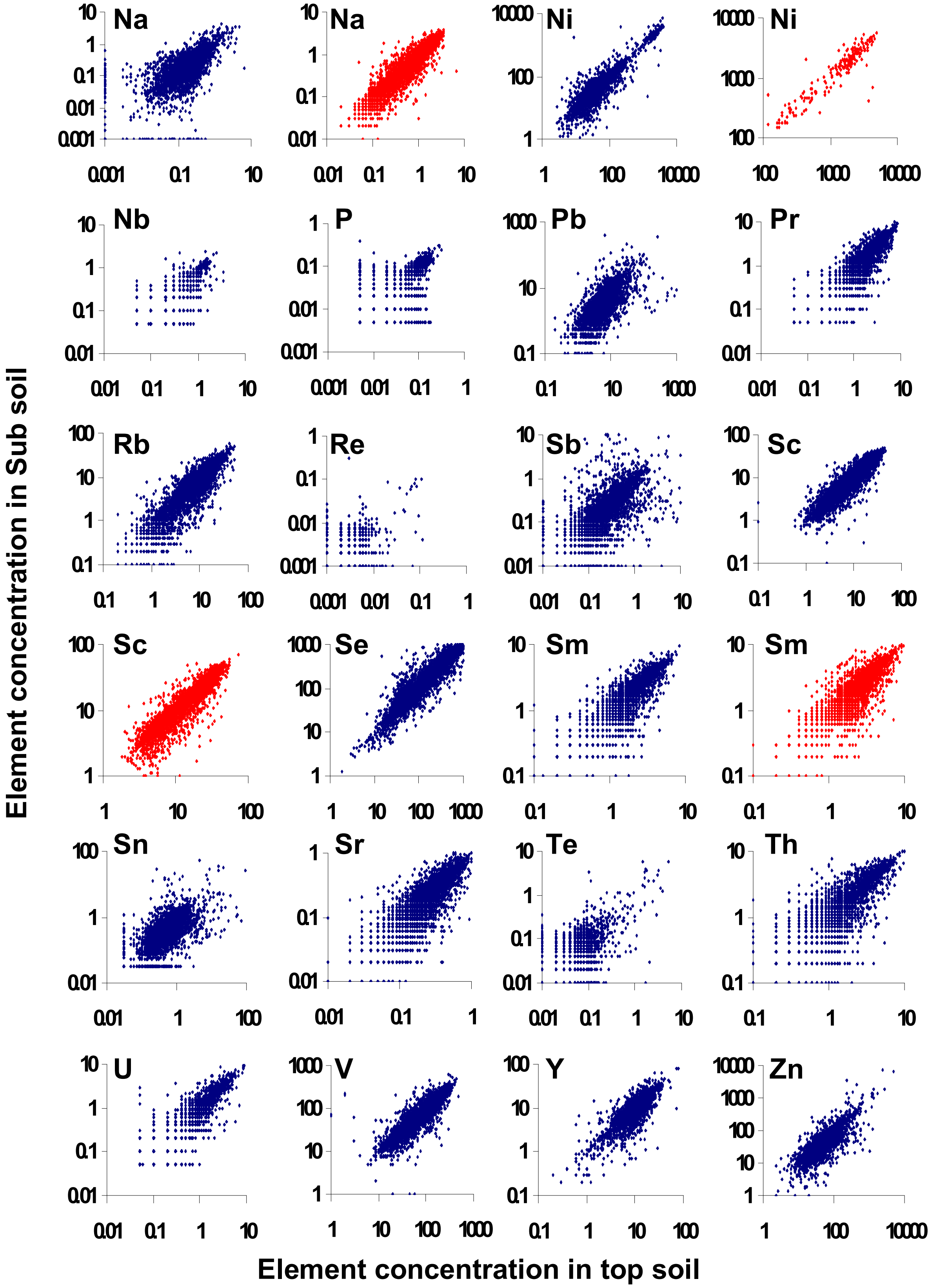

Figure 5.3 Plot of aqua regia-extractable (blue) or total (red) element values in top soil versus sub soil for selected elements.

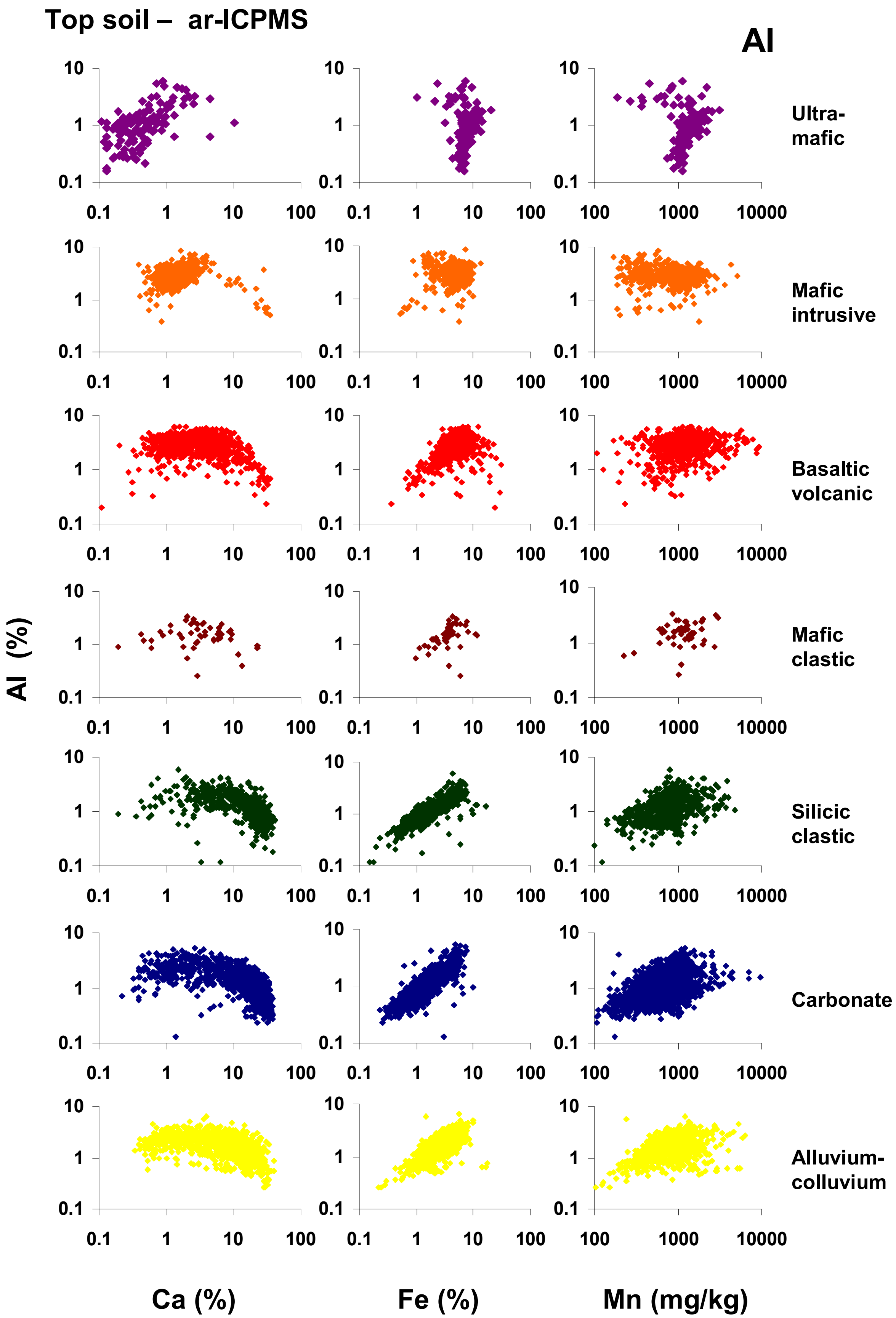

Figure 5.4 Plot of aqua regia-extractable Al versus Ca, Fe and Mn in top soils, separated by underlying lithology group.

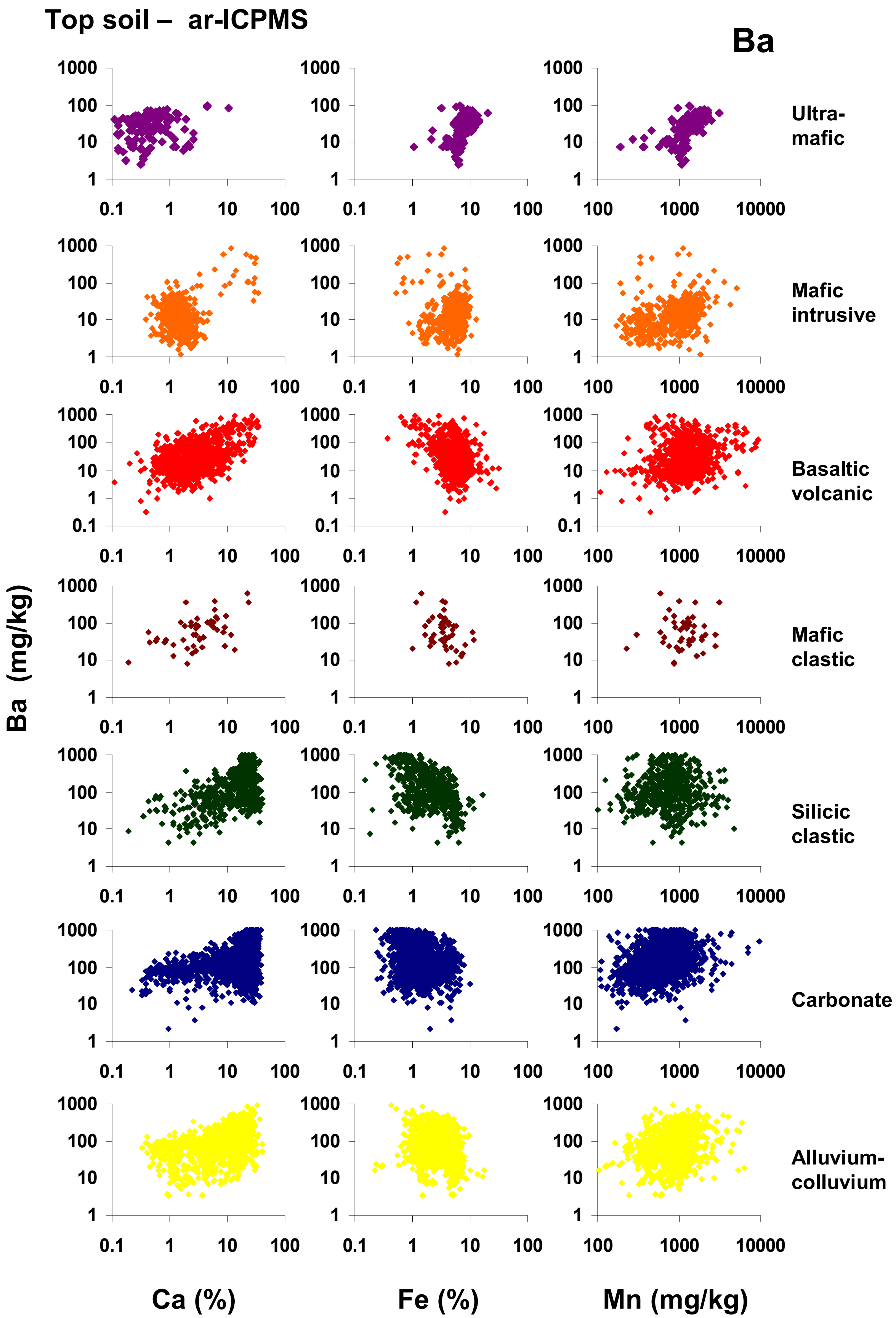

Figure 5.5 Plot of aqua regia-extractable Ba versus Ca, Fe and Mn in top soils, separated by underlying lithology group.

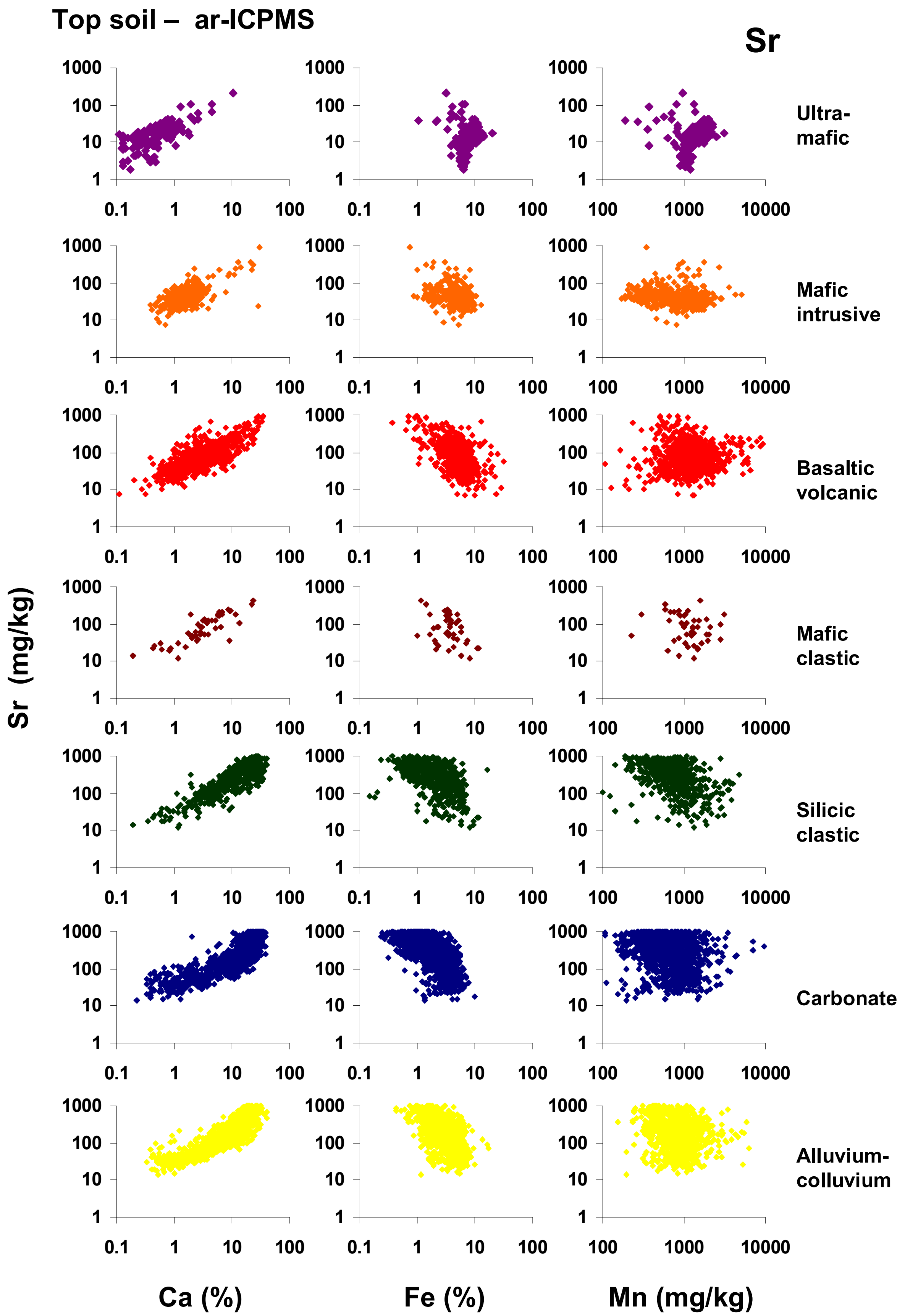

Figure 5.6 Plot of aqua regia-extractable Sr versus Ca, Fe and Mn in top soils, separated by underlying lithology group.

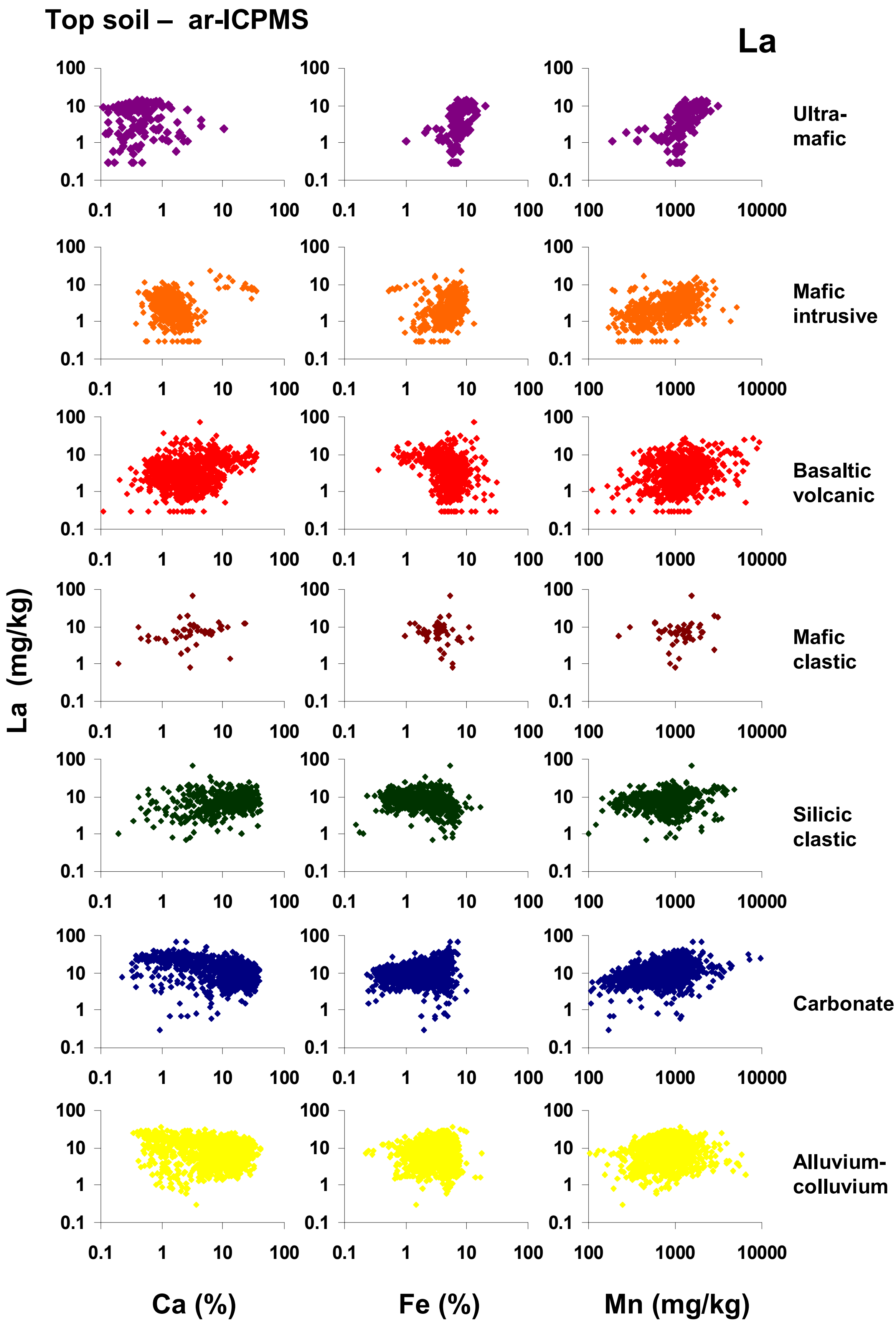

Figure 5.7 Plot of aqua regia-extractable La versus Ca, Fe and Mn in top soils, separated by underlying lithology group.

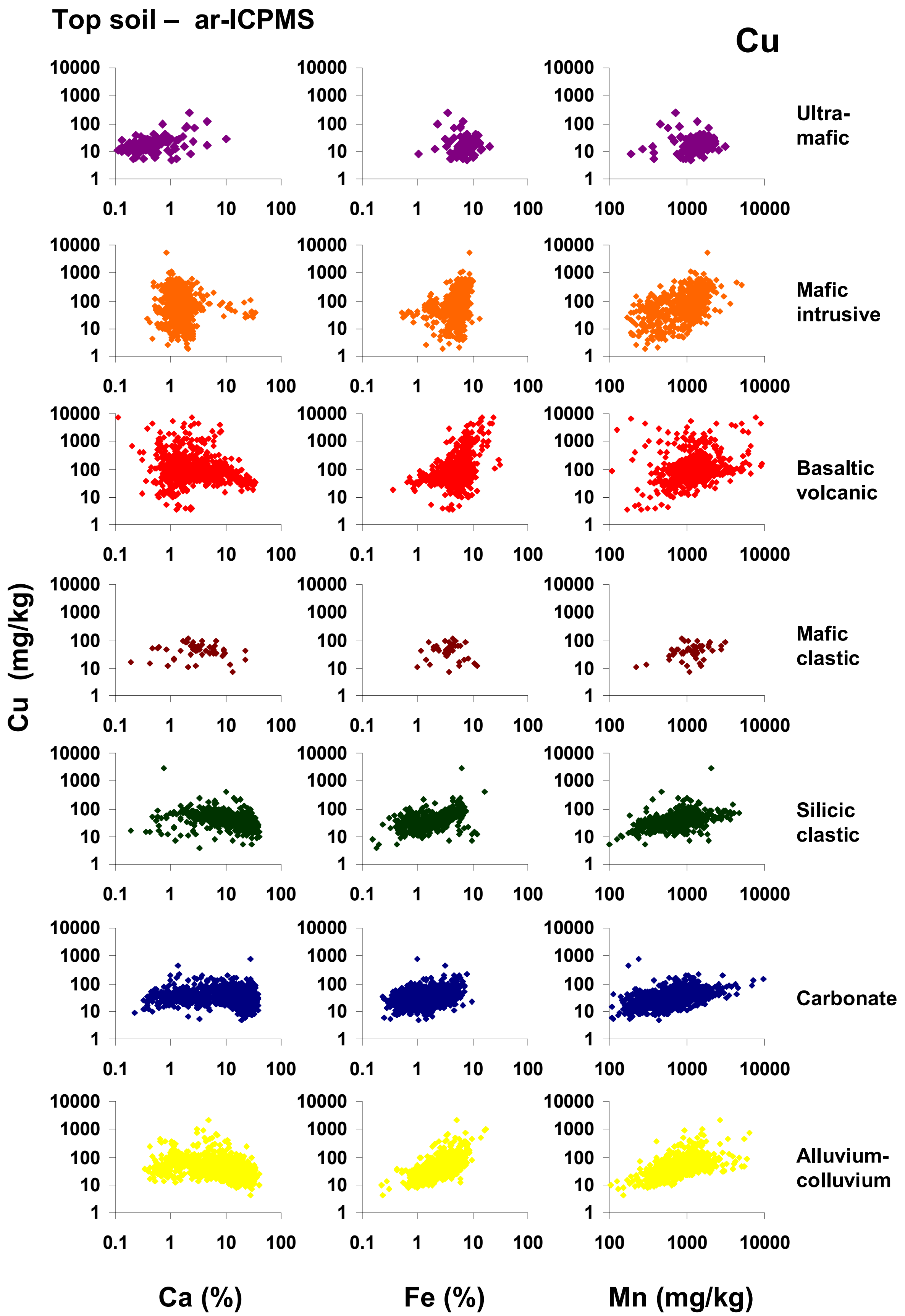

Figure 5.8 Plot of aqua regia-extractable Cu versus Ca, Fe and Mn in top soils, separated by underlying lithology group.

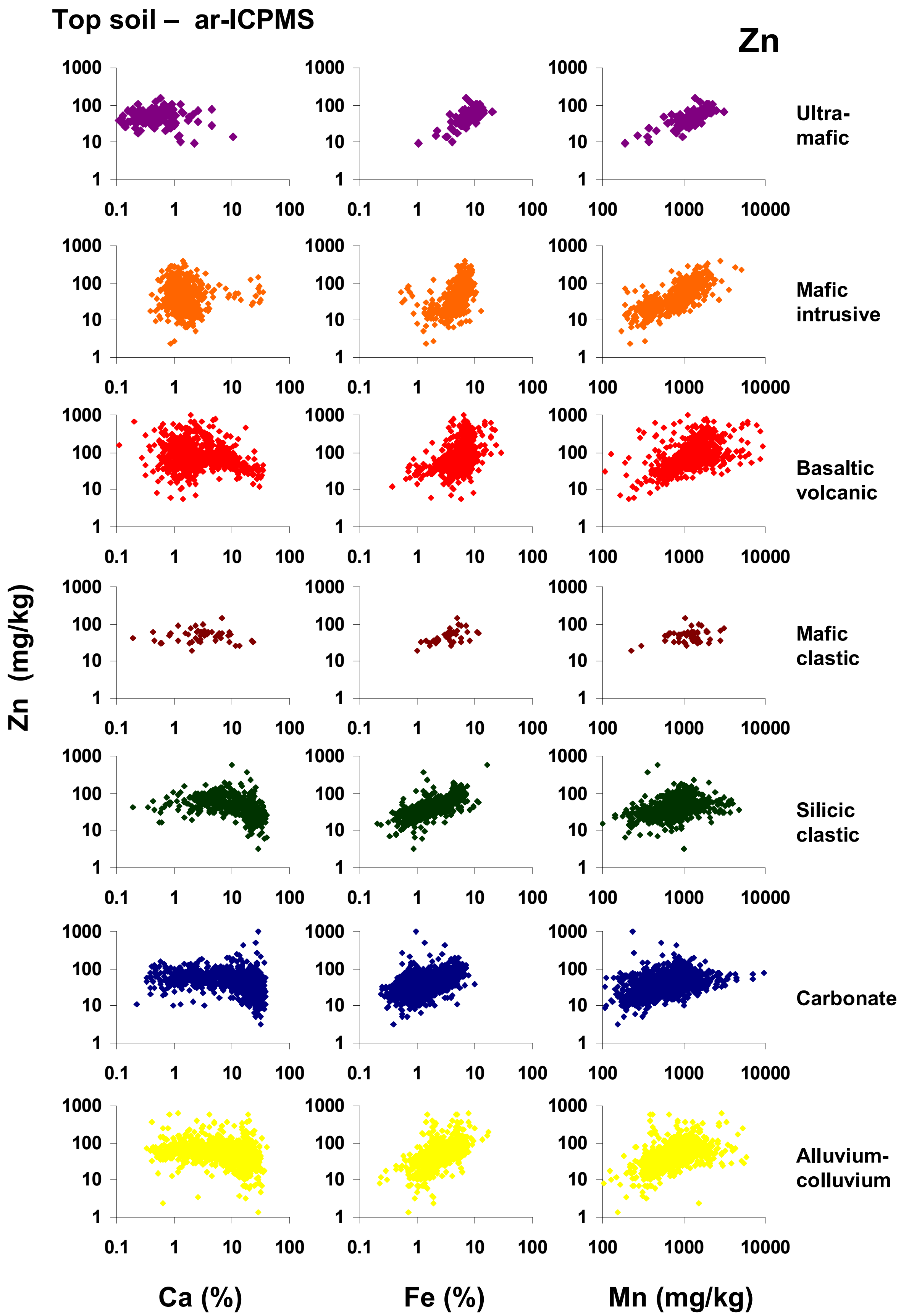

Figure 5.9 Plot of aqua regia-extractable Zn versus Ca, Fe and Mn in top soils, separated by underlying lithology group.

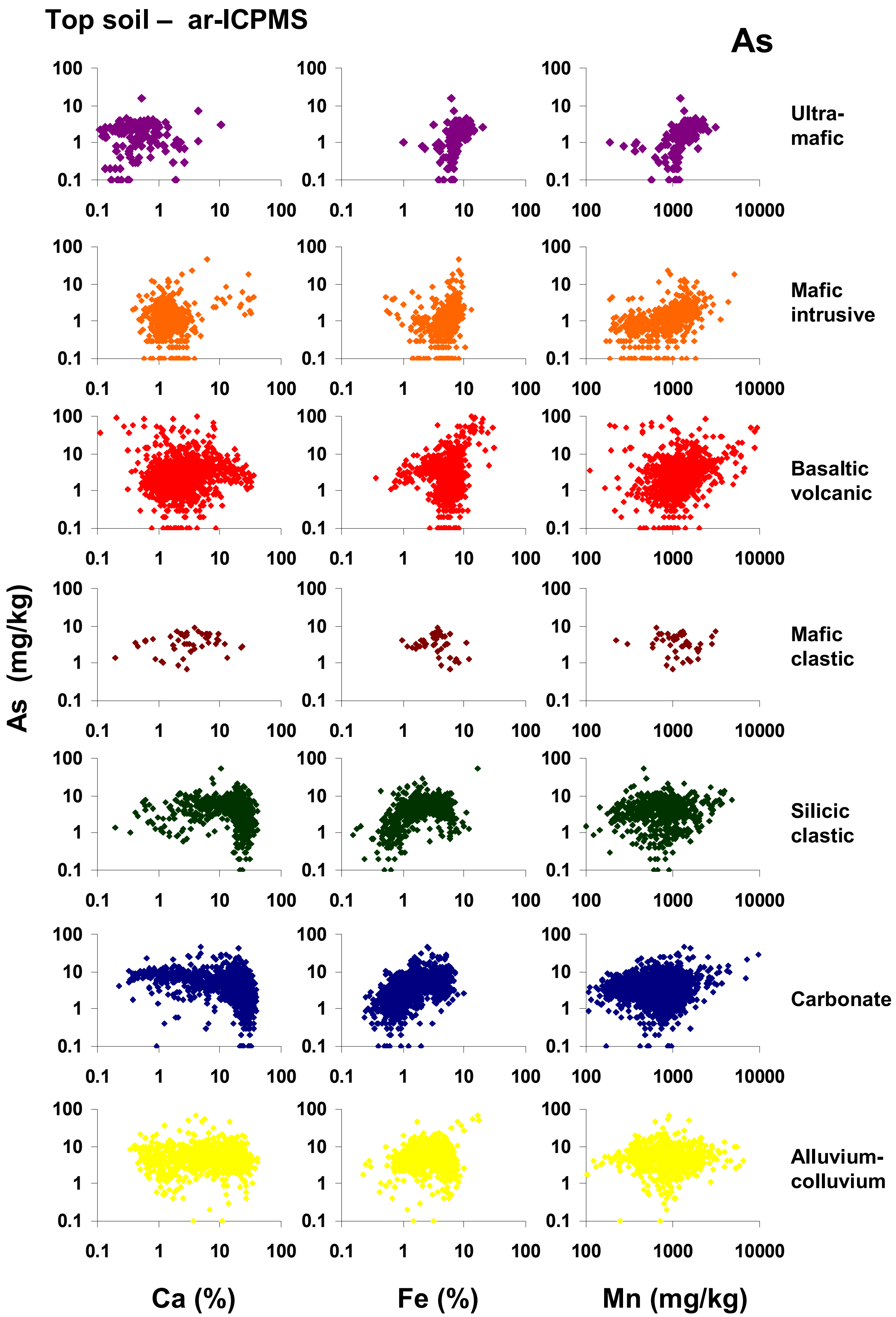

Figure 5.10 Plot of aqua regia-extractable As versus Ca, Fe and Mn in top soils, separated by underlying lithology group.

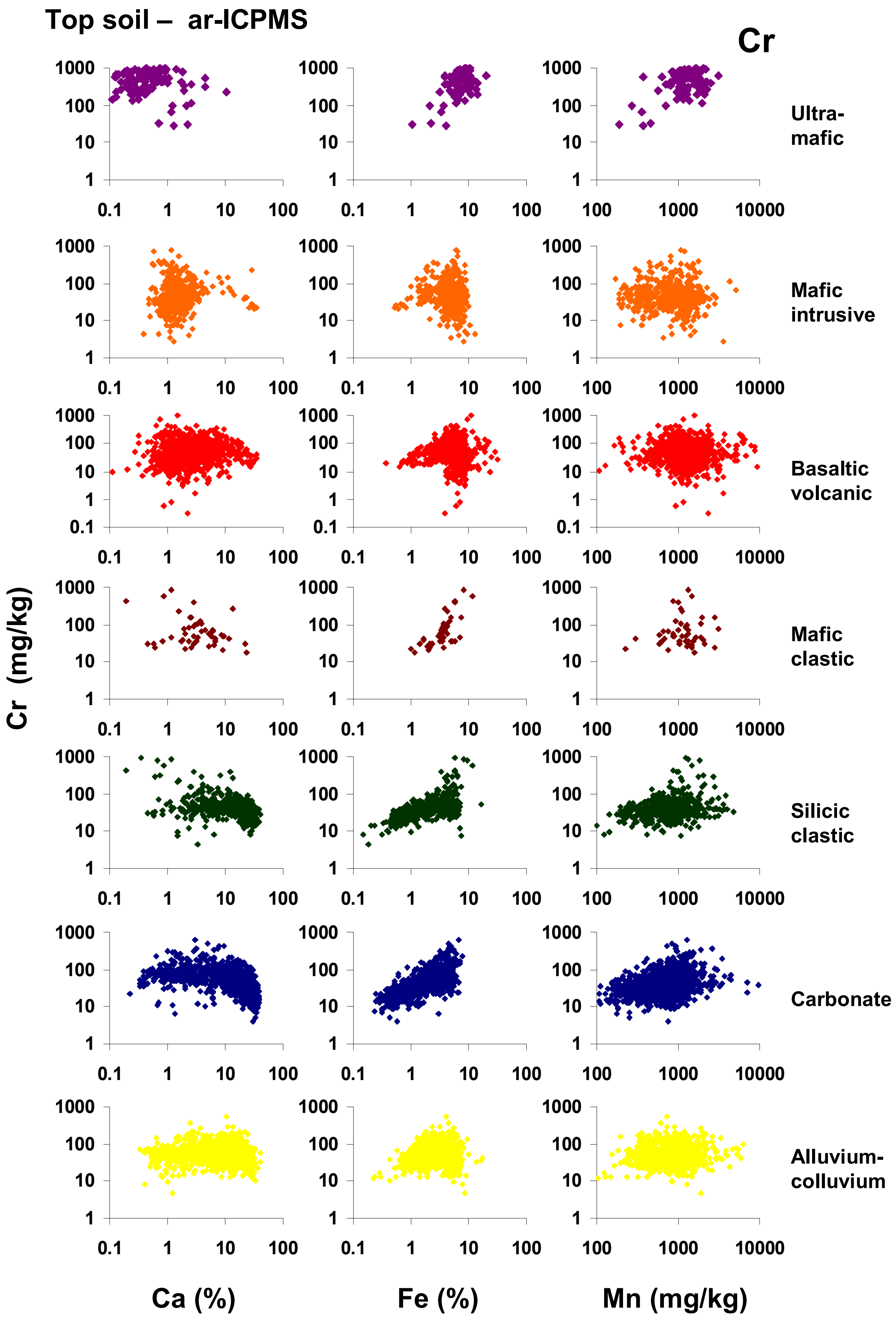

Figure 5.11 Plot of aqua regia-extractable Cr versus Ca, Fe and Mn in top soils, separated by underlying lithology group.

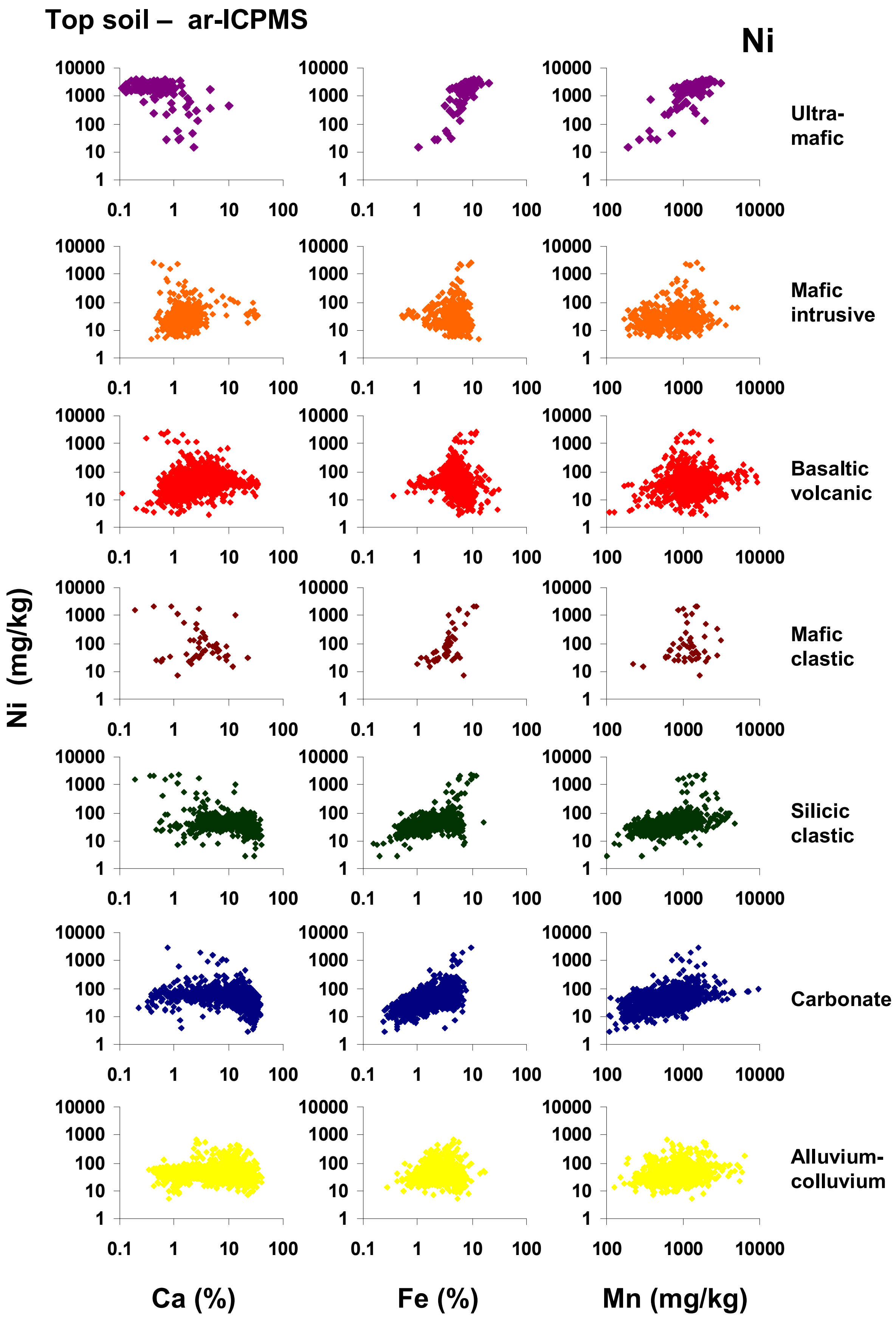

Figure 5.12 Plot of aqua regia-extractable Ni versus Ca, Fe and Mn in top soils, separated by underlying lithology group.

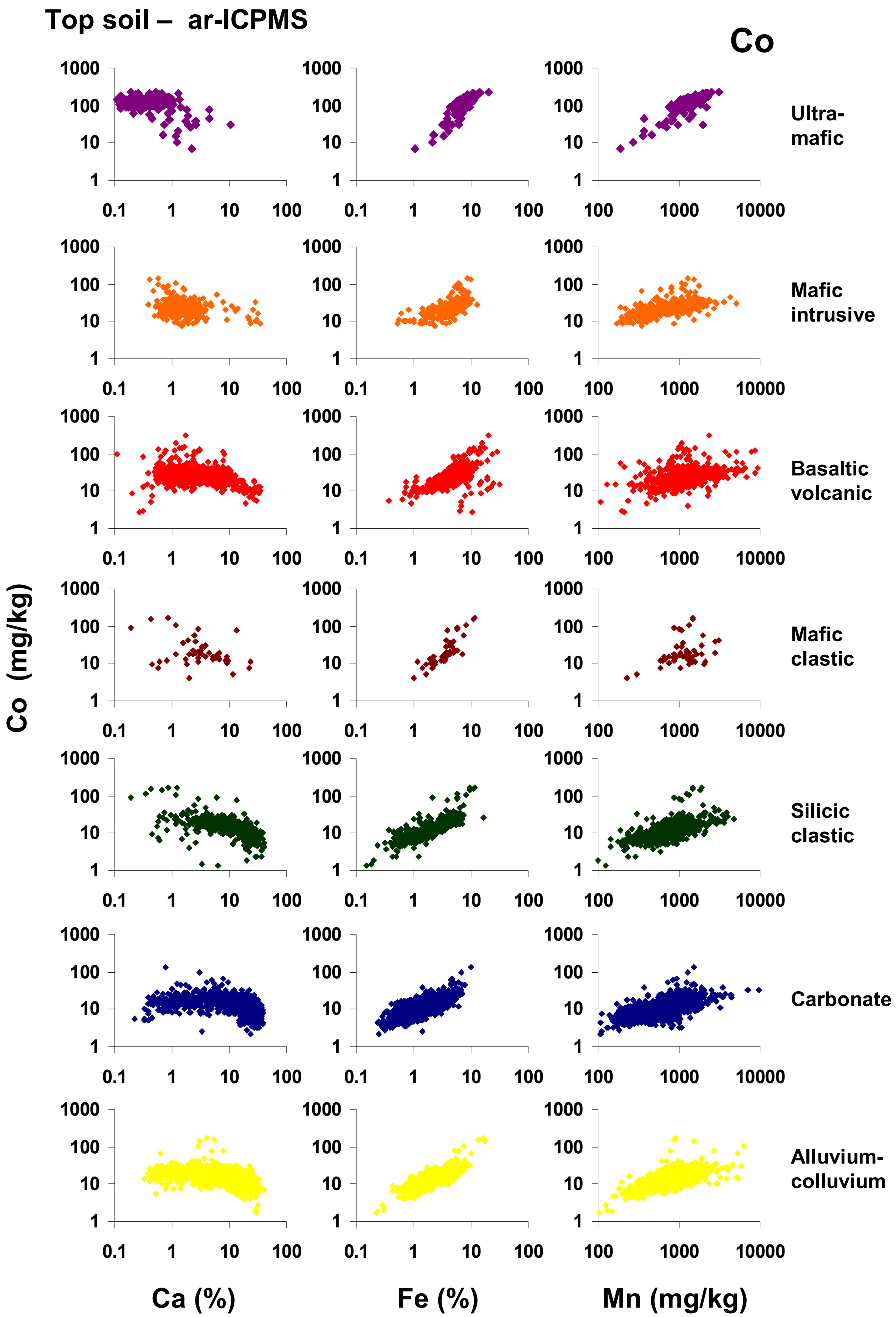

Figure 5.13 Plot of aqua regia-extractable Co versus Ca, Fe and Mn in top soils, separated by underlying lithology group.

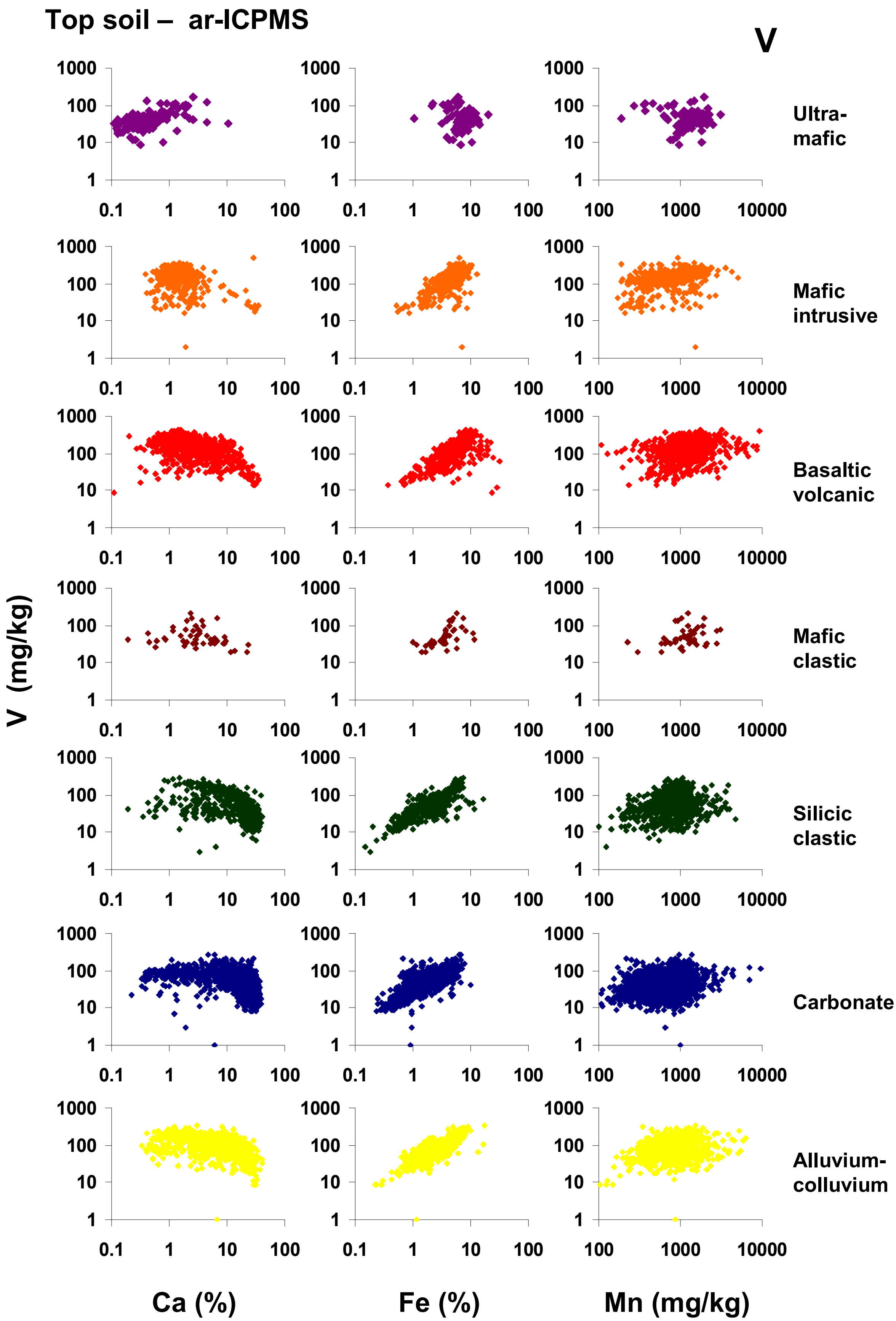

Figure 5.14 Plot of aqua regia-extractable V versus Ca, Fe and Mn in top soils, separated by underlying lithology group.

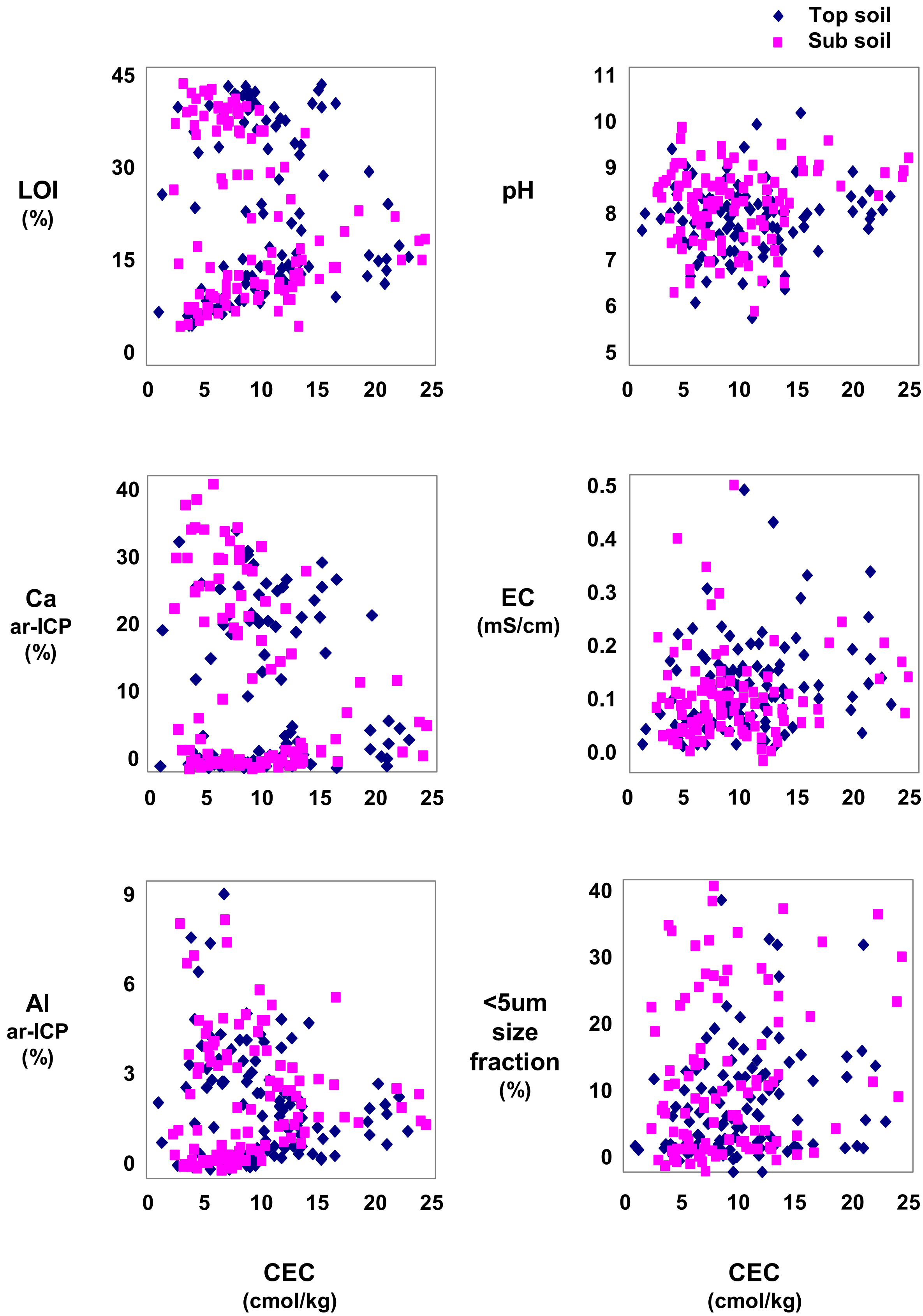

Figure 5.15 Plot of selected variables agains catio exchange capacity (CEC).

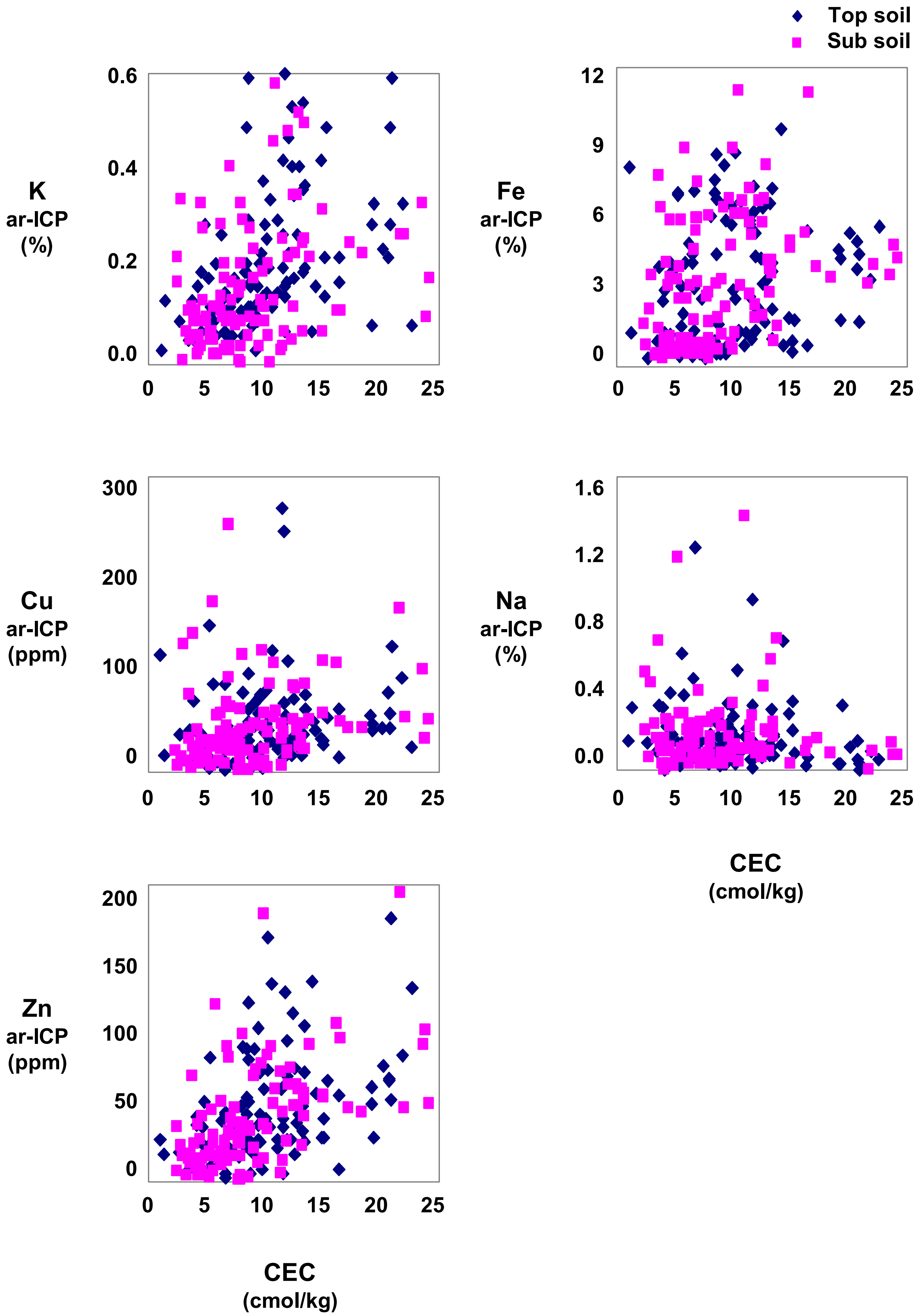

Figure 5.16 Plot of selected variables agains catio exchange capacity (CEC).

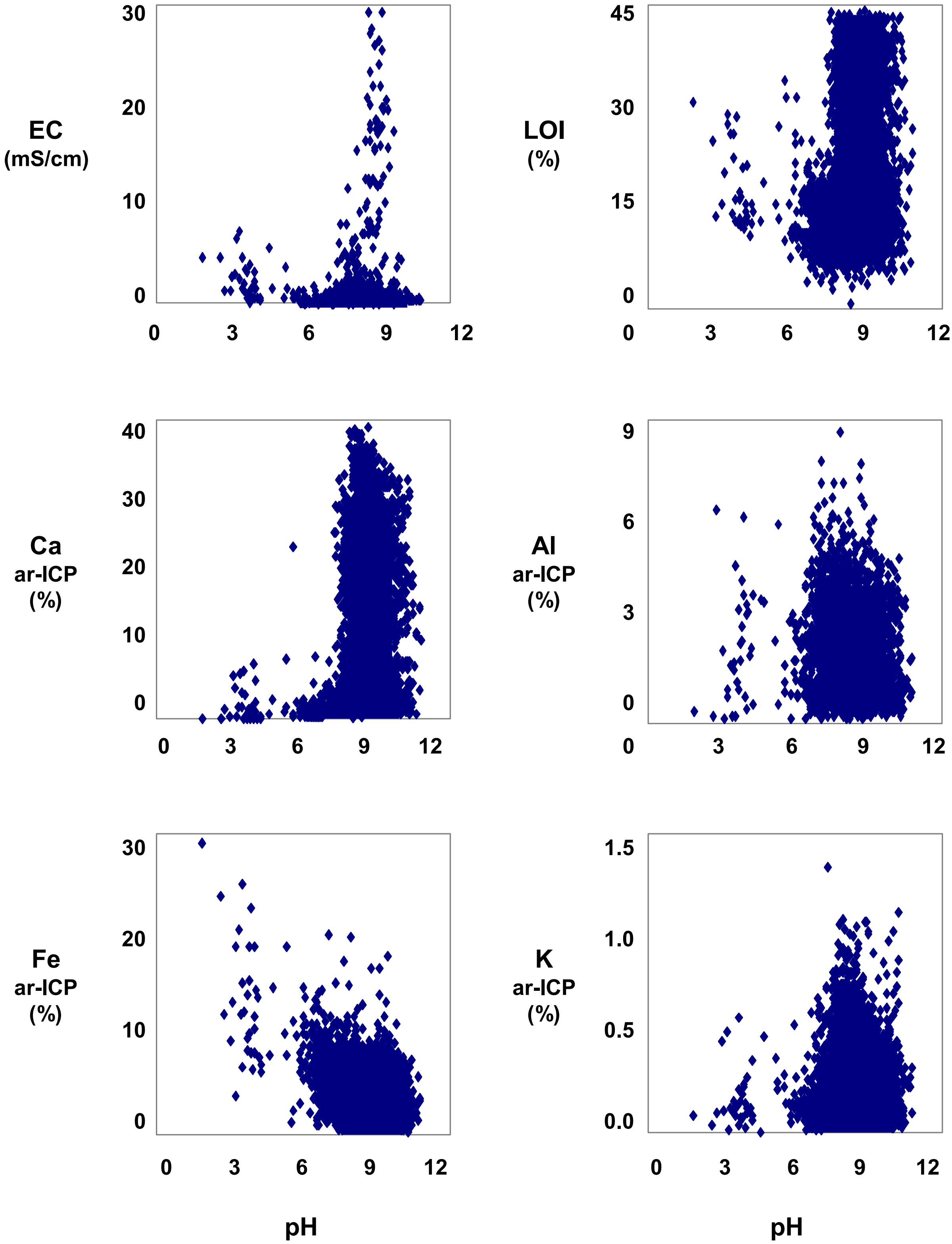

Figure 5.17 Plot of selected variables agains pH.

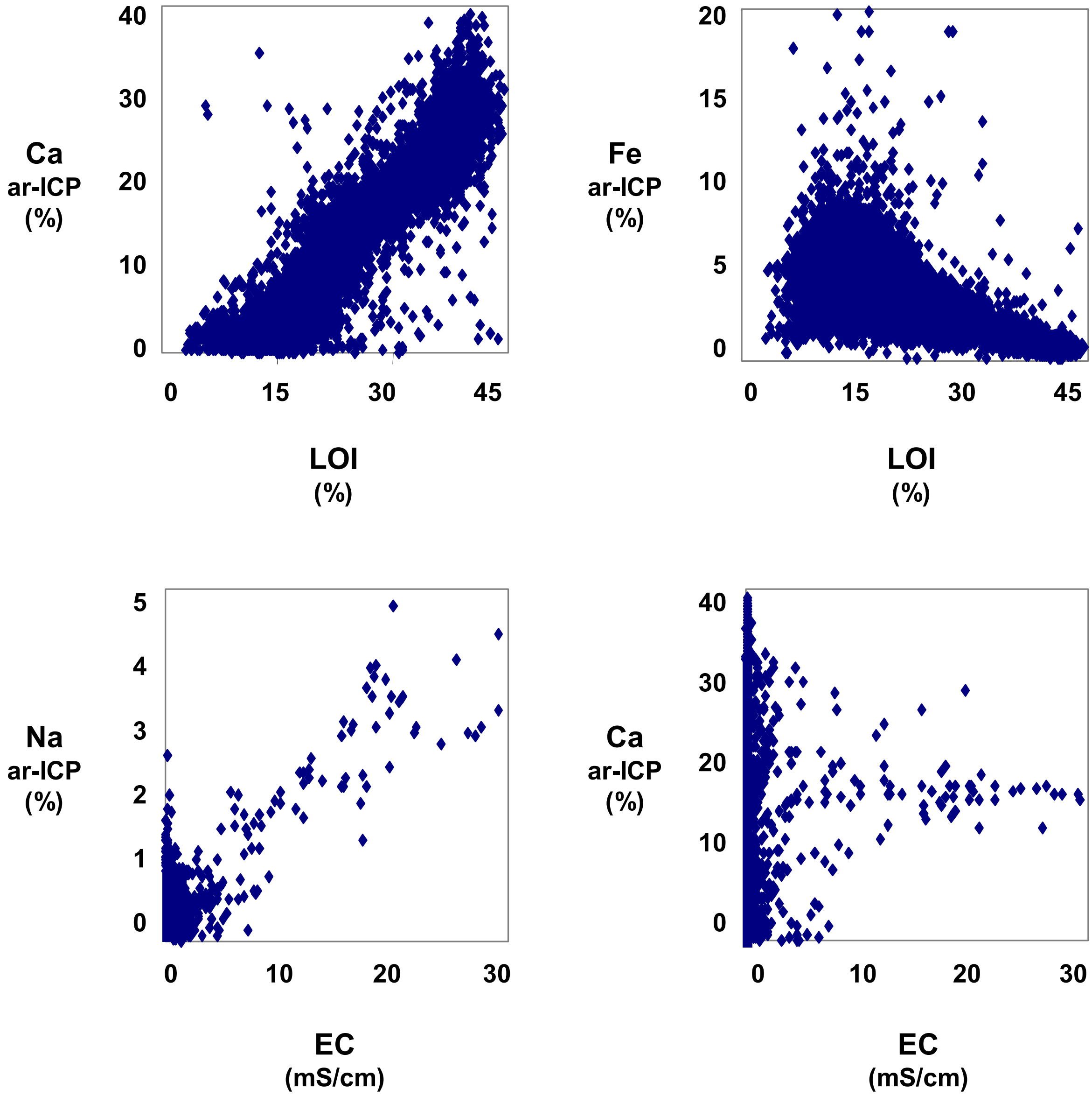

Figure 5.18 Plot of selected variables agains loss on ignition (LOI) and electrical conductivity (EC).

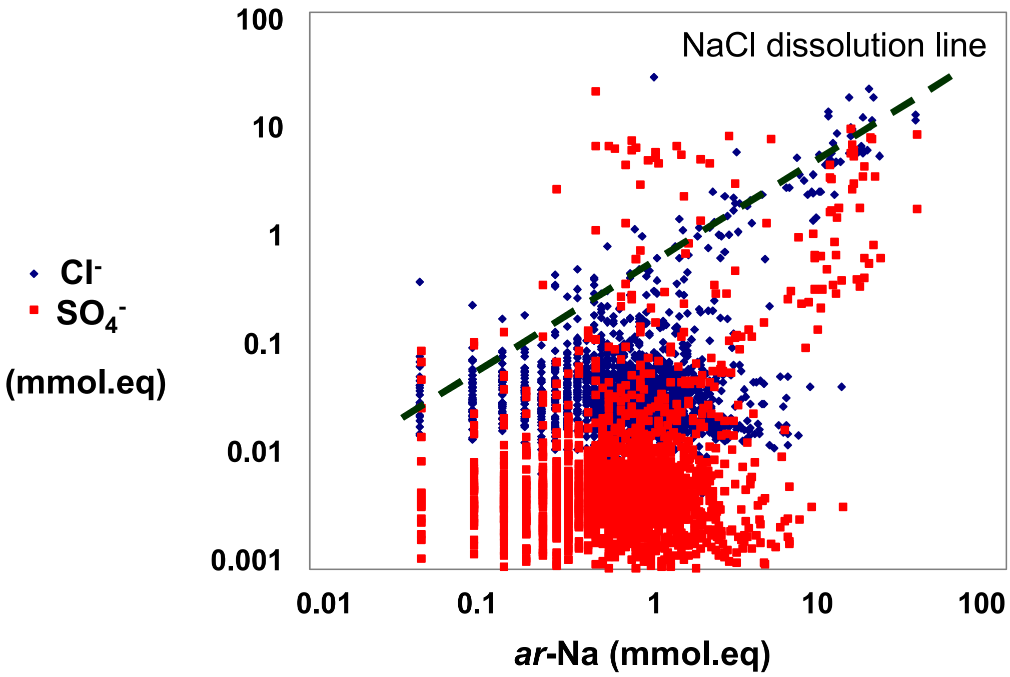

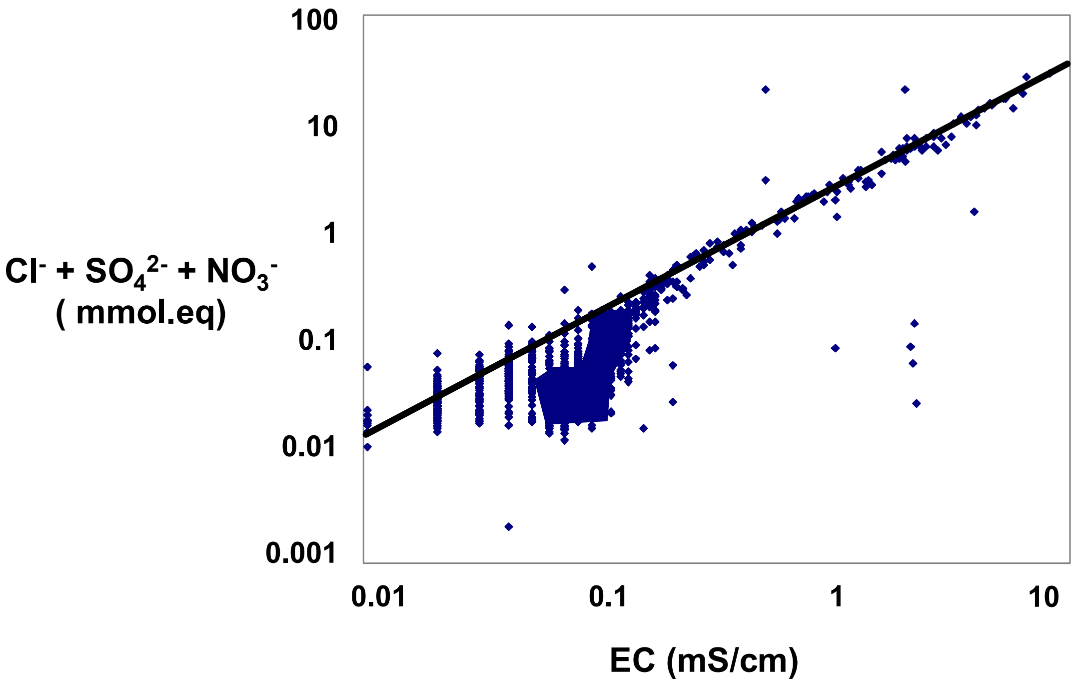

Figure 5.19 (a) Plot of soluble Cl^- and SO_4^{2-} versis *ar*-Na for top soil samples (mmol.eq). (b) Sum of soluble Cl^-, SO_4^{2-} and NO_3^- (mmol.eq) versus EC.

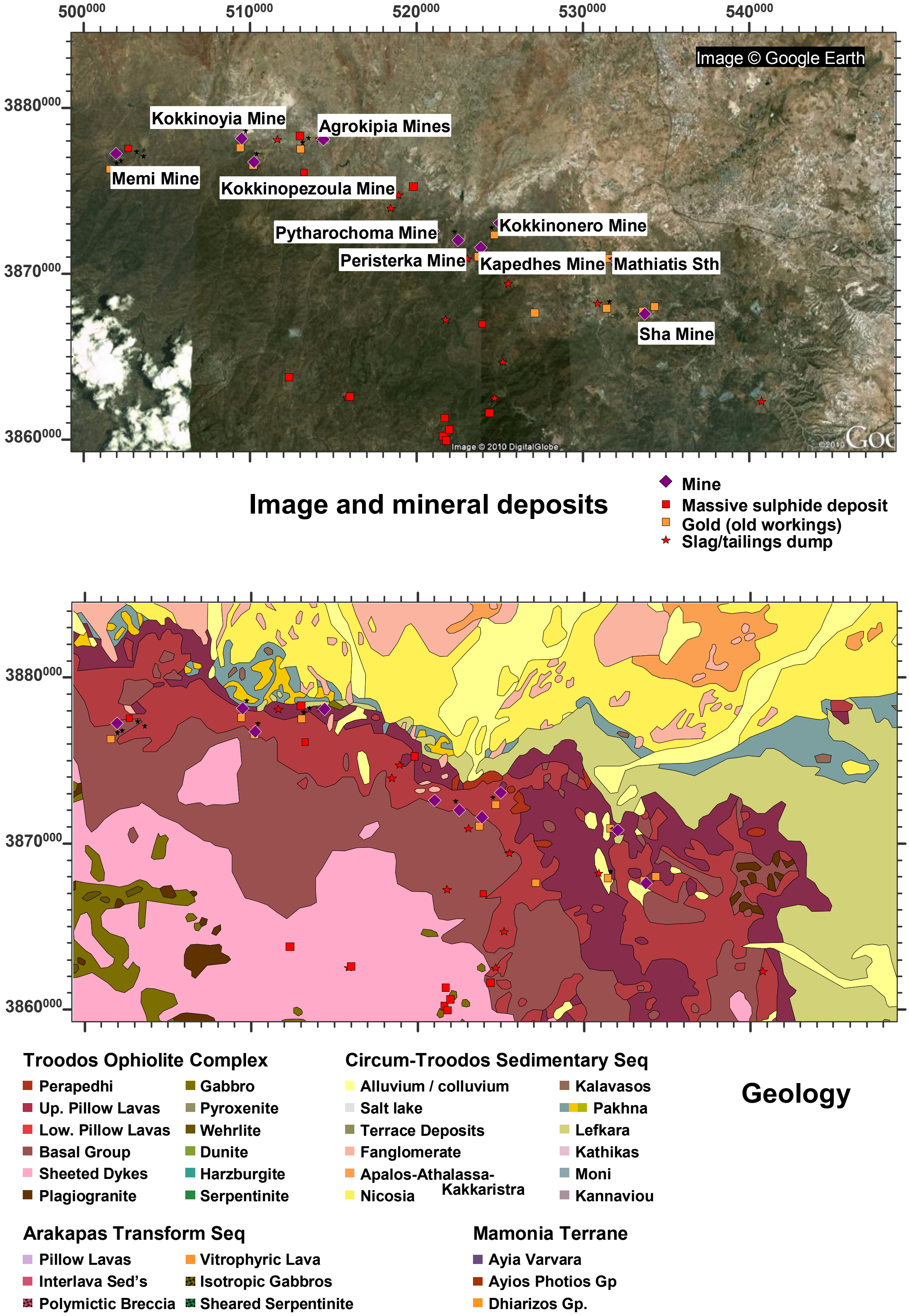

Figure 5.20 Google image and geology of the NE mines group, with mines and known mineralisation indicated.

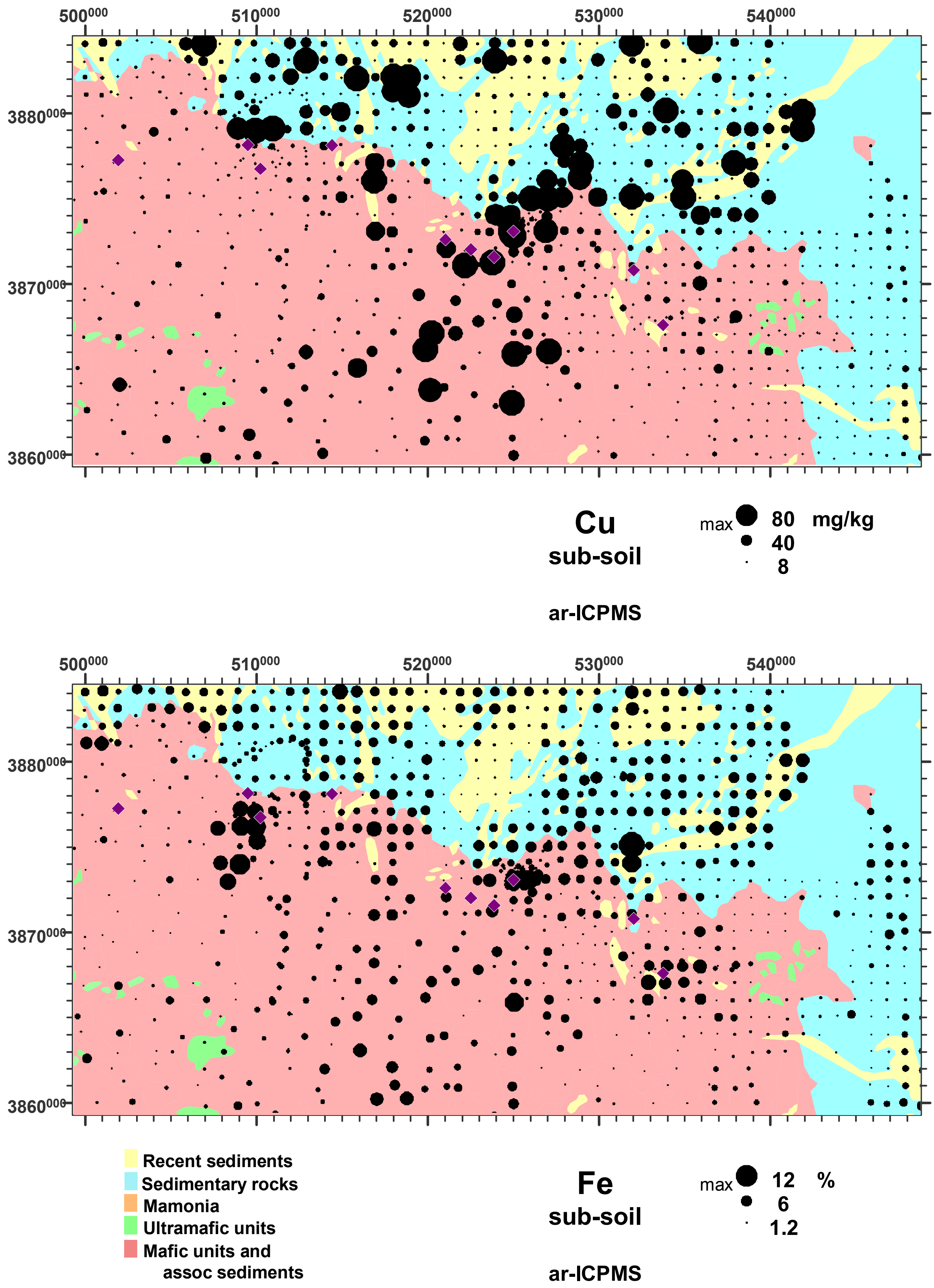

Figure 5.21 Dot-plots of *ar*-Cu and *ar*-Fe in top soil, NE mines group.

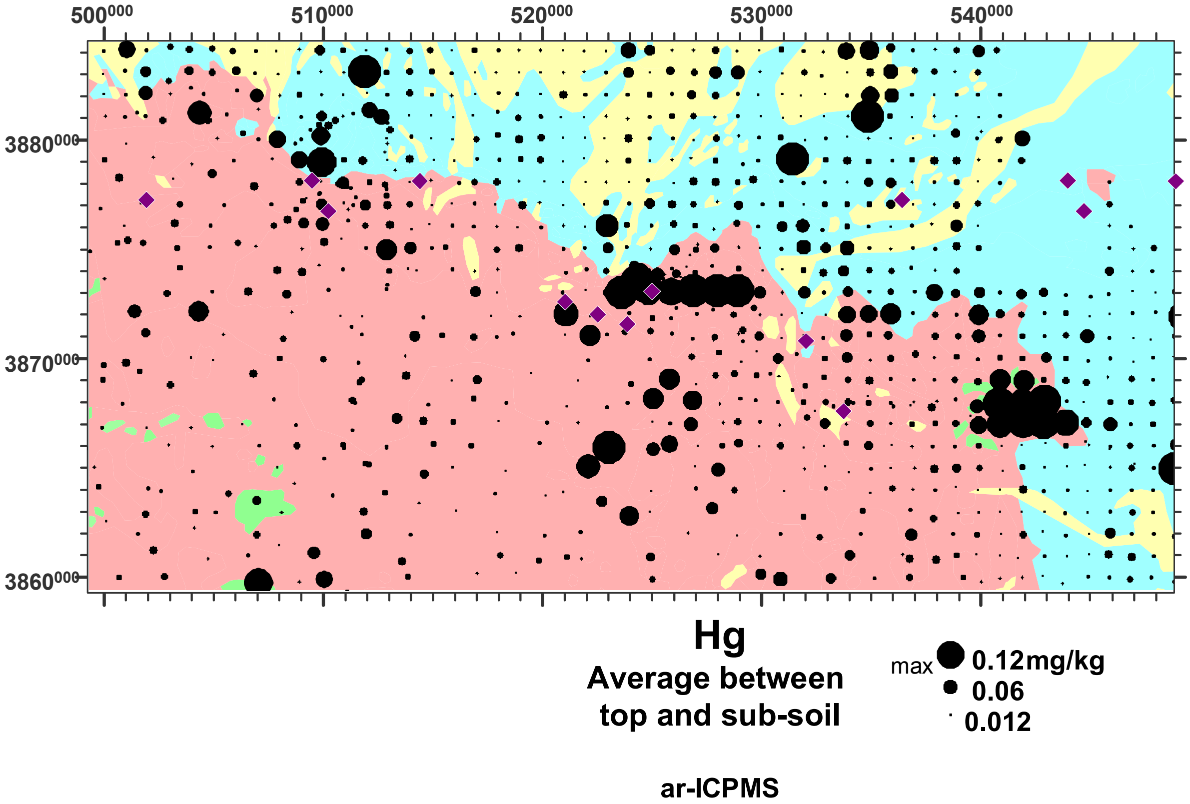

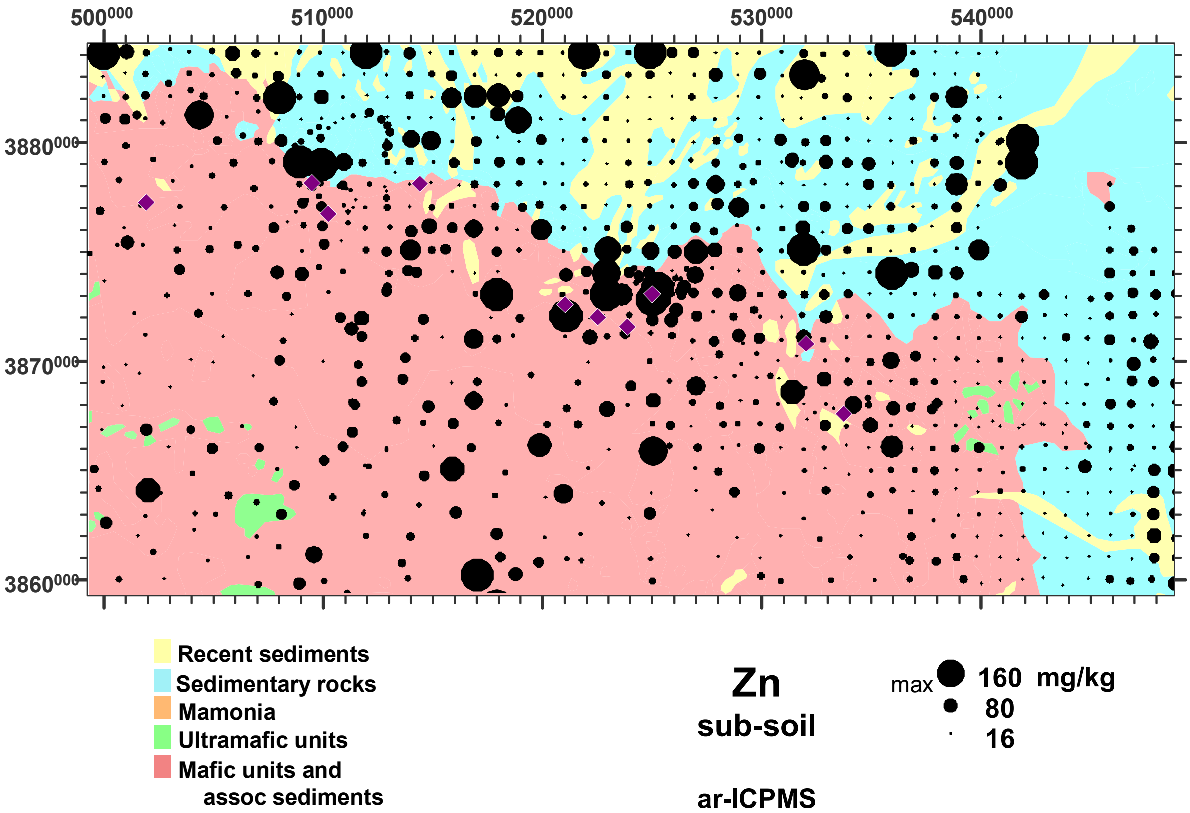

Figure 5.22 Dot-plots of average *ar*-Hg in top and sub soil and *ar*-Zn in sub soil, NE mines group.

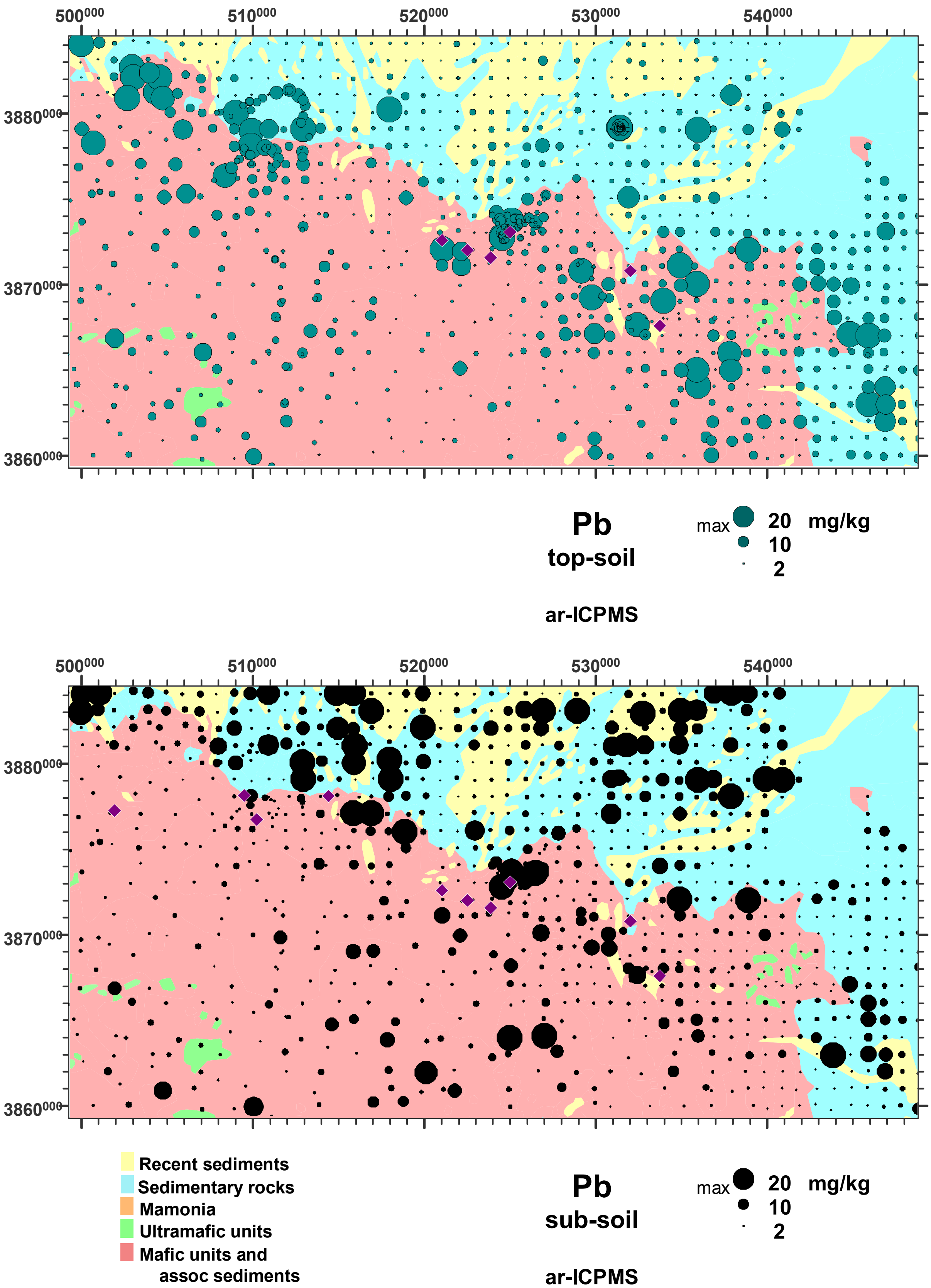

Figure 5.23 Dot-plots of *ar*-Pb in top soil and sub soil, NE mines group.

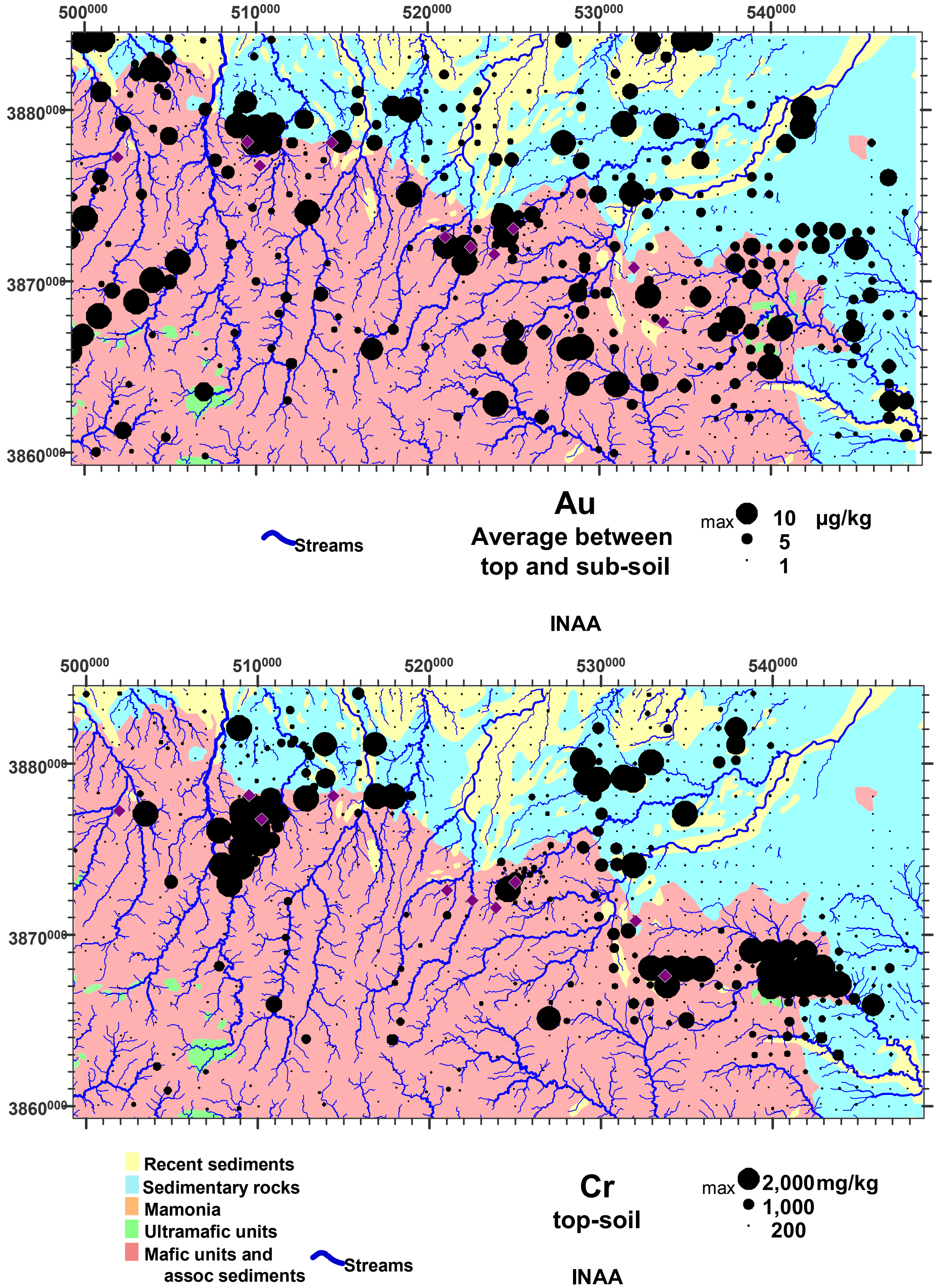

Figure 5.24 Dot-plots of average *tot*-Au in top and sub soil and *tot*-Cr in top-soil, NE mines group.

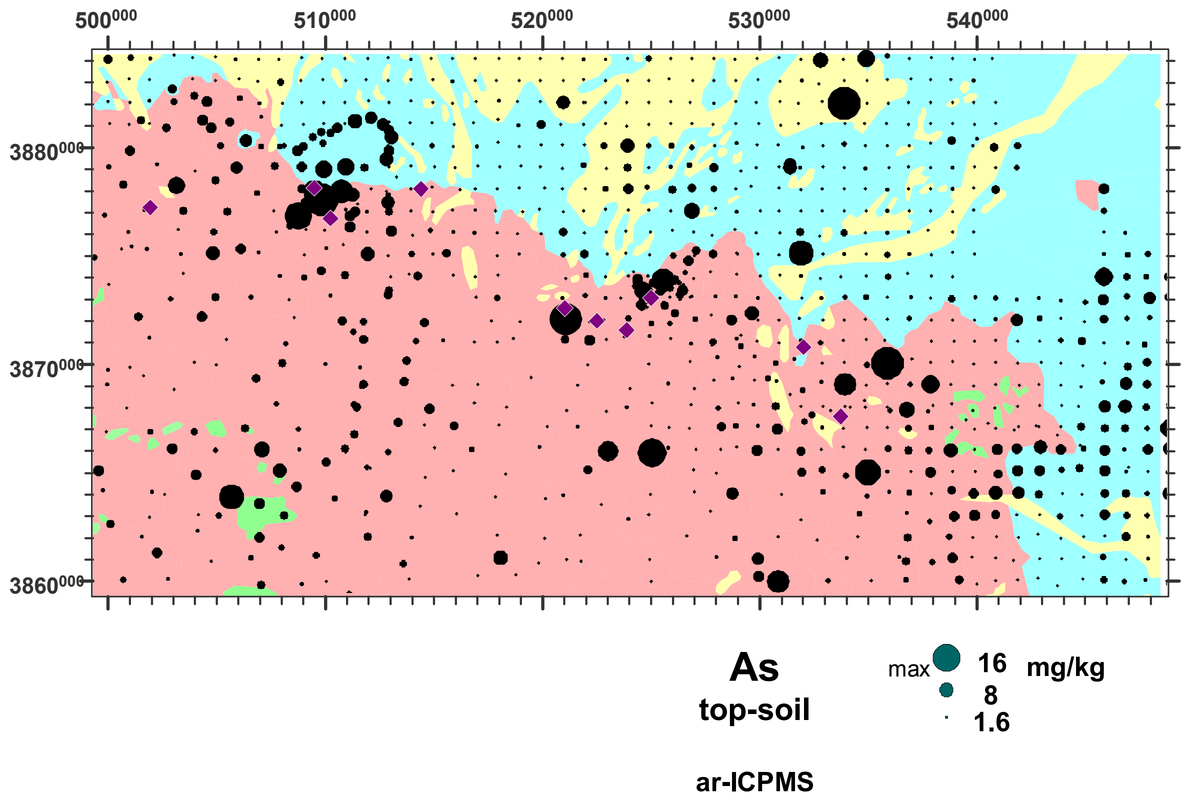

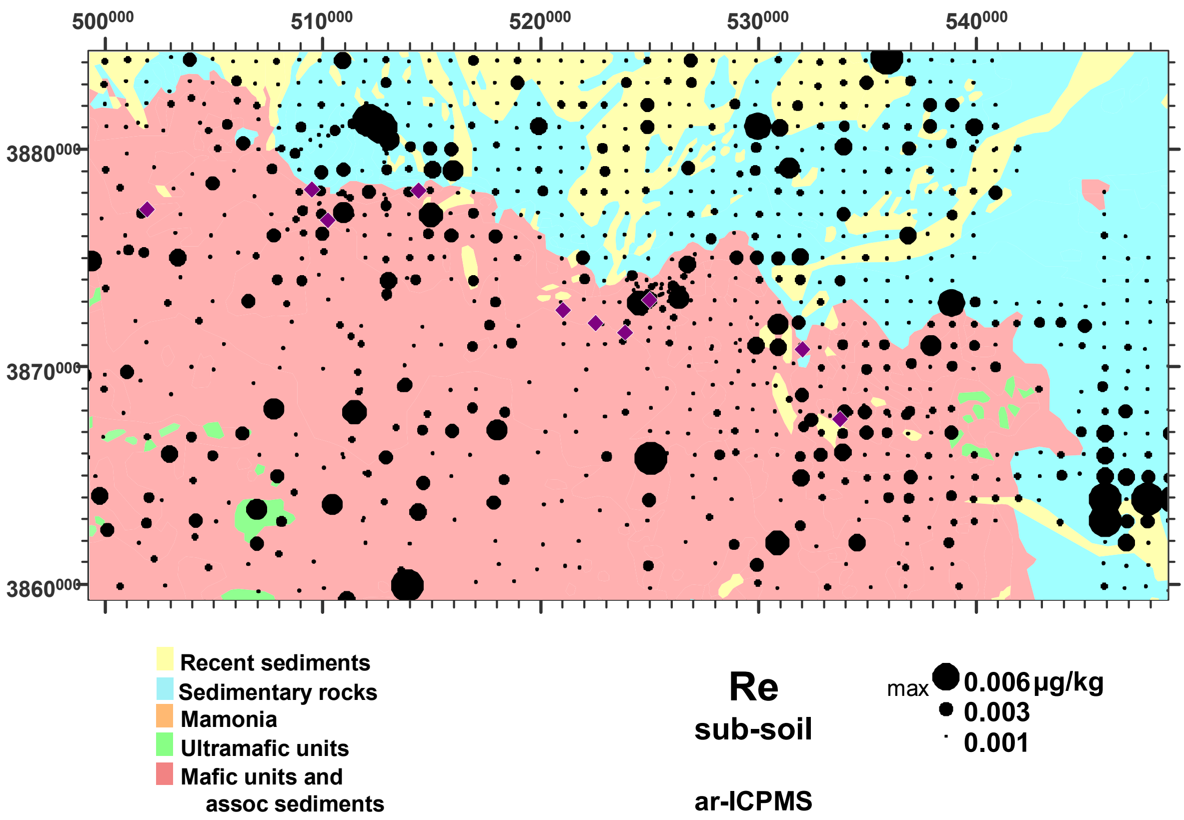

Figure 5.25 Dot-plots of *ar*-As in top soil and *ar*-Re in sub soil, NE mines group.

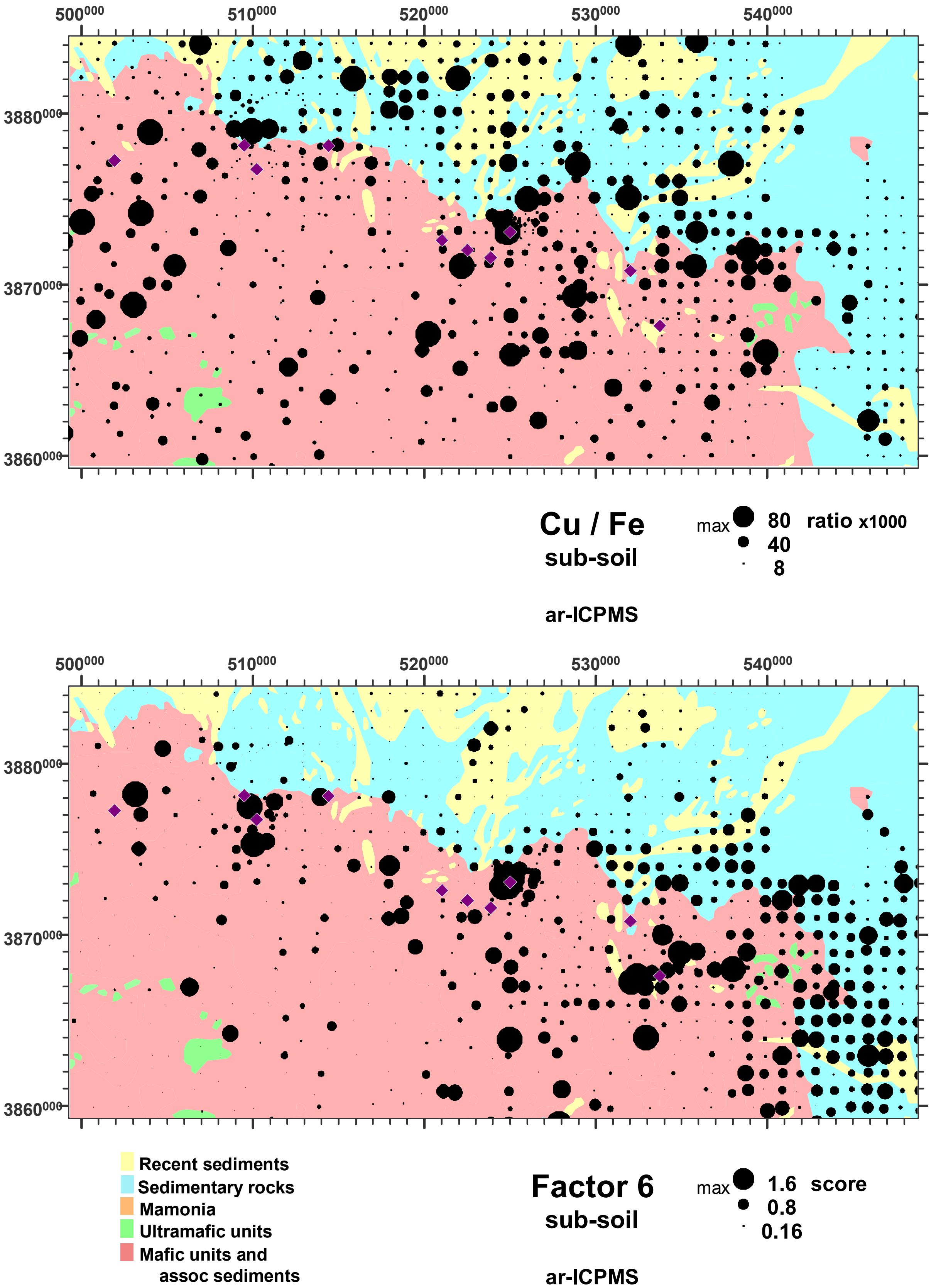

Figure 5.26 Dot-plots of *ar*-Cu/*ar*-Fe ratio and *ar-ICPMS factor 6* in sub soil, NE mines group.

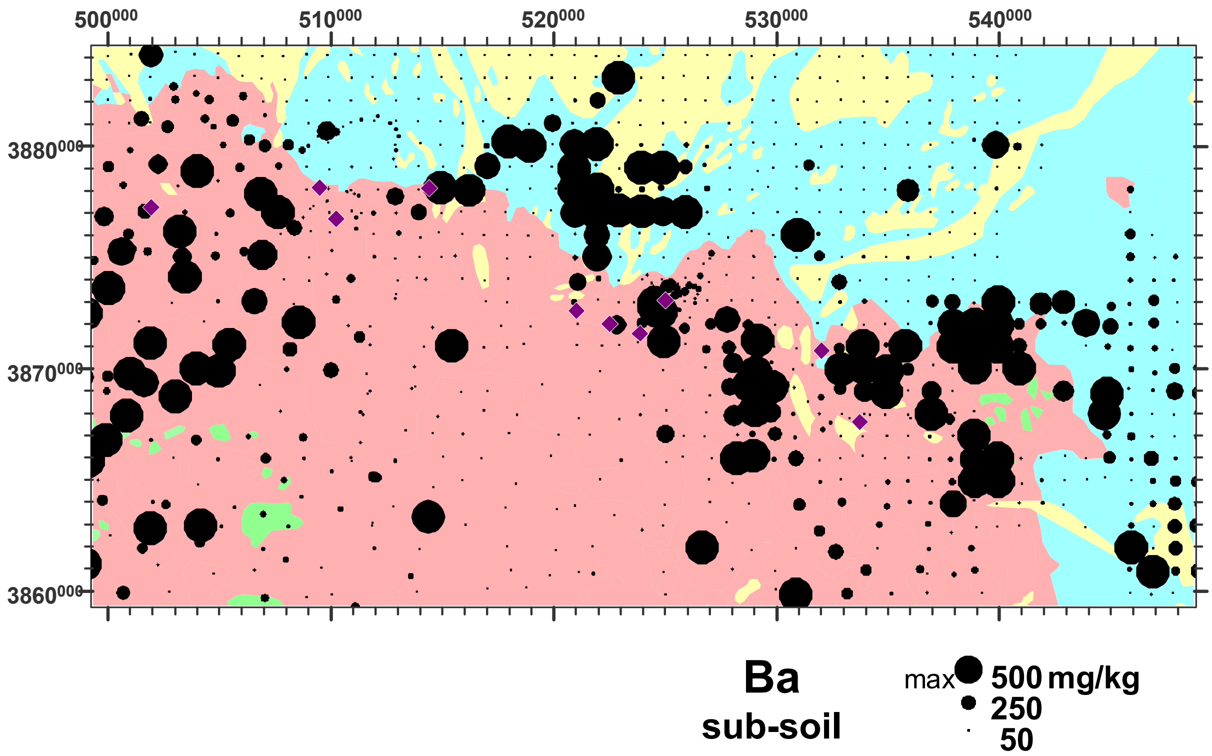

ar-ICPMS

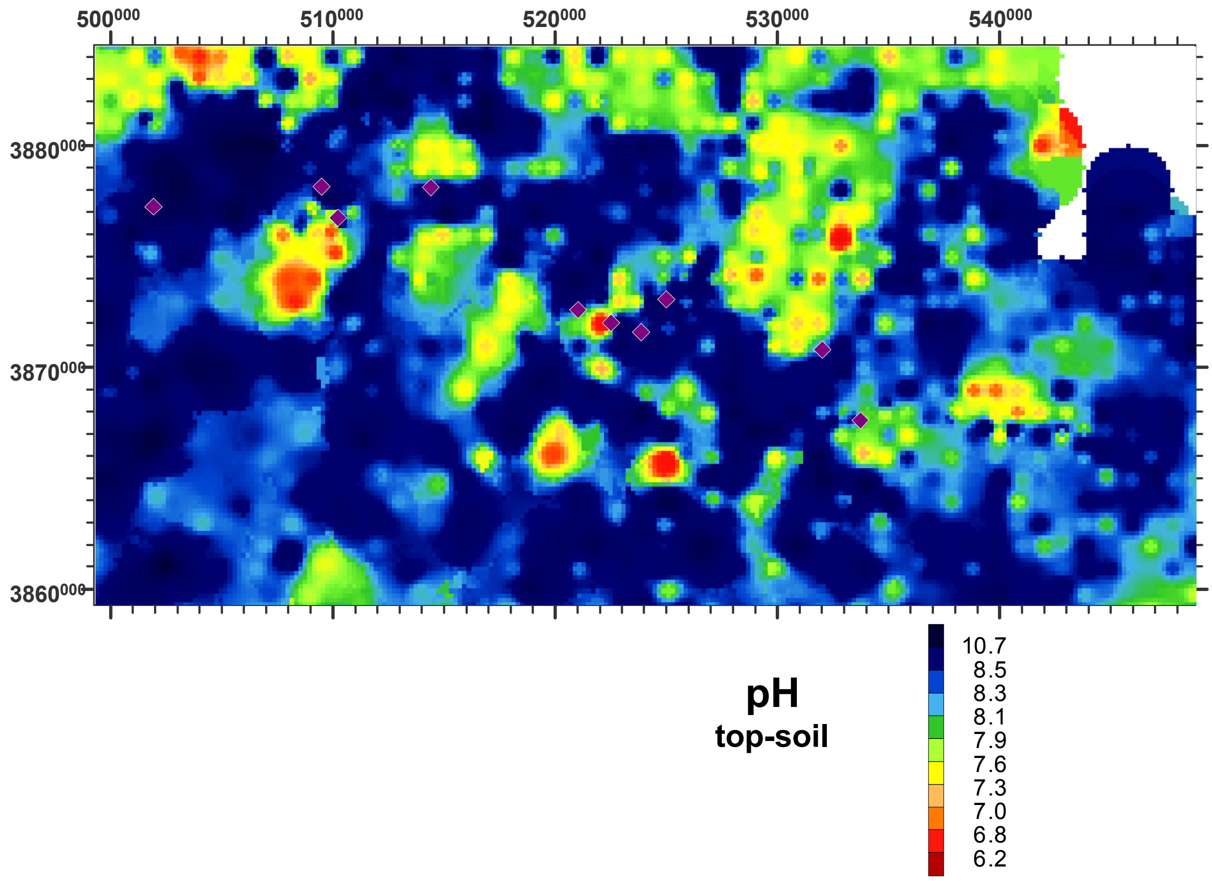

Figure 5.27 Dot-plots of *ar*-Ba in sub soil and regional pH patterns in top soil, NE mines group.

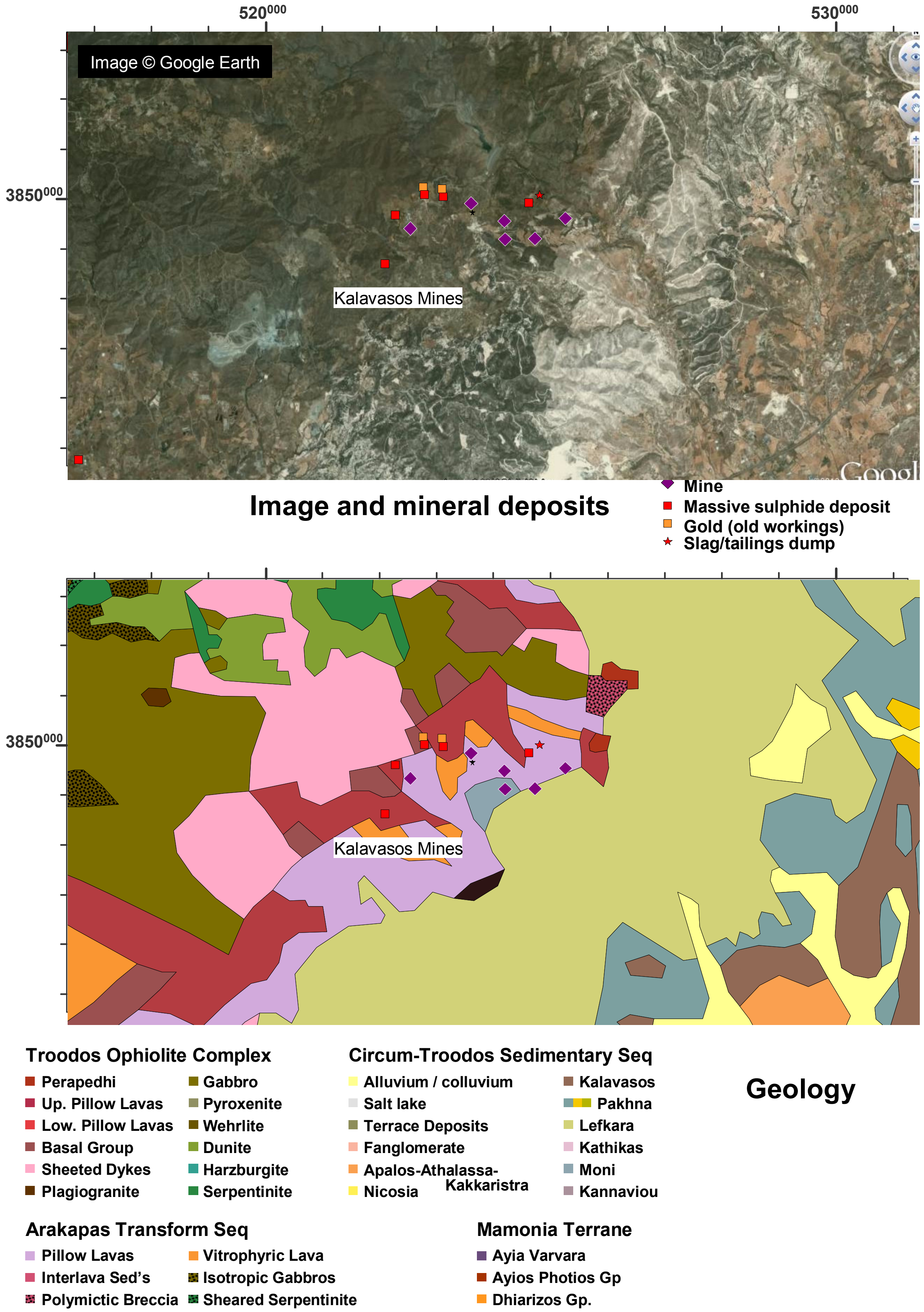

Figure 5.28 Google image and geology of the Kalavasos Mine area, with mines and known mineralisation indicated.

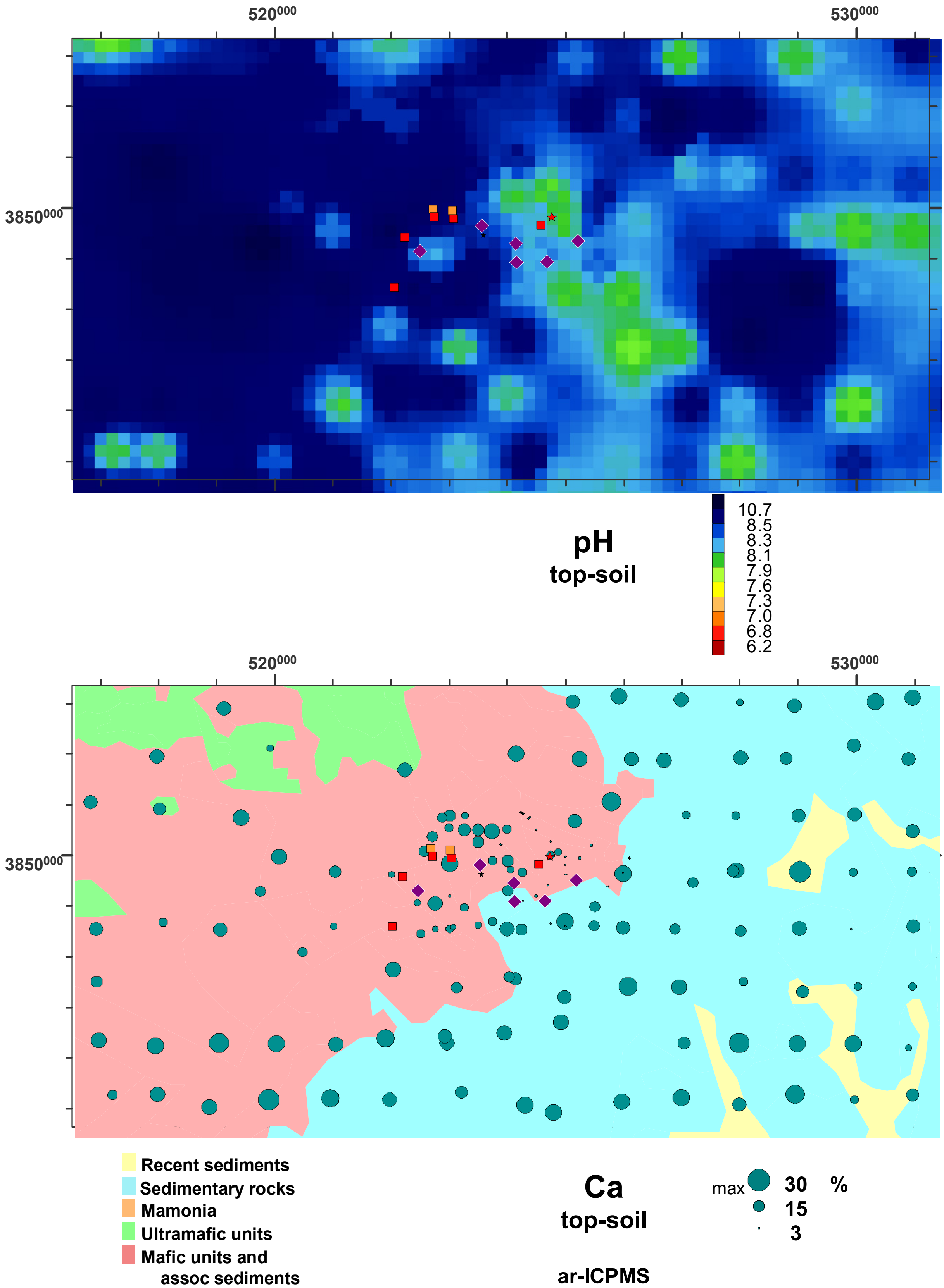

Figure 5.29 Dot-plots of *ar*-Ca in sub soil and regional pH patterns in top soil, Kalavasos Mine area.

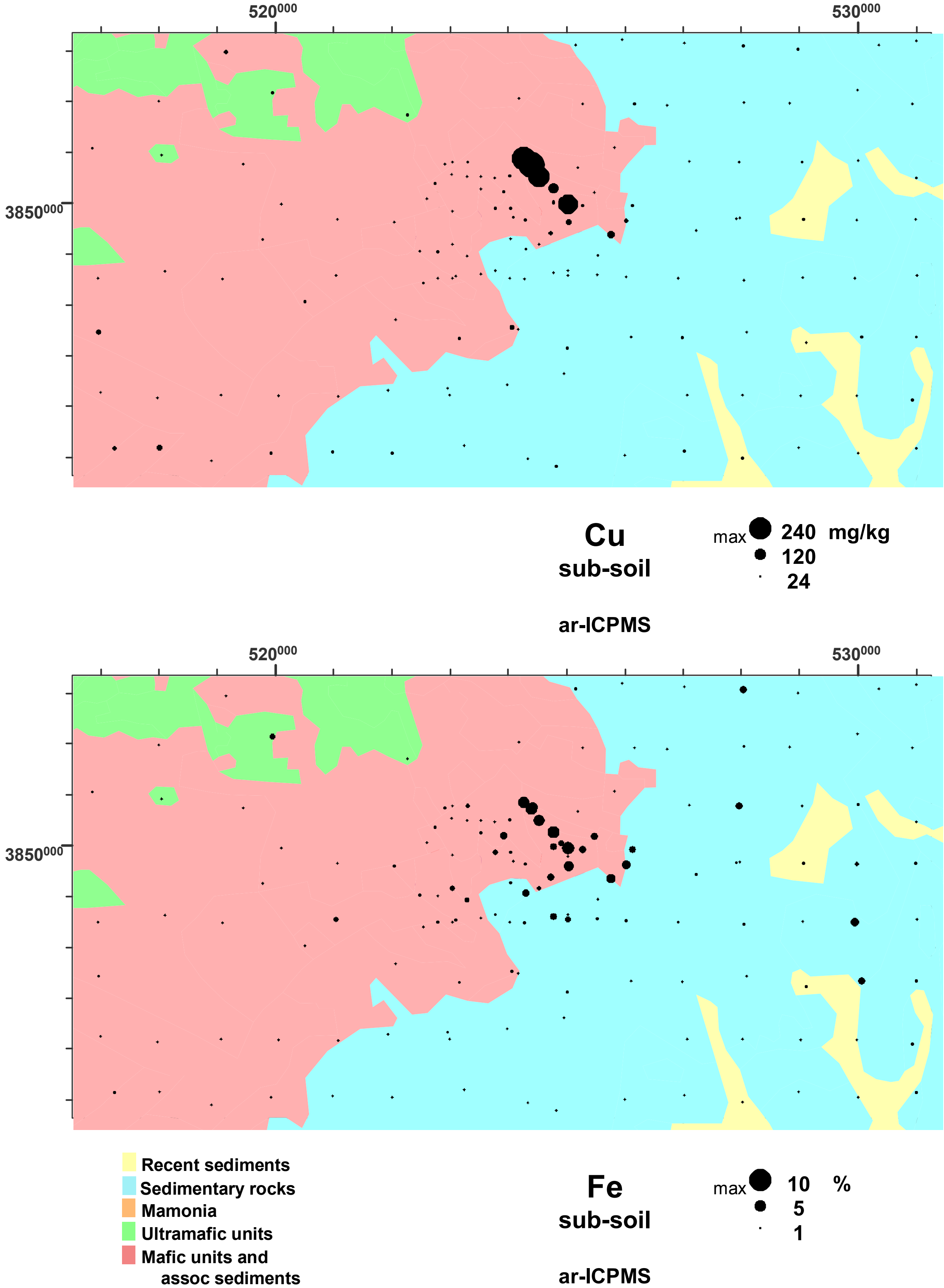

Figure 5.30 Dot-plots of *ar*-Cu and *ar*-Fe in sub soil, Kalavasos Mine area.

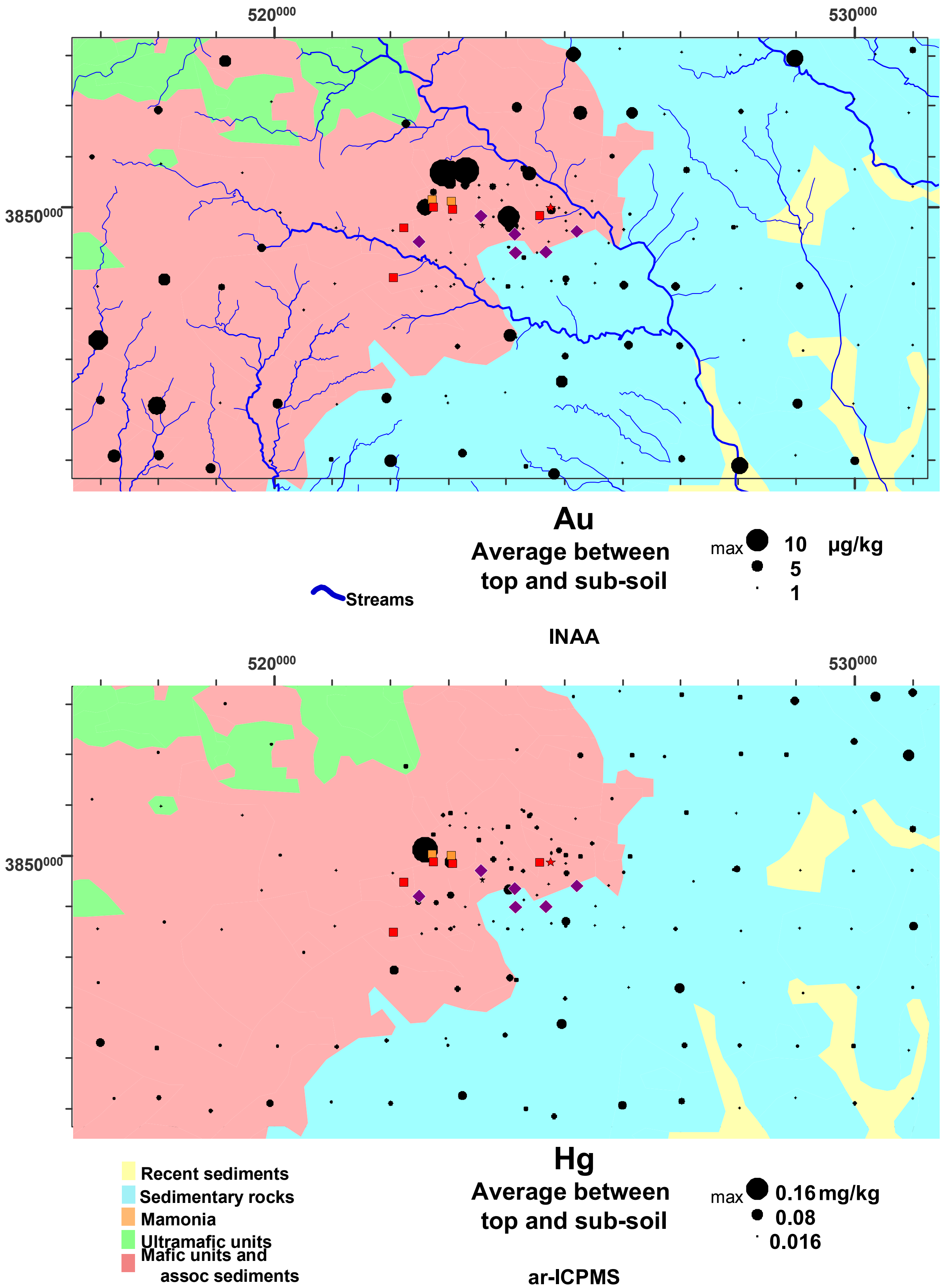

Figure 5.31 Dot-plots of average *tot*-Au and average *ar*-Hg within top and sub soil, Kalavasos Mine area.

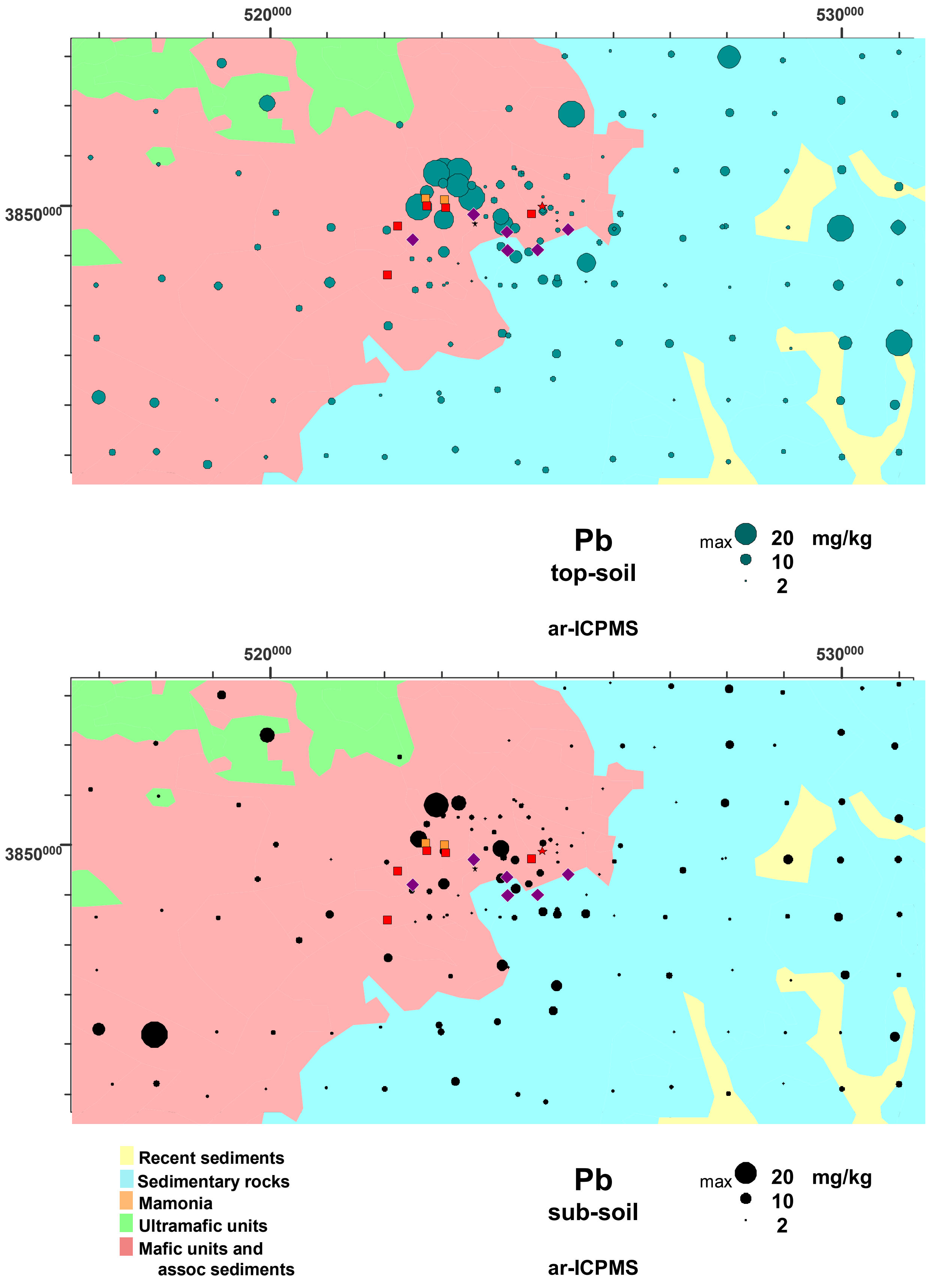

Figure 5.32 Dot-plots of *ar*-Pb in top soil and sub soil, Kalavasos Mine area.

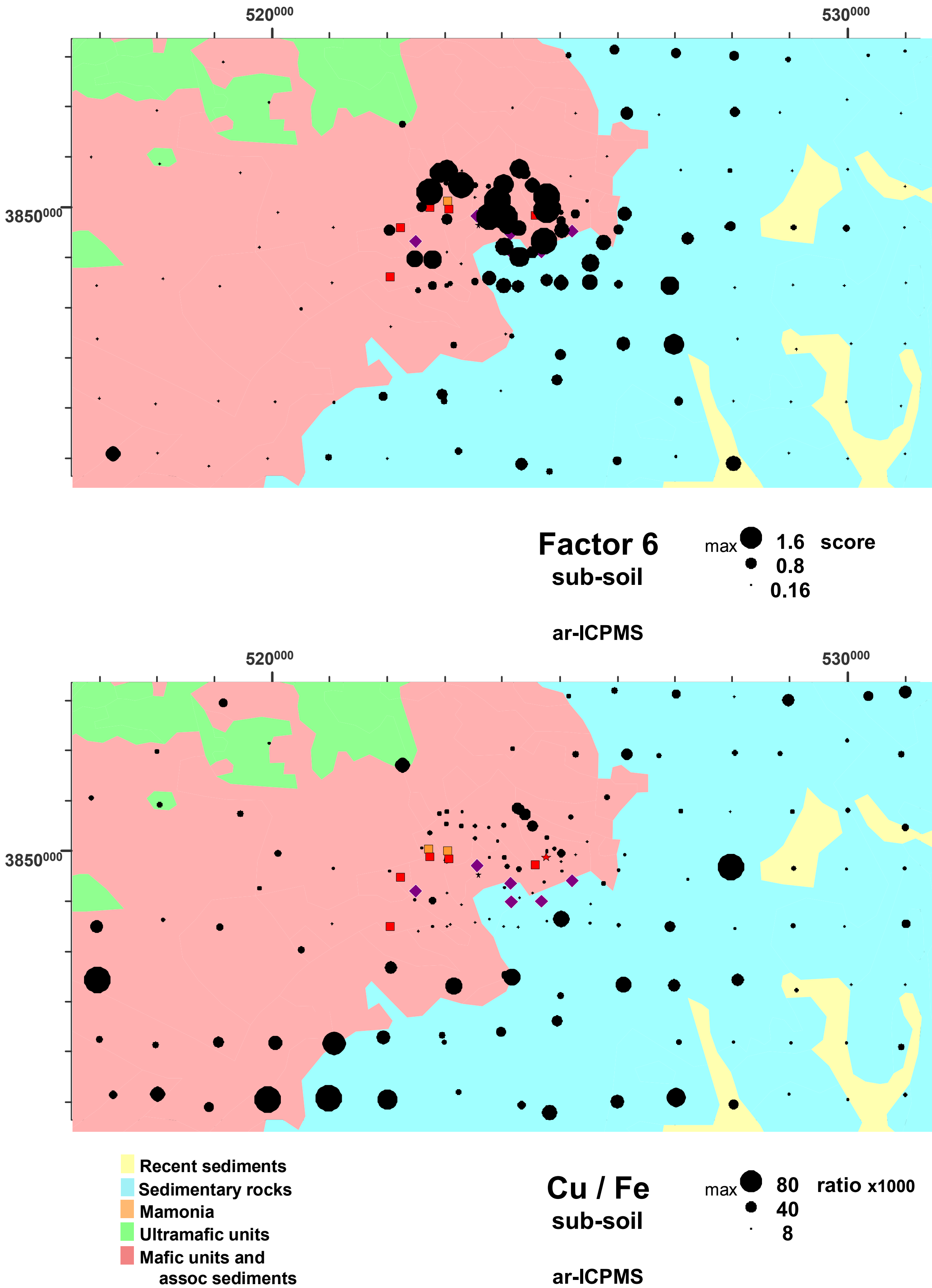

Figure 5.33 Dot-plots of *ar*-Cu/*ar*-Fe ratio and *ar-ICPMS factor 6* in sub soil, Kalavasos Mine area.

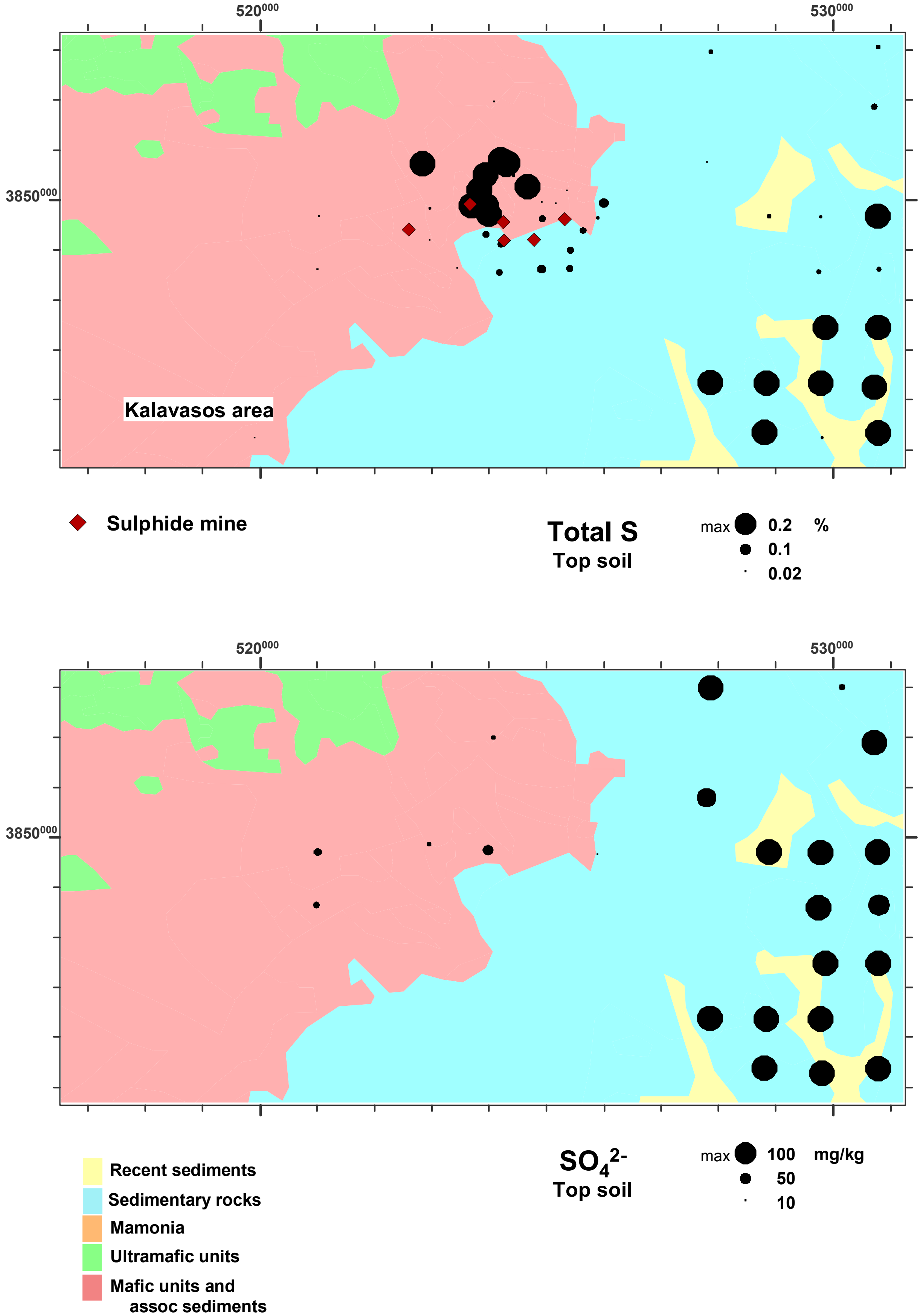

Figure 5.34 Dot-plots of tot-S and soluble SO_4^{2-} in top soil, Kalavasos Mine area.

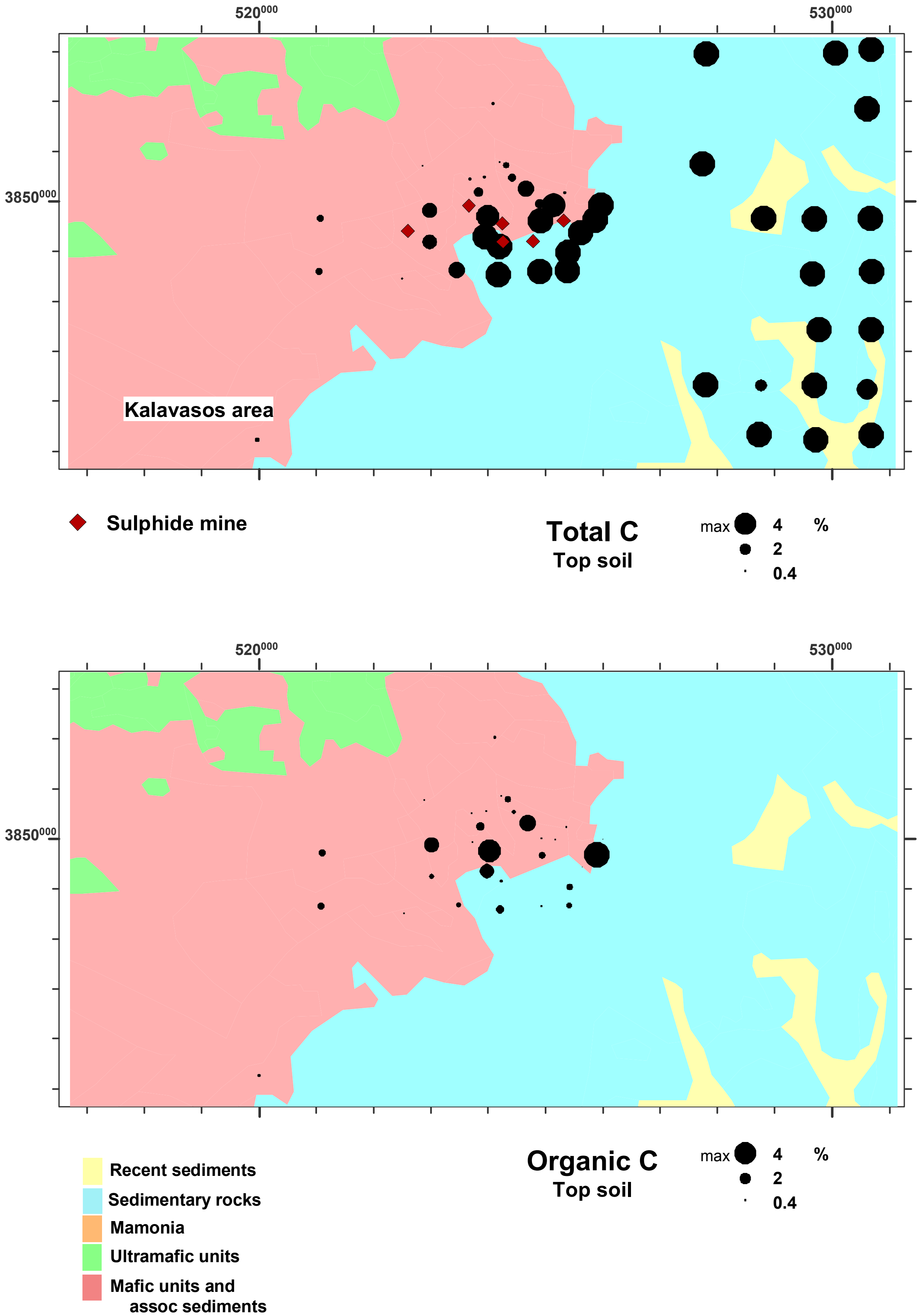

Figure 5.35 Dot-plots of tot-C and org-C in top soil, Kalavasos Mine area.

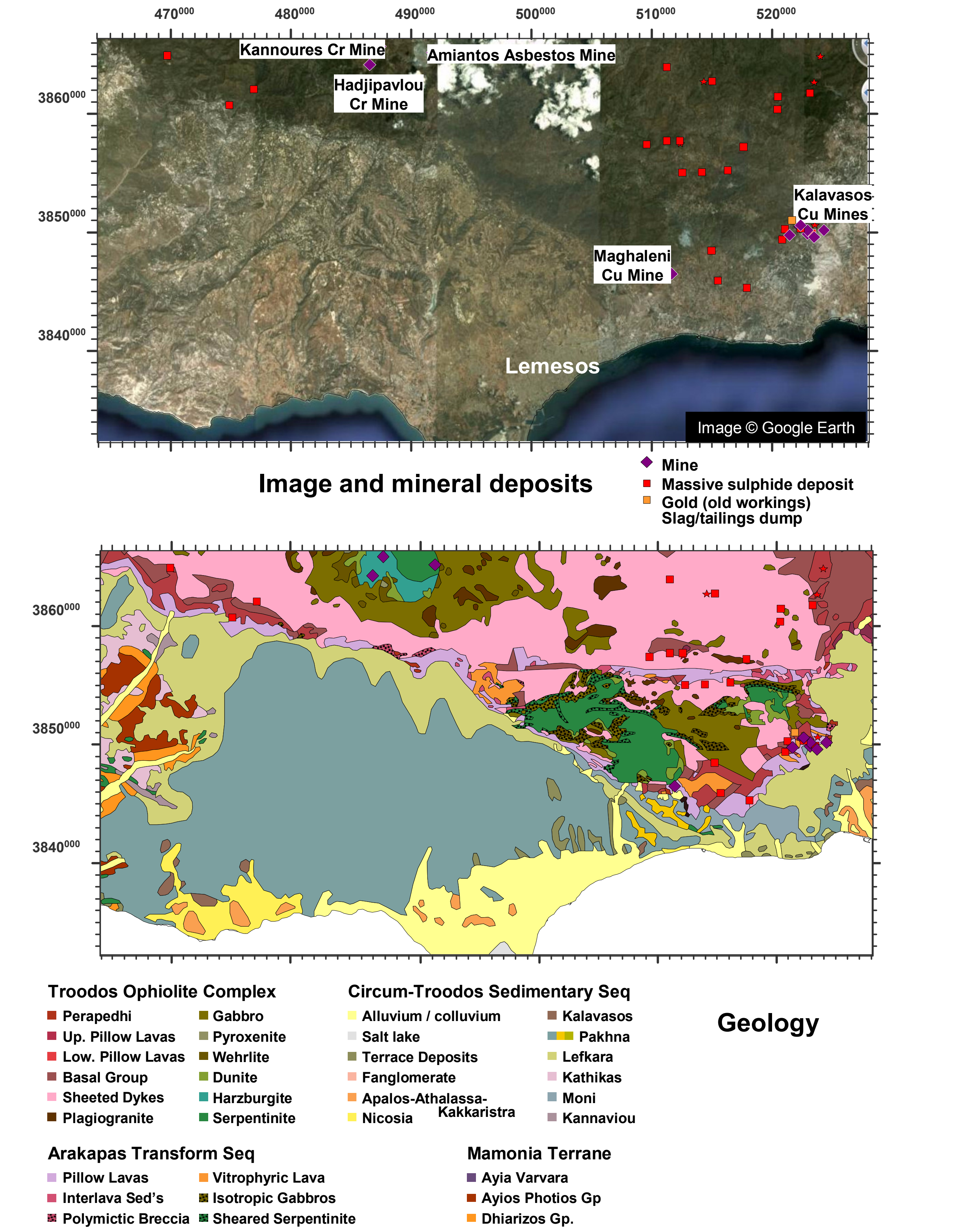

Figure 5.36 Google image and geology of the South Coast region, with mines and known mineralisation indicated.

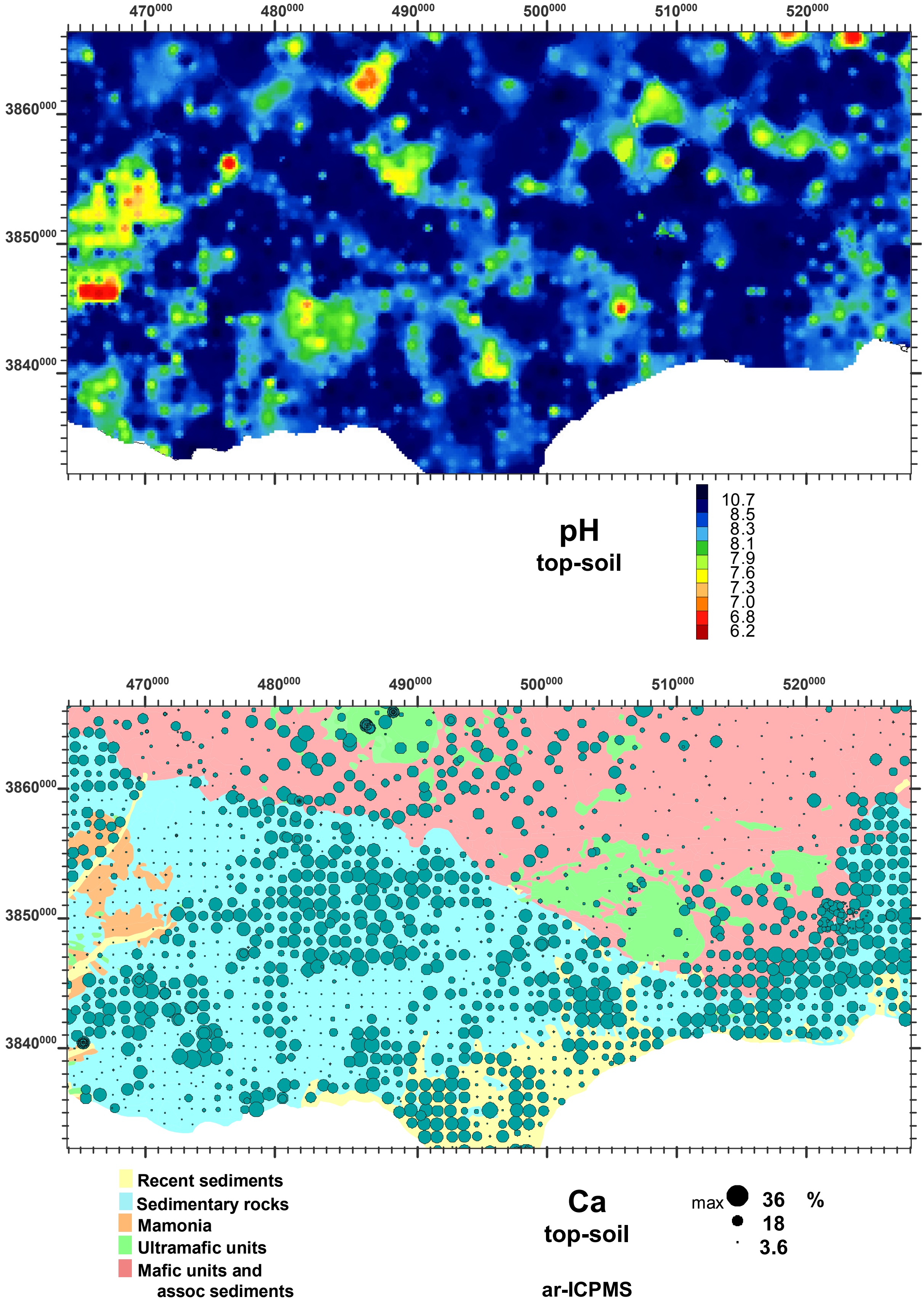

Figure 5.37 Dot-plots of *ar*-Ca in sub soil and regional pH patterns in top soil, South Coast region.

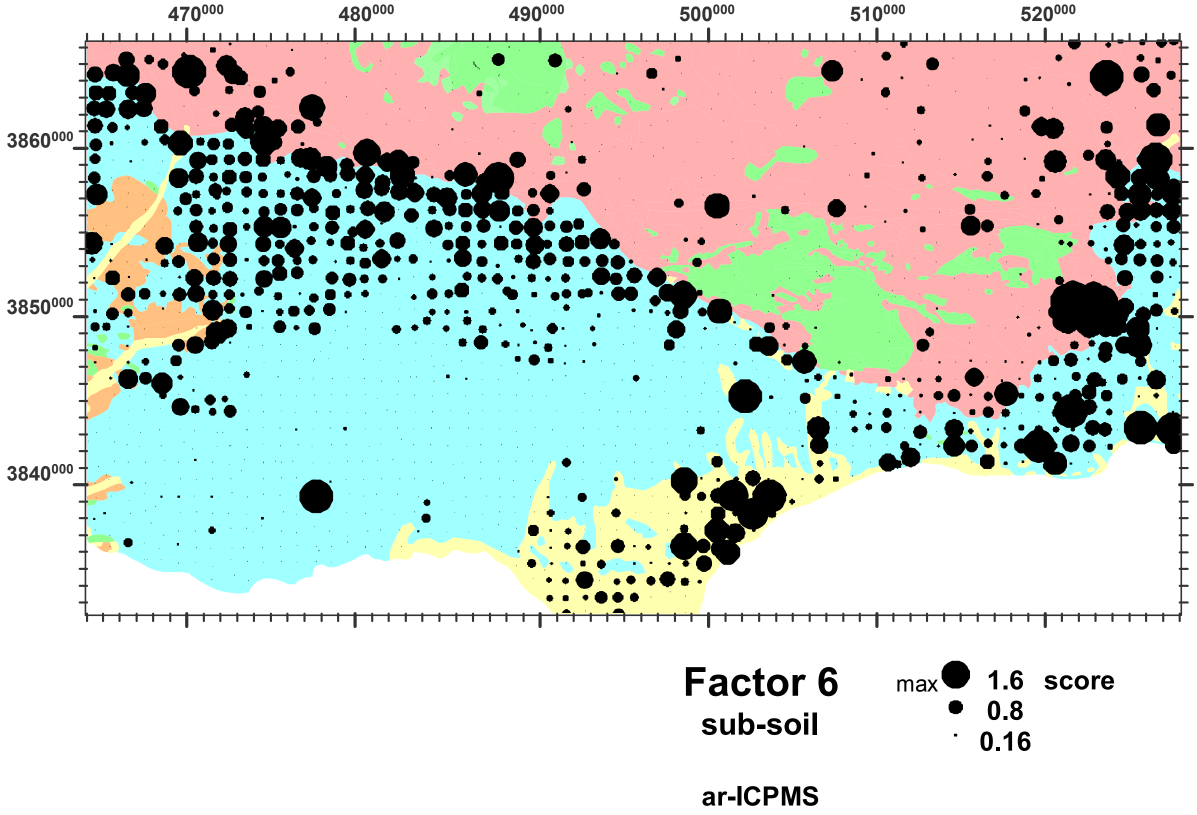

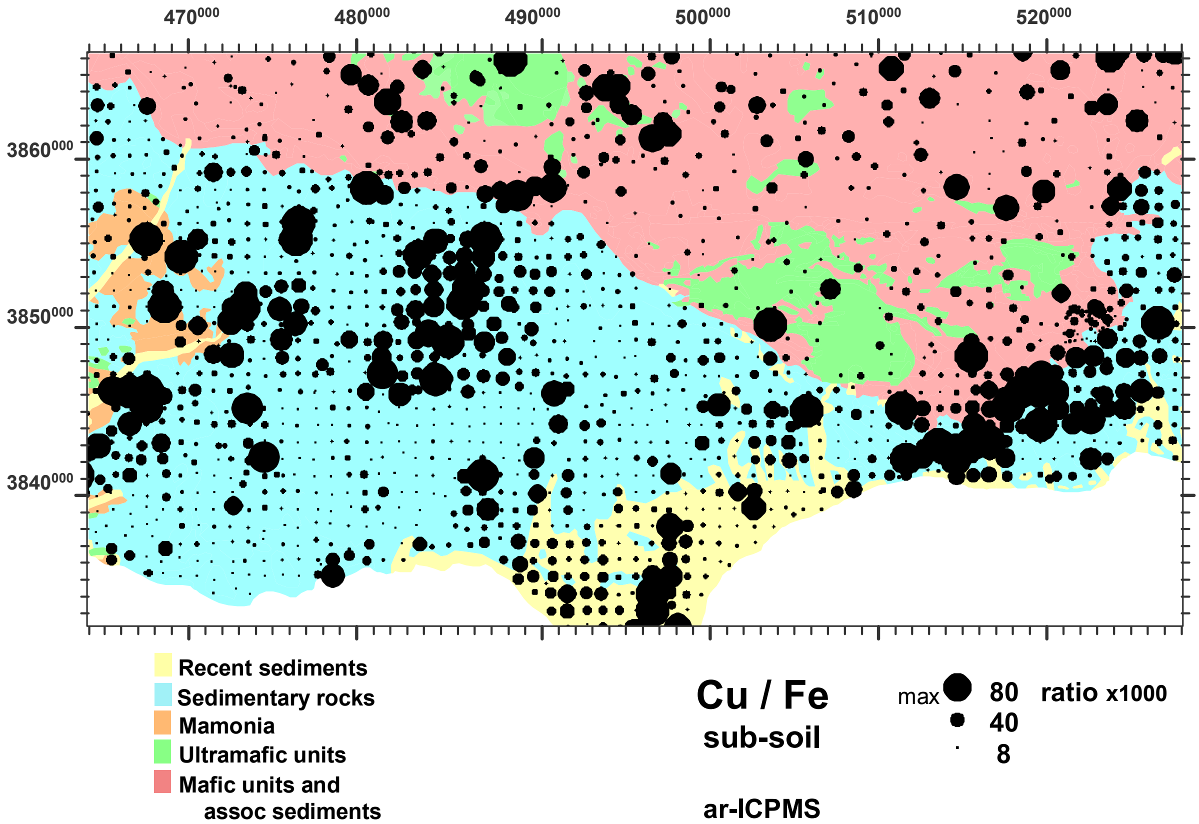

Figure 5.38 Dot-plots of *ar*-Cu/*ar*-Fe ratio and *ar-ICPMS factor 6* in sub soil, South Coast region.

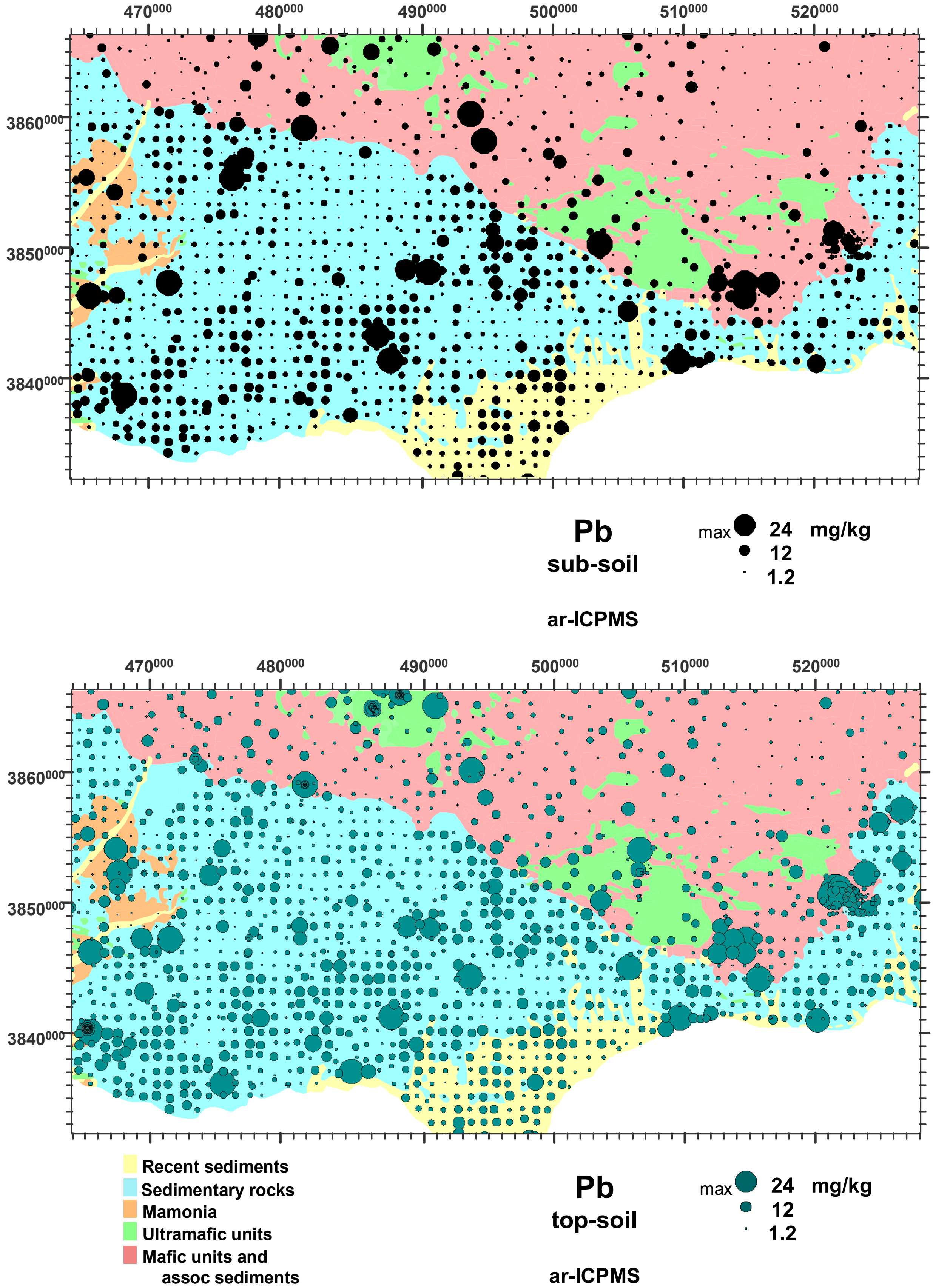

Figure 5.39 Dot-plots of *ar*-Pb in top soil and sub soil, South Coast region.

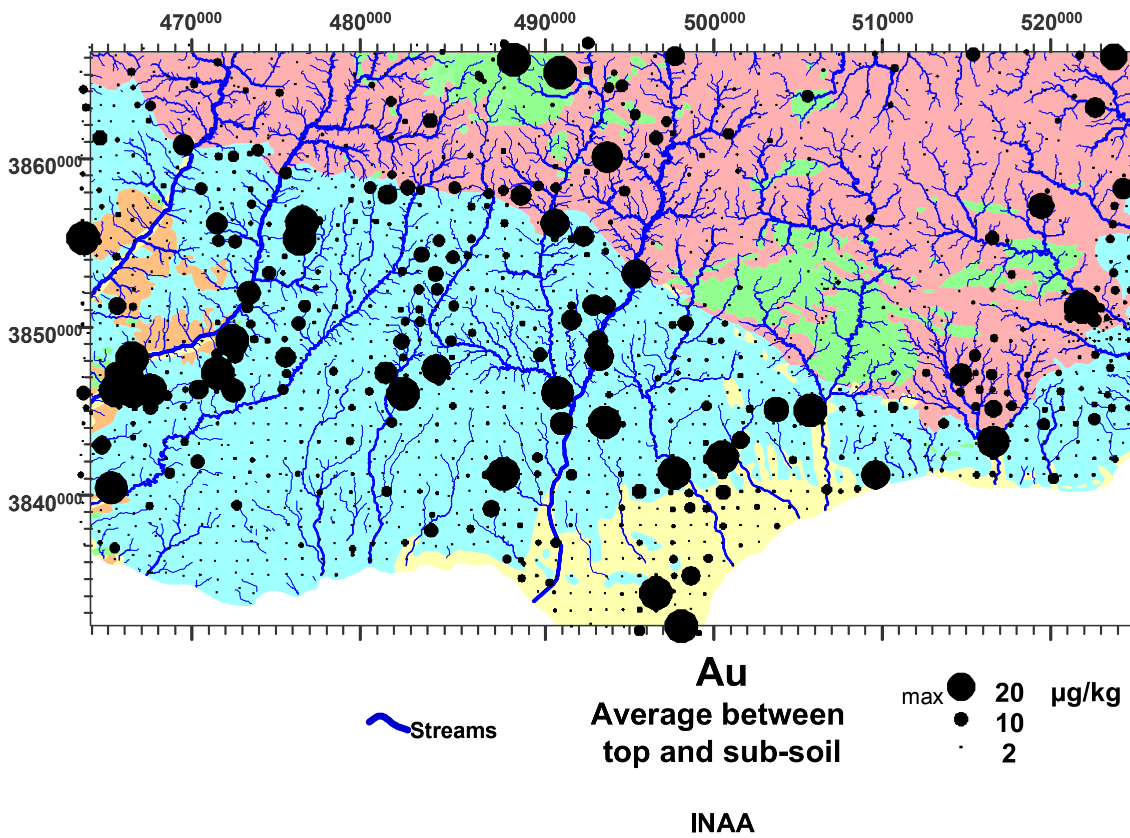

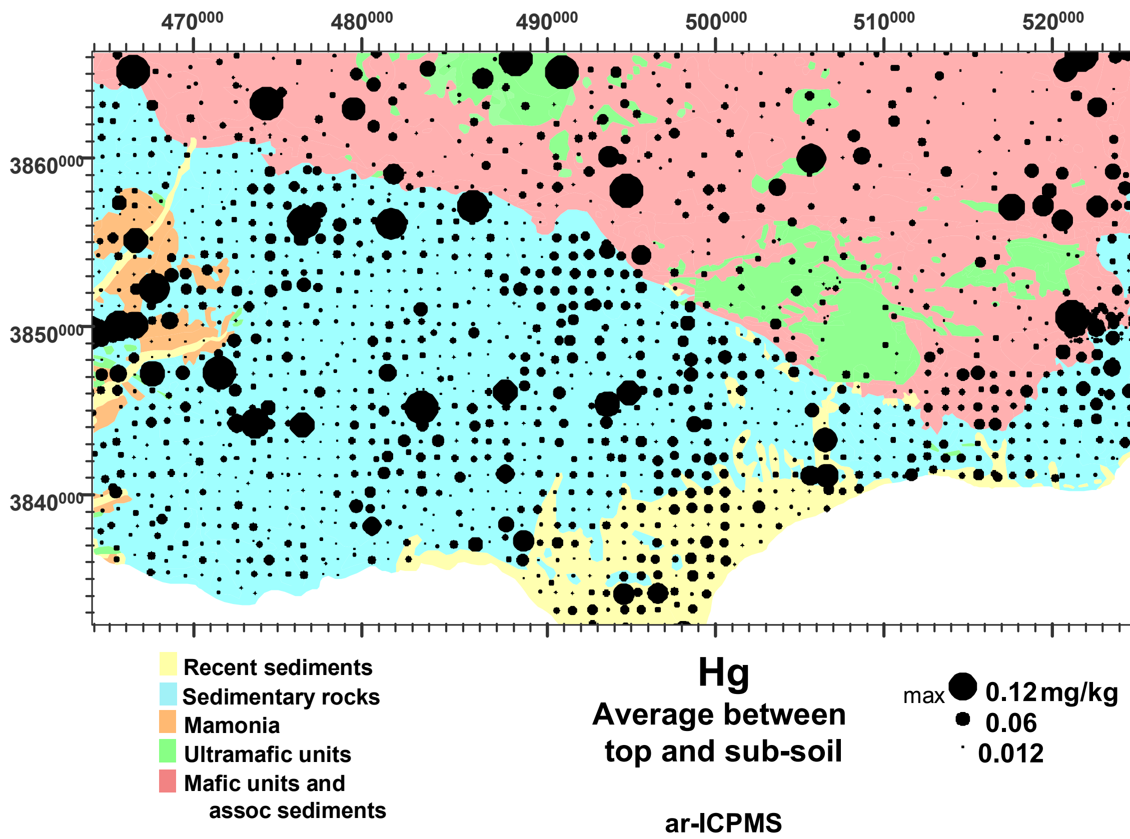

Figure 5.40 Dot-plots of average *tot*-Au in top and average *ar*-Hg in top-soil, South Coast region.

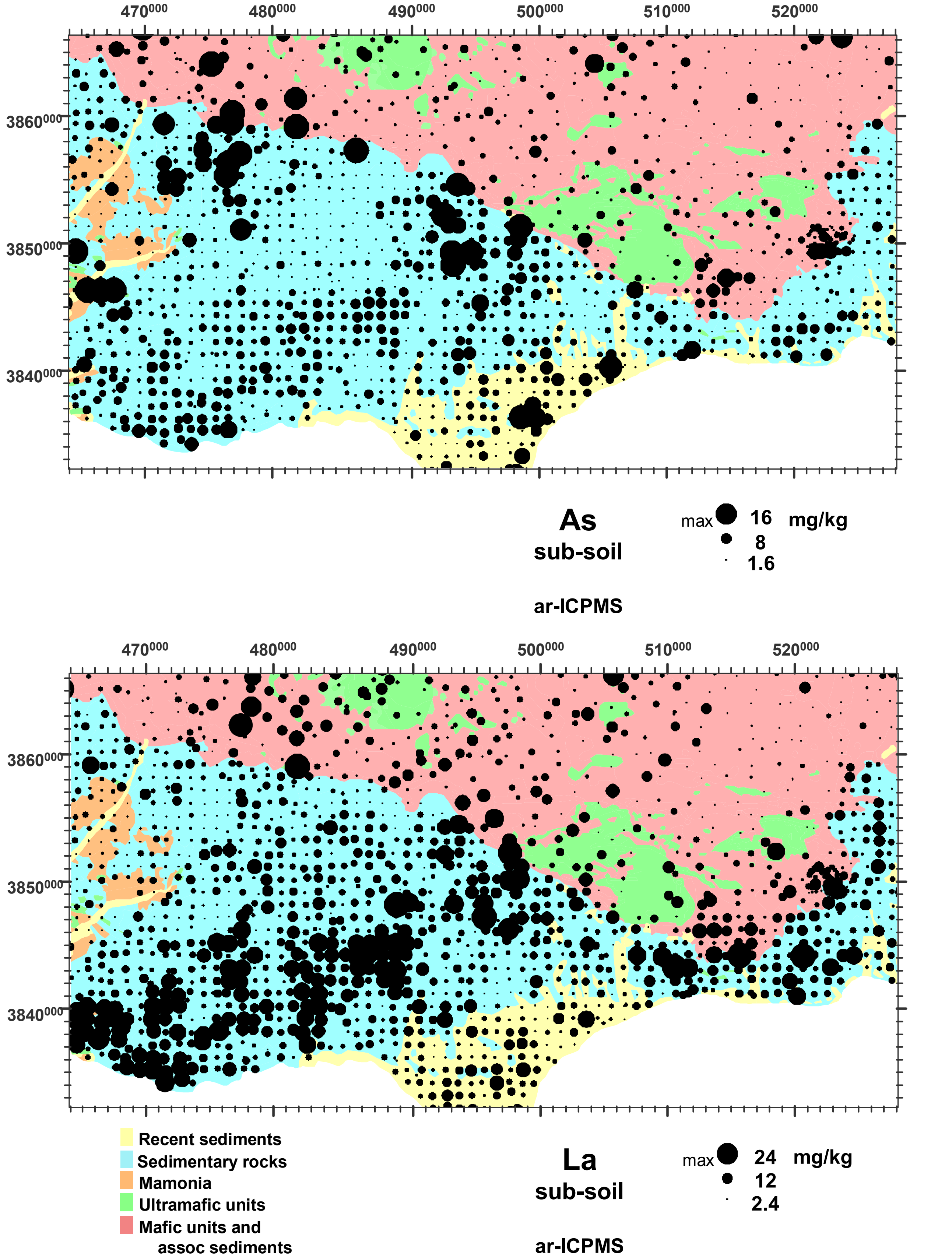

Figure 5.41 Dot-plots of *ar*-As and *ar*-La in sub soil, South Coast region.

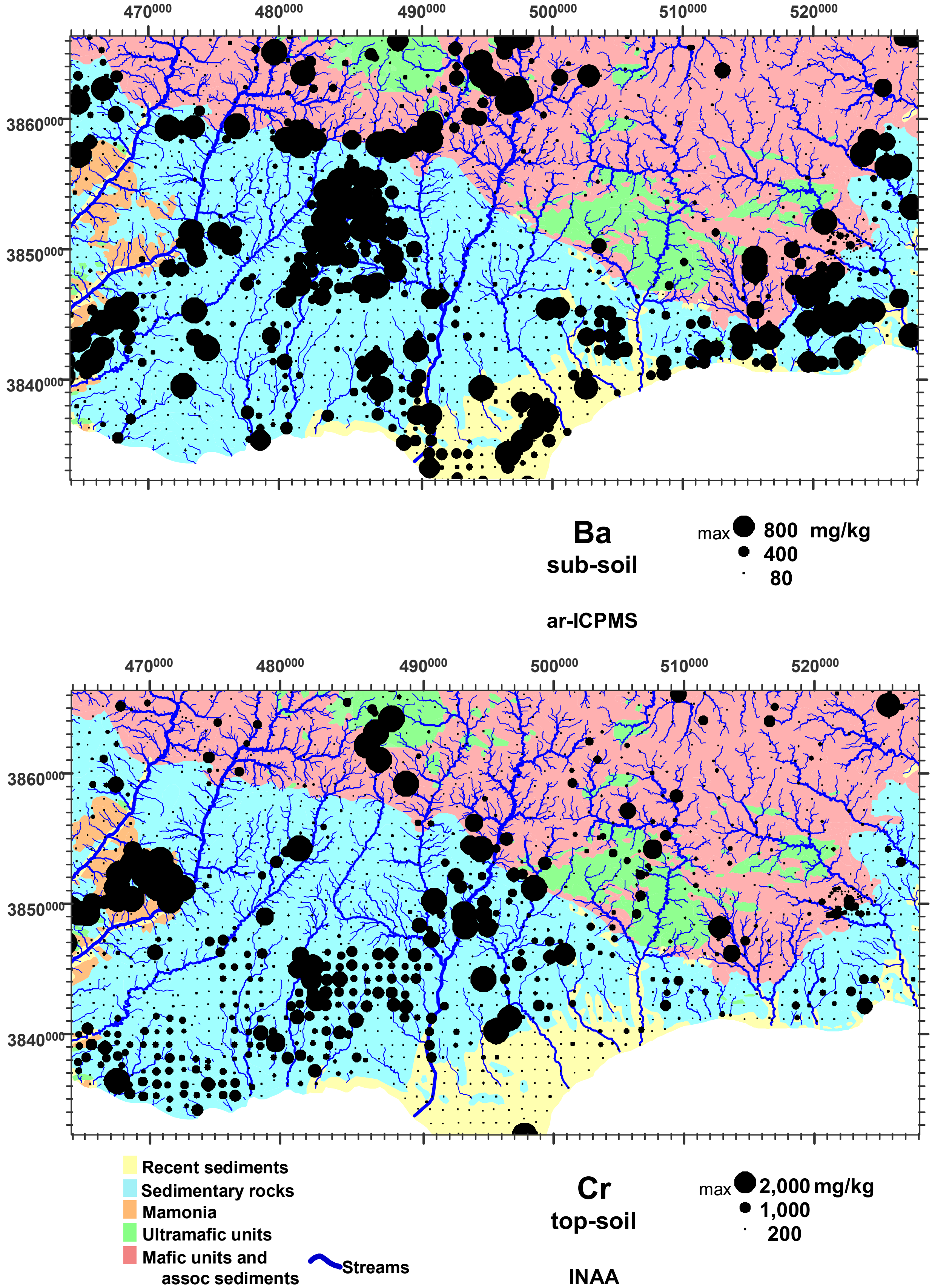

Figure 5.42 Dot-plots of *ar*-Ba and *tot*-Cr in sub soil, South Coast region.

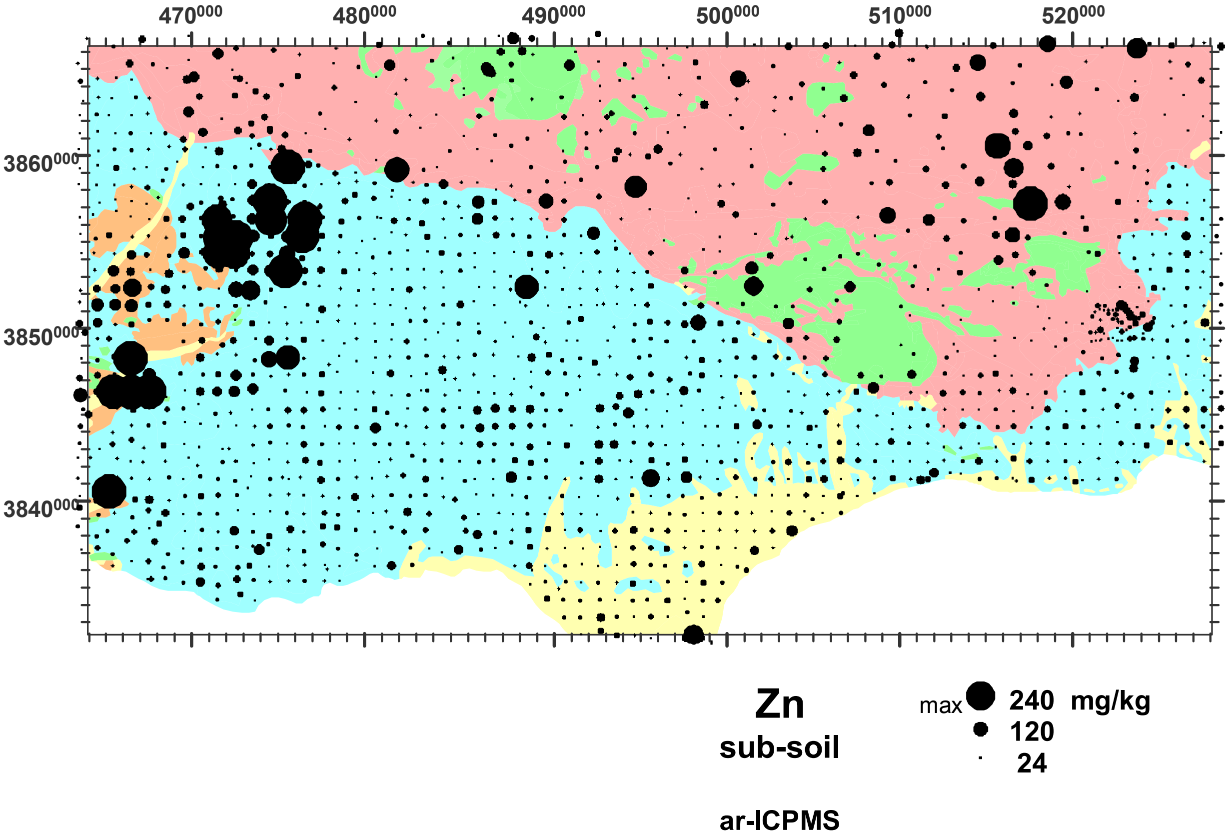

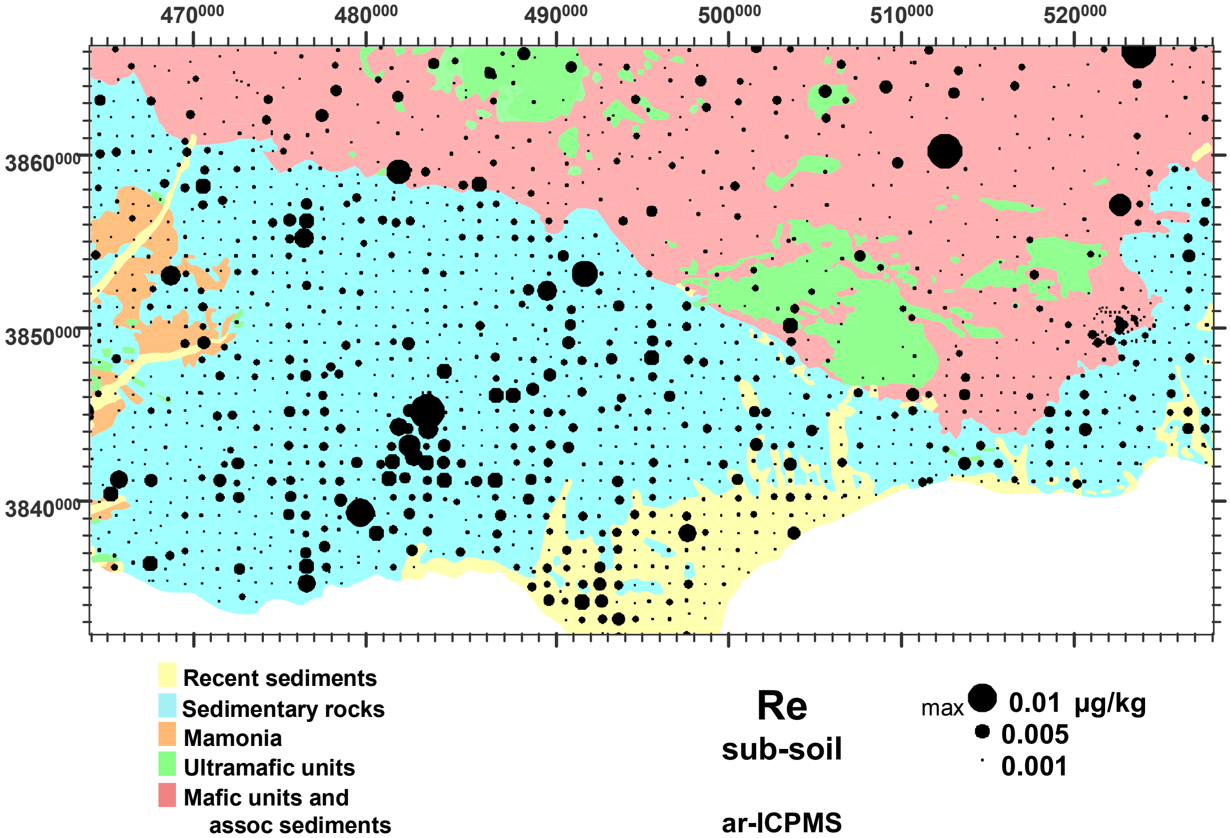

Figure 5.43 Dot-plots of *ar*-Zn and *ar*-Re in sub soil, South Coast region.

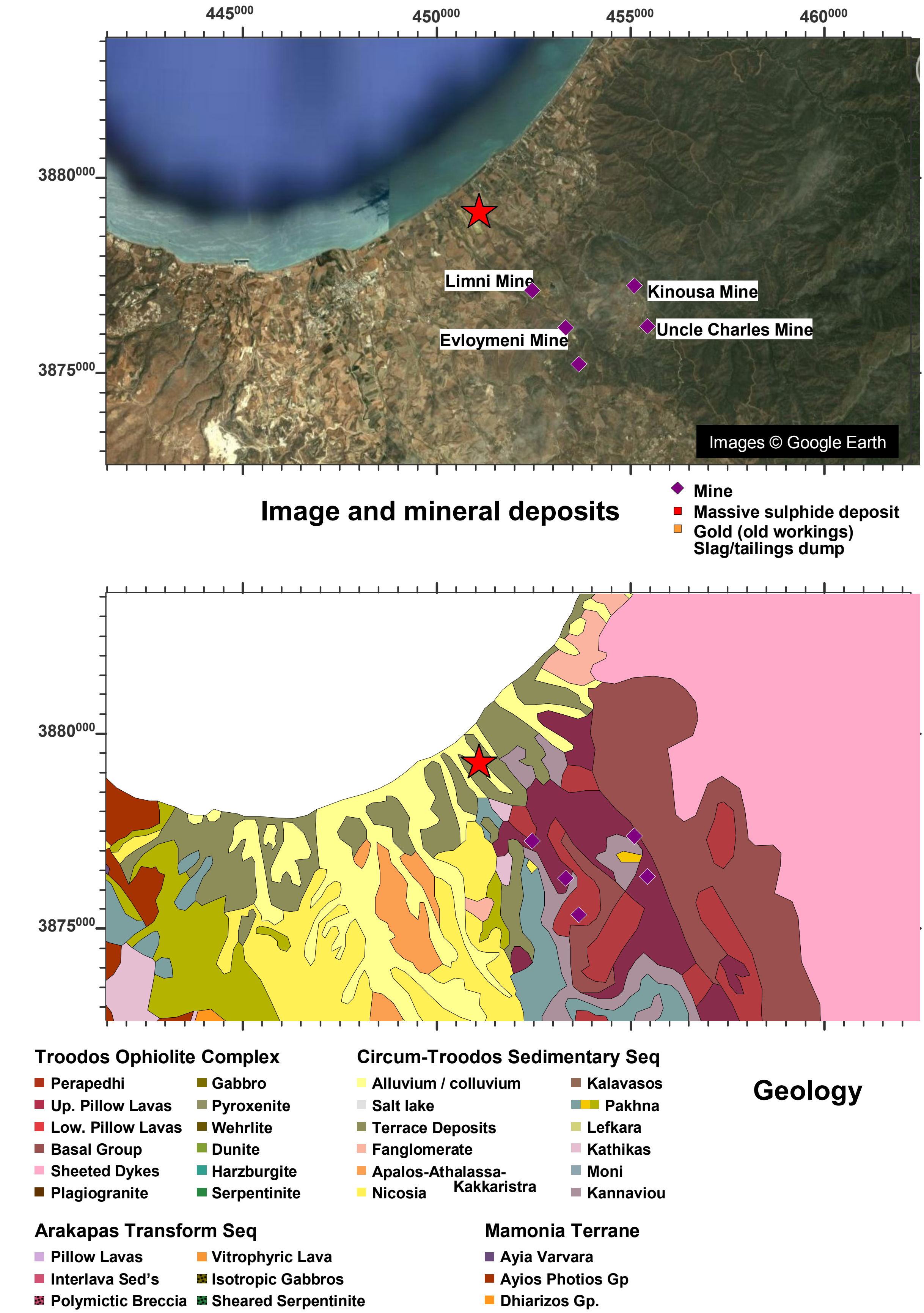

Figure 5.44 Google image and geology of the Limni Mines area, with mines and known mineralisation indicated.

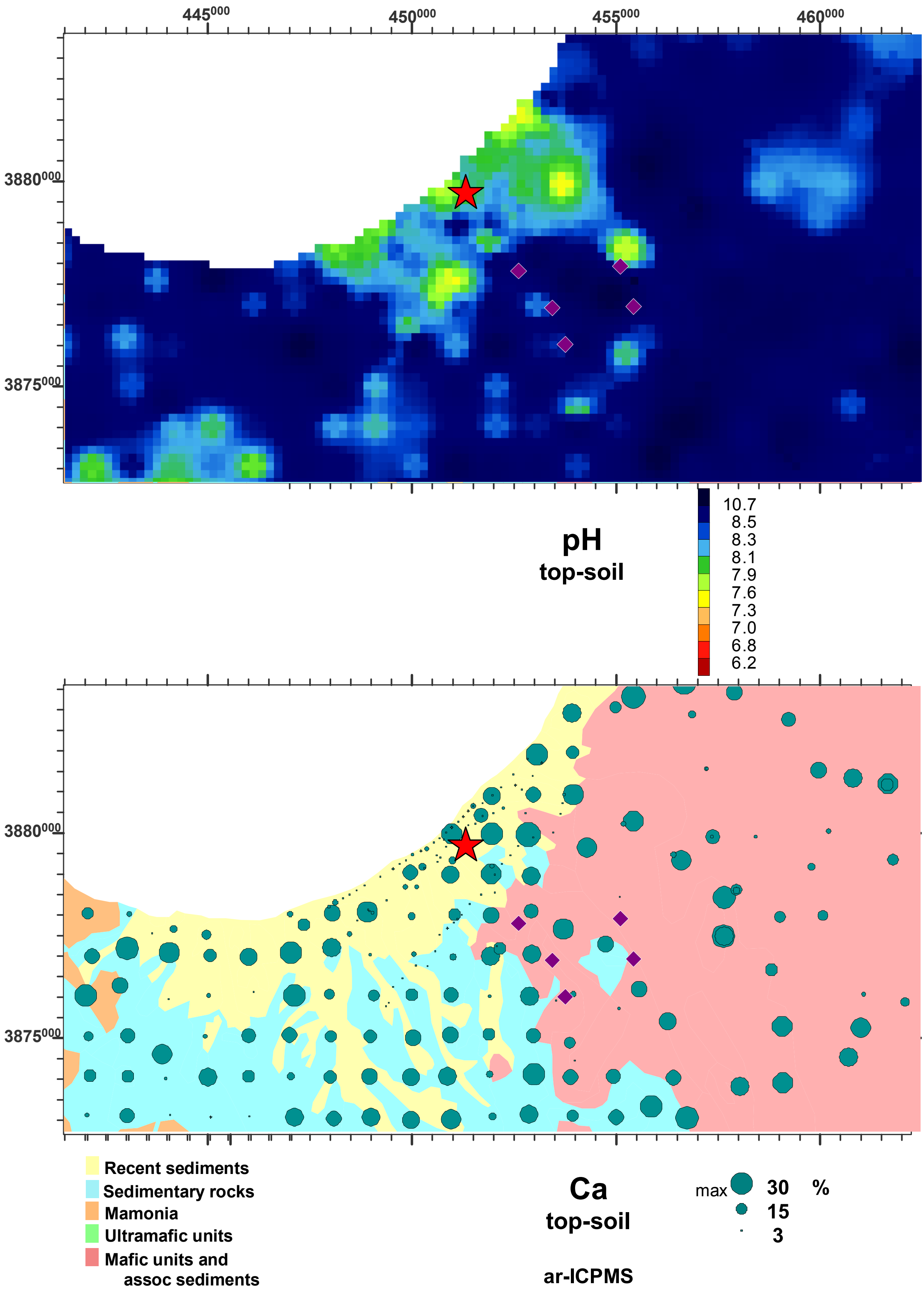

Figure 5.45 Dot-plots of *ar*-Ca in sub soil and regional pH patterns in top soil, Limni Mines area.

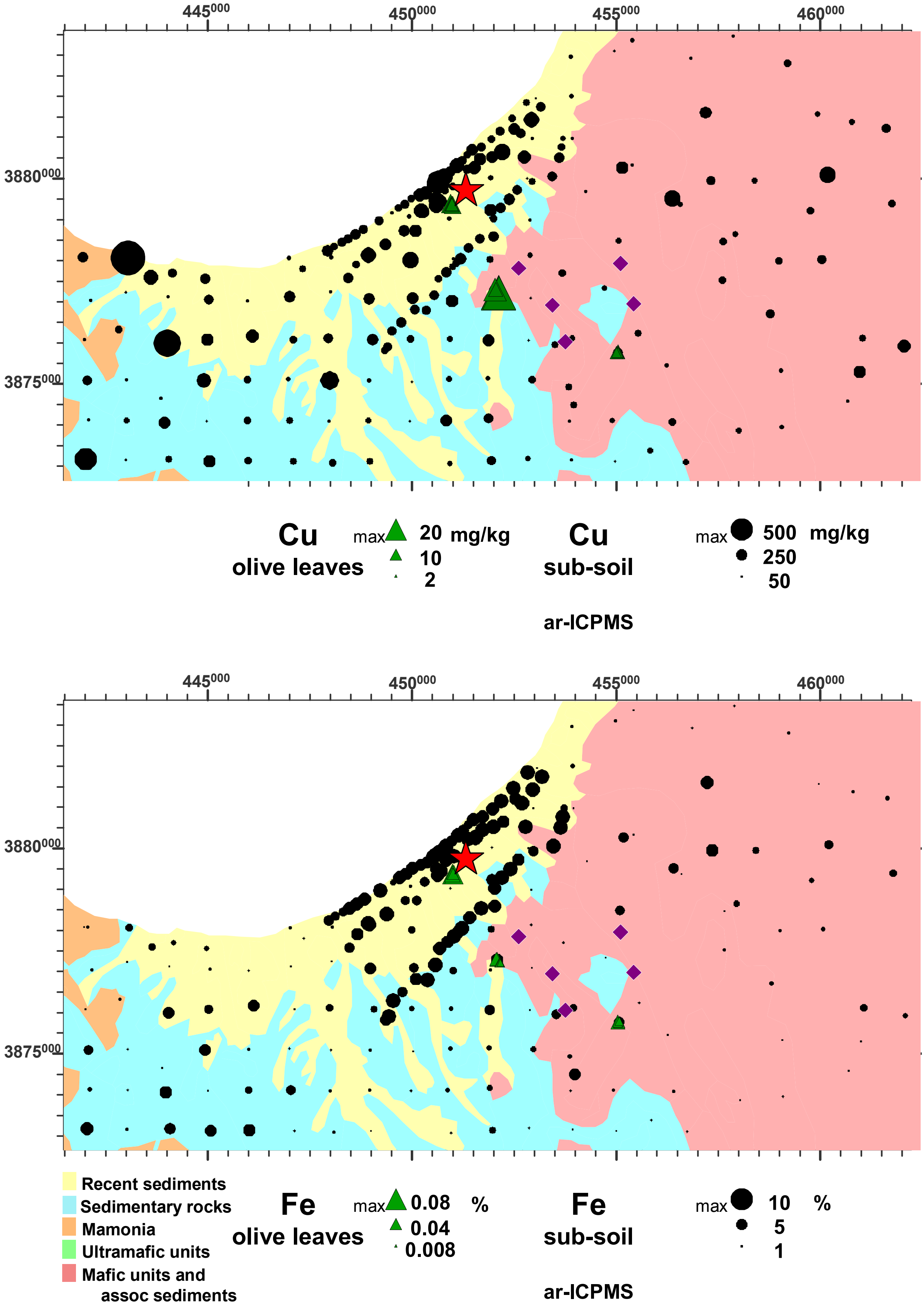

Figure 5.46 Dot-plots of *ar*-Cu and *ar*-Fe in top soil, Limni Mines area.

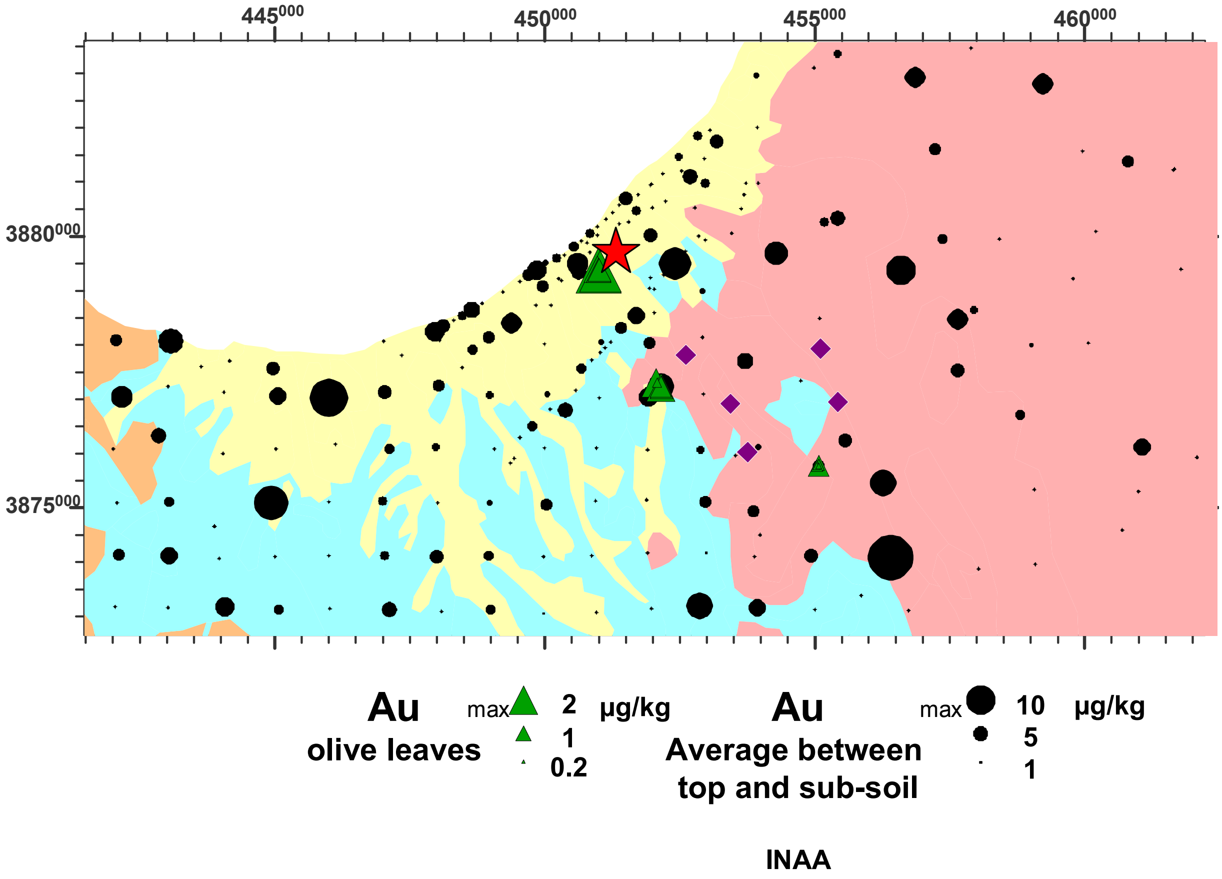

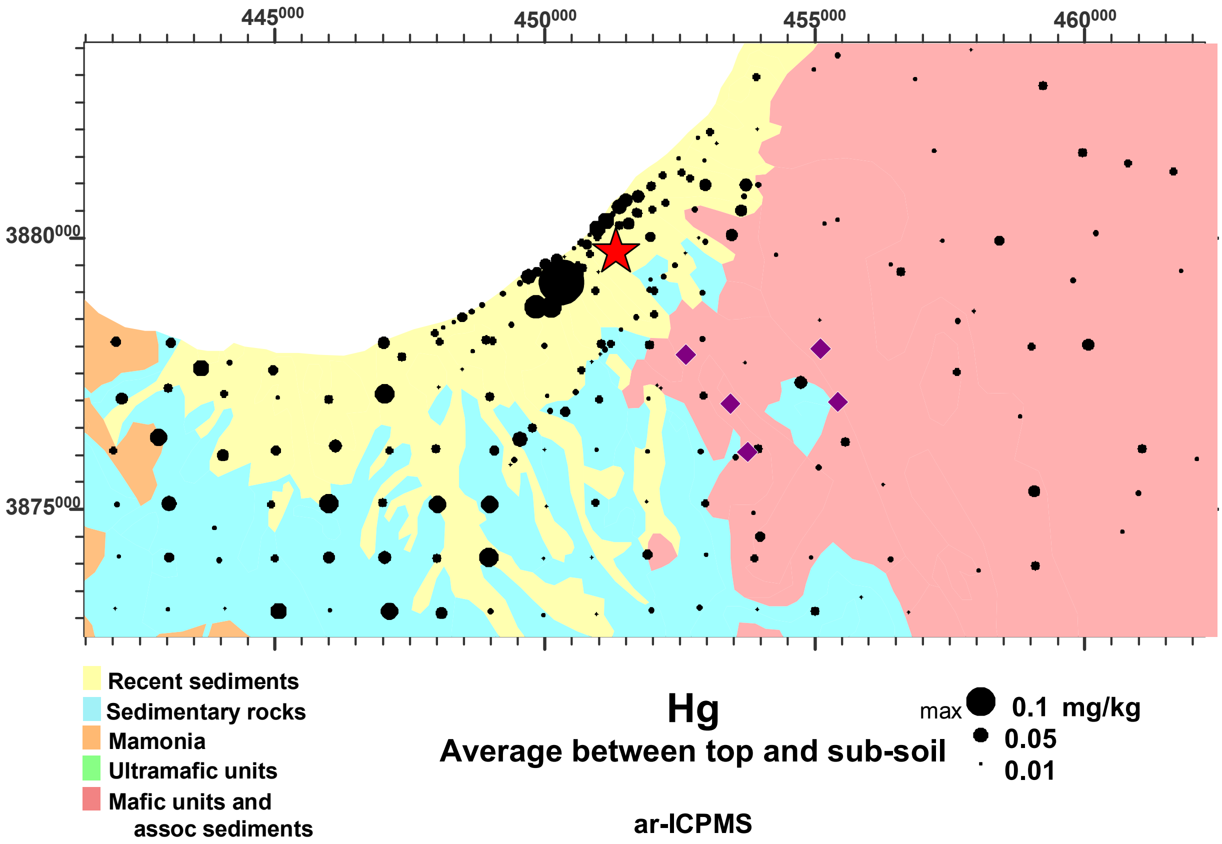

Figure 5.47 Dot-plots of average *tot*-Au in top and sub soil and average *ar*-Hg in top and sub soil, Limni Mines area.

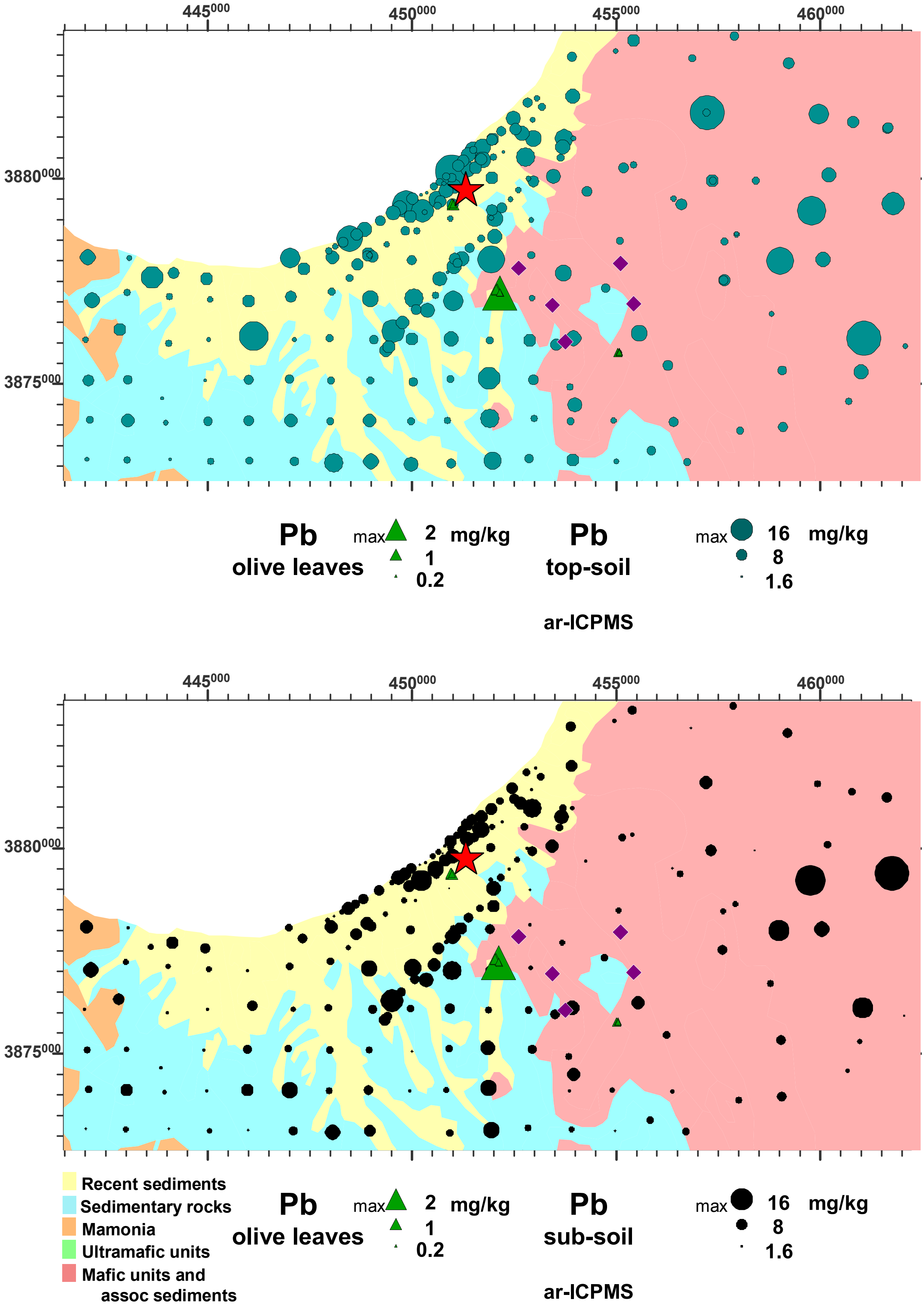

Figure 5.48 Dot-plots of *ar*-Pb in top soil and sub soil, Limni Mines area.

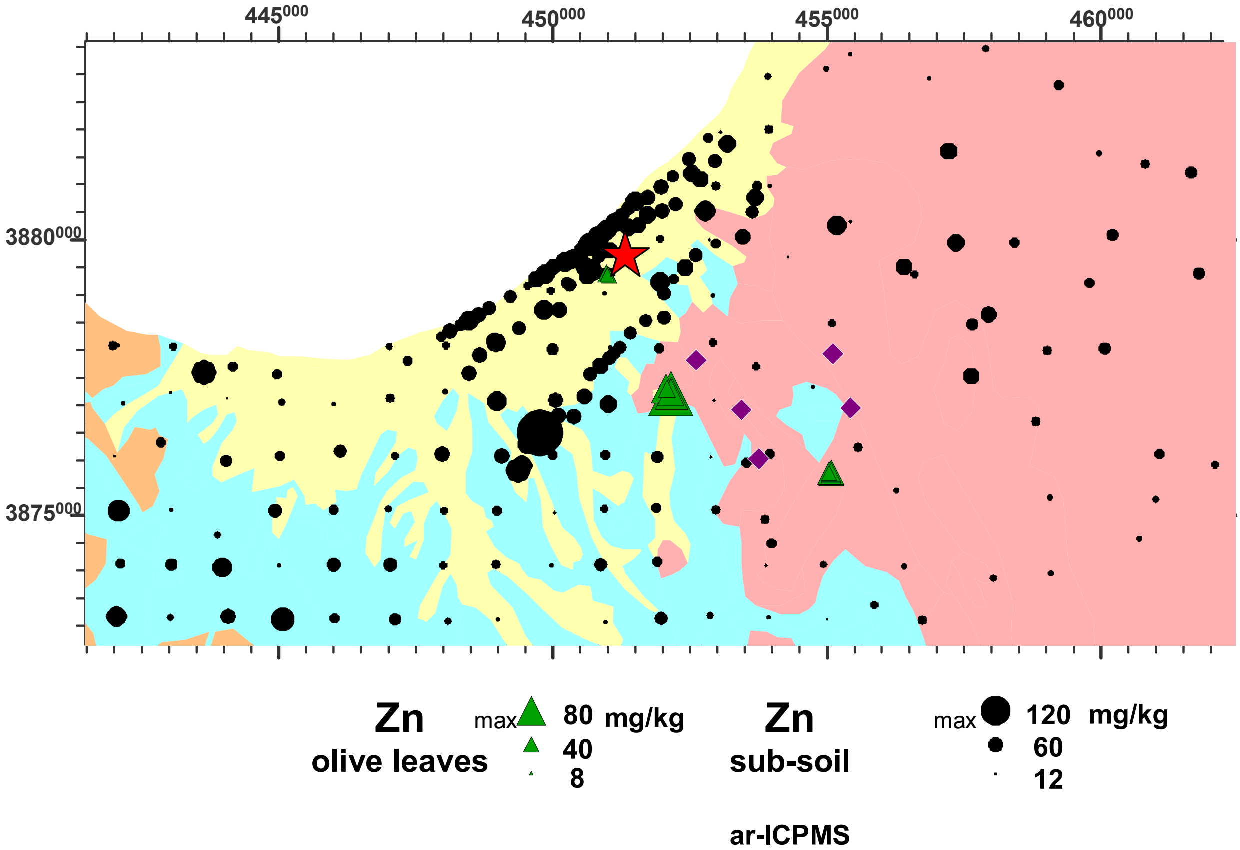

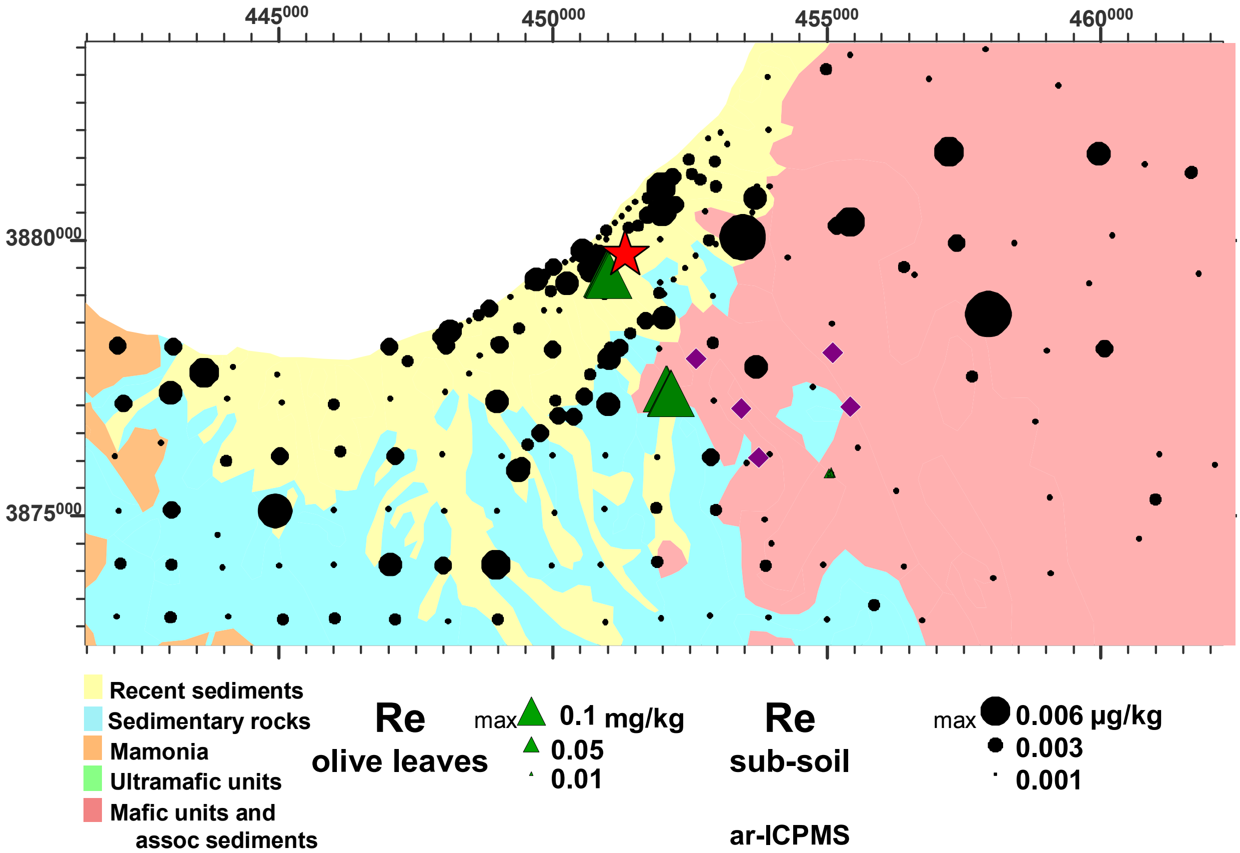

Figure 5.49 Dot-plots of *ar*-Zn and *ar*-Re in sub soil, Limni Mines area.

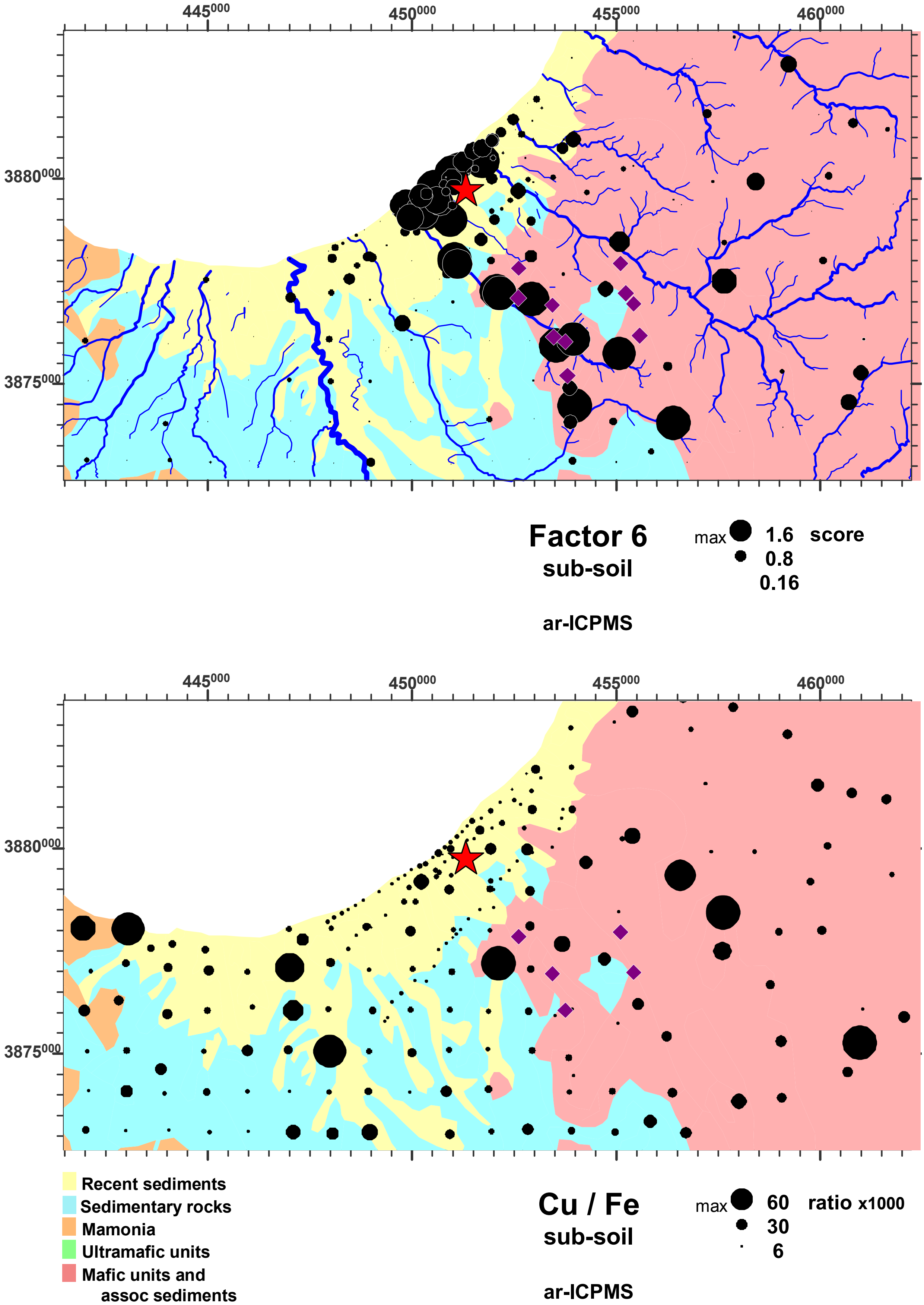

Figure 5.50 Dot-plots of *ar*-Cu/*ar*-Fe ratio and *ar-ICPMS factor 6* in sub soil, Limni Mines area.

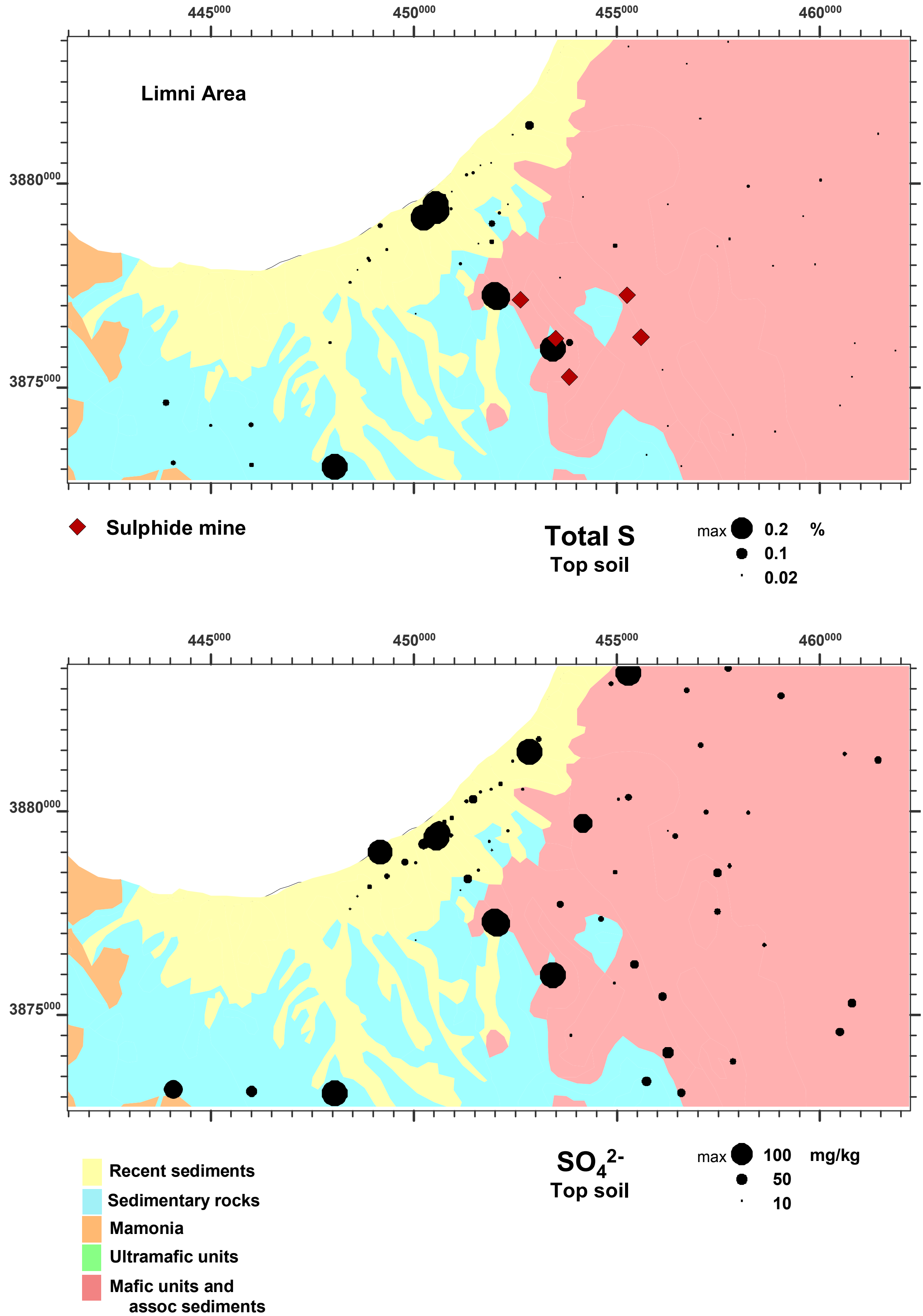

Figure 5.51 Dot-plots of tot-S and soluble SO_4^{2-} in top soil, Limni Mines area.

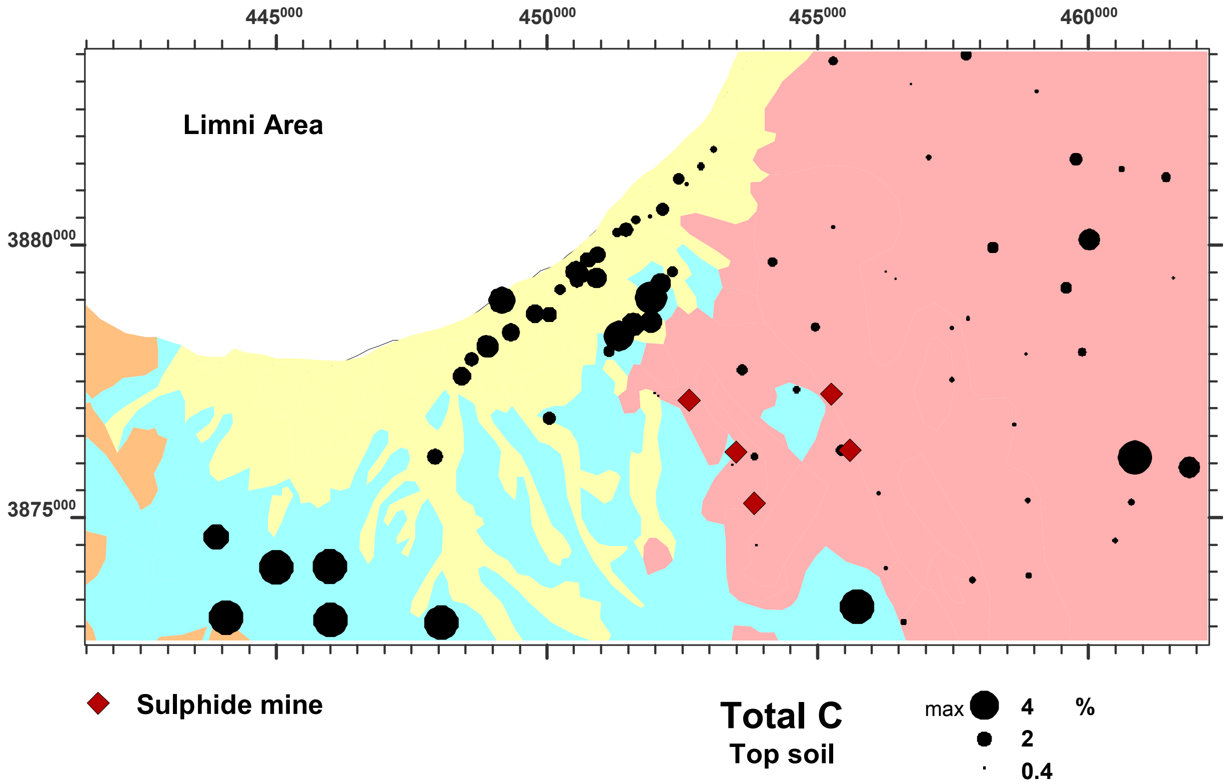

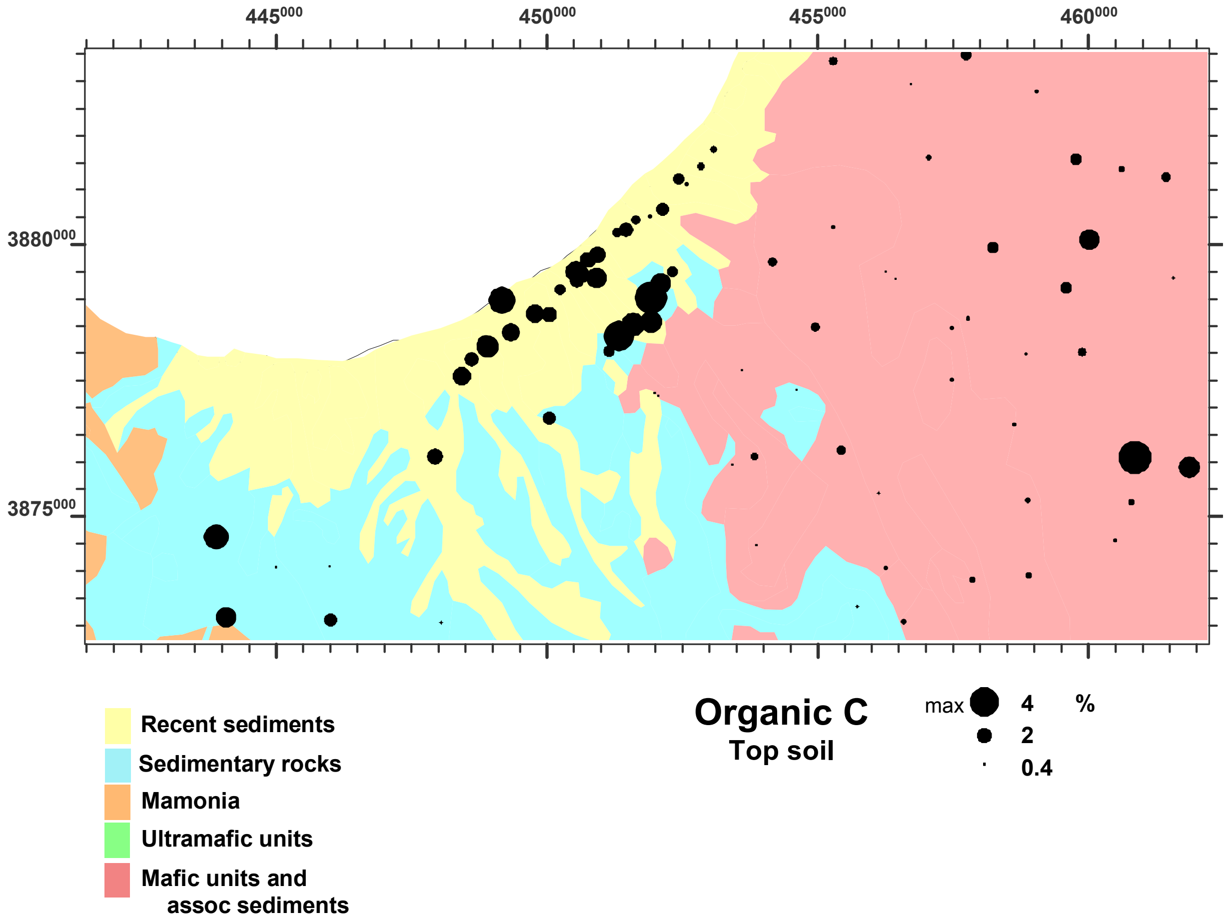

Figure 5.52 Dot-plots of tot-C and org-C in top soil, Limni Mines area.

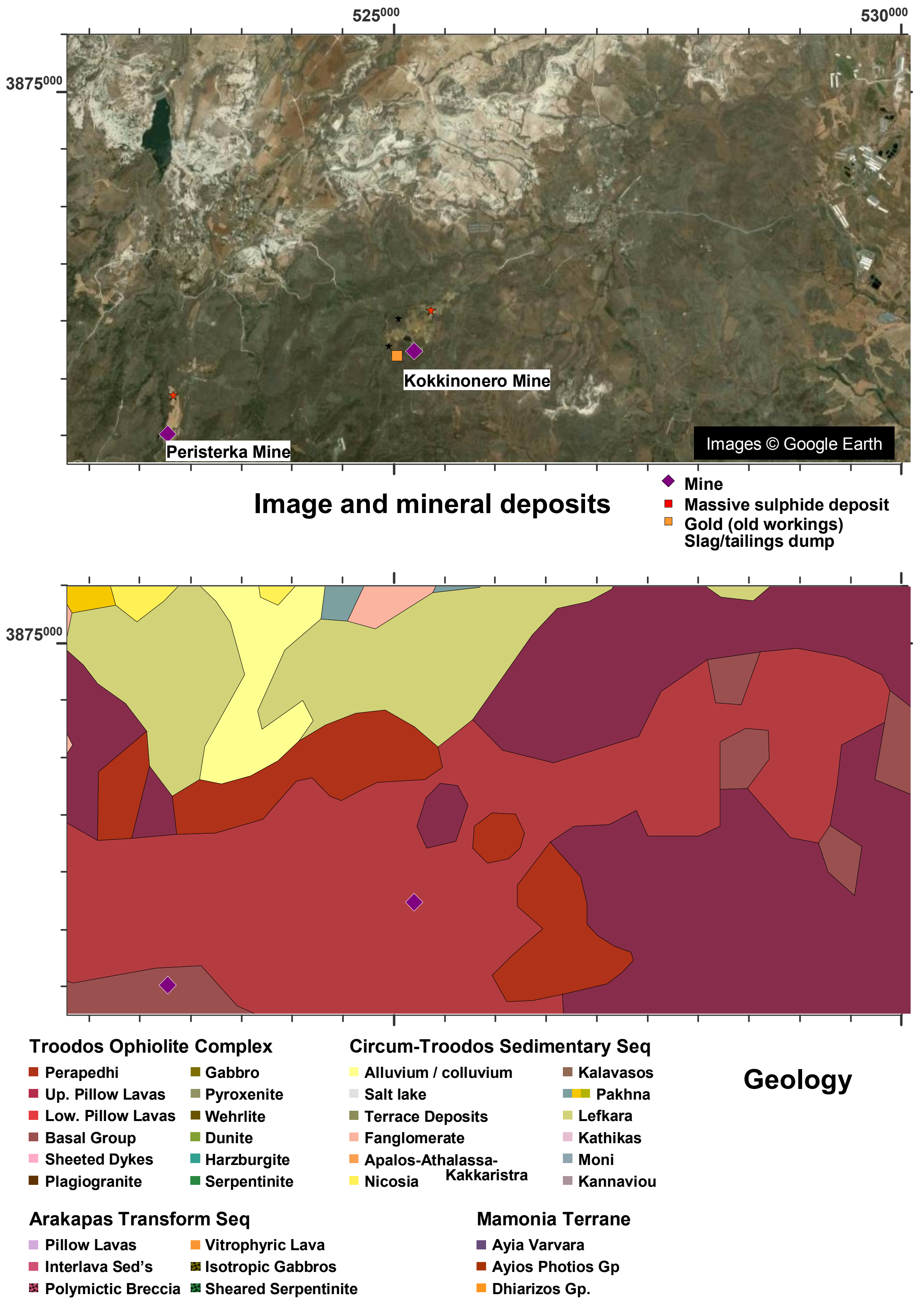

Figure 5.53 Google image and geology of the Kokkinonero Mine area, with mines and known mineralisation indicated.

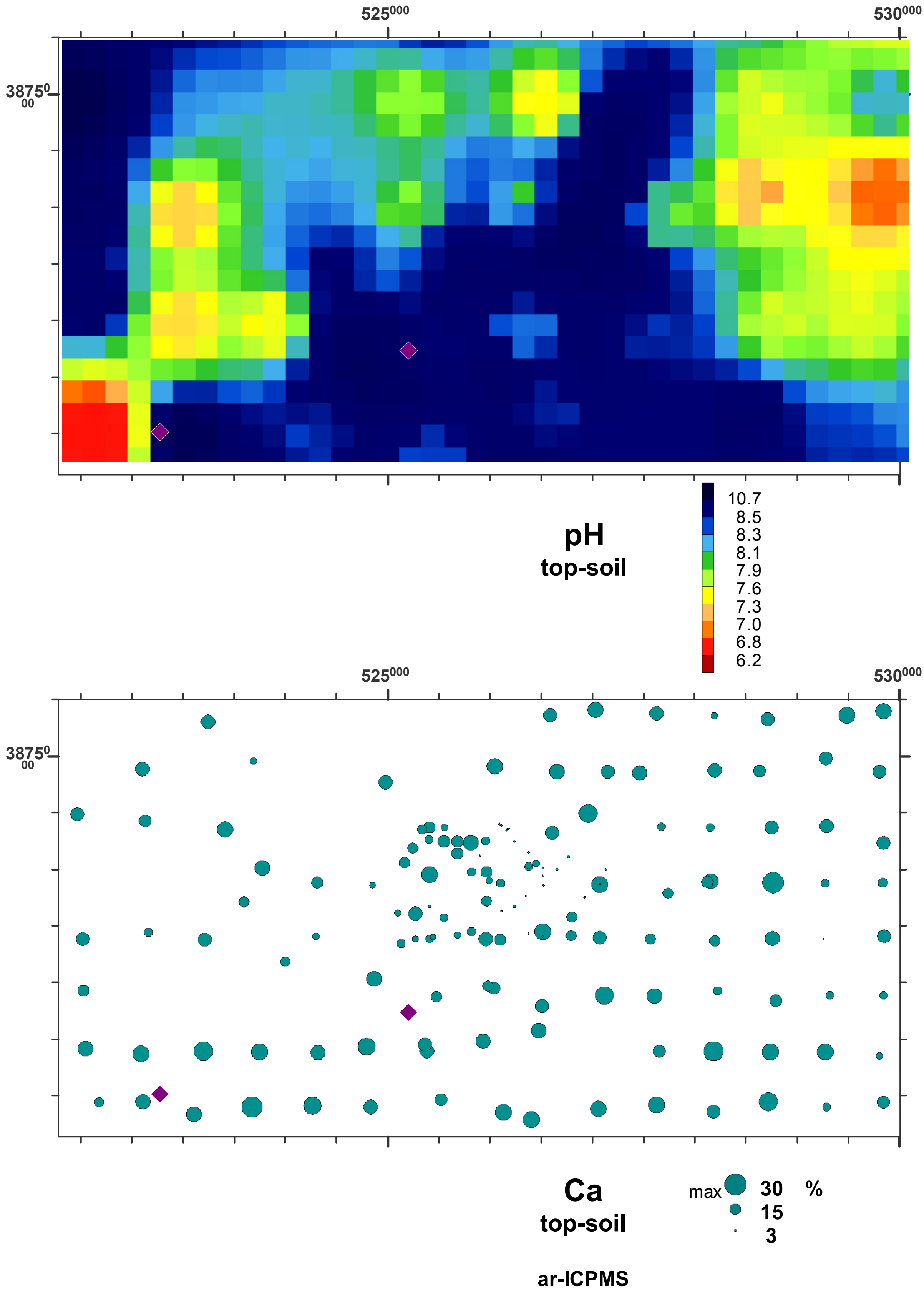

Figure 5.54 Dot-plots of *ar*-Ca in sub soil and regional pH patterns in top soil, Kokkinonero Mine area.

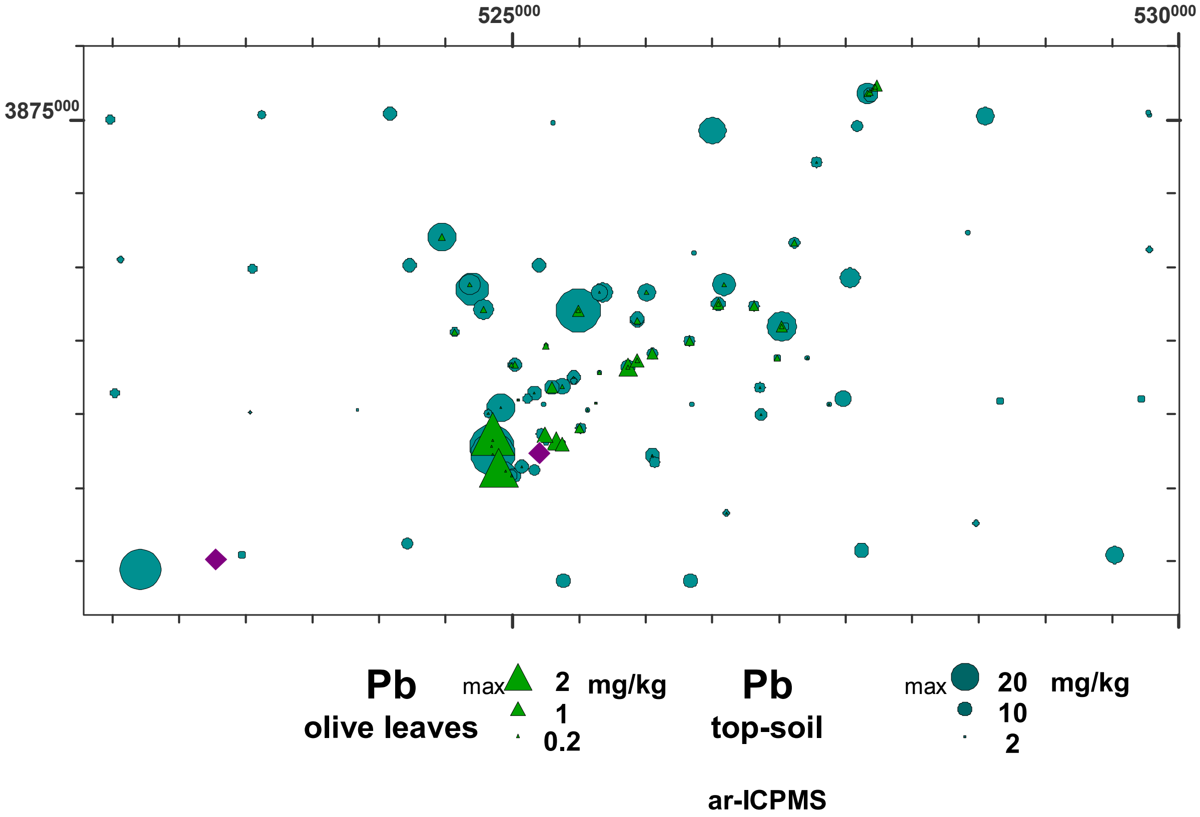

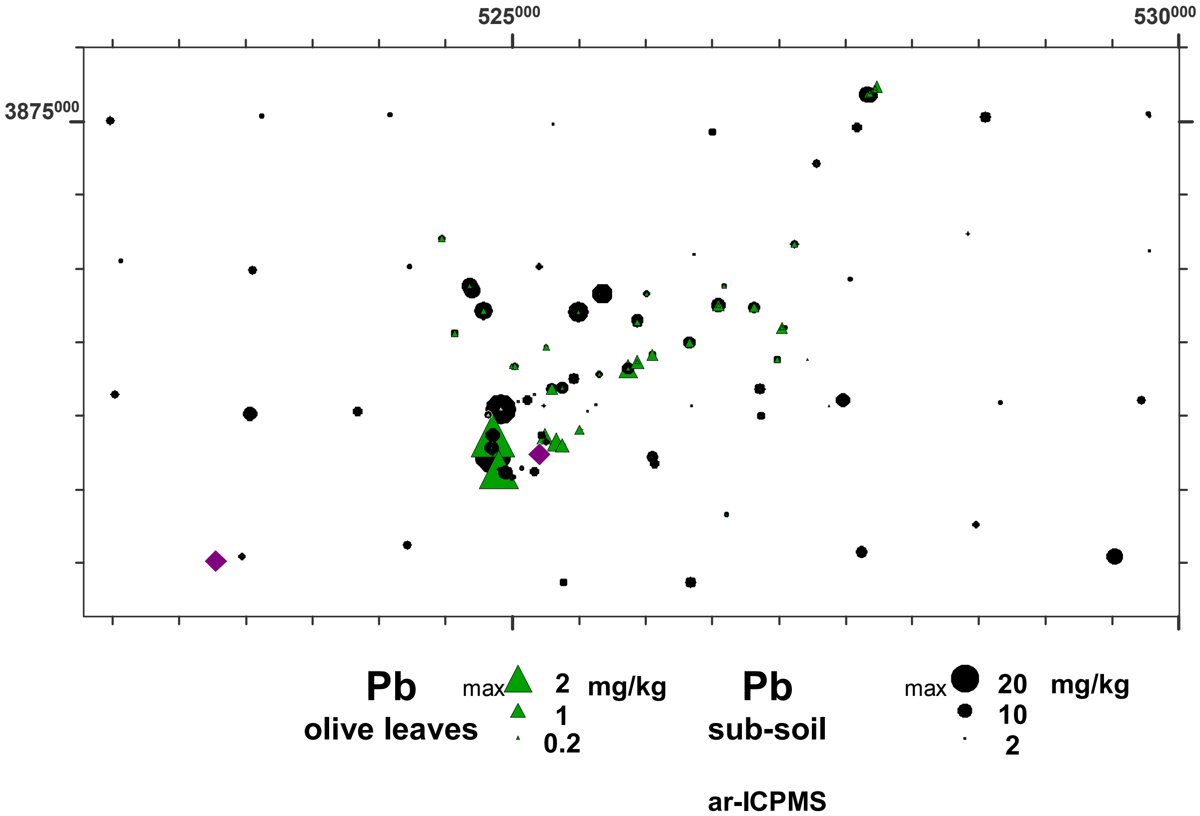

Figure 5.55 Dot-plots of *ar*-Pb in top soil and sub soil and in olive leaves, Kokkinonero Mine area.

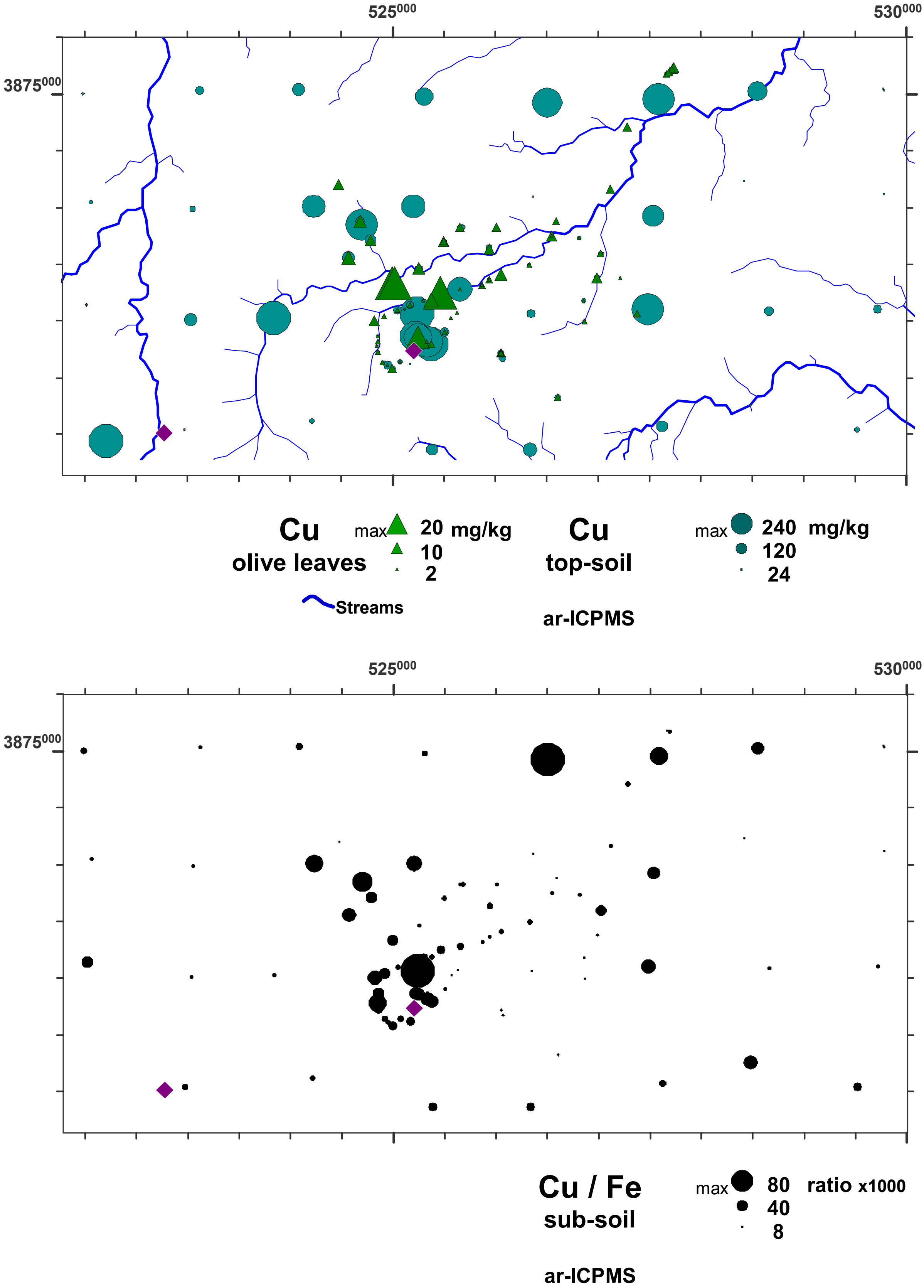

Figure 5.56 Dot-plots of *ar*-Cu in top soil and *ar*-Cu/*ar*-Fe ratio in sub- soil, and Cu in olive leaves, Kokkinonero Mine area.

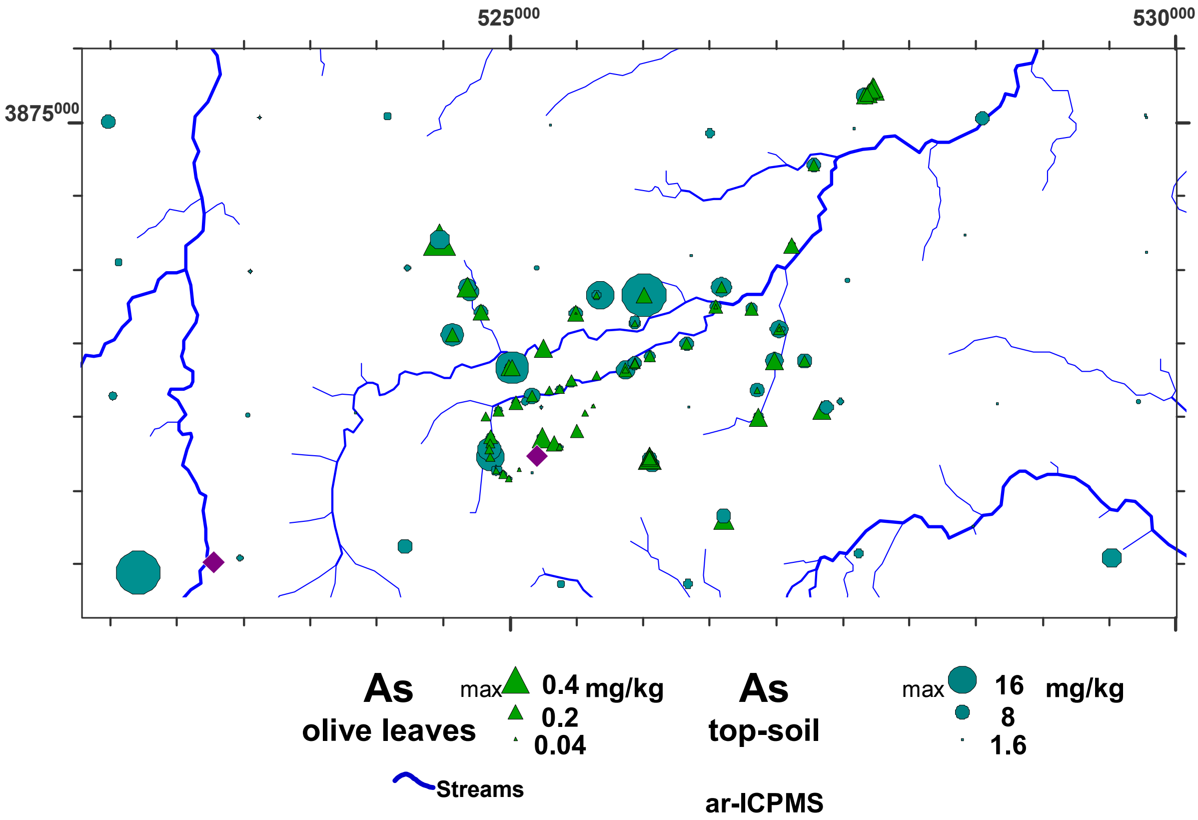

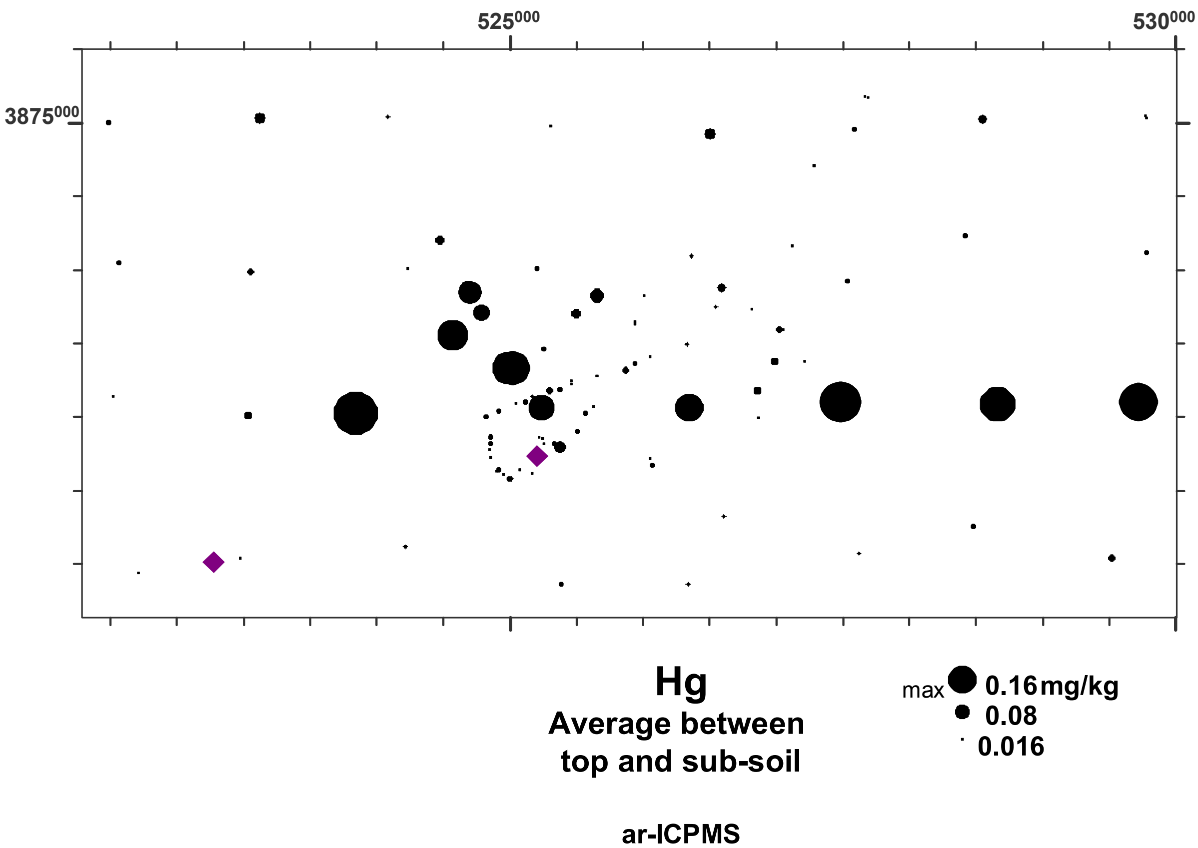

Figure 5.57 Dot-plots of ar-As in top soil and average *ar*-Hg in top-soil, and Au and Hg in olive leaves, Kokkinonero Mine area.

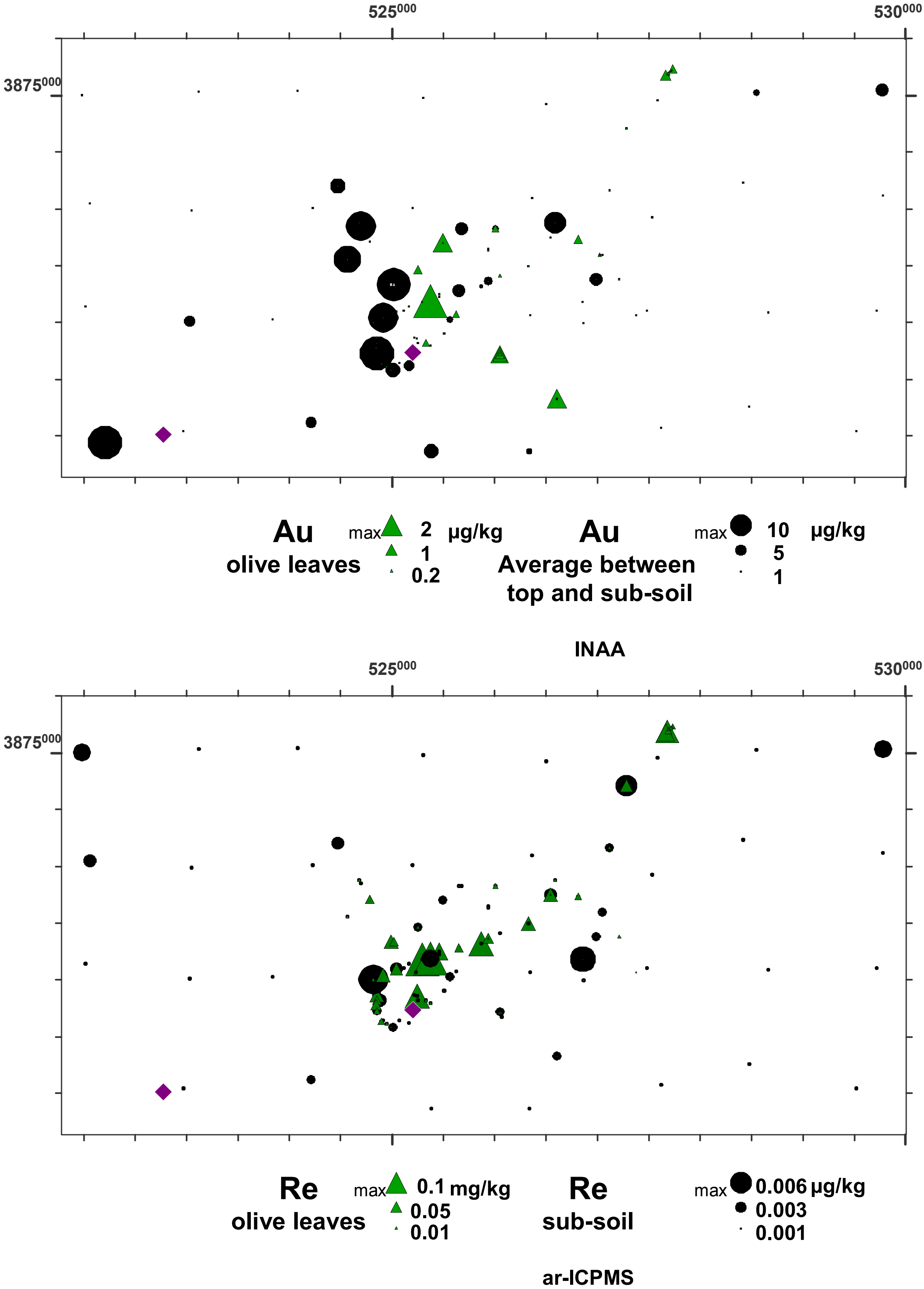

Figure 5.58 Dot-plots of *tot*-Au and *ar*-Re in sub soil, and Au and Re in olive leaves, Kokkinonero Mine area.

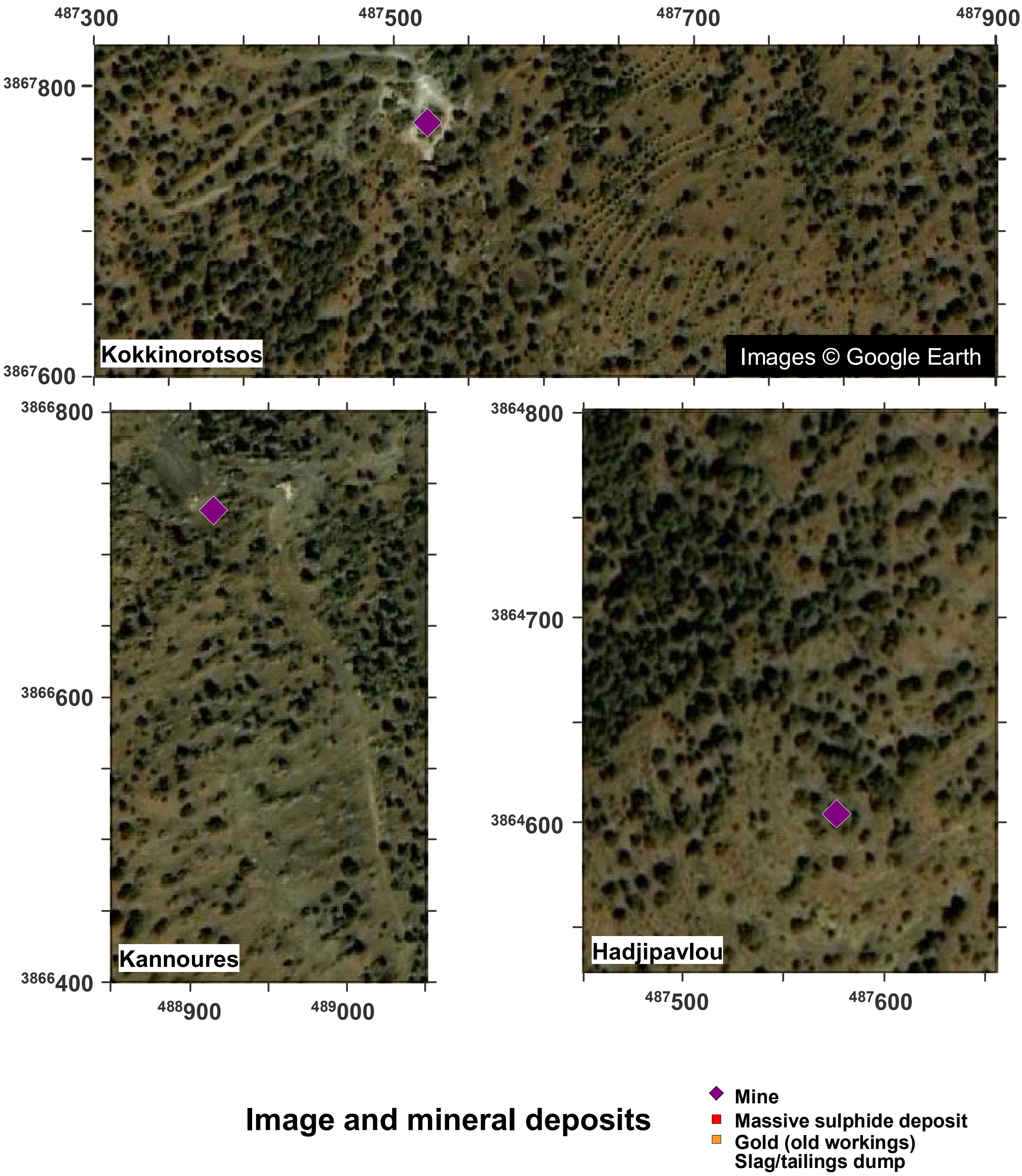

Figure 5.59 Google image of the Kokkinorotsos, Kannoures and Hadjipavlou Cr Mines area.

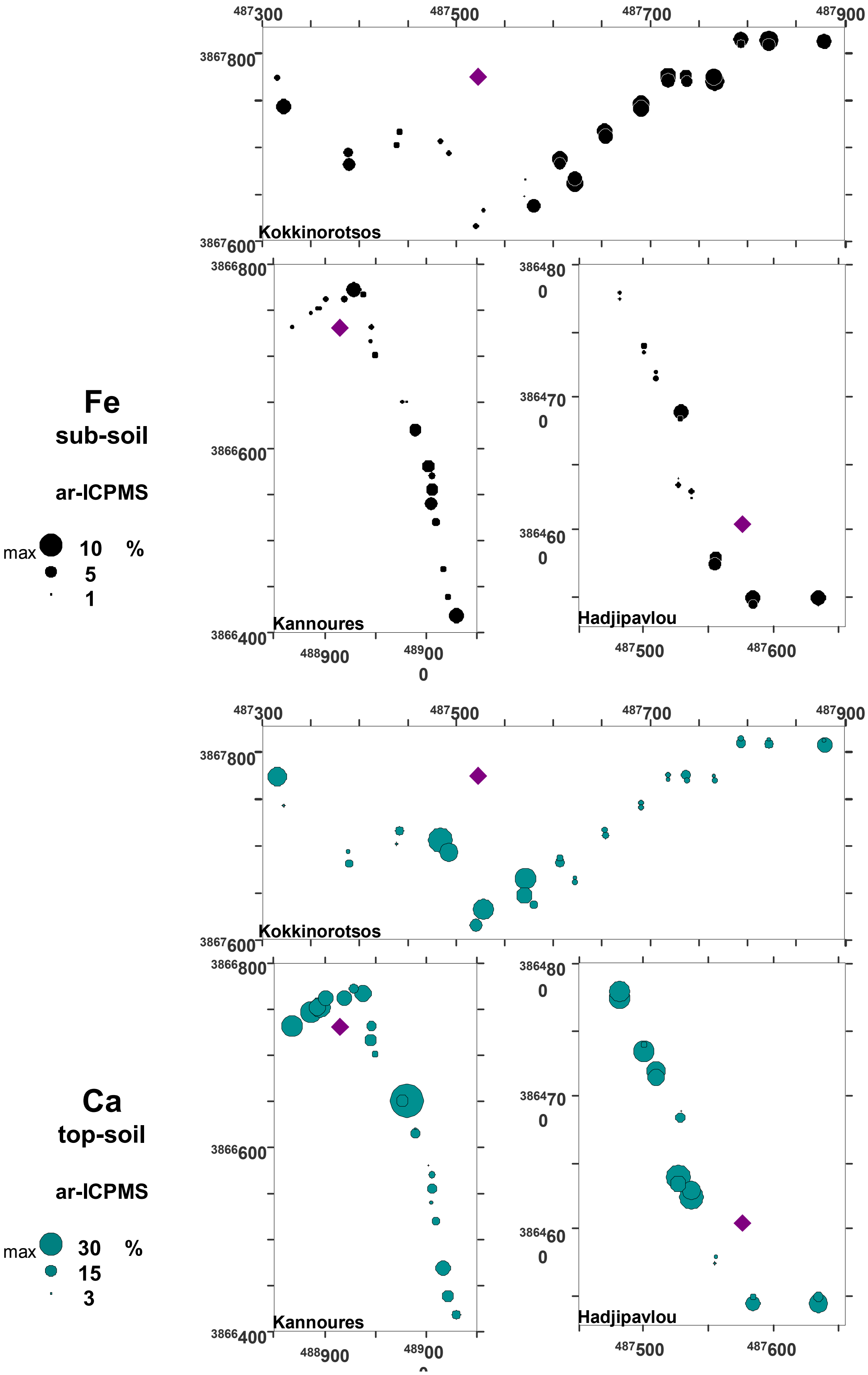

Figure 5.60 Dot-plots of *ar*-Ca in top soil and ar_Fe in sub soil, Chromite mines area.

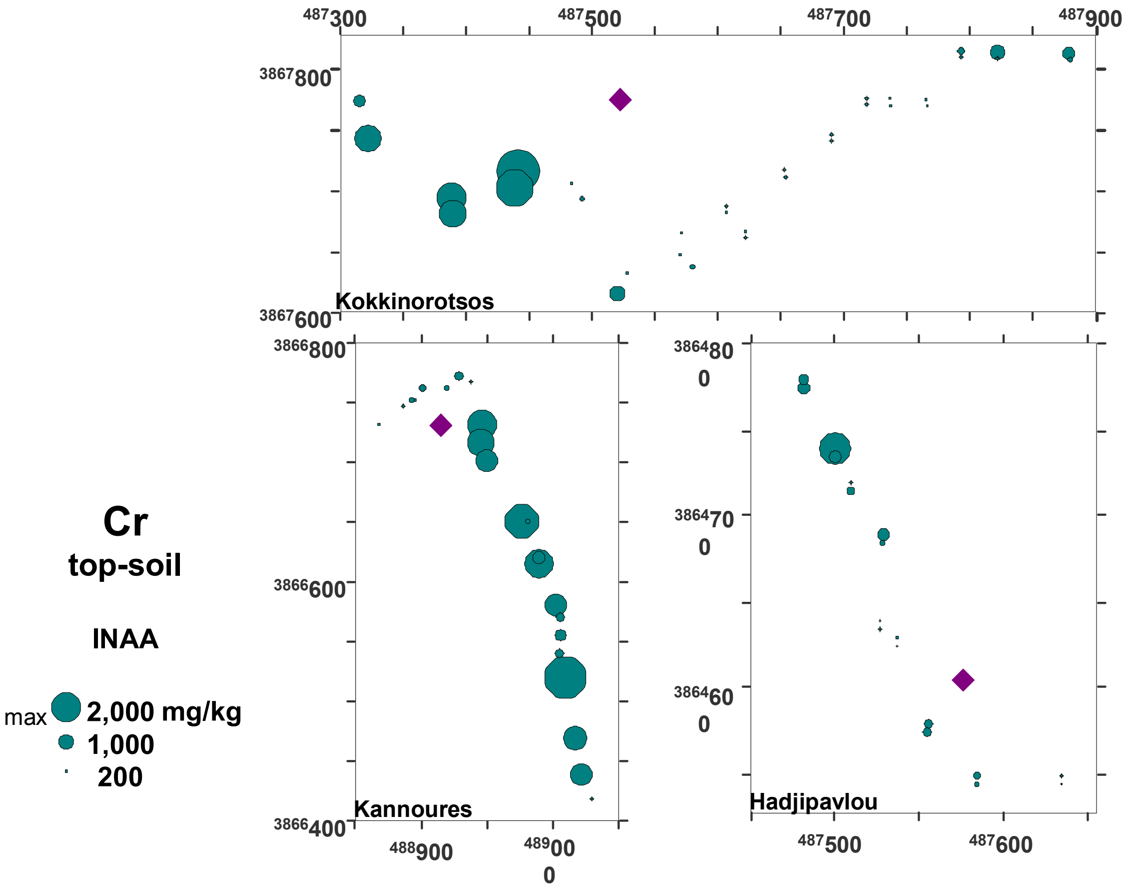

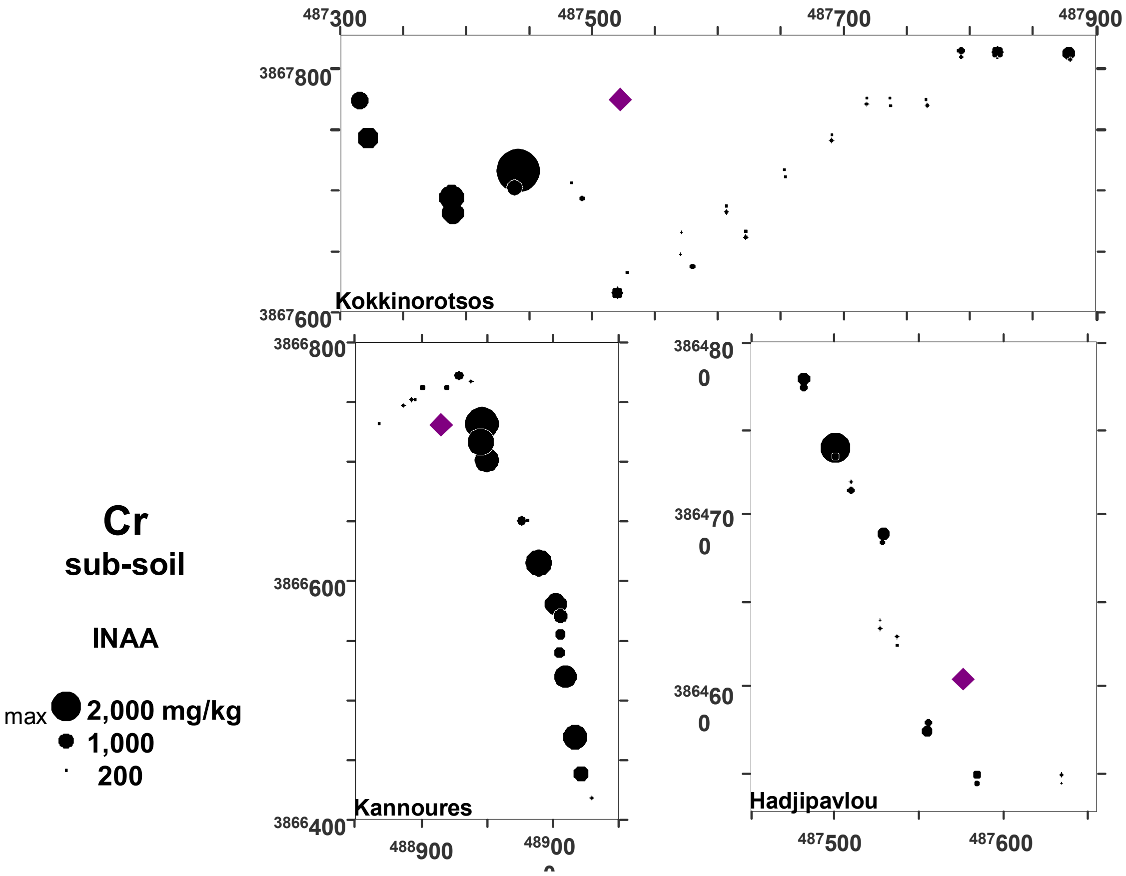

Figure 5.61 Dot-plots of *tot*-Cr in top soil and sub soil, Chromite mines area.

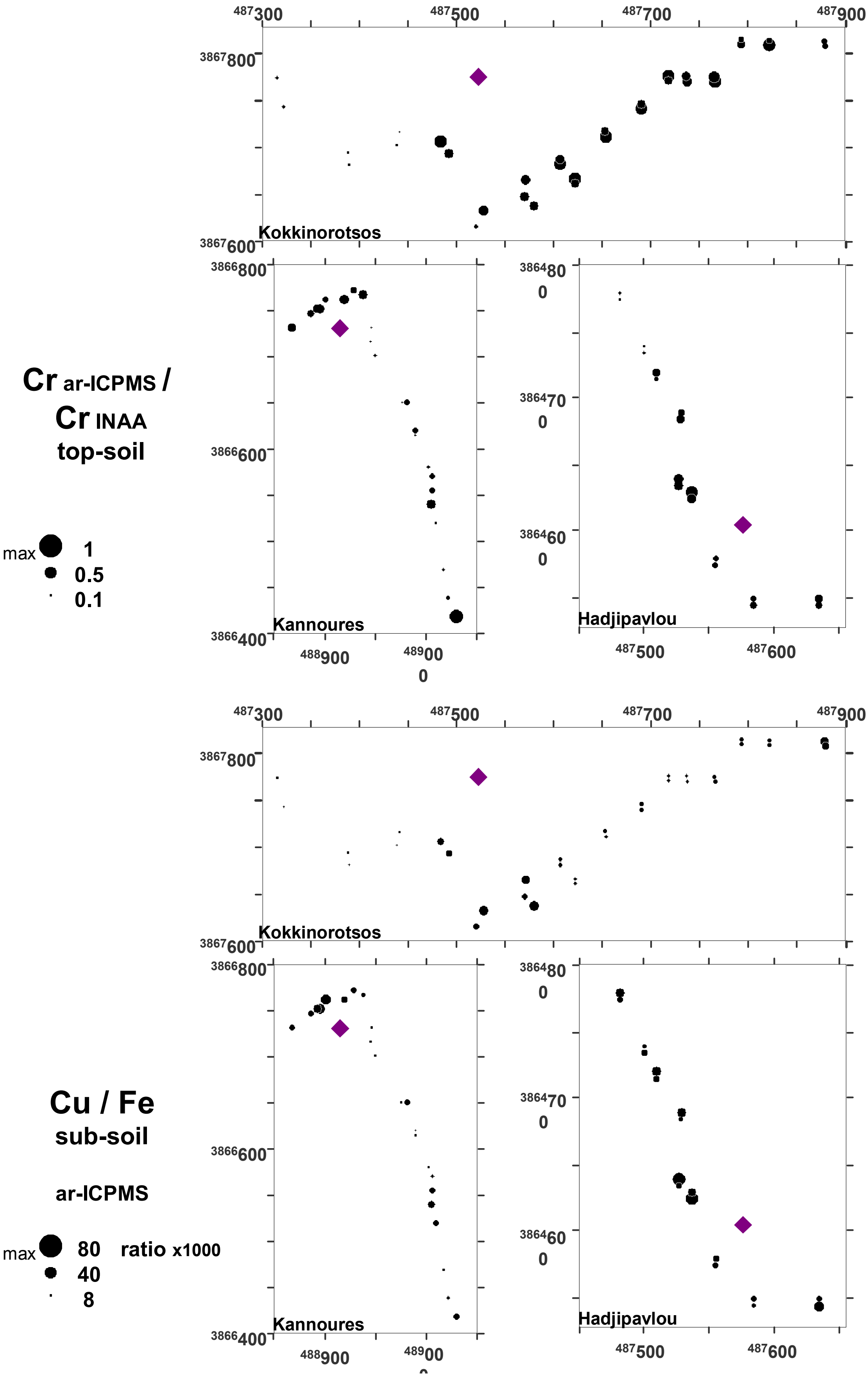

Figure 5.62 Dot-plots of *ar*-Cr/*tot*-Cr ratio in top soil, and *ar*-Cu/*ar*-Fe in sub soil, Chromite mines area.

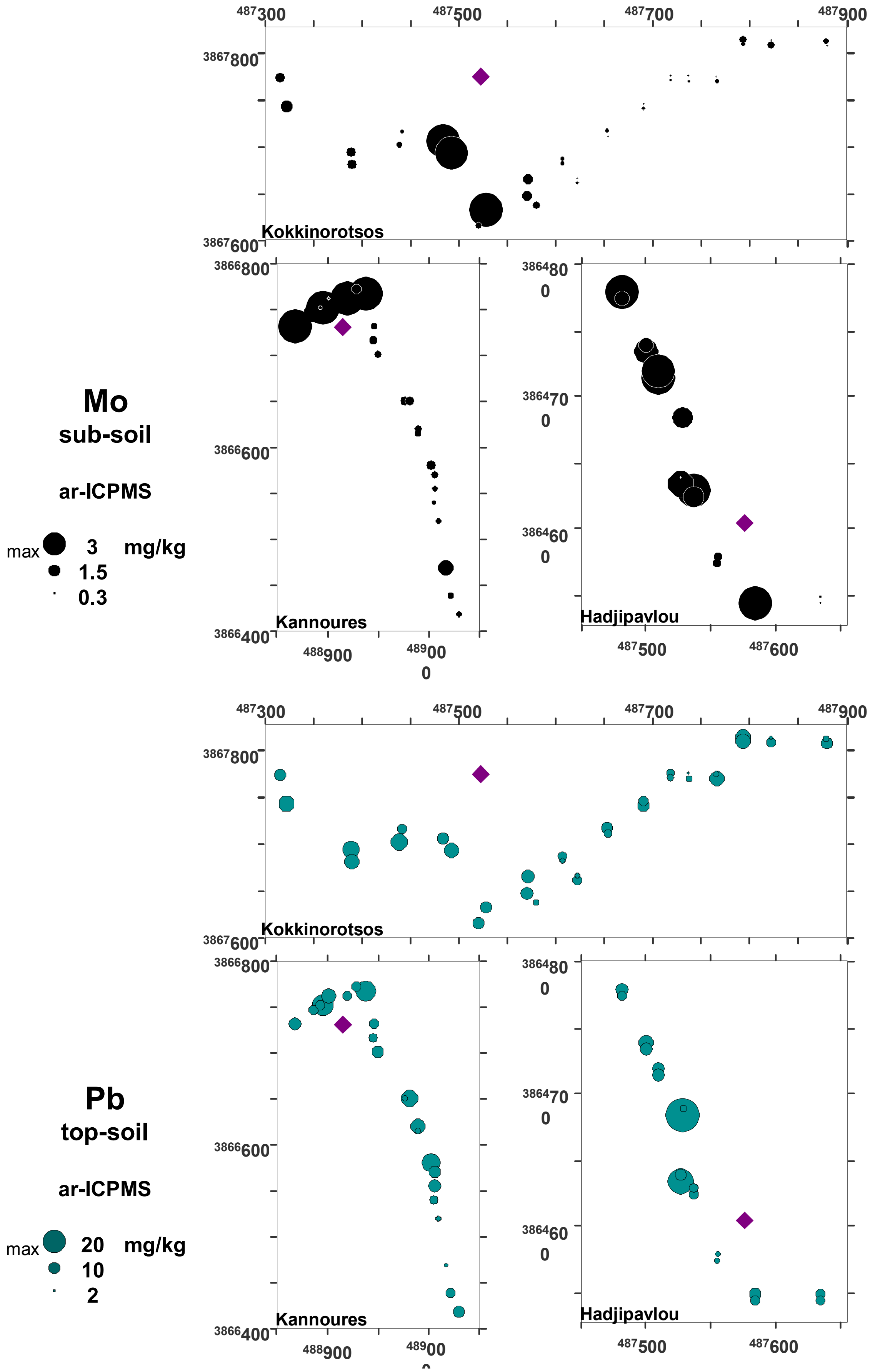

Figure 5.63 Dot-plots of *ar*-Mo in sub soil and *ar*-Pb in top soil, Chromite mines area.

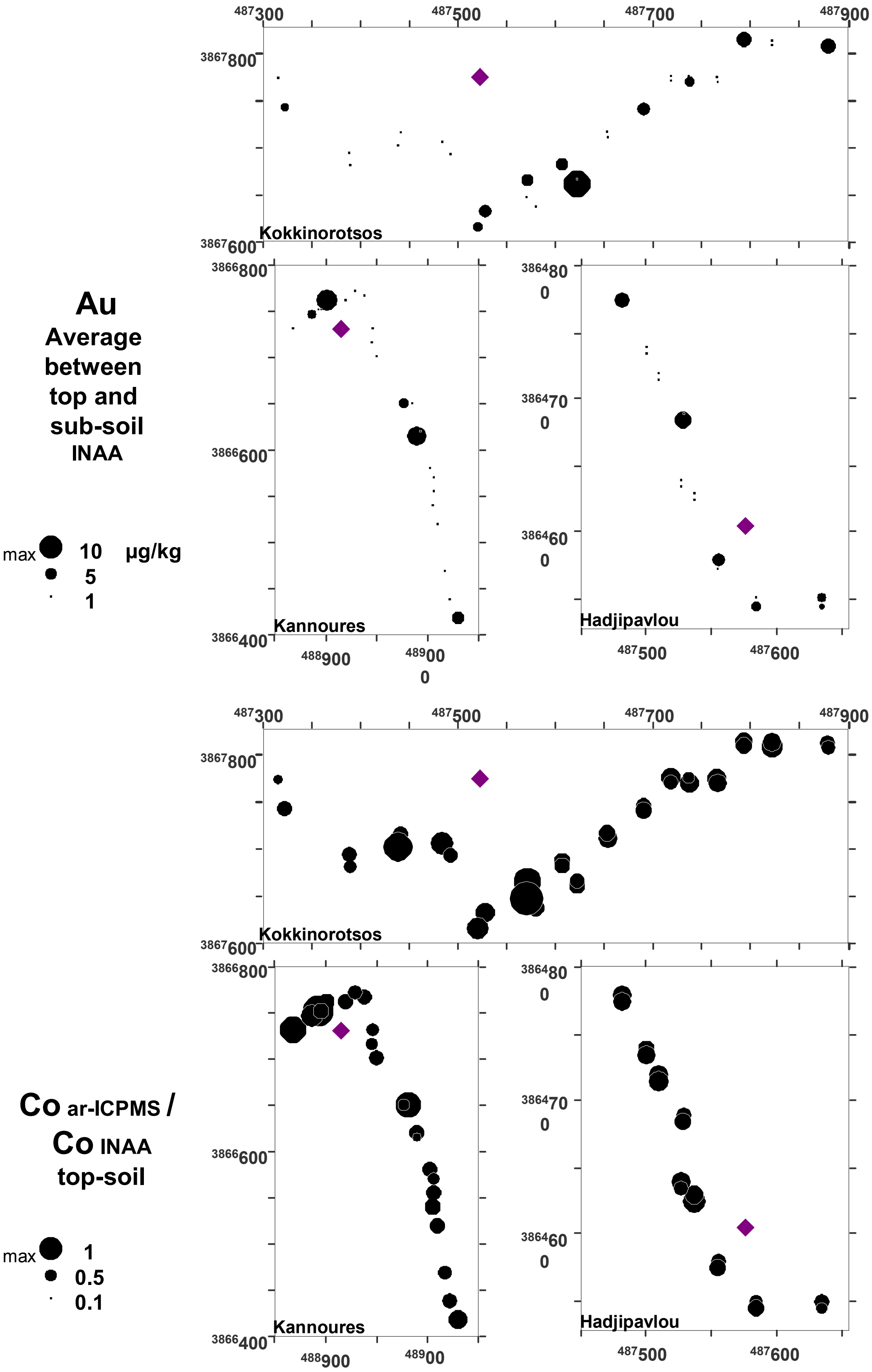

Figure 5.64 Dot-plots of average *tot*-Au in top and sub soil and *ar*-Co/*tot*-Co ratio in top soil, Chromite mines area.

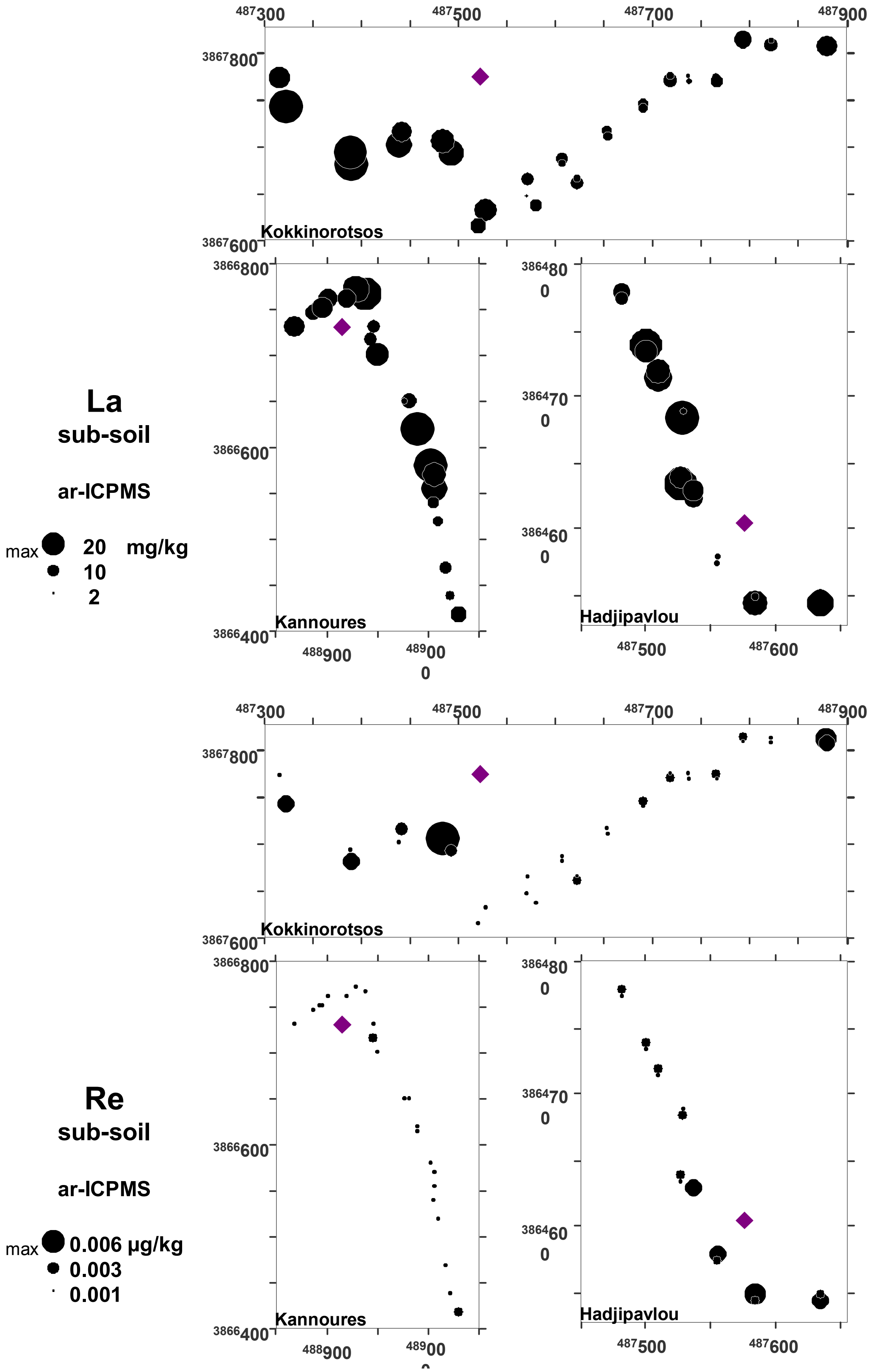

Figure 5.65 Dot-plots of *ar*-La and *ar*-Re in sub soil, Chromite mines area.

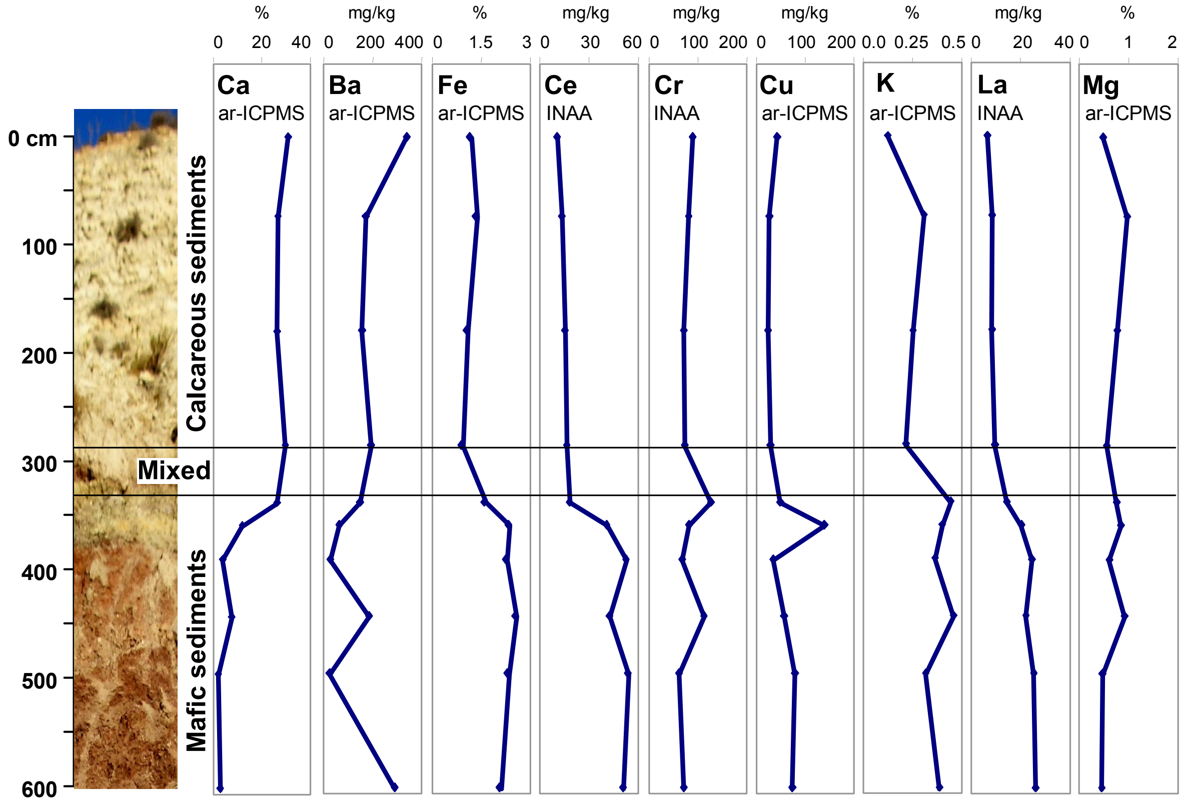

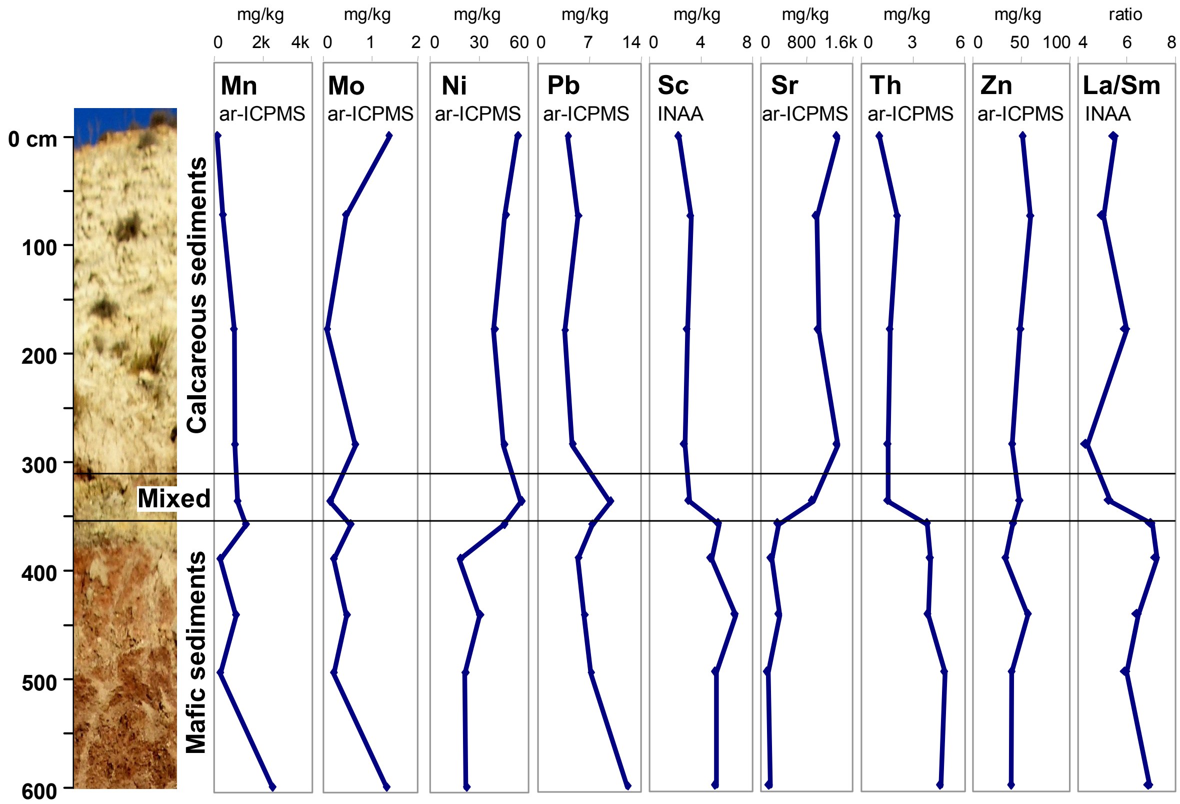

Figure 5.66 Vertical sampling profiles for selected elements across transition between the Dhiarizos Fmn ferruginous mudstones and calcareous colluvium derived from the Lefkara Fmn, near Mamonia (GR 463070, 3843600).

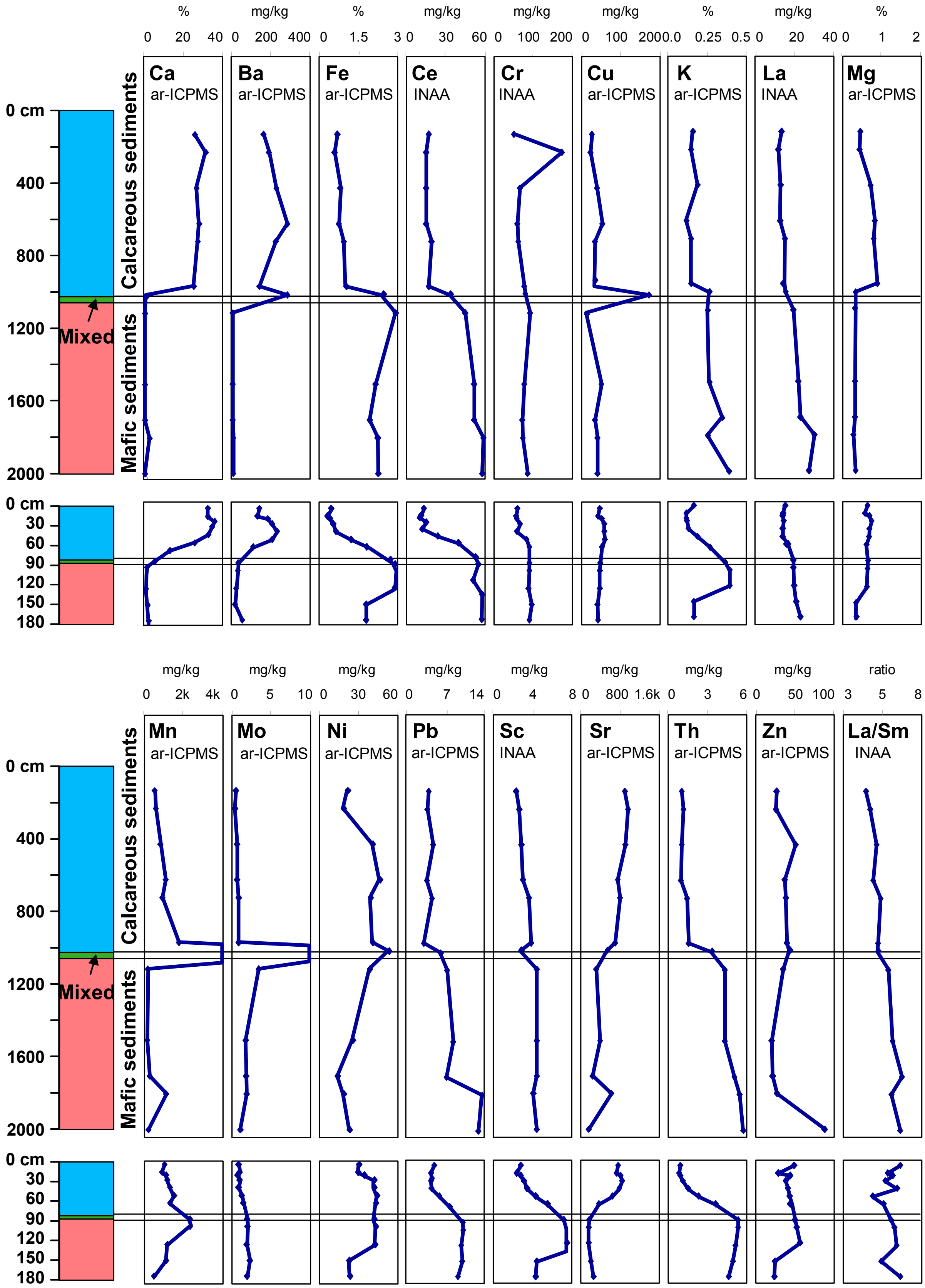

Figure 5.67 Vertical sampling profiles for selected elements across the transition between Dhiarizos Fmn ferruginous mudstones and the Lefkara Fmn-derived calcareous sediment, Secret Valley (GR 465691, 3840260).

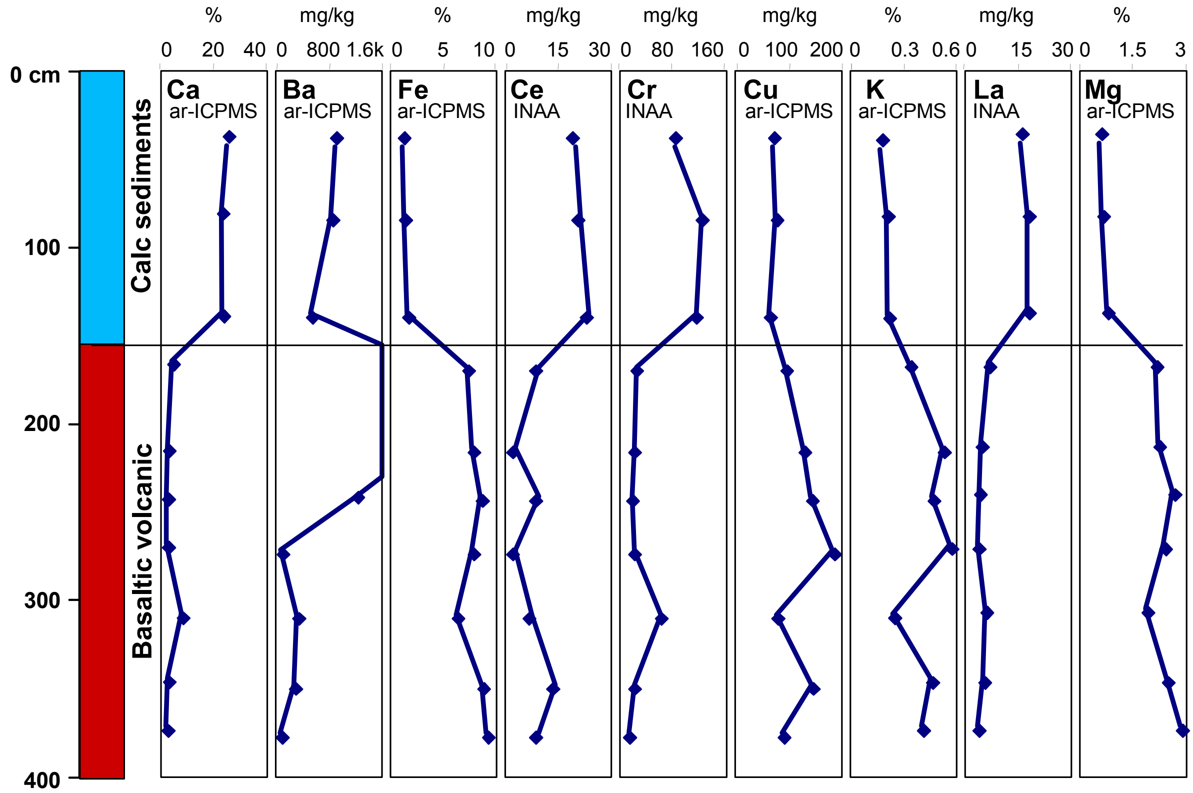

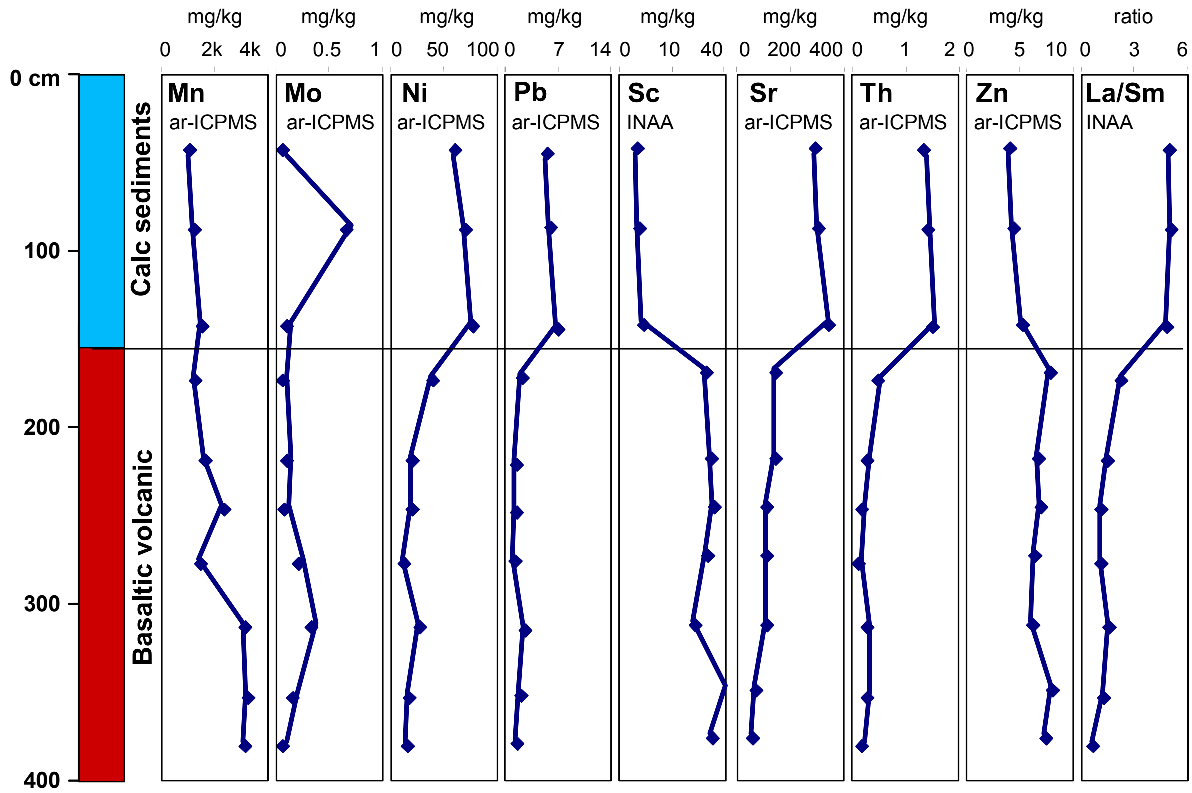

Figure 5.68 Vertical sampling profiles for selected elements across the transition between the Upper Pillow Lava basalts and overlying Pakhna Fmn calcareous siltstone, near Prodromos (GR 482350, 3858850).

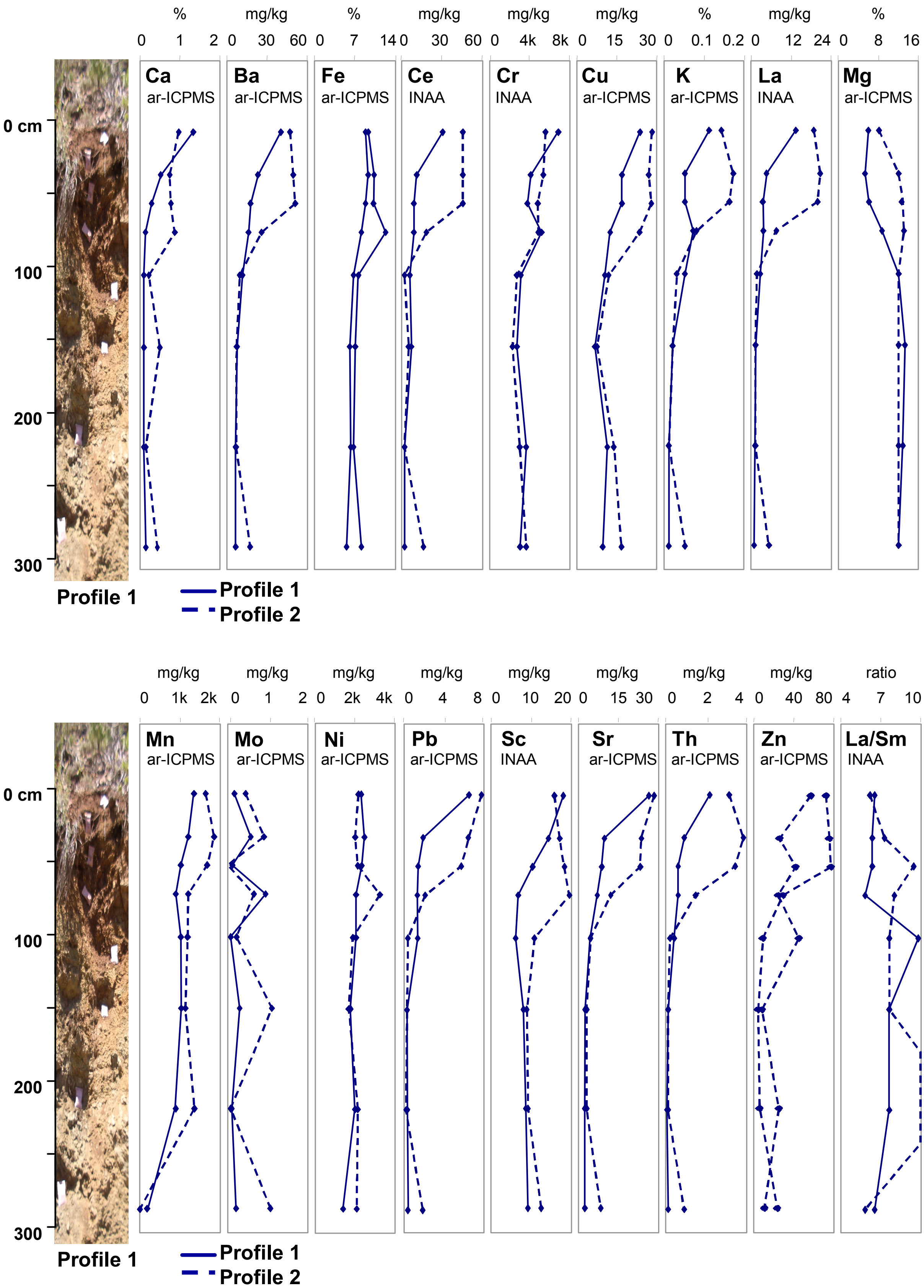

Figure 5.69 Duplicate vertical sampling profiles from C to B(r) horizons, near Kannoures Cr mine (GR 489570, 3865670).

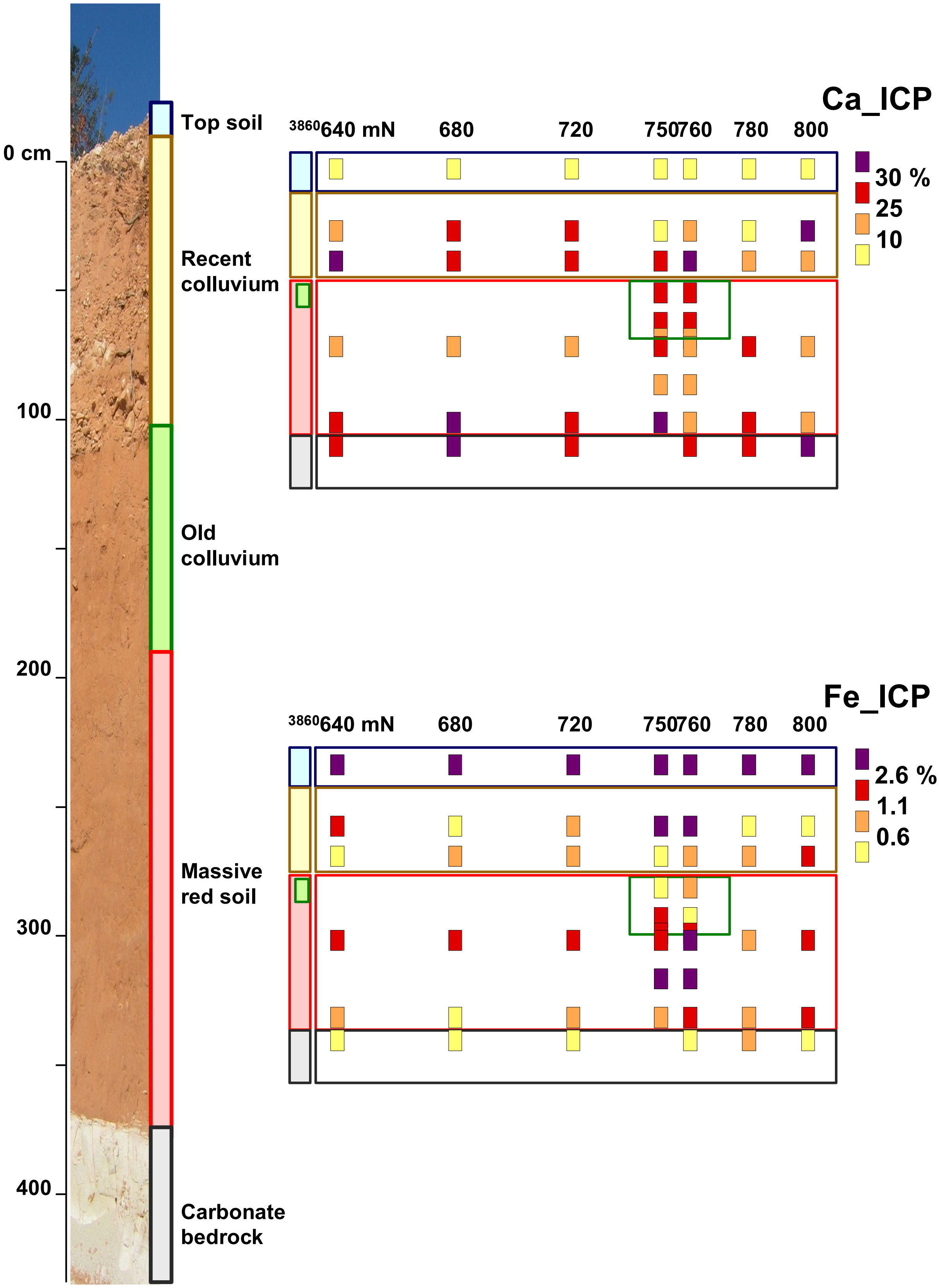

Figure 5.70 Geochemical profiles for Fe and Ca in multi-layer transported regolith, Coral Bay.

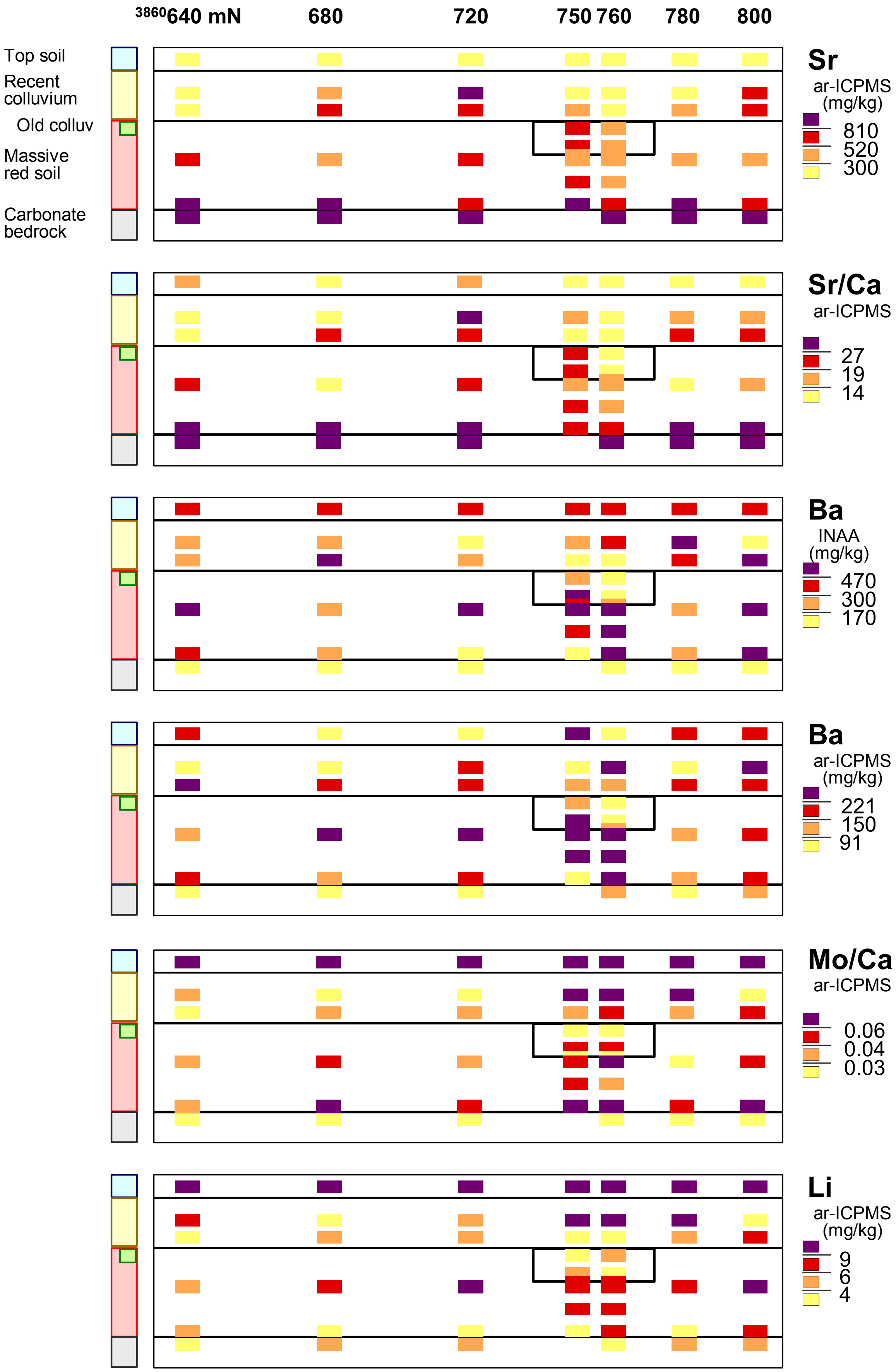

Figure 5.71 Geochemical profiles in multi-layer transported regolith, Coral Bay.

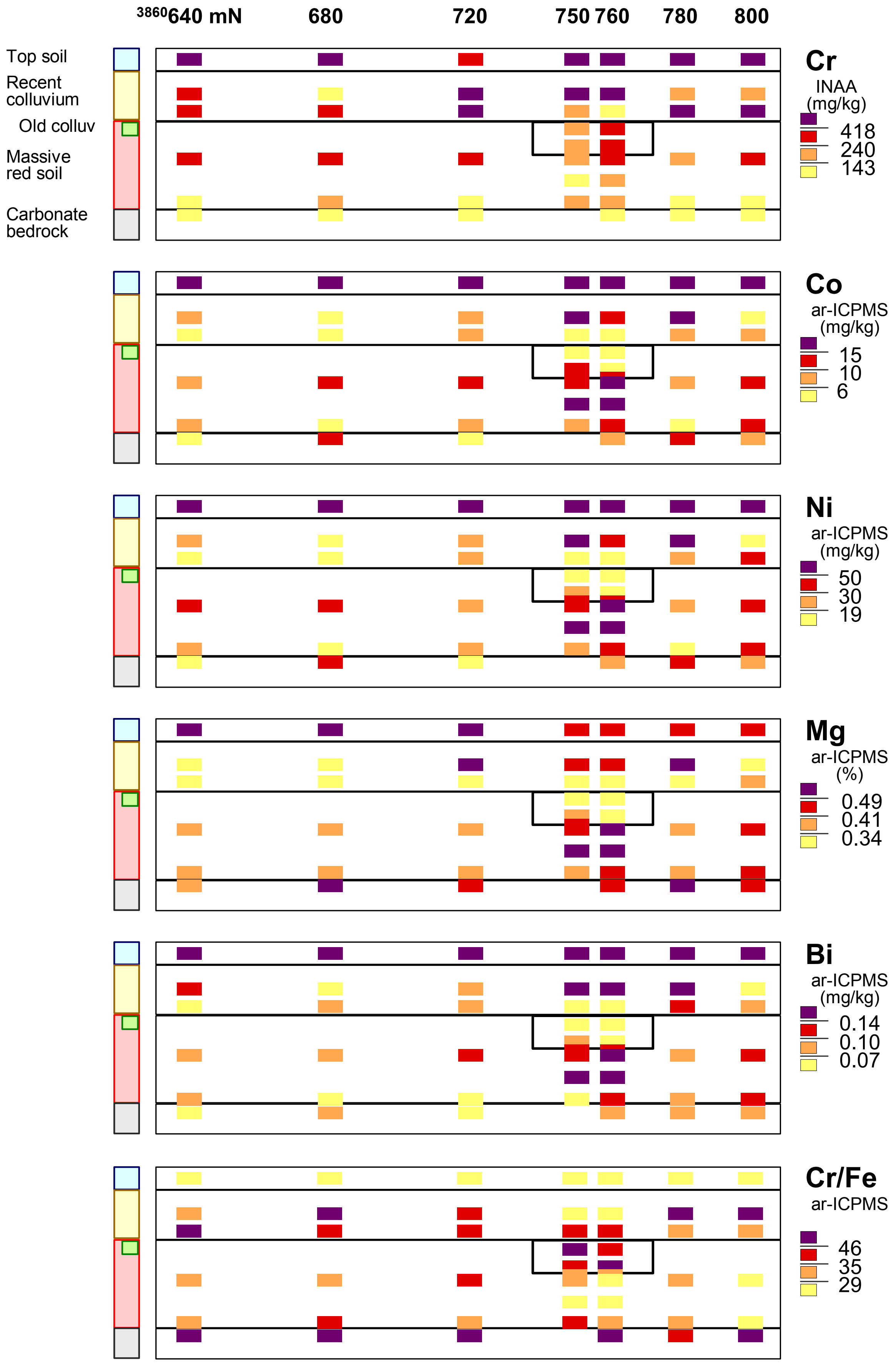

Figure 5.72 Geochemical profiles in multi-layer transported regolith, Coral Bay.

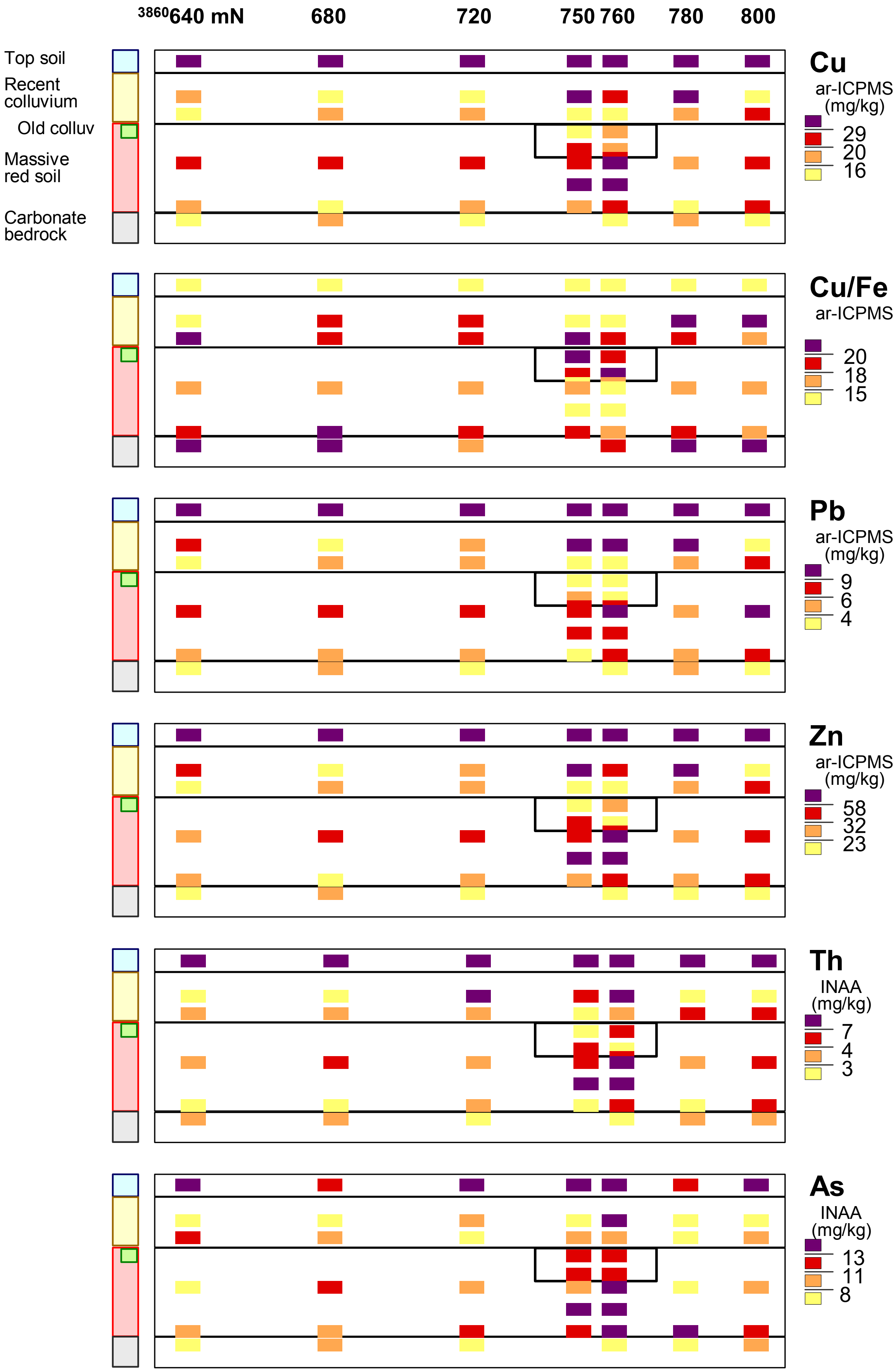

Figure 5.73 Geochemical profiles in multi-layer transported regolith, Coral Bay.

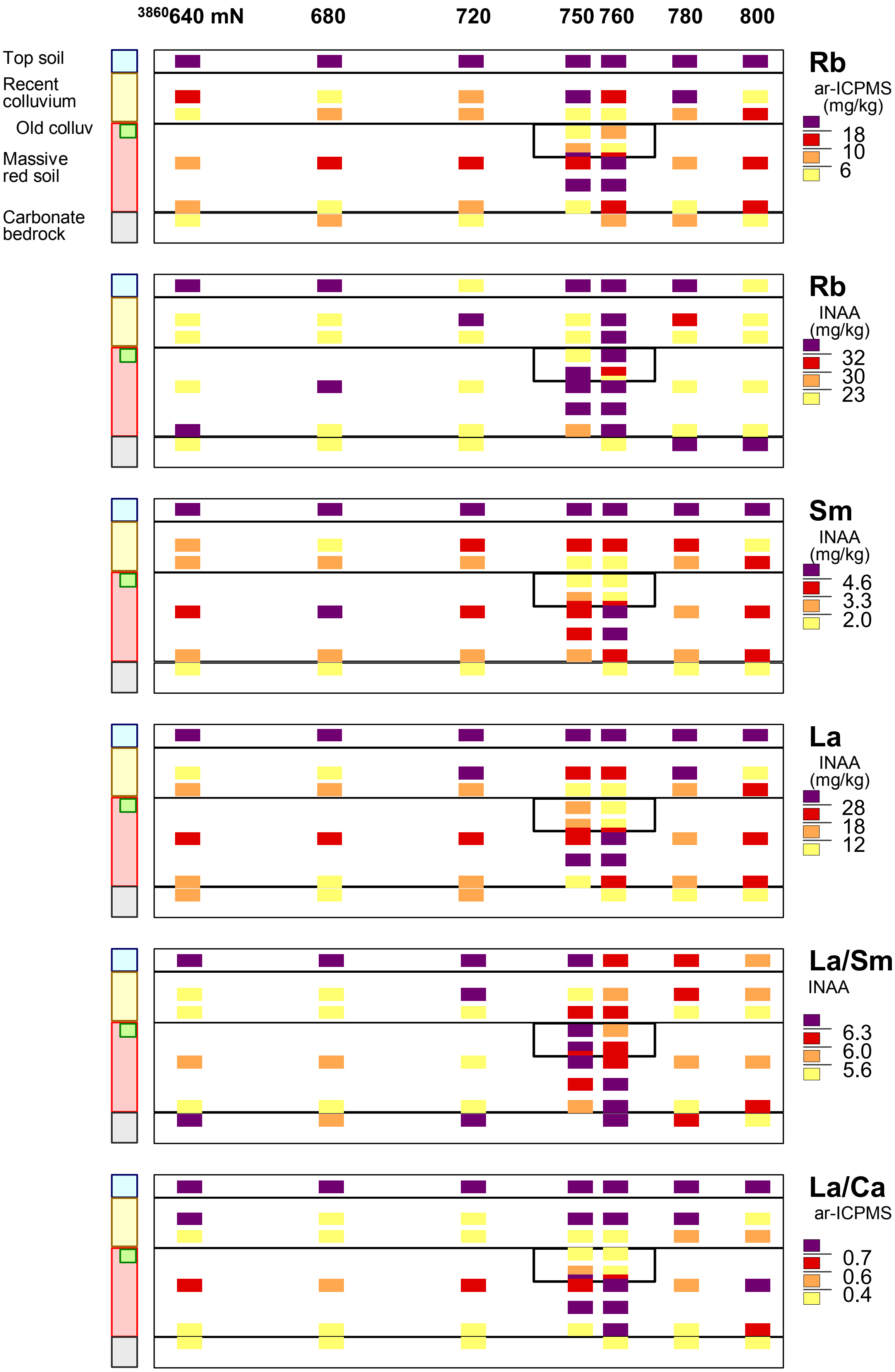

Figure 5.74 Geochemical profiles in multi-layer transported regolith, Coral Bay.

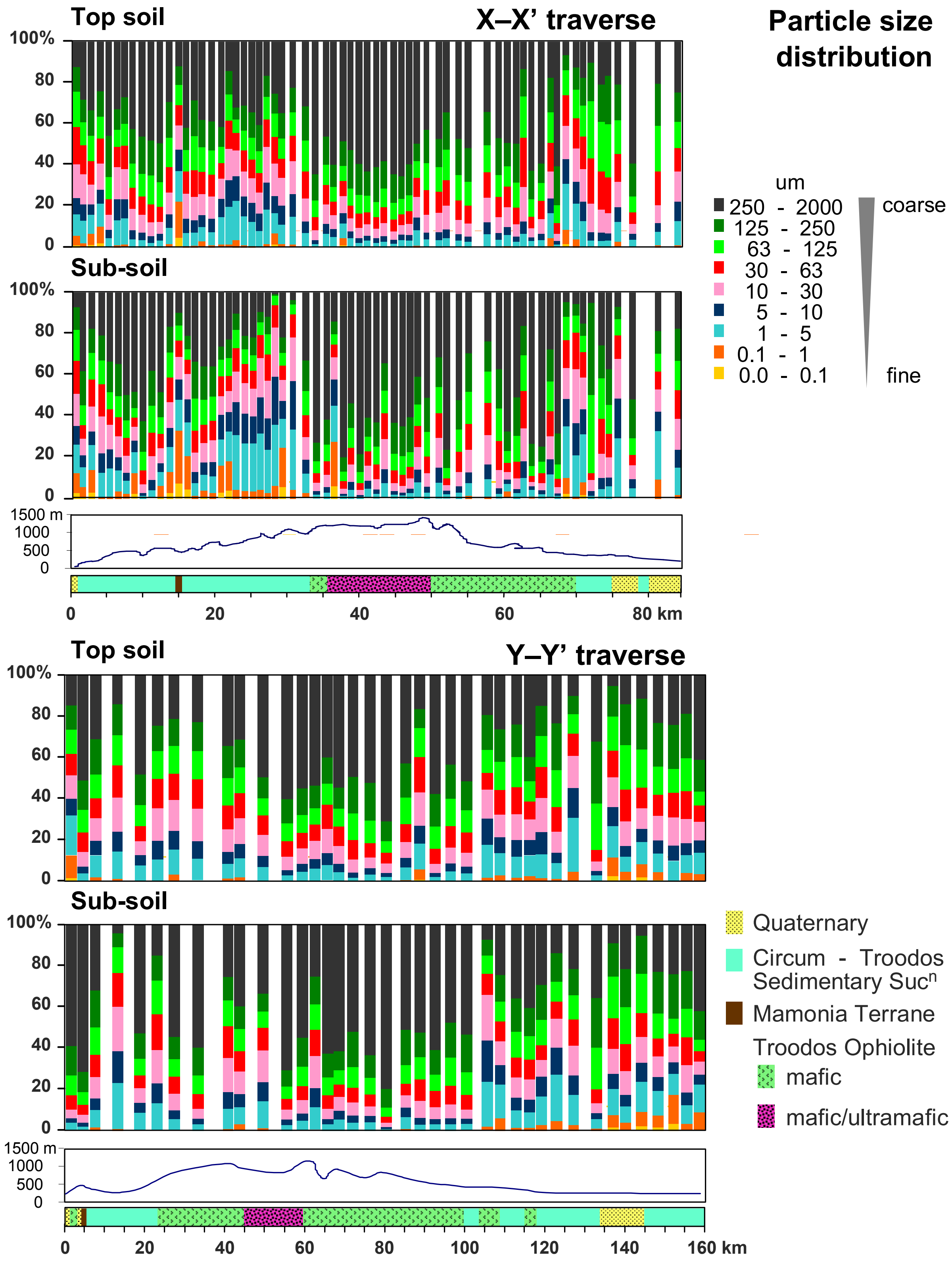

Figure 5.75 Particle size distribution in top soil and sub soil samples from the two orientation traverses.

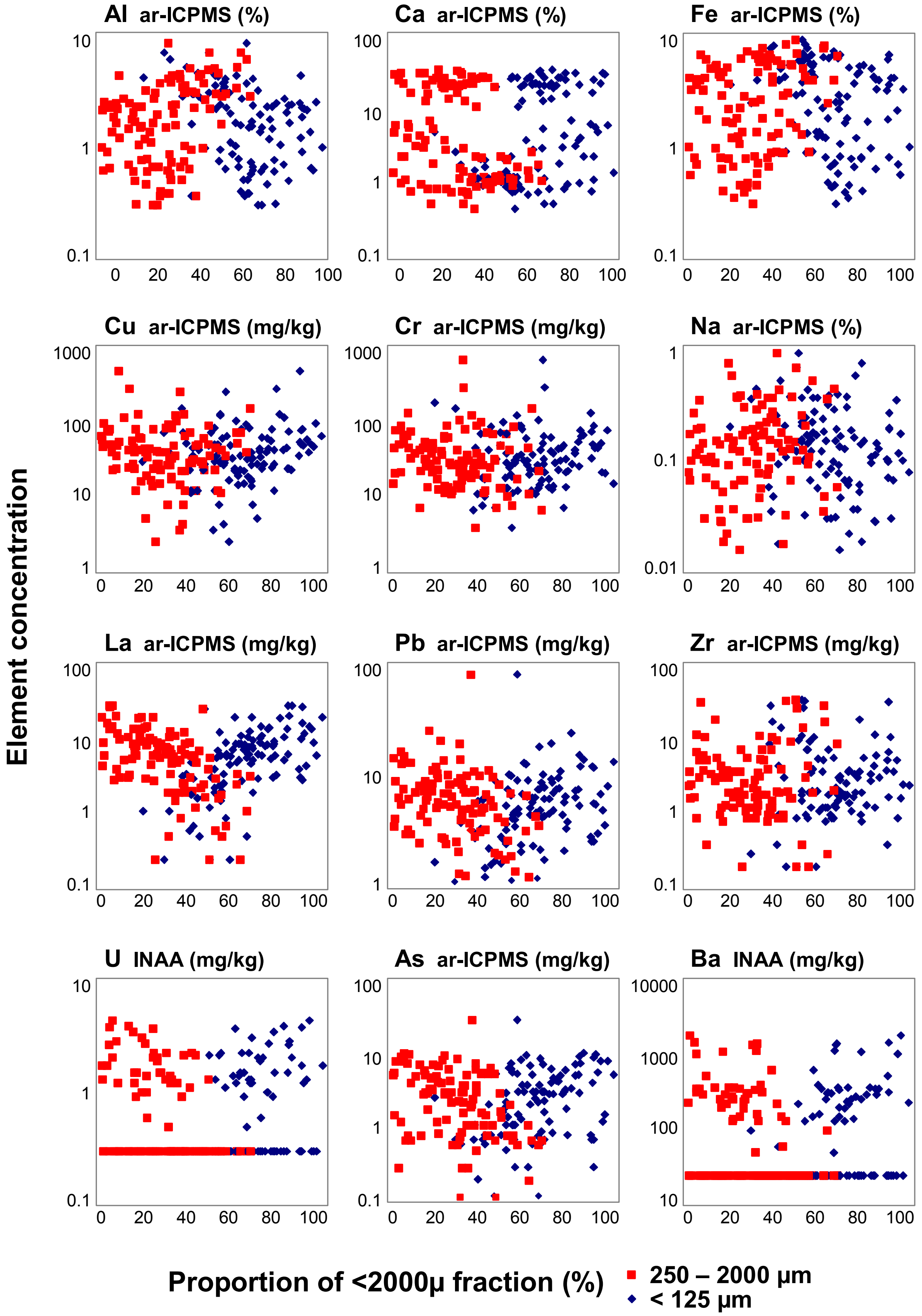

Figure 5.76 Plot of selected elements values against the proportion of coarse and fine fraction in orientation suite samples.

Loss-on-ignition (%)

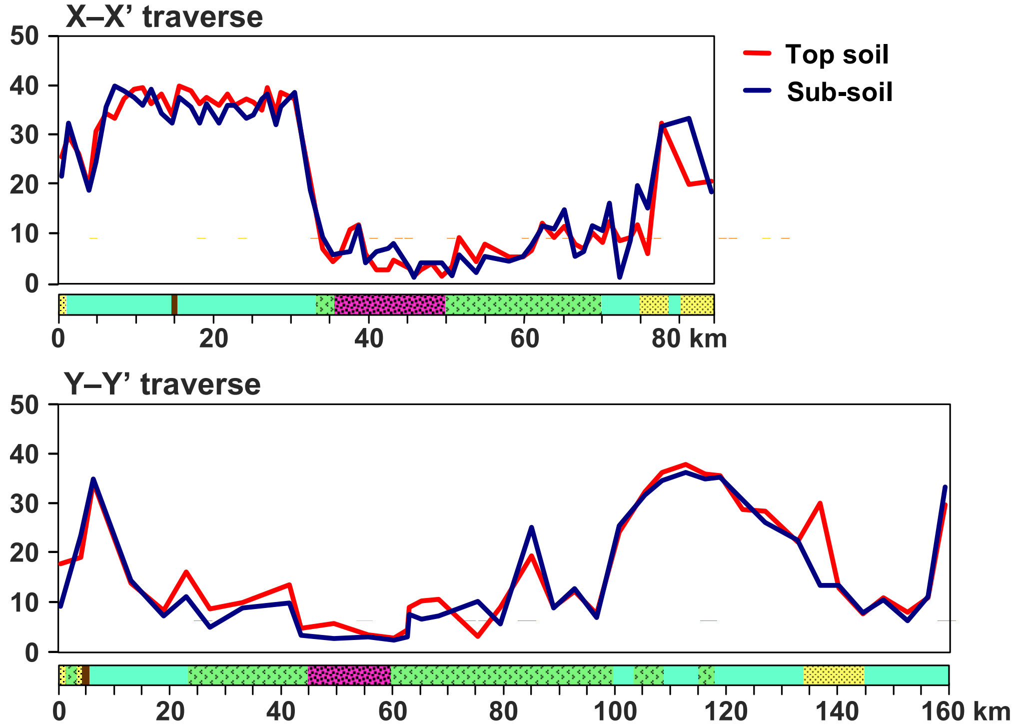

pH

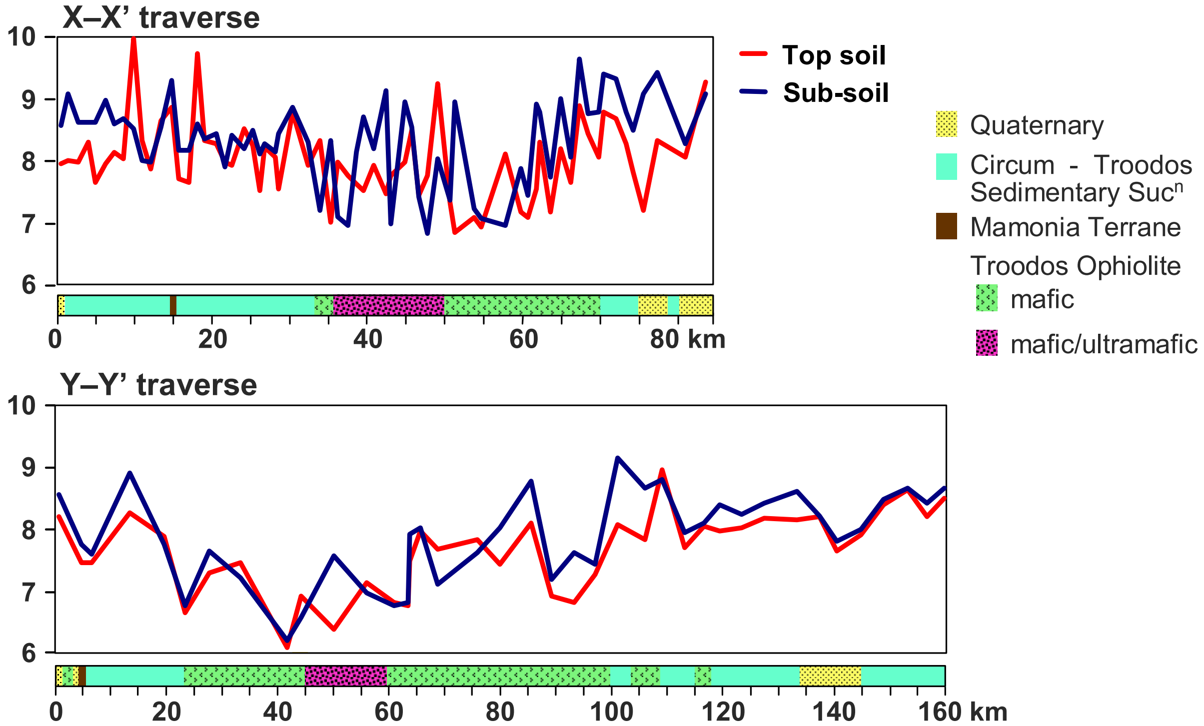

Figure 5.77 Loss-on-ignition and pH in top soil samples from the X-X′ and Y-Y′ orientation traverses.

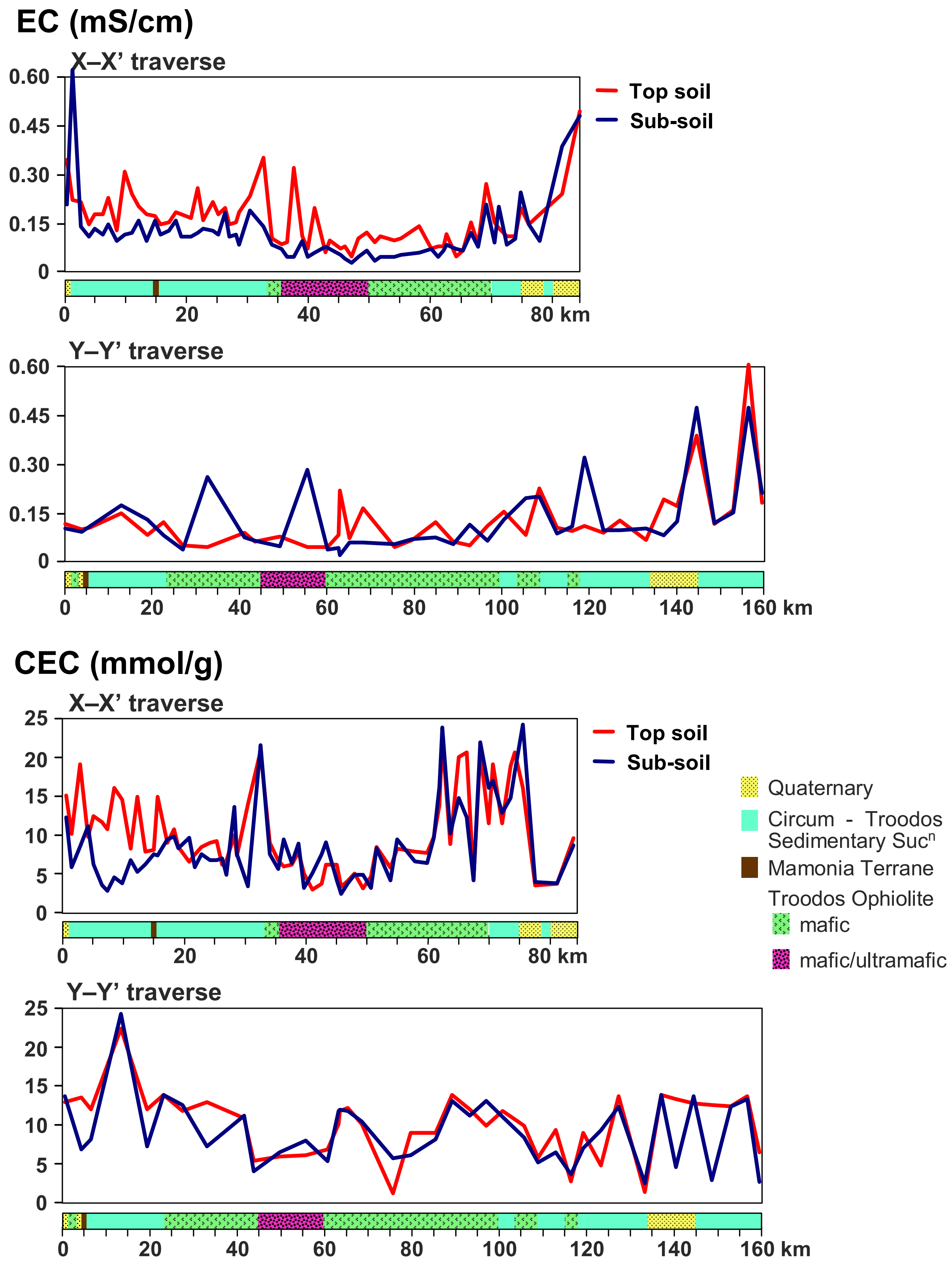

Figure 5.78 Electrical conductivity and cation exchange capacity in top soil samples from the X-X′ and Y-Y′ orientation traverses.

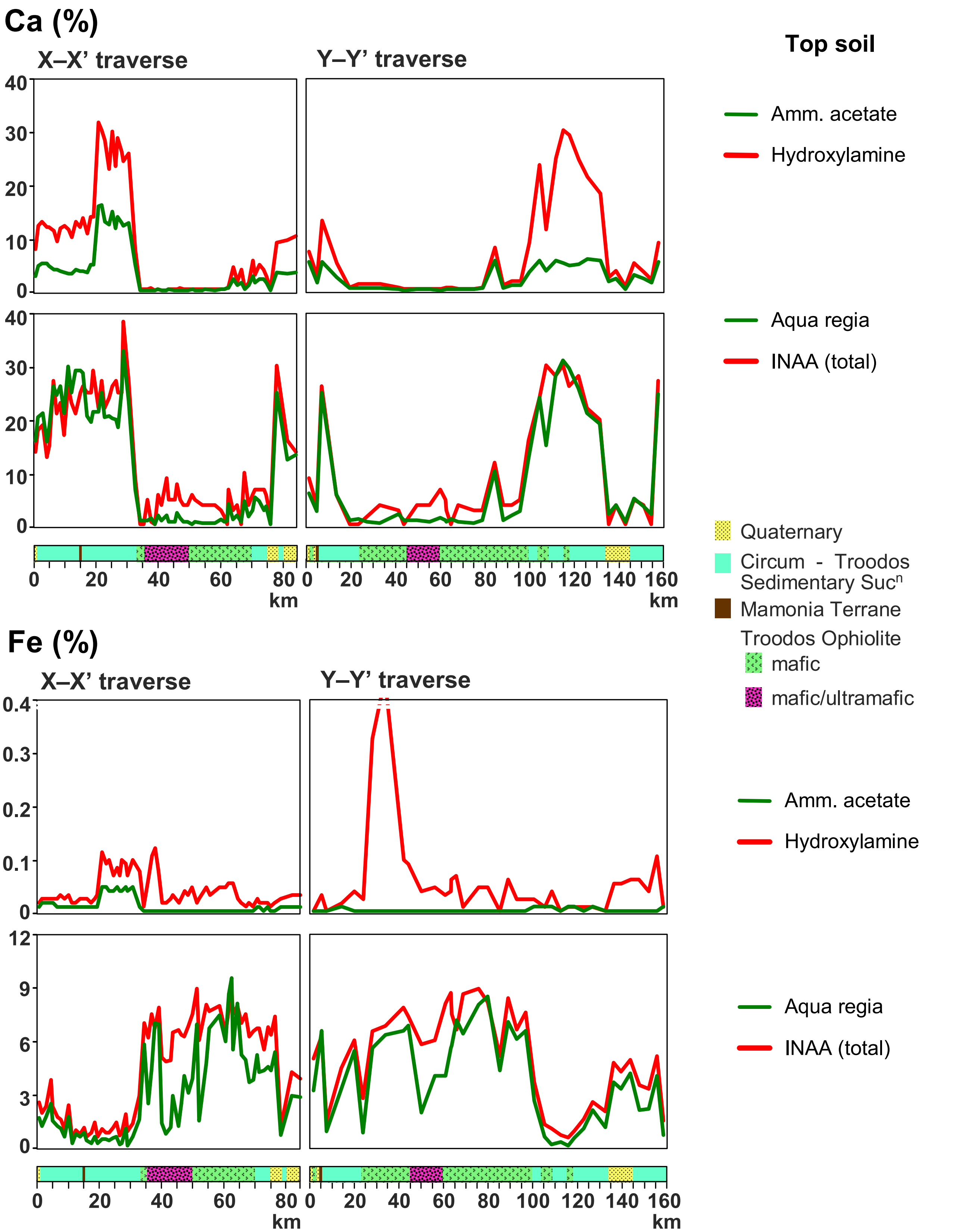

Figure 5.79 Comparison of aqua regia, ammonium acetate and hydroxylamine extractable Ca and Fe versus total contents (INAA) in top soil samples from the X-X′ and Y-Y′ orientation traverses.

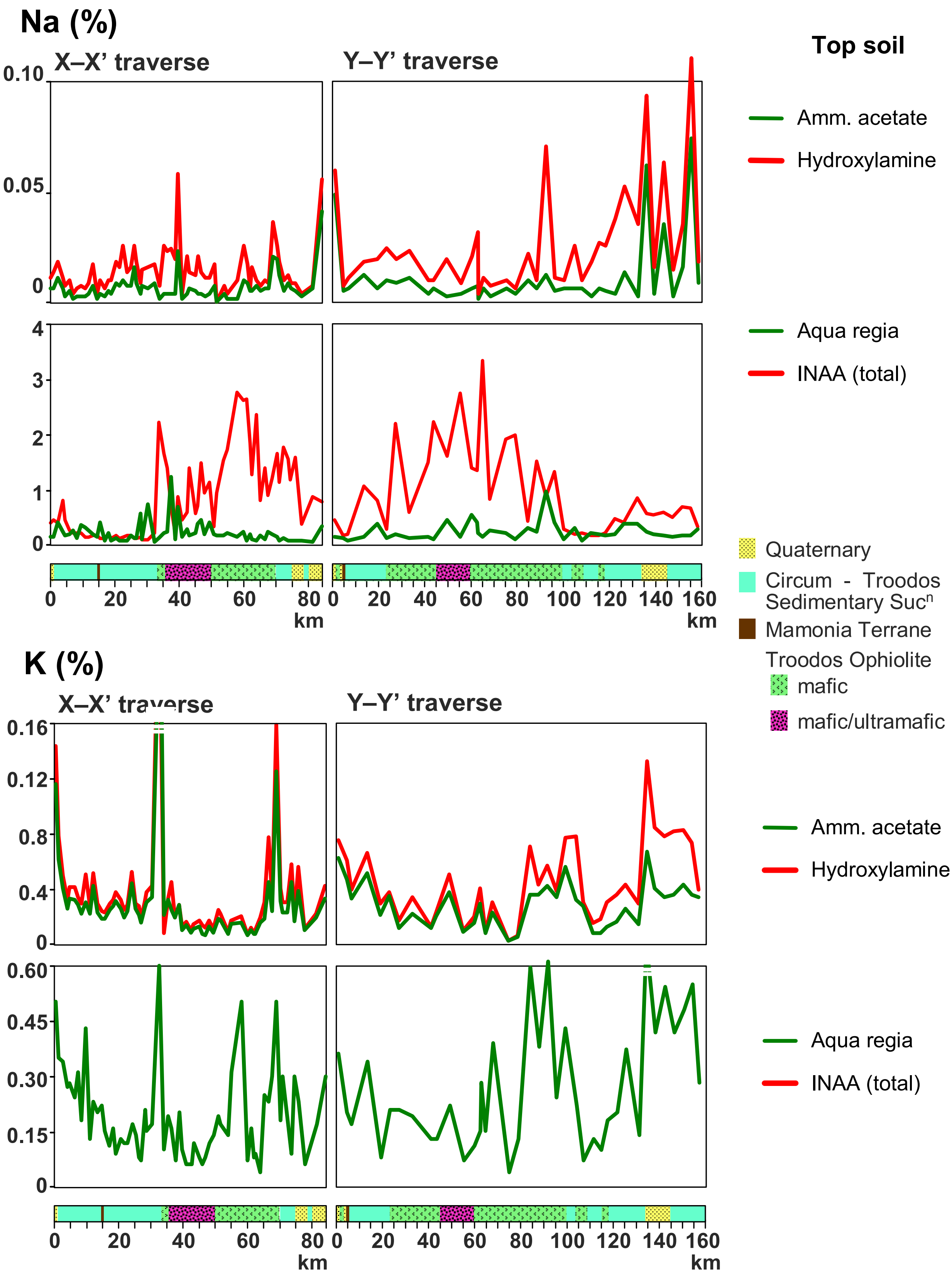

Figure 5.80 Comparison of aqua regia, ammonium acetate and hydroxylamine extractable Na and K versus total contents (INAA) in top soil samples from the X-X′ and Y-Y′ orientation traverses.

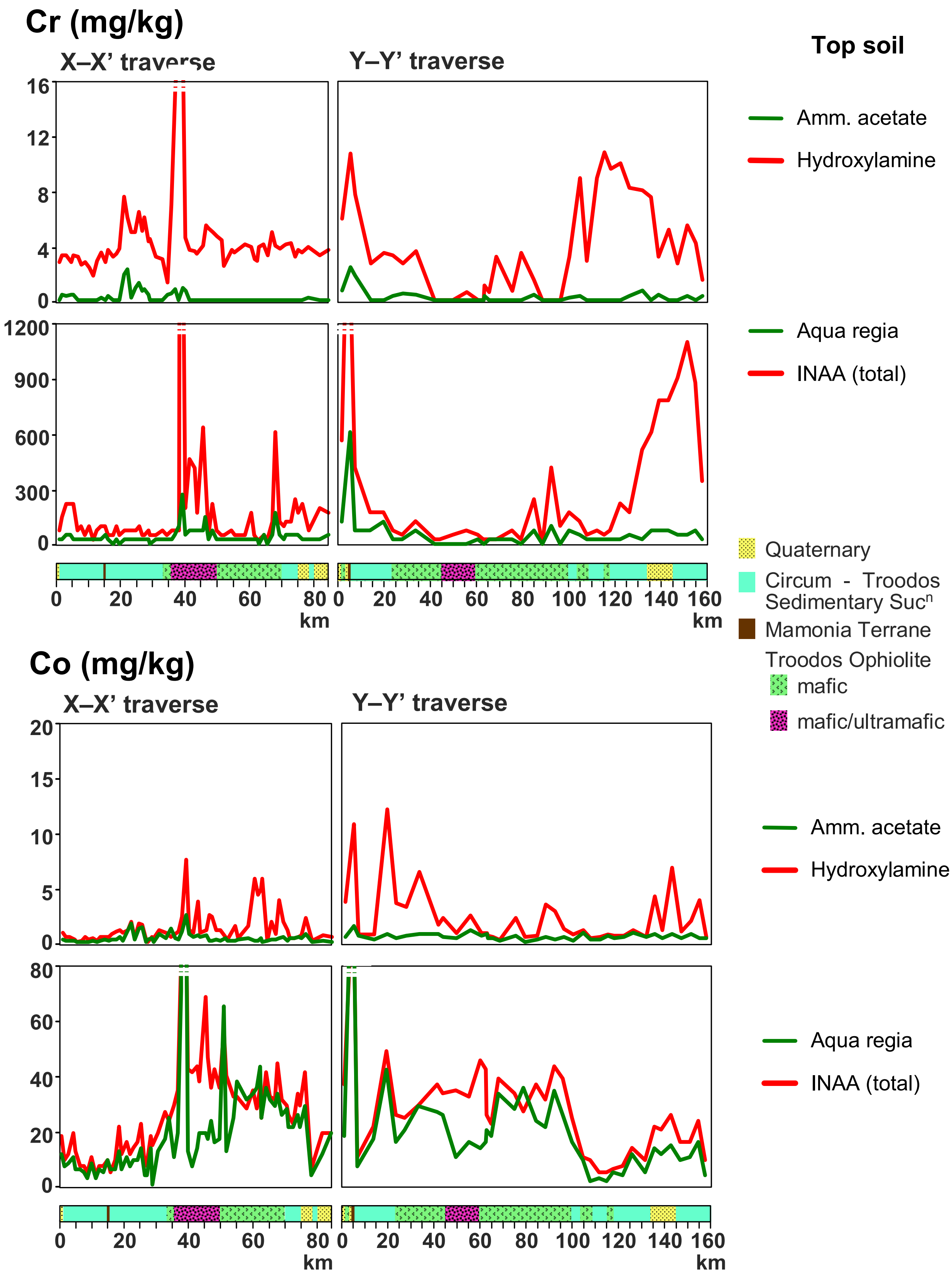

Figure 5.81 Comparison of aqua regia, ammonium acetate and hydroxylamine extractable Cr and Co versus total contents (INAA) in top soil samples from the X-X′ and Y-Y′ orientation traverses.

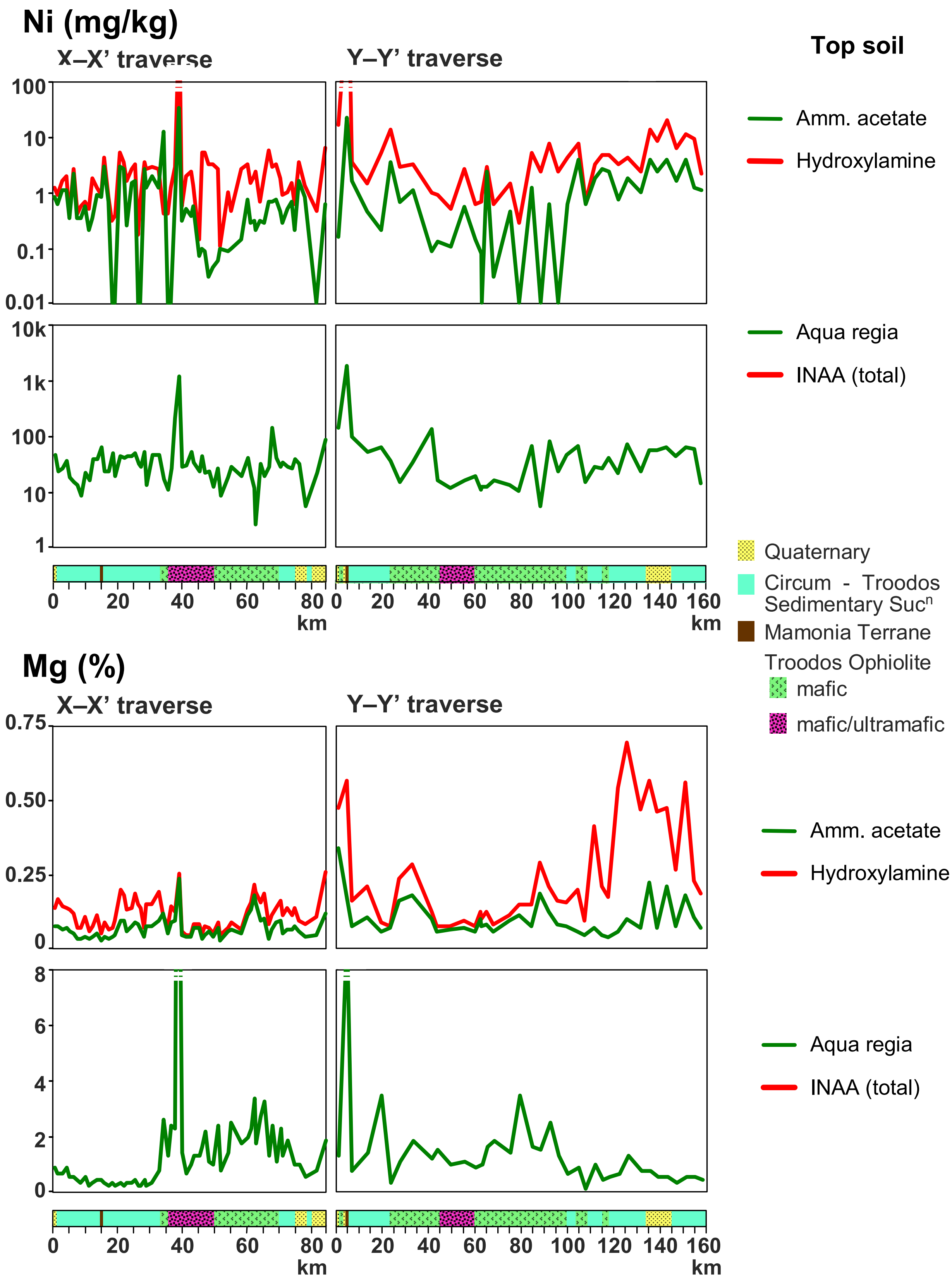

Figure 5.82 Comparison of aqua regia, ammonium acetate and hydroxylamine extractable Ni and Mg versus total contents (INAA) in top soil samples from the X-X′ and Y-Y′ orientation traverses.

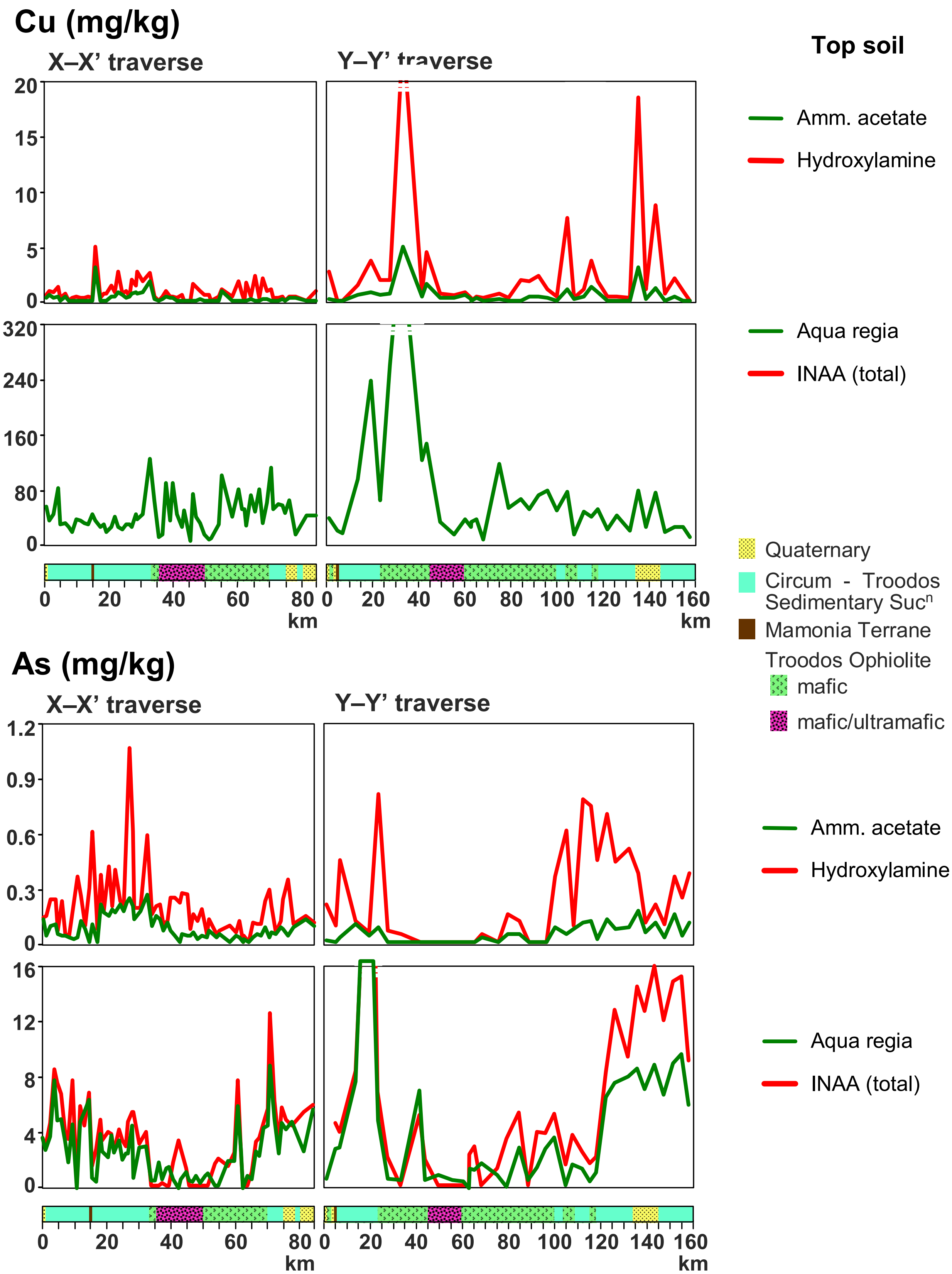

Figure 5.83 Comparison of aqua regia, ammonium acetate and hydroxylamine extractable Cu and As versus total contents (INAA) in top soil samples from the X-X′ and Y-Y′ orientation traverses.

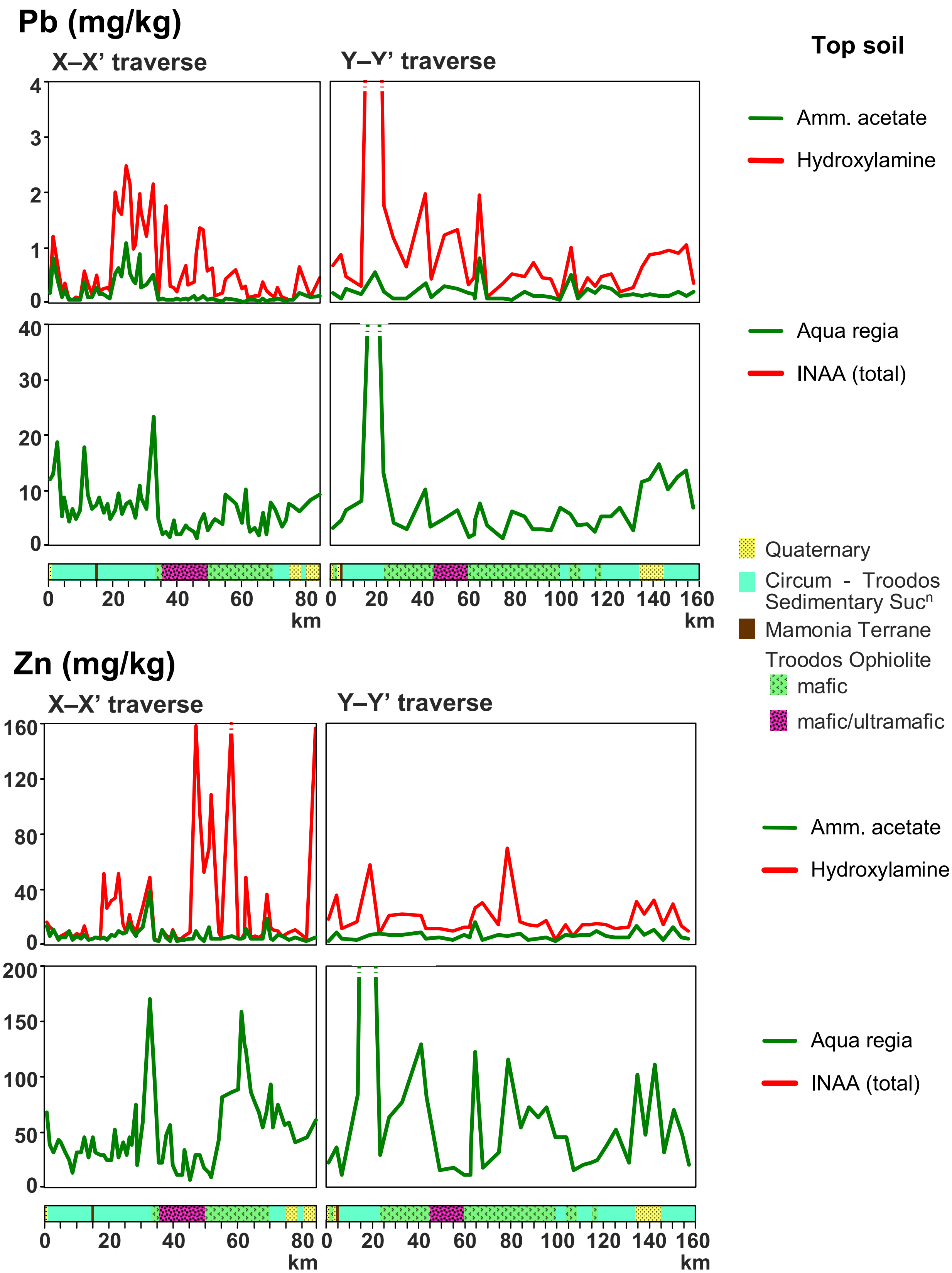

Figure 5.84 Comparison of aqua regia, ammonium acetate and hydroxylamine extractable Pb and Zn versus total contents (INAA) in top soil samples from the X-X′ and Y-Y′ orientation traverses.

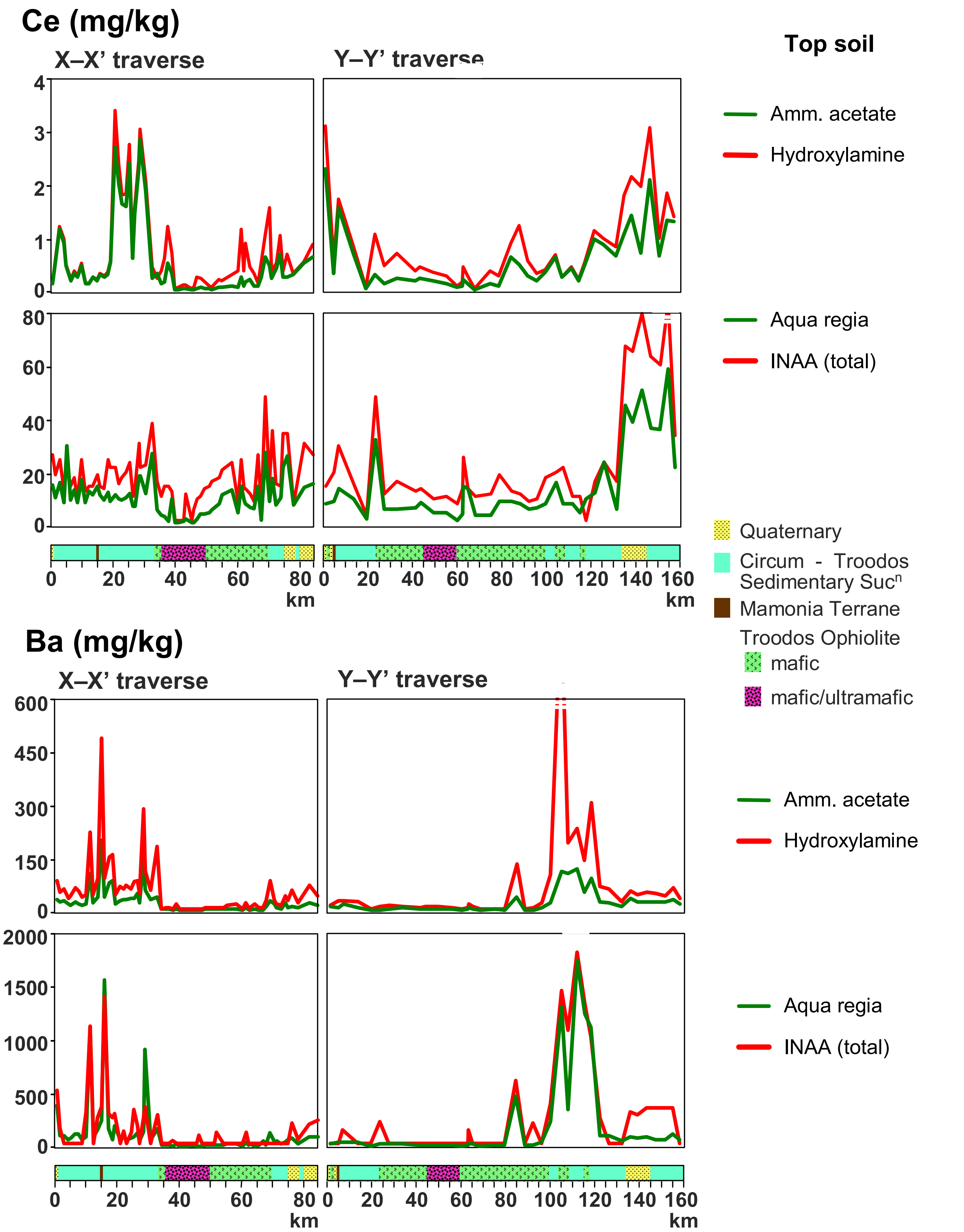

Figure 5.85 Comparison of aqua regia, ammonium acetate and hydroxylamine extractable Ce and Ba versus total contents (INAA) in top soil samples from the X-X′ and Y-Y′ orientation traverses.

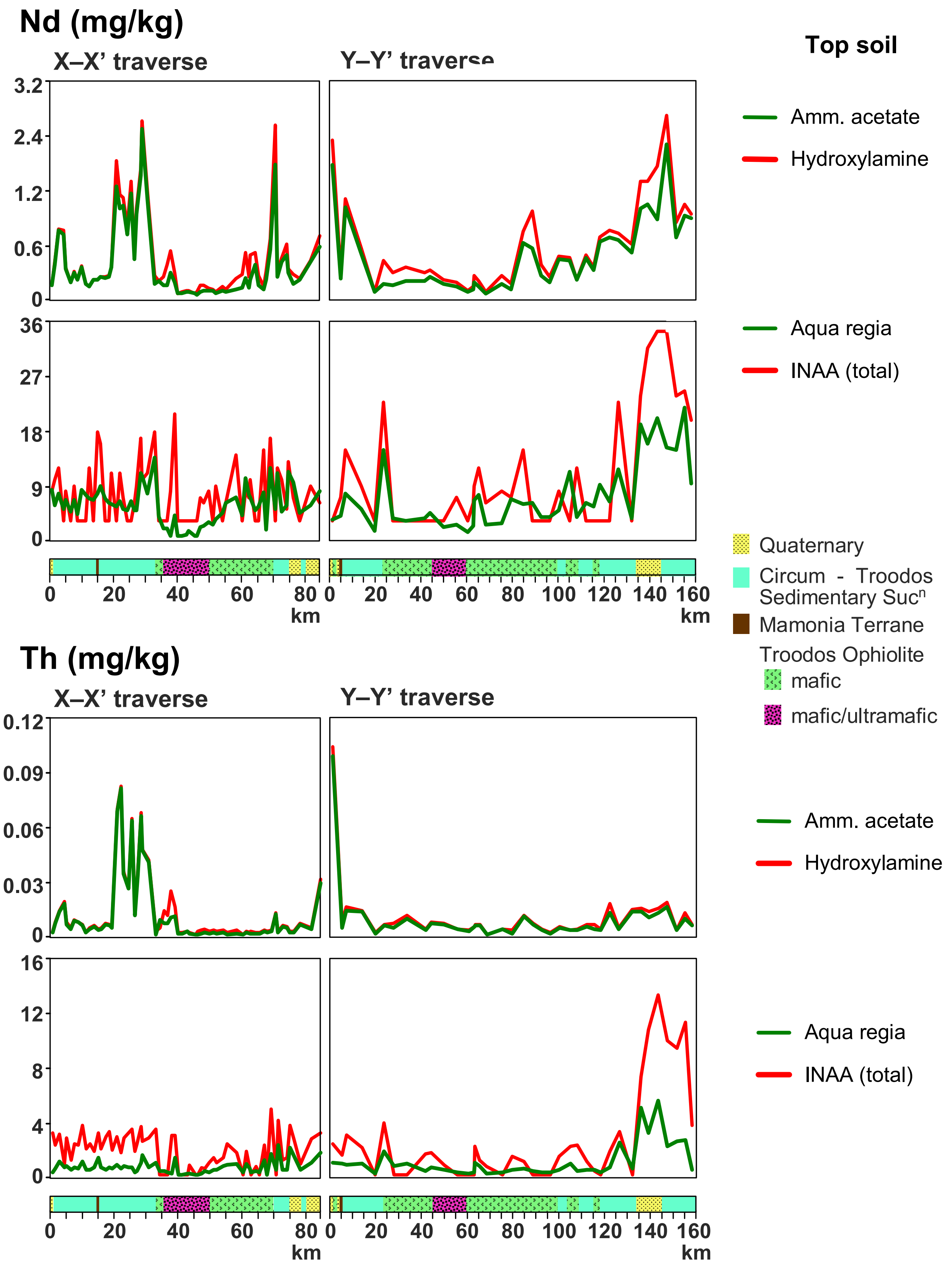

Figure 5.86 Comparison of aqua regia, ammonium acetate and hydroxylamine extractable Nd and Th versus total contents (INAA) in top soil samples from the X-X′ and Y-Y′ orientation traverses.

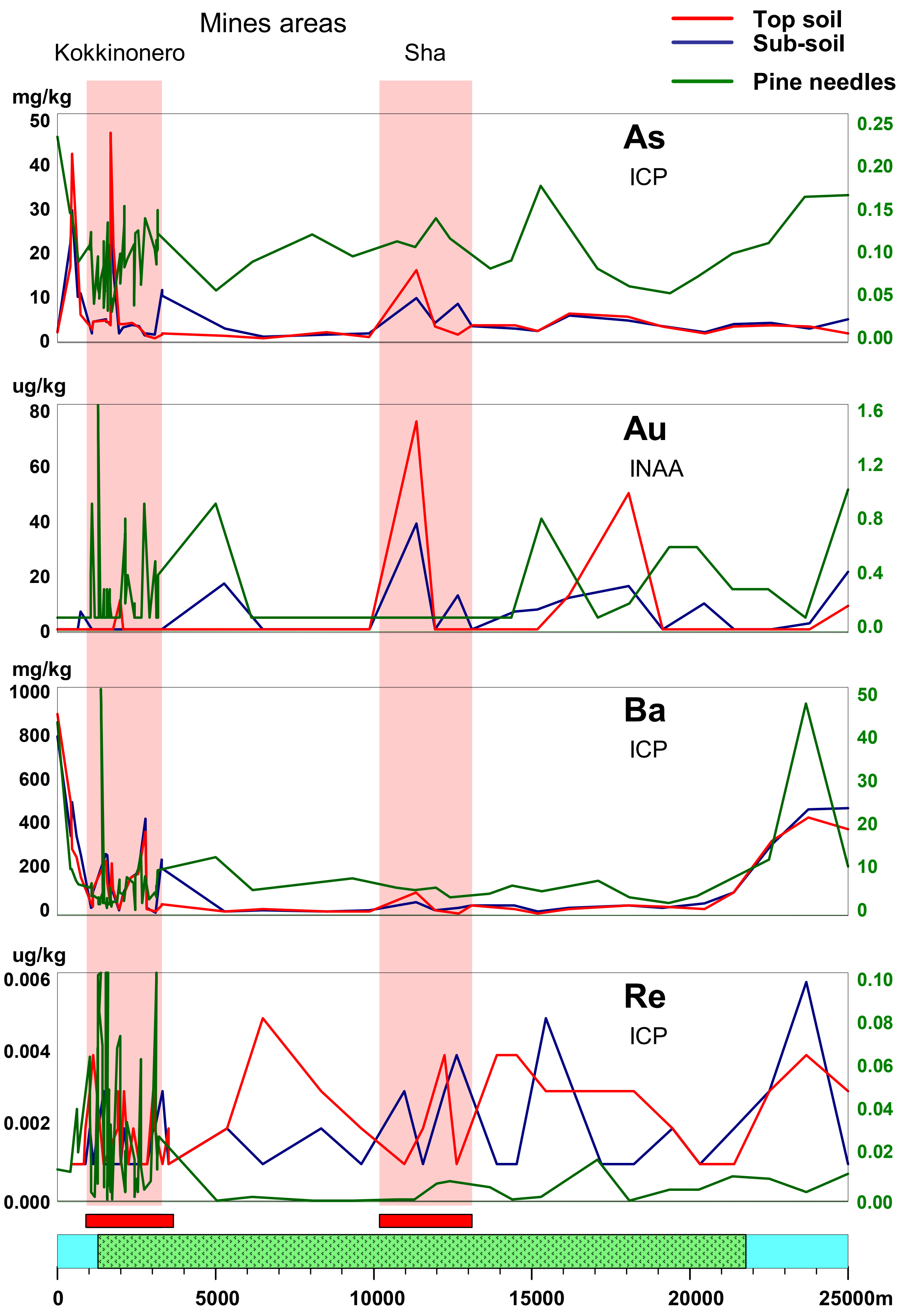

Figure 5.87 Soil and vegetation element concentrations along Kokkinonero-Sha traverse.

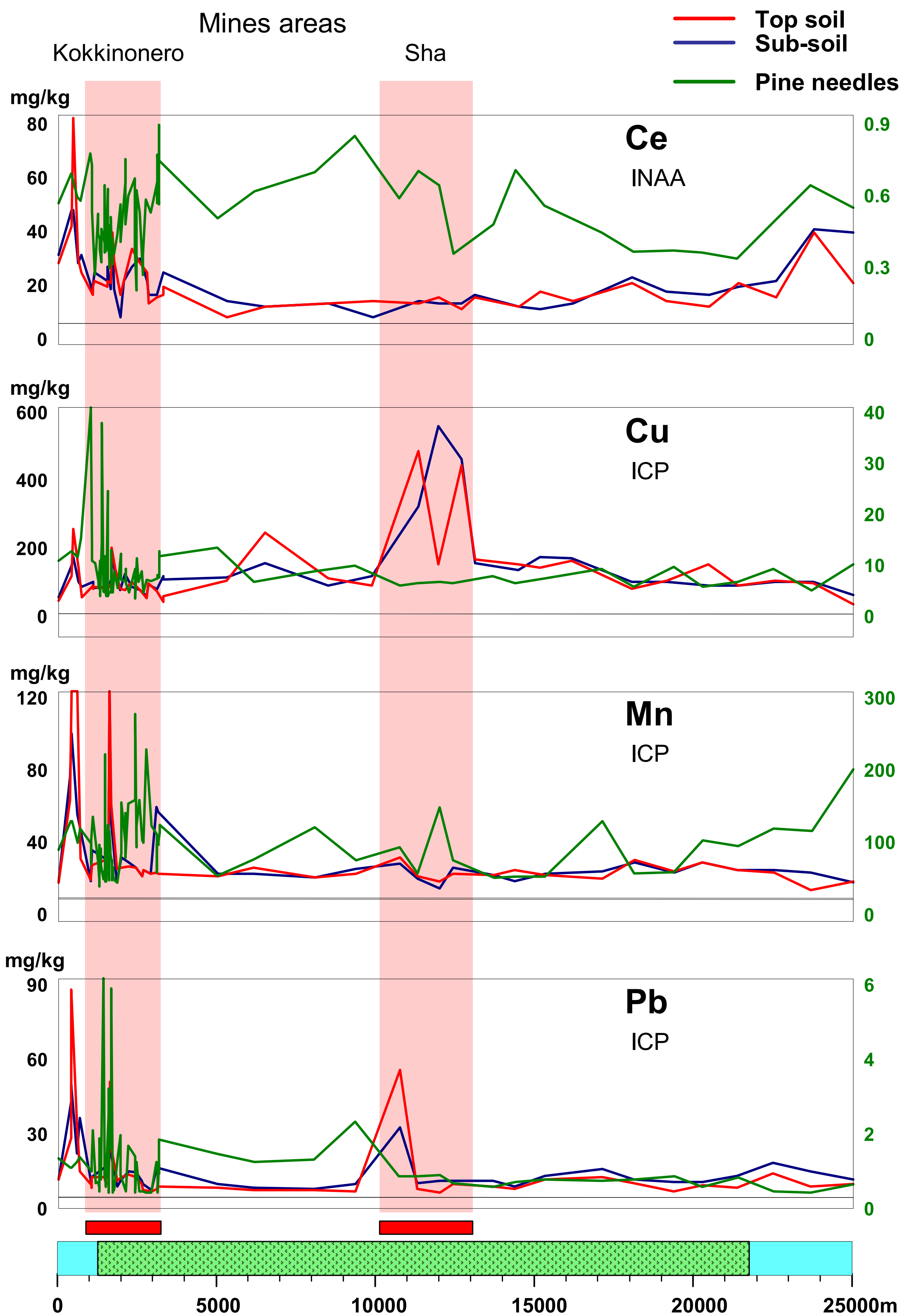

Figure 5.88 Soil and vegetation element concentrations along Kokkinonero-Sha traverse.

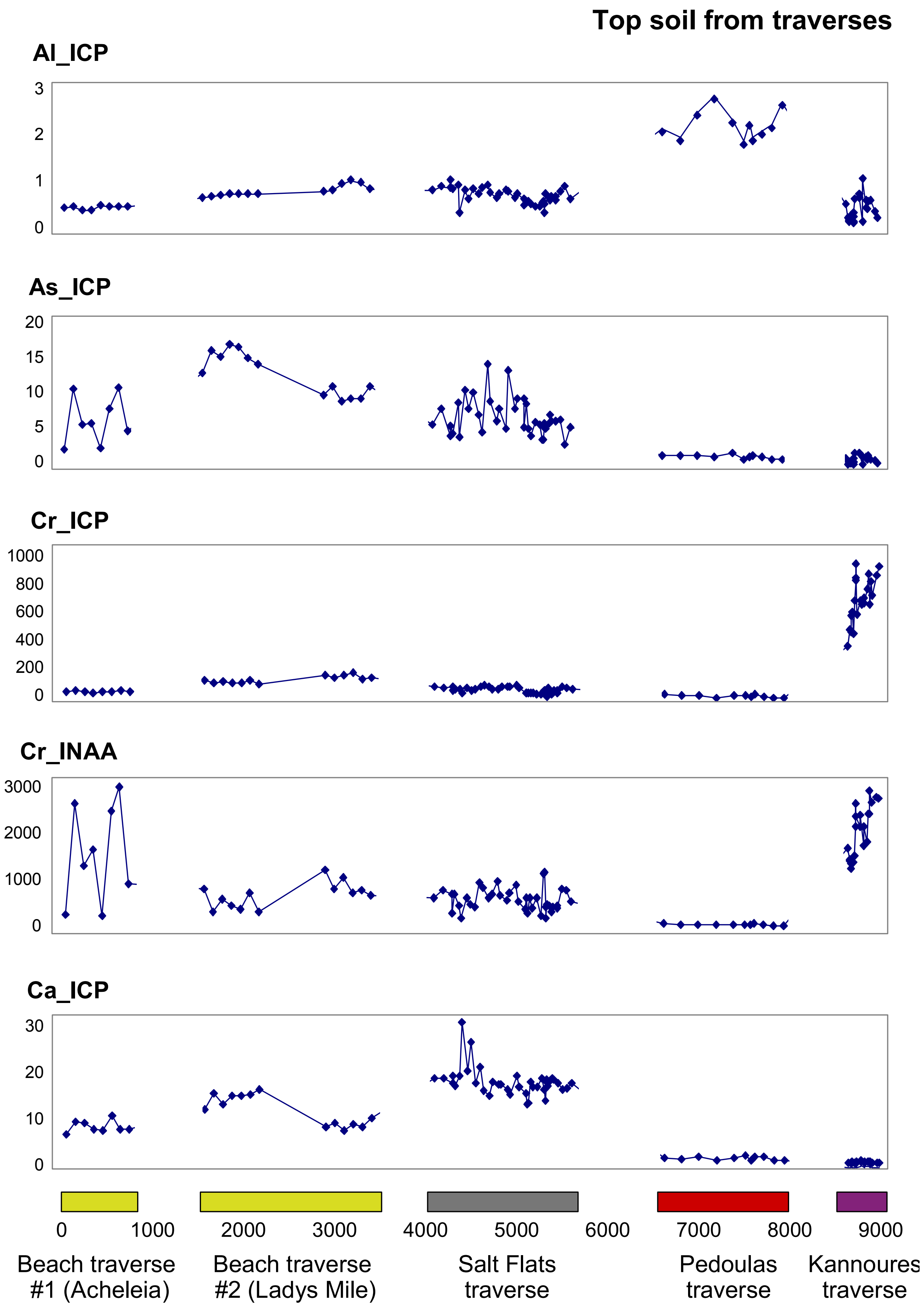

Figure 5.89 Soil geochemistry along various traverses in different geology-landform settings.

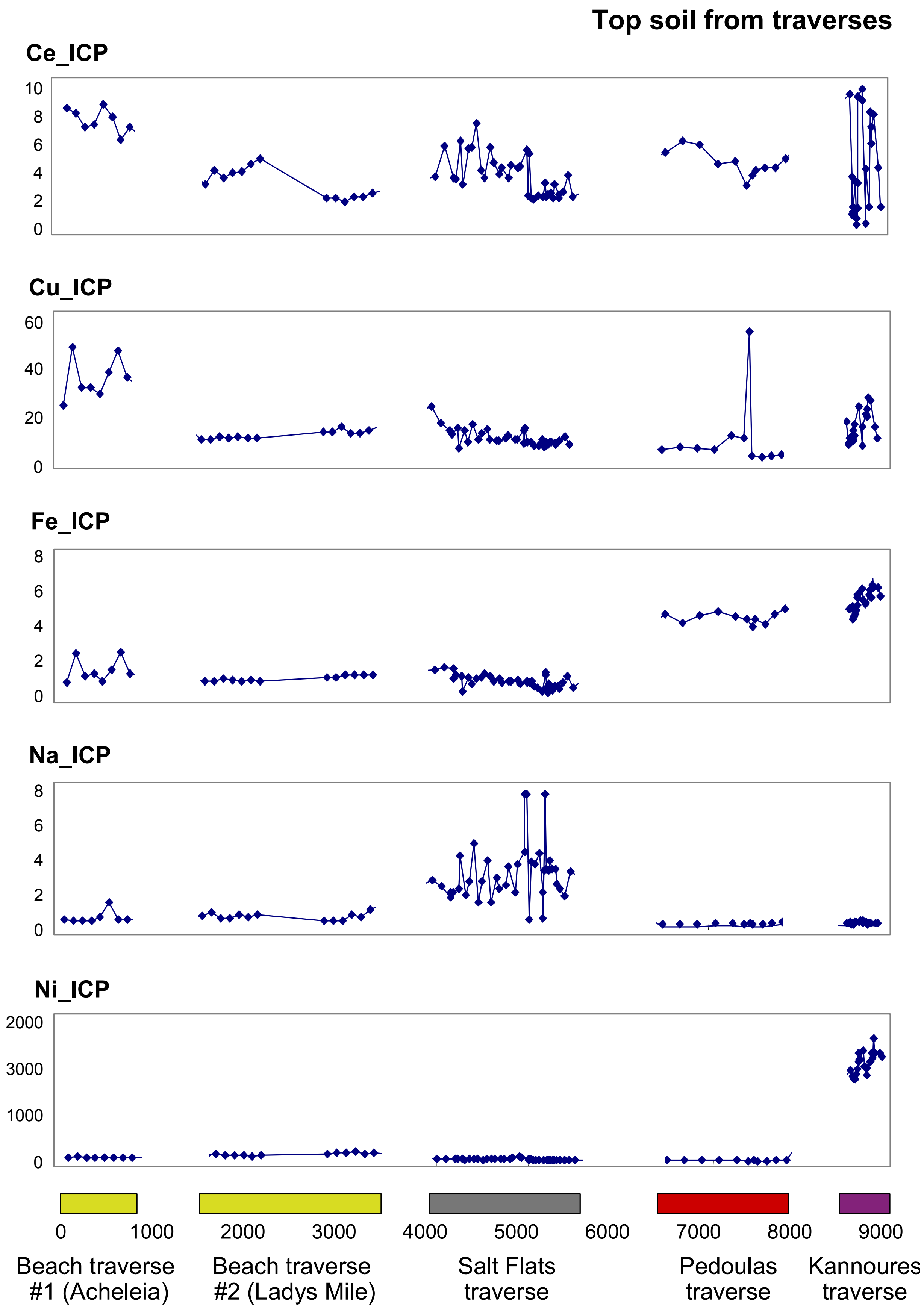

Figure 5.90 Soil geochemistry along various traverses in different geology-landform settings.

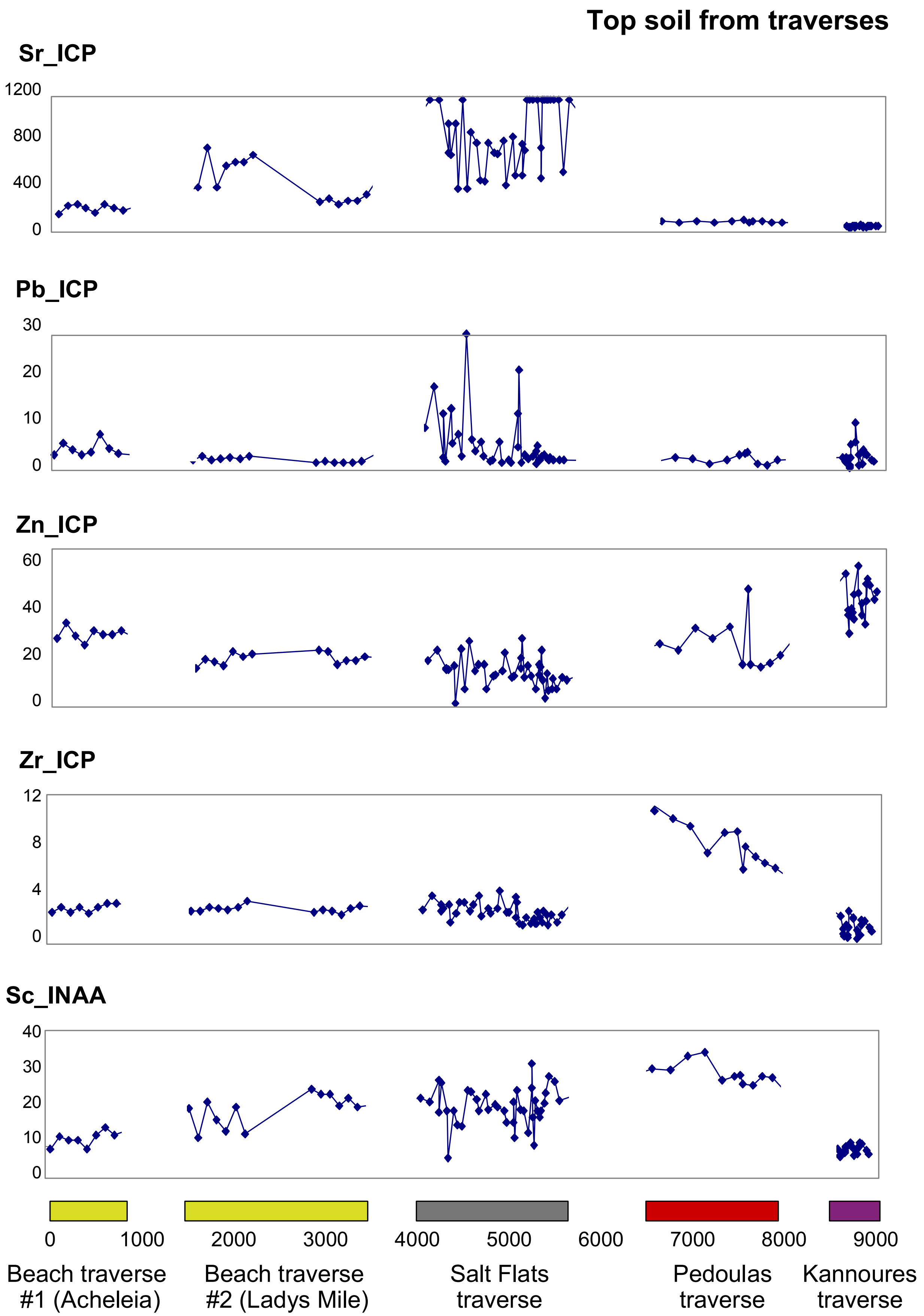

Figure 5.91 Soil geochemistry along various traverses in different geology-landform settings.

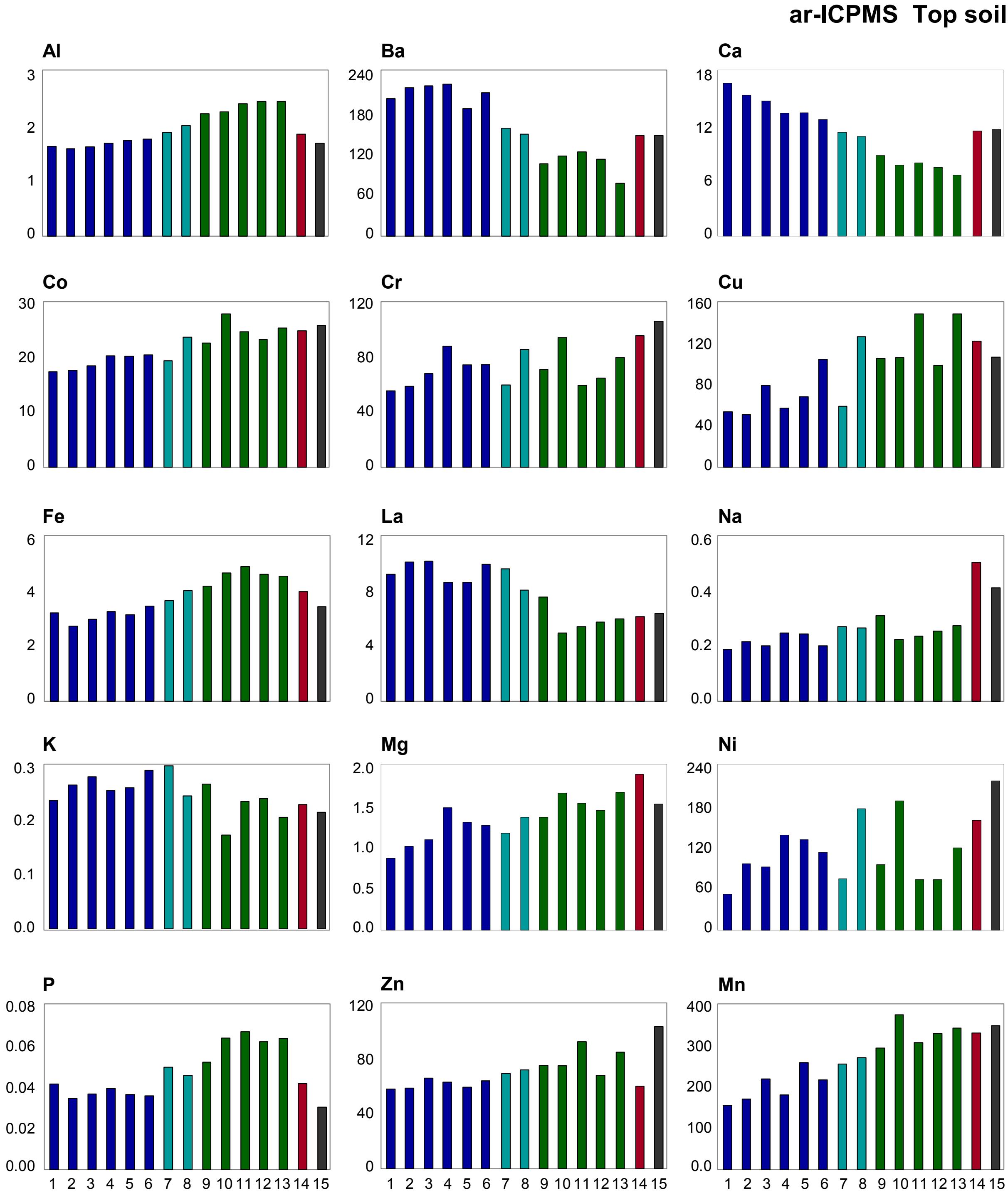

1 gypsiric-regosols + leptic-gypisols
2 calcaric-rendzic-leptosols + calcaric-leptic-cambisols
3 skeletic-calcaric-regosols + calcaric-lithic-leptosols
4 eutric-gambisols + eutric-anthropic-regosols
5 eutric-lithic-leptosols + eutric-skeletic-regosols
6 skeletic-leptic-regosols
7 calcaric-cambisols + calcaric-regosols
8 calcaric-fluvic-cambisols + vertic-cambisols
9 lithic-leptosols + epipetric-calcisols
10 vertic-cambisols + calcaric-regosols
11 calcic-luvisols + chromic-vertic-luvisols
12 epipetric-calcisols + leptic-chromic-luvisols
13 calcaric-lithic-leptosols + calcaric-leptic-regosols
14 vertic-leptic-cambisols + chromic-vertisols
15 gleyic-solonchalks

Figure 5.92 Variation in selected element content by soil type, Cyprus

Pine needles

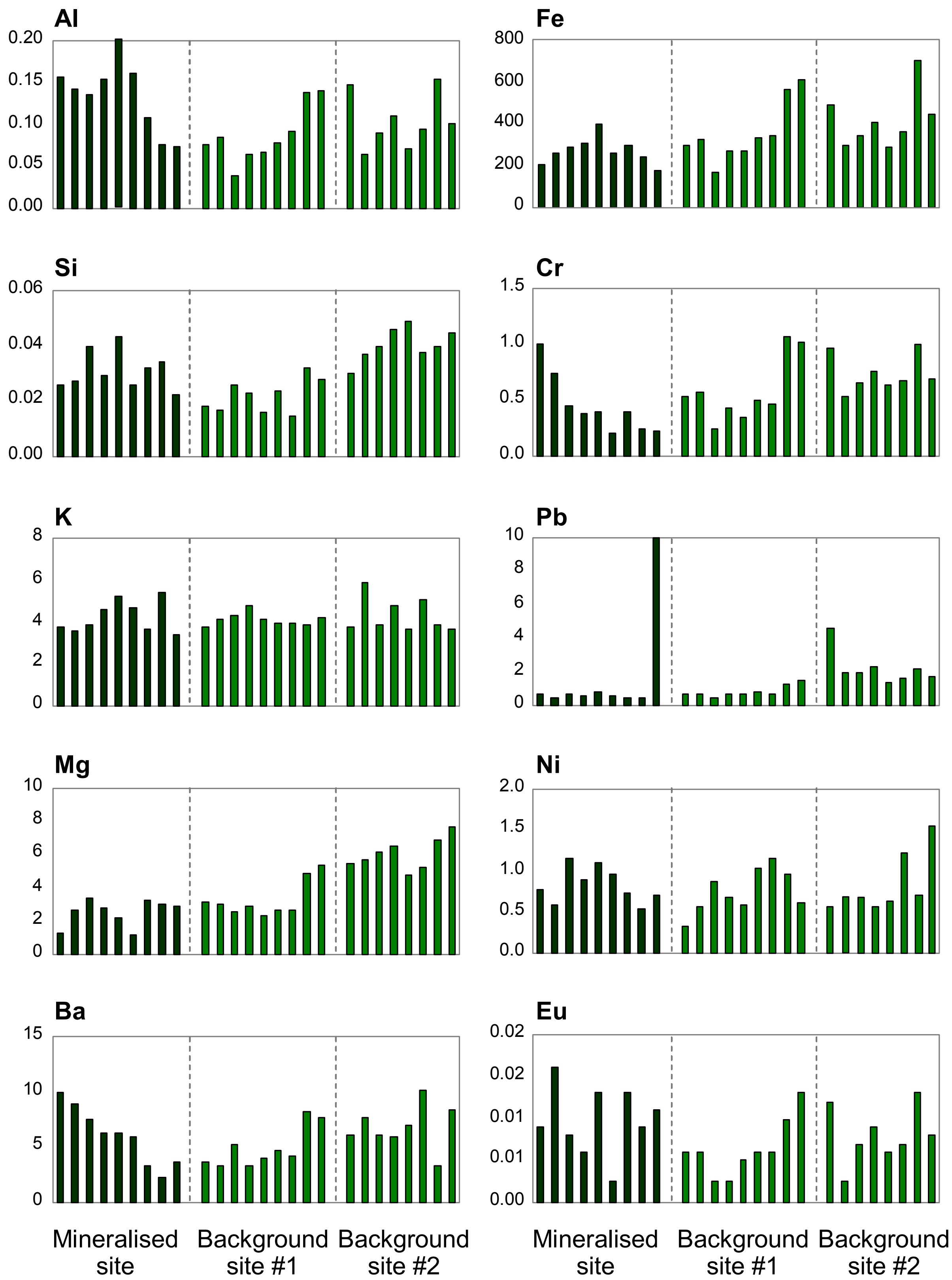

Figure 5.93 Variation in trace element concentrations in olive leave from three test sites in Mitsero (one near mineralisation and two from areas away from mineralisation) .

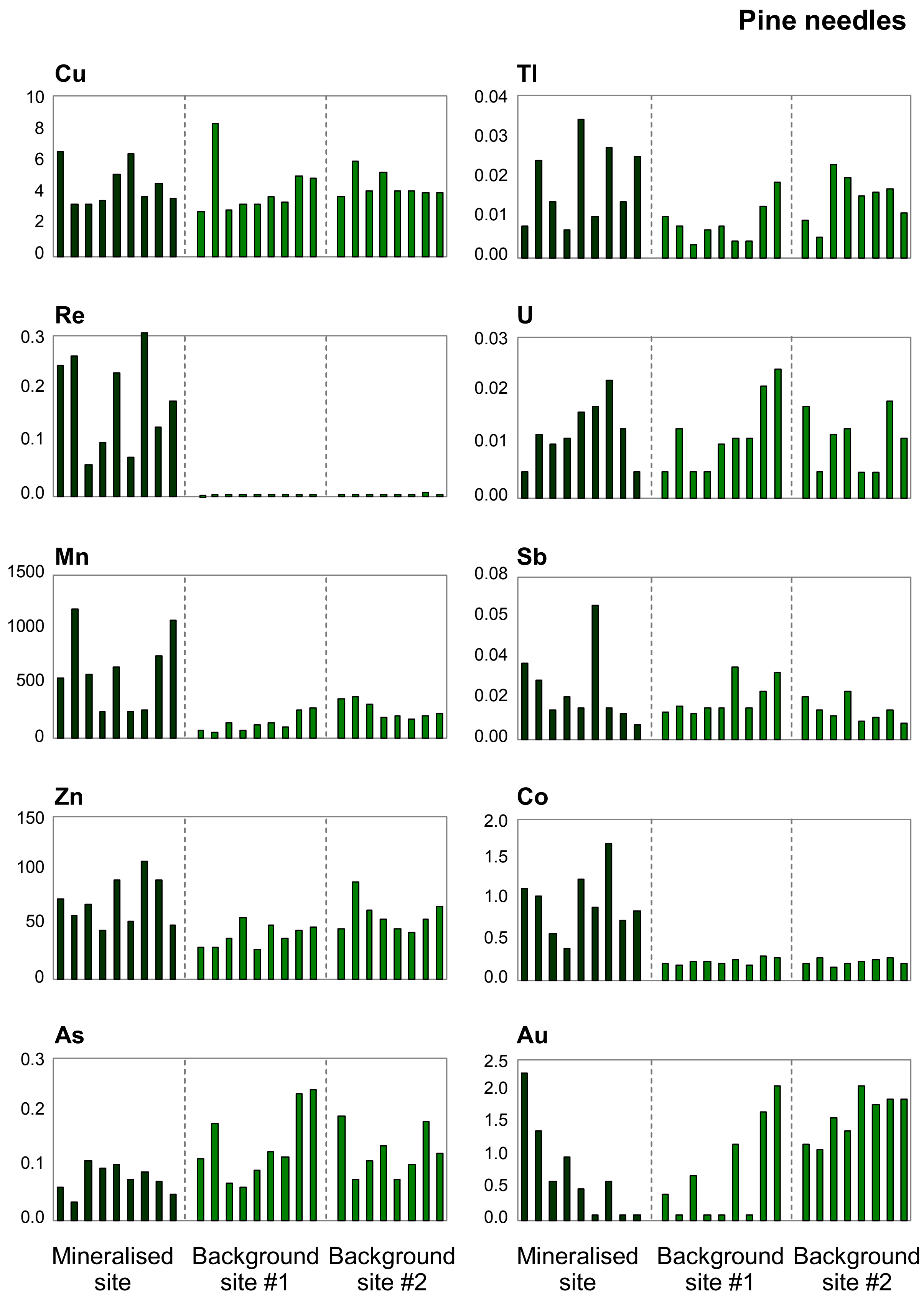

Figure 5.94 Variation in trace element concentrations in olive leave from three test sites in Mitsero (one near mineralisation and two from areas away from mineralisation).

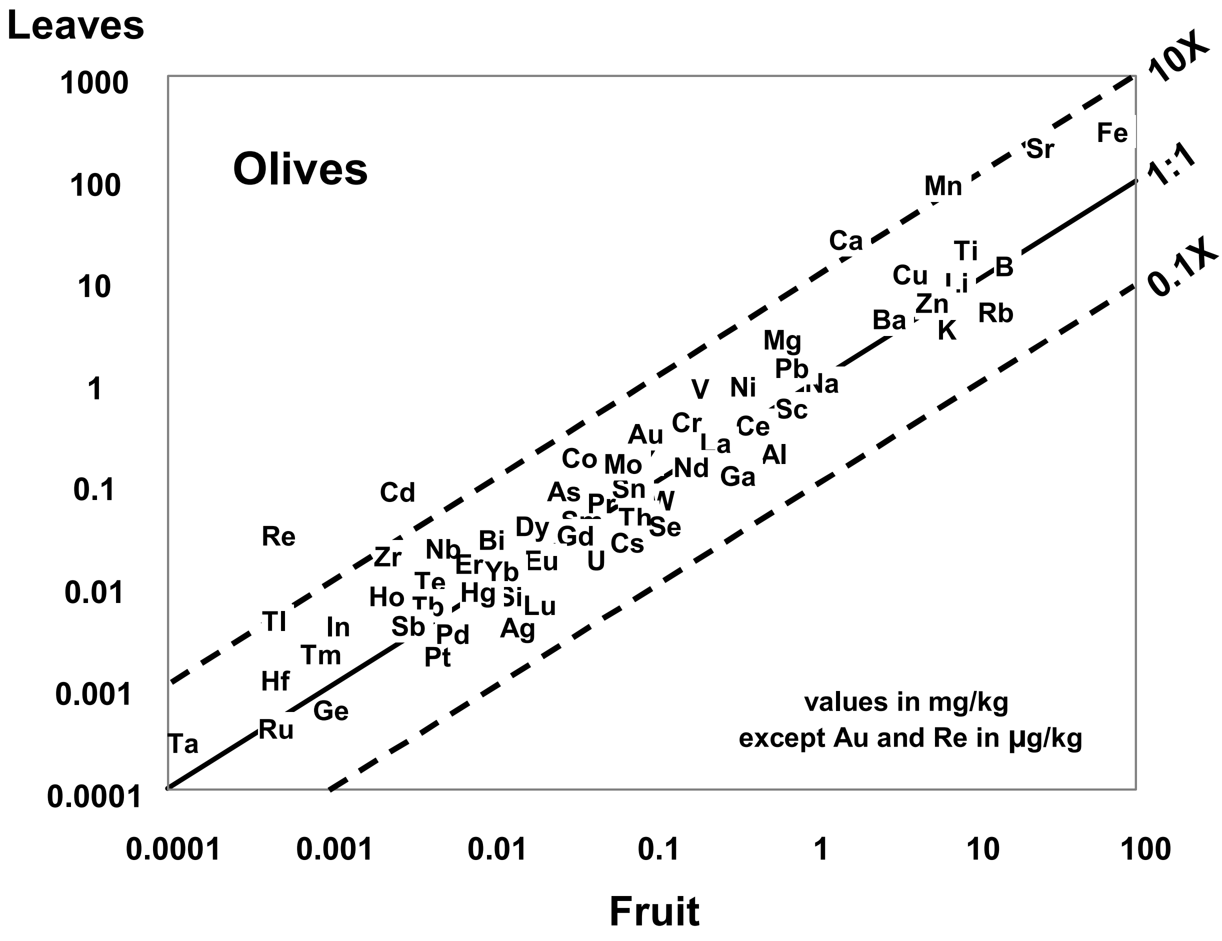

Figure 5.95 Comparison of element contents in fruit and leaves of olive leaves collected near Sha (n=6).

Table 5.7 Factor patterns after varimax rotation (λ-transformed variables, ar-ICPMS average for topsoil and subsoil ,8-factor model). Only significant loadings shown.

Factor	**1**	**2**	**3**	**4**	**5**	**6**	**7**	**8**	**Communality**
Ag				*0.36*		*0.39*			0.31
Al		0.85							0.84
As				0.73					0.68
B					0.43				0.28
Ba		-0.67							0.73
Be	0.67								0.72
Bi	0.49			*0.36*		*0.36*	-0.43		0.82
Ca		-0.88							0.92
Cd				0.49		*0.35*			0.63
Co		0.73	0.50						0.87
Cr			0.69						0.69
Cs	*0.37*				0.52				0.74
Cu		0.49				0.63			0.68
Fe		0.93							0.92
Ga		0.88							0.91
Hg									0.10
K	0.43				0.77				0.83
Li					0.67				0.65
Mg		0.64	0.43						0.78
Mn		0.47				*0.35*			0.65
Mo				0.73					0.58
Na									0.21
Nb	*0.36*							0.50	0.67
Ni			0.89						0.87
P		0.52							0.53
Pb	0.42			0.47					0.68
Rb	0.50				0.73				0.93
Sb				0.66					0.64
Sc		0.91							0.94
Se									0.16
Sn	0.52								0.50
Sr		-0.80							0.86
Te									0.18
Th	0.63								0.84
Ti		*0.38*					0.60		0.62
Tl	0.41			0.54	0.42				0.80
U		-0.51		0.58					0.74
V		0.85							0.88
Zn		0.54				0.51			0.71
Zr	0.43	0.62							0.64
Ce	0.78								0.96
Dy	0.94								0.98
Er	0.87								0.97
Eu	0.92								0.91
Gd	0.97								0.98
Ho	0.90								0.95
La	0.74	-0.41							0.94
Nd	0.86								0.97
Pr	0.82								0.97
Sm	0.93								0.97
Tb	0.93								0.93
Tm	0.74	*0.38*							0.81
Y	0.92								0.94
Yb	0.79	*0.38*							0.94
Variance %	26.3	19.0	5.0	7.4	6.3	3.6	3.6	2.8	
Cum % variance	26.3	45.3	50.3	57.7	64.0	67.6	71.2	74.0	

Factor patterns after varimax rotation (λ-transformed variables INAA average for topsoil and subsoil, 8-factor model). Only significant loadings shown.

Factor	1	2	3	4	5	6	7	8	Communality
As				0.76					0.70
Br		*-0.39*							0.38
Ca		-0.90							0.93
Co		0.90							0.94
Cr		*0.37*	-0.54						0.57
Fe		0.94							0.94
Na		0.62	*0.37*		0.43				0.79
Sb	*0.37*			0.60					0.58
Sc		0.85							0.93
Th	0.89								0.89
Ce	0.94								0.92
Eu	0.69		0.43						0.77
La	0.94								0.96
Lu		0.49	0.53						0.67
Nd	0.69								0.58
Sm	0.83		*0.36*						0.90
Yb	0.40	0.50	0.70						0.97
Variance %	29.4	27.5	10.5	6.4	2.4	1.4	0.8	0.6	
Cum % variance	29.4	56.9	67.4	73.8	76.2	77.6	78.4	79.0	

See Volume 3 of the Report for Maps

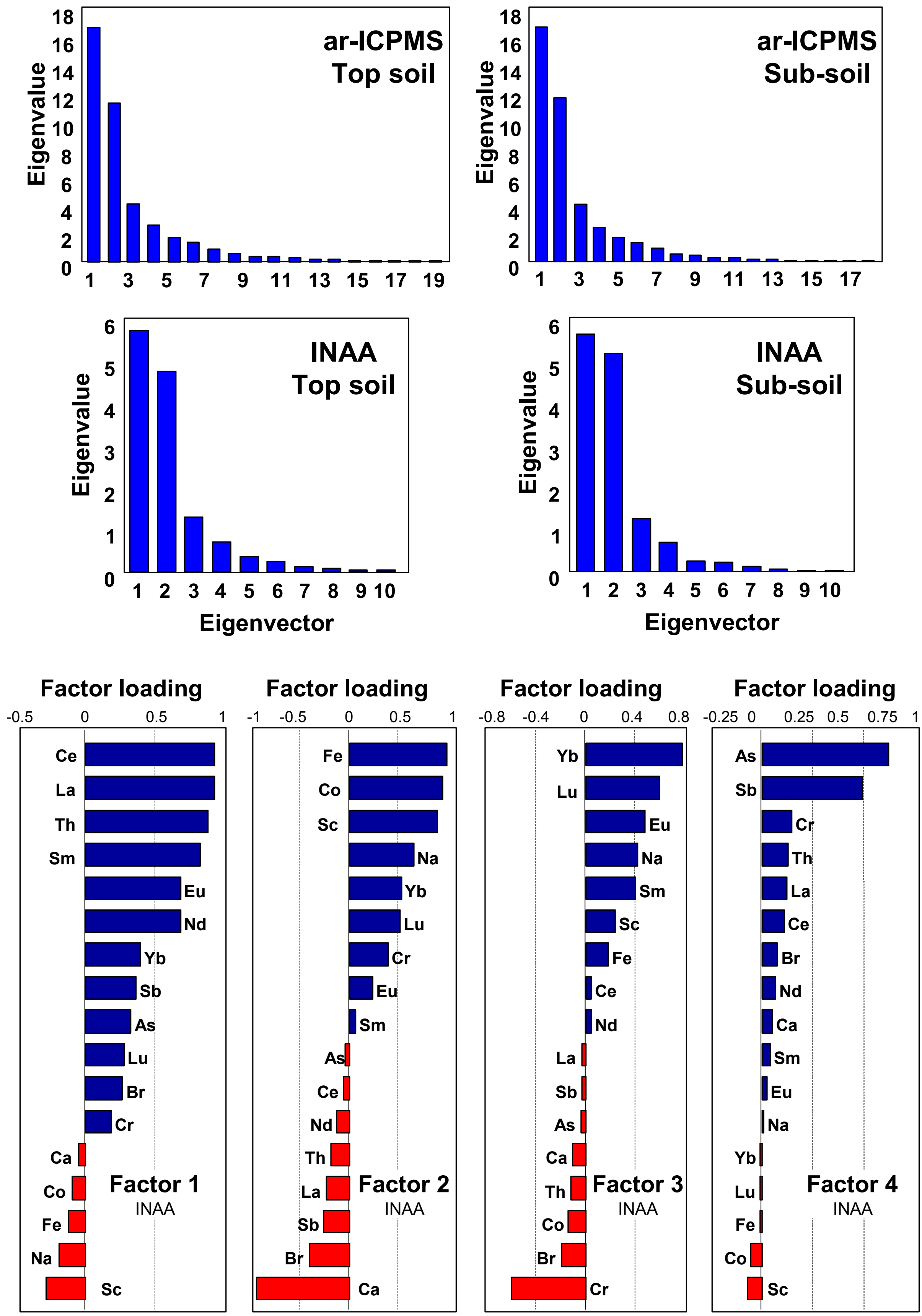

Figure 5.96 Scree plots and significant factor loadings for the first four factors from an eight-factor model for top soil INAA data. Varimax rotation on λ-transformed data.

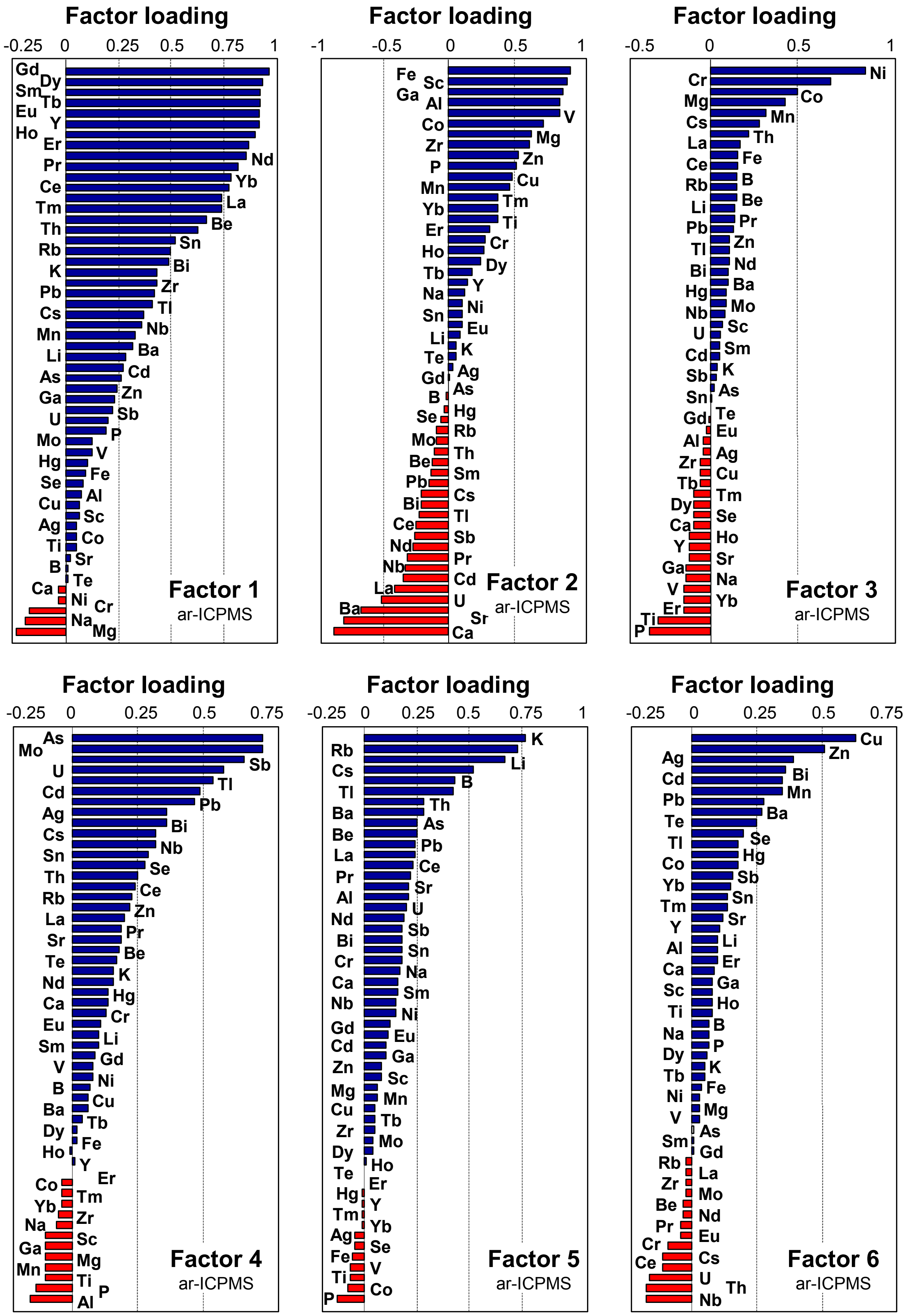

Figure 5.97 Significant factor loadings for the first six factors from an eight-factor model for top soil ar-ICPMS data. Varimax rotation on λ-transformed data.

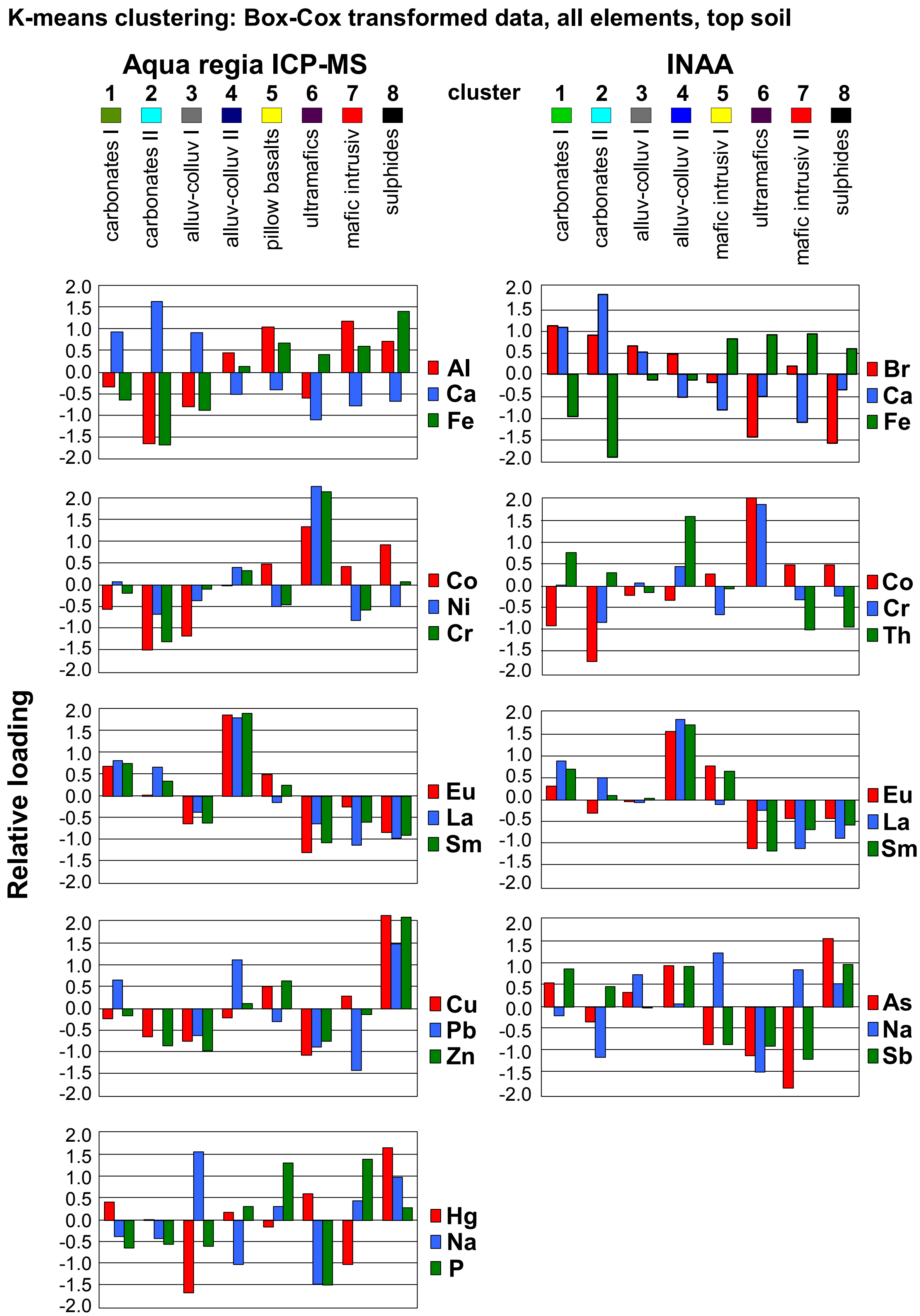

Figure 5.98 Mean element values for selected variables in 8– cluster k-mean analysis for ar-ICPMS and INAA data from top soil (λ-transformed data).

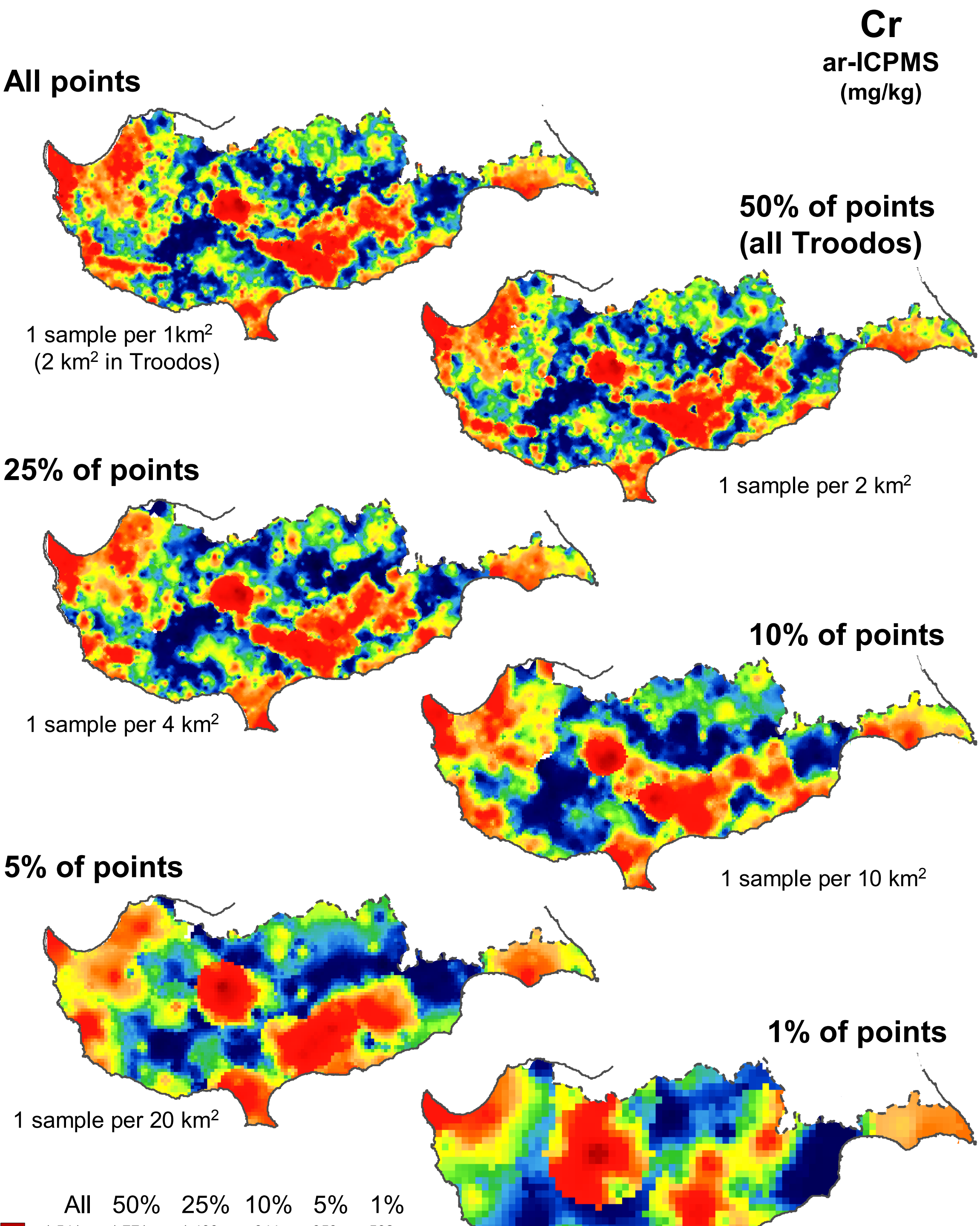

All	50%	25%	10%	5%	1%
1,541	1,771	1,490	944	950	532
111	110	114	110	130	118
77.5	76.4	80.5	78.8	86.3	85.9
61.6	60.5	64.6	63.1	67.5	75.7
52.5	51.6	54.0	53.4	53.4	64.0
45.7	46.3	46.9	46.2	47.1	55.4
41.2	41.0	41.6	40.1	42.4	47.5
36.6	35.7	38.0	36.5	39.2	43.6
32.1	30.4	32.7	31.7	36.1	37.4
25.3	25.1	27.4	25.6	31.4	31.1
0.3	0.3	2.7	2.7	9.0	6.6

Figure 5.99 Variations in spatial patterns for Ba_ICP_A as the sampling density is progressively reduced from the original 1 per 1 km² to 1 per 100 km².

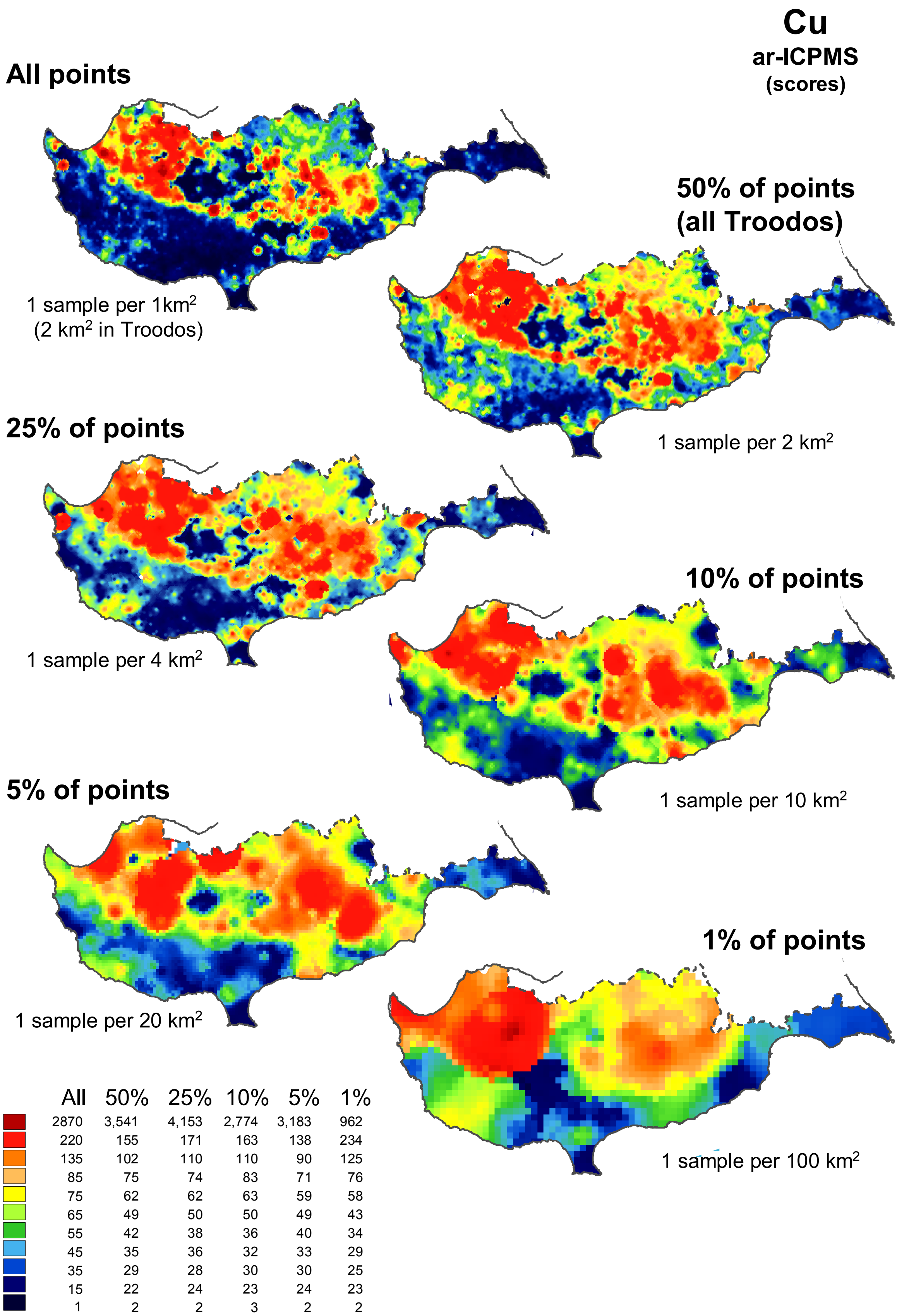

All	50%	25%	10%	5%	1%
2870	3,541	4,153	2,774	3,183	962
220	155	171	163	138	234
135	102	110	110	90	125
85	75	74	83	71	76
75	62	62	63	59	58
65	49	50	50	49	43
55	42	38	36	40	34
45	35	36	32	33	29
35	29	28	30	30	25
15	22	24	23	24	23
1	2	2	3	2	2

Figure 5.100 Variations in spatial patterns for Cr_ICP_A as the sampling density is progressively reduced from the original 1 per 1 km² to 1 per 100 km².

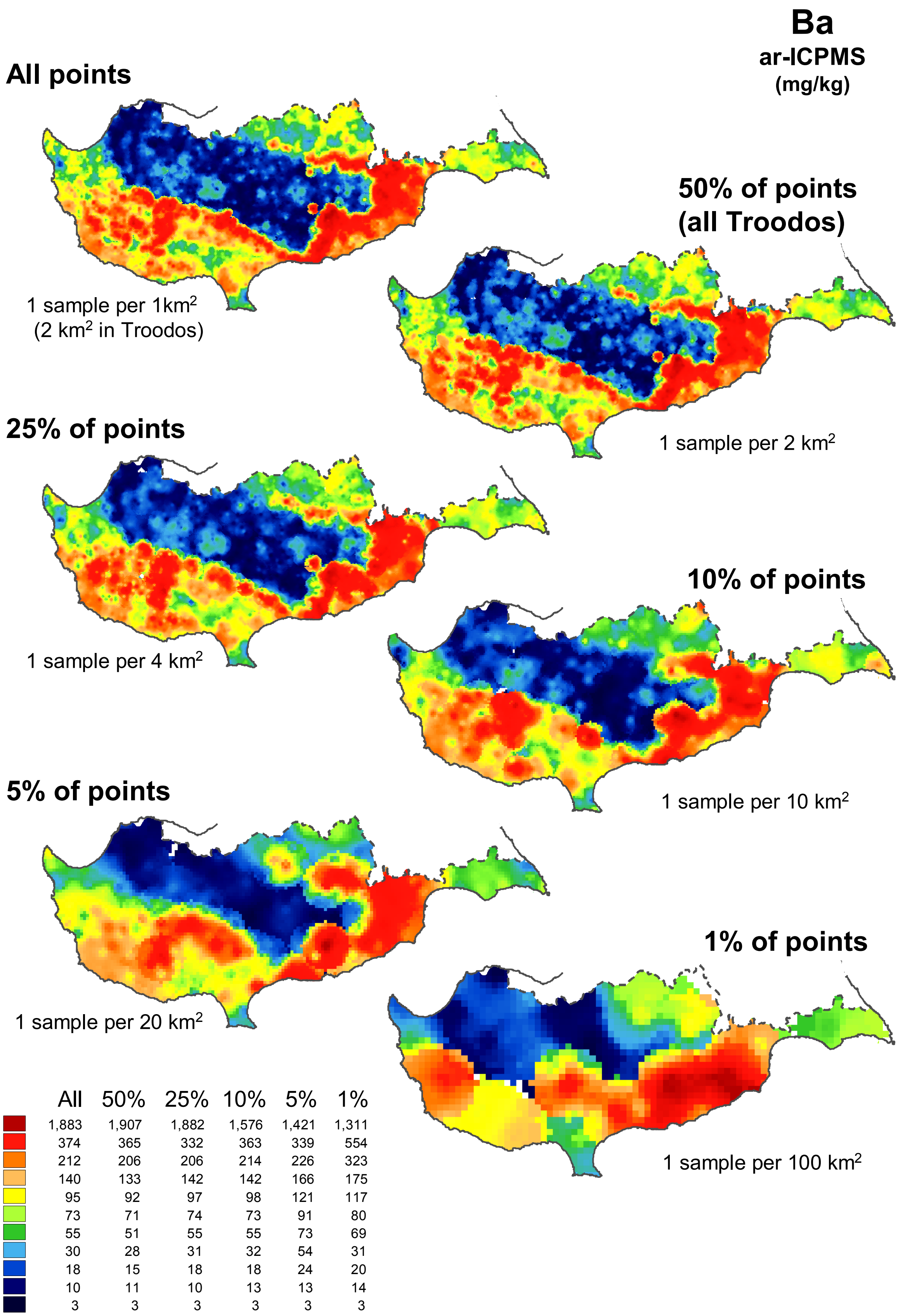

All	50%	25%	10%	5%	1%
1,883	1,907	1,882	1,576	1,421	1,311
374	365	332	363	339	554
212	206	206	214	226	323
140	133	142	142	166	175
95	92	97	98	121	117
73	71	74	73	91	80
55	51	55	55	73	69
30	28	31	32	54	31
18	15	18	18	24	20
10	11	10	13	13	14
3	3	3	3	3	3

Figure 5.101 Variations in spatial patterns for Cu_ICP_A as the sampling density is progressively reduced from the original 1 per 1 km² to 1 per 100 km².

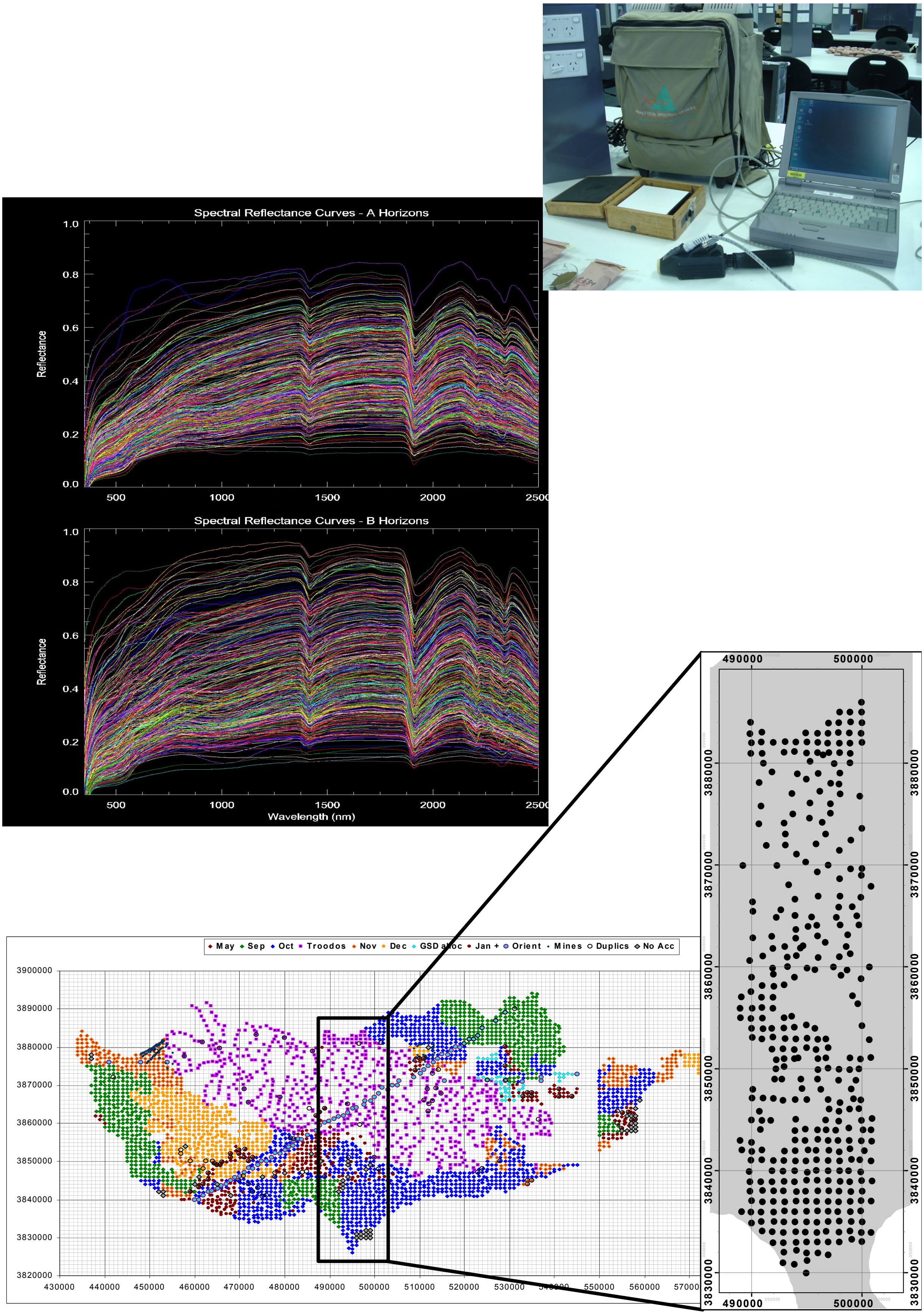

Figure 5.102 Spectral Reflectance Curves for A and B horizons, set up of the FieldSpec infrared spectrometer and locations of sample sites.

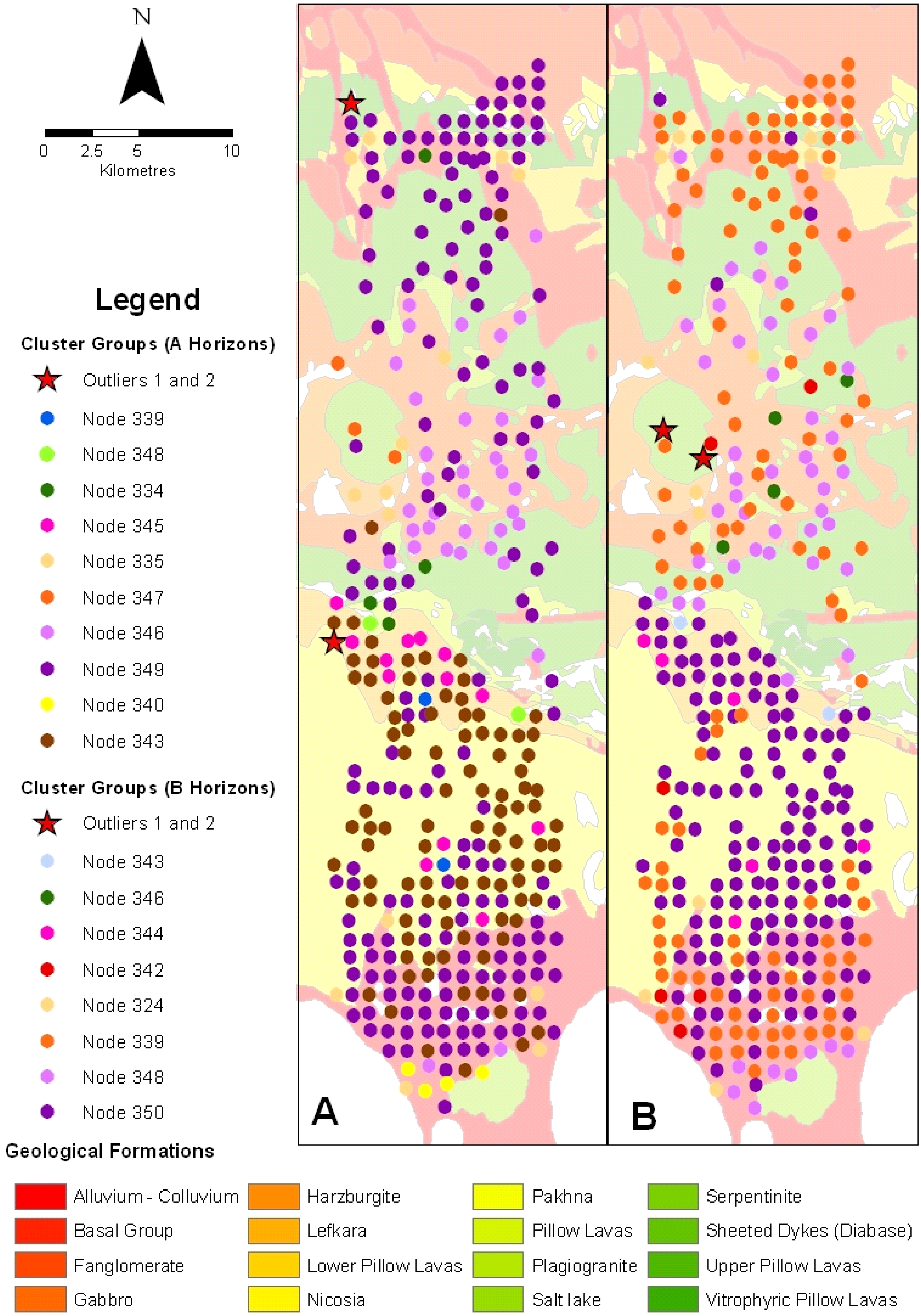

Figure 5.103 An overlay map of cluster nodes and lithological units for A and B horizons.

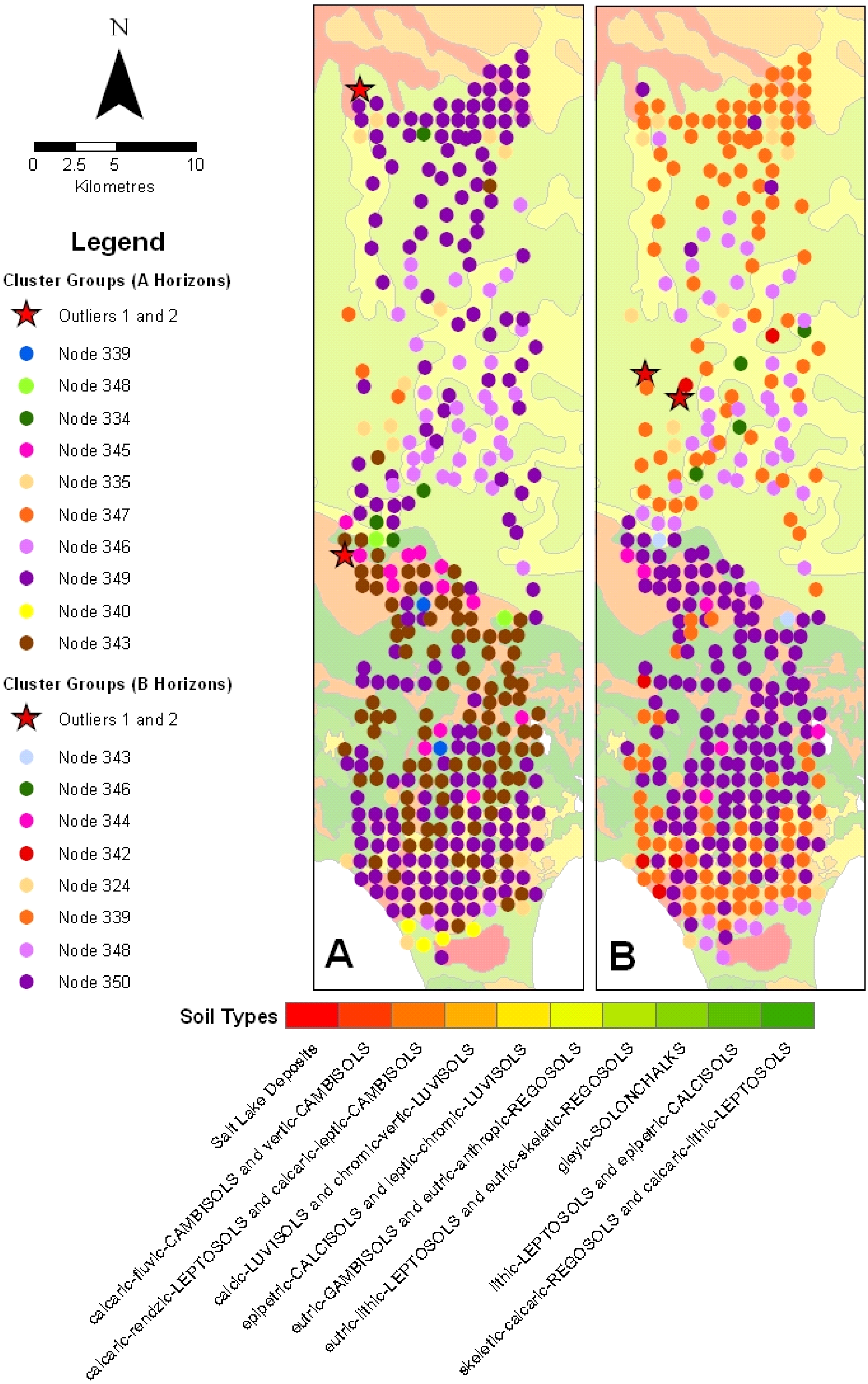

Figure 5.104 An overlay map of cluster nodes and soil units for A and B horizons.